Operational Characteristics of Thermoelectric Refrigeration.

VOLUME I

By

Wallace Shakun, B.S.M.E., M.S.M.E.

A Thesis submitted for the degree of Doctor of Philosophy.

April 1969.

Department of Aeronautics and Fluid Mechanics,
University of Glasgow.

TABLE OF CONTENTS:

The thesis consists of two bound volumes. Volume I contains: Chapter 1.0 to Chapter 9.0 (inclusive). Volume II contains: Chapter 10.0 to Chapter 13.0 (inclusive), Computer Program Index and Appendix.

Pg.

COMPUTER PROGRAMME INDEX.

APPENDICES.

I PREFACE.

This research thesis is concerned with the operational characteristics of thermoelectric effects in solids. It covers thermoelectric cooling modular design from a parametric-phenomalogical aspect as opposed to a mechanical method of construction or assembly point of view. -- The research constitutes a comprehensive engineering/research effort to develop the mathematical relationships required for the design of a thermoelectric cooling system.

The thesis has been written as an engineering tool inabling the designer to utilize or evaluate the thermoelectric refrigeration process. Care has been exercised in defining functions, differential equations/solutions; in particular the author has presented the implications of a particular form of the solution. Avoiding such expressions as "it is evident that", "it is clear that" since to the utilizer the statement that is supposed to be self evident rarely is. In the technological world the interrelated changing entities and variable dictate to some extent the conclusions presented at this time.

The research was sponsored by the University of Glasgow, Department of Aeronautics and Fluid Mechanics, Glasgow, Scotland.

The author is indebted to Professor T.R.F. Nonweiler and to Dr. H.Y. Wong for their academic encouragement. The research was conducted while the author was a research student at the University of Glasgow, Scotland.

The manufacturing and assembly of the components were under the admiral control of Mr. J.F. Kinnear. His coöperation and extreme care during the program is herewith proclaimed.

( ) Numbers in brackets refer to similarly numbered items in the reference chapter (13.0).

II SUMMARY.

Advancements in contemporary physics in the field of semiconductors now make it possible to effectively utilize thermoelectric phenomenon for cooling and environment heating. Refrigerator applications using thermoelectric cooling effect are being built and introduced into industrial and military engineering design. Calculations on semiconductor thermoelectric refrigeration systems are based on relationships derived from considering the basic thermoelectric couple to be in an isolated control volume. In this pseudo environment the cooling capacity and coefficient of performance are based on the assumption that junction temperatures of the thermoelements are independent of the current. Test results on semiconductor refrigeration systems indicate however that the C.O.P. characteristic* with the absence of artifical restraints do not have extremal values. Such conclusions can only be observed if an experiment is conducted in which the junction temperatures are controlled (constant). Conclusions which are obtained account only for internal energy processes occuring within the control volume. However in actual practice the cooling capability, performance level are functions of the applied current. The results available (within the thesis proper) indicate that there is a direct functional relation between the thermoelectric couple and the environment to be regulated.

* C.O.P. = f(I)

The object of the thesis is to present the various operational parameters that relate system performance to the environment in which the thermoelectric module is required to perform and control. The mathematical coupling between the thermoelectric junctions and the environments are assumed to be represented by a N^{th} order function.

The technique of utilizing a parametric analysis model enables a comprehensive engineering effort to establish the mathematical tools for competitive evaluation.

Four major subcomponents sharply influence the design/performance of thermcouples for modular assembly. The thermal and electrical material properties of the elements fall into the most fundamental category. Power supply and regulation control are in a second major category. Properties and technique of material construction and processing are a third consideration. Heat exchanger devices provide further requirements to be considered. The various problems to be encountered are considered and the inter-acting of the major components are indicated. The extent to which these conditions limit the design/performance and the determination of the most advantageous comprimise is essentially the task considered.

Methods are developed to determine the quantative effects of parametric adjustment. The design problems considered result in the requirements for the solution of the heat transfer equation in which the boundary conditions are stated. The solution to this class of problem is offered by the application of numerical analysis. The technique for solution is by the method termed, "overrelaxation" thereby effectively increasing the convergence rate of the finite difference equations. Advances and more sophisticated methods of digital computer utilization resulted in a comprehensive mathematical tool being afforded to the design engineer.

1.0 INTRODUCTION.

This section is an introduction to the parametric/ operational methods of designing a heat pumping module for cooling applications. The applications would generally be of low capacity per module assembly, specialized devices. Most basic or fundamental design problems for large capacity systems are similiar for small capacity modules. The various problems to be considered in designing a heat-pumping modular assembly are stated, and the limits presently imposed by interacting effects are indicated. Mathematical methods are developed to determine the quantitative effects of parametric adjustments. The results are described by use of these operational methods.

The research is explicit, but considers a more complete design range of current thermoelectric element devices. Use of the digital computer (English Electric KDF9) for program solutions are profuse; in order to afford the engineer the ability to perform "trade off studies" at a more accurate level. The use of sophisticated method of analysis coupled with advances in material technology results in an approach philosophy not previously reported or available in literature.

2.0 OBJECTIVES.

The thermoelectric cooling devices considered are intended primarly for two types of operation:

(1) Refrigeration or heat pumping <u>against</u> a thermal gradient

(2) Heat pumping <u>along</u> a thermal gradient

In general the thermoelectric cooling devices must compete functionally and be economically competitive with other cooling methods. At present it appears that the application in which the thermoelectric heat pump can favorable compete are limited to those having low capacity requirements. A number of thermoelectric cooling devices have been built both in this country and overseas. Home refrigerators of the type used in private homes have been built in Russia, and in the United States by the Radio Corp. of America, Westinghouse and others. However, these early devices on a cost per cooling capacity cannot compete favorable with vapor-compression systems. Elementary thermoelectric cooling devices have been incorporated into infrared detectors for "spot" cooling of the detection head. In this application the required cooling capacity per installed volume (weight) was more effective than other cooling proposals.

The fact that thermoelectric cooling systems can not at present compete among high capacity devices (Commercial freezers) where initial costs are important appears to be reflected in the requirements of the material properties of the thermoelements.

The highest figure of merit[(1)] available at present is approximate 3×10^{-3} $^{o}C^{-1}$ and for an idealized cooling couple (chapter 6) results in a coefficient of performance (C.O.P.) for a refrigeration cycle of about 0.5 the value for a conventional compressor-type refrigerator. Hence, it can be presumed that operating costs should be greater than twice as for a compressor assembly, and hence an important design limitation for high capacity systems.

The fact that thermoelectric cooling systems can compete in low capacity applications is partially contributed to the fact that operating economy is not usually a major consideration for low capacity modules. In addition the packing requirements for many military applications excludes other cooling systems. Furthermore, thermoelectric heat pumps can be designed over a large variation in capacity with the C.O.P. being generally

(1) Figure of merit is a term defined by equation 6.5.2.13. The figure of merit is a material parameter affecting system performance.

invariant of capacity. Other types of heat pumps which which are not normally designed for cooling capacities of a few watts, have poor efficiences when designed for small heat loads and still poorer when operated at less than rated capacity. Hence for small heat load requirements thermoelectric devices may have the lowest operating cost or the highest C.O.P. per unit cost. Since thermoelectric materials are still relatively expensive thereby requiring high material utilization (watts/mass of thermoelectric material). In striving for high material utilization, the C.O.P. must not be sacrificed. For although the power consumption and operating cost may be tolerable because of the requirement for a low capacity system, the C.O.P. also determines the heat rejection requirements and hence the size and weight of the heat exchangers (interface with surroundings) increasing rapidly as the C.O.P. decreases. Furthermore efficiency degradation of the basic heat pump increases the size and weight of the regulated power supply.

A further design objective in order to minimize the power supply is to limit the ratio of the thermoelement area to the element height. The result is a smaller current and relatively high voltage for which power supplies by design are smaller, lighter, more efficient and cheaper.

3.0 DESIGN CONSIDERATIONS.

Although thermoelectric effects have been known and investigated for over a century (1820), practical thermoelectric energy-conversion devices have become possible very recent. Modern developments in semiconductors, statistical thermodynamics have made feasible the fabrication of thermoelectric generators and heat pumps or refrigerators that have significant utility.

Modern research into thermoelectric effects can be divided into two broad areas. The first of these is the materials for thermoelectric application. The research in this area has been to investigate and understand the thermal and interrelated electrical phenomina in semiconductors and to develop materials having characteristics better suited for this application. The second is the area of device development and application. Research in this area is directed towards utilizing available materials towards an understanding of system performance in order to optimize device response. The research reported in this thesis falls in the category of device performance.

Four major categories or operational conditions sharply influence the design of thermoelement arrays used in modules.

The thermal and electrical properties of the thermo-element material fall into the most fundamental category. Cost of fabrication, interrelated material processing are a second major category. Power supplies and output regulation, heat exchanger design provide further requirements to be considered.

The extent to which these parameters influence and limit the ultimate design of the thermoelectric device and the determination of the most advantageous compromise is essentially the research undertaken. The following subsections will indicate and review the general areas considered. Some quantative estimates will be presented to indicate the seriousness of the limitations imposed. These estimates will not be fully justified in these early sections.

3.1 Thermoelectric Material Properties.

The thermal and interrelated electrical material properties of the thermoelements define the ultimate limits on system design and performance. The material figure of merit, for example determine directly the maximum junction temperature difference that can be attained and defines the maximum C.O.P. for given operating junction temperatures. Specific properties, such as ρ, density; K, thermal conductivity collectively influence design potential. For materials to be suitable for thermoelectric applications they must exhibit a high figure of merit, Z . The three properties that effect the figure of merit; the electrical conductivity, thermal conductivity, the absolute couple Seebeck coefficient are not independent of each other or invariant with temperature. All three are functions of the free charge carrie density (1) . In fact most design objectives depend ultimately on these specific properties and not simply on the figure of merit. For example: determining the length and cross sectional of materials required to optimize performance, specifying configuration for a prescribed heat load, decreasing the effect of junction resitivity (discontinuity).

The operational calculations did not assume any major changes from present day material properties, in fact some of the illustrations employed, average values measured on materials were employed. However, the parametric results and presentation format allows for easy extrapolation. Substantial improvements in material properties would yield obviously more useful designs and hence this research can be applied for "advancements" in material state of art.

Since high quality or 'doping' of semiconductor materials are expensive, design which minimize material requirements will be extremely important. In general, this requires the use of short couple arms, figure 7.1.2.1. It will be shown equation 7.2.5.8. that the amount of material required to pump a given heat load (watts, BTU/time) decreases as the square of the length of thermoelement arm.

3.2 Construction Materials and Processing.

A practical thermoelectric device would normally consist of thermoelectric couples connected electrically in series and thermally in parallel. It is required that the electrical resistance of any inactive materials connected in a series circuit should be as low as possible in order to minimize the joule heat (I^2R, watts). The joule heat an irreversible phenomena is the heating effect arising in a current carrying conductor. This requires low electrical resistivity and high area to length ratio (if compatable with other requirements) coupled with low junction resistivity. Electrical resistance of shunting circuits must be kept relatively high. Similarily the thermal impedence of the thermo-elements should be as low as possible, while the heat path inter-element is required to have a high thermal impedence.

Structural integrity of a module assembly is also important, the severity of the problem depending on the application. Environment stability may require some form of encapsulation.

Chemical compatibility and adequate matched thermal expansion coefficients are additional construction considerations.

When thermoelements are used in a module, it is necessary to join or bound them to metal conductors or to other module components. The basic requirement for these contacts or junctions is that they must have little effect on electrical and thermal conduction. If high or any impedence exists joule heat losses and temperature drops across the contacts will reduce system efficiency. The effect of contact resistance is discussed in section 7.2.

Many considerations may only become important or recognized in the actual process of construction. Developing reliable, performance repetitive devices or automating production can influence the final design. These considerations are referred to as a practical design compromise as opposed to a parametric consideration.

The main concern of this research program is "phenomenological" in approach; where real properties and material characteristics are evaluated but where difficulties of construction are not the prime consideration.

3.3 Power Supplies and Controls.

Thermoelectric heat pumps operate only with unidirectional current and any alternating current component represents pure loss. Any alternating component of the current would produce joule heating and would pump no heat. The requirements for steady direct current at the impedence levels for a thermoelectric couple is not a commonly encountered problem. At the present state of development, thermoelectric cooling devices operate at relatively high currents and low voltages, i.e. from 5 to 40 amps and from fraction of volts to 30 volts. Since most commercial consumers would use A.C. as a prime power supply rectifying power supplies are essential.

Conventional power supplies become less efficient, larger and heavier when designed for high currents and low voltages. The burden is further increased when ample filtering networks are encorporated.

The most desirable current form can be determined after considering the source of direct current, the ratio of thermoelement height to cross sectional area whether the C.O.P. or refrigeration capacity is more important. Usually a 10% ripple will be satisfactory which represents a loss of 4% in system efficiency (2).

Assuming the resistivity of modern thermoelectric elements of the order of 10^{-3} ohm-cm; with a ratio of area to length of a thermcouple arm of $\simeq$ 1 results in a resistance of the order of 10^{-3} ohms. This will require high current, low voltage power supply even with a large number of thermocouples connected in series. By proper adjustment of the area to length ratio operation can be reduced to a few amperes with a subsequent reduction in the cooling capacity per couple and thereby requiring more couples for a given application. The net result may be to increase fabrication and reliability problems.

With low current devices filtering would not be perfect and the residual ripple would decrease the heat pump performance. Section 7.3.2. discusses ripple effect and presents graphically the effects of current ripple on system performance.

3.4 Heat Exchangers.

Two design considerations influence the interface between the heat pumping module and the heat exchangers. The first is the problem of electrically isolating (insulation) the conducting straps on the thermoelements from the heat exchange surface and maintain consistant thermal contact. This is partly a problem of construction and material assembly and was partly reviewed in (3)

The second problem is that of 'matching' the heat pump capacity with the heat exchangers and balancing the requirements of the surroundings. From an engineering viewpoint the determination of the rate of heat transfer at a specified temperature difference is dependent on the characteristic of the heat exchanger. Consequently the design of the heat exchanger will greatly influence the response and steady state behavior of the thermoelectric assembly. The thermoelectric cooling system when analyzed with the aid of control volume is influenced by the surroundings via the medium of heat transfer, a non-reversible process. Using economically short thermoelements the heat pumping capacity per unit area (watts/cm^2) of thermoelectric material is expected to be a few watts/cm^2, a flux difficult to achieve with small junction temperature differences. In order to decrease the heat flux packing densities[2] less than unity are introduced. This however allows for inter-element heat leakage where there is no thermoelectric material. Thermoelectric couples supported on pedestals (figure 8.2.1) can be used to minimize inter-element heat leakage by increasing the effective height of the thermocouple junctions. The pedestals allow the use of short thermoelements with the increased effective height between the thermocouple junctions. An extensive analysis of the proposed mathe-

(2) Packing density (ω) is defined as:

$$\omega = \frac{\text{cross sectional area of thermoelement}}{\text{Total module cross sectional area}}$$

Section 7.2.2. introduces ω as an operational parameter.

matical models was conducted with the aid of a digital computer. The computer programs were compiled on an English Electric KDF9 machine. Appendicies (C.P.I.1,8) describe the programs that have been developed for studying various configurations. Section 7.4. contains the analysis technique for determining the heat leakage when pedestal modules are employed.

4.0 TECHNICAL APPROACH.

Unfortunately there does not appear to be a general formula that will yield the best, or even good designs. Logical configurations can be assumed, evaluated, modified and further evaluated. On the other hand, an inspiration may provide a physical arrangement that is easy to construct and performs well and reliable. In any case it is necessary to have a valid means of evaluating a functional design without having to build and test it.

The technique of analysis proposed requires the development of mathematical models that represent the physical model to the required level of approximation. Mathematical manipulation of the parameters and variables then gives a means of evaluating the design which the model represents. Variation or adjustment of the variables is representative of configuration changes, which may be subsequently evaluated.

The thesis evaluation can perhaps most logically be described in order of the extent to which the complete physical situation is accurately described by the mathematical model(s) employed. Thus the research considered first the design evaluation of an idealized thermoelectric system with several simplifying-limiting assumptions. This is primarily to define a common background for the understanding of the subsequent analysis.

The effect of electrical ripple on performance is one of the practical aspects taken into account. Other practical considerations deal with treating the idealized thermoelectric couple as part of a heat pumping system in which some of the early assumptions used to discuss the basic idealized couple are no longer valid. In the analysis of the basic idealized couple the material properties are assumed to be invariant with temperature. This assumption may not be realistic for the materials presently used in device fabrication.

Consequently, its variation may cause errors or deviations from the theoretical calculations of device performance. The mathematical models developed allow for the thermoelectric material parameters to be defined functions of temperature. For a final solution of a practical heat pumping module the problem of matching heat fluxes across the heat exchangers with the capability of the basic thermoelectric module must be considered.

5.0 THERMOELECTRIC EFFECTS.

5.1 Introduction.

This section reviews the laws and effects of thermoelectric behavior with specific regard to thermoelectric cooling. The direct utilization of electricity to produce useful work (refrigeration) with no moving parts is now a reality. Although thermoelectric effects have been known for over a century, practical thermoelectric energy-conversion devices made little progress for over a century. Further development had to await the understanding of semi-conductor behavior and in methods of material preparation which occured in the 1950's.

5.2 Thermoelectric Laws and Effects.

In order to introduce the various reversible and irreversible effects which may occur in a non-isothermal system or circuit three thermoelectric effects are introduced. The three dominant effects, the Seebeck, Peltier, and the Thomson effect have been observed in the early 1820's. Each of these measurable effects is a result of the direct reversible interchange of electrical energy and thermal energy.

5.2.1. Seebeck Effect.

5.2.1.1 Description.

Of the reversible effects it appears most convenient to treat the Seebeck effect first. In 1821, Seebeck reported experimental results to the Prussian Academy of Science. Seebeck observed then when a closed circuit consists of two different metals, and the two junctions of these metals are at different temperatures, there will be a flow of electric current in the circuit. The current is a function of the type of metals and is approximately proportional to the temperature difference between junction and inversely proportional to the circuit resistance. If the circuit is opened then an open circuit voltage (V_{AB}) results. The voltage is proportional to the temperature difference and is expressible in differential form as:

$$\alpha_{AB}(T) \equiv \lim_{\Delta T \to 0} \frac{\Delta V_{AB}}{\Delta T} \qquad 5.2.1.1.1.$$

and

$$\alpha_{AB}(T) = \frac{dV_{AB}}{dT} \qquad 5.2.1.1.2.$$

where:

V_{AB} Seebeck emf, volts

T temperature at junction, ^{o}K

$\alpha_{AB}(T)$ Seebeck coefficient for the two materials, volts/^{o}C

The Seebeck coefficient may be defined as

$\alpha_{AB}(T) = \alpha_A(T) - \alpha_B(T)$ where $\alpha_A(T) - \alpha_B(T)$ is referred to as the thermoelectric power of the couple. The Seebeck or thermoelectric voltage of a couple is:-

$$V_{AB} = \int_{T_0}^{T} (\alpha_A - \alpha_B)\, dT \qquad 5.2.1.1.3.$$

where:

α_A entropy transport factor material A

α_B entropy transport factor material B

5.2.1.2 Illustration.

Thermocouples use this principle for measuring a very wide range of temperatures.

5.2.1.3 Magnitude.

A Chromel-Alumel thermocouple develops approximately 20u v per ^{o}C difference in junction temperatures. In general, when two metals are selected at random the variation of emf with temperature is far from linear. If one junction of an iron-copper thermcouple is held at $0^{o}C$, the variation of emf developed by the thermcouple versus the temperature of the second junction is as follows:

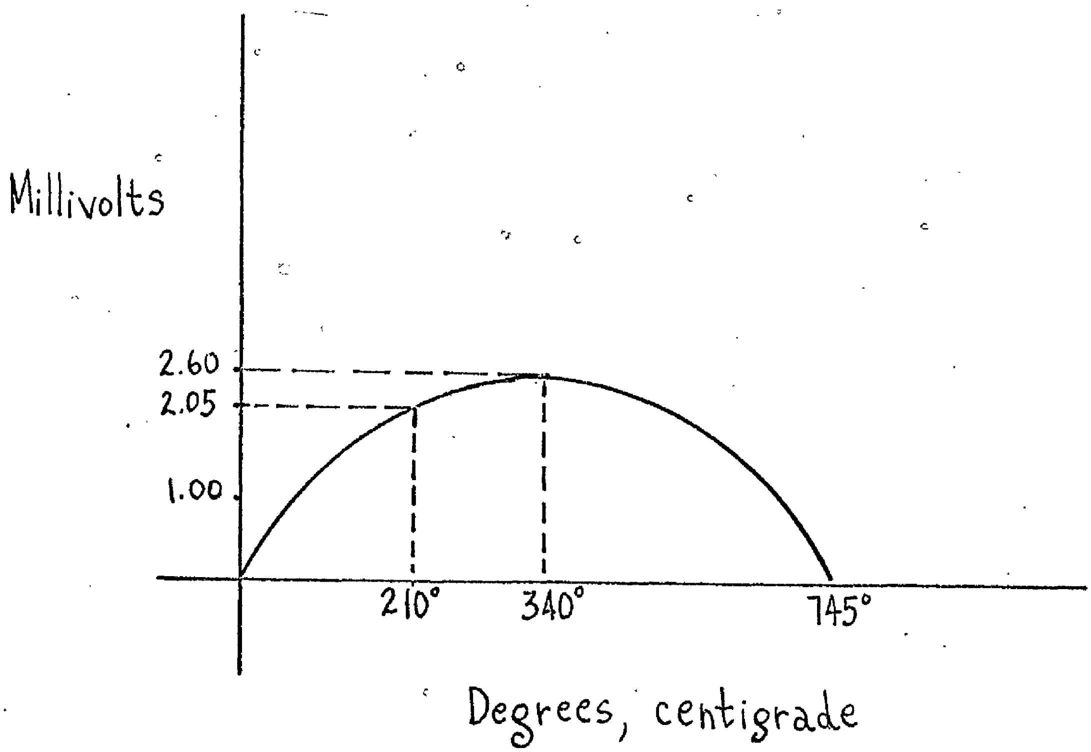

Figure 5.2.1.3.1.

Thermcouple emf as a Function of Temperature.

Figure 5.2.1.3.1 emplies that current will flow across the hot junction from iron to copper at temperatures between 0^{+} and $745^{o}C$. Current would flow in the opposite direction at temperatures above or below the limits.

Figure 5.2.1.3.2 illustrates the circuit exhibiting the Seebeck effect.

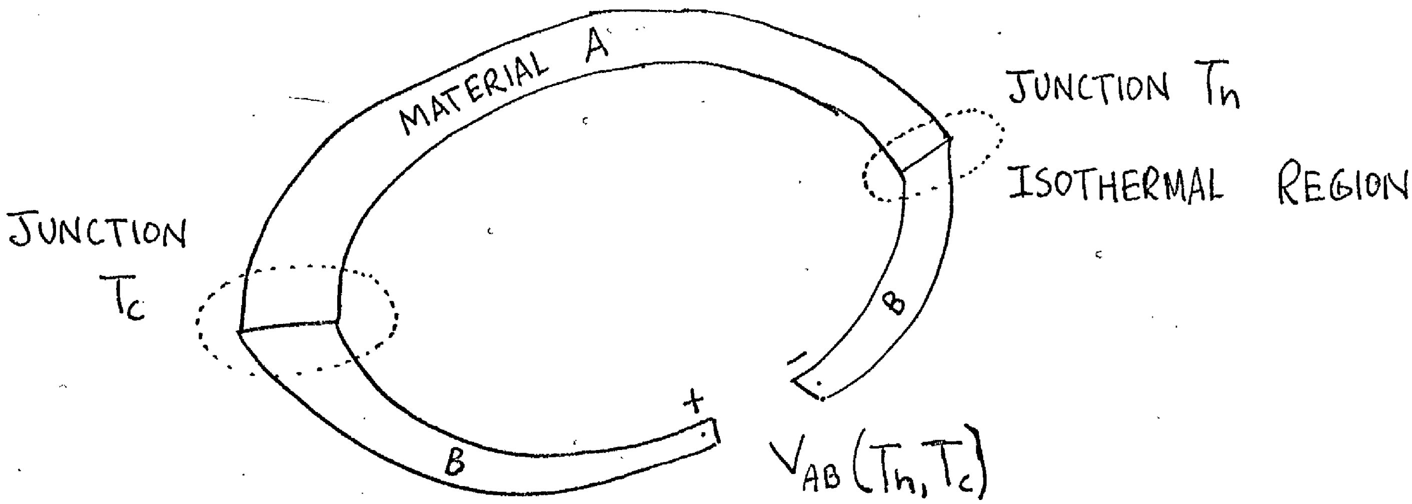

Figure 5.2.1.3.2.

Seebeck - Voltage Coefficient.

5.2.2. Peltier Effect.

5.2.2.1 Description.

In 1834, Peltier observed the complementary effect of the Seebeck phenomenon. When a current flows across a junction of two unlike metals, it gives rise to an absorption or liberation of heat. If the current flows in the same direction as the current at the hot junction of a thermoelectric circuit of the two metals, heat is absorbed, if it flows in the same direction as the current at the cold junction of the thermoelectric circuit, heat is liberated. The Peltier effect may be defined as a reversible transformation of electrical potential energy at a junction of dissimilar conductors.

The heat developed in a junction of two materials is proportional to the first power of the current, and depends on the direction of the current.

The quantity of heat absorbed or liberated is given by the following equation

$$Q_{AB} = \Pi_{AB}(T)I \qquad 5.2.2.1.$$

where:

Q_{AB} is the rate at which Peltier heat is absorbed or liberated at the junction, watts

$\Pi_{AB}(T)$ relative Peltier coefficient between conductor A and B, watts/amps

I current, amps

5.2.2.2 Illustration.

The Peltier effect is an aspect of the thermoelectric effect and the magnitude is directly proportional to the thermoelectric power of the combination of the metals used, as well as the current through the junction. Figure 5.2.2.2.1 illustrates the Peltier effect.

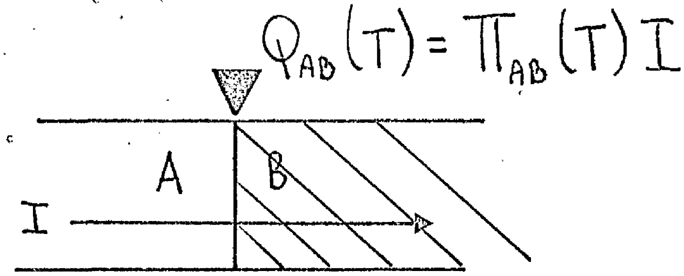

Figure 5.2.2.2.1.

Peltier - Heat Coefficient.

The fundamental requirements for an efficient Peltier couple are

(1) High contrasting thermoelectric power
(2) Low heat conductivity
(3) High electric conductivity

The Peltier couple is used as a calibrated refrigerator in radiation detectors where current required to hold temperature constant is a measure of heat input.

5.2.2.3 Magnitude.

At a junction of Fe-Ni at 273^{o}K, there would be liberated or absorbed 9.4×10^{-3} joule/second for each ampere of current. (This does not consider I^2R loss which will liberate heat). In general by the use of ordinary metal it is possible to cool a small amount of metal by approximately $10^{o}C$. This figure has been substantially improved by the use of semi-conducting materials. These semi-conducting materials are used to build refrigerators.

5.2.3. Thomson Effect.

5.2.3.1. Description.

The third effect, occurs when a current flows in a conductor which has a temperature gradient as illustrated by figure 5.2.3.1. In unequally heated conductors (such as Copper), heat is liberated at points where the current

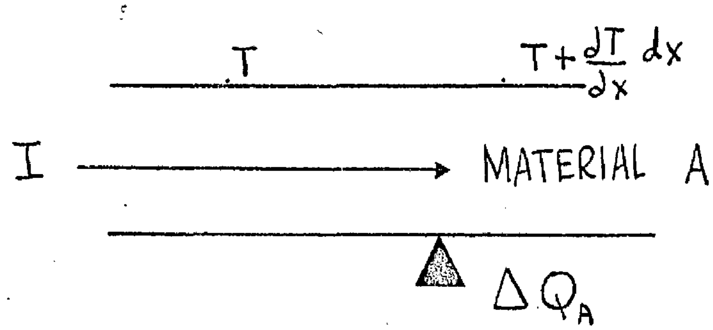

Figure 5.2.3.1.
Thomson - Heat Coefficient.

and heat flow in the same direction and are absorbed when they flow in opposite directions. For Cu this tends to decrease the inequality of temperature while for iron it tends to increase the difference. The Thomson coefficient of a material is defined by:

$$Q_A(T) = \tau_A(T)\, I \frac{dT}{dx} \qquad 5.2.3.1.$$

where:

$Q_A(T)$ is the rate of heat absorption per unit length of conductor, watts/cm

$\tau_A(T)$ Thomson coefficient of conductor A, Volts/^{o}K

$\frac{dT}{dx}$ temperature gradient, ^{o}C/cm

5.2.3.2. Illustration.

This effect can be used to generate a small but accurate temperature difference. If a thin sheet of copper is suspended vertically between the poles of a horseshoe magnet and one corner of the sheet is heated, the copper will tend to rotate because of the interaction of the circulating currents and the magnetic field. Lead has no measurable Thomson effect.

5.2.3.3. Magnitude.

From the second Kelvin relation, the Seebeck coefficient α and the Thomson coefficient τ can be related in the following manner:

$$\frac{d\alpha}{dT} = \frac{\tau}{T} \qquad 5.2.3.3.1.$$

If τ is invariant with temperature, equation 5.2.3.3.1 integrates to yield:

$$\alpha = \tau \ln\left(\frac{T}{T_0}\right) \qquad 5.2.3.3.2.$$

Where T_0 is a constant of integration. If the Seebeck coefficient is plotted as a function of the of temperature, the slope at any temperature ($^{\circ}$K) is interpreted as the Thomson coefficient at that temperature. From a representative plot of the Seebeck coefficient with temperature for bismuth telluride (4) a representative value appears to be $|5 \times 10^{-5}\ \text{V}/^{\circ}\text{K}| \leq \tau \leq |25 \times 10^{-5}\ \text{V}/^{\circ}\text{K}|$

5.2.4. Kelvin's Relations; Absolute Seebeck and Peltier Coefficients.

Thomson, later Lord Kelvin, determined the relationship between the Seebeck Coefficient and the Peltier Effect, by applying the classical laws of thermodynamics (1) . Subsequent measurements have supported the results of Lord Kelvin. The resulting equations have been experimentally verified by direct observations to within acceptable limits. The first (often referred) equation relates the Seebeck coefficient and the Thomson coefficient and is given by:

$$\frac{d\alpha_{AB}}{dT} = \frac{\tau_A - \tau_B}{T} \qquad 5.2.4.1.$$

Equation 5.2.4.1. relates the junction property of two materials (left-side) and on the other side are quantities which refer to the bulk phases of A and B. The absolute Seebeck coefficient of A at temperature T will be expressed as:

$$\alpha_A = \int_0^T \frac{\tau_A}{T} \, dT \qquad 5.2.4.2.$$

The second Kelvin relates the Peltier coefficient to the Seebeck coefficient giving:

$$\Pi_{AB}(T) = T\alpha_{AB}(T) \qquad 5.2.4.3.$$

and the absolute Peltier coefficient of A at temperature T by:

$$\Pi_{A}(T) = T\alpha_{A}(T) \qquad 5.2.4.4.$$

It is noted that the assumption of the Seebeck coefficient being invariant with temperature implies (5.2.4.1) zero net Thomson heat. Such a model is convenient for analyzing and optimizing simple thermoelectric devices.

5.2.5. Irreversible Effects.

In addition to the three reversible effects which occur in conductors two other thermodynamic irreversible processes take place; these are joule heating and heat conduction.

Consider first joule heating arising in a current carrying conductor. The magnitude of this effect is proportional to the square of the current. The rate at which joule heat can be written is:

$$Q_J = RI^2 \qquad 5.2.5.1.$$

where:

R resistance, ohms

I current, amps

Equation 5.2.5. can also be written as:

$$\frac{Q_J}{VOL} = \frac{J^2}{\sigma} \qquad 5.2.5.2.$$

where:

J current density, amps/cm^2

σ electrical conductivity, $(ohm\text{-}cm)^{-1}$

VOL volume, cm^3

The second irreversible process, thermal conduction results in a heat flux when a temperature gradient is present in a material, and can be given by

$$Q_K = -k \cdot \nabla T \qquad 5.2.5.3.$$

The heat flux is a vector and is not necessarily parallel to the direction of the temperature gradient. It is the tensor property of the thermal conductivity of an anisotropic material. The sections that follow will be concerned only with isotropic (1) material where all thermodynamic properties are scalar. In applications involving magnetic fields (5) the tensor properties of the medium as well as the three-dimensional nature of the problem, must be considered.

(1) Isotropic material exhibit properties at any point independent of direction.

6.0 IDEALIZED THERMOELECTRIC COUPLE PERFORMANCE.

6.1 Introduction.

In this section the relationships required to establish the parametric performance of an idealized thermoelectric couple will be considered. The principle device is the Peltier heat pump couple. In this device the electric power is an external input to the couple. Heat is absorbed from the cold reservoir (T_{c_∞}) because of the Peltier effect (5.2.2.1.) at the junction of the n - and p type semiconductor/ thermoelectric material. Semiconductors in which the electrical conduction is predominately due to free electrons are called n-type semiconductors and in those in which holes are predominate are classified as p-types. The n-type refers to negative carriers and the p-type for positive carriers.

The efficiencies achievable with thermoelectric heat pumps are limited by the Peltier effect an aspect of the thermoelectric effect. The magnitude is directly proportional to the thermoelectric power of the combination of metals used, as well as the current through the junction. Semiconductor materials exhibit the fundamental requirements for a Peltier couple.

The basic requirements for a Peltier couple are:

(1) High contrasting thermoelectric power

(2) Low heat conductivity

(3) High electric conductivity

The useful Peltier cooling effect is less than the to heat abstraction because of:

(1) I^2R_j loss in the junction

(2) I^2R loss in the materials

(3) Heat from the surrounding medium

(4) Conduction of heat from the hot junction (T_{hj})

It is noted that the first two (above) depend on the square of the current while the Peltier cooling is proportional to the first power of the current (5.2.2.1). Therefore, for a given couple there is an optium current (I_Q) for the maximum attainable cooling.

The performance of an ideal thermoelectric heat pump will be determined using simplifying/limiting assumptions. The assumptions primarily concern, material properties being invariant with temperature and isolation of the cold junction by a control volume. The basic couple configuration figure 6.2.1. consists of an n- and p-type Peltier device connected to electrical conductors.

6.2. Couple Configuration and Assumptions.

The analysis of the mathematical model illustrated by figure 6.2.1 is a basic thermoelectric couple.

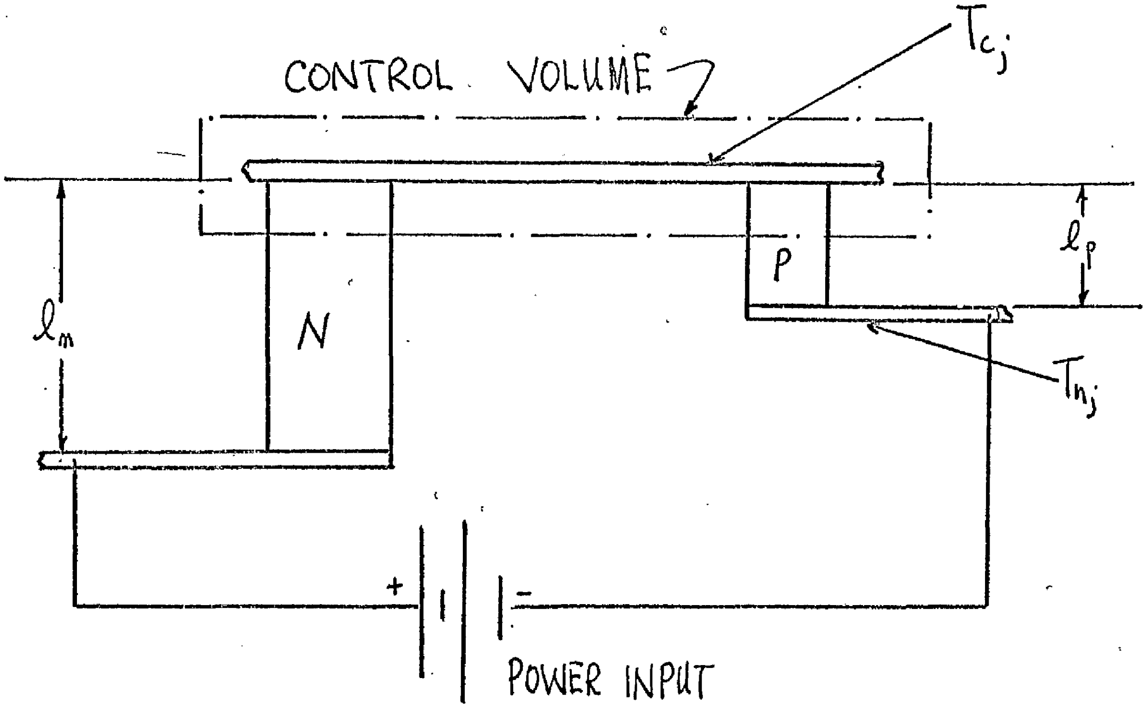

Figure 6.2.1.

Basic Thermoelectric Peltier Couple.

The simplifying assumptions are:

(1) Electrical resistivity of the n- and p-type semiconductors are equal $\rho_n = \rho_p$

(2) Thermal conductivity are equal $k_n = k_p$ watts/cm - ^oC

(3) The Seebeck coefficients are equal in magnitude and opposite in sign, $|\alpha_m| + |\alpha_p| = \alpha_{mp}$
$\alpha_M = \alpha_p$, watts/°C

(4) All material properties are invariant of temperature

(5) The problem of heat transfer to the ambient is not considered, i.e. the couple is an isolated module

(6) The couple is operating between T_{hj}, T_{cj} (°K), which are the junction temperatures of the active semiconductor elements

(7) The inter-element thermal insulation is perfect

(8) No heat transfer between junctions except through the thermoelement arms, i.e. no shunt heat paths

(9) The flow of heat and electricity in the elements are one-dimensional, X-direction

(10) Convection and radiation effects from the thermoelements are neglected. A condition difficult to achieve in the expected operational temperatures

(11) Junction resistance is neglible compared to the bulk resistance of the elements

(12) Arms are of constant cross-sectional area

(13) The ancillary components of the electrical circuit is zero, all shunt resistances are ∞

6.3 Steady State.

Consider the thermoelectric couple as shown in figure 6.2.1. representing the physical system. A D.C. power supply is affixed to the hot junction and an electric Peltier circuit is completed. The resulting device will be capable of pumping heat from T_{cj} to T_{hj} For the control volume about the cold junction, the Peltier heat removed (Q_p , watts) must work against the following irreversible effects.

1. Q_s , heat supplied by source, watts
2. Q_k , thermal conduction from T_{hj} to T_{cj} , watts
3. Q_J , joule heat produced in circuit, watts

For steady state operation the heat balance at T_{cj} is:

$$Q_p = Q_s + \frac{1}{2} Q_J + Q_k \qquad 6.3.1.$$

The right hand side of equation 6.3.1. indicates that exactly 0.5 of the total joule heating produced flows to each end of the bar. It is shown in appendix A that this is not an approximation but exact for the case considered (assumption (4)). The Thomson effect has been omitted from the steady state heat balance. The Thomson coefficient is zero due to invariance of the Seebeck coefficient with temperature (equation 5.2.4.1).

Equation 6.3.1. is rearranged to become

$$Q_S = Q_p - \frac{1}{2} Q_J - Q_k \qquad 6.3.2.$$

The Peltier absorption rate is expressed as:

$$Q_p = T_{c_j} \alpha_{mp} I \qquad 6.3.3.$$

which results from equation 5.2.2.1 and 5.2.4.3.

The joule heating term is expressed as

$$Q_J = I^2 \left[R_m + R_p \right] \qquad 6.3.4.$$

where:

R_m, R_p , thermoelement resistance, ohms

The thermoelement resistance can be expressed in terms of element resistivity:

$$R_m = \frac{\rho_m l}{A} \qquad 6.3.5.$$

$$R_p = \frac{\rho_p l}{A} \qquad 6.3.6.$$

where:

A element cross-sectional area, cm^2
ℓ element height, cm

The thermal conduction term is expressed as

$$Q_k = K\left[T_{h_j} - T_{c_j}\right] \qquad 6.3.7.$$

and:

$$\Delta T_j = T_{h_j} - T_{c_j} \qquad 6.3.8.$$

where:

K thermal conductance of thermocouple, watts/$^{\circ}C$
T_{h_j} hot junction temperature, $^{\circ}K$
T_{c_j} cold junction temperature, $^{\circ}K$

The thermal couple conductance is:

$$K = \frac{A k_n}{\ell} + \frac{A k_p}{\ell} \qquad 6.3.9.$$

where:

k_n, k_p element conductivity watts/cm-$^{\circ}C$

Substituting 6.3.3., 6.3.4., 6.3.7. into equation 6.3.2. results as follows:

$$Q_s = T_{cj}\alpha_{mp} I - \frac{1}{2} I^2 \left[\frac{\rho_n l}{A} + \frac{\rho_p l}{A} \right] - K \Delta T_j \qquad 6.3.10.$$

Equation 6.3.10 is similiar to equation A.19 derived in Appendix A Figure 6.3.1. presents the heat pump rate as a function of current for fixed junction temperatures.

Equation 6.3.10 may be rearranged and expressed in terms of junction temperature difference.

$$\Delta T_j = \frac{T_{cj}\alpha_{mp} I - \frac{1}{2} I^2 R - Q_s}{K} \qquad 6.3.11.$$

Equation 6.3.11 indicates that under otherwise equal operating conditions, i.e. the material properties equal the maximum junction temperature when the cold junction is "perfectly" insulated ($Q_s = 0$). For an internal chamber or home refrigerator where the cold junction is in thermal contact with the environment ΔT_j will be smaller as $Q_s > 0$. Equation 6.3.11 indicates that the increase in junction temperature is in accord with the material requirements for a Peltier couple (Section 5.2.2.2)

HEAT PUMP RATE AS A FUNCTION OF CURRENT, SINGLE COUPLE
Fig. 6.3.1.

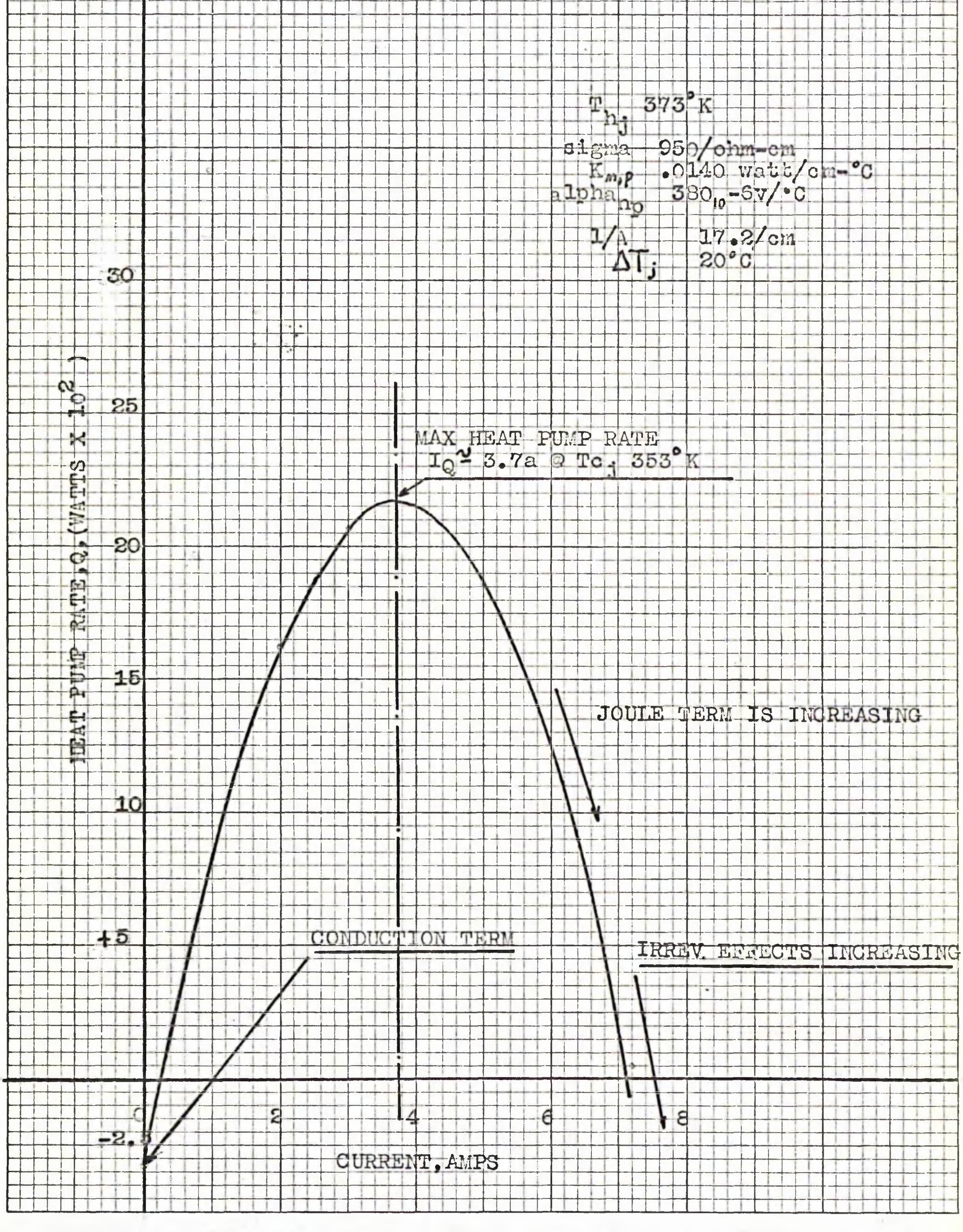

6.4. Coefficient of Performance.

Effectiveness parameters for evaluating the operation of refrigerators are: the coefficient of performance (C.O.P), heat pump rate (watts), maximum junction temperature difference ($\Delta T_{j,max}$) and those relating output to the operation burden (watts/mass).

In a power cycle, heat is received by the working fluid at an elevated temperature and rejected at a lower temperature, while a net amount of work is done 'by' the fluid. Thermodynamic cycles in which the reverse occurs are called heat pumps or refrigeration cycles. The criterion of performance of the cycle can be expressed as the ratio of output to input (depends upon what is regarded as output). In a refrigerator, the extraction of heat (Q_s , equation 6.3.2) for a net expenditure of work (W) is defined as the coefficient of performance (C.O.P). The parameter is defined as:

$$C.O.P \equiv \frac{Q_s}{W} \qquad 6.4.1.$$

From the axioms of Sadi Carnot, "Second Law of Thermodynamics" a summary conclusion is:

The thermal efficiency of a reversible cycle depends (only) upon the source and sink temperatures (^{o}K). The maximum C.O.P. for a refrigerator under reversible operation is expressed as:

$$\gamma_{max} = \frac{T_{c_j}}{T_{h_j} - T_{c_j}} \qquad 6.4.2.$$

where:

T_{c_j}, T_{h_j} junction temperatures (^{o}K)

For the operation of a thermoelectric couple the C.O.P. can be determined as follows:

The heat removed is expressed as:

$$Q_s = T_{c_j}\alpha_{mp} I - \frac{1}{2} I^2 R - K\Delta T_j \qquad 6.4.3.$$

The power consumption consists of two parts:

$$P = W_s + W_J \qquad 6.4.4.$$

where:

P , total power consumption, watts

W_s , power consumption due to Seebeck emf, watts

W_J , power consumption due to joule heating, watts

The Seebeck voltage from equation 5.2.1.1.3 is:

$$V_s = \alpha_{mp}\left[T_{h_j} - T_{c_j}\right] \qquad 6.4.5.$$

The required Seebeck power is:

$$W_s = I V_s \qquad 6.4.6.$$

then

$$W_s = I \alpha_{np} \left[T_{hj} - T_{cj} \right] \qquad 6.4.7.$$

The required joule power is:

$$W_J = I^2 R \qquad 6.4.8.$$

from equation 6.4.1. then

$$\text{C.O.P.} = \frac{T_{cj} \alpha_{np} I - \frac{1}{2} I^2 R - K \Delta T_j}{I \alpha_{np} \Delta T_j + I^2 R} \qquad 6.4.9.$$

Figure 6.4.1. presents the C.O.P. and Q_s as a function of current (I) for fixed junction temperature difference. The result indicates that at the maximum heat pump rate the C.O.P. is approximately .40. In some applications a large heat pump rate is more important than a large C.O.P.

HEAT PUMP RATE AND C.O.P. AS A FUNCTION OF CURRENT FOR A THERMOELECTRIC COUPLE

Fig. 6.4.1.

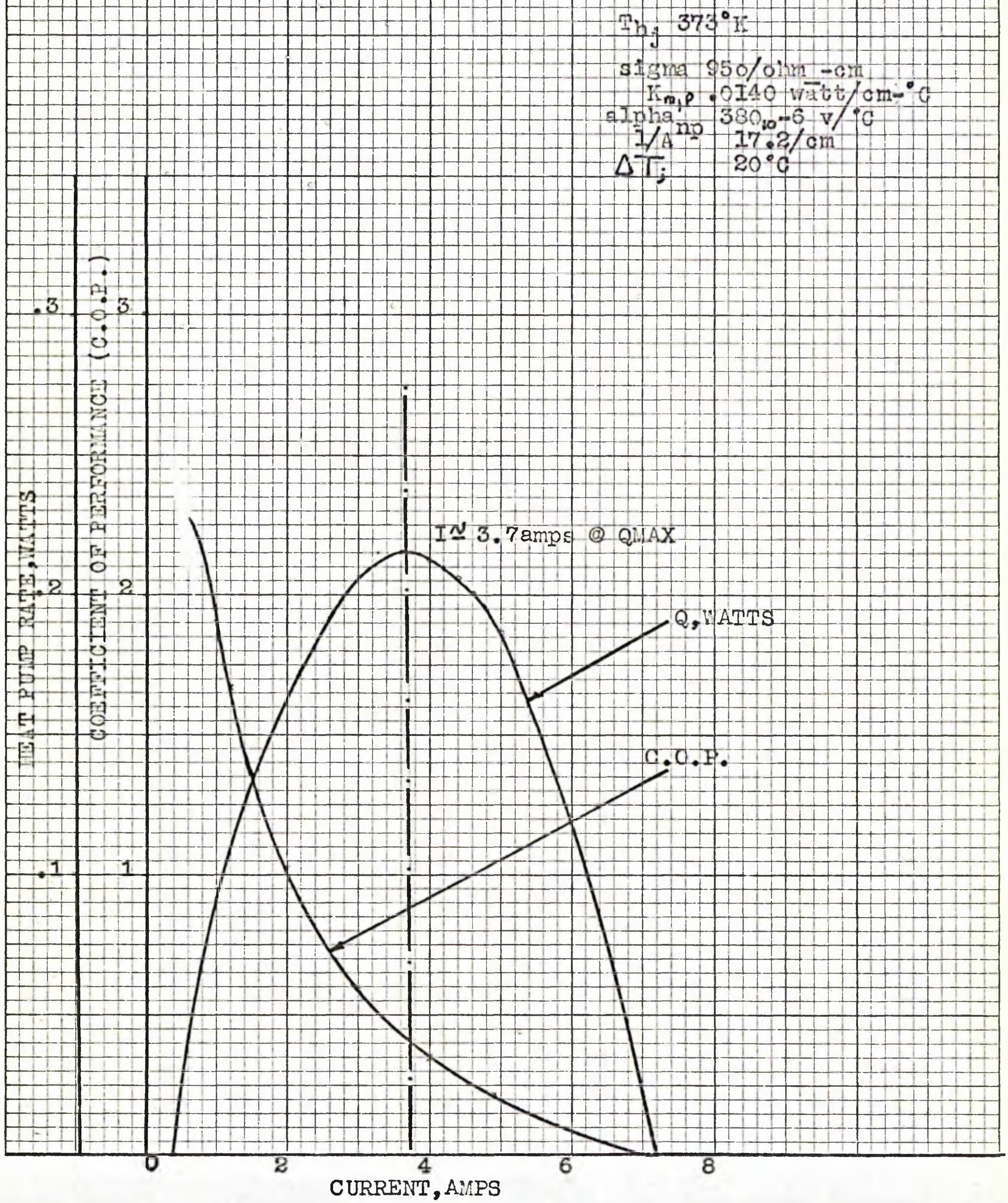

6.5. Parametric Optimization.

6.5.1 Maximizing C.O.P. (I)

From equation 6.4.9. the C.O.P. is a dependent function of the operating current (I). The optimum value of the current can be found by equating the first derivative to zero and solving for the current (I_ϕ). Appendix* presents the mathematical concept of maximizing controllable variables.

The current maximizing the C.O.P. is expressed as:

$$I_\phi = \frac{\alpha_{np}\,\Delta T_j}{R(\sqrt{B}-1)} \qquad 6.5.1.1.$$

where:

$$B = 1 + \frac{1}{2}\frac{\alpha_{np}^2}{RK}\left(T_{h_j} + T_{c_j}\right) \qquad 6.5.1.2.$$

and the maximum C.O.P. resulting is ;

$$C.O.P._{max} = \frac{T_{c_j}}{T_{h_j} - T_{c_j}}\left[\frac{\sqrt{B} - \frac{T_{h_j}}{T_{c_j}}}{\sqrt{B} + 1}\right] \qquad 6.5.1.3.$$

* B.

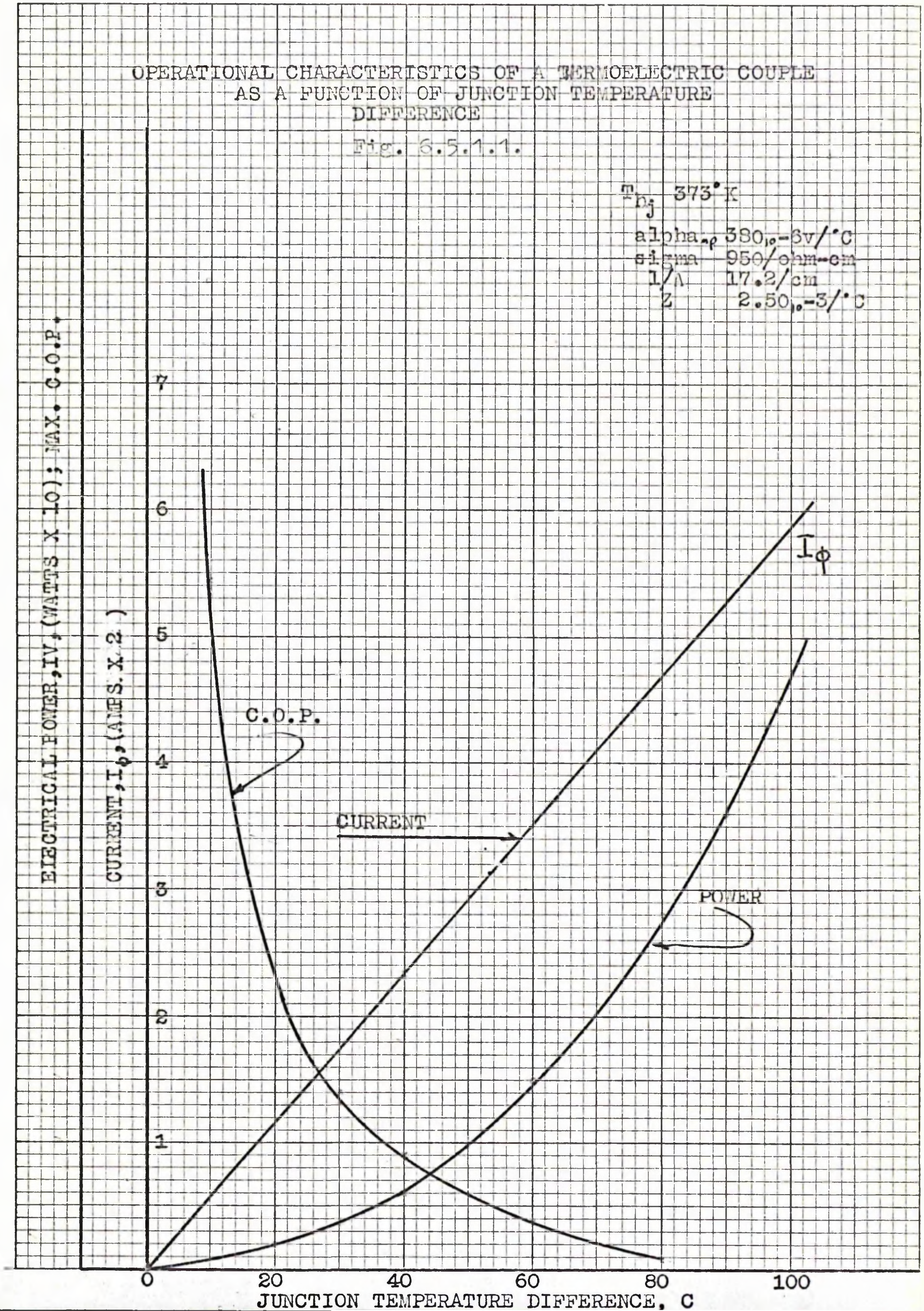

OPERATIONAL CHARACTERISTICS OF A THERMOELECTRIC COUPLE AS A FUNCTION OF JUNCTION TEMPERATURE DIFFERENCE

Fig. 6.5.1.1.

comment:

(There is a limitation with regard to the maximizing relationships in this section (6.5 Parametric Optimization) and results from the invariance of the junction temperatures with current. In section 8.6 and section 11.2.2. the proposed mathematical models consider the thermoelectric module to be operating between known heat source and heat sink temperatures. The resulting interative procedures determine the current required to maintain thermal equilibrium with the surroundings. Determination of the junction temperatures are resulting functions of the current and hence not arbitrary).

The derivation of equations 6.5.1.1. - 6.5.1.3. are found in Appendix C. From equation 6.5.1.3. the resulting C.O.P.(max) is a function of the Carnot efficiency (6.4.2) and a factor containing material properties and the temperature boundries of the thermoelectric couple. The factor [ ] will be less than unity and positive.

In figure 6.5.1.1., the C.O.P., current, power input are shown as a function of junction temperature difference. For each temperature difference the applied current is adjusted to maximize the C.O.P. As the temperature difference approaches zero the power input which maximizes the C.O.P. approaches zero, and hence the heat pump rate rapidly decrease (figure 6.5.1.2).

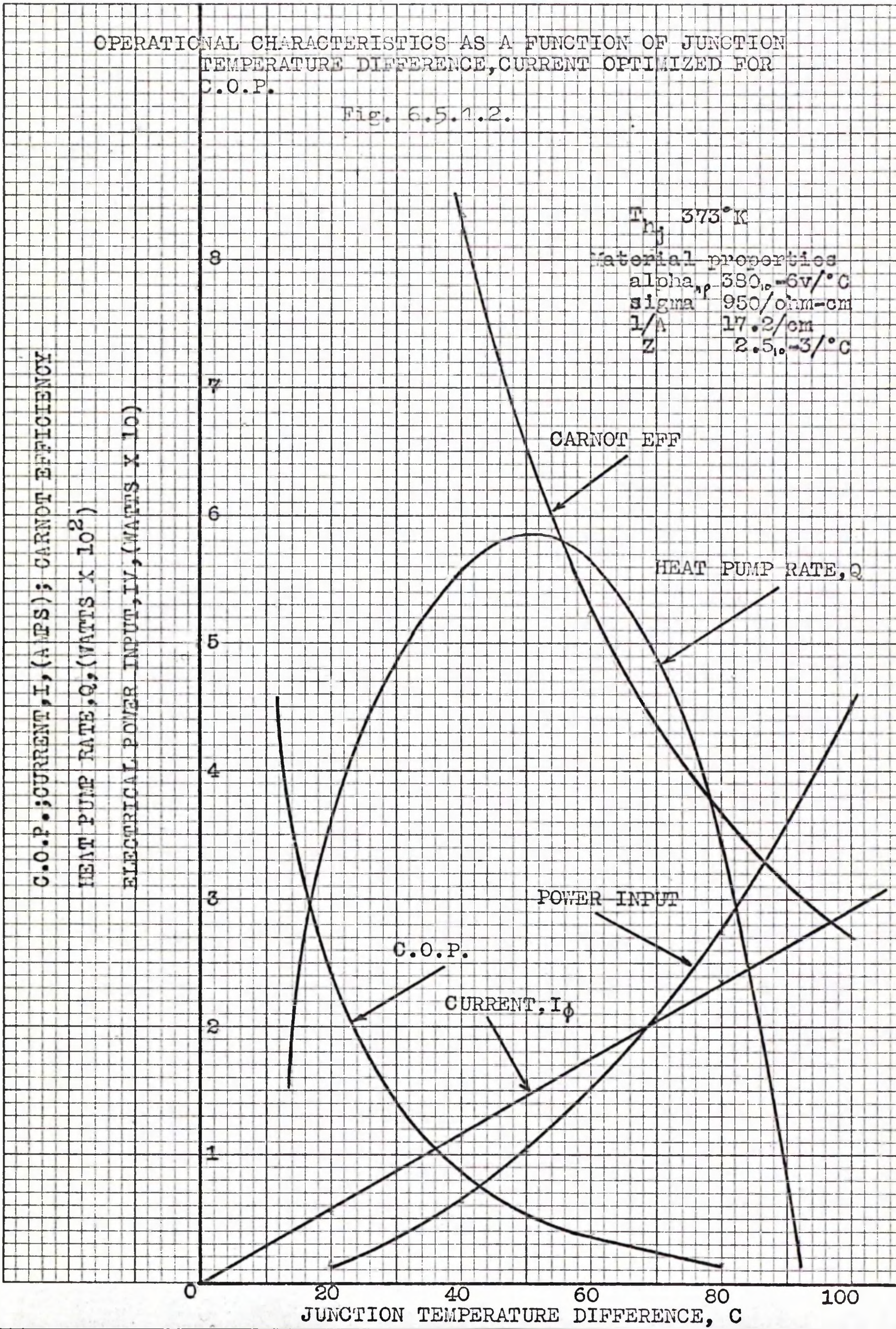

OPERATIONAL CHARACTERISTICS AS A FUNCTION OF JUNCTION TEMPERATURE DIFFERENCE, CURRENT OPTIMIZED FOR C.O.P.

Fig. 6.5.1.2.

Figure 6.5.1.2. illustrates the irreversible nature of the thermoelectric heat pump. The C.O.P. is approximately one sixth of the carnot efficiency. The current (I_ϕ) appears as a linear function of ΔT_j and the power[1] required, non-linear in presentation.

(1) The power required to operate at maximum C.O.P. The derivation appears in section 6.5.4.

6.5.2 Maximizing C.O.P. (Configuration Geometry).

From equation 6.4.9. the current that maximizes the C.O.P. was determined. (equation 6.5.1.1) to be dependent upon the junction temperatures and material properties. Equation 6.5.1.2. indicates that the product of the parallel thermal conductance and series electrical resistance (Configuration Geometry) can be adjusted to maximize the C.O.P. From equation 6.5.1.2. the (RK) product is expanded as follows:

$$RK = \left(K_n + K_p\right)\left(R_p + R_n\right) \qquad 6.5.2.1.$$

The subscripts refer to the n- and p- thermoelement expanding 6.5.2.1. and inserting 6.3.5 (R_n), 6.3.6. (R_p), 6.3.9. (K_n, K_p) results:

$$RK = k_n \rho_n + \frac{A_n l_p k_n \rho_p}{A_p l_n} + \frac{A_p l_n \rho_n k_p}{A_n l_p} + k_p \rho_p \qquad 6.5.2.2.$$

Defining the shape factor as:

$$f_n \equiv \frac{A_n}{l_n} \qquad 6.5.2.3.$$

$$f_p \equiv \frac{A_p}{l_p} \qquad 6.5.2.4.$$

introducing 6.5.2.3. and 6.5.2.4. into 6.5.2.2.

$$RK = k_m \rho_m + k_m \rho_p \left(\frac{f_m}{f_p}\right) + k_p \rho_m \left(\frac{f_p}{f_m}\right) + k_p \rho_p \qquad 6.5.2.5.$$

Introducing $\left(\frac{R}{\alpha_{mp}^2}\right)$ into equation 6.4.9.

$$C.O.P. = \frac{\frac{T_{cj} I R \alpha}{\alpha^2} - \frac{1}{2}\frac{I^2 R^2}{\alpha^2} - \frac{K \Delta T_j R}{\alpha^2}}{\frac{I \alpha \Delta T_j R}{\alpha^2} + \frac{I^2 R^2}{\alpha^2}} \qquad 6.5.2.6.$$

Note:

For simplicity of presentation $\alpha \equiv \alpha_{mp}$

The joule voltage parameter(1) (ρ) is defined as:

$$\rho \equiv \frac{IR}{\alpha} \qquad 6.5.2.7.$$

Equation 6.5.2.6. simplifies to:

$$C.O.P. = \frac{T_{cj}\rho - \frac{1}{2}\rho^2 - \frac{RK\Delta T_j}{\alpha^2}}{\rho^2 + \rho \Delta T_j} \qquad 6.5.2.8.$$

(1) term defined by author

Since the C.O.P. is $> 0(+)$ it can be maximized by minimizing the product (RK). The product (RK) is defined by equation 6.5.2.5. From equation 6.5.2.5. the partial derivative of (KR) with respect to the ratio (f_m/f_p) will be set to zero to determine the value of (f_m/f_p) which optimizes (KR).

$$\frac{\partial(KR)}{\partial\left(\frac{f_m}{f_p}\right)} = k_m \rho_p \left(\frac{f_m}{f_p}\right)^2 - k_p \rho_m \qquad 6.5.2.9.$$

Setting 6.5.2.9. to zero and solving:

$$\frac{f_m}{f_p} = \left(\frac{k_p \rho_m}{k_m \rho_p}\right)^{\frac{1}{2}} \qquad 6.5.2.10.$$

Substituting 6.5.2.10 into equation 6.5.2.5.

$$(KR)_{MIN} = k_m \rho_m + k_m \rho_m \left[\frac{k_p \rho_m}{k_m \rho_p}\right]^{\frac{1}{2}} + k_p \rho_m \left[\frac{k_m \rho_p}{k_p \rho_m}\right]^{\frac{1}{2}} + k_p \rho_p \qquad 6.5.2.11.$$

Expanding and noting that the right side is a perfect square.

then

$$(KR)_{MIN} = \left[(\rho_n k_n)^{\frac{1}{2}} + (\rho_p k_p)^{\frac{1}{2}} \right]^2 \qquad 6.5.2.12.$$

The term $(KR)_{MIN}$ is incorporated into a material parameter called the material figure of merit. The material figure of merit (Z)[1] becomes:

$$Z = \frac{\alpha_{np}^2}{\left[(\rho_n k_n)^{\frac{1}{2}} + (\rho_p k_p)^{\frac{1}{2}} \right]^2} \qquad 6.5.2.13.$$

The material figure of merit (Z) contains the material properties of the thermoelements, but not their dimensions. In future sections the use of the material figure of merit will be as indicated.

For the condition of $\rho_n = \rho_p = \rho$, $k_n = k_p = k$ and $|\alpha_n| + |\alpha_p| = 2\alpha$ then equation 6.5.2.13 reduces to:

$$Z = \frac{\alpha^2}{\rho k} \qquad 6.5.2.14.$$

where:

Z is the material figure of merit of the couple, $^{o}C^{-1}$

(1) This term is called figure of merit (6). In section 7.2.5. an effective figure of merit is introduced

CURRENT TO MAXIMIZE C.O.P AS A FUNCTION OF
JUNCTION TEMPERATURE DIFFERENCE

Fig. 6.5.2.1.

T_{hj} 373°K

ΔT_j 20°C

Material properties

alpha 380$_{10}$-6V/°C

sigma 950/ohm-cm

l/A 17.2/cm

Z 2.5$_{10}$-3/°C

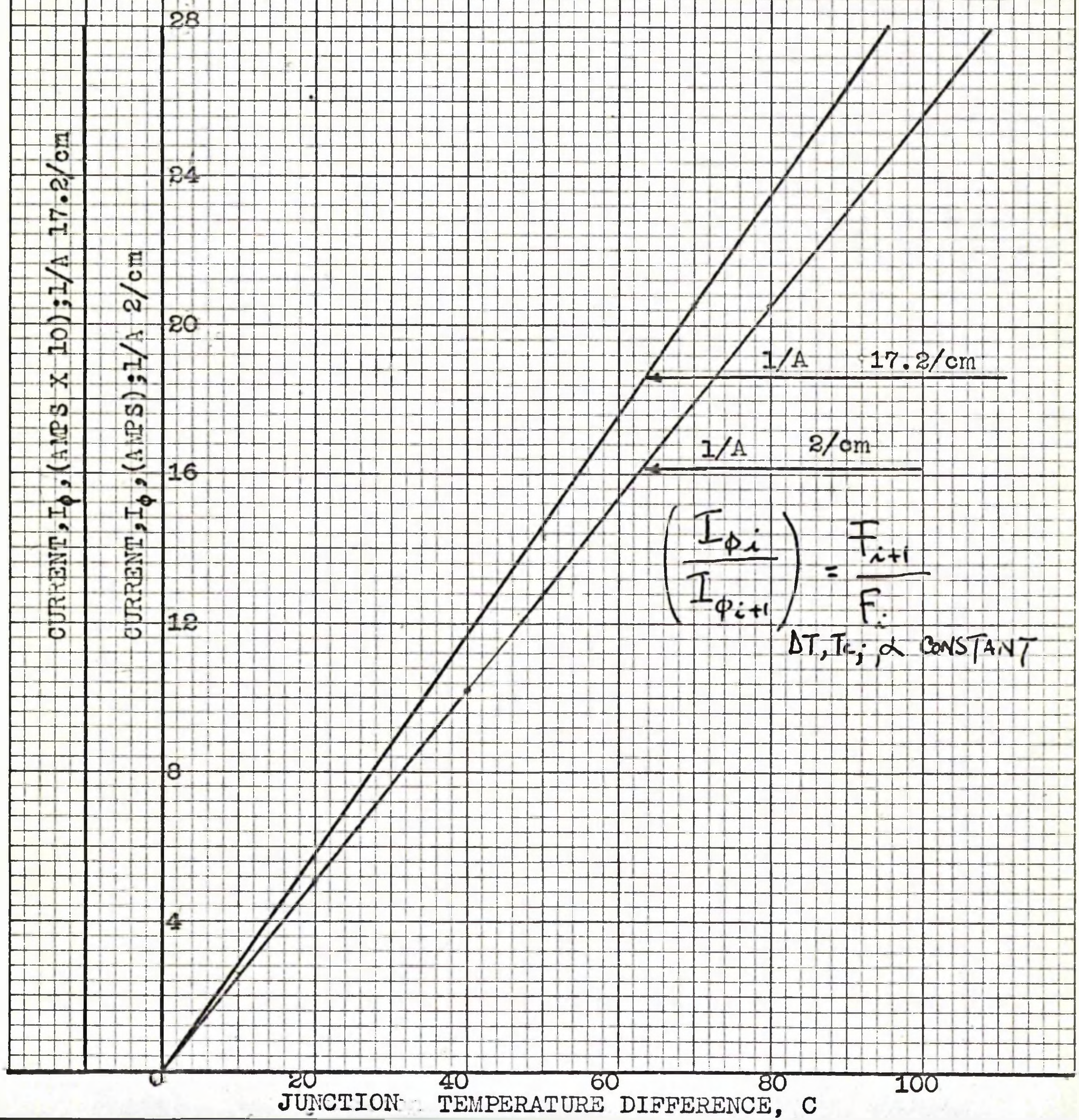

From equation 6.5.1.1. (I_ϕ) and 6.5.1.3. (C.O.P.$_{max}$) the parameter (B) can be expressed as follows:

$$\beta = 1 + \tfrac{1}{2} Z \left(T_{h_j} + T_{c_j}\right) \qquad 6.5.2.15.$$

Noting that $T_{MEAN} = \dfrac{T_{h_j} + T_{c_j}}{2}$ 6.5.2.16.

then:

$$\beta = 1 + Z\,T_{MEAN} \qquad 6.5.2.17.$$

The maximum C.O.P. expressed by equation 6.5.13. incorporating equation 6.5.2.17 results as follows:

$$C.O.P._{max} = \frac{T_{c_j}}{T_{h_j} - T_{c_j}} \left[\frac{\left(1 + Z T_{MEAN}\right)^{0.5} - \dfrac{T_{h_j}}{T_{c_j}}}{\left(1 + Z T_{MEAN}\right)^{0.5} + 1} \right] \qquad 6.5.2.18.$$

and the current which maximizes the C.O.P. is:

$$I_\phi = \frac{\alpha_{mp}\,\Delta T_j}{R\left(\sqrt{1 + Z T_{MEAN}} - 1\right)} \qquad 6.5.2.19.$$

Figure 6.5.2.1. shows the variation of current to maximize the C.O.P. as a function of junction temperature difference. The current (I_ϕ) is a linear function of

VOLTAGE WHICH MAXIMIZES C.O.P. AS A FUNCTION OF JUNCTION TEMPERATURE DIFFERENCE

Fig. 6.5.2.2.

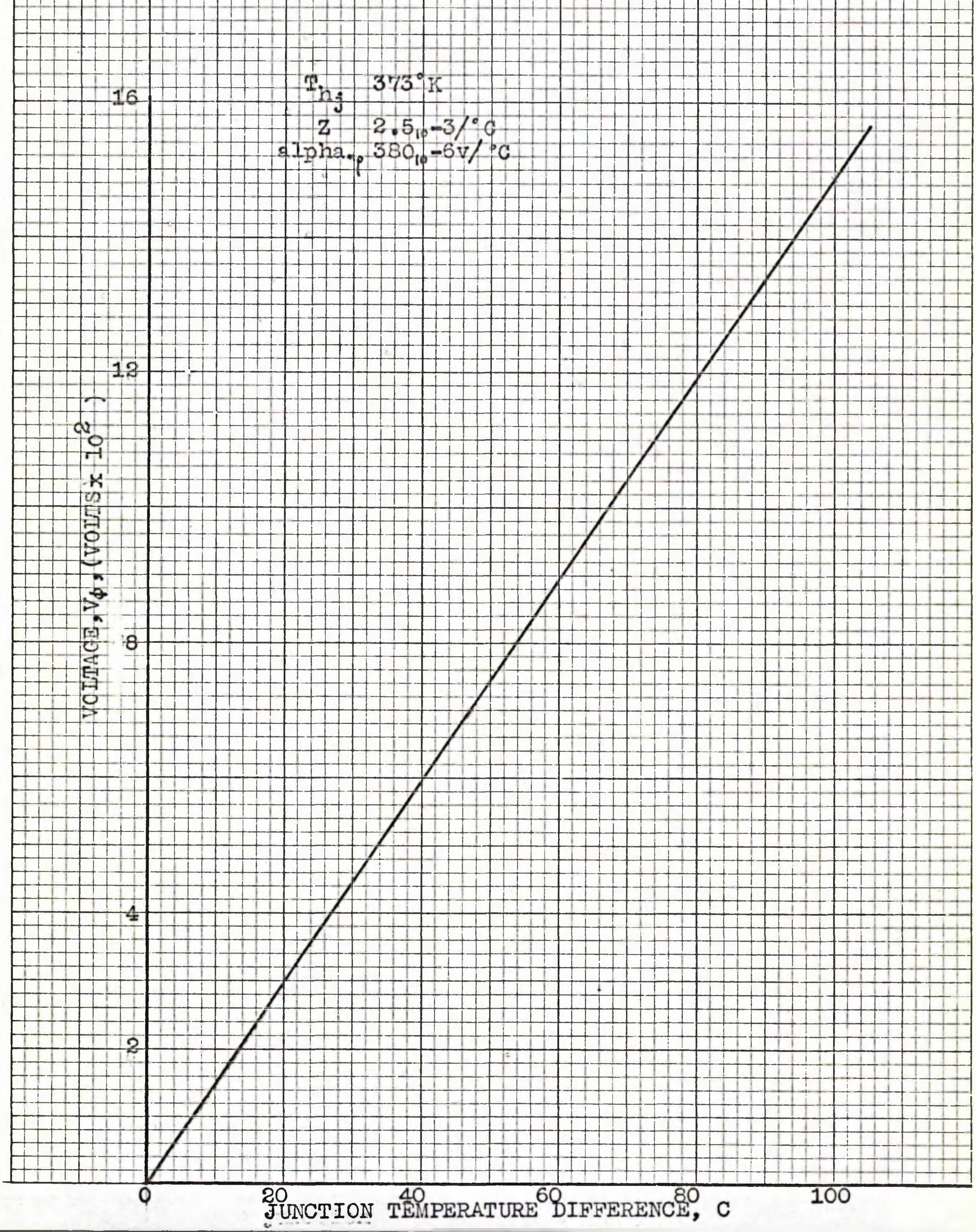

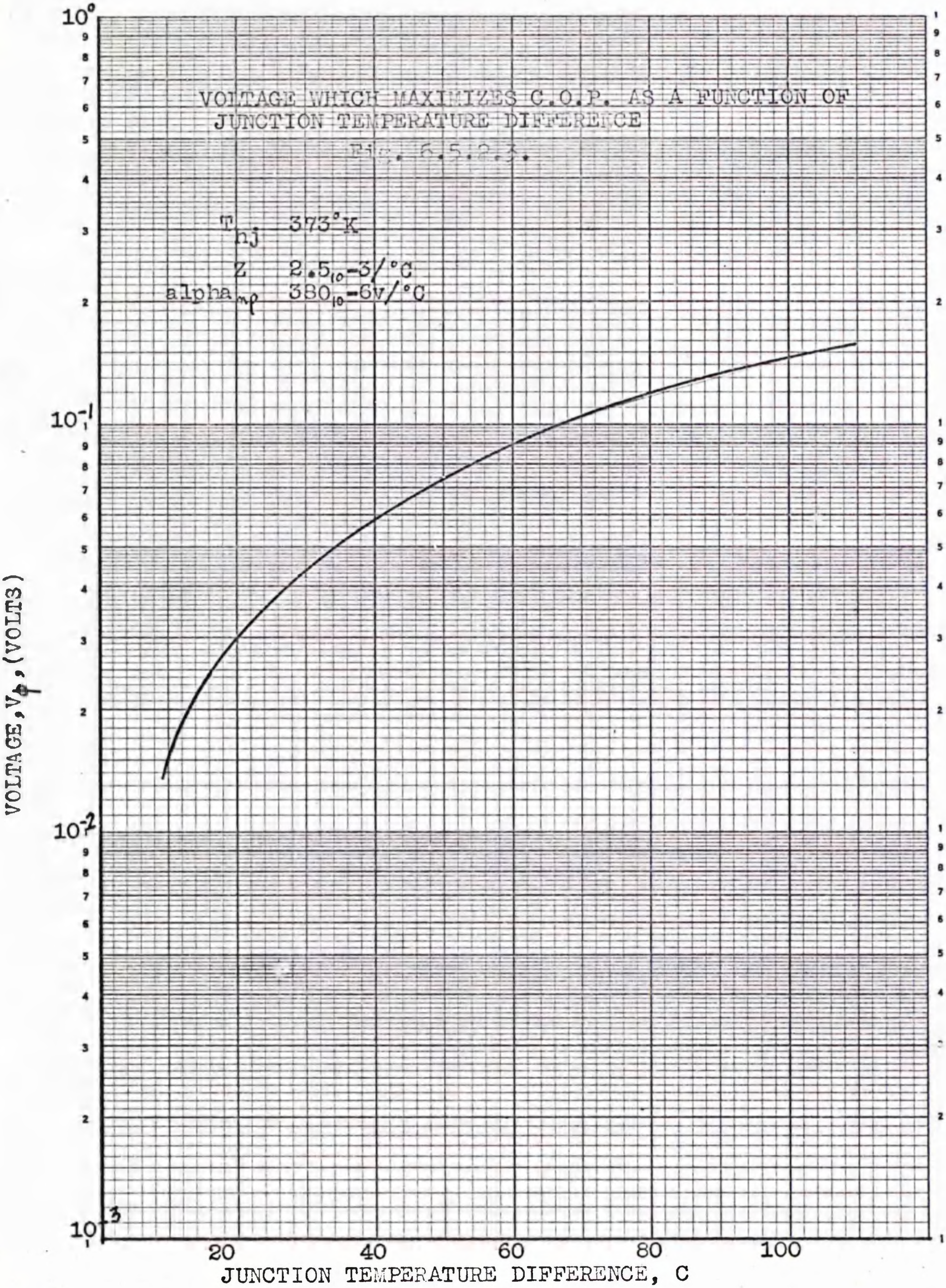

VOLTAGE WHICH MAXIMIZES C.O.P. AS A FUNCTION OF JUNCTION TEMPERATURE DIFFERENCE

Fig. 6.5.2.3.

junction temperature difference, the parameter is the thermoelement height to cross sectional area.

The maximum C.O.P. (equation 6.5.2.18) depends on the material properties only through the material figure of merit (Z).

From appendix C the required voltage is expressed as:

$$V_\phi = \frac{\alpha_{mp} \Delta T_j \sqrt{B}}{\sqrt{B} - 1} \qquad 6.5.2.20.$$

where:

B is defined by 6.5.2.17.

Figure 6.5.2.2 and figure 6.5.2.3 illustrate the voltage required to maximize the C.O.P. as a function of junction temperature difference.

The maximum C.O.P. (equation 6.5.2.18) as a function of junction temperature difference with the variation of the material figure of merit (Z) is shown in figure 6.5.2.4. An appropriate value of Z would be approximately $3.0_{10} - 3$ /°C (state of art) resulting in a maximum C.O.P. approximately one eigth (@ ΔT_j = 20°C) of the carnot efficiency.

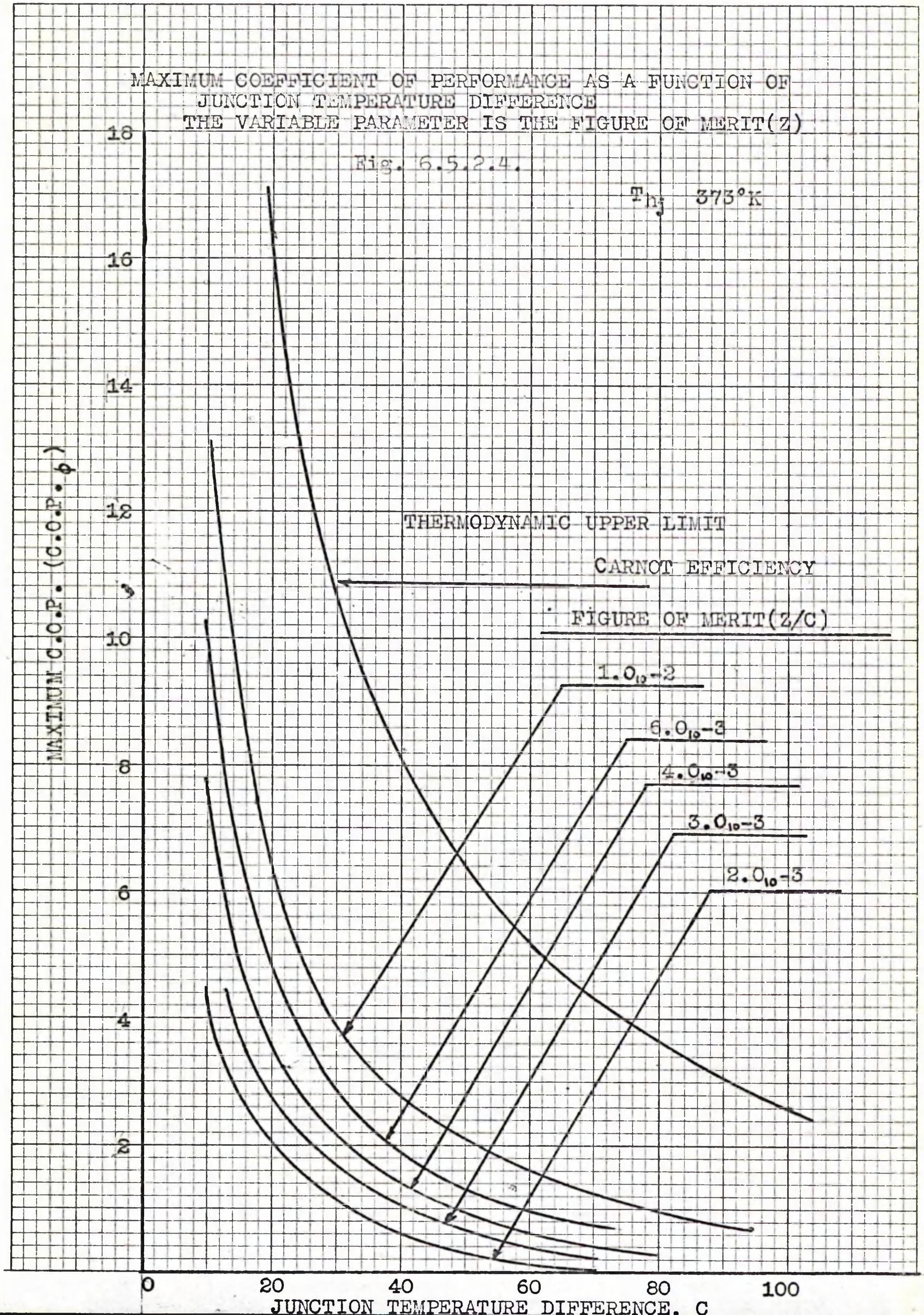
MAXIMUM COEFFICIENT OF PERFORMANCE AS A FUNCTION OF JUNCTION TEMPERATURE DIFFERENCE
THE VARIABLE PARAMETER IS THE FIGURE OF MERIT(Z)
Thj 373°K
THERMODYNAMIC UPPER LIMIT
CARNOT EFFICIENCY
FIGURE OF MERIT(Z/C)
1.0₁₀-2
6.0₁₀-3
4.0₁₀-3
3.0₁₀-3
2.0₁₀-3
MAXIMUM C.O.P. (C.O.P. φ)
18
16
14
12
10
8
6
4
2
0
20
40
60
80
100
JUNCTION TEMPERATURE DIFFERENCE, C

Fig. 6.5.2.4.

Equation 6.5.2.18 may be transposed into a form as in (3) to illustrate the maximum C.O.P. as a function of the parameter ZT_{MEAN} (dimensionless) with variation of (T_{h_j} / T_{c_j}). At the present state of the art a ZT_{MEAN} value of approximately unity (3) results at $(T_{h_j} / T_{c_j}) = 1.110$ of a maximum C.O.P. of 1.15 (somewhat encouraging). Fig. 6.5.25 illustrates the above relation.

The required voltage (equation 6.5.2.20) is independent of the termocouple geometry. The power required to operate at maximum C.O.P. is expressed as:

$$P_\phi = I_\phi V_\phi \qquad 6.5.2.21.$$

and

$$P_\phi = \frac{\alpha_{mp}^2 \, \Delta T_j^2 \sqrt{B}}{R(\sqrt{B} - 1)^2} \qquad 6.5.2.22.$$

Figure 6.5.1.2. shows the variation of the power required at maximum C.O.P. as a function of the junction temperature difference. The resulting value of P_ϕ is $\propto \Delta T_j^2$; and hence non-linear in format.

Equation 6.5.2.10 represents the configuration geometry required for maximizing the C.O.P. For the

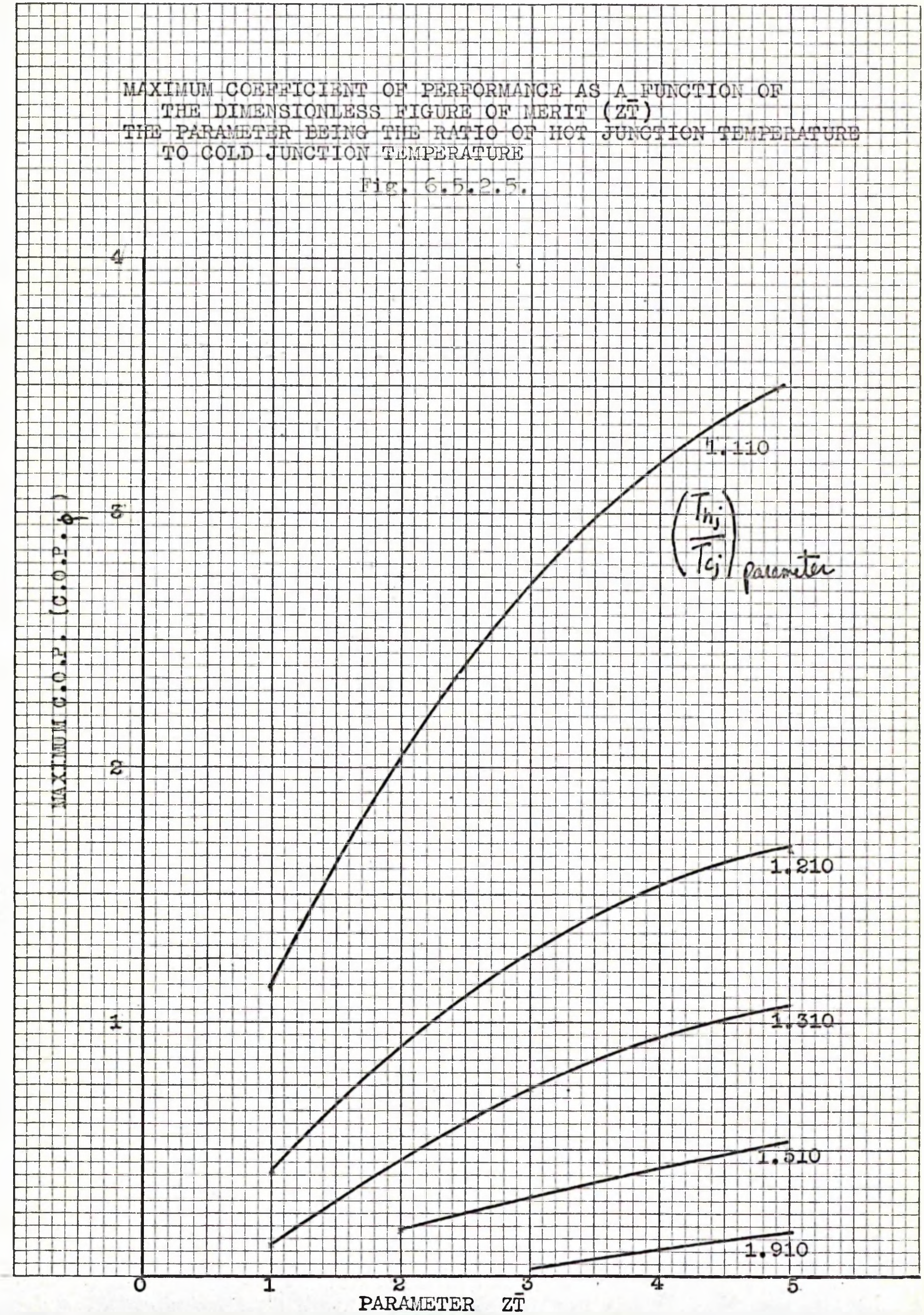

MAXIMUM COEFFICIENT OF PERFORMANCE AS A FUNCTION OF THE DIMENSIONLESS FIGURE OF MERIT ($Z\bar{T}$)
THE PARAMETER BEING THE RATIO OF HOT JUNCTION TEMPERATURE TO COLD JUNCTION TEMPERATURE

Fig. 6.5.2.5.

condition where the thermoelement heights are equal, equation 6.5.2.10 becomes:

$$\frac{A_m}{A_p} = \left[\frac{k_p \rho_m}{k_m \rho_p}\right]^{0.5} \qquad 6.5.2.23.$$

To illustrate the performance sensitivity for deviation from the above relationship computer program C.P.1 was developed. The computer program is found in the section titled 'Computer Programs'. The dimensionless performance ratios as a function of the shape factor modification term are shown in figure 6.5.2.6. The performance ratios are derived on the basis of operational approximations. The derivation and limit controls are found in section 6.6. Figure 6.5.2.6 introduces an ordinate term called "factor". The term factor is utilized as a multiplication variable applied to equation 6.5.2.23 resulting in:

$$\frac{A_m}{A_p} = \left[\frac{k_p \rho_m}{k_m \rho_p}\right]^{0.5} \times \text{"factor"} \qquad 6.5.2.24.$$

Equation 6.5.2.24 requires particular material values in order to determine the area ratio. Because of this fact, values of each material parameter was selected on the quality level readily available at present.

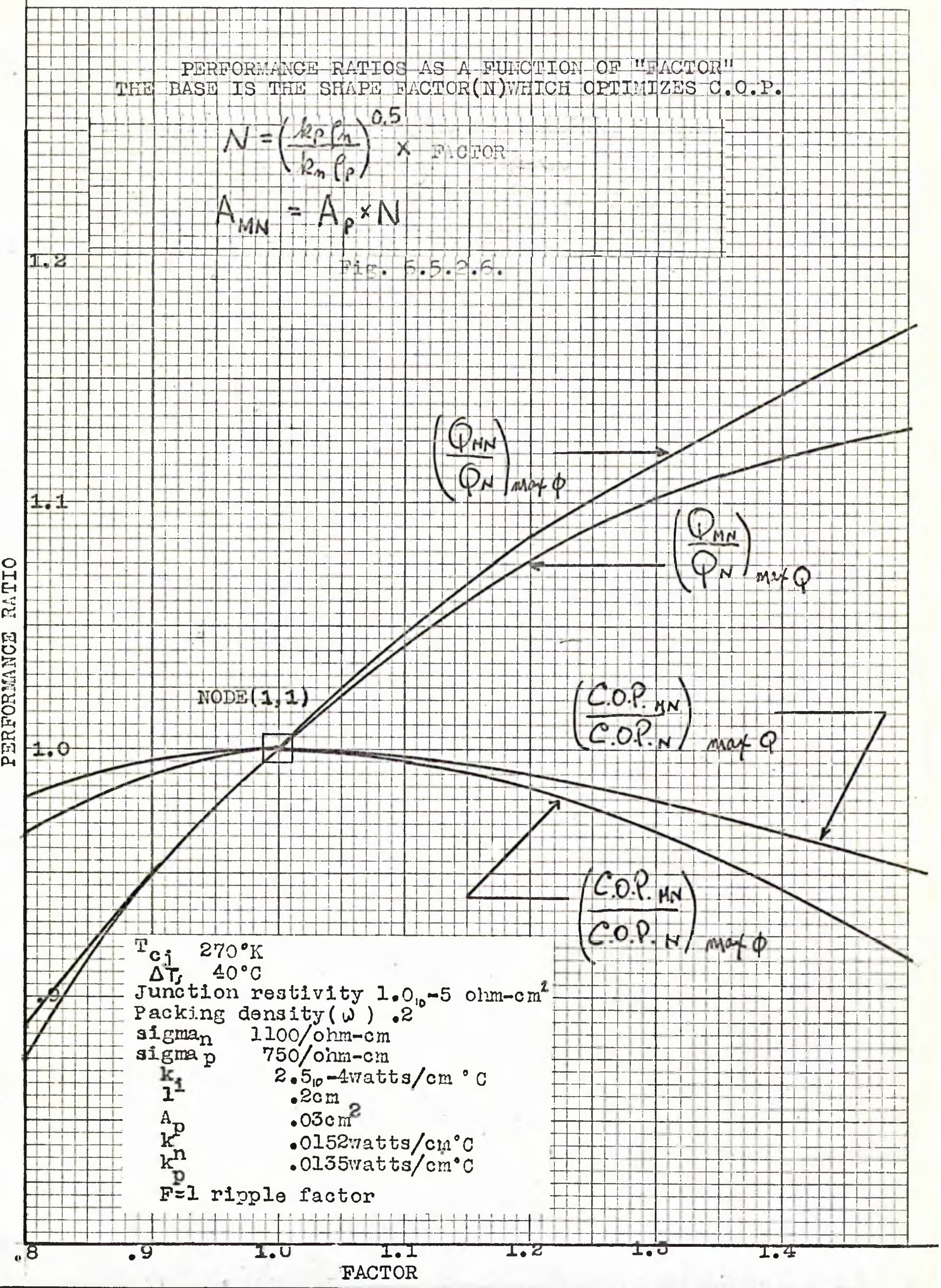
PERFORMANCE RATIOS AS A FUNCTION OF "FACTOR"
THE BASE IS THE SHAPE FACTOR(N)WHICH OPTIMIZES C.O.P.
$N = \left(\frac{k_p \rho_n}{k_n \rho_p}\right)^{0.5} \times$ FACTOR
$A_{MN} = A_p \times N$
$\left(\frac{Q_{MN}}{Q_N}\right)_{max\,\phi}$
$\left(\frac{Q_{MN}}{Q_N}\right)_{max\,Q}$
NODE(1,1)
$\left(\frac{C.O.P._{MN}}{C.O.P._N}\right)_{max\,Q}$
$\left(\frac{C.O.P._{MN}}{C.O.P._N}\right)_{max\,\phi}$
T_{cj} 270°K
ΔT_j 40°C
Junction restivity $1.0_{10}{-5}$ ohm-cm^2
Packing density(ω) .2
$sigma_n$ 1100/ohm-cm
$sigma_p$ 750/ohm-cm
k_i $2.5_{10}{-4}$watts/cm °C
l^1 .2cm
A_p .03cm^2
k^n .0152watts/cm°C
k_p .0135watts/cm°C
F=1 ripple factor
PERFORMANCE RATIO
FACTOR
1.2
1.1
1.0
.9
.8
.9
1.0
1.1
1.2
1.3
1.4

Fig. 6.5.2.6.

Figure 6.5.2.6 indicates the performance ratio when the factor is applied to the shape ratio (equation 6.5.2.24) which maximizes the C.O.P. The figure illustrates the degradation in performance of maximum C.O.P. and the C.O.P. at maximum heat pump rate

The numerator subscripts (MN) indicating the application of the factor (i.e. not equal to unity). The data indicates that at a factor of 1.5 the decrease in performance is not expected to exceed $\simeq$ 8%. Production tolerances (8) indicate that a factor of 1.3 is expected which results in a nominal $\simeq$ 3% performance fall off. The curves representing the performance ratios of heat pump rate at maximum C.O.P. and maximum heat pump rate $\left(Q_{MN}/Q_N\right)_{Q_{max}}$ indicate a decrease in performance for the factor less than unity. However, for the factor greater than unity there is an increase in the heat pump rate output. The rational for this increase in performance is considered in appendix D . The net effect appears to be an increase in element cross sectional and hence an expected increase in heat pump rate output.

6.5.3 Heat Pump Rate at Maximized C.O.P. (Configuration Geometry).

The heat pump with the current adjusted for the maximized C.O.P. operation can be expressed as follows:

$$Q_{s\phi} = T_{cj} I_\phi \alpha_{mp} - \frac{1}{2} I_\phi^2 R - K \Delta T_j \qquad 6.5.3.1.$$

Equation 6.5.3.1 requires the evaluation of R and K (with the element geometry consistant with 6.5.2.10). From equation 6.5.2.10 the n- element shape factor can be expressed:

$$f_n = \left(\frac{k_p \rho_n}{k_n \rho_p}\right)^{\frac{1}{2}} \times f_p \qquad 6.5.3.2.$$

The total electrical series resistance is expressed:

$$R = \frac{\rho_n l_n}{A_n} + \frac{\rho_p l_p}{A_p} \qquad 6.5.3.3.$$

and from 6.5.2.3 and 6.5.2.4:

$$R = \frac{\rho_n}{f_n} + \frac{\rho_p}{f_p} \qquad 6.5.3.4.$$

Substituting 6.5.3.2 into 6.5.3.4 results:

$$R = \frac{\rho_n k_n^{\frac{1}{2}} \rho_p^{\frac{1}{2}}}{k_p^{\frac{1}{2}} \rho_n^{\frac{1}{2}} f_p} + \frac{\rho_p}{f_p} \qquad 6.5.3.5.$$

Operating on the first term the removal of $\rho_m^{\frac{1}{2}}$ in the denominator and introducing into the second term $\frac{k_p^{\frac{1}{2}}}{k_p^{\frac{1}{2}}}$ with a splitting of ρ_p into $\rho_p^{\frac{1}{2}} \times \rho_p^{\frac{1}{2}}$

The purpose of the algebraic manipulation is to express the material variable (R) in terms of the figure of merit (Z)

Factoring 6.5.3.5 results:

$$R = \frac{\rho_p^{\frac{1}{2}}}{f_p k_p^{\frac{1}{2}}}\left[(\rho_m k_m)^{\frac{1}{2}} + (\rho_p k_p)^{\frac{1}{2}}\right] \qquad 6.5.3.6.$$

from equation 6.5.2.13

$$\frac{\alpha_{np}}{Z^{\frac{1}{2}}} = \left[(\rho_m k_m)^{\frac{1}{2}} + (\rho_p k_p)^{\frac{1}{2}}\right] \qquad 6.5.3.7.$$

and

$$R = \frac{\rho_p^{\frac{1}{2}}}{f_p k_p^{\frac{1}{2}}}\left[\frac{\alpha_{np}}{Z^{\frac{1}{2}}}\right] \qquad 6.5.3.8.$$

A similiar derivation can be performed resulting in a slightly different form for the series resistance. The solution starts at equation 6.5.3.2 by solving for f_p and proceeding as indicated above. This results in the series resistance being expressable as:

$$R = \frac{\rho_m^{\frac{1}{2}}}{f_m k_m^{\frac{1}{2}}}\left[\frac{\alpha_{np}}{Z^{\frac{1}{2}}}\right] \qquad 6.5.3.9.$$

The parallel thermal conductance (K) can be expressed as:

$$K = \frac{A_m k_m}{l_m} + \frac{A_p k_p}{l_p} \qquad 6.5.3.10.$$

From equation 6.5.2.3. and 6.5.2.4 (K) becomes:

$$K = f_m k_m + f_p k_p \qquad 6.5.3.11.$$

Introducing equation 6.5.3.2. into the first term

$$K = \frac{k_p^{\frac{1}{2}} \rho_m^{\frac{1}{2}} f_p k_m}{k_m^{\frac{1}{2}} \rho_p^{\frac{1}{2}}} + f_p k_p \qquad 6.5.3.12.$$

Performing on the first term the removal of $k_m^{\frac{1}{2}}$ from the denominator and introducing into the second term $(\rho_p^{\frac{1}{2}}/\rho_p^{\frac{1}{2}})$ with a splitting of k_p into $k_p^{\frac{1}{2}}$ x $k_p^{\frac{1}{2}}$ The purpose of the algebraic manipulation is to express the material variable (K) in terms of the figure of merit (Z).

Factoring and combining like terms:

$$K = \frac{k_p^{\frac{1}{2}} f_p}{\rho_p^{\frac{1}{2}}} \left[k_m^{\frac{1}{2}} \rho_m^{\frac{1}{2}} + k_p^{\frac{1}{2}} \rho_p^{\frac{1}{2}} \right] \qquad 6.5.3.13.$$

introducing equation 6.5.3.7 into 6.5.3.13 results:

$$K = \frac{k_p^{\frac{1}{2}} f_p}{\rho_p^{\frac{1}{2}}} \left[\frac{\alpha_{np}}{Z^{\frac{1}{2}}} \right] \qquad 6.5.3.14.$$

A similiar derivation can be performed resulting in:

$$K = \frac{k_n^{\frac{1}{2}} f_n}{\rho_n^{\frac{1}{2}}} \left[\frac{\alpha_{np}}{Z^{\frac{1}{2}}} \right] \qquad 6.5.3.15.$$

(The derivation is similiar which resulted in equation 6.5.3.9)

The heat pump rate at maximum C.O.P. can be expressed as:

$$Q_{s\phi} = T_{c_j} I_\phi \alpha_{np} - \frac{1}{2} I^2 \frac{\rho_p^{\frac{1}{2}}}{f_p k_p^{\frac{1}{2}}} \left[\frac{\alpha_{np}}{Z^{\frac{1}{2}}} \right] - \frac{k_p^{\frac{1}{2}} f_p}{\rho_p^{\frac{1}{2}}} \left[\frac{\alpha_{np}}{Z^{\frac{1}{2}}} \right] \Delta T_j \qquad 6.5.3.16.$$

or

$$Q_{s\phi} = T_{c_j} I_\phi \alpha_{np} - \frac{1}{2} I^2 \frac{\rho_n^{\frac{1}{2}}}{f_n k_n^{\frac{1}{2}}} \left[\frac{\alpha_{np}}{Z^{\frac{1}{2}}} \right] - \frac{k_p^{\frac{1}{2}} f_p}{\rho_p^{\frac{1}{2}}} \left[\frac{\alpha_{np}}{Z^{\frac{1}{2}}} \right] \Delta T_j \qquad 6.5.3.17.$$

In order to express the heat pump rate at maximum C.O.P. in a form more suitable for anaylsis a rederivation of $Q_{s\phi}$ was undertaken.

Repeating equation 6.5.3.1.

$$Q_{s\phi} = T_{c_j} I_\phi \alpha_{np} - \frac{1}{2} I_\phi^2 R - K \Delta T_j$$

and from equation 6.5.2.19

$$I_\phi = \frac{\alpha_{mp} \Delta T_j}{R(\sqrt{B}-1)}$$

where:

$$B = 1 + \frac{Z(T_{hj} + T_{cj})}{2} \qquad 6.5.2.17.$$

Substituting 6.5.2.19 into 6.5.3.1 results:

$$Q_{s\phi} = \frac{T_{cj}\alpha_{mp}^2 \Delta T_j}{R(\sqrt{B}-1)} - \frac{\alpha_{mp}^2 \Delta T_j^2}{2R(\sqrt{B}-1)^2} - K\Delta T_j \qquad 6.5.3.18.$$

Combining the first and second term

$$Q_{s\phi} = \frac{T_{cj}\alpha_{mp}^2 \Delta T_j(\sqrt{B}-1) - \frac{1}{2}\alpha_{mp}^2 \Delta T_j^2}{R(\sqrt{B}-1)^2} - K\Delta T_j \qquad 6.5.3.19.$$

From equation 6.5.2.13

$$ZK = \alpha_{mp}^2 / R \qquad 6.5.3.20.$$

Introducing equation 6.5.3.20 into equation 6.5.3.19 results:

$$Q_{s\phi} = \frac{T_{cj}\Delta T_j ZK(\sqrt{B}-1) - \frac{1}{2}\Delta T_j^2 ZK}{(\sqrt{B}-1)^2} - K\Delta T_j \qquad 6.5.3.21.$$

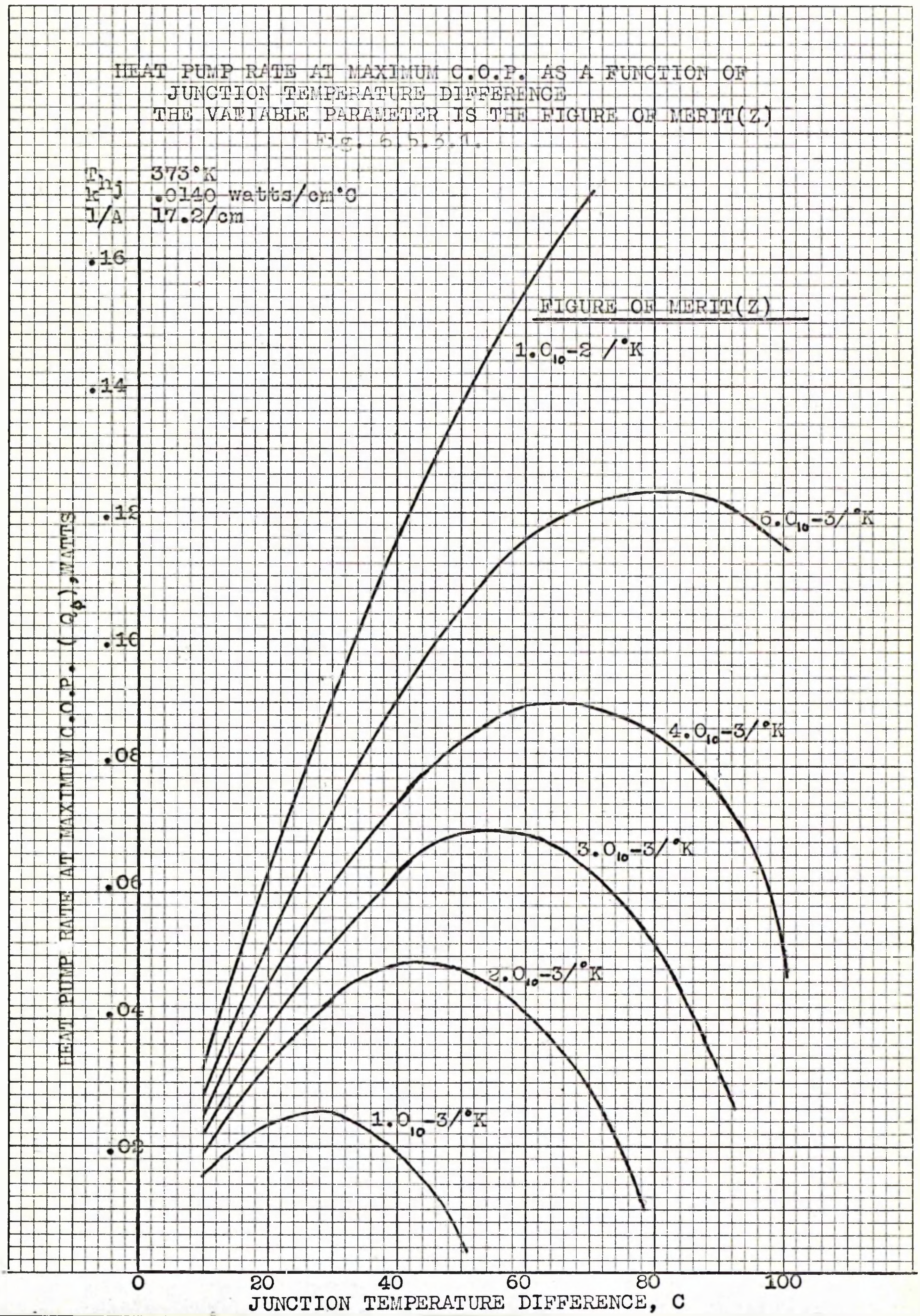
HEAT PUMP RATE AT MAXIMUM C.O.P. AS A FUNCTION OF
JUNCTION TEMPERATURE DIFFERENCE
THE VATIABLE PARAMETER IS THE FIGURE OF MERIT(Z)
Fig. 6.5.3.1.
T_{hj} 373°K
k .0140 watts/cm°C
l/A 17.2/cm
FIGURE OF MERIT(Z)
1.0_{10}-2 /°K
6.0_{10}-3/°K
4.0_{10}-3/°K
3.0_{10}-3/°K
2.0_{10}-3/°K
1.0_{10}-3/°K
HEAT PUMP RATE AT MAXIMUM C.O.P. (Q_p), WATTS
.16
.14
.12
.10
.08
.06
.04
.02
0
20
40
60
80
100
JUNCTION TEMPERATURE DIFFERENCE, C

Expanding the first and second term, while introducing

$\Delta T_j = T_{h_j} - T_{c_j}$ and factoring $K \Delta T_j$ results:

$$Q_{s\phi} = K\Delta T_j \left[\frac{Z T_{c_j}\sqrt{B} - Z T_{MEAN}}{(\sqrt{B}-1)^2} + 1 \right] \qquad 6.5.3.22.$$

Equation 6.5.3.22 can be expressed as a dimensionless parameter by expressing:

$$\frac{Q_{s\phi}}{K\Delta T_j} = \left[\frac{Z T_{c_j}\sqrt{B} - Z T_{MEAN}}{(\sqrt{B}-1)^2} - 1 \right] \qquad 6.5.3.23.$$

Figure 6.5.3.1 shows the heat pump rate at maximum C.O.P. as a function of junction temperature difference for variation in the figure of merit. The hot side junction temperature was fixed at 100^{o}C (B.P. water). At the present state of art a figure of merit of 3.0_{10} - 3/^{o}K will result in a heat pump rate of $\simeq$ .07 watts/ couple at a ΔT_j of approximately 58^{o}C.

6.5.4 Maximizing Heat Pump Rate (I).

The net rate of heat removal, i.e. the heat pumping capacity is

$$Q_s = T_{c_j} I \alpha_{np} - \frac{1}{2} I^2 R - K\Delta T_j \qquad 6.4.3.$$

The current that yields maximum cooling is the value satisfying the condition $\frac{dQ_s}{dI} = 0$ The current corresponding to Qsmax is designated I_Q , and is

$$I_Q = \frac{\alpha_{np} T_{cj}}{R} \qquad 6.5.4.1.$$

Substituting 6.5.4.1 into 6.4.3 results (Qsmax):

$$Q_{s_{max}} = \frac{T_{cj}^2 \alpha_{np}^2}{2R} - K \Delta T_j \qquad 6.5.4.2.$$

With the cold junction "perfectly" insulated (Qs = 0) and the current (I_Q), the maximum junction temperature ($\Delta T_{j_{max}}$) the couple can provide can be determined as follows:

$$0 = T_{cj} I_Q \alpha_{np} - \frac{1}{2} I_Q^2 R - K \Delta T_{j_{max}} \qquad 6.5.4.3.$$

Solving for $\Delta T_{j_{max}}$ the expression becomes:

$$\Delta T_{j_{max}} = \frac{\alpha_{np}^2 T_{cj}^2}{2RK} - \frac{T_{cj}^2 \alpha_{np}^2}{RK} \qquad 6.5.4.4.$$

then:

$$\Delta T_{j_{max}} = \frac{T_{cj}^2 \alpha_{np}^2}{2RK} \qquad 6.5.4.5.$$

introducing the figure of merit (equation 6.5.2.13)

$$\Delta T_{j_{max}} = \frac{1}{2} T_{cj}^2 Z \qquad 6.5.4.6.$$

A complete derivation for determining the maximum temperature difference is presented in section 6.5.6. The maximum heat pump rate can be simplified by introducing equation 6.5.4.5 into equation 6.5.4.2 resulting

$$Q_{s_{max}} = K\left[\Delta T_{j_{max}} - \Delta T_j\right] \qquad 6.5.4.7.$$

rearranging equation 6.5.4.7 results

$$Q_{s_{max}} = K\,\Delta T_{j_{max}}\left[1 - \frac{\Delta T_j}{\Delta T_{j_{max}}}\right] \qquad 6.5.4.8.$$

The voltage required to operate at the maximum heat pump rate can be expressed as:

$$V_Q = I_Q R + \alpha_{np}\,\Delta T_j \qquad 6.5.4.9.$$

Introducing equation 6.5.4.1 into equation 6.5.4.9 results as follows:

$$V_Q = \alpha_{np} T_{c_j} + \alpha_{np}\,\Delta T_j \qquad 6.5.4.10.$$

and

$$\Delta T_j = T_{h_j} - T_{c_j}$$

then:

$$V_Q = \alpha_{np} T_{h_j} \qquad 6.5.4.11.$$

where:

T_{h_j} hot junction temperature, ^{o}K

The power input to operate at maximum heat pump rate is expressable as:

$$P_Q = I_Q V_Q \qquad 6.5.4.12.$$

and

$$P_Q = \frac{\alpha_{mp}^2 T_{h_j} T_{c_j}}{R} \qquad 6.5.4.13.$$

It is possible to express P_Q by utilizing equation 6.5.4.9 and 6.5.4.1 to become:

$$P_Q = I_Q^2 R + I_Q \alpha_{mp} \Delta T_j \qquad 6.5.4.14.$$

substituting 6.5.4.1 into 6.5.4.14 and introducing (K/K) into the first and second term:

$$P_Q = \frac{\alpha_{mp}^2 T_{c_j}^2 K}{RK} + \frac{\alpha_{mp}^2 T_{c_j} \Delta T_j K}{RK} \qquad 6.5.4.15.$$

using 6.5.4.5 into equation 6.5.4.15 results:

$$P_Q = 2K\Delta T_{j_{max}} + \frac{2K\Delta T_j \Delta T_{j_{max}}}{T_{c_j}} \qquad 6.5.4.16.$$

Factoring, results in the power required at maximum heat pump rate as:

$$P_Q = 2K\Delta T_{j_{max}}\left[1 + \frac{\Delta T_j}{T_{c_j}}\right] \qquad 6.5.4.17.$$

6.5.5. C.O.P. at Maximized Heat Pump Rate (I).

The C.O.P. can be expressed when the current (I_Q) is adjusted to maximize the heat pump rate ($Q_{s_{max}}$) by utilizing equation 6.5.4.8 and 6.5.4.17. The C.O.P. becomes:

$$C.O.P._Q = \frac{\left[1 - \frac{\Delta T_j}{\Delta T_{j_{max}}}\right]}{2\left[1 + \frac{\Delta T_j}{T_{c_j}}\right]} \qquad 6.5.5.1.$$

Equation 6.5.5.1 indicates that the C.O.P. when the current is adjusted to maximize the heat pump rate is invariant with the thermoelement geometry. Material properties are reflected in the determination of (equation 6.5.4.5).

6.5.6. Maximum Junction Temperature Difference ($\Delta T_{j_{max}}$)

The maximum junction temperature difference can be determined by evaluating the current that satisfies $d(\Delta T_j)/dI$ = 0 and solving for ΔT_j Equation 6.4.3 is transposed as follows:

$$\Delta T_j = \frac{T_{c_j} \alpha_{np} I - \frac{1}{2} I^2 R - Q_s}{K} \qquad 6.5.6.1.$$

taking the derivative then:

$$\frac{d(\Delta T_j)}{dI} = T_{c_j} \alpha_{np} - IR \qquad 6.5.6.1.$$

and solving for I with $d(\Delta T_j)/dI = 0$ results:

$$I_{\Delta T} = \frac{T_{cj}\,\alpha_{np}}{R} \qquad 6.5.6.2.$$

Comparing equation 6.5.4.1 (I_Q) and 6.5.6.2. ($I_{\Delta T}$) indicates that the value of the current maximizing the required parameters are equal. Substituting equation 6.5.6.2 into equation 6.5.6.1 for Q_s = 0 results:

$$\Delta T_{j_{max}} = \frac{T_{cj}^2\,\alpha_{np}^2}{2RK} \qquad 6.5.6.3.$$

Equation 6.5.6.3. is identical to equation 6.5.4.5 as derived in section 6.5.4.

There are two additional techniques that will yield identical results to equation 6.5.6.3. The algebraic manipulations are found in appendix A. The techniques employed are:

(1) Take $dQ/dI = 0$ solve for I_Q (6.5.4.1), substitute I_Q into equation 6.4.3 resulting in $Q_{s_{max}}$ (equation 6.5.4.2) and solve for $\Delta T_{j_{max}}$ at $Q_{s_{max}}$ = 0.

(2) Take $d(COP)/dI = 0$ solve for I_ϕ (6.5.1.1), substitute I_ϕ into equation 6.4.9 resulting in C.O.P.$_{max}$ (equation 6.5.1.3) and solve for $\Delta T_{j_{max}}$ at C.O.P.$_{max}$ =0.

The minimum cold junction temperature ($T_{cj_{MIN}}$, ^{o}K) with fixed hot-junction temperature can be obtained from equation 6.5.4.6

$$\Delta T_{j_{max}} = \frac{T_{cj_{MIN}}^{2} \times Z}{2} \qquad 6.5.4.6.$$

and

$$\Delta T_{j_{max}} = T_{hj_{max}} - T_{cj_{MIN}} \qquad 6.5.6.4.$$

then

$$2 T_{hj_{max}} - 2 T_{cj_{MIN}} = T_{cj_{MIN}}^{2} \times Z \qquad 6.5.6.5.$$

Avoiding a quadratic solution by introducing Z to both sides of equation 6.5.6.5 and rearranging results:

$$T_{cj_{MIN}}^{2} \times Z^{2} + 2 T_{cj_{MIN}} Z = 2 T_{hj_{max}} Z \qquad 6.5.6.6.$$

Adding unity to both sides of equation 6.5.6.6 and the left side is a perfect square then:

$$\left(1 + Z T_{cj_{MIN}}\right)^{2} = 2 Z T_{hj_{max}} + 1 \qquad 6.5.6.7.$$

and

$$T_{cj_{min}} = \frac{\sqrt{2 Z T_{hj_{max}} + 1} - 1}{Z} \qquad 6.5.6.8.$$

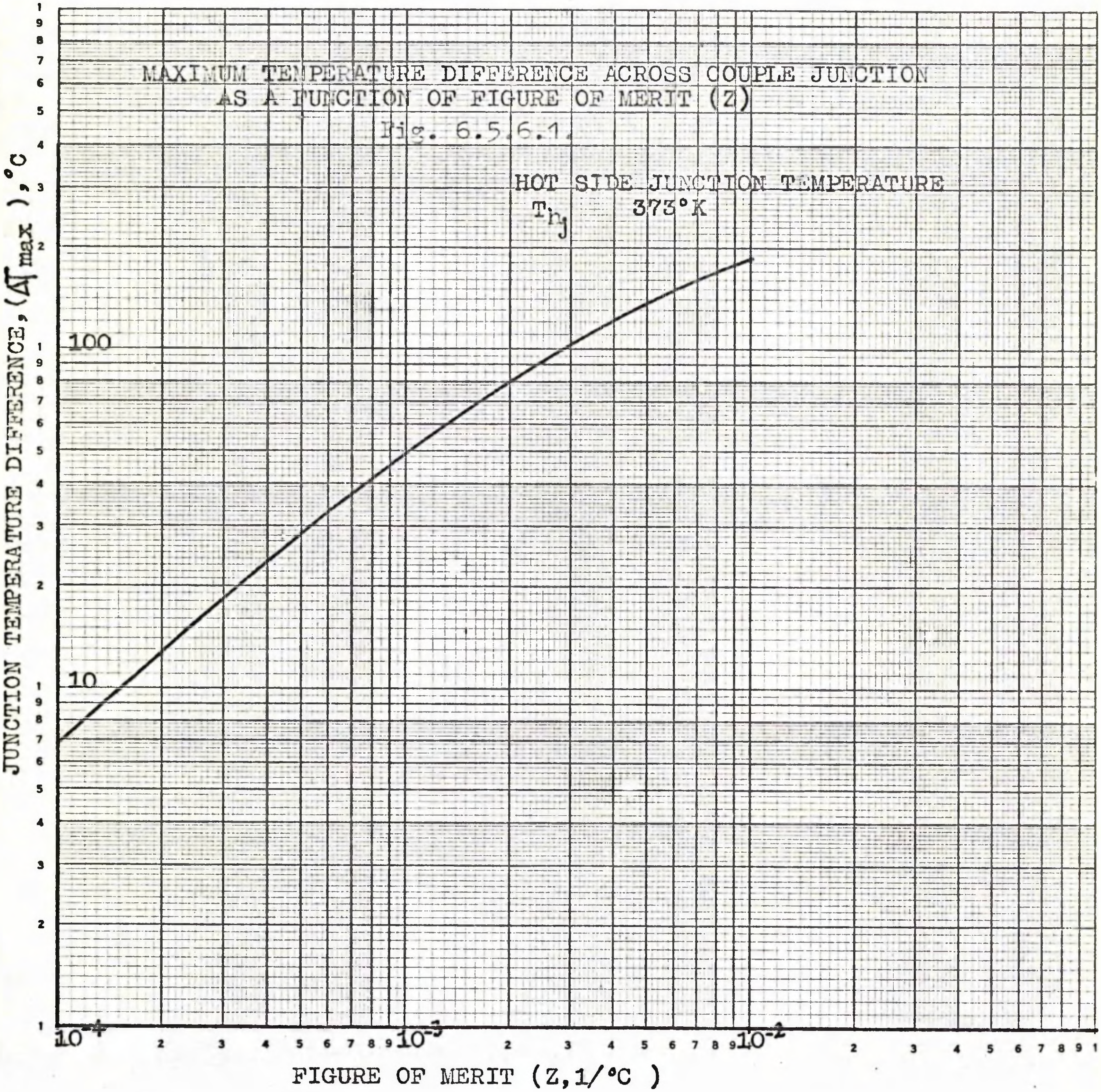
MAXIMUM TEMPERATURE DIFFERENCE ACROSS COUPLE JUNCTION
AS A FUNCTION OF FIGURE OF MERIT (Z)
Fig. 6.5.6.1.
HOT SIDE JUNCTION TEMPERATURE
T_{h_J} 373°K
JUNCTION TEMPERATURE DIFFERENCE, (ΔT_{max}), °C
100
10
10^{-4}
10^{-3}
10^{-2}
FIGURE OF MERIT (Z,1/°C)

Figure 6.5.6.1 illustrates the maximum junction temperature difference as a function of the figure of merit for a hot junction temperature of 100°C (B.P. water).

6.5.7 Maximized (Heat Pump Rate/Configuration Geometry).

The maximum heat pump rate ($Q_{s_{max}}$) is:

$$Q_{s_{max}} = \frac{T_{c_j}^2 \alpha_{np}^2}{2R} - K \Delta T_j \qquad 6.5.4.2.$$

where:

$$R = \frac{\rho_n l_n}{A_n} + \frac{\rho_p l_p}{A_p} \qquad 6.5.3.3.$$

and

$$K = \frac{A_n k_n}{l_n} + \frac{A_p k_p}{l_p} \qquad 6.5.3.10.$$

For military or space/satellite operation it is desirable to maximize the heat pump rate with respect to system weight. In order to determine the thermoelement configuration required for this operational condition the geometry of the element must be considered.

The thermoelement weight for the n- and p- thermoelements of the same length (l) can be expressed as:

$$W_{TOTAL} = l\left[\gamma_n A_n + \gamma_p A_p\right] \qquad 6.5.7.1.$$

where:

ℓ thermoelement height, cm.

γ_n, γ_p thermoelement density, grams/cm^3

W_{TOTAL} thermoelectric couple weight, grams

Equation 6.5.7.1 indicates that in order to minimize the thermoelectric couple weight the height of the element (ℓ) should be restricted and A_n, A_p be consistent with the required heat pump rate. It is proposed to maximize the heat pump rate with respect to system weight by equating the first derivative to zero and solving for the configuration variable. The equation to be solved can be expressed as:

$$\frac{d\left(\frac{Q_{s\,max}}{A_T}\right)}{d(A)} = 0 \qquad 6.5.7.2.$$

where:

A represents the cross sectional area of the n- or p- thermoelement. (p- utilized)

Appendix E presents the complete mathematical manipulations required to solve equation 6.5.7.2. The operational parameter considered was to find the area ratio maximizing $(Q_{s\,max}/A_T)$ this is found to be:

$$\frac{A_n}{A_p} = \left[\frac{\left(\frac{\rho_n + \rho_n^2 \xi - \rho_n \rho_p \xi}{\rho_p}\right)^{\frac{1}{2}} + \rho_n \xi}{(1 - \xi \rho_p)}\right] \qquad 6.5.7.3.$$

where:

$$\zeta = \frac{2(k_p - k_n)\Delta T_j}{\alpha_{np}^2 T_{c_j}^2} \qquad 6.5.7.4.$$

From appendix E equation E.1 the maximum heat pump rate is expressable as:

$$Q_{S_{max}} = \frac{\alpha_{np}^2 T_{c_j}^2 [A_n A_p]}{2\ell [A_p \rho_n + A_n \rho_p]} - \frac{1}{\ell}\left[k_n A_n + k_p A_p\right] \Delta T_j$$

Expanding the first term and combining the second results:

$$Q_{S_{max}} = \frac{\alpha_{np}^2 T_{c_j}^2 A_n A_p - 2\Delta T_j [k_n A_n + k_p A_p][A_p \rho_n + A_n \rho_p]}{2\ell [A_p \rho_n + A_n \rho_p]} \qquad 6.5.7.5.$$

Dividing numerator and denominator by $(A_n A_p)$

$$Q_{S_{max}} = \frac{\alpha_{np}^2 T_{c_j}^2 - 2\Delta T_j \left[\frac{k_n}{A_p} + \frac{k_p}{A_n}\right]\left[\frac{\rho_n}{A_n} + \frac{\rho_p}{A_p}\right]}{2\ell \left[\frac{\rho_n}{A_n} + \frac{\rho_p}{A_p}\right]} \qquad 6.5.7.6.$$

Equation 6.5.7.6. will fulfill the requirements of equation 6.5.7.2 by utilizing equation 6.5.7.3 to determine the area of the n- element given the cross sectional area of the p- element.

The total cross sectional area is expressable as:

$$A_T = A_m + A_p \qquad 6.5.7.7.$$

and

$$A_T = A_p\left[\begin{pmatrix}\text{EQUATION}\\ 6.5.7.3\end{pmatrix} + 1\right] \qquad 6.5.7.8.$$

with $\left(Q_{s_{max}}/A_T\right)$ being maximized by equation 6.5.7.6 and equation 6.5.7.8.

Assuming the following simplifications:

(1) $A_m = A_p = A \;;\; A_T = 2A$

(2) $(\rho_m + \rho_p)/2 = \bar{\rho}$

(3) $(k_m + k_p)/2 = \bar{k}$

Incorporating the simplifications into equation 6.5.7.6. results in:

$$Q_{s_{max}} = \frac{\alpha_{np}^2 T_{cj}^2 A_T}{8 l \bar{\rho}} - \frac{\Delta T_j A_T \bar{k}}{l} \qquad 6.5.7.9.$$

when $\Delta T_j \longrightarrow 0$

$$Q_{s_{max}} \longrightarrow \frac{\alpha_{np}^2 T_{cj}^2 A_T}{8 l \bar{\rho}} \qquad 6.5.7.10.$$

and from equation 6.5.5.1.

$$\text{C.O.P.}_Q \longrightarrow \tfrac{1}{2} \qquad 6.5.7.11.$$

The circuit resistance can be expressed as

$$R = \frac{(\rho_n + \rho_p)\, l 4}{2 A_T} \qquad 6.5.7.12.$$

then

$$R = \frac{\bar{\rho}\, l 4}{A_T} \qquad 6.5.7.13.$$

Substituting equation 6.5.7.13 into equation 6.5.7.10 results:

$$Q_{s\,max} \longrightarrow \frac{\alpha_{np}^{2}\, T_{cj}^{2}}{2R} \qquad 6.5.7.14.$$

Equation 6.5.4.7 for $\Delta T_j \longrightarrow 0$ indicates that:

$$Q_{s\,max} \longrightarrow K \Delta T_{j\,max} \qquad 6.5.7.15.$$

Equation 6.5.7.14 is identical to equation 6.5.7.15 which follows from equation 6.5.4.5. For $k_n = k_p$ ($\varphi = 0$) equation 6.5.7.3 reduces to:

$$\frac{A_n}{A_p} = \left(\frac{\rho_n}{\rho_p}\right)^{0.5} \qquad 6.5.7.16.$$

Equation 6.5.7.16 is equivalent to equation 6.5.2.10 for the condition where $l_n = l_p = l$

6.6 Simplified Design Approximations.

The relationship between the current for maximizing the C.O.P (I_ϕ) and the current for maximizing the heat pump rate (I_Q) will be developed as follows:

The current heat maximizes the C.O.P. is expressed as:

$$I_\phi = \frac{\alpha_{mp} \Delta T_j}{R(\sqrt{B}-1)} \qquad 6.5.2.19.$$

The current that maximizes the heat pump rate is expressed as:

$$I_Q = \frac{\alpha_{mp} T_{cj}}{R} \qquad 6.5.4.1.$$

combining equation 6.5.4.1 and equation 6.5.2.19 then it follows:

$$I_\phi = \frac{I_Q \Delta T_j}{T_{cj}(\sqrt{B}-1)} \qquad 6.6.1.$$

Equation 6.6.1 indicates that the current maximizing the C.O.P. (I_ϕ) is inversely proportional to the figure of merit.

Introducing $\frac{(\sqrt{B}+1)}{(\sqrt{B}+1)}$ into equation 6.6.1 and performing the multiplication results:

$$I_\phi = \frac{I_Q \Delta T_j(\sqrt{B}+1)}{T_{cj}(B-1)} \qquad 6.6.2.$$

Introducing: $$B = 1 + \frac{\Delta T_{j_{max}}}{T_{c_j}^2}\left[T_{h_j} + T_{c_j}\right] \qquad 6.6.3.$$

into the denominator and expanding the numerator:

$$I_\phi = \frac{I_\varphi \Delta T_j \sqrt{B} + I_\varphi \Delta T_j}{\frac{\Delta T_{j_{max}}}{T_{c_j}}\left[T_{h_j} + T_{c_j}\right]} \qquad 6.6.4.$$

Introducing equation 6.6.3 into the numerator and factoring ($I_\varphi \Delta T_j$) results:

$$I_\phi = \frac{I_\varphi \Delta T_j \left[1 + \left(1 + \frac{\Delta T_{j_{max}}}{T_{c_j}^2}\left[T_{h_j} + T_{c_j}\right]\right)^{\frac{1}{2}}\right]}{\Delta T_{j_{max}}\left[\frac{T_{h_j}}{T_{c_j}} + 1\right]} \qquad 6.6.5.$$

Operating on denominator by introducing:

$$T_{h_j} = \Delta T_j + T_{c_j} \qquad 6.6.6.$$

then:

$$\Delta T_{j_{max}}\left[\frac{\Delta T_j + T_{c_j}}{T_{c_j}} + 1\right] = \Delta T_{j_{max}}\left[\frac{\Delta T_j}{T_{c_j}} + 2\right] \qquad 6.6.7.$$

Expanding the terms in the numerator bracket and utilizing equation 6.6.6 transforms equation 6.6.5 into:

$$I_\phi = \frac{I_\varphi \Delta T_j}{\Delta T_{j_{max}}}\left[\frac{1 + \left[1 + \frac{2\Delta T_{j_{max}}}{T_{c_j}} + \frac{\Delta T_j \Delta T_{j_{max}}}{T_{c_j}^2}\right]^{\frac{1}{2}}}{\left[\frac{\Delta T_j}{T_{c_j}} + 2\right]}\right]$$

6.6.8.

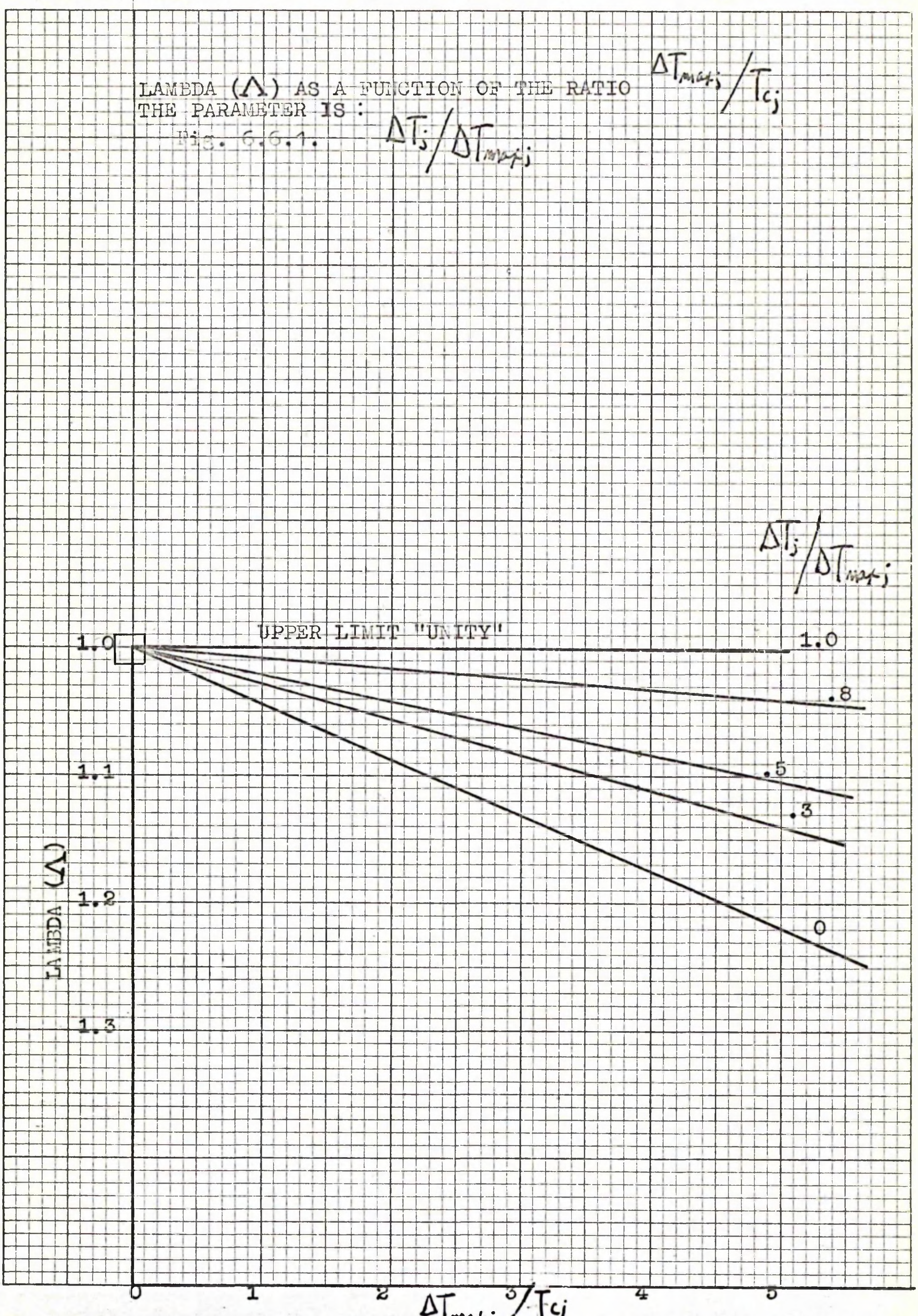
LAMBDA (Λ) AS A FUNCTION OF THE RATIO $\Delta T_{max\,j} / T_{cj}$
THE PARAMETER IS : $\Delta T_j / \Delta T_{max\,j}$
Fig. 6.6.1.
$\Delta T_j / \Delta T_{max\,j}$
UPPER LIMIT "UNITY"
1.0
.8
.5
.3
0
LAMBDA (Λ)
1.0
1.1
1.2
1.3
0
1
2
3
4
5
$\Delta T_{max\,j} / T_{cj}$

Assigning Λ to replace the terms in the bracket then equation 6.6.8 becomes:

$$I_\phi = \frac{I_Q \Delta T_j}{\Delta T_{j_{max}}} \Lambda \qquad 6.6.9.$$

Figure 6.6.1 illustrates the magnitude of Λ as a function of ($\Delta T_{j_{max}} / T_{c_j}$) with ($\Delta T_j / \Delta T_{j_{max}}$) a variable parameter. For Λ = 1 then equation 6.6.9 reduces to:

$$I_\phi = \frac{I_Q \Delta T_j}{\Delta T_{j_{max}}} \qquad 6.6.10.$$

From equation 6.5.3.1:

$$Q_{s\phi} = T_{c_j} I_\phi \alpha_{np} - \frac{1}{2} I_\phi^2 R - K \Delta T_j$$

Substituting equation 6.6.10 into equation 6.5.3.1 and introducing:

$$\frac{\alpha_{np}^2}{R} = \frac{2 \Delta T_{j_{max}} K}{T_{c_j}^2} \qquad 6.6.11.$$

transforms equation 6.5.3.1 into:

$$Q_{s\phi} = K \Delta T_j \left[2\Lambda - \frac{\Lambda^2 \Delta T_j}{\Delta T_{j_{max}}} - 1 \right] \qquad 6.6.12.$$

when Λ = 1 then equation 6.6.12 reduces to:

$$Q_{s\phi} = K \Delta T_j \left[1 - \frac{\Delta T_j}{\Delta T_{j_{max}}} \right] \qquad 6.6.13.$$

Equation 6.6.13 expresses the heat pump rate when the current has been adjusted so as to maximize the C.O.P. (I_ϕ). Equation 6.5.4.8 can be combined with equation 6.6.13 resulting:

$$Q_{s\phi} = \frac{\Delta T_j}{\Delta T_{j_{max}}} Q_{s_{max}} \qquad 6.6.14.$$

The limits on $Q_{s_{max}}$ and $Q_{s\phi}$ can be obtained by equating ΔT_j = 0 results in $Q_{s\phi}$ = 0 (equation 6.6.13) and when $\Delta T_j = \Delta T_{j_{max}}$ results in $Q_{s_{max}}$ = 0 (equation 6.5.4.8).

The power required to operate at maximum C.O.P. can be expressed by equation 6.6.10 and equation 6.5.2.21 resulting:

$$P_\phi = I_\phi^2 R + I_\phi \alpha_{np} \Delta T_j \qquad 6.6.15.$$

utilizing 6.6.11 and factoring:

$$P_\phi = 2K\Delta T_j \left[\frac{\Delta T_j \Lambda}{T_{c_j}} + \frac{\Delta T_j \Lambda^2}{\Delta T_{j_{max}}} \right] \qquad 6.6.16.$$

with Λ = 1 then equation 6.6.16 reduces to:

$$P_\phi = 2K\Delta T_j \left[\frac{\Delta T_j}{T_{c_j}} + \frac{\Delta T_j}{\Delta T_{j_{max}}} \right] \qquad 6.6.17.$$


THE RATIO OF POWER REQUIRED AT MAXIMUM C.O.P.
TO THE POWER TO OPERATE AT MAXIMUM HEAT PUMP RATE
AS A FUNCTION OF $\Delta T_j / \Delta T_{max\,j}$
THE PARAMETER IS : $\Delta T_j / T_{cj}$
Fig. 6.6.2.
$\Delta T_j / T_{cj}$
.1
.5
RATIO: POWER ϕ / POWER Q
$\Delta T_j / \Delta T_{max\,j}$
0
.1
.2
.3
.4
.5
.6
.7
.8
.9
1.0

Combining equation 6.6.17 and equation 6.5.4.17 to form a dimensionless power ratio, expressable as:

$$\frac{P_\phi}{P_Q} = \frac{\left[\frac{\Delta T_j}{T_{c_j}} + \frac{\Delta T_j}{\Delta T_{j\,max}}\right]}{\left[1 + \frac{\Delta T_j}{T_{c_j}}\right]} \qquad 6.6.18.$$

Figure 6.6.2 shows the power ratio P_ϕ / P_Q as a function of $\Delta T_j / \Delta T_{j\,max}$ with $\Delta T_j / T_{c_j}$ a variable parameter.

For the condition of $\Delta T_j \rightarrow \Delta T_{j\,max}$ the power ratio $\longrightarrow$ unity. The maximum C.O.P. can be expressed by equation 6.6.12 and equation 6.6.16 resulting:

$$C.O.P._{max} = \frac{2K\Delta T_j \left[2 - \frac{\Lambda \Delta T_j}{\Delta T_{j\,max}} - \frac{1}{\Lambda}\right]}{4\Lambda K \Delta T_j \left[\frac{\Delta T_j}{T_{c_j}} + \frac{\Delta T_j \Lambda}{\Delta T_{j\,max}}\right]} \qquad 6.6.19.$$

for $\Lambda = 1$ then equation 6.6.19 reduces to:

$$C.O.P._{max} = \frac{\left[1 - \frac{\Delta T_j}{\Delta T_{j\,max}}\right]}{2\left[\frac{\Delta T_j}{T_{c_j}} + \frac{\Delta T_j}{\Delta T_{j\,max}}\right]} \qquad 6.6.20.$$

Appendix F indicates that the right hand side may be transposed by an identity.

$$C.O.P._{max} = \frac{\Delta T_{j\,max}}{2\Delta T_j}\left[1 - \frac{\Delta T_j}{\Delta T_{j\,max}}\right]\left[1 - \frac{\Delta T_j}{T_{h_j}}\right]\left[\frac{1}{1 + \frac{\Delta T_{j\,max} - \Delta T_j}{T_{h_j}}}\right] \qquad 6.6.20.$$

The last term in the right side will be called the

RECIPROCAL VALUE AS A FUNCTION OF $\Delta T_{maxj}/T_{hj}$

THE PARAMETER IS : $\Delta T_j/T_{hj}$

Fig. 6.6.3

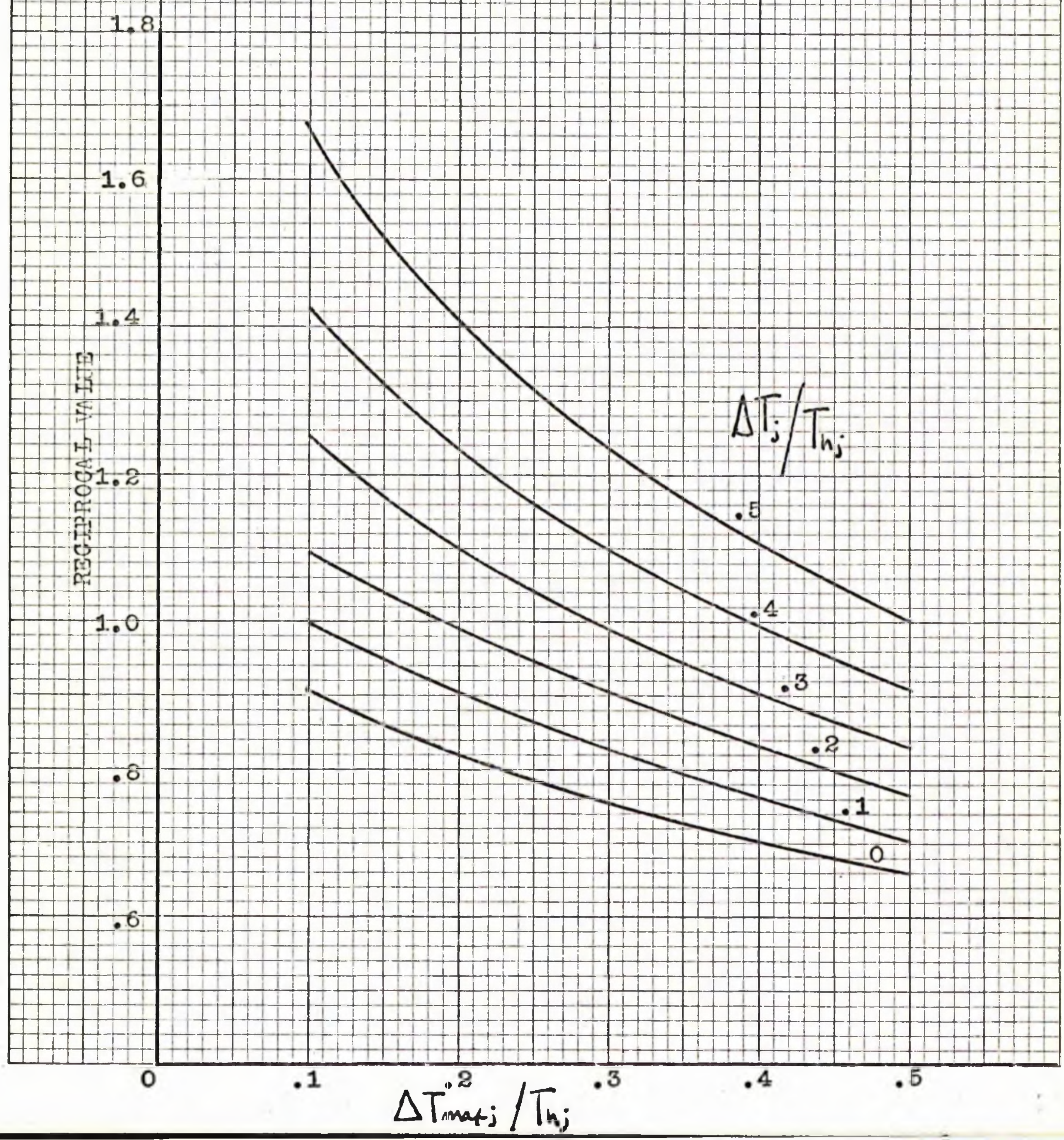

reciprocal value. Figure 6.6.3 shows the reciprocal value as a function of $\Delta T_{j_{max}} / T_{h_j}$ with $\Delta T_j / T_{h_j}$ a variable parameter. Neglecting the last term (i.e. = 1) equation 6.6.20 reduces to:

$$C.O.P._{max} = \frac{\Delta T_{j_{max}}}{2\Delta T_j}\left[1 - \frac{\Delta T_j}{\Delta T_{j_{max}}}\right]\left[1 - \frac{\Delta T_j}{T_{h_j}}\right] \qquad 6.6.21.$$

Equation 6.5.5.1 (C.O.P.$_Q$) can be transposed by an identity derived in Appendix H. The C.O.P. when the current has been maximized for the heat pump rate can be expressed as:

$$C.O.P._Q = \frac{1}{2}\left[1 - \frac{\Delta T_j}{\Delta T_{j_{max}}}\right]\left[1 - \frac{\Delta T_j}{T_{h_j}}\right] \qquad 6.6.22.$$

Equation 6.6.21 and equation 6.6.22 can be combined to form:

$$C.O.P._{max} = \frac{\Delta T_{j_{max}} \times C.O.P._Q}{\Delta T_j} \qquad 6.6.23.$$

Repeating equation 6.6.10 for comparison:

$$I_\phi = \frac{\Delta T_j}{\Delta T_{j_{max}}} I_Q \qquad 6.6.10.$$

The resulting relationship (equation 6.6.23) is approximate by virtue of Λ and the reciprocal value being equal to unity.

6.7. Operational Performance Parameters.

In the previous sections performance equations have been developed with current as a controllable variable. A current dimensionless parameter is introduced in this section in order to facilitate a general engineering approach. The current dimensionless parameter is defined as the ratio of the actual operating current (I) to the current required to operate at maximum heat pump rate (I_Q). This can be expressed as

$$\Theta = \frac{I}{I_Q} \qquad 6.7.1.$$

where:

$$I_Q = \frac{\alpha_{np} T_{cj}}{R} \qquad 6.5.4.1.$$

The heat pump rate (Q_s) is:

$$Q_s = T_{cj} I \alpha_{np} - \frac{1}{2} I^2 R - K \Delta T_j \qquad 6.4.3.$$

Expressing the maximum junction temperature difference in terms of equation 6.5.4.1 results;

$$T_{cj} \alpha_{np} = \frac{2K \Delta T_{j\,max}}{I_Q} \qquad 6.7.2.$$

and from equation 6.5.4.1

$$R = \frac{\alpha_{np} T_{cj}}{I_Q} \qquad 6.7.3.$$

Substituting equation 6.7.2 and 6.7.3 into equation 6.4.3 results:

$$Q_s = K\Delta T_{j_{max}}\left[\frac{2I}{I_Q} - \frac{I^2}{I_Q^2} - \frac{\Delta T_j}{\Delta T_{j_{max}}}\right] \tag{6.7.4.}$$

Introducing:

$$\theta = I / I_Q \tag{6.7.1.}$$

then:

$$Q_s = K\Delta T_{j_{max}}\left[2\theta - \theta^2 - \frac{\Delta T_j}{\Delta T_{j_{max}}}\right] \tag{6.7.5.}$$

Figure 6.7.1 shows the heat pump rate as a function of the dimensionless current ratio (θ) with (ΔT_j) a variable parameter. The C.O.P. can be expressed in a form similar to equation 6.7.5 by the following approach:

The power required from equation 6.4.7 and 6.4.8 can be expressed as:

$$P = I^2R + I\alpha_{mp}\Delta T_j \tag{6.7.6.}$$

Substituting equation 6.7.3 into equation 6.7.6 and introducing $2K\Delta T_{j_{max}} / 2K\Delta T_{j_{max}}$ into the second term:

$$P = I^2R + \frac{I\alpha_{mp}\Delta T_j\, 2K\Delta T_{j_{max}}}{2K\Delta T_{j_{max}}} \tag{6.7.7.}$$

then:

$$P = 2K\Delta T_{j_{max}}\left[\frac{I^2}{I_Q^2} + \frac{I}{I_Q}\Delta T_j\right] \tag{6.7.8.}$$

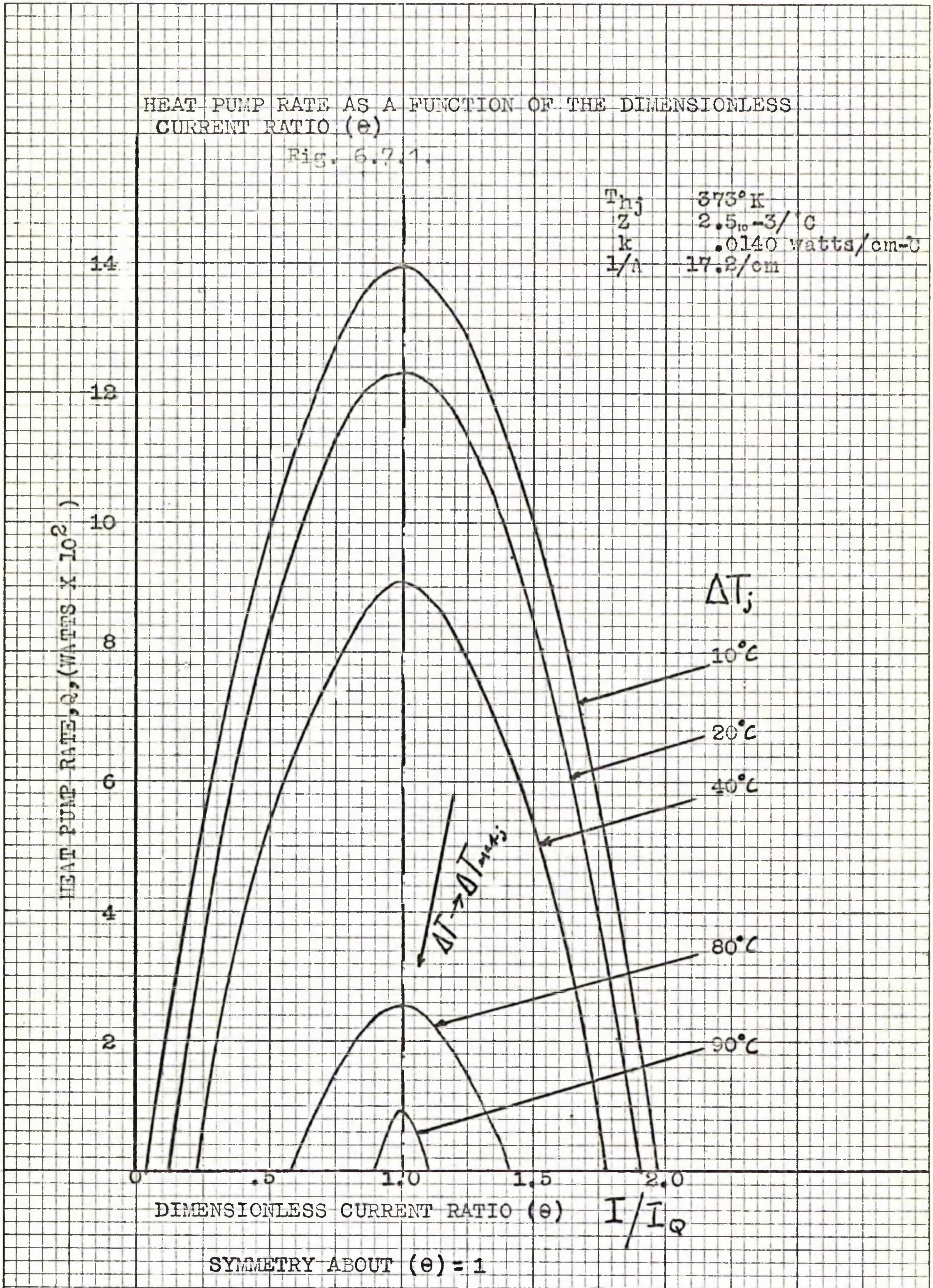
HEAT PUMP RATE AS A FUNCTION OF THE DIMENSIONLESS CURRENT RATIO (θ)
Fig. 6.7.1.
T_{hj} 373°K
Z 2.5$_{10}$-3/°C
k .0140 watts/cm-C
1/A 17.2/cm
14
12
10
8
6
4
2
HEAT PUMP RATE, Q, (WATTS X 10^2)
ΔT$_j$
10°C
20°C
40°C
80°C
90°C
ΔT → ΔT$_{max_j}$
0
.5
1.0
1.5
2.0
DIMENSIONLESS CURRENT RATIO (θ) I/I$_Q$
SYMMETRY ABOUT (θ) = 1

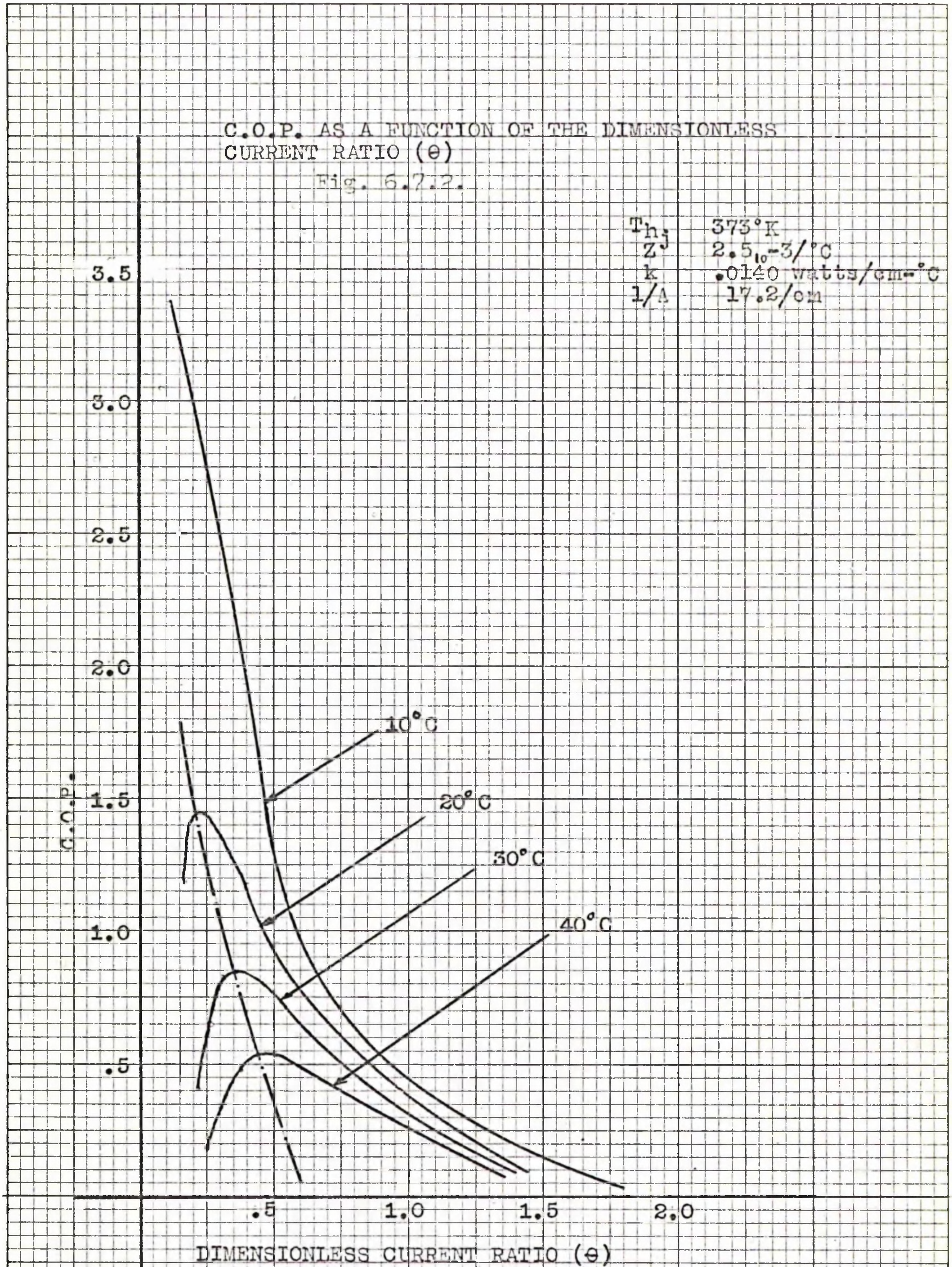
C.O.P. AS A FUNCTION OF THE DIMENSIONLESS CURRENT RATIO (θ)
Fig. 6.7.2.
Th, 373°K
Z 2.5₁₀-3/°C
k .0140 watts/cm-°C
l/A 17.2/cm
10°C
20°C
30°C
40°C
C.O.P.
3.5
3.0
2.5
2.0
1.5
1.0
.5
.5
1.0
1.5
2.0
DIMENSIONLESS CURRENT RATIO (θ)

Substituting $\theta = I/I_Q$ 6.7.1.

results :

$$P = 2K\Delta T_{j_{max}}\left[\theta^2 + \theta\,\Delta T_j\right] \qquad 6.7.9.$$

then by equation 6.4.1:

$$C.O.P. = \frac{\left[2\theta - \theta^2 - \frac{\Delta T_j}{\Delta T_{j\,max}}\right]}{2\left[\theta^2 + \theta\,\Delta T_j\right]} \qquad 6.7.10.$$

Appendix F indicates that equation 6.7.10 can be used as a basic equation for determining equation 6.6.19 (6.6.20). Figure 6.7.2 shows the C.O.P. as a function of the dimensionless current ratio (θ) with ΔT_j a variable parameter. Equation 6.6.10 indicates (Λ = 1) that for a ΔT_j = 40°C and a $\Delta T_{j\,max} \simeq$ 90°C ($\Delta T_{j\,max} = 0.5\,T_{c_j}^2 Z$)* the maximum C.O.P. occurs at $\theta(I_\phi/I_Q) \cong .444$ which corresponds to graphical display from equation 6.7.10. Figure 6.7.1 and figure 6.7.2 may be employed to determine figure 6.7.3

* figure 6.5.6.1.

Figure 6.7.4 is a sketch of the basic information appearing in figure 6.7.3. The heat pump rate (Q_5) is shown as a function of the C.O.P. for a specific temperature difference (ΔT_j). The dimensionless current ratio (θ) does not appear explicity but varies along the curve.

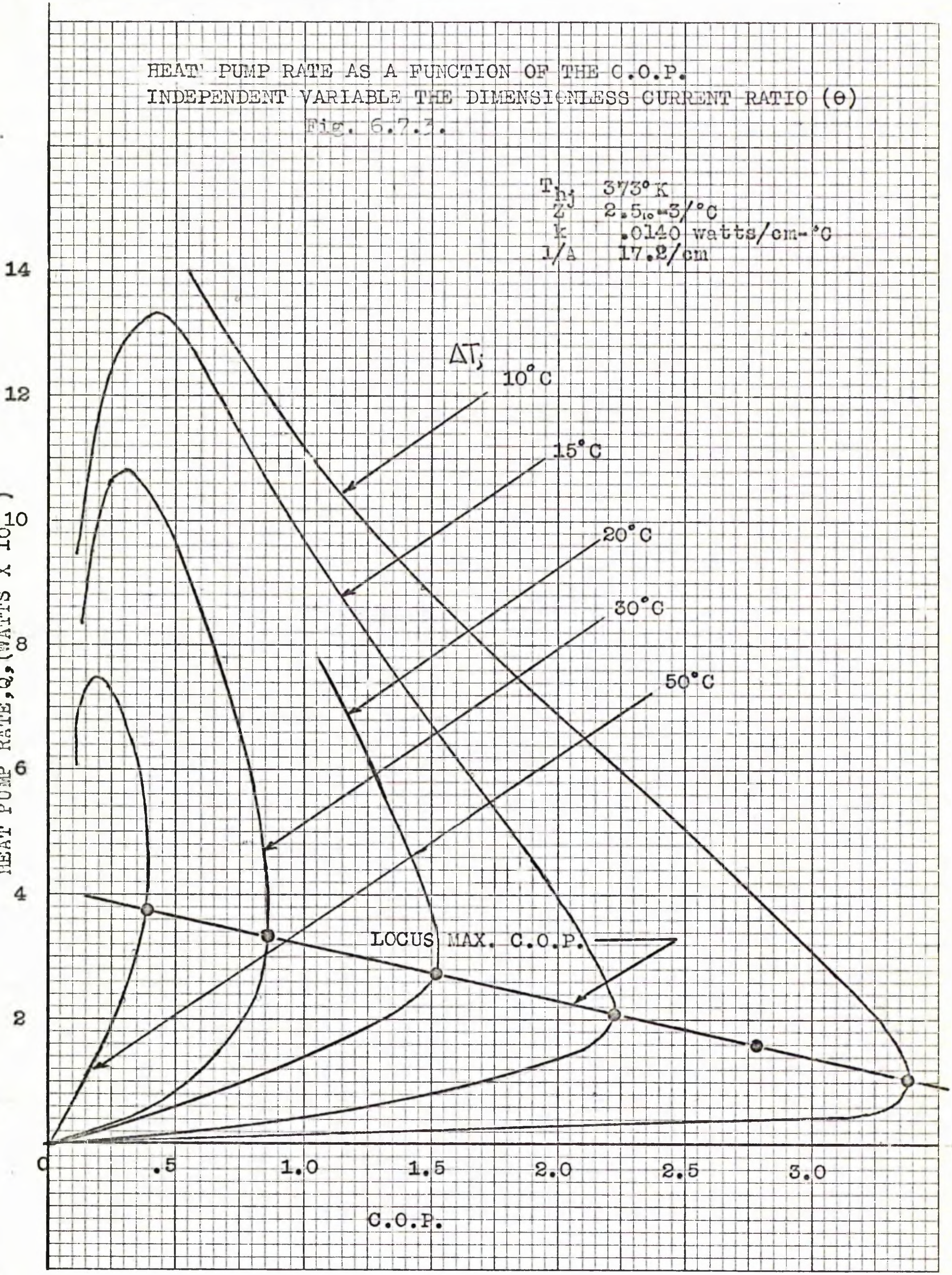

HEAT PUMP RATE AS A FUNCTION OF THE C.O.P.
INDEPENDENT VARIABLE THE DIMENSIONLESS CURRENT RATIO (θ)
Fig. 6.7.3.
T hj 373° K
Z 2.5₁₀-3/°C
k .0140 watts/cm-°C
l/A 17.2/cm
ΔTj
10°C
15°C
20°C
30°C
50°C
LOCUS MAX. C.O.P.
HEAT PUMP RATE, Q, (WATTS X 10²)
14
12
10
8
6
4
2
0
.5
1.0
1.5
2.0
2.5
3.0
C.O.P.

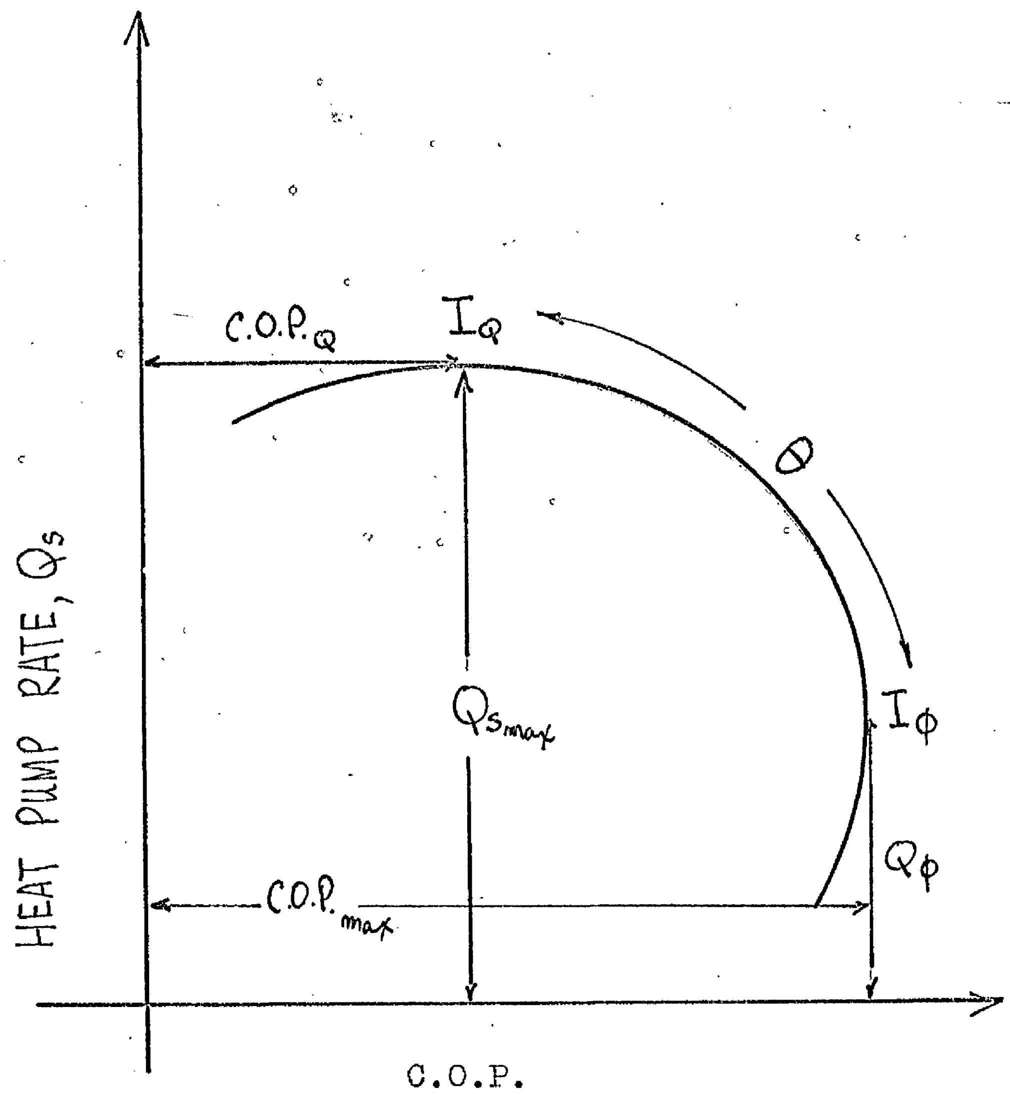

Figure 6.7.4.

Heat Pump Rate as a function of the C.O.P.

The following performance equations were derived in the previous sections; with current as an operational parameter. The symbol $\cong$ will denote that suitable approximations were employed.

(a) $Q_{s_{max}}$, heat pump rate maximum

$$Q_{s_{max}} = K \Delta T_{j_{max}} \left[1 - \frac{\Delta T_j}{\Delta T_{j_{max}}} \right] \qquad 6.5.4.8.$$

(b) C.O.P.$_Q$, C.O.P. at maximum heat pump rate

$$C.O.P._Q = \frac{1}{2} \left[1 - \frac{\Delta T_j}{\Delta T_{j_{max}}} \right] \left[1 - \frac{\Delta T_j}{T_{h_j}} \right] \qquad 6.6.22.$$

neglecting

$$\left[1 - \frac{\Delta T_j}{T_{h_j}} \right] \longrightarrow 1 \qquad 6.7.11.$$

then:

$$C.O.P._Q \cong \frac{1}{2} \left[1 - \frac{\Delta T_j}{\Delta T_{j_{max}}} \right] \qquad 6.7.12.$$

(c) C.O.P.$_\phi$, maximum C.O.P.

$$C.O.P._\phi \cong \frac{1}{2} \frac{\Delta T_{j_{max}}}{\Delta T_j} \left[1 - \frac{\Delta T_j}{\Delta T_{j_{max}}} \right] \left[1 - \frac{\Delta T_j}{T_{h_j}} \right] \qquad 6.6.21.$$

(for Λ and reciprocal value of unity)

employing equation 6.7.11 then:

$$C.O.P._\phi \cong \frac{1}{2} \left[\frac{\Delta T_{j_{max}}}{\Delta T_j} - 1 \right] \qquad 6.7.13.$$

and

$$C.O.P._\phi \cong \frac{\Delta T_{j_{max}}}{\Delta T_j} \times C.O.P._Q \qquad 6.6.23.$$

HEAT PUMP RATE RATIO Q/Q_{max} AS A FUNCTION OF THE DIMENSIONLESS CURRENT RATIO (θ)

Fig. 6.7.5.

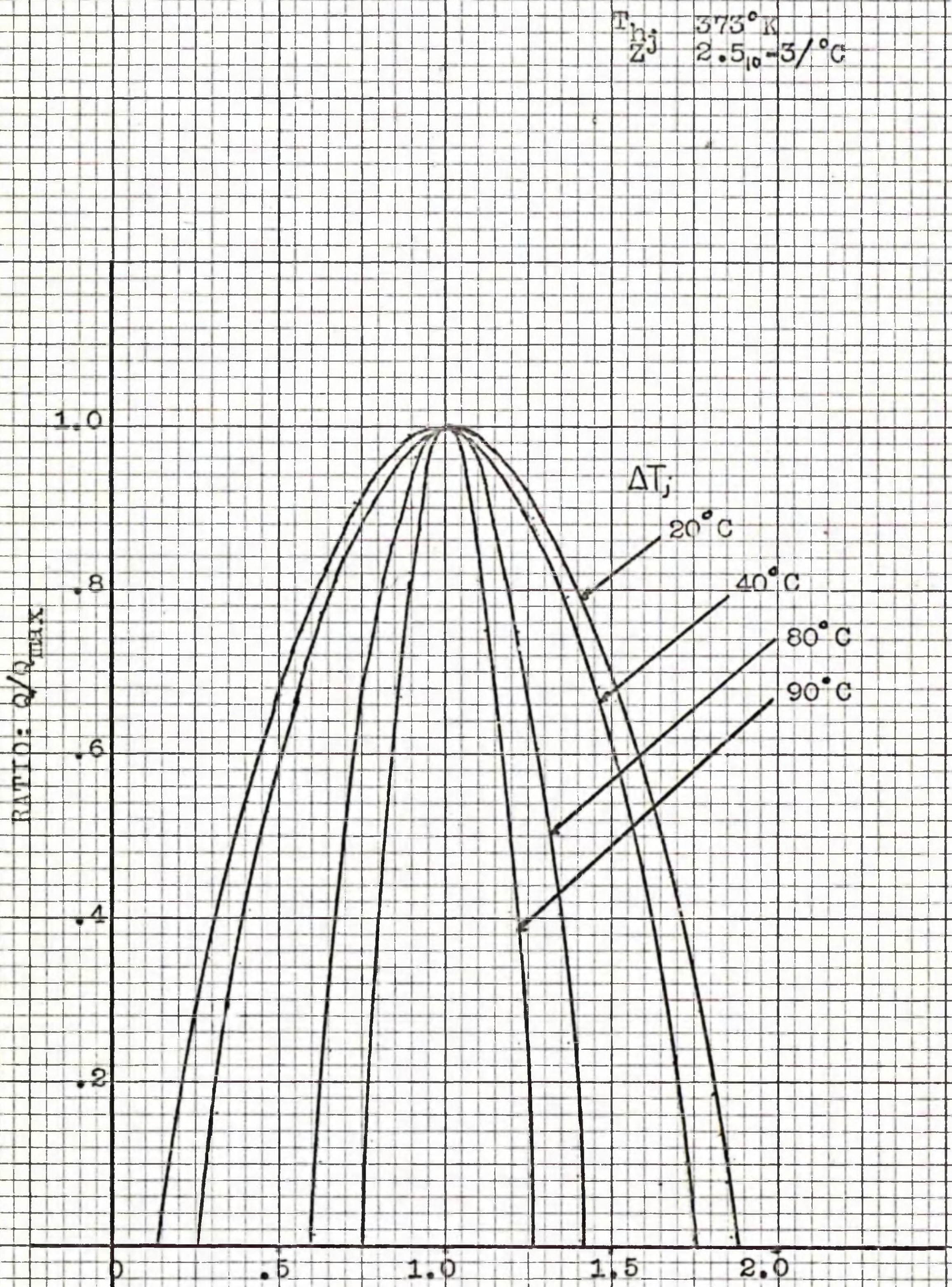

(d) $Q_{s\phi}$ heat pump rate optimized for maximum C.O.P. for $\Lambda = 1$.

$$Q_{s\phi} \cong K \Delta T_j \left[1 - \frac{\Delta T_j}{\Delta T_{j\,max}} \right] \qquad 6.6.13.$$

and

$$Q_{s\phi} \cong \frac{\Delta T_j}{\Delta T_{j\,max}} \times Q_{s\,max} \qquad 6.6.14.$$

(e) I_Q current maximizing heat pump rate

$$I_Q = \frac{\alpha_{np} T_{c_j}}{R} \qquad 6.5.4.1.$$

(f) I_ϕ current maximizing C.O.P. for $\Lambda = 1$

$$I_\phi \cong \frac{\Delta T_j}{\Delta T_{j\,max}} \; I_Q \qquad 6.6.10.$$

It is advantageous to present four performance ratios based on the approximate relations intoduced in section 6.6.

The ratio of $Q_{s\,max}$: C.O.P.$_Q$ can be expressed as:

$$\frac{Q_{s\,max}}{C.O.P._Q} \cong 2K\Delta T_{j\,max} \cong \frac{\alpha_{np}^2}{R} \qquad 6.7.14.$$

The ratio of heat pump rate at maximum C.O.P:

C.O.P.$_{max}$ can be expressed as:

$$\frac{Q_\phi}{C.O.P._{max}} \cong \frac{2K\Delta T_j \left[1 - \frac{\Delta T_j}{\Delta T_{j\,max}} \right]}{\left[\frac{\Delta T_{j\,max}}{\Delta T_j} - 1 \right]} \qquad 6.7.15.$$

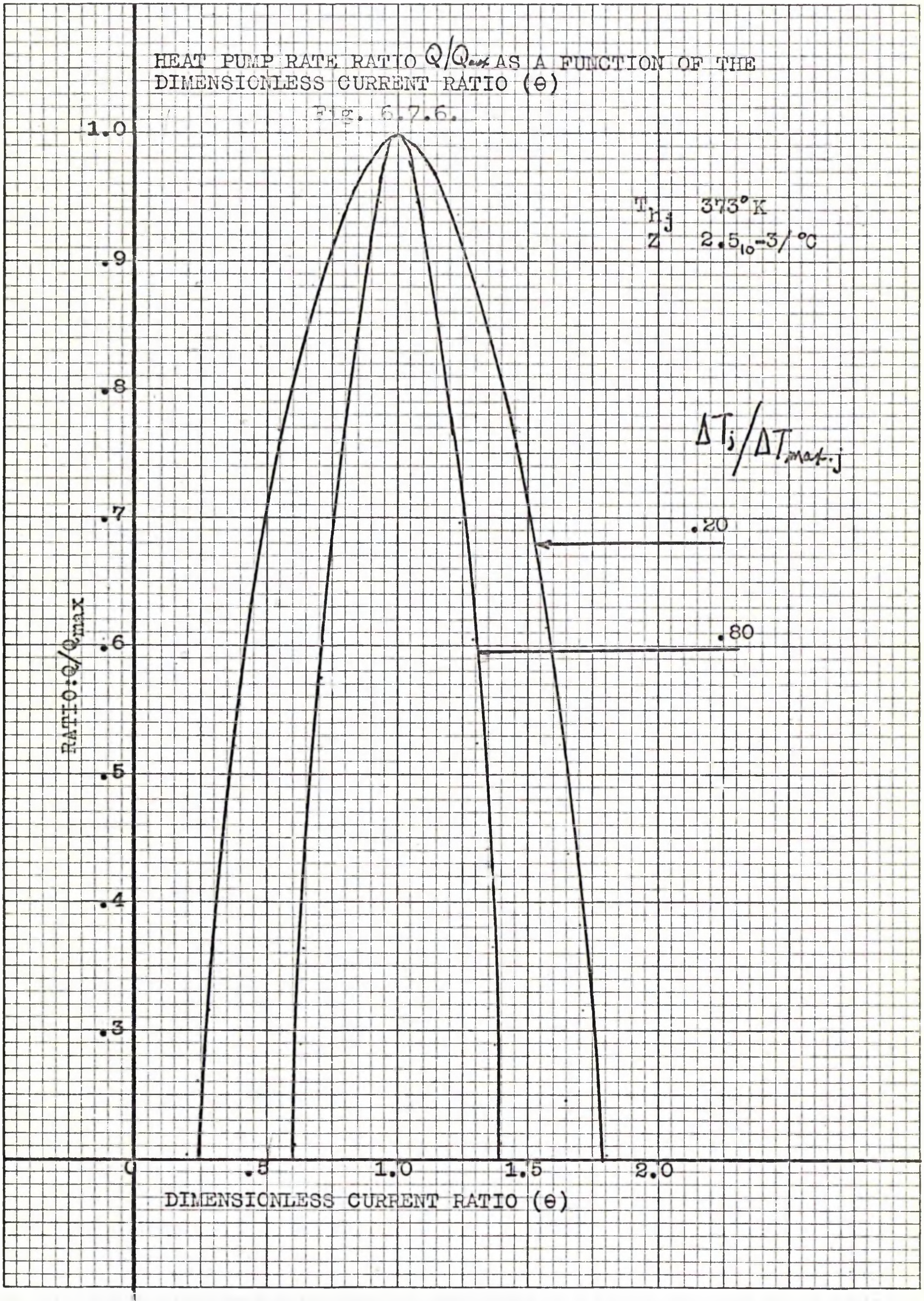
HEAT PUMP RATE RATIO Q/Qmax AS A FUNCTION OF THE DIMENSIONLESS CURRENT RATIO (θ)
Fig. 6.7.6.
1.0
.9
.8
.7
.6
.5
.4
.3
RATIO:Q/Qmax
Thj 373°K
Z 2.5 10-3/°C
ΔTj/ΔTmax.j
.20
.80
0
.5
1.0
1.5
2.0
DIMENSIONLESS CURRENT RATIO (θ)

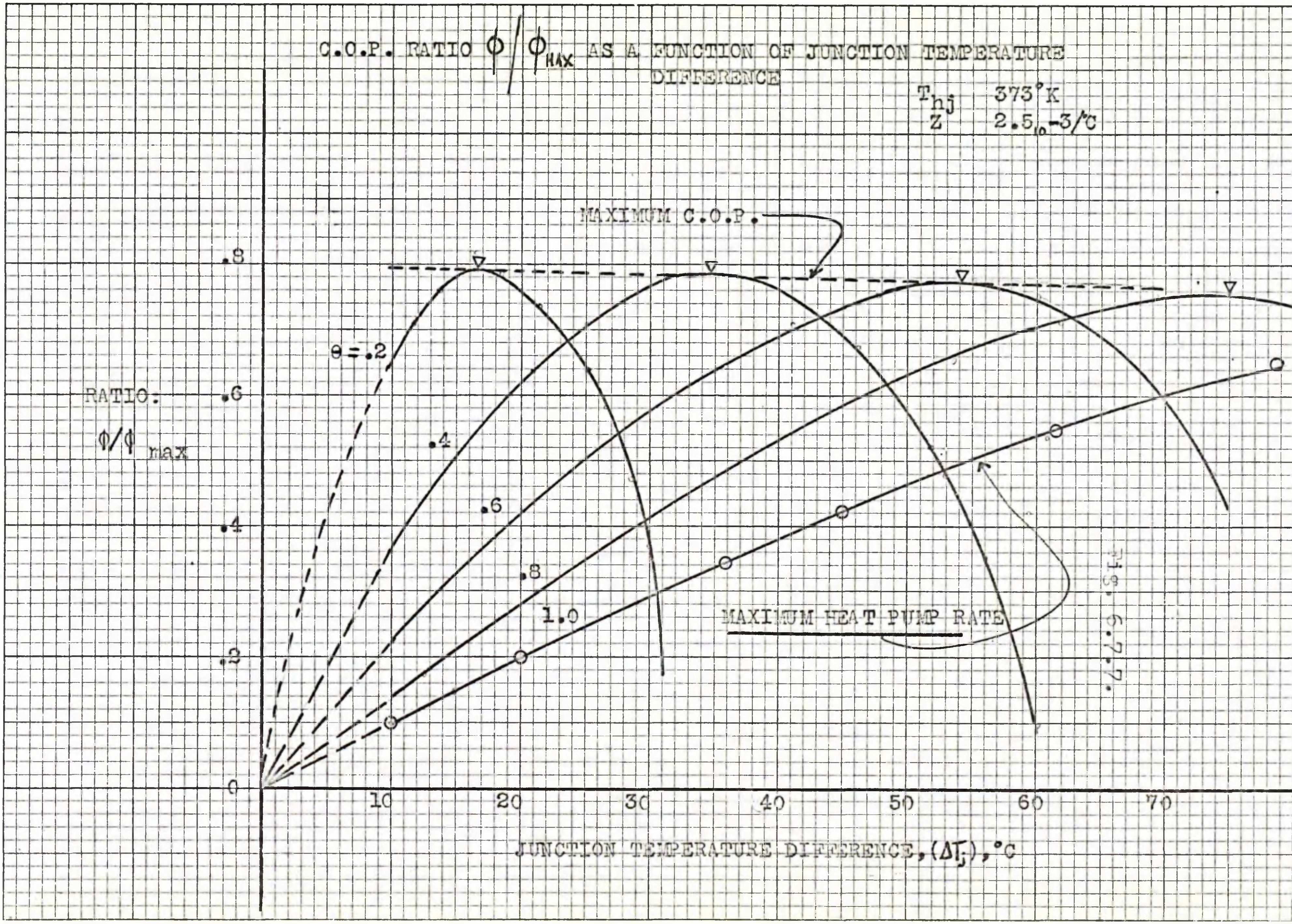

C.O.P. RATIO ϕ / ϕ_{MAX} AS A FUNCTION OF JUNCTION TEMPERATURE DIFFERENCE
T_{hj} 373°K
Z 2.5_{10}-3/°C
MAXIMUM C.O.P.
θ = .2
.4
.6
.8
1.0
MAXIMUM HEAT PUMP RATE
RATIO: ϕ/ϕ_{max}
.8
.6
.4
.2
0
10
20
30
40
50
60
70
JUNCTION TEMPERATURE DIFFERENCE, (ΔT_j), °C

Fig. 6.7.7.

The heat pump rate ratio can be expressed as:

$$\frac{Q_s}{Q_{s_{max}}} = \frac{\left[2\theta - \theta^2 - \frac{\Delta T_j}{\Delta T_{j_{max}}} \right]}{\left[1 - \frac{\Delta T_j}{\Delta T_{j_{max}}} \right]} \qquad 6.7.16.$$

The numerator is equation 6.7.5 and the denominatr equation 6.5.4.8. Equation 6.7.16 is exact and therefore no approximations are utilized. Figure 6.7.5 shows $(Q_s / Q_{s_{max}})$ as a function of the dimensionless current ratio (θ) for variation in the junction temperature difference. Figure 6.7.5 may be modified by introducing the variable $\Delta T_j / \Delta T_{j_{max}}$ as a replacement for (ΔT_j)

resulting in figure 6.7.6.

The C.O.P. performance ratio is expressed as:

$$\frac{C.O.P.}{C.O.P._{max}} \cong \frac{\left[2\theta - \theta^2 - \frac{\Delta T_j}{\Delta T_{j_{max}}} \right]}{\left[\theta^2 + \theta \frac{\Delta T_j}{T_{c_j}} \right] \left[\frac{\Delta T_{j_{max}}}{\Delta T_j} - 1 \right]} \qquad 6.7.17.$$

The approximation is introduced into equation 6.7.17 by C.O.P.$_{max}$ (equation 6.7.13). Figure 6.7.7 illustrates the C.O.P. performance ratio as a function of the junction temperature difference for variation in the dimensionless current ratio (θ). Figure 6.7.8 and figure 6.7.9 illustratesthe parameter ($Q_s / K \Delta T_{j_{max}}$) (equation 6.7.5) and the C.O.P. (equation 6.7.10) as a function of the dimensionless current parameter (θ) with parameter $\Delta T_j / \Delta T_{j_{max}} = .20, .02$ respectfully. Each figure

OPERATIONAL PARAMETERS ASA FUNCTION OF THE DIMENSIONLESS CURRENT RATIO (θ)

Fig. 6.2.3.

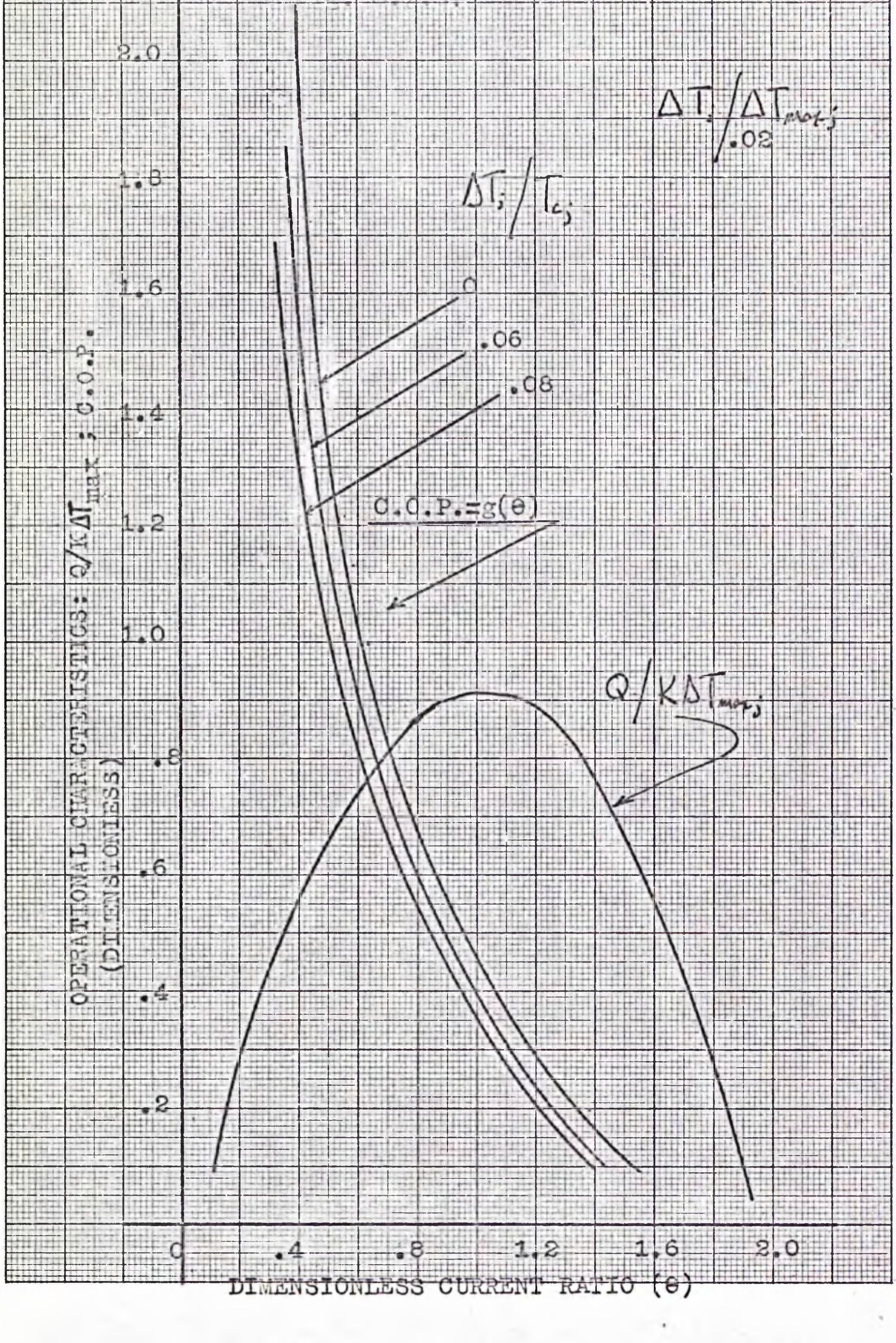

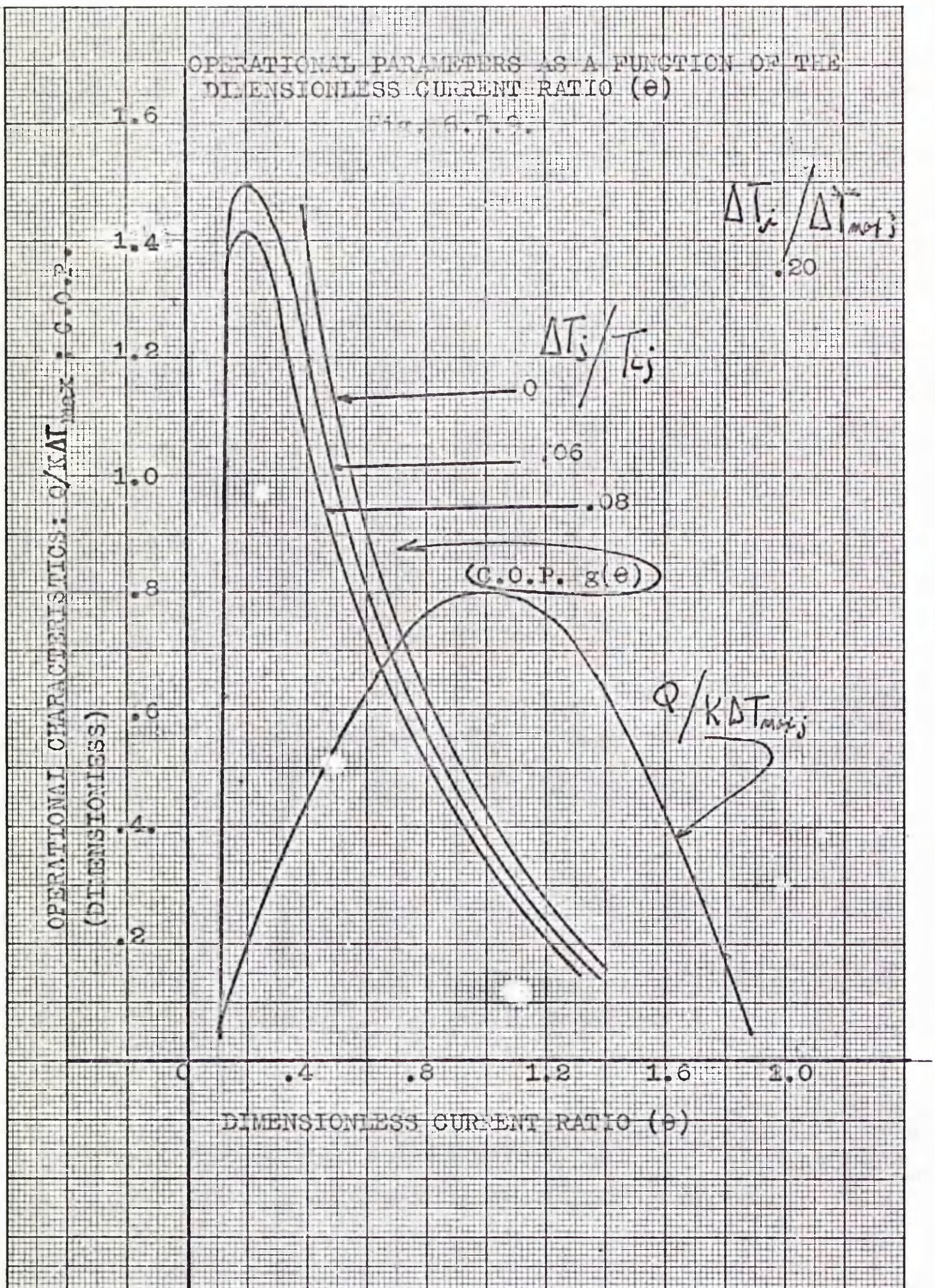

OPERATIONAL PARAMETERS AS A FUNCTION OF THE DIMENSIONLESS CURRENT RATIO (θ)
OPERATIONAL CHARACTERISTICS: Q/KΔT max, C.O.P.
(DIMENSIONLESS)
1.6
1.4
1.2
1.0
.8
.6
.4
.2
0
.4
.8
1.2
1.6
2.0
DIMENSIONLESS CURRENT RATIO (θ)
ΔTj/ΔTmaxj
.20
ΔTj/TLj
0
.06
.08
(C.O.P. g(θ))
Q/KΔTmaxj

includes a family of curves for $0 \leq \frac{\Delta T_j}{T_{cj}} \leq .08$ The peak of ($K \Delta T_{j\,max}$) occurs at $\Theta = 1$ which is in accord with equation 6.7.5. The maximum C.O.P. occurs at a dimensionless current ratio less than required for maximizing ($K \Delta T_{j\,max}$). Figure 6.7.10 and figure 6.7.11 shows the C.O.P. as a function of $(Q_s / K \Delta T_{j\,max})$ The graphical presentation appears as a convenient format for reviewing the general thermoelectric couple performance. The lines radiating from the origin (0,0) are the dimensionless current ratios, while the loops are for constant $\Delta T_j / \Delta T_{j\,max}$ The dashed line (figure 6.7.10) is the locus of the maximum C.O.P. function. The maximum C.O.P. is expressible as:

$$C.O.P._{max} \cong .5 \times \left[\frac{\Delta T_{j\,max}}{\Delta T_j} - 1 \right] \qquad 6.7.13.$$

and occurs at:

$$\Theta \cong \Delta T_j / \Delta T_{j\,max}$$

The maximum heat pump rate ($Q_{s\,max}$) occurs at $\Theta = 1$. The power required ratio can be expressed by equation 6.5.4.17 for P_Q as:

$$P_Q = 2K \Delta T_{j\,max} \left[1 + \frac{\Delta T_j}{T_{cj}} \right] \qquad 6.5.4.17.$$

and

$$P_\phi \cong 2K \Delta T_j \left[\frac{\Delta T_j}{T_{cj}} + \frac{\Delta T_j}{\Delta T_{j\,max}} \right] \qquad 6.6.17.$$

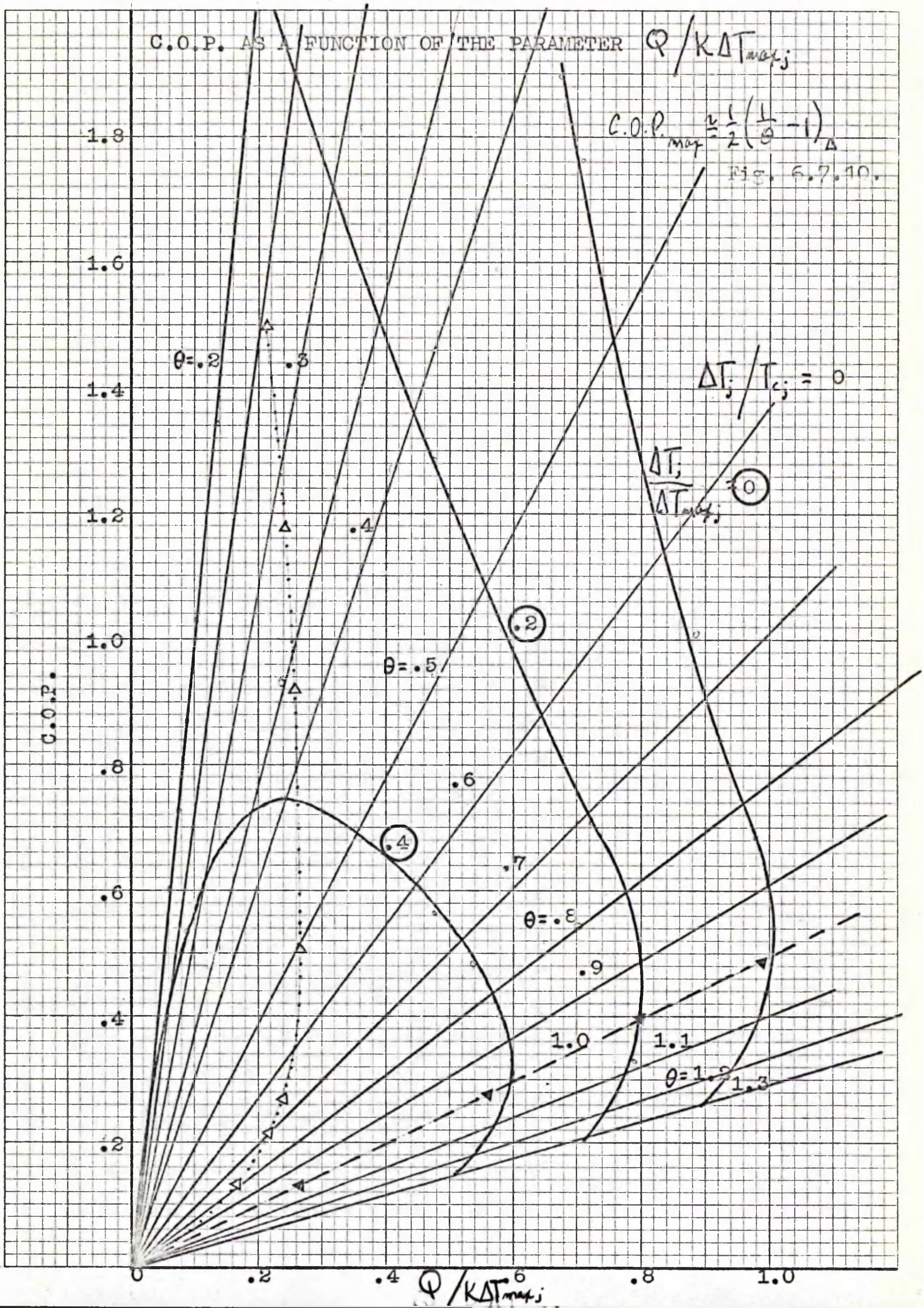
C.O.P. AS A FUNCTION OF THE PARAMETER $Q/K\Delta T_{max_j}$
$C.O.P._{max} \simeq \frac{1}{2}\left(\frac{1}{\theta}-1\right)_{\Delta}$
Fig. 6.7.10.
$\Delta T_j / T_{c_j} = 0$
$\frac{\Delta T_j}{\Delta T_{max_j}} = 0$
.2
.4
θ=.2
.3
.4
θ=.5
.6
.7
θ=.8
.9
1.0
1.1
θ=1.2
1.3
C.O.P.
1.8
1.6
1.4
1.2
1.0
.8
.6
.4
.2
0
.2
.4
.6
.8
1.0
$Q/K\Delta T_{max_j}$

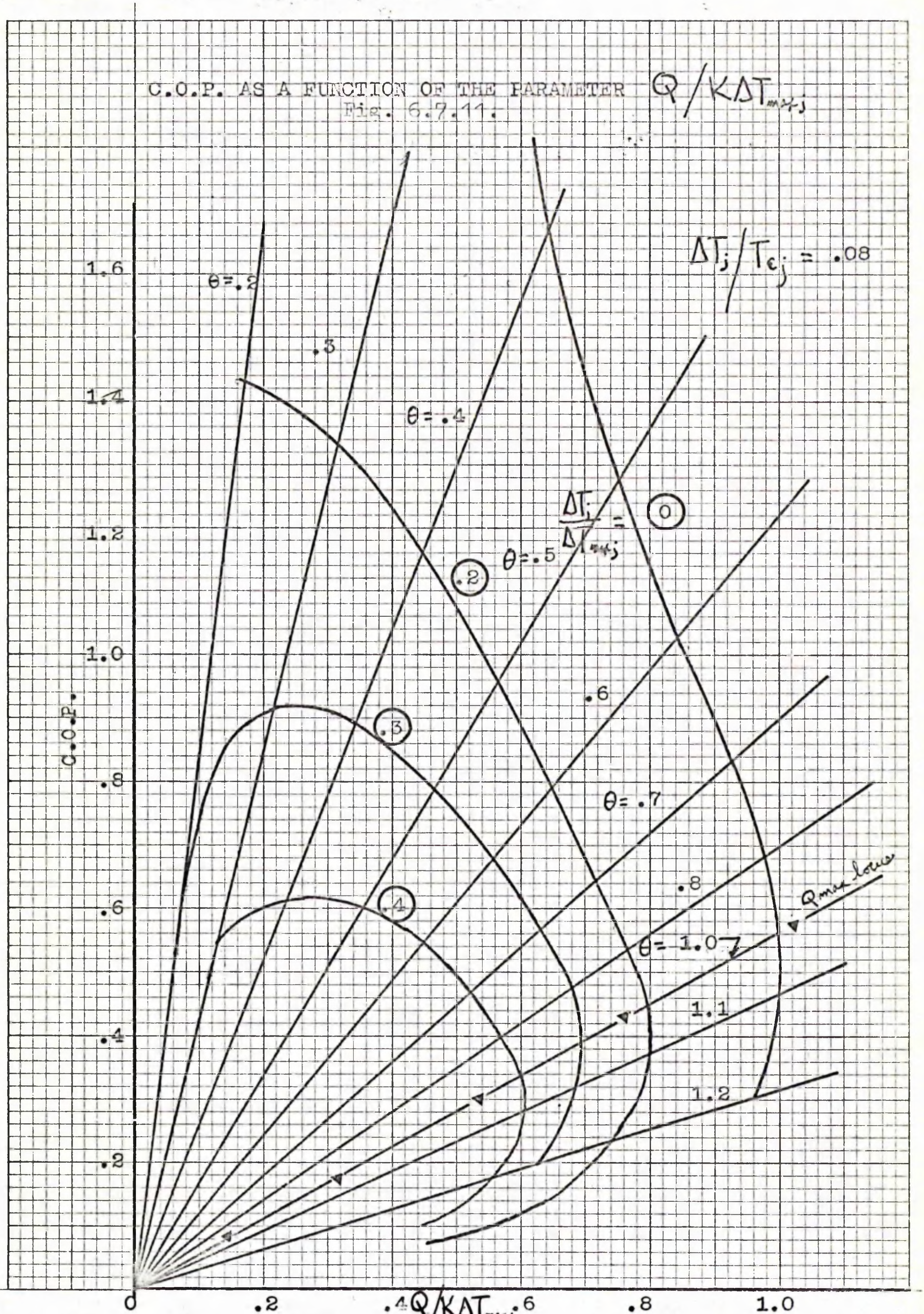
C.O.P. AS A FUNCTION OF THE PARAMETER $Q/K\Delta T_{max_j}$
Fig. 6.7.11.
$\Delta T_j / T_{c_j} = .08$
$\frac{\Delta T_j}{\Delta T_{max_j}} =$ 0
.2
.3
.4
θ=.2
.3
θ=.4
θ=.5
.6
θ=.7
.8
θ=1.0
1.1
1.2
Qmax locus
C.O.P.
1.6
1.4
1.2
1.0
.8
.6
.4
.2
0
.2
.4
.6
.8
1.0
$Q/K\Delta T_{max_j}$

Factoring and rearranging equation 6.6.17 results:

$$P_\phi = 2K\,\Delta T_{j_{max}}\left[\frac{\Delta T_j^{\,2}}{T_{c_j}\,\Delta T_{j_{max}}} + \frac{\Delta T_j}{\Delta T_{j_{max}}^{\,2}}\right] \qquad 6.7.18.$$

Equation 6.7.9 is:

$$P = 2K\,\Delta T_{j_{max}}\left[\theta^2 + \theta\,\Delta T_j\right]$$

Expressing the power ratios as:

$$\frac{P}{P_\phi} = \frac{\left[\theta^2 + \theta\,\Delta T_j\right]}{\left[1 + \frac{\Delta T_j}{T_{c_j}}\right]} \qquad 6.7.19.$$

and

$$\frac{P}{P_\phi} = \frac{\left[\theta^2 + \theta\,\Delta T_j\right]}{\left[\frac{\Delta T_j^{\,2}}{T_{c_j}\,\Delta T_{j_{max}}} + \frac{\Delta T_j}{\Delta T_{j_{max}}^{\,2}}\right]} \qquad 6.7.20.$$

Figure 6.7.12 illustrates the power: power at maximum heat pump rate (equation 6.7.19) as a function of the dimensionless current ratio (θ) with $\Delta T_j / T_{c_j}$ = .80 and .10 as a variable parameter.

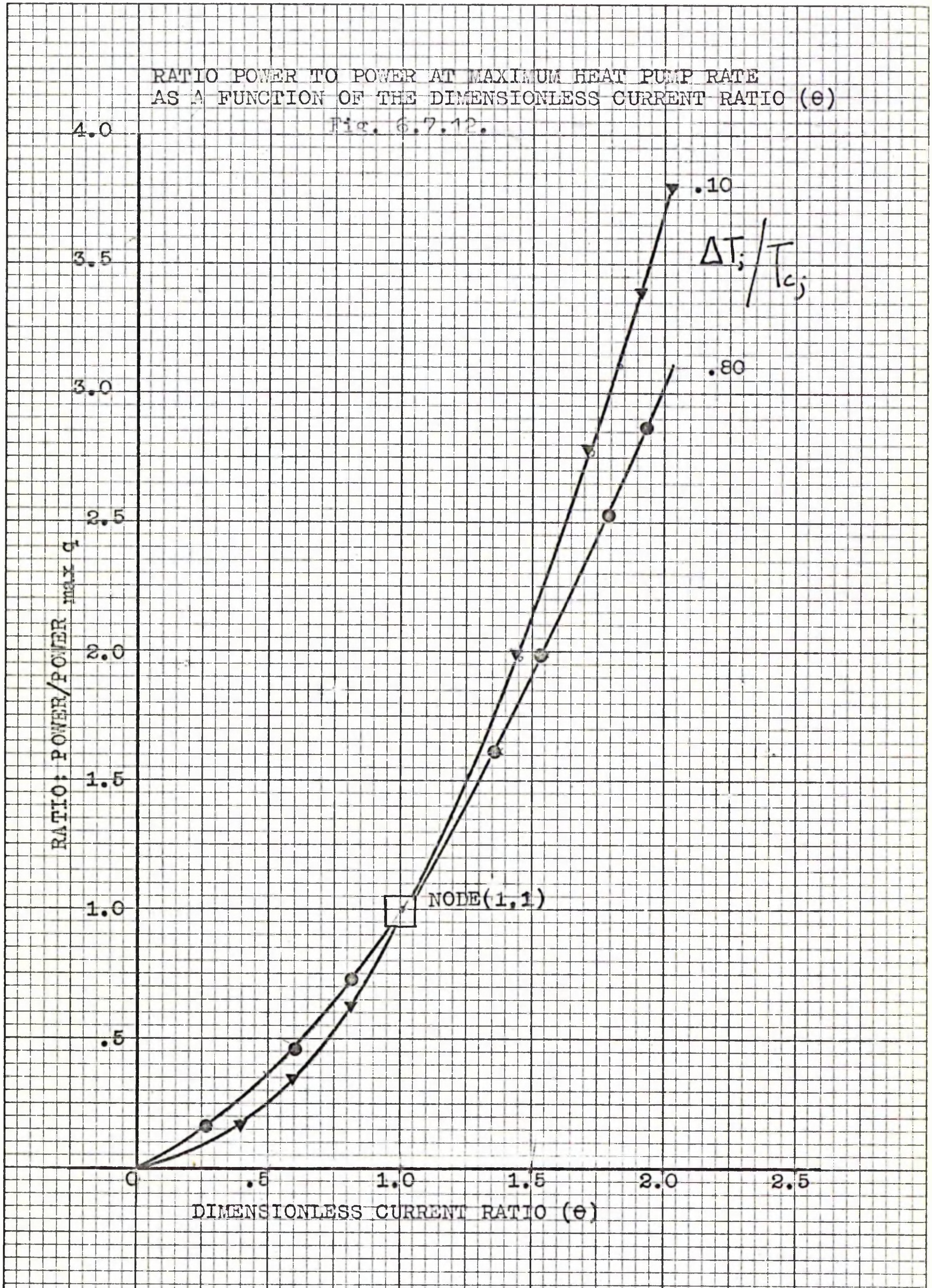
RATIO POWER TO POWER AT MAXIMUM HEAT PUMP RATE
AS A FUNCTION OF THE DIMENSIONLESS CURRENT RATIO (θ)
Fig. 6.7.12.
4.0
3.5
3.0
2.5
2.0
1.5
1.0
.5
0
.5
1.0
1.5
2.0
2.5
.10
.80
ΔTj/Tcj
NODE(1,1)
RATIO: POWER/POWER max q
DIMENSIONLESS CURRENT RATIO (θ)

7.0 QUASI-IDEAL PERFORMANCE.

7.1 General Characteristics.

A thermoelectric module in its simplest form consists of an electrical circuit of several thermoelements in series which are thermally in parallel between two surfaces. In this section the surfaces are assumed to have perfect thermal contact with the heat source ($T_{c\infty}$) and heat sink ($T_{h\infty}$) environment. The additional electrical resistance and shunt thermal conductances introduced when utilizing "real" thermoelectric devices in practical refrigeration can significantly alter the system performance. The expressions derived in section 6.0 representing the level of attainable performance can be used if modifications are introduced into the material definitions. It appears reasonable to include junction resistance, connecting strap resistance for defining an "effective resistance" term. Simarily, conductance from hot to cold plate through the thermal interelement insulation can be factored into an "effective thermal conductance" term. "Effective figure of merit" and "effective maximum junction temperature" can be introduced into the equations of Chapter 6.0, thereby utilizing the previous sections.

The equations appearing in Chapter 6.0 are approximate and in many cases are based on currents that provide maximum heat pump rate or maximum C.O.P. operation. In section 7.2 more accurate analysis are performed using "complete" expressions. The results indicate that the basic concept of using "effective" values as a condition for expressing "real" couple performance is adequate and practical for the present/state of art material.

Mathematical models are developed to determine the feasibility of supporting the thermocouple onto a conducting pedestal (figure 8.2.1). The thermocouple/pedestal configuration introduces an analysis problem that has not been considered in earlier module calculations. The proposed solution employs characteristic dimensionless parameters and thus the solution is applicable in subsequent module analysis. Appendix M contains a complete description of the mathematical evolution and subsequent numerical solution of the pedestal/thermoelement model.

Since the evaluation of various designs is a process of repeated calculations with different parameters in similar equations extensive utilization of the digital computer resulted.

7.1.1 Ripple Effect.

The computer programs developed incorporate the effect of current ripple on system performance. It is frequently desirable to estimate the changes in performance resulting from the degree of power supply filtering or to determine the system burden by an imposed ripple level.

The expressions of section 6.0 can be modified from an idealized ripple-free direct current thermoelectric couple to indicate couple performance for operation where the current has an alternating component. In appendix J the effect of ripple is introduced by a 'ripple form factor'. The ripple form factor is defined as the ratio of the rms value of current to the d.c. component. The wave form of the current ripple is assumed sinusoidal. The resulting relationship between form factor and ripple directly relates system performance to percent ripple. Section 7.3.2. illustrates this form of presentation. From the graphical results of section 7.3.2 ripple becomes relatively more important as the ratio $\Delta T_j / \Delta T_{j\,max}$ increases.

7.1.2 Thermal Impedence Effects.

In chapter 6.0 a major assumption is the condition of perfect thermal contact between the thermoelectric junctions and the surrounding environment. During the operation of a real system the thermoelement junction temperature would not be the same as the corresponding heat sink and heat source temperature. It is the "real" system that this research is primarily seeking to define and solve.

The junction temperature difference (ΔT_j), i.e. the difference between T_{h_j} (hot junction temperature) and T_{c_j} (cold junction temperature) is larger than

the overall (ΔT_{∞})temperature difference. The overall temperature difference between the heat source (T_{c_∞}) and heat sink (T_{h_∞}) is less than the junction temperature difference by the temperature drops on the hot and cold sides respectfully (ΔT_{h_j} , ΔT_{c_j})
The temperature differences on a side of the thermocouple is composed of:

(1) electrical link
(2) electrical insulation
(3) heat exchanger
(4) thermal boundary layer

Figure 7.1.2.1 shows the basic temperatures and indicates a general configuration.

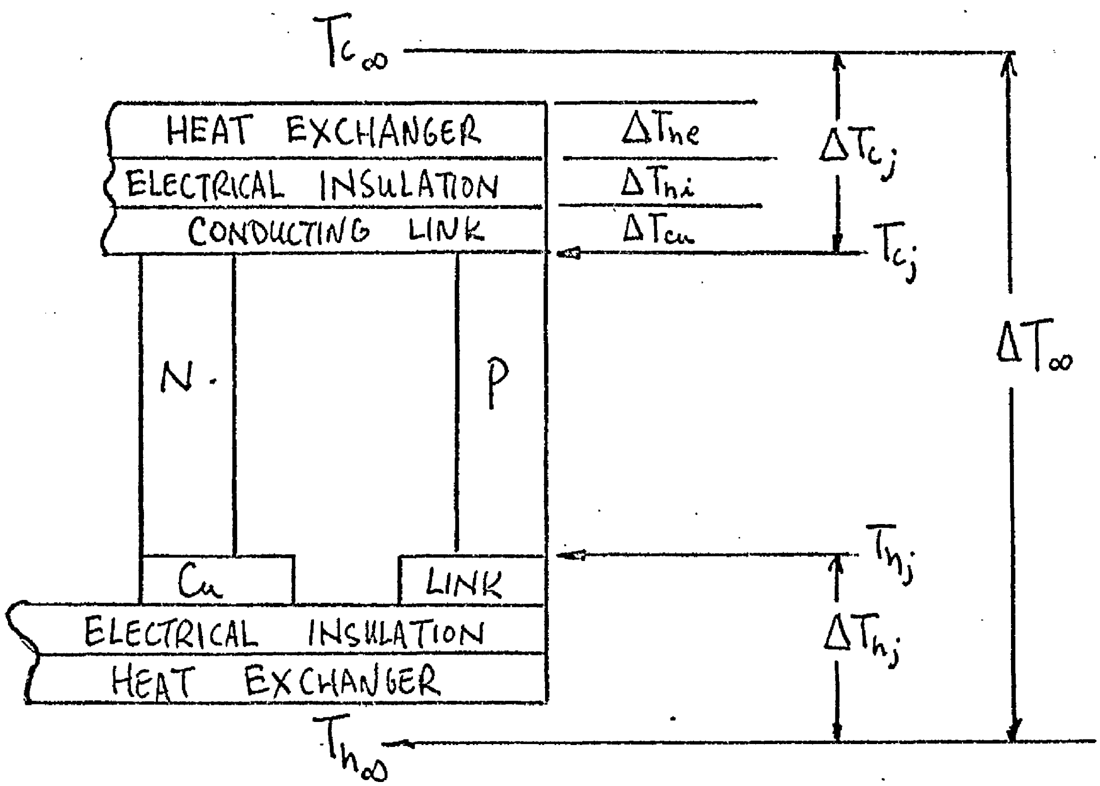

Figure 7.1.2.1.
Thermocouple Temperature Differences.

The effect of thermal impedence can be illustrated by figure 7.1.2.2. The temperature profile excludes discontinuties at the interfaces.

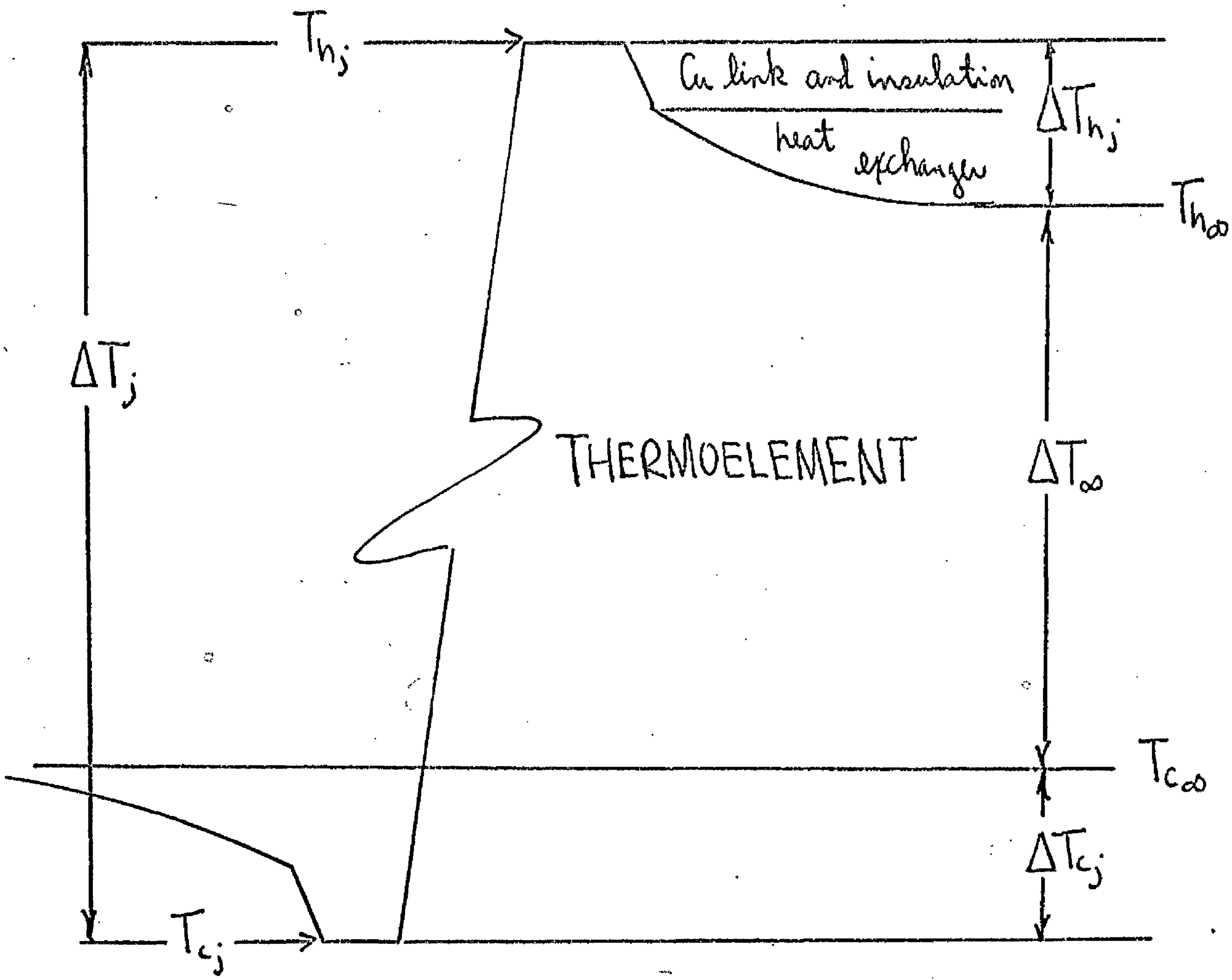

Figure 7.1.2.2.

Temperature Distribution.

7.2 Effectiveness Parameters.

7.2.1 Introduction.

This section contains the equations that describe the operation of the "quasi" ideal thermoelectric couple. The mathematical model includes the modifications to the equation developed in chapter 6.0 by the introduction of "effectiveness" values. In general the equations describing ideal couple performance may be used to describe the performance of a thermoelectric couple with losses, if the terms representing electrical resistance and thermal conductance are suitable modified. The equations (i.e. 6.5.2.18, 6.5.2.13) indicate that the performance of the idealized is independent of the height of the thermo-element. This conclusion results from the exclusion of contact resistance at the junctions. The inclusion of contact resistance(1) transforms the idealized analysis into a practical problem considered in the performance of the "quasi" ideal thermoelectric couple.

7.2.2 Packing Density (ω).

The electrical series resistance resulting in equation 6.5.3.3 neglects the resistance introduced by contact effects and element electrical linkages. In addition to

(1) a representative problem.

the increase in electrical resistance; shunt thermal paths exist between (T_{hj}) the hot junction temperature and the (T_{cj}) cold junction temperature. In this section and in the developed computer programs these effects will be considered.

A module is considered of total area A_T, containing N uniformly spaced couples thus the area associated with each couple is (A_T/N). A portion (A_i) consists of inter-element thermal insulation and the remaining (A_n+A_p) occupied by the n- and p- thermoelement. The packing density (ω) is defined as the fraction of the total module area (A) occupied by the thermal insulation. The packing density is expressable as:

$$\omega \equiv \frac{A_n+A_p}{A_n+A_p+A_i} \qquad 7.2.2.1.$$

assuming(1) (for simplicity in presentation):

$$2A = A_n+A_p \qquad 7.2.2.2.$$

then:

$$A_i = \frac{2A(1-\omega)}{\omega} \qquad 7.2.2.3.$$

(1) This type of assumption is to simplify written expression. The computer programs do not employ this form of limitation.

7.2.3 Effective Thermal Conductance.

The thermal couple conductance can be expressed as:

$$K = \frac{A_m k_m}{l_m} + \frac{A_p k_p}{l_p} \qquad 6.5.3.10.$$

assuming:

$$k = k_m = k_p$$
$$A = A_m = A_p$$
$$l = l_m = l_p$$

The inter-element thermal conductance is:

$$K_\omega = \frac{k_i A_i}{l} \qquad 7.2.3.1.$$

where:

k_i the thermal conductivity of the insulation material, watts/cm - ^oC

K_ω thermal conductance of the insulation material, watts/^oC

The effective thermal conductance is expressible as:

$$K_{EFF} = \frac{k_i A_i}{l_i} + \frac{2kA}{l} \qquad 7.2.3.2.$$

Introducing equation 7.2.2.3 into equation 7.2.3.2 results:

$$K_{EFF} = \frac{k_i 2A(1-\omega)}{l\omega} + \frac{2kA}{l} \qquad 7.2.3.3.$$

Factoring equation 7.2.3.3 results:

$$K_{EFF} = \frac{2kA}{l}\left[1 + \frac{k_i(1-\omega)}{k\omega}\right] \qquad 7.2.3.4.$$

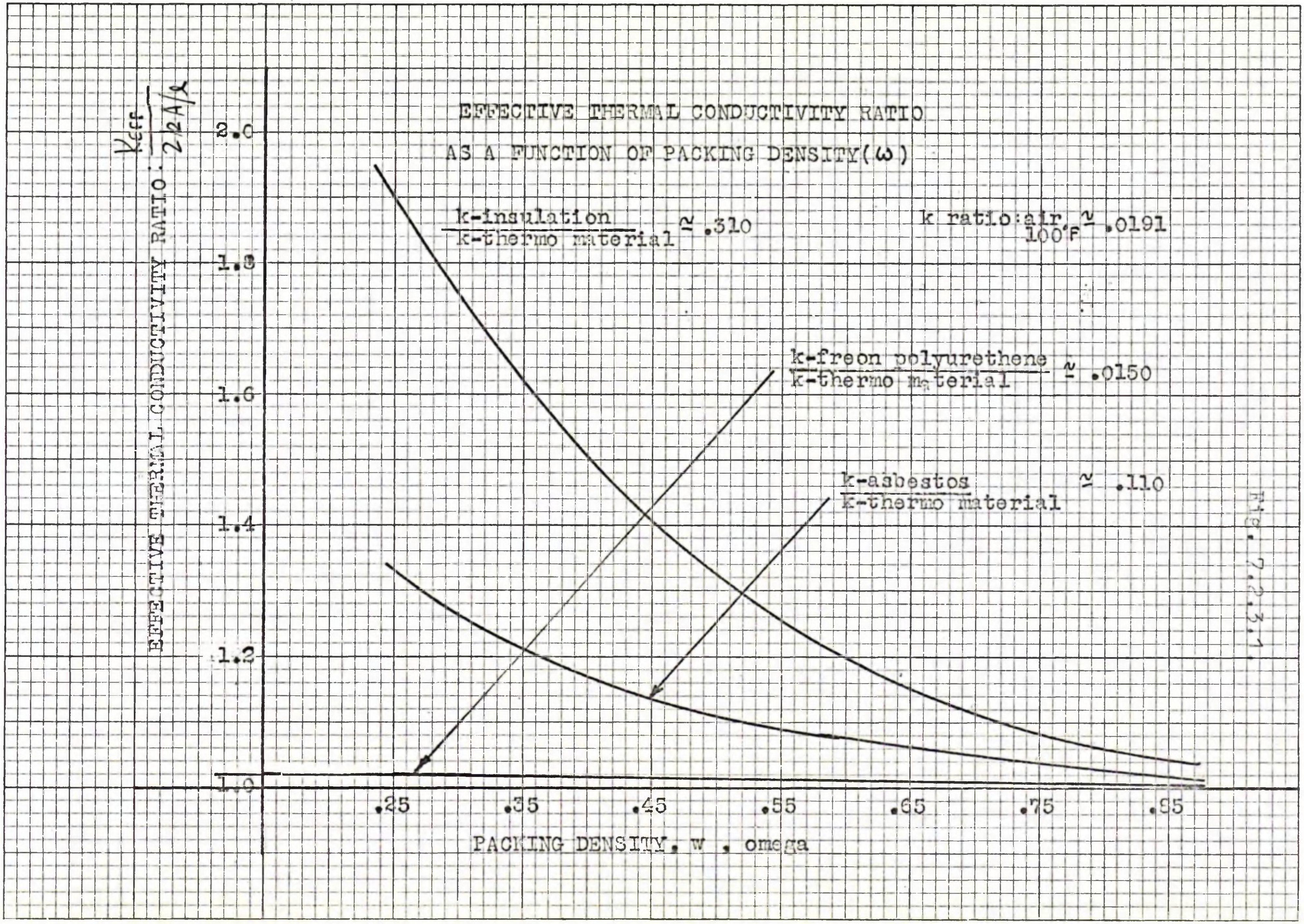
EFFECTIVE THERMAL CONDUCTIVITY RATIO
AS A FUNCTION OF PACKING DENSITY(ω)
k-insulation / k-thermo material ≃ .310
k ratio: air 100°F ≃ .0191
k-freon polyurethene / k-thermo material ≃ .0150
k-asbestos / k-thermo material ≃ .110
EFFECTIVE THERMAL CONDUCTIVITY RATIO: $\frac{K_{eff}}{2kA/l}$
2.0
1.8
1.6
1.4
1.2
1.0
.25
.35
.45
.55
.65
.75
.85
PACKING DENSITY, w , omega

Fig. 7.2.3.1

Figure 7.2.3.1 shows the effective thermal conductance ratio $\left(K_{EFF} l / 2kA\right)$ as a function of the packing density for variation in the ratio $\left(k_i / k\right)$.

7.2.4 Effective Electrical Resistance.

The effective electrical resistance is assumed to be composed of:

$$R_{EFF} = R + R_j + R_{STRAPS} \qquad 7.2.4.1.$$

where:

R couple electrical resistance (equation 6.5.4.2), ohms

R_j junction resistance for a couple, ohms

R_{STRAP} electrical strap resistance for a couple, ohms

Poor junction contact resulting in high junction resistance can cause a large decrease in couple performance (figure 7.4.4.9.5.) In a thermoelectric device, joule heat generated at a poor contact can result in a significant decrease in design expectation. Improper contact can distort the material properties by creating localized joule heating effects.

From reference (7) the junction resistance is defined in terms of "specific-contact resistivity". The specific contact resistivity is expressed as:

$$\rho_j \equiv R_{ji} A_{ii} \qquad 7.2.4.2.$$

where:

ρ_j specific contact resistivity, ohm-cm^2

R_{ji} contact resistance, ohms

A_{ii} cross sectional contact area, cm^2

For example:

A specific contact resistivity (state of the art) of the order 10^{-5} ohm-cm^2 on each end of a 1 cm length element of 10^{-3} ohm-cm (electrical resistivity) represents approximately 2% of the total element resistance. The elements tested in section 12.0 had an element height of .20 cm hence the contact resistance can represent 20% of the total element resistance. With short elements the effect of contact resistance (figure 7.4.4.9.6.) must be considered. The effect of poor element contact at the cold side of the basic thermoelectric device may significantly add to the heat load at the cold junction interface. The effect at the hot junction may not be critical, since the local joule heat generated is adjacent to the heat rejection surface. The total couple effective resistance is expressed as:

$$R_{EFF} = R + \frac{4\rho_j}{A} + R_s \qquad 7.2.4.3.$$

where:

R internal couple electrical resistance, ohms

A cross sectional element area, cm^2

and:

$$R_s = \rho_s l_s / A_s \qquad 7.2.4.4.$$

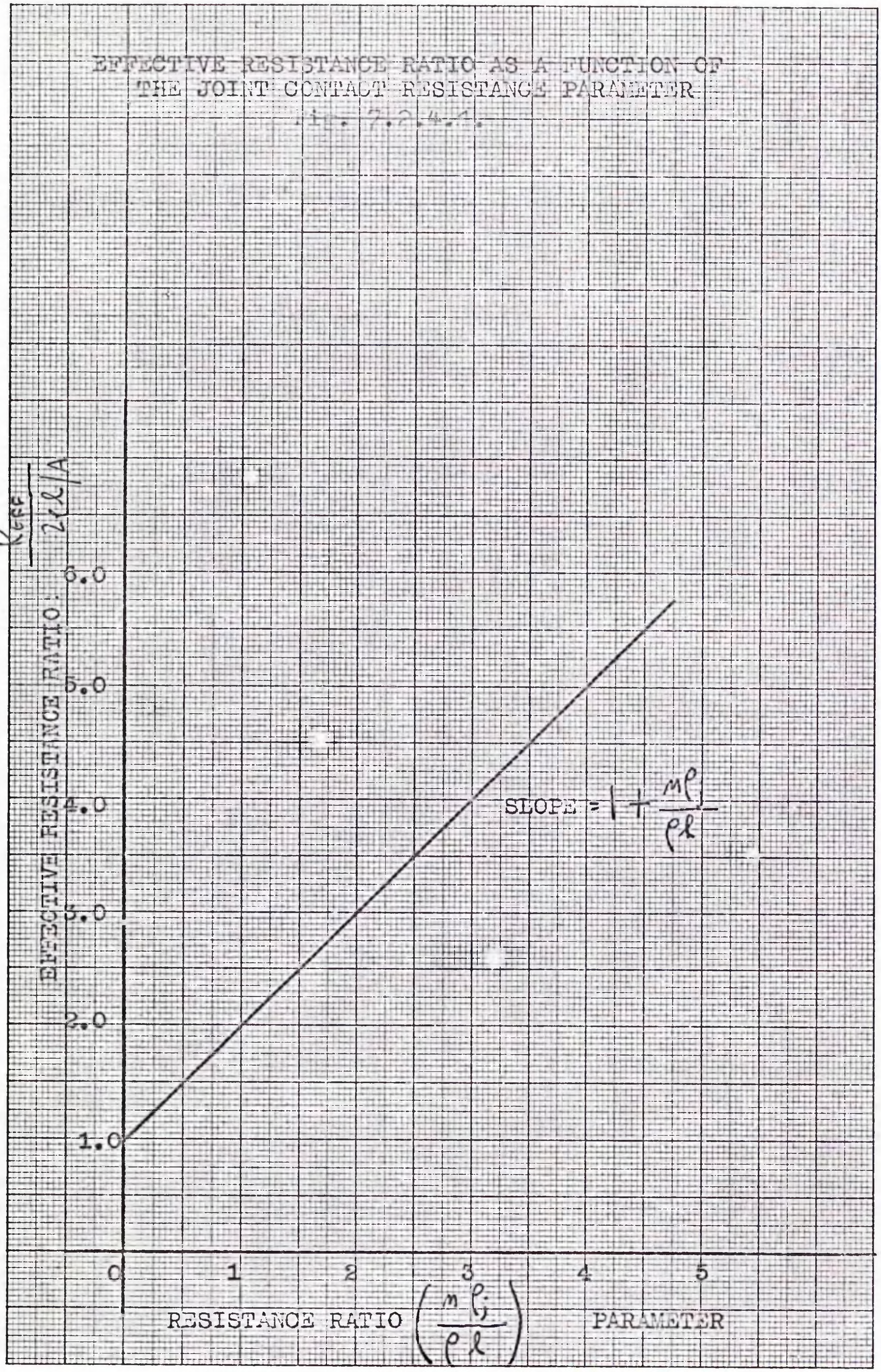

EFFECTIVE RESISTANCE RATIO AS A FUNCTION OF
THE JOINT CONTACT RESISTANCE PARAMETER
Fig. 7.2.4-1.
EFFECTIVE RESISTANCE RATIO: $\frac{R_{eff}}{2\rho l/A}$
1.0
2.0
3.0
4.0
5.0
6.0
SLOPE = $1+\frac{n\rho_i}{\rho l}$
0
1
2
3
4
5
RESISTANCE RATIO $\left(\frac{n\rho_i}{\rho l}\right)$ PARAMETER

where:

R_s strap resistance, ohms

ρ_s effective strap resistivity, ohm-cm

A_s effective cross sectional area, cm^2

Introducing equation 6.5.3.3 and equation 7.2.4.4 into equation 7.2.4.3 with the assumptions of section 7.2.3 results:

$$R_{EFF} = \frac{2\rho l}{A} + \frac{4\rho_j}{A} + \frac{\rho_s l_s}{A_s} \qquad 7.2.4.5.$$

Factoring and combining:

$$R_{EFF} = \frac{2\rho l}{A}\left[1 + \frac{2\rho_j}{\rho l} + \frac{\rho_s l_s A}{A_s 2\rho l}\right] \qquad 7.2.4.6.$$

Figure 7.2.4.1 shows the effective resistance ratio $(R_{EFF} A / 2\rho l)$ as a function of the contact resistance parameter $(m\rho_j / \rho l)$ (the strap resistance term has been neglected).

7.2.5 Effective Figure of Merit.

The effective parameters relating material properties can be combined with the Seebeck coefficient to define an effective figure of merit (Z_{EFF}). The concept of using effective parameters establishes the relationship for effective maximum junction temperature difference

The effective figure of merit is defined as:

$$Z_{EFF} = \frac{\alpha_{mp}^{2}}{R_{EFF} \cdot K_{EFF}} \qquad 7.2.5.1.$$

The effective maximum junction temperature is expressed as:

$$\Delta T_{j_{max_{EFF}}} = 0.5 \times T_{c_j} Z_{EFF} \qquad 7.2.5.2.$$

From equation 7.2.5.1 expanding denominator into basic material parameters:

$$R_{EFF} = \frac{2\rho l}{A}\left[1 + \frac{2\rho_j}{\rho l}\right] \qquad 7.2.5.3.$$

Letting (ω) = 1 then equation 7.2.3.4 reduces to:

$$K_{EFF} = \frac{2kA}{l} \qquad 7.2.5.4.$$

Equation 7.2.5.7 is essentially equation 6.5.3.10 with suitable material assumptions. Introducing equation 7.2.5.3 and equation 7.2.5.4 into equation 7.2.5.1 results:

$$Z_{EFF} = \frac{\alpha_{mp}^{2}}{4k\rho\left[1 + \frac{2\rho_j}{\rho l}\right]} \qquad 7.2.5.5.$$

assuming

$$\alpha_{mp} = |\alpha_m| + |\alpha_p|$$

and

$$\alpha = \alpha_m = \alpha_p$$

therefore

$$\alpha_{mp}^{2} = 4\alpha^{2} \qquad 7.2.5.6.$$

EFFECTIVE FIGURE OF MERIT RATIO AS A FUNCTION OF THE RATIO:CONTACT RESISTIVITY TO MATERIAL CHARACTERISTIC

Fig. 7.7.5.1

EFFECTIVE FIGURE OF MERIT RATIO = $Z_{EFFECTIVE} / Z_{MATERIAL}$

PROPERTY PARAMETER = $\dfrac{m\rho_i}{\rho l}$

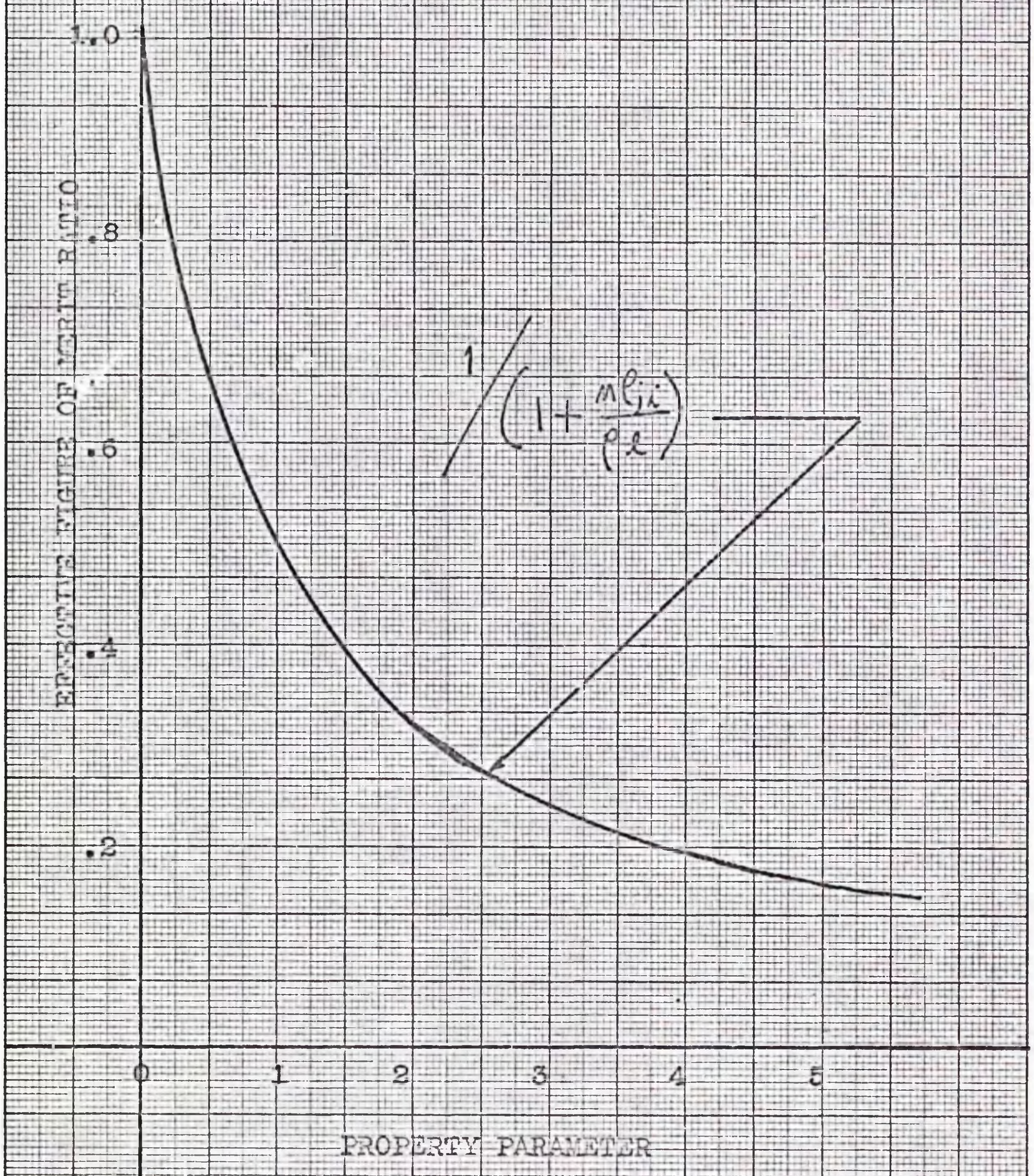

Introducing equation 7.2.5.6 into equation 7.2.5.5 and utilizing the basic definition of figure of merit results:

$$Z_{EFF} = \frac{Z}{\left[1 + \frac{2\rho_j}{\rho l}\right]} \qquad 7.2.5.7.$$

Figure 7.2.5.1 illustrates the effective figure of merit ratio (Z_{EFF}/Z) as a function of the contact property parameter $(m\rho_j/\rho l)$. In section 7.2.1 it was stated, " the equations derived for the ideal thermoelectric couple may be utilized to describe performance of a couple with electrical and thermal losses by suitable modification of the material properties". To illustrate: (consider figure 6.5.3.1), the figure of merit (Z) can be replaced by Z_{EFF} (equation 7.2.5.7) resulting in an effective heat pump rate at maximum C.O.P. The effective maximum junction temperature can be determined by figure 6.5.6.1 with the supstitution of Z by Z_{EFF}.

For a given performance level there is a required ratio of (Z_{EFF}/Z). With the material property $\bar{\rho}$ constant then it follows from figure 7.2.5.1 that (ρ_j/l) must remain constant. If improvement in contact resistance is obtained l must decrease in order to maintain (ρ_j/l) fixed. From equation 6.5.7.9 the maximum cooling rate per unit volume can be expressed as:

$$\frac{Q_{s\,max}}{A_T l} = \frac{\alpha_{np}^2 T_{cj}^2}{8 l^2 \bar{\rho}} - \frac{\Delta T_j \bar{k}}{l^2} \qquad 7.2.5.8.$$

From equation 7.2.5.8. the maximum cooling per unit volume will decrease as the square of the height of the thermoelement (l) and is proportional to the contact resistance. The volume of an element is (Al) which can be expressed in terms of the shape factor (equation 6.5.2.3) as ($f_i l^2$) inferring that the volume of the thermoelectric couple will decrease proportionally to a decrease in contact resistance (figure 7.4.4.9.5).

Contact resistivity (ρ_j) is a difficult value to obtain experimentally within an acceptable level of accuracy. A review of data indicates (Author's opinion coupled with statistical analysis) sufficient scatter to warrant additional investigation. What may be established is the general trends or expected limits on contact resistivity. The present state of the art data indicates a contact resistivity of the order 10^{-5} ohm-cm^2 per contact. Thermoelectric material with a resistivity of 10^{-3} ohm - cm as a representative value combined with equation 7.2.5.7. can yield an effective figure of merit ratio.

$$\frac{Z_{EFF}}{Z} = \frac{1}{\left[1 + \frac{2\times10^{-5}}{(.2)(10^{-3})}\right]} \qquad 7.2.5.9.$$

$$Z_{EFF} \cong Z\,(.906) \qquad 7.2.5.10.$$

The percent decrease in Z is expressed as:

$$\% = \left(1 - Z_{EFF}/Z\right) \times 100 \qquad 7.2.5.11.$$

Equation indicates that an expected decrease in the figure of merit is approximately 9.4% ($\omega = 1$). The expression introducing the effective figure of merit (equation 7.2.5.7) permits the use of the idealized performance equations of chapter 6.0. Thus the effectiveness quantities can be utilized with the equations of the idealized couple to compensate for losses. These equations can be utilized to determine module performance since the module is a group of couples with losses. The relations developed in the previous sections assume that material properties are invariant with temperature. The computer programs developed incorporate provisions to account for material properties being function of temperature. The foregoing performance equations have been expressed in terms of junction temperatures (T_{hj}, T_{cj}). These equations may be adequate for a first order approximation if estimates of junction temperatures are correct. In section 8.4 the thermoelectric couple is considered part of an over-all heat transfer problem with junction temperatures resulting functions of current and hence are not arbitrary.

7.3 Power Supply Ripple.

7.3.1 Introduction.

The performance equations presented in the previous sections have been derived with the assumption that the thermoelectric couple is powered by a steady direct current source. There are numerous cooling applications where the primary power supply would be alternating current. It then becomes necessary to know how 'completely' the required current must be rectified as device performance decreases by imperfect filtering.

The essential problem is that any alternating current component is pure loss. The A.C. current generates heat but develops no heat pumping capability by the Peltier effect. It is necessary to estimate the magnitude of loss relative to the unavoidable loss (i.e. joule heat) terms. The effect of current ripple has been evaluated by direct integration of power supply filtering for limited performance parameters. Fourier transformations (8) were employed to evaluate transient behavior with power supply ripple. The analysis presented in this section is parametric in concept and hence introduces a mathematical tool to be utilized for a wide variety of performance criteria.

The concept of the form factor (F) (2) is proposed as a measure of the joule heating current (rms current or effective current) relative to the average (D.C) current. The form factor (F) is introduced into the basic heat pumping equation (equation 7.3.2.5.) and is proposed as an approximate expression accounting for power supply ripple. The method presented results in a mathematical tool for evaluating thermoelectric design development. The concept is to present not only the simplified equations but an appreciation of the effect of power supply ripple. The presentation format (graphs) is proposed as a technique for providing utilizable information on which economic decisions can be made.

7.3.2 Analysis and Results.

The procedure proposed is to present the equations for heat pumping capacity, C.O.P. in terms of the effective material properties and current. The effective parameters (section 7.2) introduce material properties which account for controllable losses as well as losses which are inherent in irreversible processes (Thermoelectric devices). The resulting parametric equations can be simplified to include the direct current and the form factor (F).

The form factor is defined (2) as:

$$F \equiv \frac{I_{RMS}}{I_{D.C.}(I)} \qquad 7.3.2.1.$$

It is advantageous to convert (F) in terms of ripple or percent ripple in order to establish a common terminology with the power supply manufacturer. A relationship can be developed between ripple and form factor if the ripple wave form is assumed. The assumption proposed is that the small ripple from a filtered power supply will be sinusodial. Percent ripple (%) is defined as the peak-to-peak value of the alternating component divided

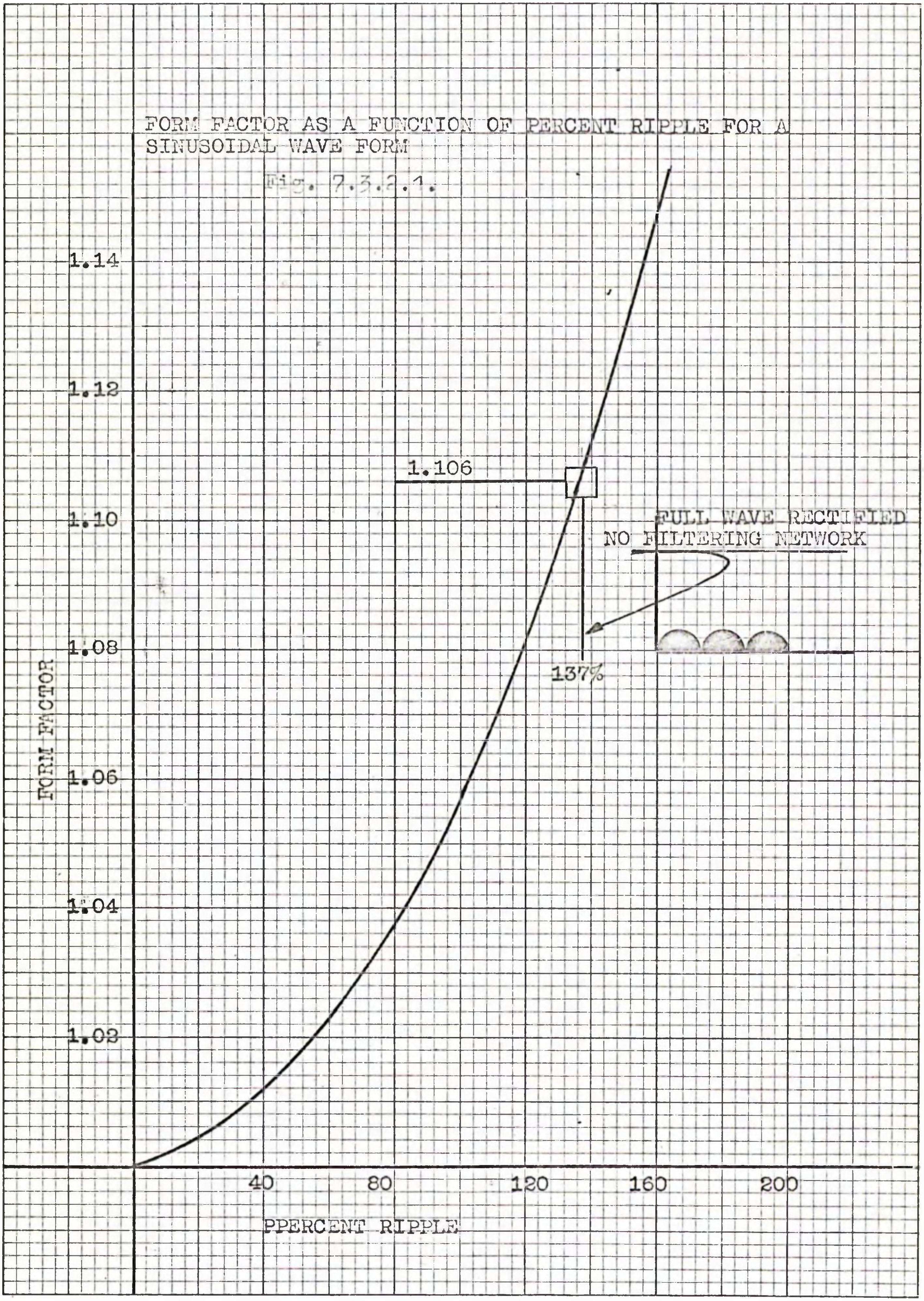

FORM FACTOR AS A FUNCTION OF PERCENT RIPPLE FOR A SINUSOIDAL WAVE FORM

Fig. 7.3.2.1.

by the average current (d.c) times 100. In appendix I the derivation relating form factor is developed and is given by:

$$F^2 = 1 + \frac{(\%\ \text{RIPPLE})^2}{8 \times 10^4} \qquad 7.3.2.2.$$

Figure 7.3.2.1 illustrates the form factor (F) as a function of percent ripple. For an unfiltered, full wave rectified output (Appendix I) the form factor is approximately 1.10 and the corresponding percent ripple of $\cong$ 136%. This limit affixes a number to a recognizable wave-form. The effect of power supply ripple will be determined for the following operational conditions:

(1) Maximum junction temperature difference $(\Delta T_{j\,max})$
(2) Current for maximizing heat pump rate (I_Q)
(3) Current for maximizing C.O.P. (I_ϕ)
(4) Capacity at maximum heat pump rate $(Q_{s\,max})$
(5) Heat pump rate at maximum C.O.P. (Q_ϕ)
(6) C.O.P. at maximum heat pump rate $(C.O.P._Q)$
(7) Maximum C.O.P. $(C.O.P._{max})$

The computer programs developed introduce the effect of form factor (F) as an operational term. Figure 7.4.4.9.7. illustrates the effect of power supply ripple on material utilization (watts/cm^3) as a function of C.O.P. The expressions develop present the ratio of the variable with current ripple to its value for pure d.c. operation. An asterisk (*) is used to denote the d.c. value with ripple.

From equation 6.4.3:

$$Q_s = T_{cj} I \alpha_{mp} - \frac{1}{2} I^2 R_{EFF} - K_{EFF} \Delta T_j \quad \text{(no ripple)} \qquad 7.3.2.3.$$

The current maximizing the heat pump rate is:

$$I_Q = \frac{\alpha_{mp} T_{cj}}{R_{EFF}} \qquad 7.3.2.4.$$

Introducing current ripple into equation 7.3.2.3.

$$Q_s^* = T_{cj} I^* \alpha_{mp} - \frac{1}{2} I^2_{RMS} R_{EFF} - K_{EFF} \Delta T_j \qquad 7.3.2.5.$$

Replacing: I_{RMS} by $F\, I_{d.c.}$

The current maximizing the heat pump rate with current ripple is:

$$I_Q^* = \frac{\alpha_{mp} T_{cj}}{R_{EFF} F^2} \qquad 7.3.2.6.$$

Combining 7.3.2.4 and equation 7.3.2.6 results:

$$\frac{I_Q^*}{I_Q} = \frac{1}{F^2} \quad (F \geq 1) \qquad 7.3.2.7.$$

Equation 7.3.2.7 indicates that the d.c. current required to maximize the heat pump rate is smaller when ripple is present and decreases with the square of the form factor (F). In a similiar derivation, the d.c.

current required to maximize the C.O.P. is approximately independent of any accompanying A.C. component, hence:

$$\frac{I_\phi^*}{I_\phi} \cong 1 \qquad 7.3.2.8.$$

The proof of this interesting approximate independence to (F) is derived by the following approach:

The current maximizing the C.O.P. is expressed as:

$$I_\phi = \frac{\alpha_{mp} \Delta T_j}{R(\sqrt{B}-1)} \qquad 6.5.2.19.$$

The C.O.P. can be expressed with current ripple as:

$$C.O.P.^* = \frac{T_{cj} I^* \alpha_{mp} - \frac{1}{2} R_{EFF} F^2 I^{2*} - K_{EFF} \Delta T_j}{F^2 I^{2*} R_{EFF} + I^* \alpha_{mp} \Delta T_j} \qquad 7.3.2.9.$$

and from appendix J an intermediate relationship is expressable as:

$$R_{EFF} I^* \sqrt{B} \cong \alpha_{mp} \Delta T_j + I^* R_{EFF} \qquad 7.3.2.10.$$

Factoring and combining results as indicated by equation 6.5.2.19.

$$I_\phi^* = \frac{\alpha_{mp} \Delta T_j}{R_{EFF}(\sqrt{B}-1)} \qquad 7.3.2.11.$$

Combining equation 7.3.2.11 and equation 7.3.2.4. results

$$\frac{I_\phi^*}{I_\phi} \cong 1 \qquad 7.3.2.8.$$

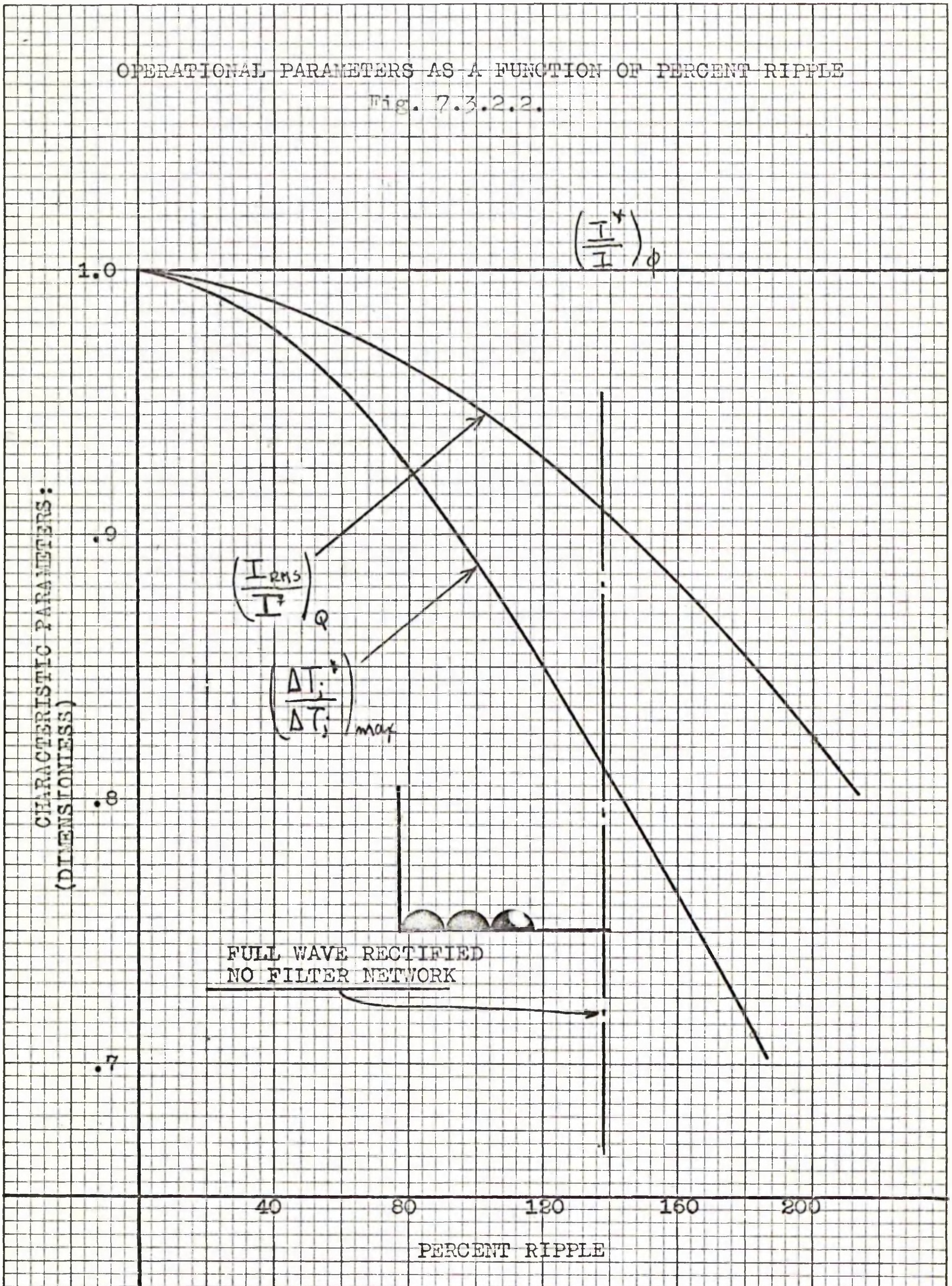
OPERATIONAL PARAMETERS AS A FUNCTION OF PERCENT RIPPLE
Fig. 7.3.2.2.
$\left(\frac{I^*}{I}\right)_\phi$
$\left(\frac{I_{RMS}}{I'}\right)_Q$
$\left(\frac{\Delta T_j^*}{\Delta T_j}\right)_{max}$
FULL WAVE RECTIFIED
NO FILTER NETWORK
CHARACTERISTIC PARAMETERS:
(DIMENSIONLESS)
1.0
.9
.8
.7
40
80
120
160
200
PERCENT RIPPLE

The maximum junction temperature ratio with ripple is expressable as: (Derivation in appendix J)

$$\frac{\Delta T_{j_{max}}^{*}}{\Delta T_{j_{max}}} = \frac{1}{F^2} \qquad 7.3.2.12.$$

From equation 7.3.2.7 and equation 7.3.2.1 expressable as:

$$\frac{I_Q^{*}}{I_Q} = \frac{1}{F^2} \qquad 7.3.2.7.$$

and

$$\frac{I_{RMS_Q}}{I_Q^{*}} \equiv F \qquad 7.3.2.1.$$

resulting:

$$\left.\frac{I_{RMS}}{I}\right|_{Q} = \frac{1}{F} \qquad 7.3.2.13.$$

Figure 7.3.2.2 illustrates the performance ripple ratios $(1/F^2, 1/F, 1)$ as a function of percent ripple.

The heat pump capacity at maximum C.O.P. (Q_ϕ) and the C.O.P. at maximum heat pump rate (C.O.P.$_Q$) performance ripple ratio are equal. The derivation is presented in appendix J. The resulting expressions are:

$$\left.\frac{C.O.P.^{*}}{C.O.P.}\right|_{Q_{max}} = \frac{\left(1 - F^2\dfrac{\Delta T_j}{\Delta T_{j_{max}}}\right)}{\left(1 - \dfrac{\Delta T_j}{\Delta T_{j_{max}}}\right)} \qquad 7.3.2.14.$$

and:

$$\left.\frac{C.O.P.^{*}}{C.O.P.}\right|_{Q_{max}} = \left.\frac{Q_s^{*}}{Q_s}\right|_{C.O.P._{max}} \qquad 7.3.2.15.$$

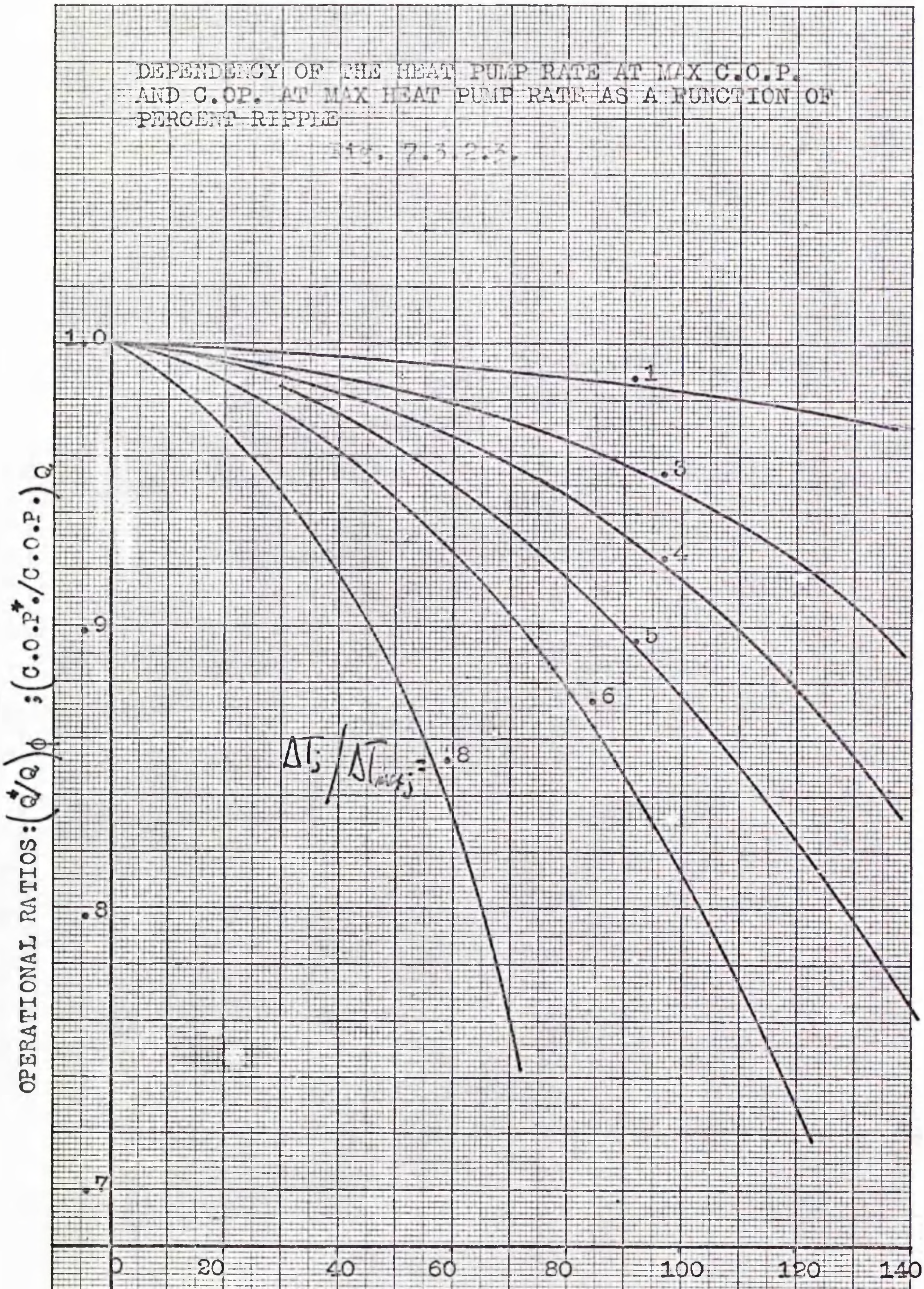

DEPENDENCY OF THE HEAT PUMP RATE AT MAX C.O.P. AND C.OP. AT MAX HEAT PUMP RATE AS A FUNCTION OF PERCENT RIPPLE

Fig. 7.3.2.3.

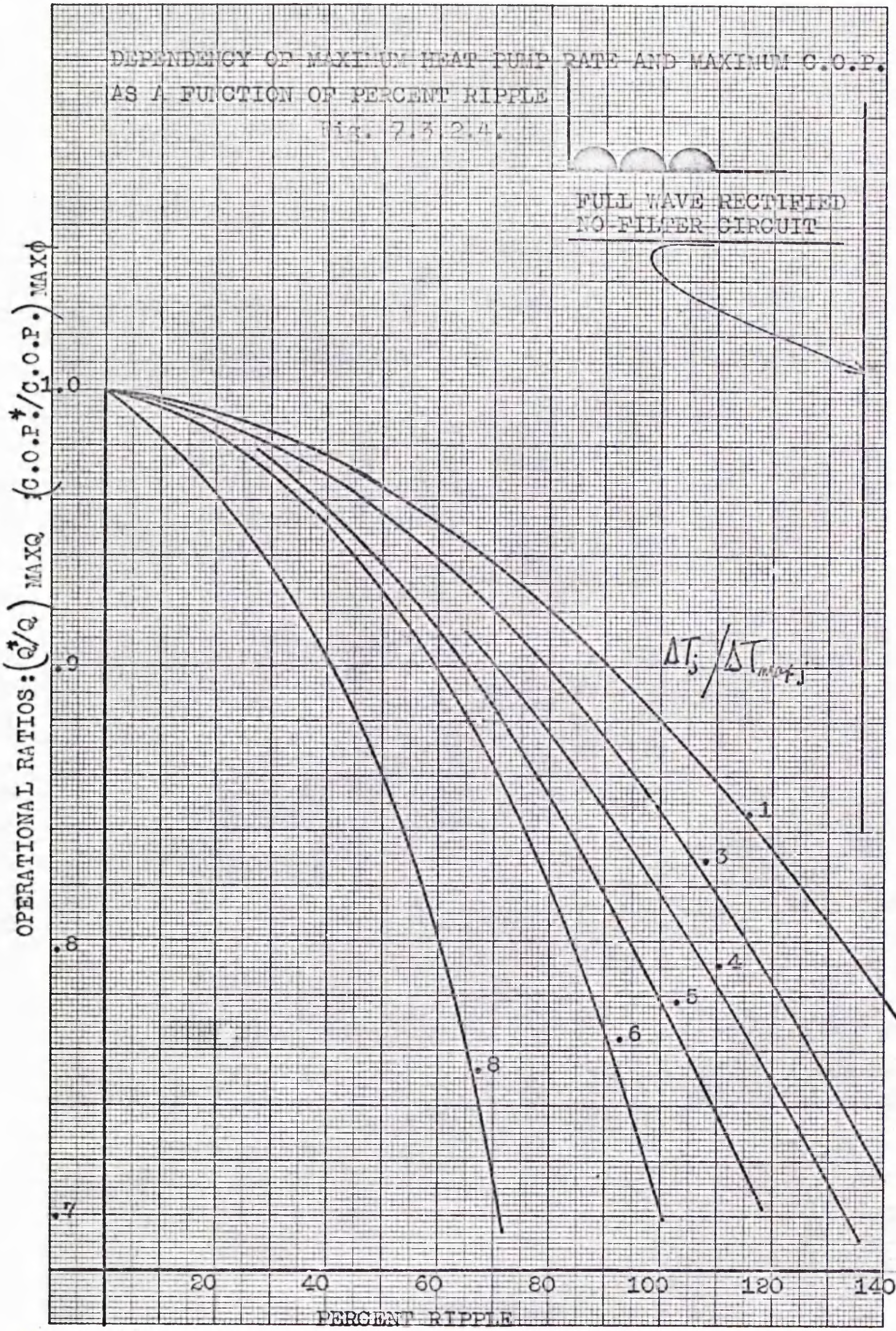
DEPENDENCY OF MAXIMUM HEAT PUMP RATE AND MAXIMUM C.O.P.
AS A FUNCTION OF PERCENT RIPPLE
Fig. 7.3.2.4.
FULL WAVE RECTIFIED
NO-FILTER CIRCUIT
$\Delta T_j / \Delta T_{max\,j}$
.1
.3
.4
.5
.6
.8
OPERATIONAL RATIOS: $(Q^*/Q)_{MAX\,Q}$ $(C.O.P.^*/C.O.P.)_{MAX\,\phi}$
1.0
.9
.8
.7
20
40
60
80
100
120
140
PERCENT RIPPLE

Equation 7.3.2.14 depends on ΔT_j and $\Delta T_{j_{max}}$ which appears reasonable as the ripple introduces additional losses not considered by equation 6.6.13 or 6.6.22. Figure 7.3.2.3 illustrates the ripple performance ratios $\left((Q^*/Q)_{C.O.P.}, (C.O.P.^*/C.O.P.)_Q\right)$ as a function of percent ripple with variable temperature ratios.

The effect of ripple for operation at maximum C.O.P. and maximum heat pump rate results in the following: (The derivation is presented in appendix J).

$$\left.\frac{Q_s^*}{Q_s}\right|_{max} = \left.\frac{C.O.P.^*}{C.O.P.}\right|_{max} = \frac{\left[1 - \frac{F^2 \Delta T_j}{\Delta T_{j_{max}}}\right]}{F^2\left[1 - \frac{\Delta T_j}{\Delta T_{j_{max}}}\right]} \qquad 7.3.2.16.$$

Figure 7.3.2.4 illustrates equation 7.3.2.16 as a function of percent ripple for variation in the temperature ratio.

A more general approach can be derived where current has been replaced by the current dimensionless parameter as defined by equation 6.7.1. The heat pumping ripple ratio is expressed as:

$$\frac{Q^*}{Q} = \frac{\left[2\theta - F^2\theta^2 - \frac{\Delta T_j}{\Delta T_{j_{max}}}\right]}{\left[2\theta - \theta^2 - \frac{\Delta T_j}{\Delta T_{j_{max}}}\right]} \qquad 7.3.2.17.$$

The C.O.P. ripple ratio is expressed as:

$$\frac{C.O.P.^*}{C.O.P.} = \frac{\left[2\theta - F^2\theta^2 - \frac{\Delta T_j}{\Delta T_{j_{max}}}\right]\left[\theta^2 + \frac{\theta \Delta T_j}{T_{c_j}}\right]}{\left[2\theta - \theta^2 - \frac{\Delta T_j}{\Delta T_{j_{max}}}\right]\left[\theta^2 F^2 + \frac{\theta \Delta T_j}{T_{c_j}}\right]} \qquad 7.3.2.18.$$

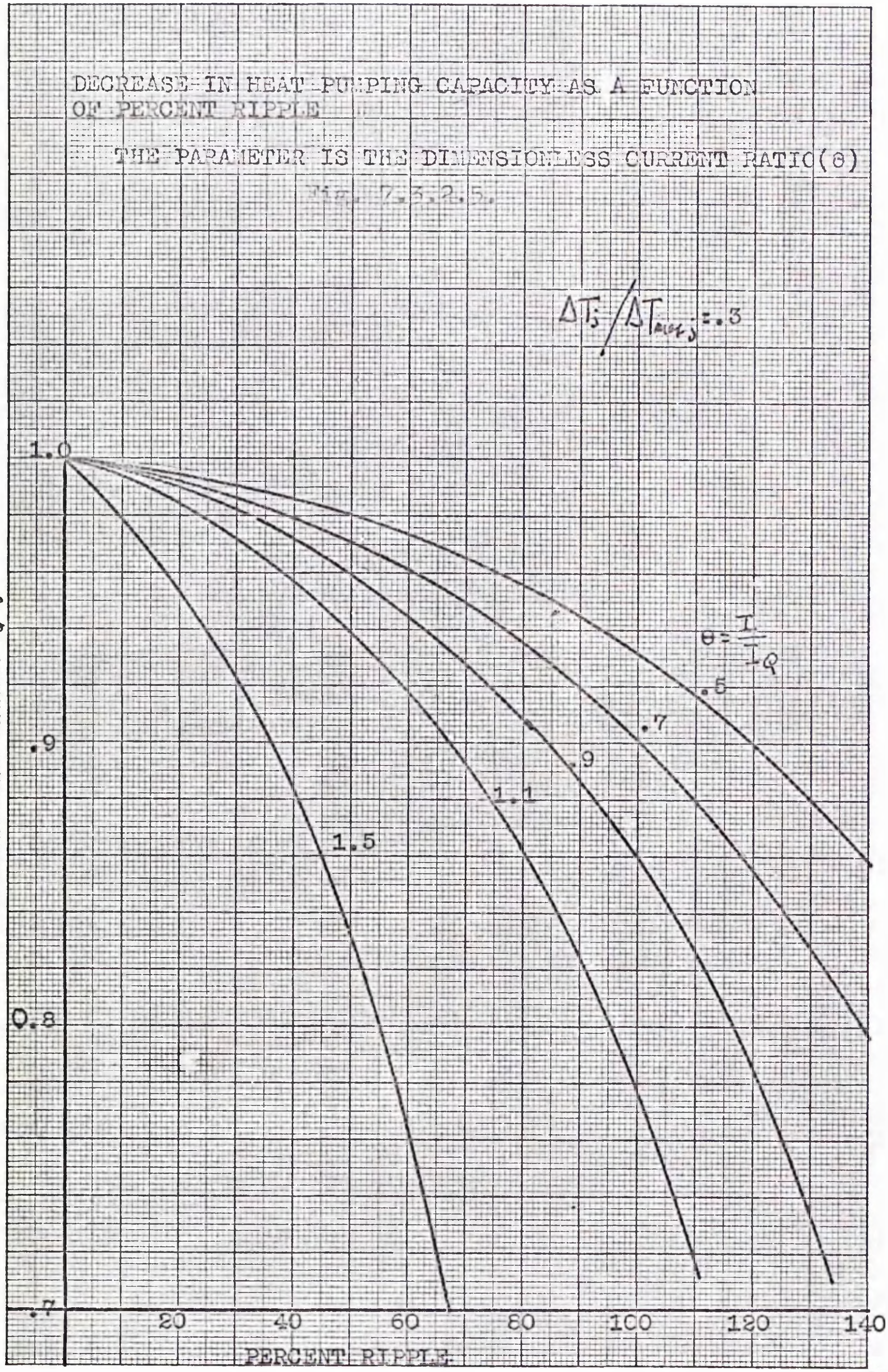
DECREASE IN HEAT PUMPING CAPACITY AS A FUNCTION OF PERCENT RIPPLE
THE PARAMETER IS THE DIMENSIONLESS CURRENT RATIO (θ)
Fig. 7.3.2.5.
ΔT/ΔT = .3
θ = I/I_Q
.5
.7
.9
1.1
1.5
1.0
.9
0.8
.7
20
40
60
80
100
120
140
PERCENT RIPPLE
OPERATIONAL RATIO: Q*/Q

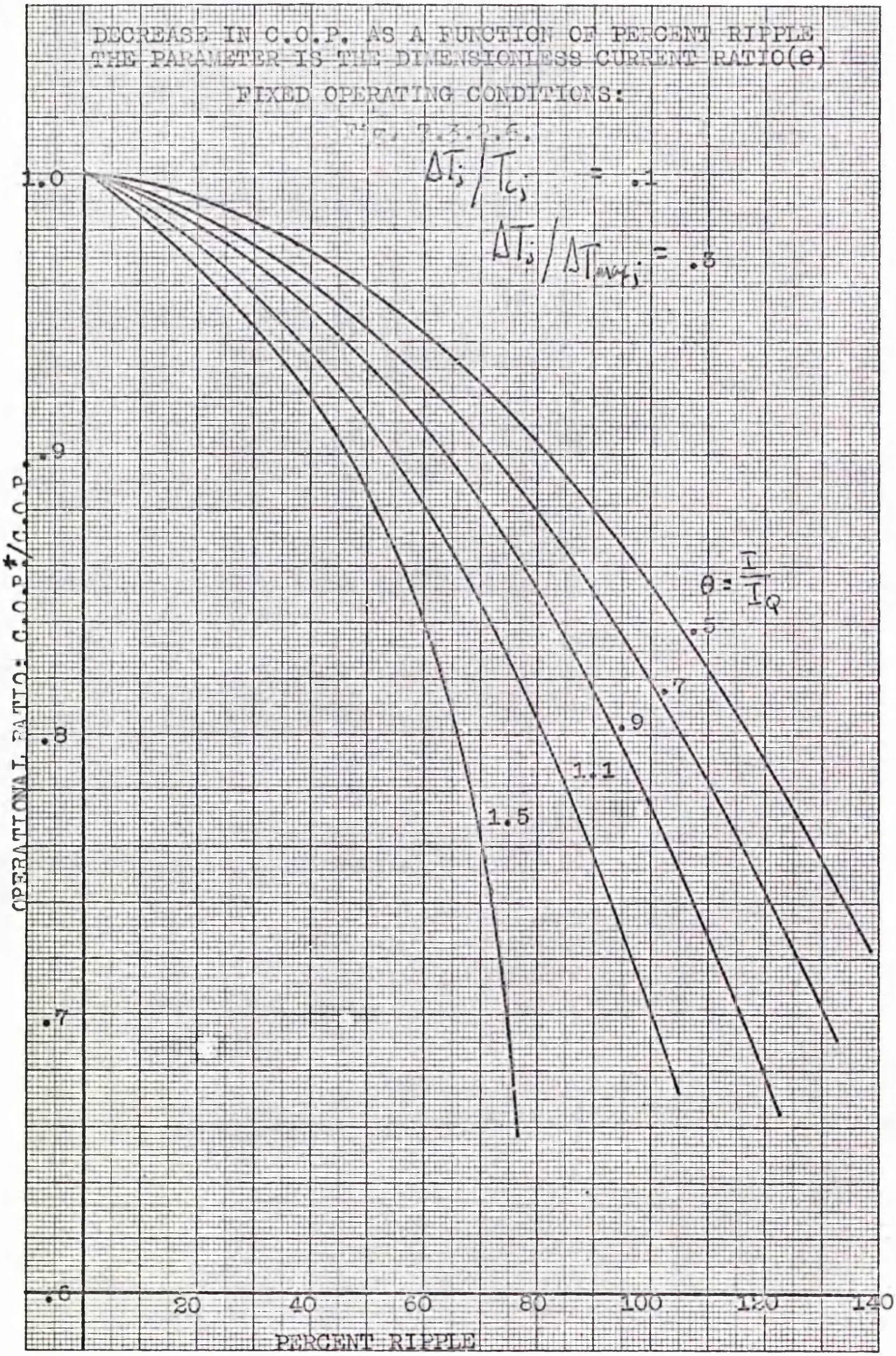
DECREASE IN C.O.P. AS A FUNCTION OF PERCENT RIPPLE
THE PARAMETER IS THE DIMENSIONLESS CURRENT RATIO(θ)
FIXED OPERATING CONDITIONS:
$\Delta T_j / T_{c_j} = .1$
$\Delta T_j / \Delta T_{max_j} = .3$
$\theta = \frac{I}{I_Q}$
.5
.7
.9
1.1
1.5
1.0
.9
.8
.7
.6
20
40
60
80
100
120
140
PERCENT RIPPLE
OPERATIONAL RATIO: C.O.P.*/C.O.P.

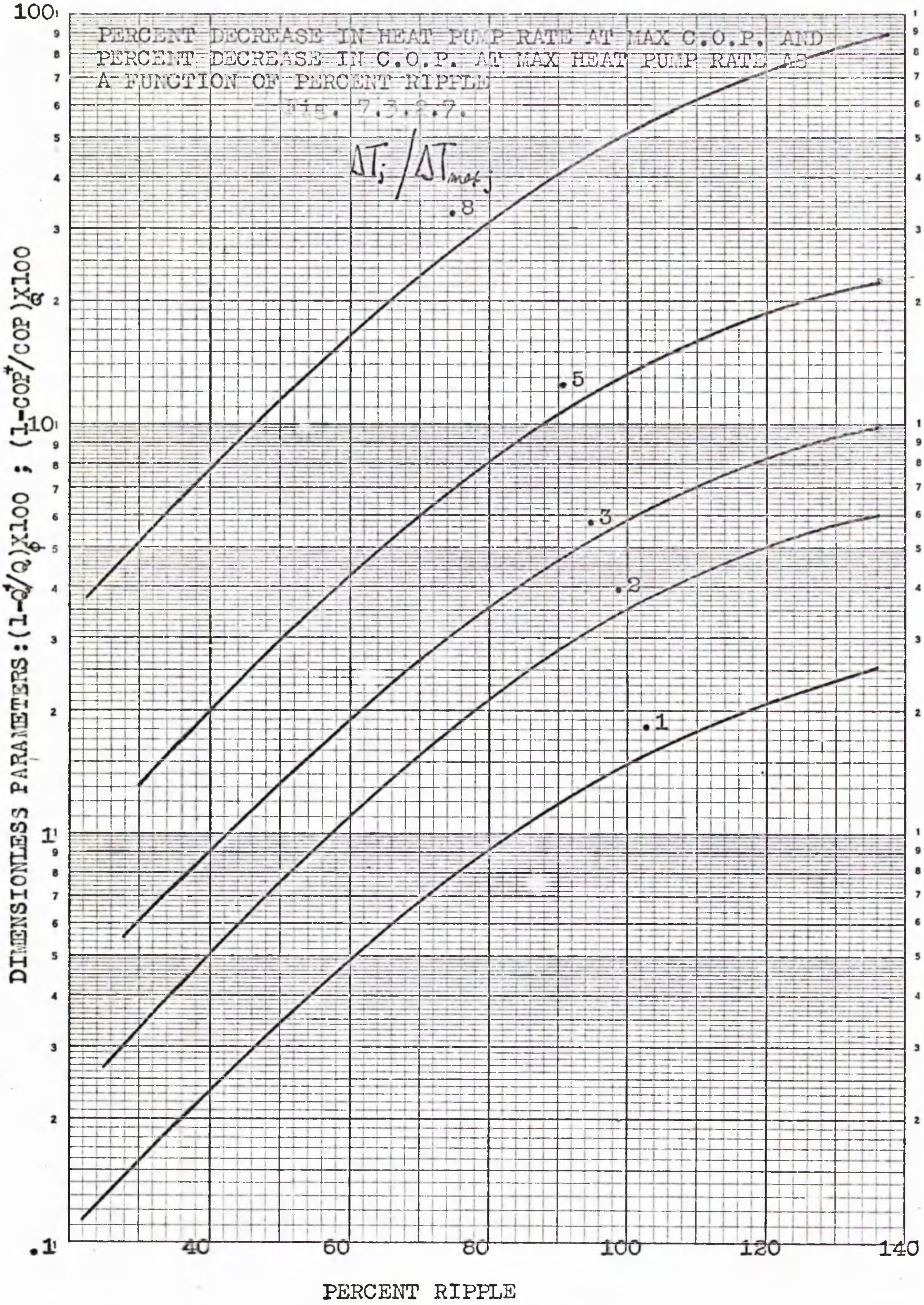
PERCENT DECREASE IN HEAT PUMP RATE AT MAX C.O.P. AND
PERCENT DECREASE IN C.O.P. AT MAX HEAT PUMP RATE AS
A FUNCTION OF PERCENT RIPPLE
Fig. 7.3.2.7.
ΔT_j / ΔT_max,j
.8
.5
.3
.2
.1
DIMENSIONLESS PARAMETERS: (1-Q*/Q)_φ X100 ; (1-COP*/COP)_Q X100
PERCENT RIPPLE
.1
1
10
100
40
60
80
100
120
140

Appendix J presents the derivations of equation 7.3.2.17 and equation 7.3.2.18. Figure 7.3.2.5 illustrates the operational ratio (Q^*/Q) as a function of percent ripple for $\Delta T_j/\Delta T_{j_{max}}$ =.3 and for variation in the dimensionless current ratio (θ). Figure 7.3.2.6 illustrates (C.O.P.*/C.O.P.) as a function of percent ripple for $\Delta T_j/\Delta T_{j_{max}}$ = .30 and $\Delta T_j/T_{cj}$ =.1 and for variation in the dimensionless current ratio (θ). Figure 7.3.2.7 illustrates that a percent ripple of 40% with $\Delta T_j/\Delta T_{j_{max}} \leq .5$ the decrease in performance is expected to be less than 2%. Figure 7.3.2.8 illustrates that for a fixed percent ripple the decrease in performance at maximum operation increases as $\Delta T_j/\Delta T_{j_{max}}$ increases.

7.4 Model Configuration.

7.4.1 Introduction.

In this section the procedure for calculating the performance of a thermoelectric cooling module is presented. The equation developed are obtained from a consideration of the internal energetic processes occuring within the control volume enclosing the basic thermoelectric couple. For a given module configuration the computer program (C.P.5.) calculates module performance for various arbitrary cold junction temperatures (T_{cj}), junction temperature differences (ΔT_j) and currents. The resulting computer programs have been programmed for

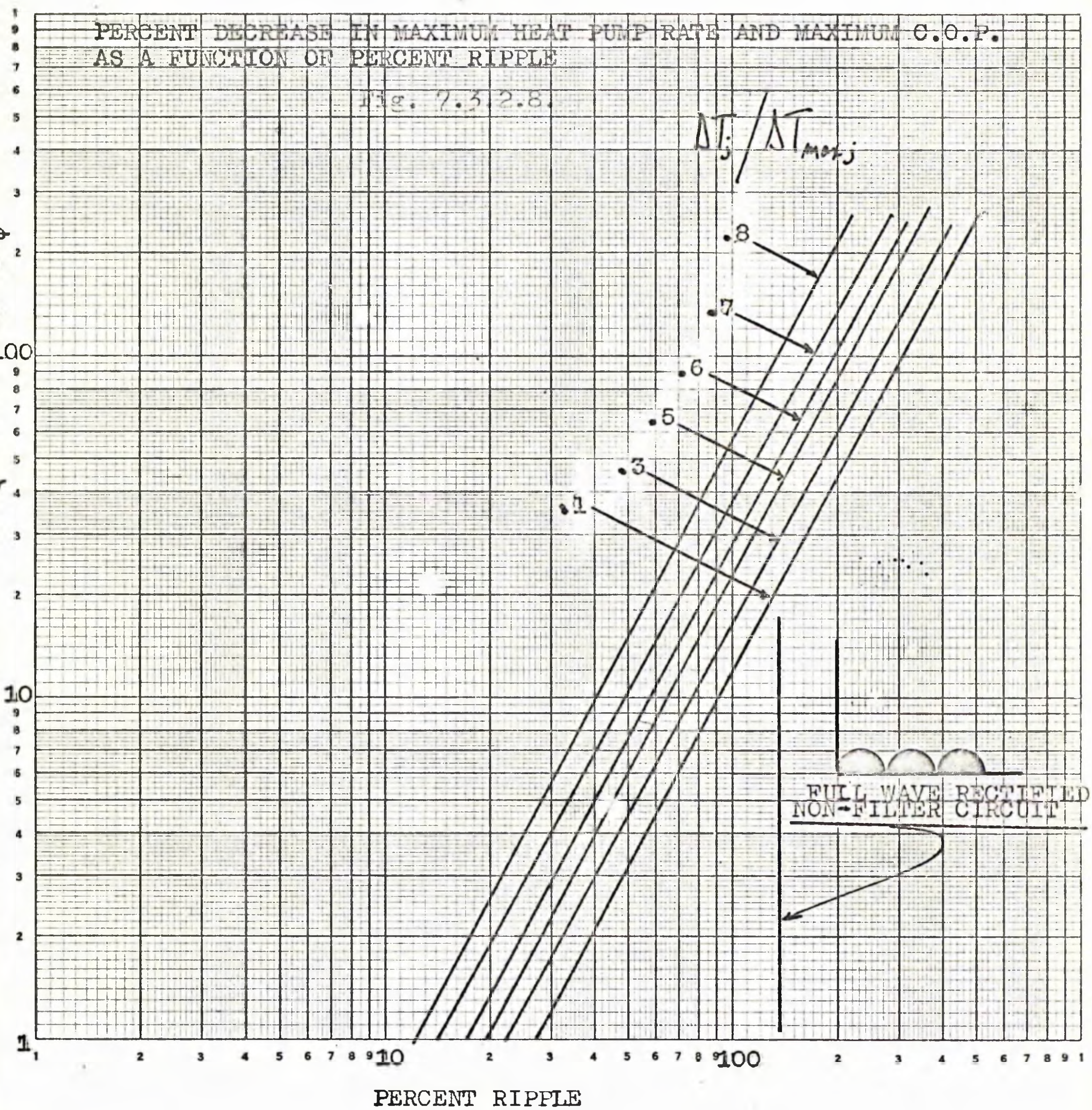
PERCENT DECREASE IN MAXIMUM HEAT PUMP RATE AND MAXIMUM C.O.P.
AS A FUNCTION OF PERCENT RIPPLE
Fig. 7.3.2.8.
$\Delta T_j / \Delta T_{max\,j}$
.8
.7
.6
.5
.3
.1
FULL WAVE RECTIFIED
NON-FILTER CIRCUIT
1
10
100
PERCENT RIPPLE

an English Electric KDF9 Computer using Algol as the basic autocode.

The configuration of the resulting mathematical model is illustrated by figure 7.4.1.1. The configuration as

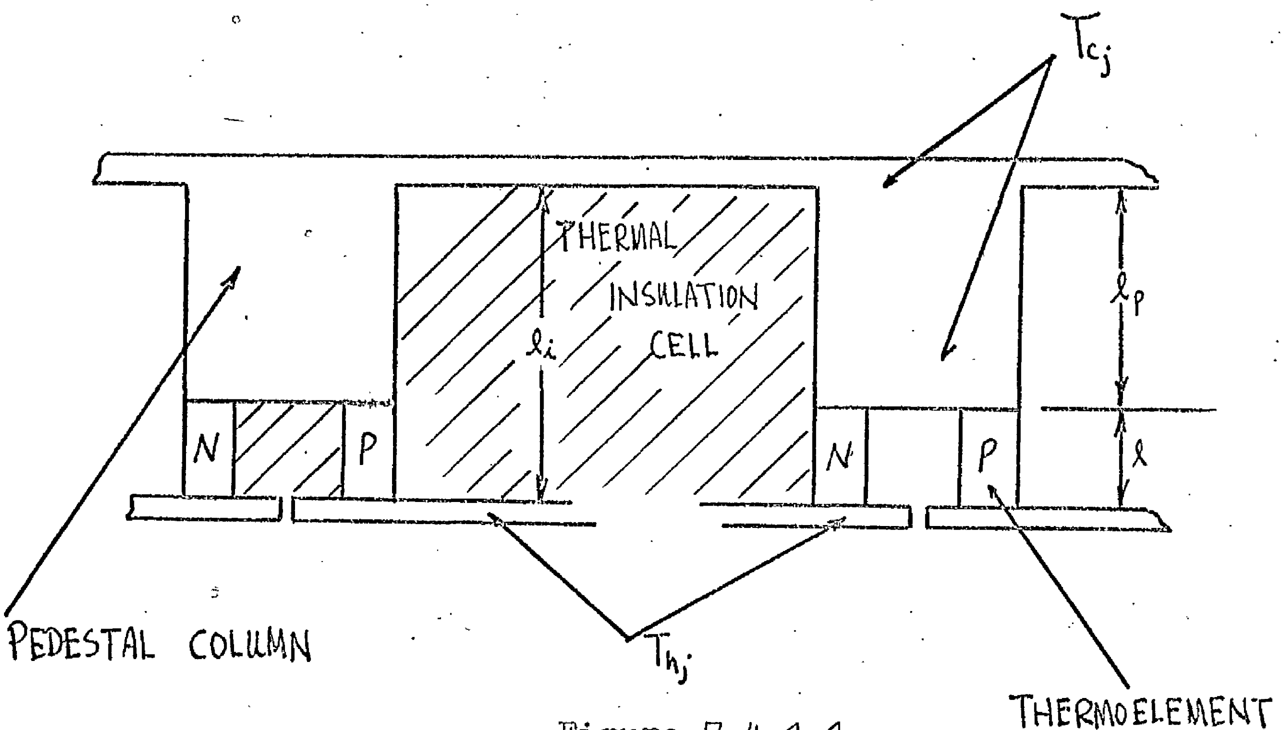

Figure 7.4.1.1.

Quasi Ideal Module Configuration.

illustrated in figure 7.4.1.1 is a cross sectional view of a low packing density module using couple pedestals. The mathematical model developed from figure 7.4.1.1 can be transformed from a pedestal configuration to a conventional Peltier couple (figure 6.2.1) by an optional procedure executed by the input data.

7.4.2 Pedestal/Thermoelectric Couple Assembly.

Pedestals have been proposed to reduce the hot to cold plate thermal leakage in low packing density modules using short thermoelements. To reduce the cost of the unit small thermoelectric elements are attached to (assumed) isothermal columns (pegs). The heat leakage from the hot to cold junction through the interelement insulation for a one-dimensional solution can be expressed as:

$$q_{mi} = \frac{K_i A_i [T_{hj} - T_{cj}]}{l_i} \qquad 7.4.2.1.$$

The one-dimensional design equation neglects the effect of the pedestal column on the heat leakage through the insulation and is replaced (appendix M) by a numerical approximation. The introduction of the pedestal reduces the thermal conductance requiring the modification of equation:

$$K_{EFF} = \frac{2kA}{l}\left[1 + \frac{k_i(1-\omega)}{k\omega}\right] \qquad 7.2.3.4.$$

The resulting configuration introduces a three-dimensional heat conduction problem. The pedestal material being of good thermal conductivity are assumed to be at the same temperature as the cold junction to which they are attached. As a general requirement the pedestal should be on the cold side of the thermoelement in order to minimize the undesirable temperature drop across the column. The problem and subsequent solution will depend on the height of the pedestal, material properties, packing density, pedestal shape etc. Section 7.4.3.3 will contain a proposed technique for determining pedestal inter-element heat leakage and the calculation of its magnitude.

However, if one element (n- or p-) is mounted on an individual pedestal (figure 7.4.1.2) the net effect is the introduction of additional electrical resistance on the cold side. Figure 7.4.1.2 illustrates the pedestal/element configuration. By mounting the two thermoelements

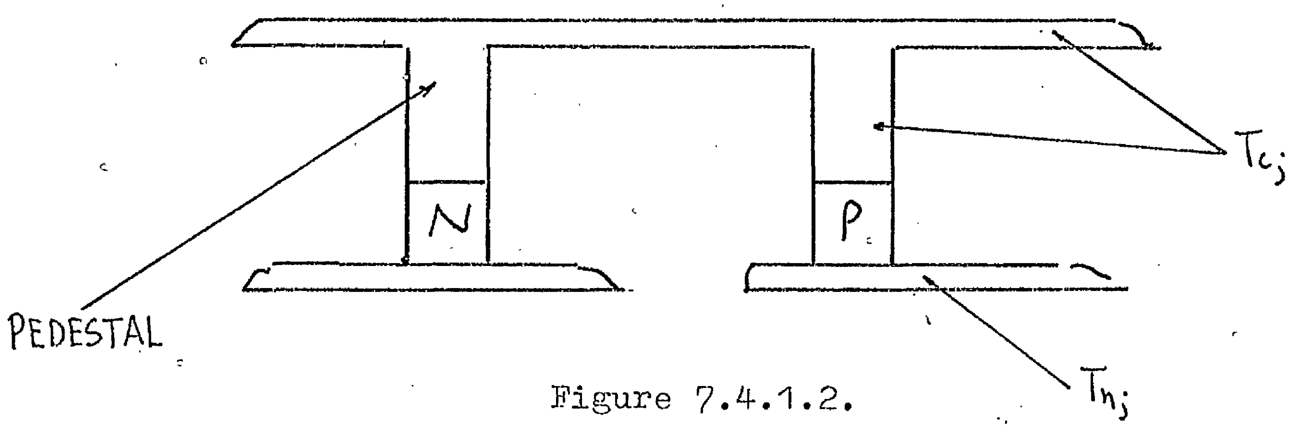

Figure 7.4.1.2.

Pedestal/Element Configuration.

as close as possible reduces the length of the electrical conductance straps on the cold side. Strap resistance will be neglected hence the effective resistance relationship (fundamentaly equation 7.2.5.3) will be utilized. The effect of strap resistance (hot side, cold side) on the C.O.P. has been investigated and the results indicate that neglecting the strap resistance ($\gamma(T)$) is of minor consequence.

7.4.3 Definition and Solution Parameters.

7.4.3.1 Solution Technique.

The configuration illustrated in figure 7.4.1.1. is a cross sectional view of a couple-pedestal assembly. The solution requires calculating the heat leakage from the hot to cold junction plates of the module through the thermal insulation cell. The total heat leakage is assumed

(1) The leakage to the cold plate through the thermal insulation cell.

(2) The leakage to the area of the pedestal end not covered by the thermoelements (heat leakage 'underneath' the pedestal.

(3) Leakage to the sides of the cold pedestal (fringe leakage)

The solution required is to evaluate the three-dimensional heat conduction effects to the cold surface composed of the cold junction plate and the sides of the pedestal/thermoelement. Heat leakage underneath the pedestal is assumed to be a one-dimensional problem.

7.4.3.2 Approach.

The approach described involves developing a mathematical model (an approximation) for the three-dimensional heat conduction problem. The inspiration for seeking a dimensionless solution associated with the heat flow model (figure 7.4.3.3.1) was based on discussions the author had with Prof. T.F. Nonweiler (Department of Aeronautics and Fluid Mechanics, University of Glasgow). The geometrical system was proposed in reference (9). The method resulting translated the geometrical system (9) into a useful form for module performance and incorporates the heat leakage underneath the pedestal.

7.4.3.3 Major Assumptions.

The major assumptions made in developing the solution of the mathematical model is as follows:

(1) All space between the hot and cold plates not occupied by the pedestal/thermoelement assembly is filled with isotropic thermal insulation.

(2) The temperature of the pedestal and the cold plate junction are equal. This assumption is based on the pedestal material being of high thermal conductivity (Cu or Alu). Figure 7.4.1.1 indicates that the cold plate is an integral part of the supporting pedestal.

(3) The hot plate junction temperature is uniform and equal to the junction temperature.

(4) The pedestals are cylindrical and arranged in a square array within the module.

(5) One pedestal supports a thermoelectric couple.

These assumptions suggest the following mathematical model. A hollow cylindrical insulation cell as shown in figure 7.4.3.3.1, with the inner radius of the cell that of the thermoelectric-pedestal and the outer radius half the distance between adjacent pedestal centres.

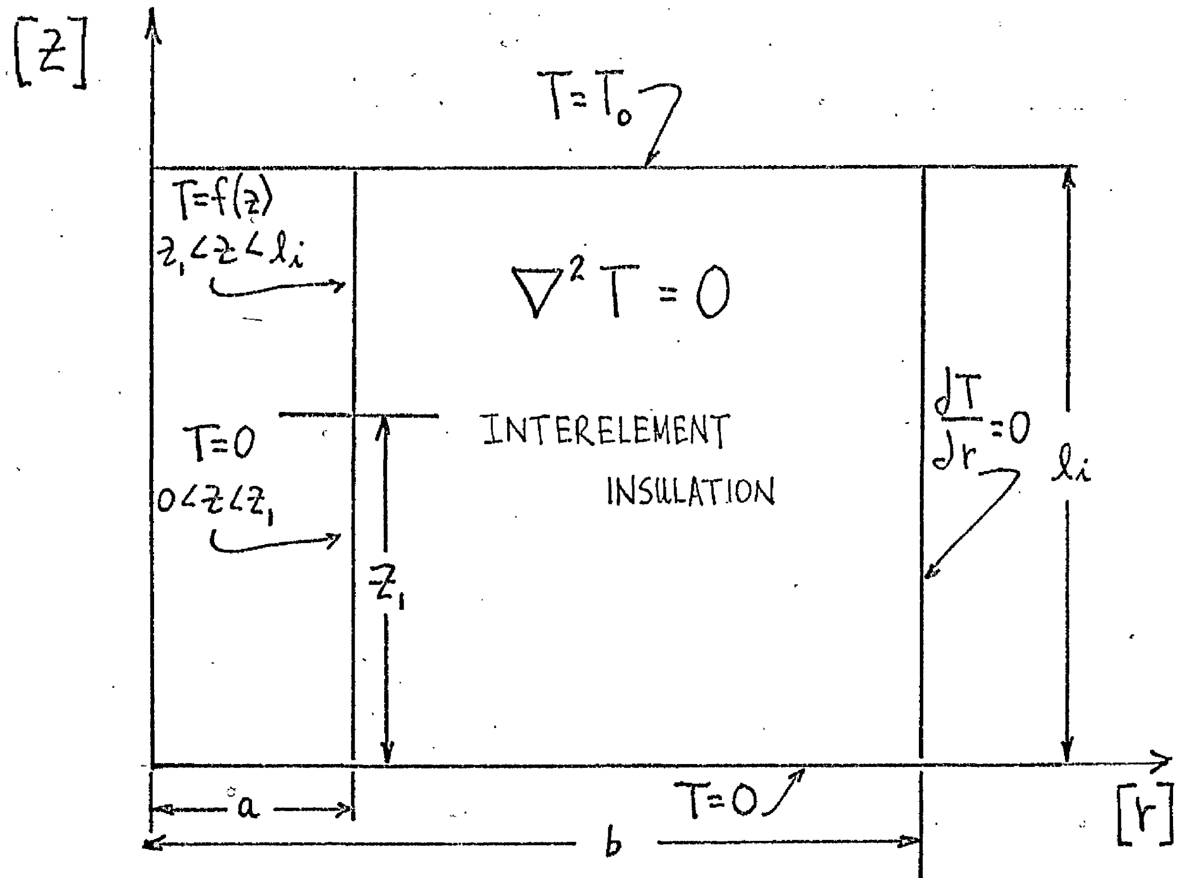

Figure 7.4.3.3.1.

Boundary Conditions for Interelement Insulation.

The following boundary conditions apply to figure 7.4.3.3.1.

(a) The top surface of the interelement insulation is isothermal at temperature, T_{h_j}

(b) The bottom surface of the interelement insulation is isothermal at temperature, T_{c_j}

(c) An adiabatic condition exists on the outer cylindrical surface

(d) The inner cylinder surface is isothermal at temperature T_{c_j} along the height of the pedestal and is subject to a linear temperature gradient from T_{h_j} to T_{c_j} along the height of the thermoelectric element.

The steady-state temperature distribution within the interelement insulation cell will be developed by a numerical determination of the finite difference equation representing the mathematical model (figure 7.4.3.3.1). The method of successive over-relaxation (modification to Gauss-Seidel method) was employed in the iterative loop to make a substantial improvement in the rate of convergence. The total insulation heat leakage is found by integrating[1] the axial derivative of the insulation temperature over the upper surface of the insulation cell.

$$q_{ACT} = -K_i \int_a^b 2\pi r \left.\frac{dT}{dz}\right|_{z=l} dr \qquad 7.4.3.3.1.$$

Design curves will be given in Appendix M for different values of the geometrical parameters associated with the heat flow model that yield the values of q_{ACT}/q_{mi} (Heat Flux Ratio).

(1) The integration is replaced by a series summation as the temperatures are at finite intervals. Appendix M contains the required transformation.

7.4.3.4 Nomenclature.

The additional symbols used are defined as follows:

A cross-sectional area of a thermoelement, cm^2

A_p cross-sectional area of a pedestal, cm^2

A_m module area per couple, cm^2

where:

$$A_m = 2A + A_i \quad \text{and}$$

A_i is defined by equation 7.2.2.3.

l thermoelement height, cm

l_i total thickness of thermal insulation, cm

where: $$l_i = l + l_p$$

l_p height of pedestal column, cm

l^* dimensionless parameter defined by equation 7.4.3.5.13

q_{iT} total heat leakage per couple through the interelement insulation, watts

q_{mi} normal one dimensional heat leakage per couple from hot junction plate to cold junction plate ignoring effects of pedestal, (q_{mi}), watts

q_{ACT} actual heat leakage per couple to cold side junction plate and pedestal sides, watts

q_{UND} heat leakage to the area of the pedestal end not covered by the thermoelements (underneath the pedestal, watts

(1) The pedestal side heat leakage is assumed to be appropriately accounted for by the left hand side boundry conditions.

r^* dimensionless parameter defined by equation 7.4.3.5.10

ΔT_j hot to cold junction temperature difference, ^oC

β^* dimensionless parameter defined by equation 7.4.3.5.5.

k_m, k_p thermal conductivity of thermoelement, watts/ cm^oC

k_i thermal conductivity of interelement insulation, watts/cm^oC

ω packing density defined by equation 7.2.2.1

7.4.3.5. Geometrical Parameters.

The heat flux ratio curves in Appendix M present the ratio q_{ACT}/q_{mi} as a function of the geometrical pedestal parameters (β^*, r^*, ℓ^*). The heat leakage parameter q_{ACT}/q_{mi} is proposed as a quantity to be utilized for estimating the total thermal heat flux from the hot junction surface to the cold junction surface.

From equation 7.3.2.3:

$$Q_s = T_{cj} I \alpha_{np} - \frac{1}{2} I^2 R_{EFF} - K_{EFF} \Delta T_j \qquad 7.3.2.3.$$

and:

$$K_{EFF} = \frac{2kA}{\ell} + \frac{k_i A_i}{\ell} \qquad 7.2.3.2.$$

Introducing equation 7.2.3.2 into equation 7.3.2.3 results:

$$Q_s = T_{cj} I \alpha_{np} - \frac{1}{2} I^2 R_{EFF} - \left[\frac{2kA}{\ell} + \frac{k_i A_i}{\ell}\right] \Delta T_j \qquad 7.4.3.5.1$$

where:

(1) The third term is the heat conducted through the thermocouple

(2) The fourth term is the heat conducted through the interelement insulation.

The heat pump rate for the pedestal supported thermoelectric couple (figure 7.4.1.1) is expressed as:

$$Q_s = T_{cj} I \alpha_{np} - \frac{1}{2} I^2 R_{EFF} - k_i \int_a^b 2\pi r \left.\frac{dT}{dz}\right|_{z=\ell} dr - \frac{2kA}{\ell} \Delta T_j - \left[\frac{A_p - 2A}{\ell}\right] k_i \Delta T_j \qquad 7.4.3.5.2.$$

where:

(1) The third term is the heat conduction through the interelement insulation cell,

(2) The fourth term is the heat conduction through the thermocouples

(3) The fifth term is the heat conducted through the insulation underneath the pedestal,

The model geometry consists of cylindrical pedestals in a square array assembly. The dimensionless parameters are as follows:

Defining bstar (β^*) as:

$$\beta^* \equiv \ell_i / b \qquad 7.4.3.5.3.$$

$$A_m = \pi b^2 \qquad 7.4.3.5.4.$$

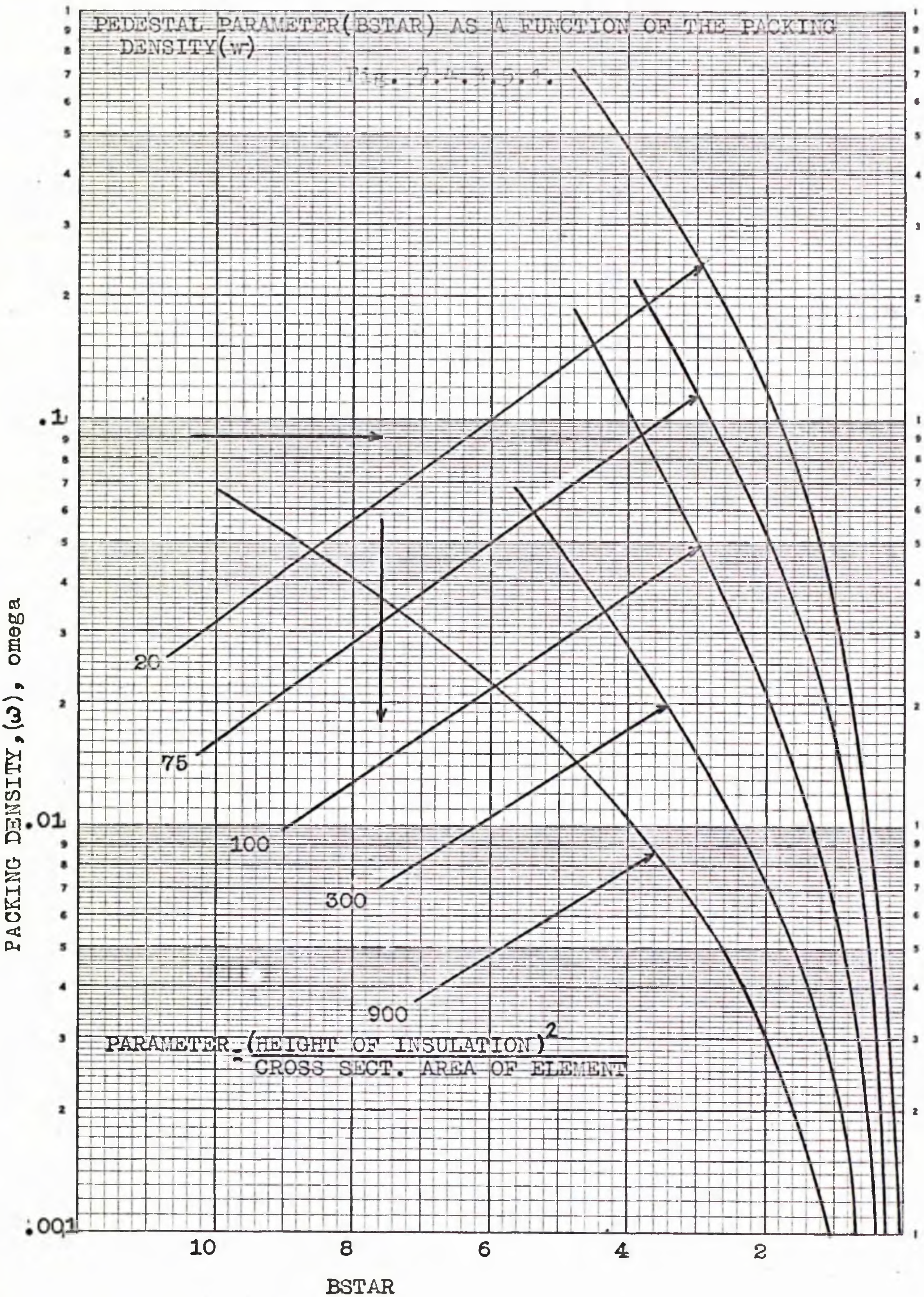
PEDESTAL PARAMETER(BSTAR) AS A FUNCTION OF THE PACKING DENSITY(w)
Fig. 7.4.3.5.4.
PACKING DENSITY,(ω), omega
.1
.01
.001
20
75
100
300
900
PARAMETER = (HEIGHT OF INSULATION)² / CROSS SECT. AREA OF ELEMENT
10
8
6
4
2
BSTAR

where:

A_m module area, cm^2

Introducing $\omega = 2A/A_m$ and combining the equations results:

$$\beta^* = l_i \sqrt{\frac{\pi\omega}{2A}} \qquad 7.4.3.5.5.$$

Figure 7.4.3.5.1 illustrates the effect of packing density (ω) as a function of β^* for variation in the parameter l_i^2/A

Defining (r^*) as:

$$r^* \equiv a/b \qquad 7.4.3.5.6.$$

with:

$$A_m = \pi b^2 \qquad 7.4.3.5.4.$$

Introducing $\omega = \frac{2A}{A_m}$ and combining the equations results:

$$r^* = \frac{a\,\pi^{\frac{1}{2}}\omega^{\frac{1}{2}}}{2^{\frac{1}{2}}A^{\frac{1}{2}}} \qquad 7.4.3.5.7.$$

The pedestal area is defined as:

$$A_p = \pi a^2 \qquad 7.4.3.5.8.$$

then:

$$a = A_p^{\frac{1}{2}} / \pi^{\frac{1}{2}} \qquad 7.4.3.5.9.$$

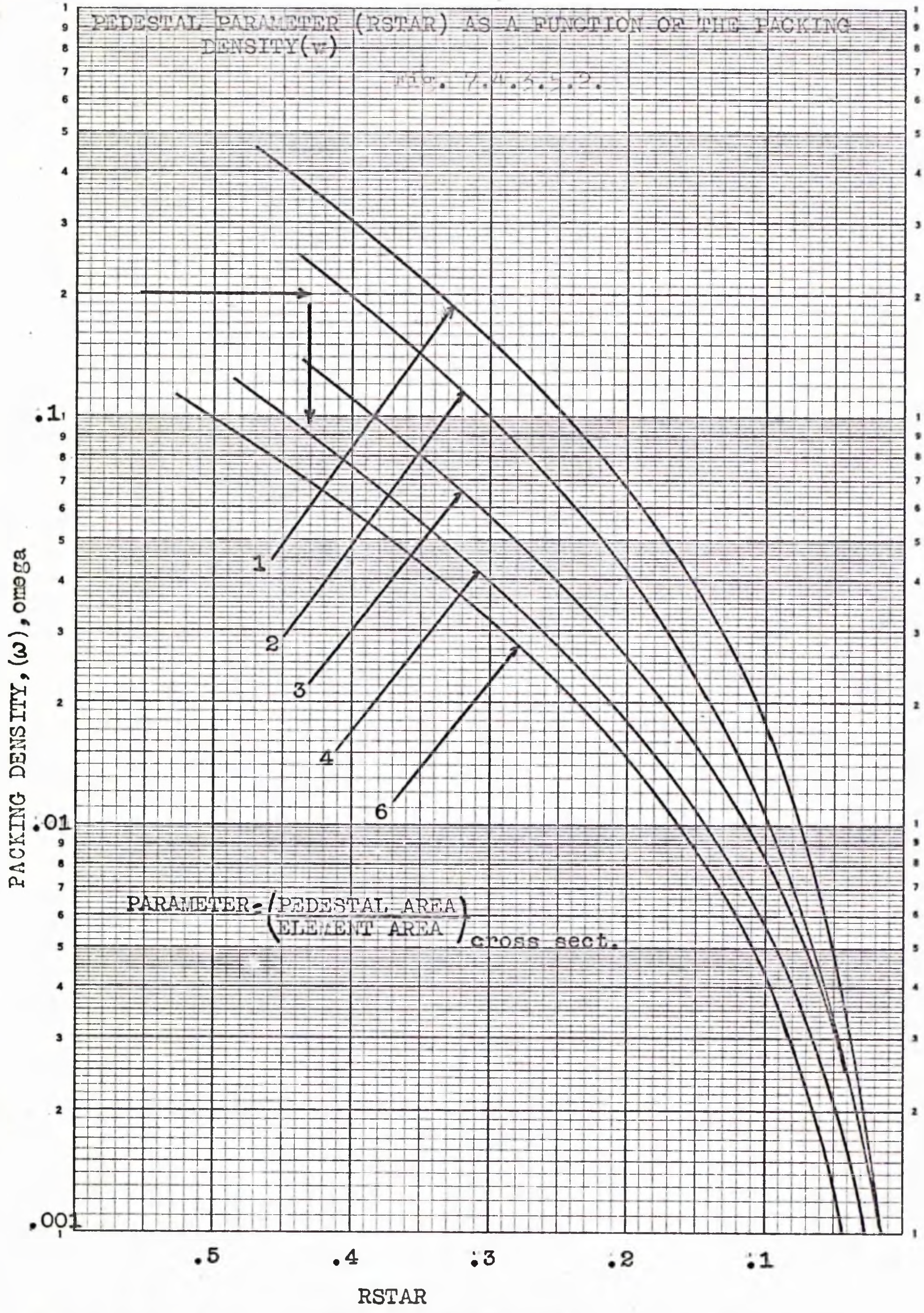

PEDESTAL PARAMETER (RSTAR) AS A FUNCTION OF THE PACKING DENSITY(w)
Fig. 7.4.3.5.2.
PACKING DENSITY, (ω), omega
.1
.01
.001
.5
.4
.3
.2
.1
RSTAR
1
2
3
4
6
PARAMETER = (PEDESTAL AREA / ELEMENT AREA) cross sect.

Introducing equation 7.4.3.5.9 into equation 7.4.3.5.7 results:

$$r^* = \sqrt{\frac{A_p \omega}{2A}} \qquad 7.4.3.5.10.$$

Figure 7.4.3.5.2 illustrates the packing density (ω) as a function of r^*, for variation in the parameter A_p/A

Defining lstar (l*) as:

$$l^* \equiv l/l_i \qquad 7.4.3.5.11.$$

and

$$l = l_i - l_p \qquad 7.4.3.5.12.$$

Combining gives:

$$l^* = 1 - l_p/l_i \qquad 7.4.3.5.13.$$

Figure 7.4.3.5.3. illustrates l* as a function of the ratio l_p/l_i.

The total heat leakage through the insulation is expressed as:

$$q_{iT} = q_{ACT} + q_{UND} \qquad 7.4.3.5.14.$$

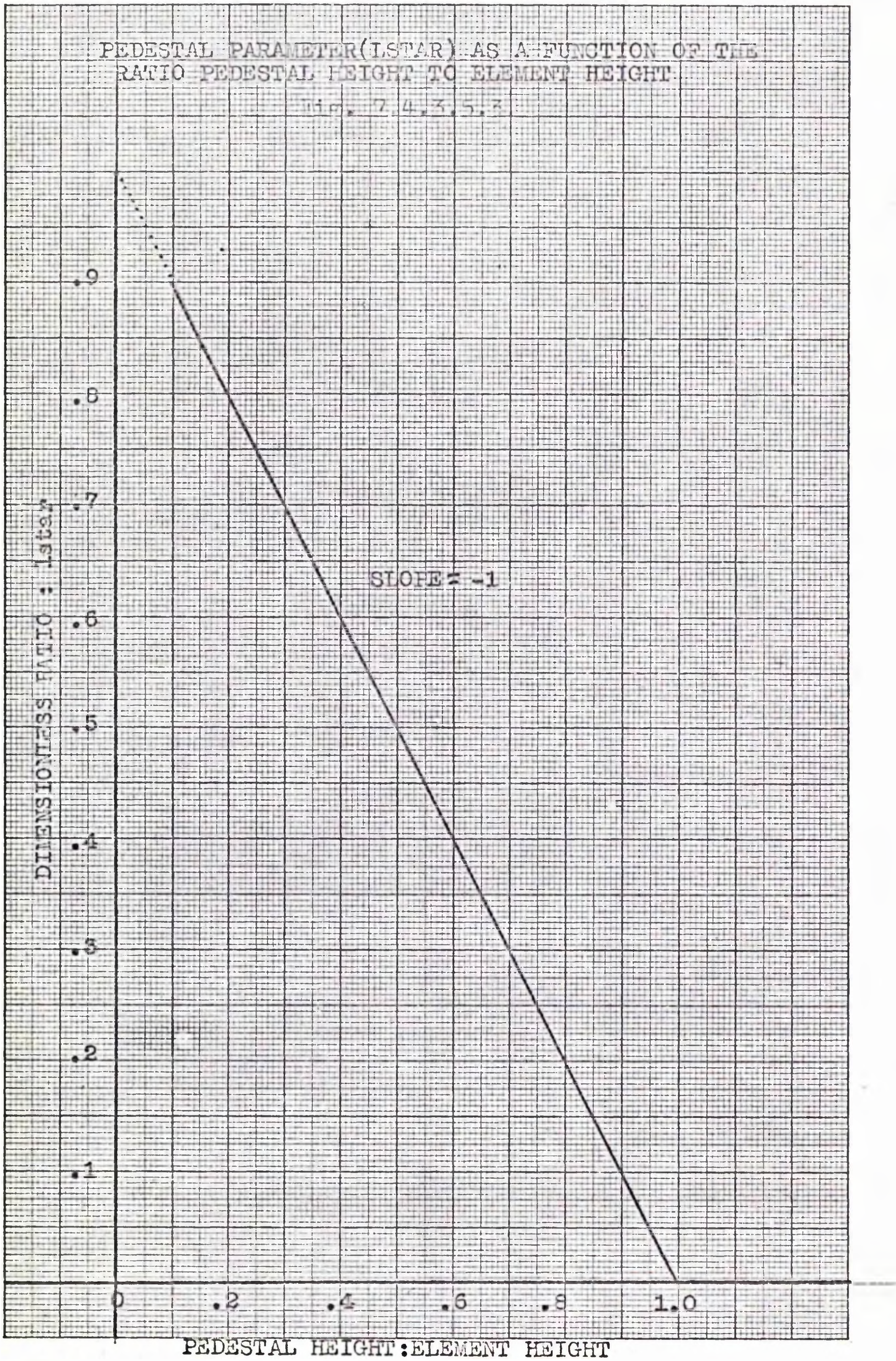
PEDESTAL PARAMETER(LSTAR) AS A FUNCTION OF THE RATIO PEDESTAL HEIGHT TO ELEMENT HEIGHT
Fig. 7.4.3.5.3
SLOPE = -1
DIMENSIONLESS RATIO : lstar
.9
.8
.7
.6
.5
.4
.3
.2
.1
0
.2
.4
.6
.8
1.0
PEDESTAL HEIGHT:ELEMENT HEIGHT

The normal one-dimensional heat leakage from the hot junction plate to the cold junction plate ignoring the pedestal effect is expressed as:

$$q_{mi} = \left[\frac{A_m - A_p}{l}\right] k_i \Delta T_j \qquad 7.4.3.5.15.$$

The heat leakage underneath the pedestal is expressed as:

$$q_{UND} = \left[\frac{A_p - 2A}{l}\right] k_i \Delta T_j \qquad 7.4.3.5.16.$$

Equation 7.4.3.5.14 is presented in the following format, taking advantage of the heat flux ratio (Appendix M)

$$q_{iT} = \left[\frac{q_{ACT}}{q_{mi}}\right] q_{mi} + q_{UND} \qquad 7.4.3.5.17.$$

Introducing the basic relations for q_{mi} and q_{UND} results:

$$q_{IT} = \frac{q_{ACT}}{q_{mi}}\left[\frac{A_m - A_p}{l}\right] k_i \Delta T_j + \left[\frac{A_p - 2A}{l}\right] k_i \Delta T_j \qquad 7.4.3.5.18.$$

factoring and introducing the packing density results:

$$\frac{q_{IT}}{k_i \Delta T_j} = \frac{q_{ACT}}{q_{mi}} \frac{2A}{l_i \omega}\left[1 - \frac{A_p \omega}{2A}\right] + \frac{2A}{l}\left[\frac{A_p}{2A} - 1\right] \qquad 7.4.3.5.19.$$

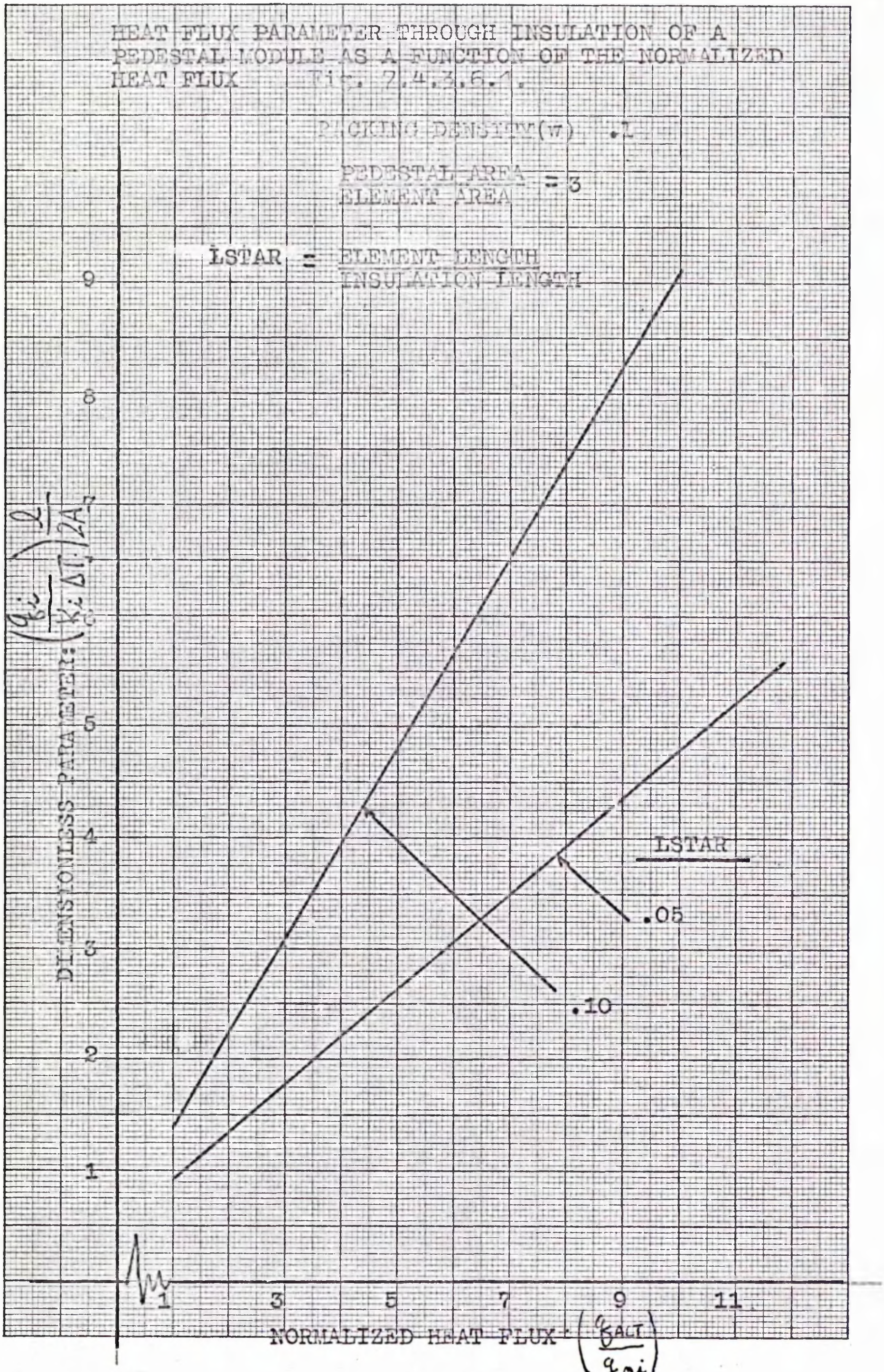
HEAT FLUX PARAMETER THROUGH INSULATION OF A PEDESTAL MODULE AS A FUNCTION OF THE NORMALIZED HEAT FLUX Fig. 7.4.3.6.1.
PACKING DENSITY(π) .1
PEDESTAL AREA / ELEMENT AREA = 3
LSTAR = ELEMENT LENGTH / INSULATION LENGTH
LSTAR
.05
.10
DIMENSIONLESS PARAMETER: $\left(\frac{q_i}{k_i \Delta T_i}\right)\frac{l}{2A_i}$
NORMALIZED HEAT FLUX $\left(\frac{q_{ALT}}{q_{ni}}\right)$
1
2
3
4
5
6
7
8
9
11

Multiply both sides of equation 7.4.3.5.19 by $(l/2A)$ results:

$$\frac{q_{IT}\,l}{k_i\,\Delta T_j\,2A} = \frac{q_{ACT}}{q_{mi}}\,\frac{l}{l_{i\omega}}\left[1-\frac{A_{p\omega}}{2A}\right] + \left[\frac{A_p}{2A}-1\right] \qquad 7.4.3.5.20.$$

7.4.3.6 Discussion and Results.

The procedure for calculating the total heat leakage (q_{IT}) through the thermal insulation all for a given pedestal module configuration is as follows:

(1) Evaluate the parameters: β^* (equation 7.4.3.5.5), r^* (equation 7.4.3.5.10), 1* (equation 7.4.3.5.11)

(2) From Appendix M the heat flux ratio q_{IT}/q_{mi} is determined from the appropriate graph.

(3) The heat leakage parameter using equation 7.4.3.5.19 or equation 7.4.3.5.20 depending upon the form of the parameter is required.

A computer program (C.P.5 procedure phaseq) has been developed to solve by finite differences (Over-Relaxation Method) the partial differential equation as required for obtaining the heat flux ratio and the subsequent solution of equation 7.4.3.5.20.

Figures 7.4.3.6.1 and 7.4.3.6.2 illustrate the heat leakage parameter $\left[q_{IT}\,l/k_i\,\Delta T_j\,2A\right]$ as a function of the heat

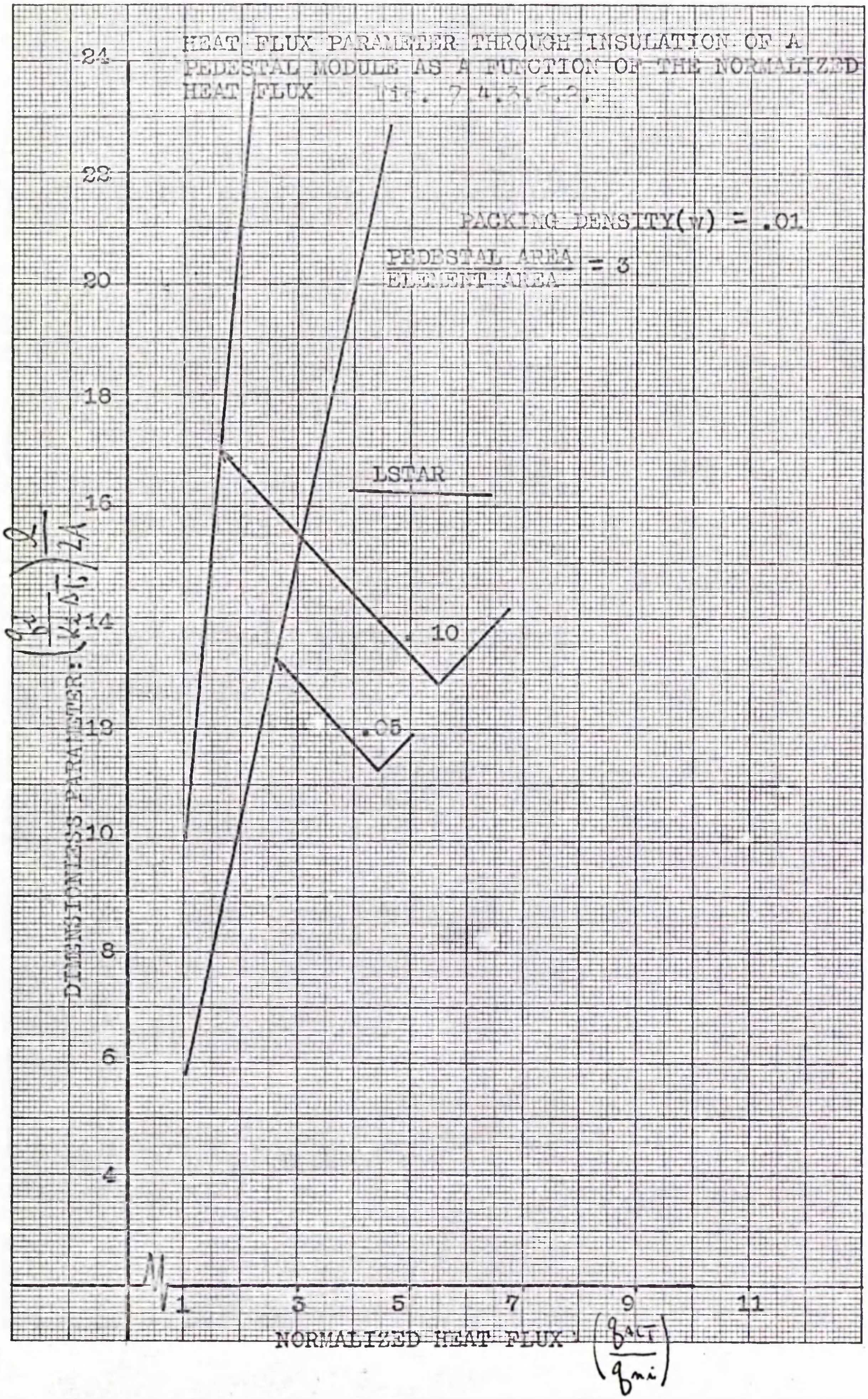

HEAT FLUX PARAMETER THROUGH INSULATION OF A PEDESTAL MODULE AS A FUNCTION OF THE NORMALIZED HEAT FLUX Fig. 7.4.3.6.2
PACKING DENSITY(v) = .01
PEDESTAL AREA / ELEMENT AREA = 3
LSTAR
.10
.05
24
22
20
18
16
14
12
10
8
6
4
1
3
5
7
9
11
DIMENSIONLESS PARAMETER: $\left(\frac{q_i}{k_i \Delta T_i}\right)\frac{l}{2A}$
NORMALIZED HEAT FLUX $\left(\frac{q_{ALT}}{q_{ni}}\right)$

flux ratio q_{iT}/q_{mi} (Normalized Heat Flux) with variation in the dimensionless parameter 1*. The results are for a Constant insulation height (l_i) of 2cm and a pedestal cross sectional area of three times the cross sectional area of a thermoelement.

The left hand side of equation 7.4.3.5.20 (ordinate of figure 7.4.3.6.1) if multiplied by the ratio of the thermal conductivity of the insulation cell (k_i) to the thermal conductivity of the thermoelement yields the ratio of the heat leakage (total) through the insulation cell to the heat conduction loss (at zero current) through the thermocouple.

From equation 7.4.3.5.20

$$\frac{q_{iT}\, l\, k_i}{k_i\, \Delta T_j\, 2 A\, k} \equiv \frac{q_{iT}}{q_{\text{COUPLE}}}$$

For example the value of the ratio (k_i/k) for Freon-foamed polyurethane insulation and bismuth telluride is approximately .015 (at room temperature). From figure 7.4.3.6.3 at 1 = .20cm, A = .03cm^2, ω = .01 and l_i = 2.0cm the heat flux parameter is approximately 20. This results in that the total heat leakage through the insulation cell is 30% of the heat conducted through the thermocouple at zero current. The percentage decreases significantly as the area of the thermoelement increases ($\omega = 2A/A_m$), since this heat flux area increases faster than the area on the sides of the pedestals.

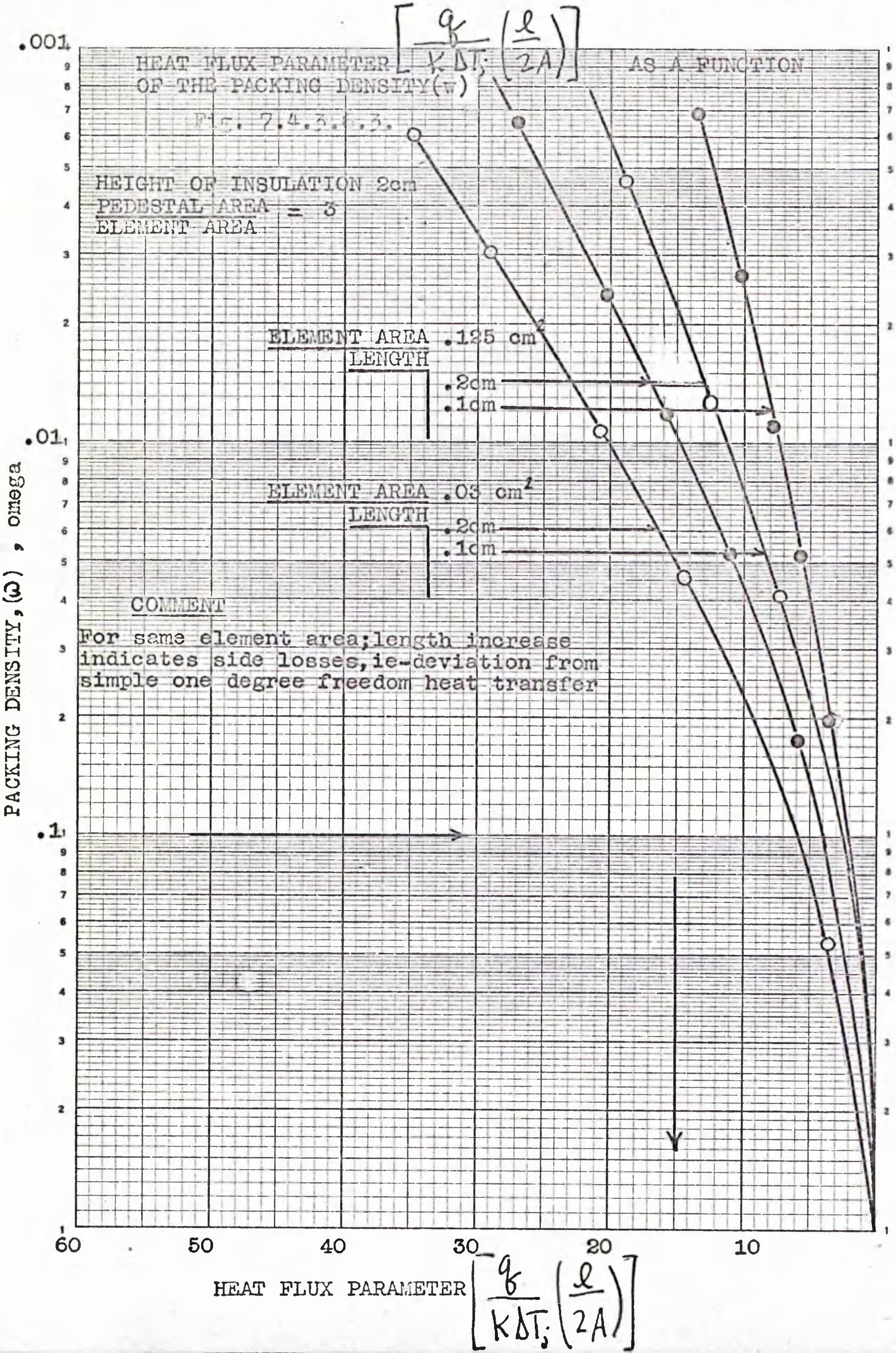
HEAT FLUX PARAMETER $\left[\frac{q}{k\Delta T_i}\left(\frac{l}{2A}\right)\right]$ AS A FUNCTION OF THE PACKING DENSITY(w)
Fig. 7.4.3.6.3.
HEIGHT OF INSULATION 2cm
PEDESTAL AREA / ELEMENT AREA = 3
ELEMENT AREA .125 cm^2
LENGTH
.2cm
.1cm
ELEMENT AREA .03 cm^2
LENGTH
.2cm
.1cm
COMMENT
For same element area; length increase indicates side losses, ie-deviation from simple one degree freedom heat transfer
PACKING DENSITY, (ω) , omega
.001
.01
.1
1
60
50
40
30
20
10
HEAT FLUX PARAMETER $\left[\frac{q}{K\Delta T_i}\left(\frac{l}{2A}\right)\right]$

Figure 7.4.3.6.4 and figure 7.4.3.6.5 illustrate the effect of packing density (ω) on the heat flux parameter. For a packing density $\longrightarrow$ unity the heat flux parameter $\longrightarrow$ zero (as the interelement cross sectional area $\longrightarrow$ 0).

For a given module configuration and material properties a technique is presented for determining the effect of pedestal geometry for improved module performance. Increasing pedestal height decreases the total heat leakage through the interelement insulation cell. On the other hand the pedestal is not isothermal (as assumed). There is associated with the pedestal a temperature drop between the cold surface and the cold junction interfacing with the thermoelectric couple. As pedestal length increases, this temperature drop increases degrading module performance. For best performance the 'optimum' pedestal height occurs at the point where the heat leakage through the insulation and pedestal temperature drop is acceptable. In this concept, there may be some advantage to use other than cylindrical pedestals. For example, a tapered pedestral with the larger end affixed to the cold plate may reduce the pedestal temperature drop at the expense of only a small increase in heat leakage.

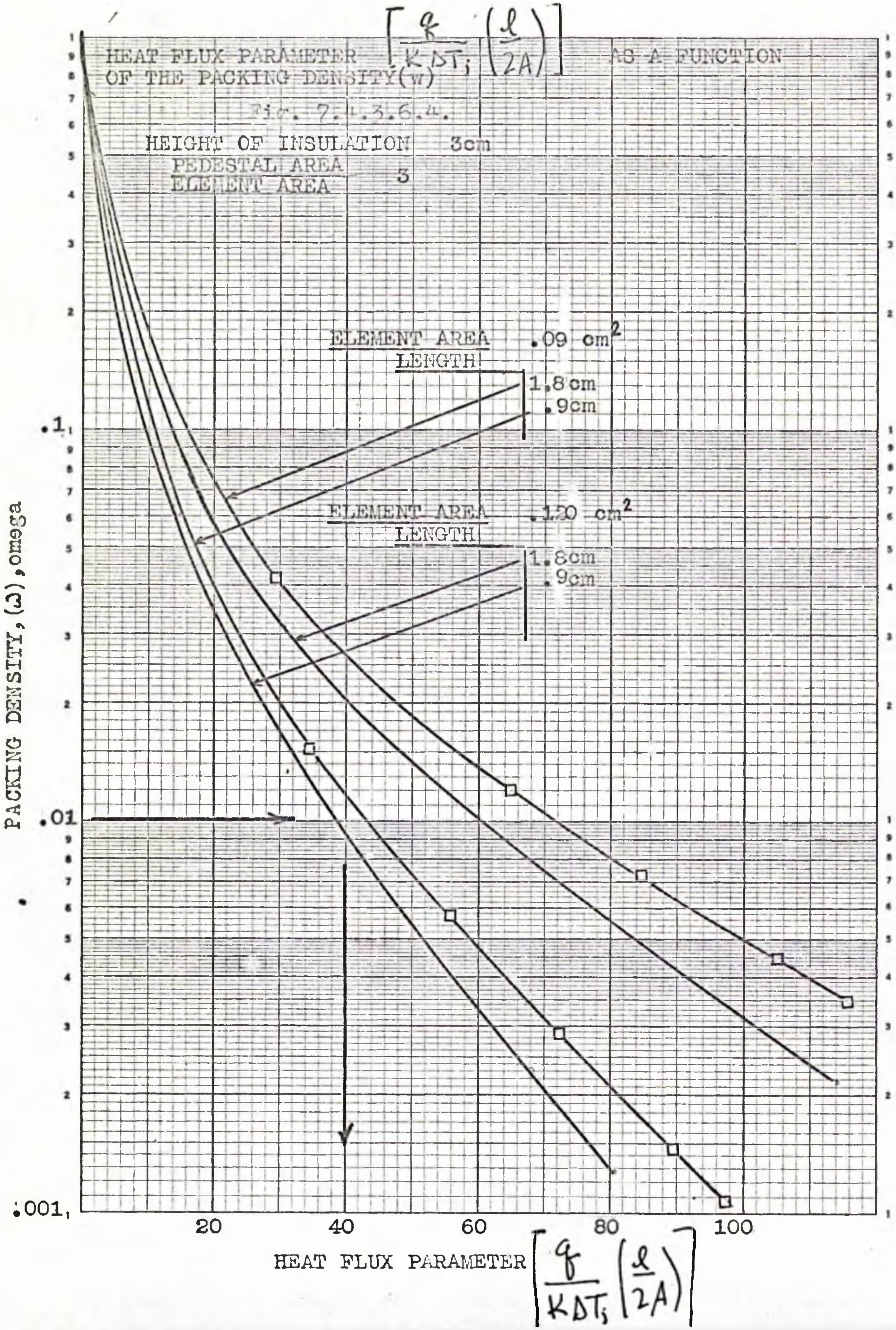

HEAT FLUX PARAMETER $\left[\frac{q}{K\Delta T_i}\left(\frac{l}{2A}\right)\right]$ AS A FUNCTION OF THE PACKING DENSITY(w)
Fig. 7.4.3.6.4.
HEIGHT OF INSULATION 3cm
$\frac{\text{PEDESTAL AREA}}{\text{ELEMENT AREA}}$ 3
$\frac{\text{ELEMENT AREA}}{\text{LENGTH}}$ .09 cm^2
1.8cm
.9cm
$\frac{\text{ELEMENT AREA}}{\text{LENGTH}}$ .120 cm^2
1.8cm
.9cm
PACKING DENSITY, (ω), omega
.1
.01
.001
20
40
60
80
100
HEAT FLUX PARAMETER $\left[\frac{q}{K\Delta T_i}\left(\frac{l}{2A}\right)\right]$

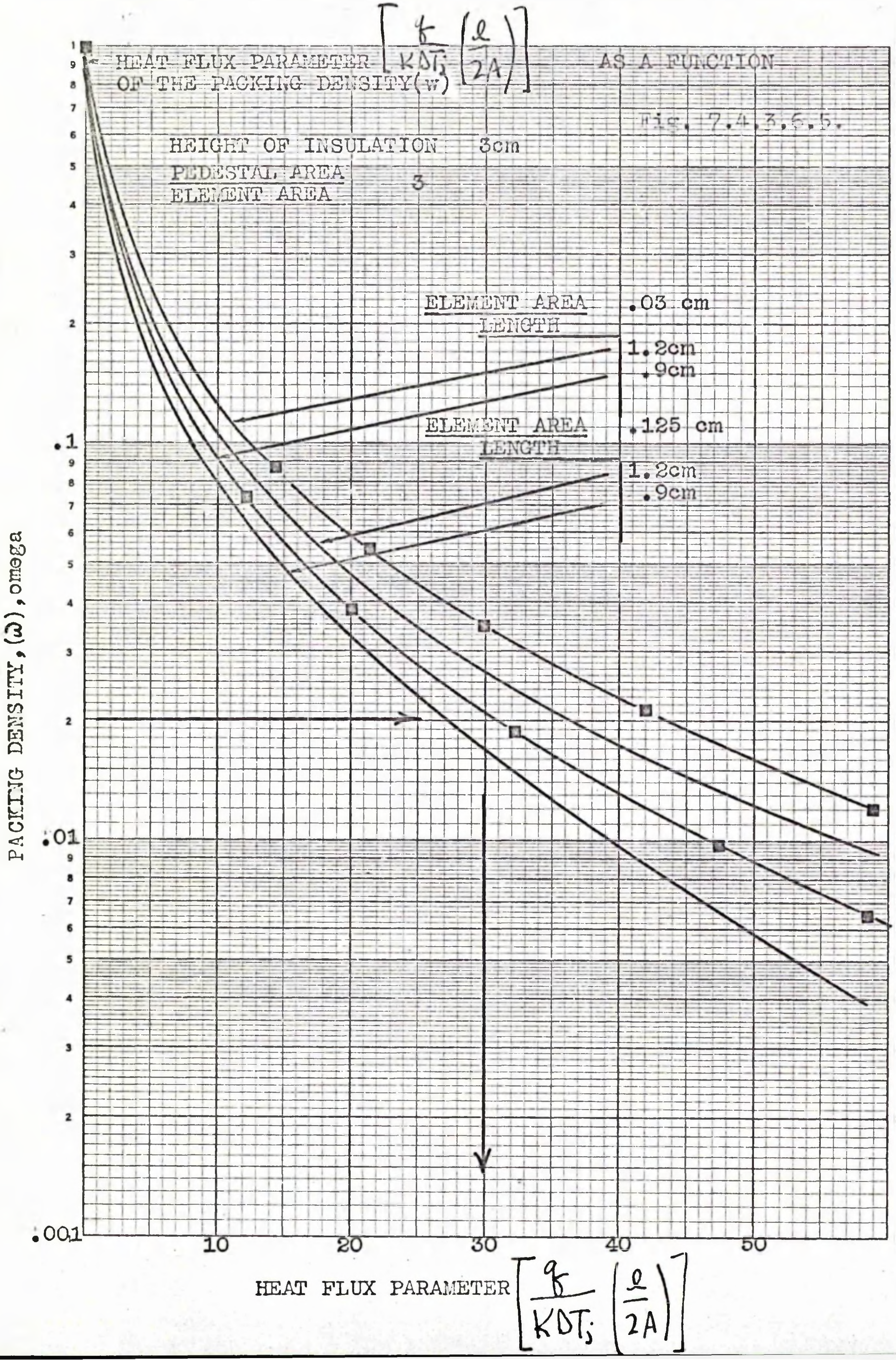
HEAT FLUX PARAMETER $\left[\frac{q}{KDT_i}\left(\frac{l}{2A}\right)\right]$ AS A FUNCTION OF THE PACKING DENSITY(w)
Fig. 7.4.3.6.5.
HEIGHT OF INSULATION 3cm
PEDESTAL AREA / ELEMENT AREA 3
ELEMENT AREA / LENGTH .03 cm
1.2cm
.9cm
ELEMENT AREA / LENGTH .125 cm
1.2cm
.9cm
PACKING DENSITY,(ω),omega
.1
.01
.001
10
20
30
40
50
HEAT FLUX PARAMETER $\left[\frac{q}{KDT_i}\left(\frac{l}{2A}\right)\right]$

7.4.4. Module Performance Program.

7.4.4.1 Introduction.

This section describes the basic relationships required for calculating the performance of thermoelectric module considering an internal energetic processes. The resulting computer program (C.P.2.) calculates for a given module design the performance characteristics for various cold junction temperature (T_{cj}), hot to cold junction temperature difference (ΔT_j) and currents.

7.4.4.2 Nomenclature.

The basic symbols utilized in this section are as follows:

- A cross sectional area of thermoelement, cm^2
- A_m module cross sectional area, cm^2
- F form factor (Section 7.3.2)
- f Switching factor (f = 1 for modules without pedestals, f = 0 for modules with pedestals)
- γ heat leakage parameter for modules with pedestals ($\gamma = q_{1T} / k_i \Delta T_j$) equation 7.4.3.5.19.
- I d.c. current, amps.
- I_Q d.c. current for maximizing heat pump rate, amps
- θ dimensionless current ratio (defined by equation 6.7.1)
- θ_ϕ dimensionless current ratio at maximum C.O.P.

(defined by equation 7.4.4.4.6)

K_{EFF} effective thermal conductance (equation 7.2.3.4), watts /^{o}C

l thermoelement height, cm

Q_S heat pump rate, watts

Q_R heat rejection rate, watts

R_{EFF} effective electrical resistance (equation 7.2.5.3) ohms

α_{np} couple Seebeck coefficient, volts/^{o}C

$$\alpha_{np} = |\alpha_n| + |\alpha_p|$$

T_{cj} cold junction temperature, ^{o}K

V d.c. voltage per couple, volts

Z_{EFF} effective figure of merit (equation 7.2.5.1)

ΔT_j junction temperature difference, ^{o}C

$\Delta T_{j\,max}$ maximum junction temperature difference, ^{o}C

$\Delta T_{j\,max\,eff}$ effective maximum junction temperature difference, ^{o}C

k thermal conductivity of thermoelement, watts/cm-^{o}C

k_i thermal conductivity of interelement insulation, watts/cm -^{o}C

ρ thermoelement electrical resistivity, ohm - cm sigma (σ) = $1/\rho$

ρ_j junction resistivity, ohm - cm^2

ϕ Coefficient of Performance

ω Packing density

7.4.4.3 Major Assumptions.

The assumptions are for simplicity in presentation. The computer program (C.P.2.) contains provisions for eliminating assumption which may limit the analysis required. The assumptions are as follows:

(1) The thermoelement materials are equal in magnitude

(2) All materials are invariant with temperature

(3) Conducting electrical straps resistance is neglected

(4) The hot and cold junction plates are isothermal

(5) The module configuration is planar

7.4.4.4 Equations.

The equations involved in the resulting computer program are listed below in the order in which they would generally be applied. The equations include the concept of effective resistance, conductance as described in section 7.2. The equations are the same or modifications of relationships appearing in the previous sections. The equations that are particular to this section are developed herein.

$$R_{EFF} = \frac{2}{A}\left[\rho l + 2\rho_j\right]F^2 \qquad 7.4.4.4.1.$$

Equation 7.4.4.4.1 defines the effective electrical resistance with the introduction of the current form factor.

The factor is introduced to permit the inclusion of power supply ripple.

The effective thermal conductance with the exclusion of the pedestal effect is expressed as:

$$K_{EFF} = \frac{2kA}{l}\left[1 + \frac{k_i(1-\omega)}{k\omega}\right] \qquad 7.2.3.4.$$

Including the effect of the pedestal supported thermocouple on the interelement heat transfer, equation 7.2.3.4 becomes:

$$K_{EFF} = \frac{2Ak}{l} + k_i\left[\frac{f2A(1-\omega)}{l\omega} + g(1-f)\right] \qquad 7.4.4.4.2.$$

where:

$$g = g_{iT} / k_i \Delta T_j$$

(as defined by equation 7.4.3.5.19)

Equation 7.4.4.4.2 represents the following terms:

(1) The first term is the couple thermal conductance, watts/$^{\circ}$C

(2) The second term is insulation thermal conductance, no pedestal

(3) The third term is insulation thermal conductance, pedestal assembly

The effective figure of merit is defined as :

$$Z_{EFF} = \frac{\alpha_{np}^2}{R_{EFF} \cdot K_{EFF}} \qquad 7.2.5.1.$$

and

$$\Delta T_{j_{max\,eff}} = 0.5\, T_{c_j}^2\, Z_{EFF} \qquad 7.2.5.2.$$

For fixed hot junction temperature (T_{h_j}) the minimum cold junction temperature ($T_{c_{j_{min\,eff}}}$) is expressed as:

$$T_{c_{j_{min\,eff}}} = \frac{\sqrt{1 + 2Z_{EFF}T_{h_j}} - 1}{Z_{EFF}} \qquad \begin{array}{c} 7.4.4.4.3 \\ (6.5.6.8) \end{array}$$

then

$$\Delta T_{j_{max\,eff}} = T_{h_j} - T_{c_{j_{min\,eff}}} \qquad 7.4.4.4.4.$$

$$I_\varphi = \frac{\alpha_{np}\, T_{c_j}}{R_{EFF}} \qquad \begin{array}{c} 7.4.4.4.5. \\ (6.5.4.1) \end{array}$$

The dimensionless current ratio $\left(I_\phi / I_\varphi\right)$ is expressed as:

$$\mu_\phi = \frac{\Delta T_j}{T_{c_j}} \left[\frac{1 + \sqrt{1 + Z_{EFF}\left[\frac{\Delta T_j}{2} + T_{c_j}\right]}}{Z_{EFF}\left[\frac{\Delta T_j}{2} + T_{c_j}\right]} \right] \qquad 7.4.4.4.6.$$

Equation 7.4.4.4.6 will be developed in section 7.4.4.5.

$$V = I R_{EFF} + \alpha_{np}\, \Delta T_j \qquad 7.4.4.4.7.$$

Introducing the dimensionless current ratio (θ) into equation 7.4.4.4.7.

$$V = \theta I_\varphi R_{EFF} + \alpha_{np}\, \Delta T_j \qquad 7.4.4.4.8.$$

Substituting equation 7.4.4.4.5 into equation 7.4.4.4.8

results:

$$V = \alpha_{np}\left[\theta T_{c_j} + \Delta T_j\right] \qquad 7.4.4.4.9$$

From equation 6.7.5

$$Q_s = K_{EFF}\,\Delta T_{j_{max_{eff}}}\left[2\theta - \theta^2 - \frac{\Delta T_j}{\Delta T_{j_{max\,eff}}}\right] \qquad 7.4.4.4.10$$

From equation 6.7.10

$$\phi = \frac{\left[2\theta - \theta^2 - \frac{\Delta T_j}{\Delta T_{j_{max\,eff}}}\right]}{2\left[\theta^2 + \theta\Delta T_j\right]} \qquad 7.4.4.4.11$$

The heat pump rate per unit volume of thermocouple material is:

$$\frac{Q_s}{2A\ell} = \frac{Q_s}{2A\ell} \qquad 7.4.4.4.12.$$

The heat pump rate per unit modular area is expressed as:

$$\frac{Q_s}{A_m} \qquad 7.4.4.4.13.$$

From the definition of packing density (ω)

$$\omega = 2A/A_m \qquad 7.2.2.1$$

Introducing equation 7.2.2.1 into equation 7.4.4.4.13 results:

$$\frac{Q_s}{A_m} = \frac{Q_s\,\omega}{2A} \qquad 7.4.4.4.14.$$

From equation 7.4.4.4.12

$$\frac{Q_s}{A_m} = \left[\frac{Q_s}{2A\ell}\right]\ell\omega \qquad 7.4.4.4.15$$

The heat rejection rate per unit of modular area can be expressed as:

$$Q_R = Q_S + P_{INPUT} \tag{7.4.4.4.16.}$$

where:

$$\phi = Q_S / P_{INPUT} \tag{7.4.4.4.17.}$$

Substituting equation 7.4.4.4.17 into equation 7.4.4.4.16 results:

$$Q_R = Q_S\left[1 + \frac{1}{\phi}\right] \tag{7.4.4.4.18.}$$

and

$$\frac{Q_R}{A_m} = \frac{Q_S\left[1 + \frac{1}{\phi}\right]}{A_m} \tag{7.4.4.4.19.}$$

The heat pump rate per unit area of the thermoelectric couple:

$$\frac{Q_S}{2A} = \left(\frac{Q_S}{2A\ell}\right)\ell \tag{7.4.4.4.20.}$$

7.4.4.5 Development of the Dimensionless Current Ratio at Maximum C.O.P.

The C.O.P. (ϕ) can be expressed as:

$$\phi = \frac{T_{cj} I \alpha_{np} - \frac{1}{2} I^2 R_{EFF} - K_{EFF} \Delta T_j}{\alpha_{np} I \Delta T_j + I^2 R_{EFF}} \qquad 7.4.4.5.1.\ (6.4.9)$$

Differentiating equation 7.4.4.5.1 with respect to I and equating the derivative to zero yields the current that maximizes the C.O.P. Appendix K indicates the technique for solution and compares equation 7.4.4.5.2. to equation 6.5.2.19 and 6.6.10. The current maximizing the C.O.P. is:

$$I_\phi = \frac{\dfrac{\alpha_{mp}\Delta T_j}{R_{EFF} Z_{EFF}}\left[1 + \sqrt{1 + Z_{EFF}\left[T_{c_j} + \dfrac{\Delta T_j}{2}\right]}\right]}{\left[\dfrac{\Delta T_j}{2} + T_{c_j}\right]} \qquad 7.4.4.5.2.$$

The sign before the $\sqrt{}$ (solution by quadratic) is required in order to have positive values of I_ϕ. The current maximizing the heat pump rate is expressed as:

$$I_Q = \frac{\alpha_{mp} T_{c_j}}{R_{EFF}} \qquad 7.4.4.4.5.$$

Defining the dimensionless current ratio at maximum C.O.P. (μ_ϕ) as

$$\mu_\phi = \frac{I_\phi}{I_Q} \qquad 7.4.4.5.3.$$

then:

$$\mu_\phi = \frac{\Delta T_j\left[1 + \sqrt{1 + Z_{EFF}\left[\dfrac{\Delta T_j}{2} + T_{c_j}\right]}\right]}{T_{c_j} Z_{EFF}\left[\dfrac{\Delta T_j}{2} + T_{c_j}\right]} \qquad \begin{array}{c}7.4.4.5.4.\\(7.4.4.4.6)\end{array}$$

7.4.4.6 Calculation Procedure.

This section describes the basic procedure for performing the calculations determining module performance with given junction temperatures and currents.

For a given module design the arbitrary selection of the variables: T_{c_j} , ΔT_j , θ will determine system performance. Accordingly a range of T_{c_j} and ΔT_j combinations are supplied to the computer as input information. For each combination of T_{c_j} and ΔT_j the calculations are performed as indicated by 7.4.4.4.1 - 7.4.4.4.20 inclusive. The third independent variable (θ) is more convenient than using the current variable (I, amps). The range of the dimensionless current ratio is expressable as:

$$\theta_{\varphi} \leq \theta \leq \mu_{\phi} \qquad 7.4.4.6.1.$$

The limit and range is applicable regardless of the individual module design. Other alternate modes of operation for restricting (or expanding) θ can be incorporated into the basic computer program. Such as:

(1) Use only $\theta = 1$ and $\theta = \mu_{\phi}$

(2) For $\Delta T_j = 0$ and $\mu_{\phi} = 0$ the C.O.P. becomes indeterminate. The singularity was overcome by introducing the computer procedure MODZERO(C.P.4)

(3) For $\Delta T_j = \Delta T_{j\,max}$ computer procedure MODMAXT is introduced as a third mode of operation(C.P.3).

7.4.4.7 Input Information.

For a given module configuration/design the following are input parameters: $\delta(1/\rho)$, l, l^*, ρ_j, F, A, $f(0,1)$ ω, k_i, k, α_{mp}, ratio (A_p/A). For modules without pedestals f is assigned by input data the value of unity (1). In modules with pedestals f is assigned by input data the value of zero (0), and g is determined for equation 7.4.4.4.4.2 by procedure phasesq. (The computer program is found in the Appendix (C.P.2 - 'Computer Programs').

The variable input parameters are T_{c_j}, ΔT_j and θ (a variable defined by equation 7.4.4.6.1). The basic program can be modified to account for variation in average material properties with temperature. A function would be required expressing (i.e.) $k, k_i, |\alpha_m| + |\alpha_p|, \rho$ as variances of T_{c_j} and ΔT_j.

7.4.4.8 Output Information.

For each module design considered and given set of junction conditions, T_{c_j}, ΔT_j the following can be output from the computer: (Economical use of the digital computer should be considered) R_{EFF}, K_{EFF}, Z_{EFF}, $\Delta T_{j\,max\,eff}$, I_φ and μ_ϕ. Module performance is then calculated as a function of θ, T_{c_j} and ΔT_j. Hence for a given set of values for T_{c_j}, ΔT_j the following can be tabulated for each stepping value of θ : Voltage, I, θ, ϕ(C.O.P.), $Q_s/2Al$, Q_s/A_m, Q_R/A_m and $Q_s/2A$.
$Q_s/2Al$ is the net heat pumped per unit volume of

THIS PROGRAM CALCULATES FOR A GIVEN MODULE DESIGN THE PERFORMANCE CHARACTERISTICS FOR VARIOUS COLD JUNCTION TEMPERATURES HOT TO COLD JUNCTION TEMPERATURES AND CURRENTS

OPERATIONAL CHARACTERISTICS OF THE GIVEN MODULE

ELEMENT HEIGHT	.1cm
JUNCTION RESISTIVITY	$2.50_{10}{-6}$ ohm cm sqrd
THERMAL CONDUCTIVITY	.0140 watts/cm °C
PACKING DENSITY	1.0
ELEMENT AREA	.03 cm sqrd
SEEBECK COEFFICIENT	$400_{10}{-6}$ volts/°C
RIPPLE FACTOR	1.0
ELECTRICAL CONDUCTIVITY	1070 $(\text{ohm cm})^{-1}$

MATERIAL MODULE PERFORMANCE

REFF	KEFF	ZEFF
+6.56n- 3	+8.40n- 3	+2.90n- 3

TSUBC = +270.0

MUPHI	ISUBQ
+0.415	+16.4537

THETA = +1.00000
VOLTAGE/COUPLE = +0.12400
CURRENT AMPS = +16.45373
HEAT PUMP RATE--WATTS = +0.55250
COEFF OF PERFORMANCE = +0.27080
HEAT PUMP RATE/VOLUME = +92.08353
HEAT PUMP RATE/MOD AREA = +9.20835
HEAT REJECTION/MOD AREA = +43.21272
HEAT PUMP RATE/ELEMENT AREA = +9.20835

THETA = +0.41494
VOLTAGE/COUPLE = +0.06081
CURRENT AMPS = +6.82728
HEAT PUMP RATE--WATTS = +0.24837
COEFF OF PERFORMANCE = +0.59821
HEAT PUMP RATE/VOLUME = +41.39493
HEAT PUMP RATE/MOD AREA = +4.13949
HEAT REJECTION/MOD AREA = +11.05932
HEAT PUMP RATE/ELEMENT AREA = +4.13949

thermoelectric material; Q_s/A_m and Q_r/A_m are respectfully, the net heat pumped and heat rejected per unit of module area; $Q_s/2A$ is the net heat pumped per unit area of thermoelectric material. Table 7.4.4.81. illustrates a portion of the computer output for $\Theta = 1$ (maximum heat pump rate) and $\Theta = \mu\phi$ (maximum C.O.P.); the junction temperature difference is constant at 40°C.

7.4.4.9 Results and Conclusions.

The computer program described in section 7.4.4.6 establishes an accurate evaluation technique for determing the effects of parametric design changes. Some of the design changes are: element height, junction resistivity, packing density, current ripple, pedestal height.

Figure 7.4.4.9.1 illustrates the material utilization parameter $Q_s/2A\ell$ as a function of C.O.P. for variation in the element height. The results indicate that as the height of the thermoelement decreases the maximum C.O.P. decreases slightly while the material utilization parameter increases rapidly. For the height of elements considered ($.1 \leq \ell \leq .6$ cm) there is a decrease in the maximum C.O.P. of about 10% and also for C.O.P. at maximum material utilization. The maximum material utilization for an element of .1cm height is approximately 85 watts/cm^3 and the material utilization at maximum C.O.P. is approximately 45 watts/cm^3. Although the junction resistance becomes relatively more important to the element resistance at short length, the heat flux also increases,

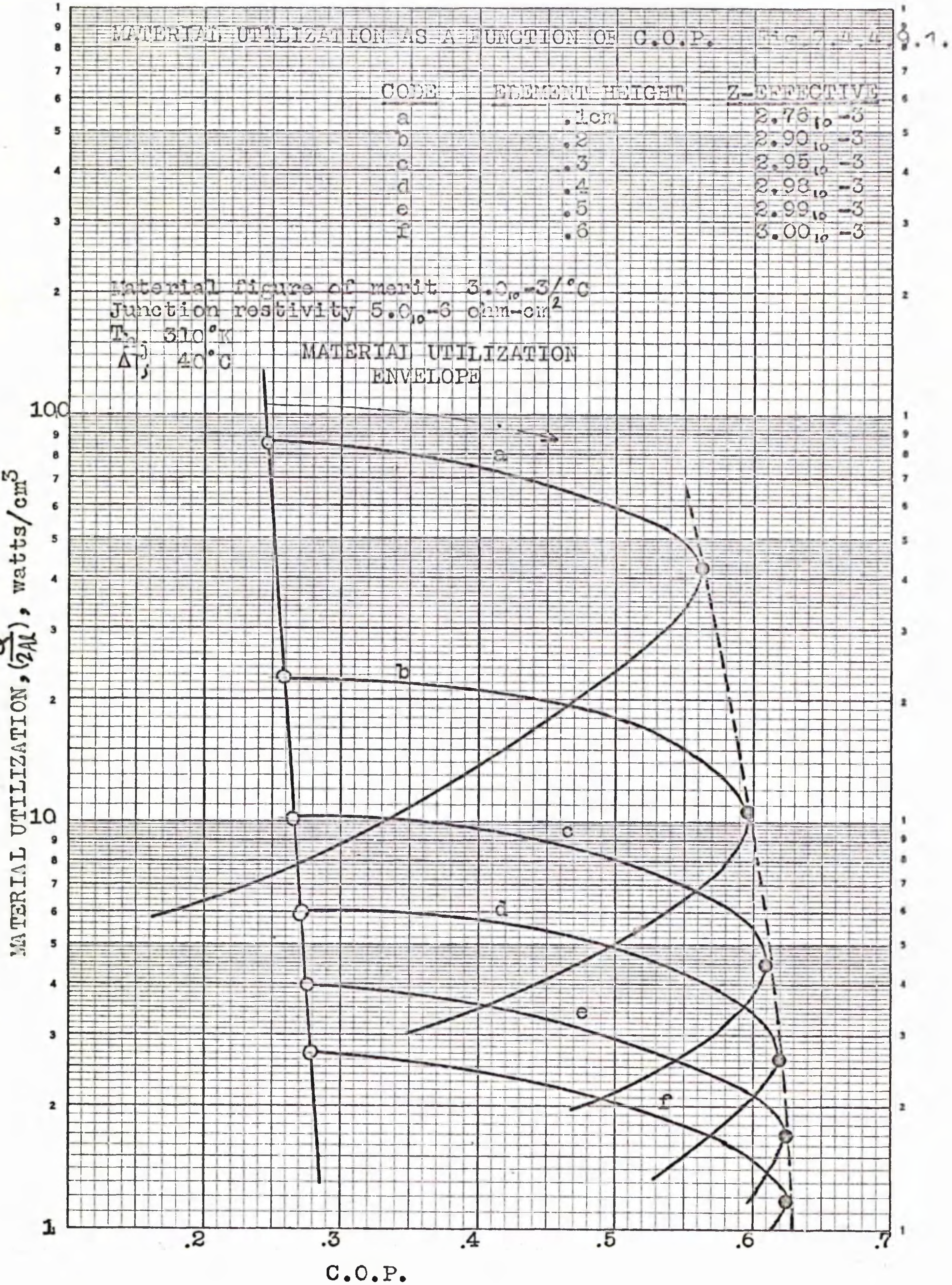
MATERIAL UTILIZATION AS A FUNCTION OF C.O.P.
CODE ELEMENT HEIGHT Z-EFFECTIVE
a .1cm 2.76 10 -3
b .2 2.90 10 -3
c .3 2.95 10 -3
d .4 2.98 10 -3
e .5 2.99 10 -3
f .6 3.00 10 -3
Material figure of merit 3.0 10 -3/°C
Junction restivity 5.0 10 -6 ohm-cm2
310°K
40°C
MATERIAL UTILIZATION ENVELOPE
a
b
c
d
e
f
100
10
1
.2
.3
.4
.5
.6
.7
MATERIAL UTILIZATION, (Q/2AL), watts/cm3
C.O.P.

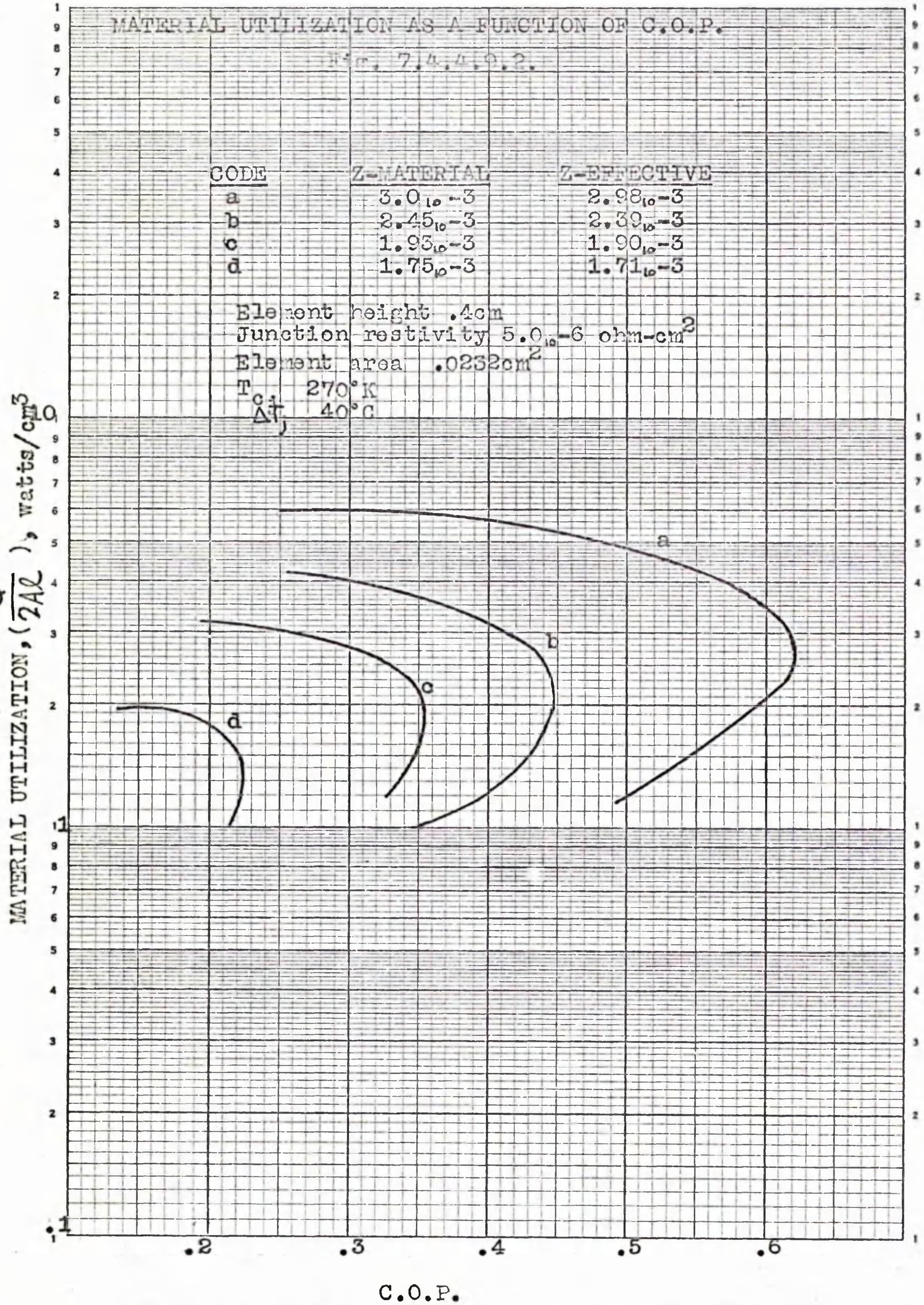
MATERIAL UTILIZATION AS A FUNCTION OF C.O.P.
Fig. 7.4.4.9.2.
CODE Z-MATERIAL Z-EFFECTIVE
a 3.0₁₀-3 2.98₁₀-3
b 2.45₁₀-3 2.39₁₀-3
c 1.93₁₀-3 1.90₁₀-3
d 1.75₁₀-3 1.71₁₀-3
Element height .4cm
Junction restivity 5.0₁₀-6 ohm-cm²
Element area .0232cm²
Tc 270°K
ΔTj 40°C
a
b
c
d
MATERIAL UTILIZATION, (Q/2Al), watts/cm³
10
1
.1
.2
.3
.4
.5
.6
C.O.P.

the net result is that the C.O.P. decreases slowly (slope of upper arm of curve).

There appears to be two related implications of decreasing the element height (ℓ). The first is that the cost of thermoelectric material for a particular heat pumping application can be kept relatively low by using short thermoelements. The dependency of material utilization on $(1/\ell^2)$ was indicated by equation 7.2.5.8. The concept of using short thermoelements had long been considered but concern over the effect of relatively large junction resistance supported high thermoelements. It appears that at the present state of the art the junction resistivity can be kept low enough to justify . 2cm high thermoelements. (The modules tested during this research program were .2cm high thermoelements). The limitation for utilizing shorter elements relates to fabrication/assembly and to the imposed heat transfer load. Correspondence with one manufacturer indicated that . 40cm is an economically/ production feasible thermoelement height. Figure 7.4.4.9.2 indicates the expected material utilization parameter as a function of C.O.P. for variation in material figure of merit.

The other related implication as illustrated by figure 7.4.4.9.1 is that for a fixed heat pumping capacity the shorter element will exhibit a higher C.O.P. The longer

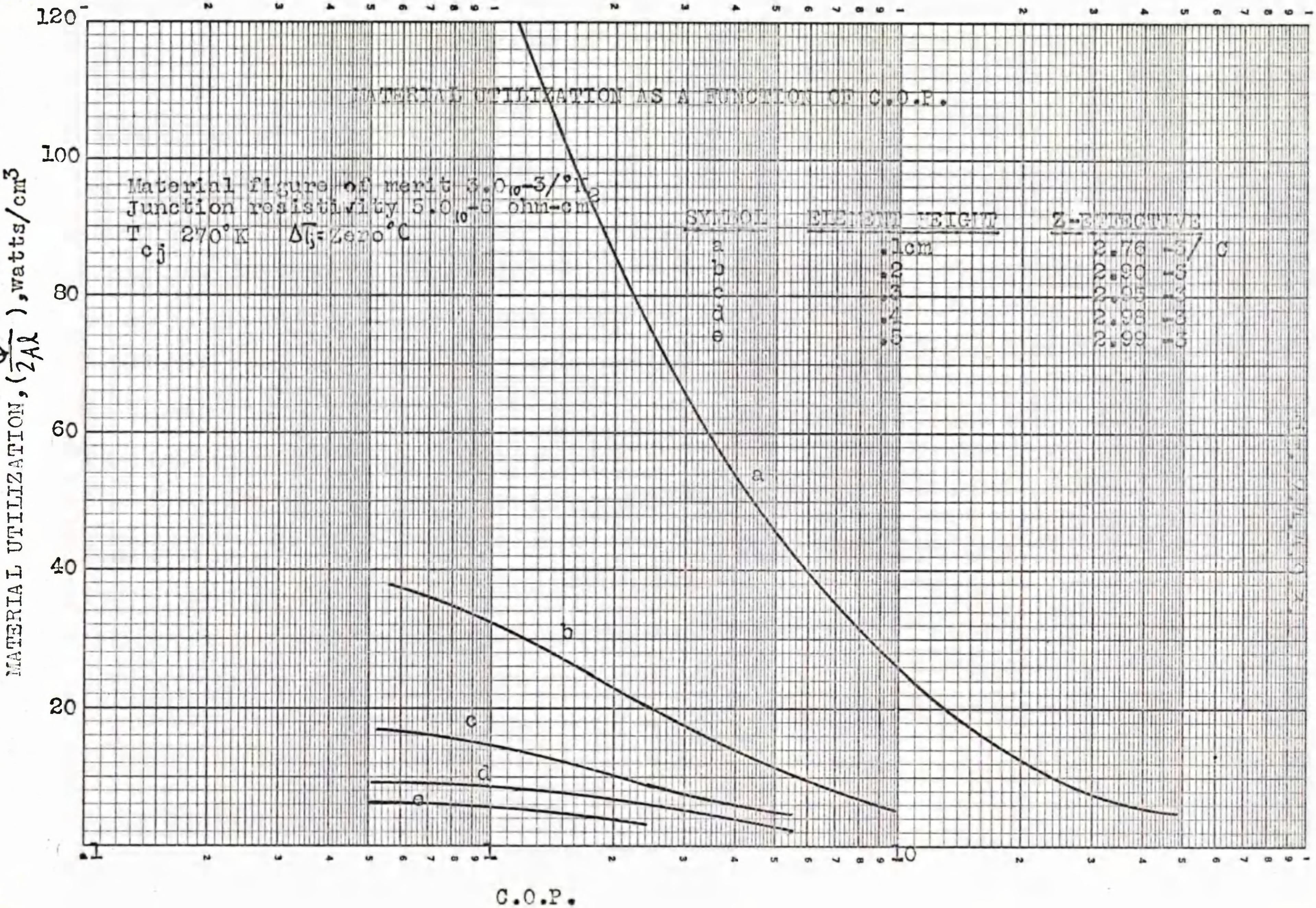
MATERIAL UTILIZATION AS A FUNCTION OF C.O.P.
Material figure of merit 3.0 10-3/°K
Junction resistivity 5.0 10-6 ohm-cm2
Tcj 270°K ΔTj=Zero°C
SYMBOL ELEMENT HEIGHT Z-EFFECTIVE
a .1cm 2.76 -3/°C
b .2 2.90 -3
c .3 2.95 -3
d .4 2.98 -3
e .5 2.99 -3
a
b
c
d
e
MATERIAL UTILIZATION, (Q/2Aλ), watts/cm3
120
100
80
60
40
20
.1
1
10
C.O.P.

element will be required to operate with higher current. This condition can be illustrated on figure 7.4.4.9.1: at $5\,\text{WATTS}/\text{cm}^3$ a .4cm thermoelement exhibits a C.O.P. of $\simeq$ .48 while a .3cm thermoelement has a C.O.P. of .61. Although longer arms are usually associated with high efficiency it has been shown from figure 7.4.4.9.1 that at a given C.O.P. a higher material utilization is achieved using shorter element arms and at a given material utilization criteria shorter arms exhibit a higher C.O.P.

Figure 7.4.4.9.3 illustrates the operational potential for a module assembly with a junction temperature difference of zero degrees (0 $^{\circ}$C). Material utilization is extremely high with corresponding increases in C.O.P. (figure 7.4.4.9.1). The required heat rejection rate to maintain the thermodynamic heat balance would impose severe design demands on the hot side heat exchanger. From figure 7.4.4.9.4 the material utilization rejection $Q_R/2A\ell$ parameter as a function of the dimensionless current ratio (θ) for variation in element height. The results presented are for $\Delta T_j = \Delta T_{j\,max\,eff}$. The heat pump rate ($Q_S$) is zero and hence the C.O.P. is zero (section 6.5.6). Another variable is introduced (θ) as a parametric term. The maximum effective junction temperature difference is $\simeq$ 105°C (most impressive for a single stage device). The large junction temperature difference results from the invariant material properties with temperature (large ΔT_j are asymptotic in form). The heat rejection term (watts/cm^2) for $\ell <$ .3cm will be in excess of (10 watts/cm^2). The operation of a module

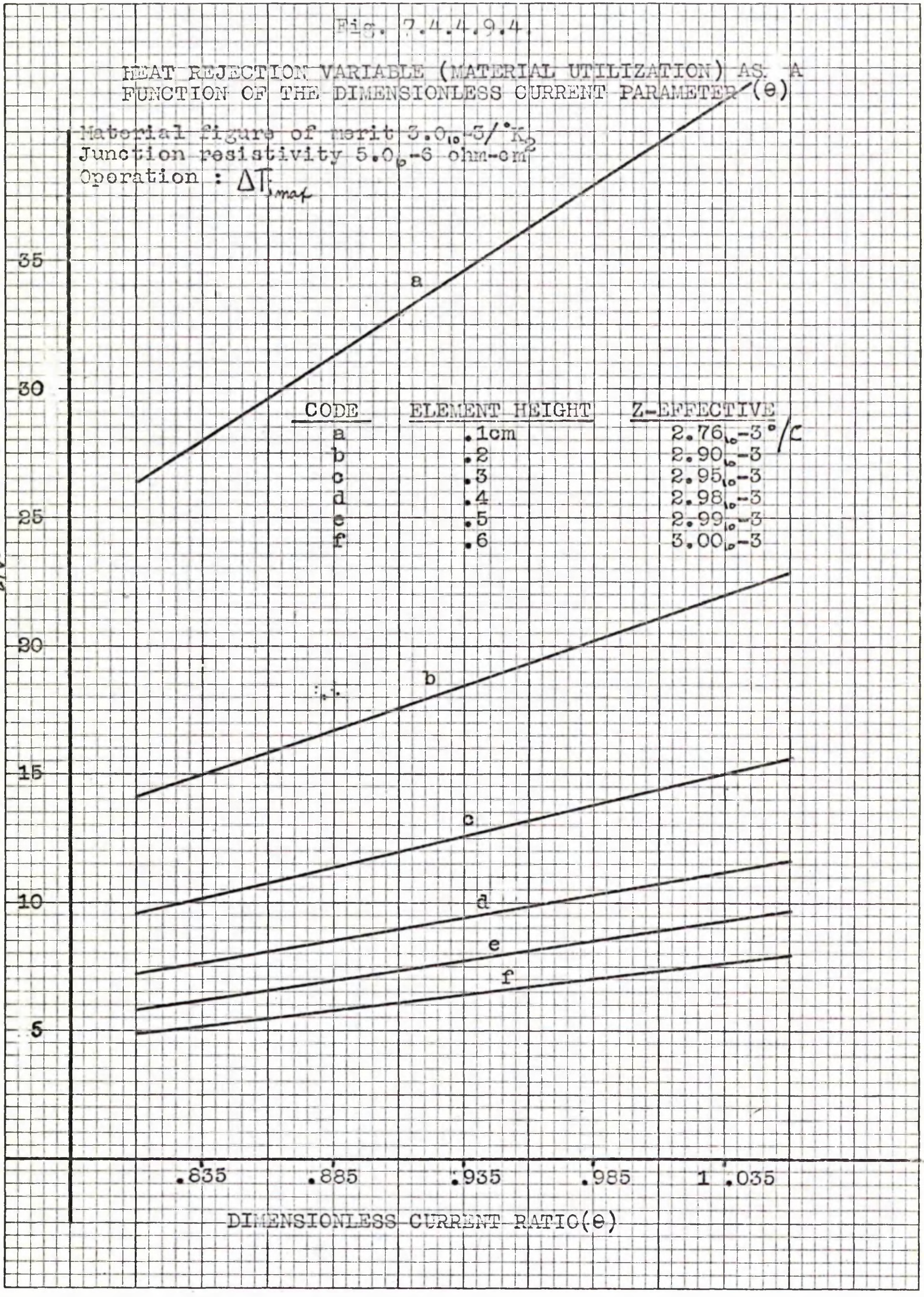

Fig. 7.4.4.9.4

HEAT REJECTION VARIABLE (MATERIAL UTILIZATION) AS A FUNCTION OF THE DIMENSIONLESS CURRENT PARAMETER (e)

Fig. 7.4.4.9.5.

MATERIAL UTILIZATION AS A FUNCTION OF C.O.P.

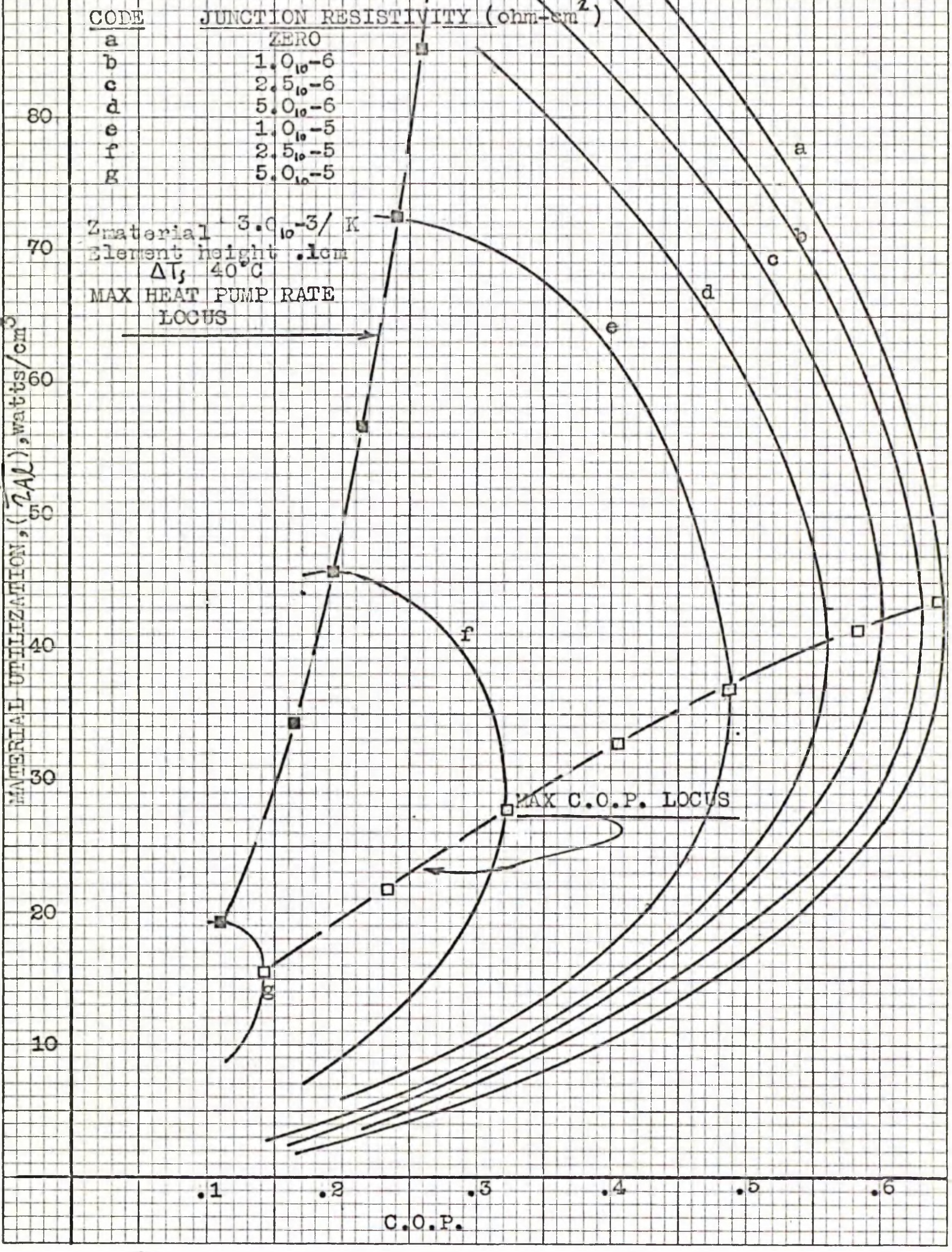

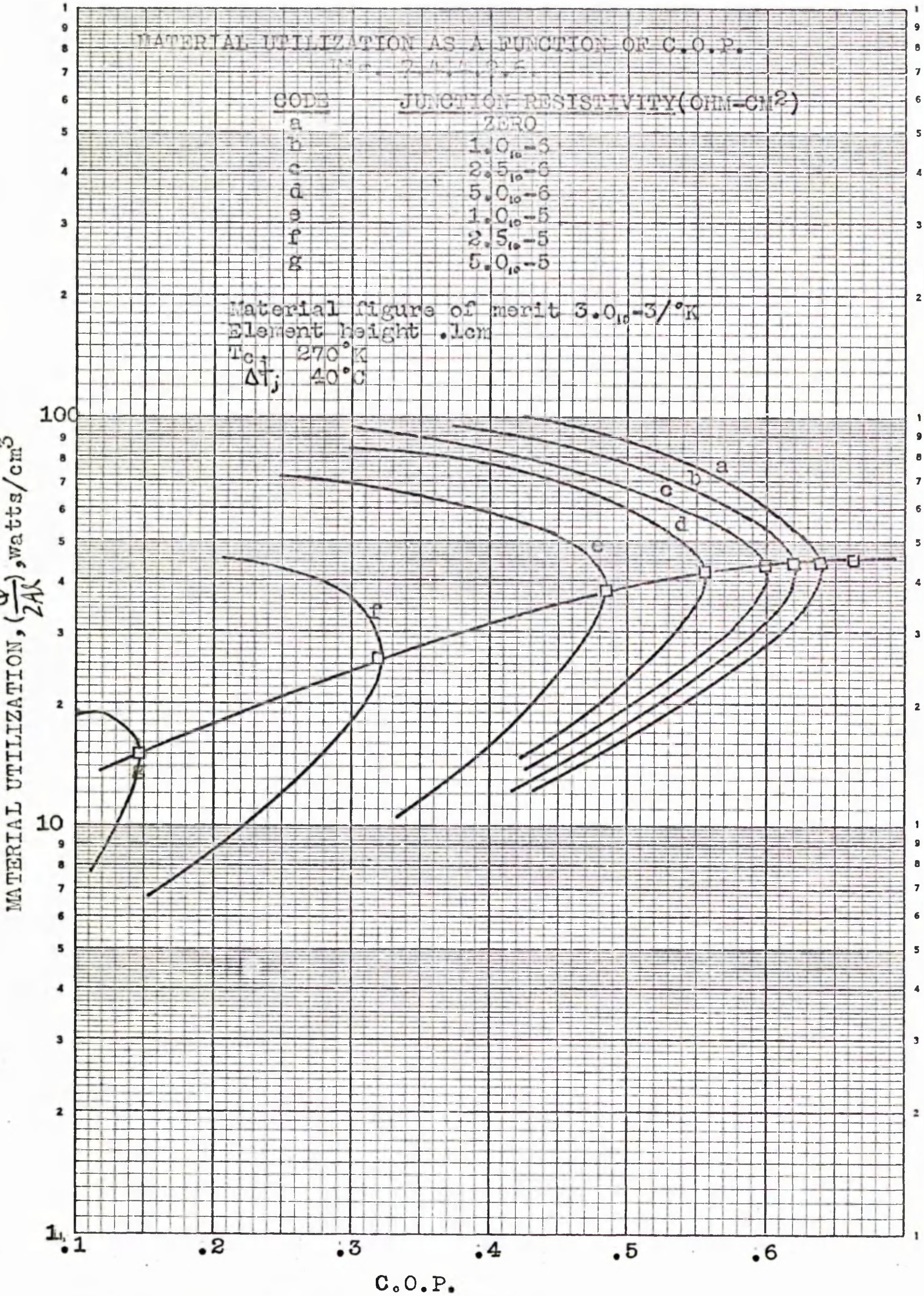

MATERIAL UTILIZATION AS A FUNCTION OF C.O.P.
CODE
JUNCTION RESISTIVITY(OHM-CM2)
a ZERO
b 1.0₁₀-3
c 2.5₁₀-6
d 5.0₁₀-6
e 1.0₁₀-5
f 2.5₁₀-5
g 5.0₁₀-5
Material figure of merit 3.0₁₀-3/°K
Element height .1cm
Tc, 270°K
Δtj 40°C
MATERIAL UTILIZATION, (Q/2Al), watts/cm3
C.O.P.

at $\simeq \Delta T_{j_{max}}$ would require the input of sufficient power to overcome the joule heating and Seebeck effect at $\simeq \Delta T_{j_{max}}$. The heat rejection is expressable as:

$Q_R = P + Q_S$, @ $Q_S = 0$ hence the heat rejection rate is equal to the power input.

Aside from the construction difficulties one requirement for supporting the use of short thermocouples is to be able to assembly the shorter arms with relatively low junction resistivity. Figure 7.4.4.9.5 and figure 7.4.4.9.6 illustrates the effect of junction resistivity (ohm-cm^2) on material utilization as a function of C.O.P. The curves indicate that for a .1cm high thermoelement with a junction resistivity (conservative) $5_{10} - 6$ ohm-cm^2 a significant decrease in performance may result for this short element height. At maximum heat pump rate and at maximum C.O.P. there is an approximate 15% decrease in material utilization, for a junction resistivity of $5_{10} - 6$ ohm-cm^2 (base ZERO). With good quality control a production junction resistivity of $10_{-}6$ ohm-cm^2 produces relatively little operational degradation.

Figure 7.4.4.9.7 illustrates the effect of power supply ripple on system performance. The effect of ripple is similiar to the degradation resulting from junction resistivity. (figures 7.4.4.9.6 and 7.4.4.9.7).

Figure 7.4.4.9.8 illustrates the effect of packing density (ω) on material utilization as a function of C.O.P.

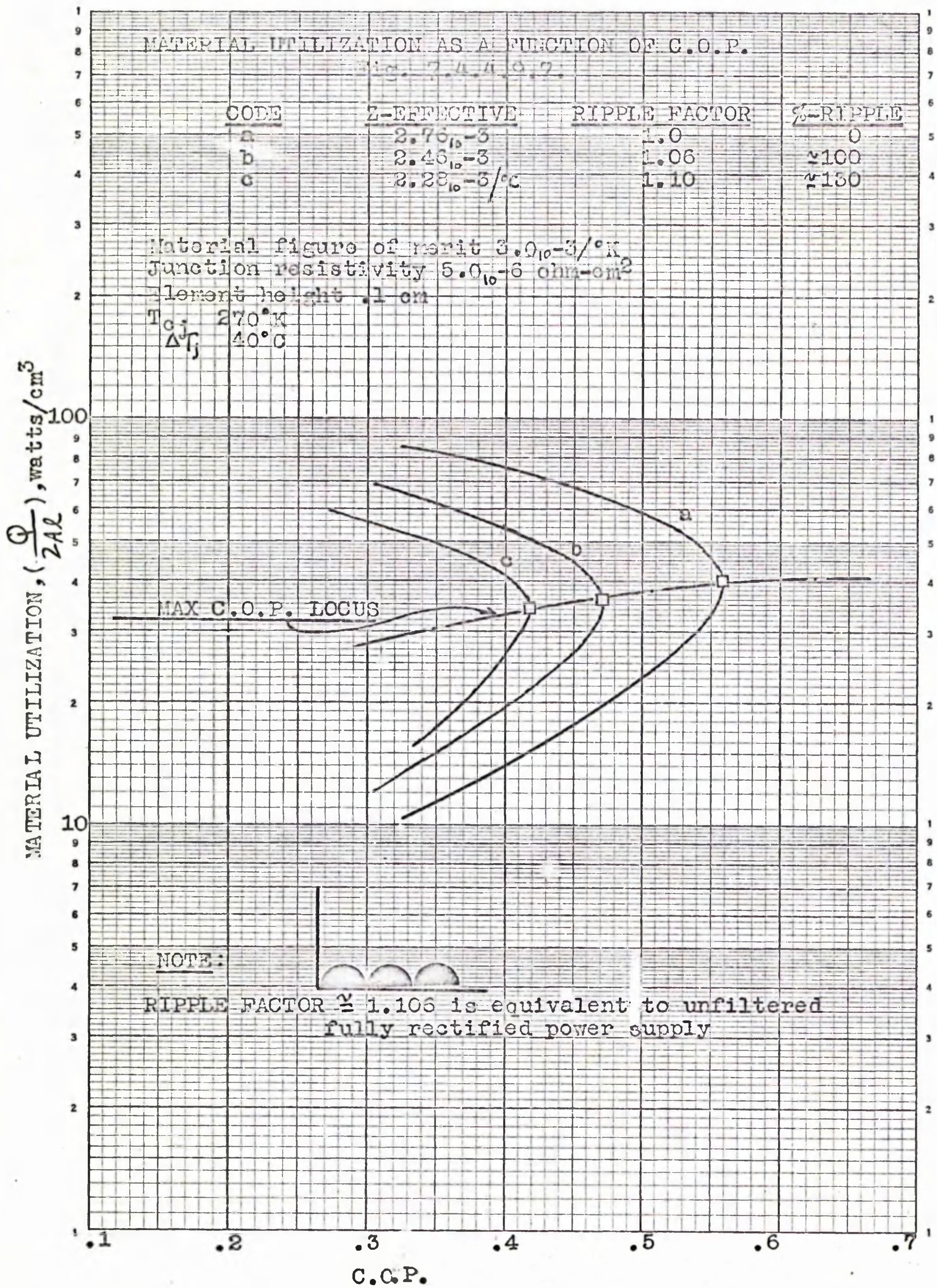

MATERIAL UTILIZATION AS A FUNCTION OF C.O.P.
Fig. 7.4.4.0.7
CODE
Z-EFFECTIVE
RIPPLE FACTOR
%-RIPPLE
a 2.76₁₀-3 1.0 0
b 2.46₁₀-3 1.06 ≃100
c 2.28₁₀-3/°C 1.10 ≃130
Material figure of merit 3.0₁₀-3/°K
Junction resistivity 5.0₁₀-6 ohm-cm²
Element height .1 cm
Tcj 270°K
ΔTj 40°C
a
b
c
MAX C.O.P. LOCUS
NOTE:
RIPPLE FACTOR ≃ 1.106 is equivalent to unfiltered fully rectified power supply
MATERIAL UTILIZATION, (Q/2Aℓ), watts/cm³
C.O.P.
.1 .2 .3 .4 .5 .6 .7
100
10

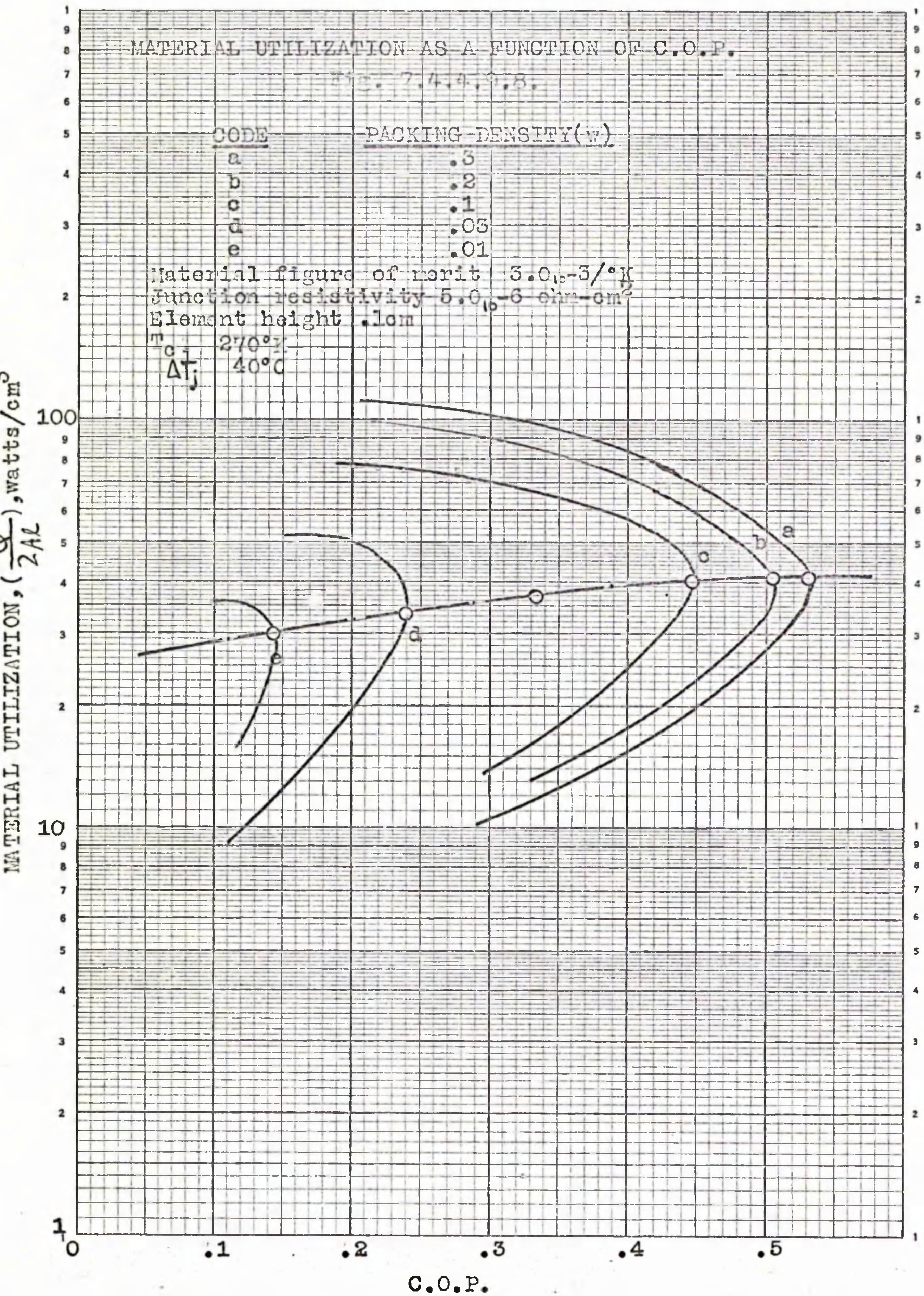
MATERIAL UTILIZATION AS A FUNCTION OF C.O.P.
CODE
PACKING DENSITY(w)
a .3
b .2
c .1
d .03
e .01
Material figure of merit 3.0₁₀-3/°K
Junction resistivity 5.0₁₀-6 ohm-cm²
Element height .1cm
Tc 270°K
ΔTj 40°C
MATERIAL UTILIZATION, (Q/2Al), watts/cm³
C.O.P.
0
.1
.2
.3
.4
.5
1
10
100
a
b
c
d
e

For packing densities $\geq$ .1 there appears to be a moduate degradation when operating in the region of maximum heat pump rate and corresponding C.O.P. Maximum C.O.P. is effected in a manner similiar to current ripple and/or junction resistivity increases.

The effect of packing density (ω), pedestal height (ℓ_p) are shown in figures 7.4.4.9.9 - figure 7.4.4.9.13 inclusive. The module configuration is composed of: .1cm high thermoelement, junction resistivity $5.0_{10} - 6$ ohm-cm^2, thermal insulation conductivity $2.5_{10} - 4$ watts/ cm - ^{o}C. Figure 7.2.3.1 illustrates the relative level of thermal insulation of polyurethane as compared to other insulation material. Figure 7.4.4.9.9 illustrates the heat flux parameter as a function of packing density for variation in the insulation cell height (ℓ_i). The values illustrated by figure 7.4.4.9.9 are utilized to produce the results of figure 7.4.4.9.10 - 7.4.4.9.13 inclusive. The heat leakage resulting from low packing density will decrease the net heat pumping capability and C.O.P. Increasing the pedestal height decreases the heat leakage and hence increases the C.O.P. and material utilization parameter. For $\omega \longrightarrow$ unity (figure 7.4.4.9.9) the effect of increasing pedestal height is greatly decreased.

Figure 7.4.4.9.10 - figure 7.4.4.9.12 illustrate the material utilization parameter as a function of C.O.P. for variation in packing density. Each curve is based on a fixed element height of .10cm with thermal insulation cell heights of: 1cm, .6cm, .4cm; resulting in pedestal heights

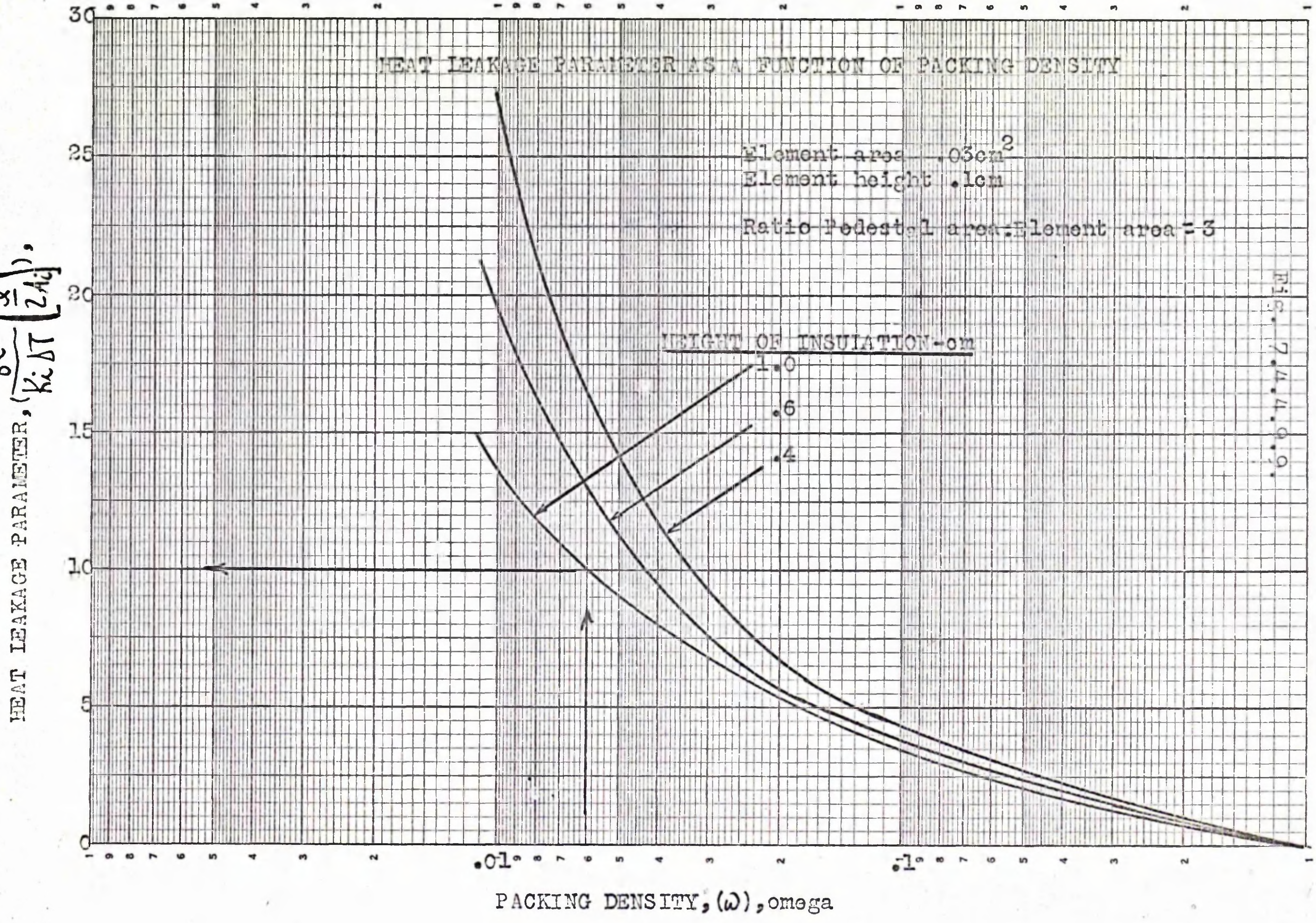
HEAT LEAKAGE PARAMETER AS A FUNCTION OF PACKING DENSITY
Element area .03cm^2
Element height .1cm
Ratio Pedestal area:Element area = 3
HEIGHT OF INSULATION-cm
1.0
.6
.4
Fig. 7.4.4.9.9.
HEAT LEAKAGE PARAMETER, $\left(\frac{q_i}{K_i \Delta T}\left[\frac{\ell}{2A_i}\right]\right)$,
PACKING DENSITY, (ω), omega
30
25
20
15
10
5
0
.01
.1
CHARTWELL GRAPH SHEET No. 5535
LOG 3 CYCLES X 10ths, ½ & 1 INCH

Fig. 7.4.4.9.10.

MATERIAL UTILIZATION AS A FUNCTION OF C.O.P.

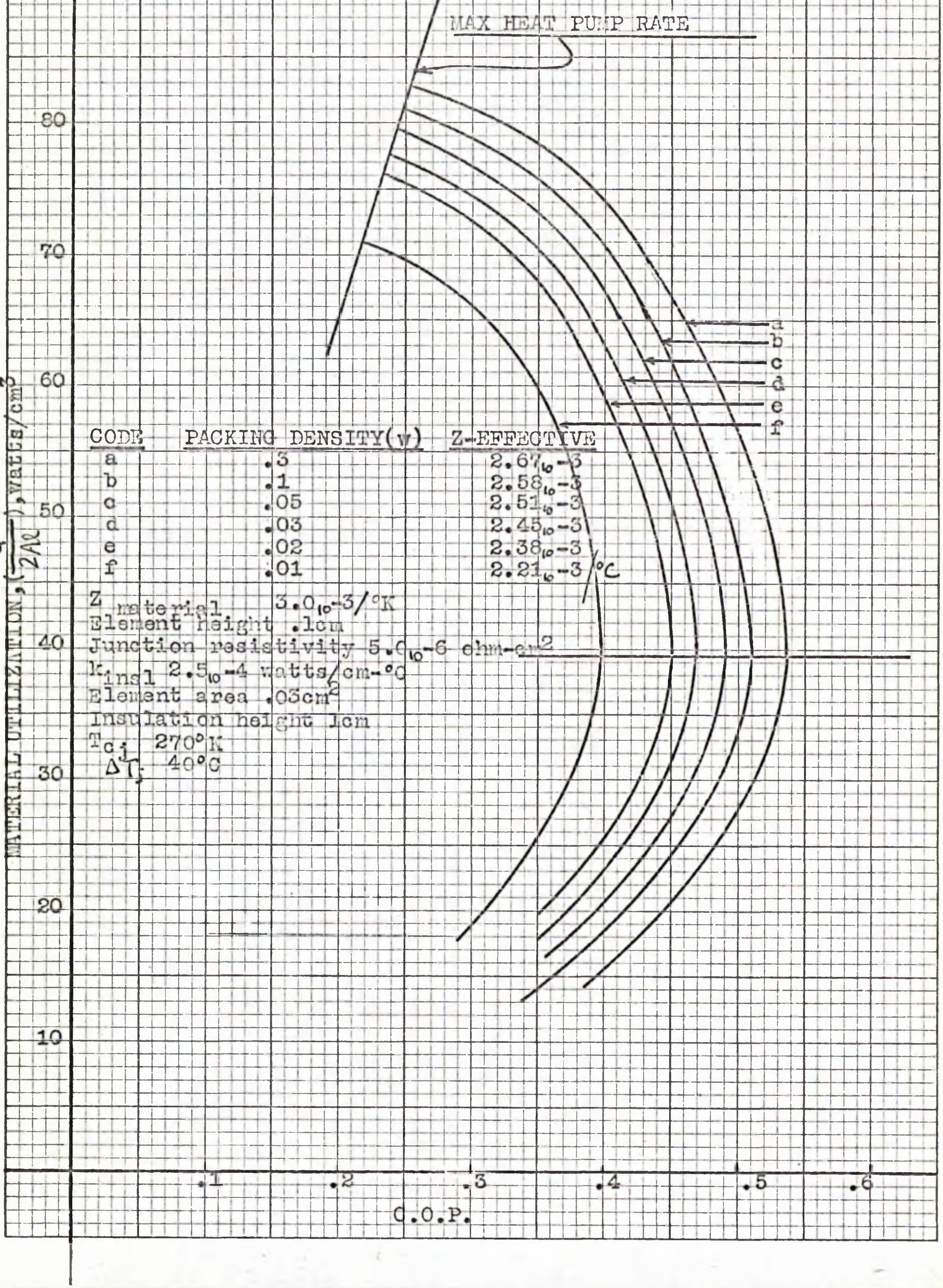

Fig. 7.4.4.9.11.

MATERIAL UTILIZATION AS A FUNCTION OF C.O.P.

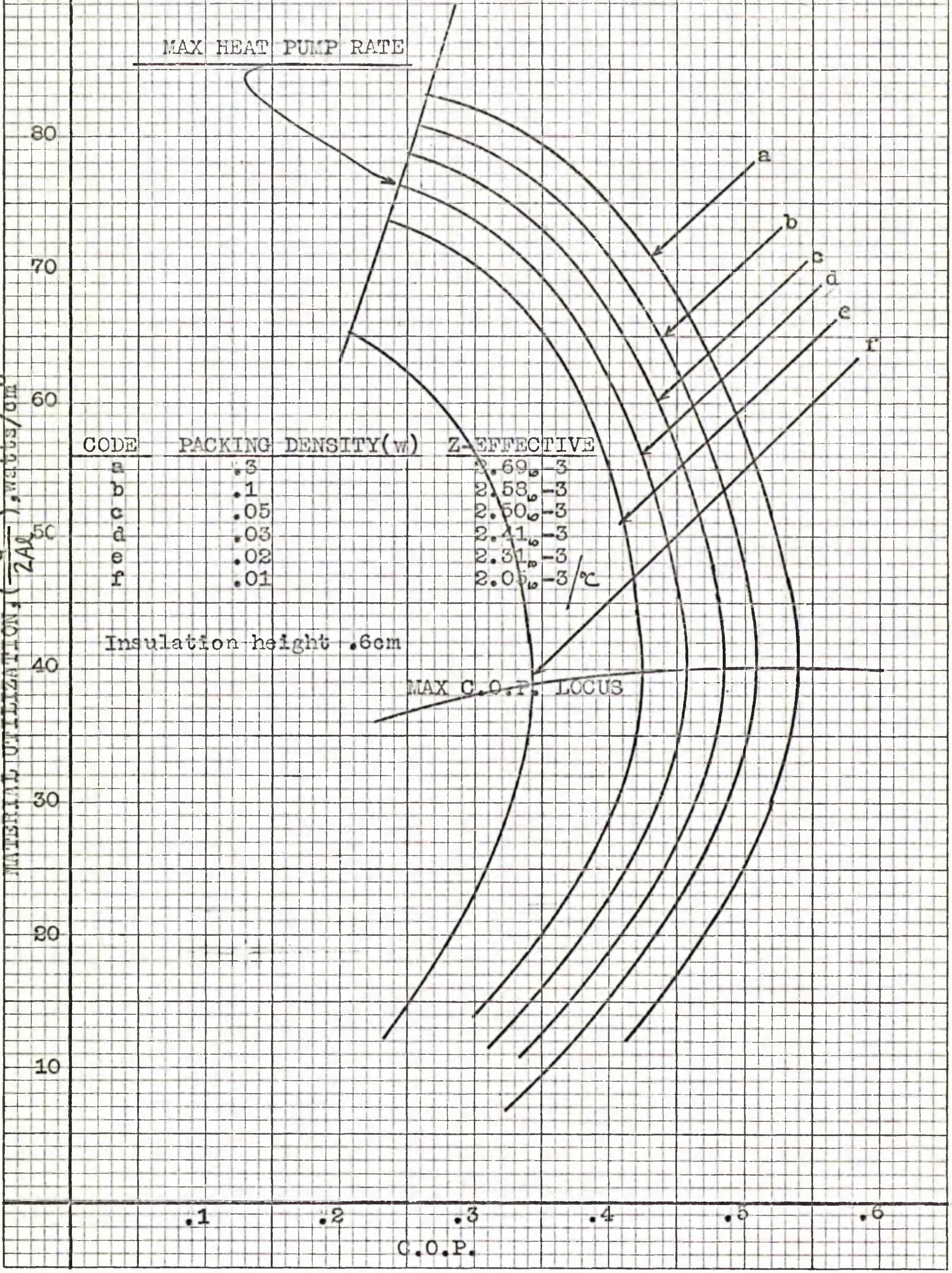

Fig. 7.4.4.9.12.

MATERIAL UTILIZATION AS A FUNCTION OF C.O.P.

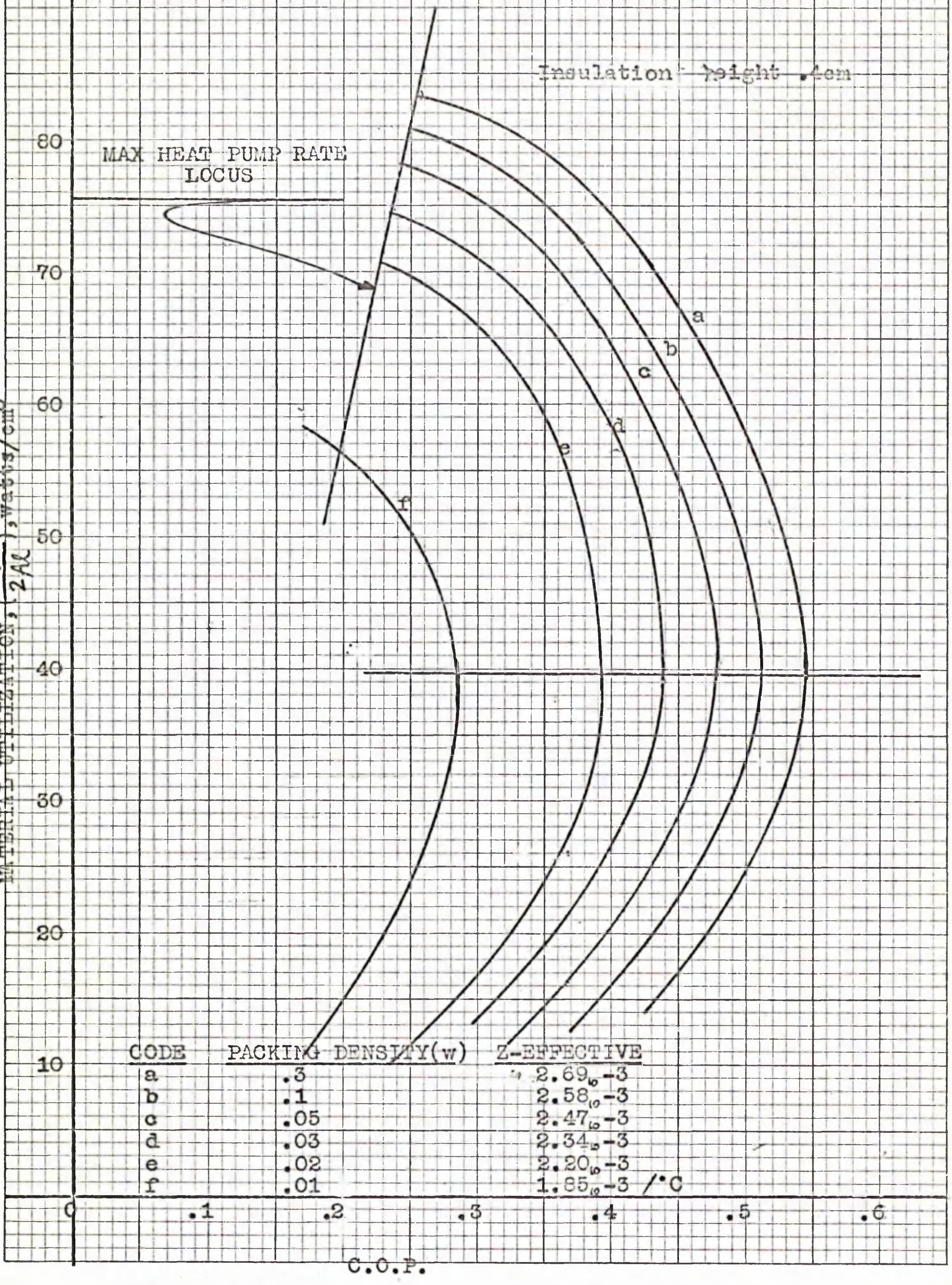

CODE	PACKING DENSITY(w)	Z-EFFECTIVE
a	.3	2.69_{10}-3
b	.1	2.58_{10}-3
c	.05	2.47_{10}-3
d	.03	2.34_{10}-3
e	.02	2.20_{10}-3
f	.01	1.85_{10}-3 /°C

of .9cm, .5cm, .3cm respectfully. The relationship between packing density (ω), insulation height (pedestal height for fixed element height) indicates that as the insulation height increases a lower packing density can be tolerated for a fixed material of utilization parameter. The maximum heat pump rate intersect is based on $\theta(I/I_\varphi)$ being equal to unity.

Figure 7.4.4.9.13 illustrates the effect of current ripple for a pedestal module of .60cm insulation cell height. The characteristic decrease in material utilization is similiar to decreasing the pedestral height (insulation height), increase in junction resistivity or packing density. Figure 7.4.4.9.13 is for a ripple percentage of 100% ($F \cong 1.056$).

Figure 7.4.4.9.14 illustrates the material utilization parameter(s) as a function of C.O.P. for $\Delta T_j = 0°C$. The heat rejection rate (watts/cm^2) for a C.O.P. of $\cong$ .5 indicates a value of $\cong$ 40 watts/cm^2 (a considerable design problem). Figures 7.4.4.9.15 and 7.4.4.9.16 indicates the heat exchanger design problem with short elements and low C.O.P. At a maximum material utilization (watts/cm^3) figure 7.4.4.9.15 indicates a heat rejection parameter of $\cong$ 32 watts/cm^2 for a material figure of merit of $2.45_{10}-3/°C$. Figure 7.4.4.9.16 for a material figure of merit of $3.00_{10}-3/°C$ indicates that at maximum material utilization (watts/cm^3) the heat rejection rate/ element area is $\cong$ 42 watts/cm^2. When the required heat rejection rate per unit area exceeds approximately

Fig. 7.4.4.9.13.

MATERIAL UTILIZATION AS A FUNCTION OF C.O.P.

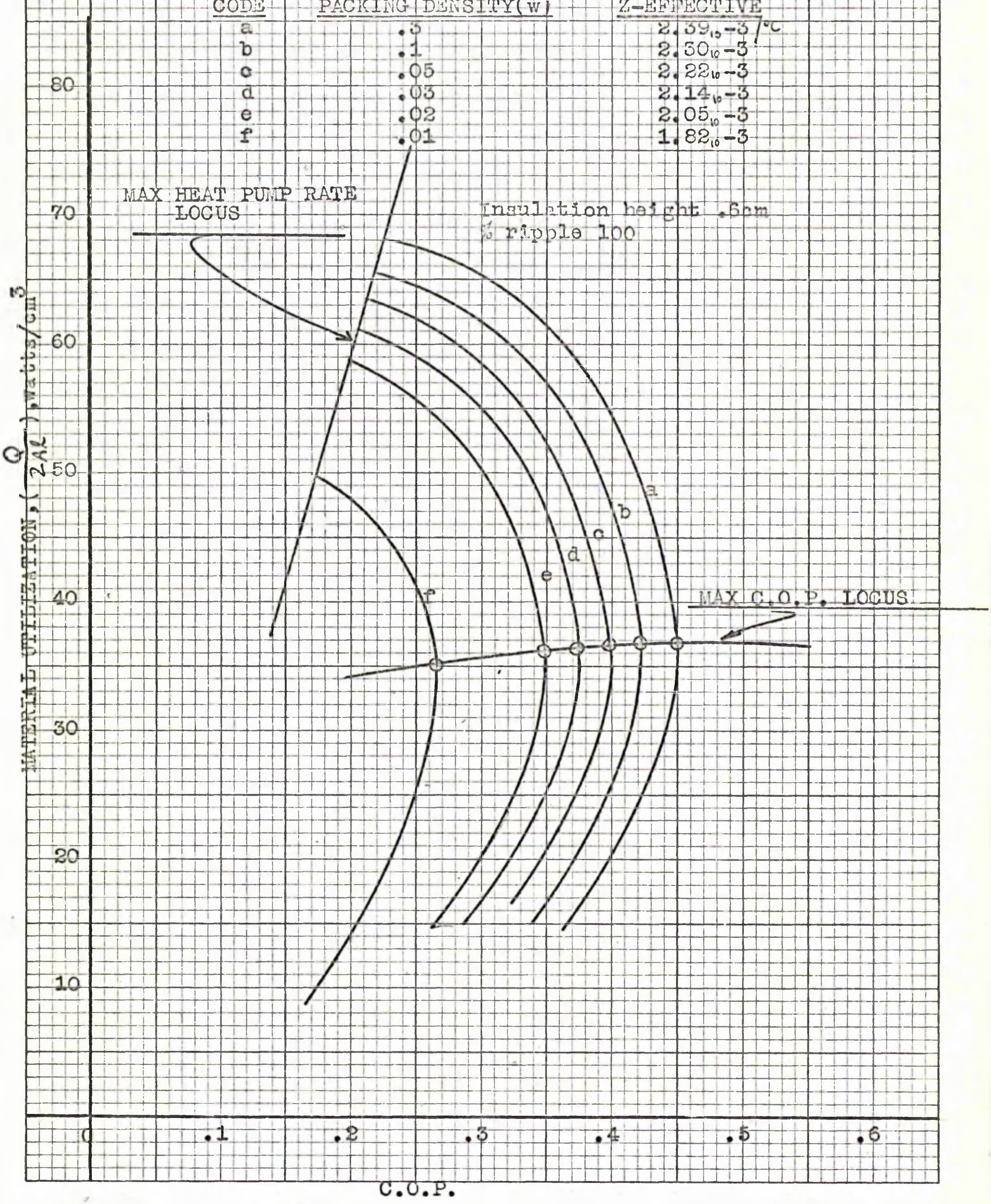

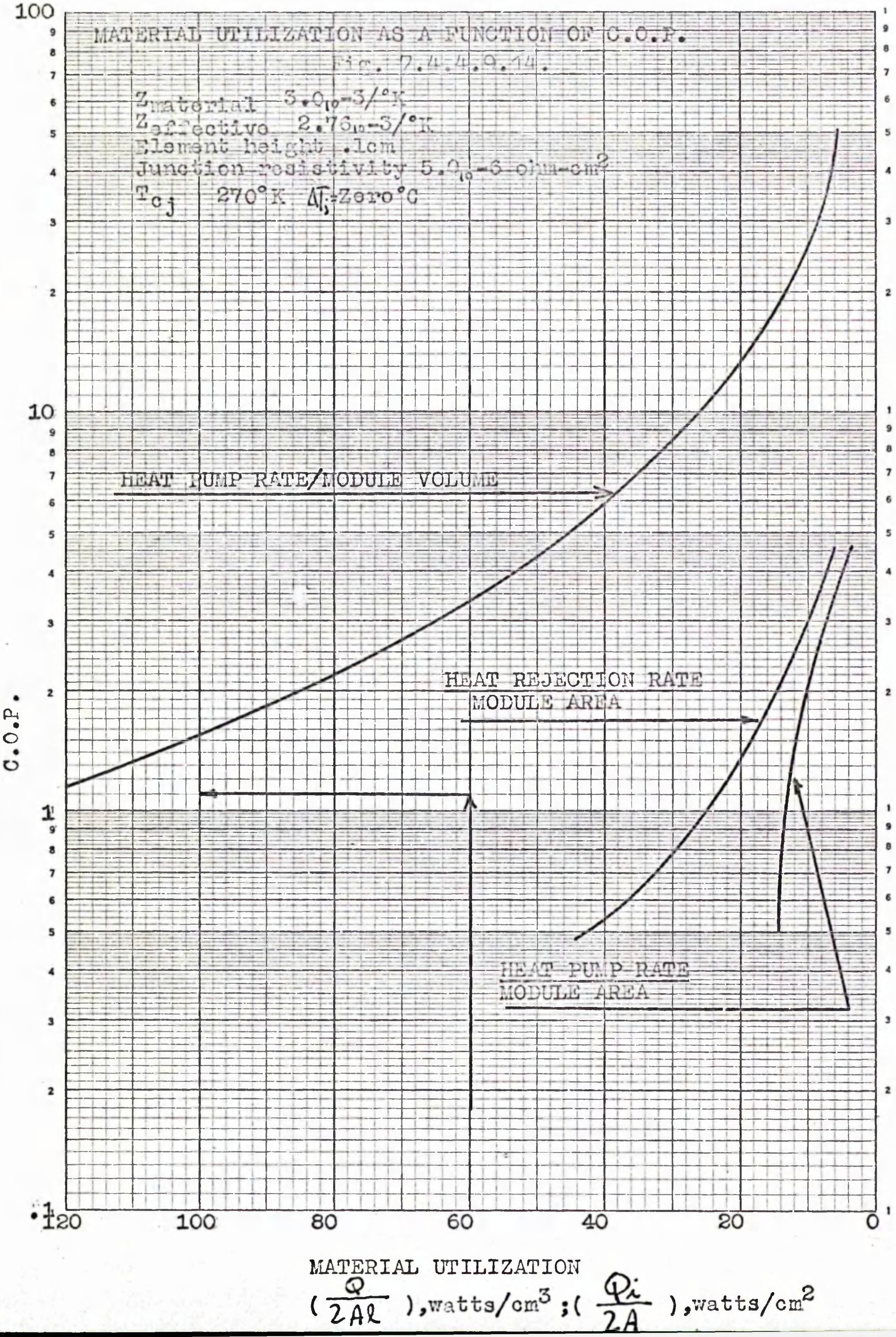

MATERIAL UTILIZATION AS A FUNCTION OF C.O.P.
Fig. 7.4.4.9.14.
$Z_{material}$ 3.0₁₀-3/°K
$Z_{effective}$ 2.76₁₀-3/°K
Element height .1cm
Junction resistivity 5.0₁₀-6 ohm-cm^2
T_{cj} 270°K ΔT_j=Zero°C
HEAT PUMP RATE/MODULE VOLUME
HEAT REJECTION RATE
MODULE AREA
HEAT PUMP RATE
MODULE AREA
C.O.P.
100
10
1
.1
120
100
80
60
40
20
0
MATERIAL UTILIZATION
$(\frac{Q}{2A\ell})$,watts/cm^3 ;$(\frac{Q_i}{2A})$,watts/cm^2

Fig. 7.4.4.9.15.

MATERIAL UTILIZATION AS A FUNCTION OF C.O.P.

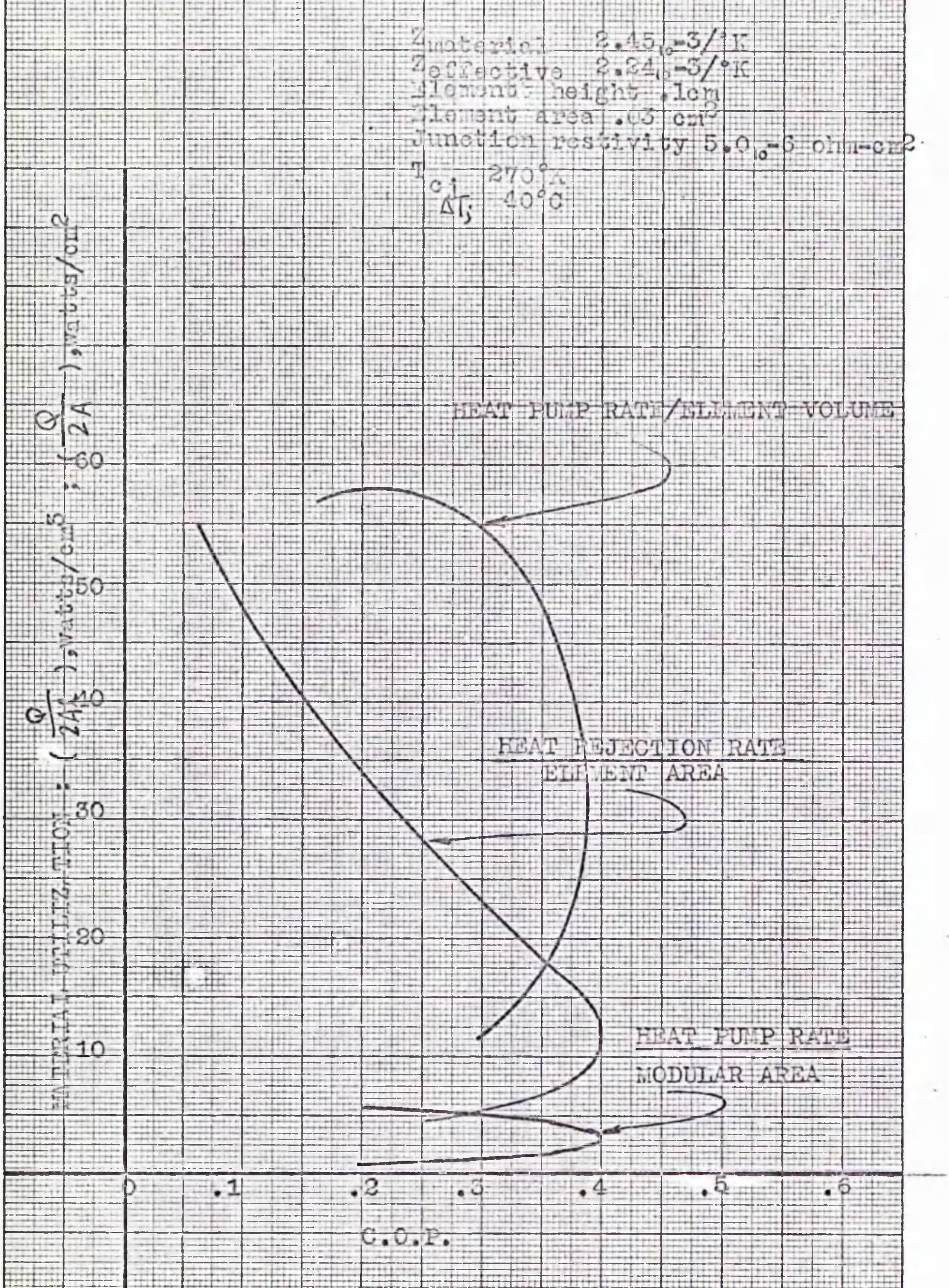

Fig. 7.4.4.9.16.

MATERIAL UTILIZATION AS A FUNCTION OF C.O.P.

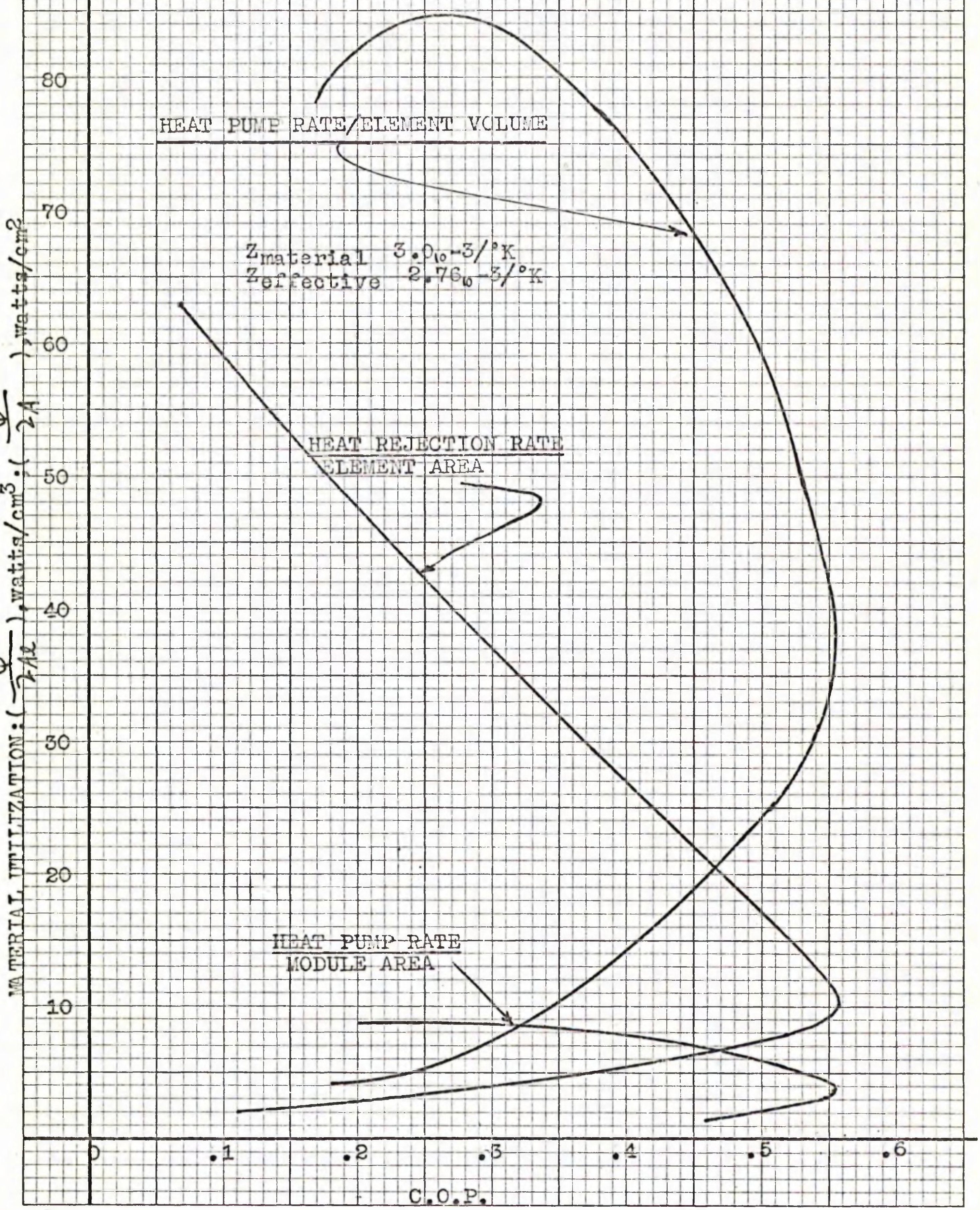

20 watts/cm^2 the heat sink/thermal electrical insulation provides an interface design problem. The heat rejection fluxes for $\ell > .1$ cm will be lower than the values stated above, however the fluxes generally are high enough to require the need for good thermal conductivity at the insulation/heat exchange interface (figure 7.1.2.1).

Basic material data for a production 48 thermocouple thermoelectric module was furnished by the manufacturer. The characteristics of a couple at room temperature (20°C) is as follows:

α_{mp}	$380_{10} - 6$ volts/°C
ℓ	.40cm (element height)
$\sigma(1/\rho)$	675/ohm-cm
A	.0232 cm^2
k	.0140 watts/cm - °C
ρ_j	$5.0_{10} - 6$ ohm - cm^2
ω	.536

Test conducted by the manufacturer indicated a $\Delta T_{j,max\ eff} \cong$ 75°C at a hot junction temperature (373°K). From figure 6.5.6.1 the effective figure of merit is $\cong 1.69_{10} - 3$/°C, $T_{cj_{min}} \cong$ 373 - 75 = 298°K. The manufacturer's test data was compared for two operational conditions $\Delta T_j = 0$, $\Delta T_j = 40$°C. Figure 7.4.4.9.17 presents the results of this analysis. The computer program out-put appears in good agreement with the manufacturer's test data. The computer program output for $\Delta T_j = 40$°C indicated a higher value than the

Fig. 7.4.4.9.17.

COMPARISON OF PUBLISHED DATA FOR A PRODUCTION THERMOELECTRIC MODULE AND THE COMPUTER MODEL AS A FUNCTION OF CURRENT

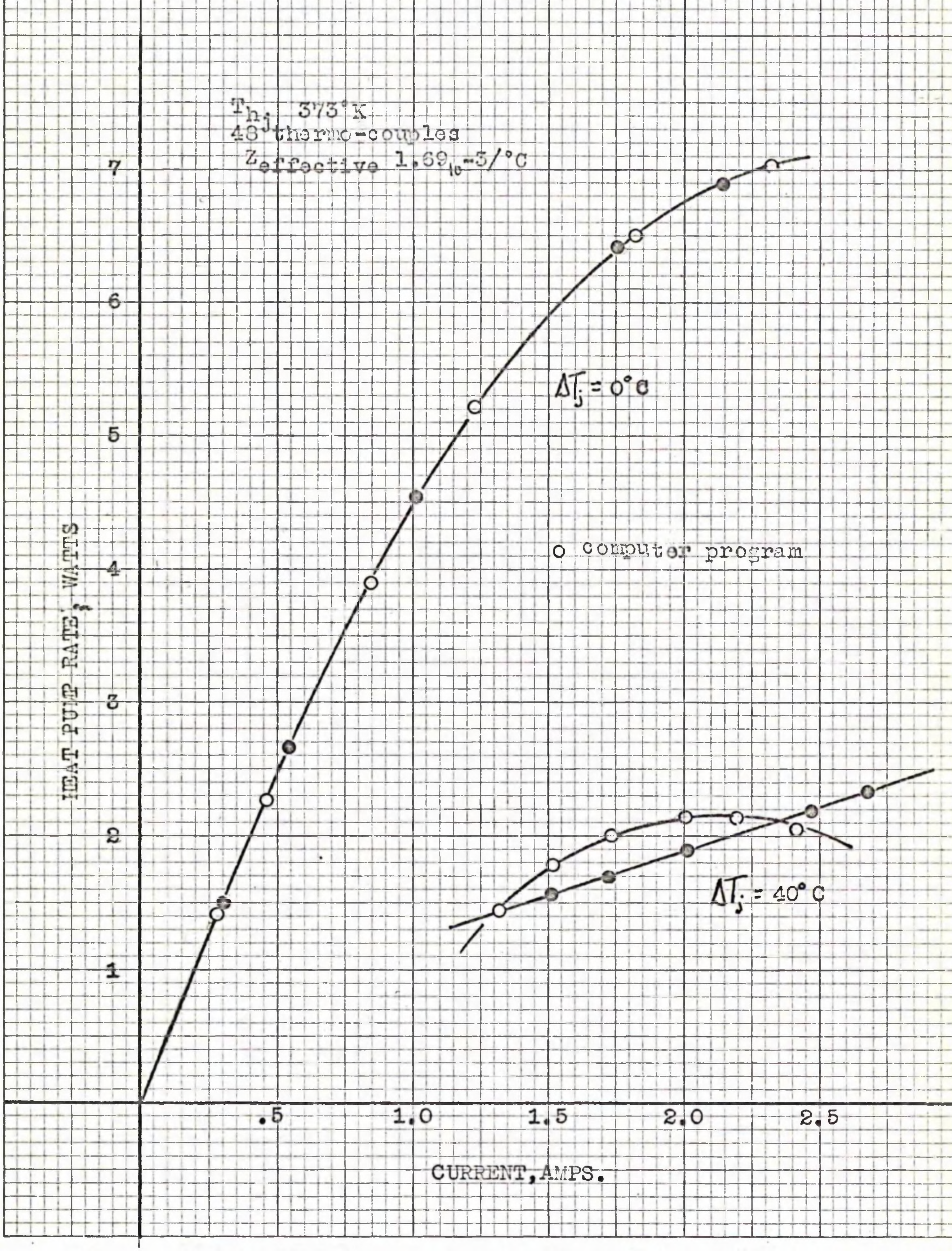

test data. The variation is related to the invariant properties of the materials with temperature and the low contact resistivity quoted by the manufacturer. Information from a Canadian manufacturer quotes a contact resistivity of $\simeq 10.0_{10} - 6$ ohm-cm^2.

Material properties extracted from a thermoelectric air-conditioner submarine application are as follows:

k	.017 watts/cm - ^oC
ρ_j	10×10^{-6} ohm-cm^2
ρ	10×10^{-4} ohm-cm
α	218×10^{-6} volts/^oC
k_i	.0003 watts/cm - oC
l	.5 cm
ω	.50
A_ϕ	.7cm (diameter)

Introducing T_{cj} 283^{o}K and ΔT_j = 45^{o}C the basic computer program (C.P.2.) output can be utilized to develop figure 7.4.4.9.18. To illustrate the data in a form readily identified by the refrigerator engineer the following conversion factors were introduced into the program:

$$K_{WATT} = \frac{NVI}{1000} \qquad 7.4.4.9.1.$$

where:

N is the number of thermoelectric couples in

Fig. 7.4.4.9.18.

C.O.P. AND HEAT PUMP RATE AS A FUNCTION OF POWER INPUT

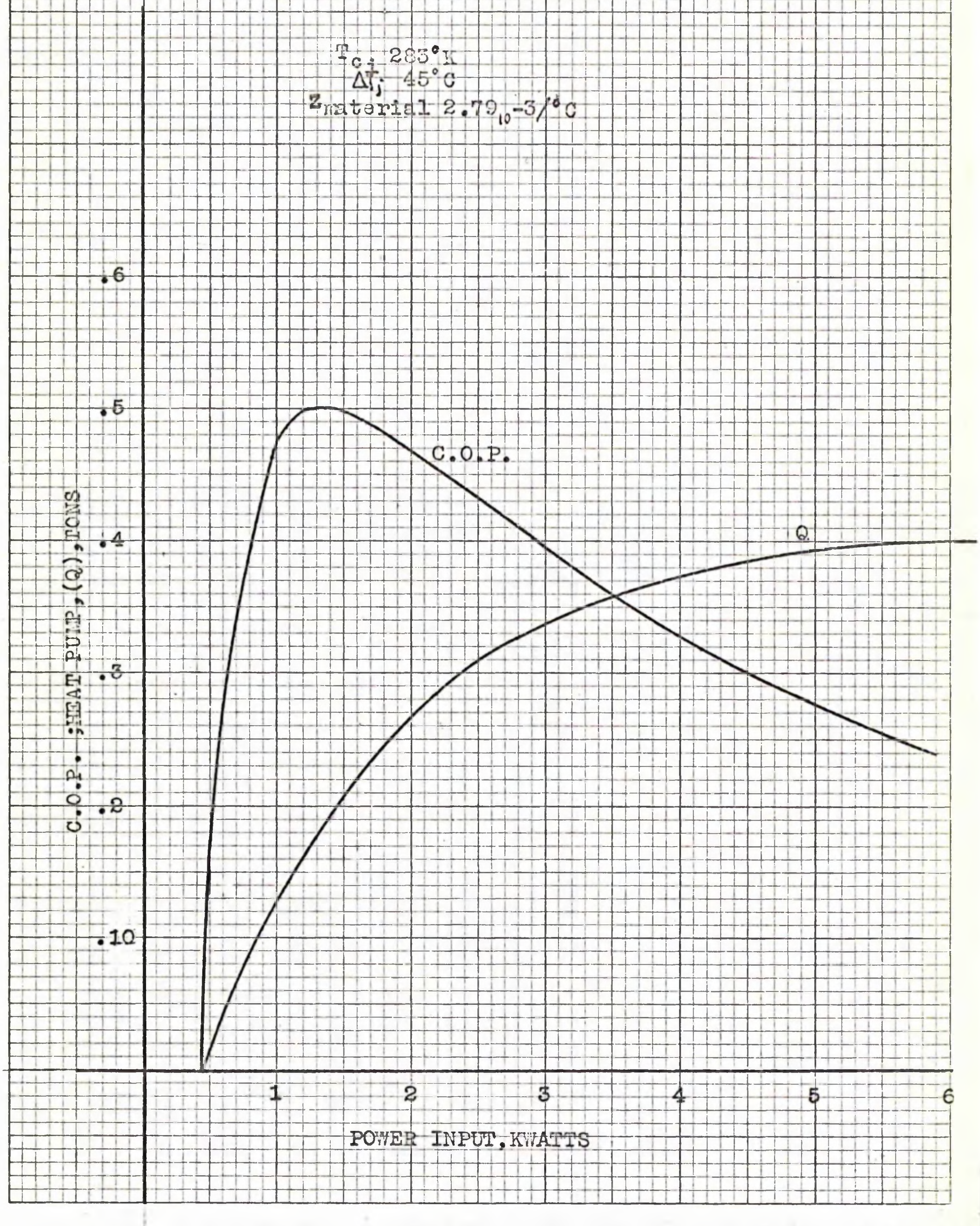

The heat pump rate will be expressed as:

Noting:

$$\frac{BTU}{MIN} \cong \frac{WATTS}{17.57} \qquad 7.4.4.9.2.$$

and

$$1 \text{ TON Refrigeration} \equiv 12{,}000 \frac{BTU}{HR} \text{ (per refrigerator)} \qquad 7.4.4.9.3.$$

therefore:

$$1 \text{ TON Refrigeration} \cong \frac{N Q_s}{(17.57)(200)} \qquad 7.4.4.9.4.$$

where:

Q_s heat pump rate per couple, watts

Figure 7.4.4.9.1.8 illustrates the C.O.P. and the Tons of refrigeration as a function of the power input, (KWATTS). The characteristic (shape, magnitude) of the curves are in good agreement with the test data appearing in reference, (12).

7.4.4.10 Generalized Design Methods.

The design of thermoelectric heat pumps generally follow the outline of chapter 4.0. Intuition and experience initiates a first design which can be effectively evaluated by the "idealized couple" analysis of chapter 6.0. Subsequent modifications in design resulting from the idealized couple analysis can be re-evaluated to the required accuracy by computing the "effective" module performance as detailed in section 7.4.4.

The computer program (C.P.2.) appears to be reasonably adequate. It would be desirable to account for material properties being temperature dependent; introduce a technique that would develop a universal design procedure, and provide for matching the thermoelectric couple to the heat source and heat sink through realistic heat exchangers. In fact, the computer program (C.P.2, 3, 4) will allow for insertion of procedures for accounting for variation in material properties resulting from temperature changes. Section 10.3.4. describes a technique for determing average material properties. Discussion with manufacturers indicate that the universal design curves developed are greatly simplified empiricaly fitted data and much remains to be done in this general area.

A computer program described in Section 8.0 and Appendix M has been developed to obtain the balanced operating point for a basic thermoelectric module with finite heat exchangers operating between a given heat source and heat sink temperature. "Off-design" operation can also be determined. The effect of changing materials or temperature parameters is determined by going through a complete computer cycle. It would be desirable to develop an approximation for more rapid semi-quantitative analysis. Two Russian papers (10) (11) present the subject but; it appears that the resulting equations are not directly applicable for rapid evaluation.

The data illustrated in this section has been programmed on an English Electric KDF9 computer utilizing the "Whetstone Computer". The average run time per set of variables (or each curve) was approximately 30 seconds. At every point (θ_{i+1}) nine outputs were required per 'state point' and there were 42 state points per curve.

7.4.4.11 Comment.

A versitile method for evaluating a given thermoelectric module has been developed and some interesting results presented. While much work has been done on material development a mathematical model is proposed to provide design information and an understanding of the various design parameters on system performance and utilization. The importance of certain parameters can be clearly indicated and the material and fabrication problems that are critical for good design can be quantitatively evaluated. Future sections will include cascaded modules and matching the heat pump requirements to that of the heat exchangers thence the junction temperatures (T_{h_j} , T_{c_j}) are not arbitrary.

The performance equations (previous sections) have been expressed in terms of arbitrary junction temperatures. The next section (chapter 8.0) will consider the effects of the over-all heat transfer coefficients at the hot and cold junction environment interface in order to determine most adequately the performance of a "real" thermoelectric refrigeration system.

8.0 SYSTEM PERFORMANCE - OPERATION BETWEEN HEAT SOURCE AND HEAT SINK WITH FINITE HEAT TRANSFER COEFFICIENTS.

8.1 Introduction.

During the past ten years considerable interest has been focused on the problem of creating useful thermoelectric devices. The rate of progress in the improvement of thermoelectric materials appears to have tapered off. Advancements in material properties indicate a plateau in which additional gains are expensive and require extreme attention to quality control. The best thermoelements from an energy-transformation viewpoint. are those with the highest figure of merit, Z. Present day materials appear to be approaching a performance asymptote. The net effect indicates that a thermoelectric module performance approaches $1/6\ (1/10)$ of the Carnot efficiency for a refrigeration cycle.

The materials which exhibit the highest (a general term) thermoelectric efficiences (to-day - 1969) are n-type $PbTe$ and p- type $BiTe - SbTe$. Present day manufacturers of thermoelectric modules are using tellunides or selenides. Present day technology will increase the application potential into commercial refrigeration systems. While many specialized devices have been demonstrated there are few thermoelectric refrigeration systems being offered for general consumer sale. Many companies offer thermoelectric modules ($\cong$ 20 watts capacity) but the costs appear too high for a general consumer oriented commercial refrigerator cycle.

It appears that through intelligent design, materials of today can within limits compete effectively with the vapor-compression machines currently used in refrigerators. It can be expected that future improvements in utilization techniques will broaden the applications both for ground and space installations.

At present most manufacturers' data related to the performance of thermoelectric devices for refrigerators are based on formulas obtained from a consideration of the internal energy processes within the control volume as illustrated by figure 6.2.1. The resulting conclusions as to cooling potential (Q_s) are drawn on the assumption that the thermocouple junction temperatures (T_{hj}, T_{cj}) do not depend on the strength of the current. Other manufacturers' suggest a 15°F (representative value) adjustment for thermal losses in the heat transfer system. In other words, heat is rejected to a given 55° F water sink temperature (70°F hot-junction temperature resulting) and absorbed from a given 0°F air source (-15°F cold junction temperature resulting). Studies performed by air-conditioning companies such as for an air-control environmental area have presented solutions "tailored" for their specific environment (submarine). The purpose of this section (section 8.0) is to develop a more general technique for solving the system heat-balance equations. The thermoelectric module is to be operating between a heat source and heat sink environment with finite heat transfer coefficients. A number of representative computer outputs are presented to illustrate the basic data available for the design engineer. In order to maintain computer run-time economy a very select number of pedestal supported modules were computed. The run-time (English Electric KDF9 Computer) required to solve the numerical analysis aspect of the pedestal problem is somewhat excessive. A more appropriate computer would be an IBM 360 or speciality machine from Univac Company. The data presented in Appendix M illustrates the dimensionless parameters for a moderate range of variables.

Comment.

Several thermoelectric modules are presented in a general fashion without explicit reference to a specific application. It is hoped that the relationships developed and presented in this section will help to make this area of consideration a little less mysterious and the relevant results a little more familiar.

8.2 Assumptions.

The major assumptions involved in the calculation procedure are as follows:

(1) Material properties are invariant with temperature, ie. within ΔT_j. Temperature dependency relations can be included into the basic computer program.

(2) Electrical conducting strap resistance are neglected.

(3) The plates on the hot side and cold side of the module are isothermal, i.e. the root cross sectional area of the heat exchanger.

(4) The module configuration is planar.

Additional assumptions and nomendature with regard to the basic thermoelectric couple are identical to those listed in section 7.4.4.3. The performance of the heat exchangers are treated in an approximate way for a general utilization of the subsequent relations (Appendix L). The resulting n^{th} order function can be interchanged with a more specific transfer function when the engineering data is developed. Figure 8.2.1 illustrates the basic cooling device considered. The diagram indicates two thermoelements per pedestal as a general concept. Solutions and illustrative examples will be for pedestal and non-pedestal assemblies.

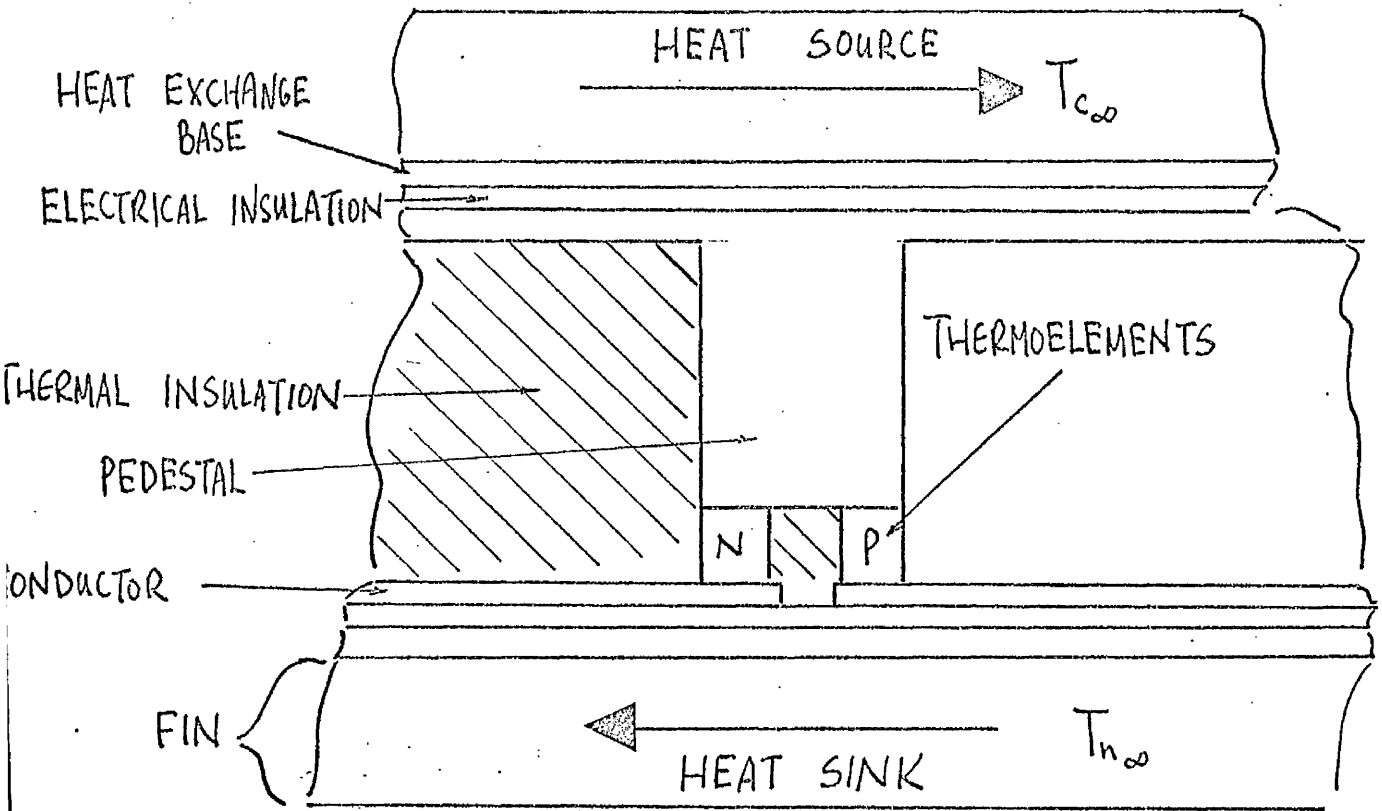

Figure 8.2.1.

Section of a Thermoelectric Cooling Device with Finite Heat Transfer Fins.

8.3 Equations.

The thermoelectric assembly is divided into three components for the purpose of this analysis:

(1) Cold-Side heat exchanger

(2) Thermocouple-Module

(3) Hot-Side heat exchanger

8.3.1 Cold-Side heat exchanger.

The heat flux per couple through the cold side heat exchanger is approximated by the expression:

$$Q_c = E_c A_m \left[T_{c\infty} - T_2 \right]^{1+N_c} \qquad 8.3.1.1.$$

where:

E_c is a constant for a given heat exchanger, heat source, and is a function of the fin effectiveness, heat transfer coefficient, watts/cm^2-^{o}C.

N_c is the exponent factor introduced to account for variation in overall heat transfer coefficients due to variation in fin effectiveness and for the mode of heat transfer, i.e. free/forced convection.

A_m module area, cm^2

$T_{c\infty} - T_2$ temperature difference between fin root and free stream source temperature, ^{o}C.

The heat flow through the electrical insulation interface is expressed as:

$$Q_c = \frac{k_c A_m}{t_c} \left[T_2 - T_{cj} \right] \qquad 8.3.1.2.$$

where:

k_c is the effective thermal conductivity of the cold side electrical insulation interface, watts/cm-°C.

t_c is the thickness of the cold side electrical insulation interface, cm

The cold side heat flux is defined as:

$$\nu_c \equiv \frac{Q_c}{A_m} \qquad 8.3.1.3.$$

where:

ν_c is defined as the heat flux, watts/cm^2

Combining equations (8.3.1.3., 8.3.1.2., 8.3.1.1) results:

$$\Delta T_c = \left[\frac{\nu_c}{E_c}\right]^{\left[\frac{1}{1+N_c}\right]M_c} + \left[\frac{t_c \nu_c}{k_c}\right] \qquad 8.3.1.4.$$

where:

$$\Delta T_c = T_{c_\infty} - T_{c_j} \qquad 8.3.1.5.$$

8.3.2 Thermocouple-Module.

The heat pump rate per couple in terms of the effective parameters can be expressed as:

$$Q_c = T_{c_j} I \alpha_{np} - \frac{1}{2} I^2 R_{EFF} - K_{EFF} \Delta T_j \qquad 8.3.2.1.$$

where:

$$R_{EFF} = \left[\frac{2\rho l}{A} + \frac{4\rho_j}{A}\right] F^2 \qquad 7.4.4.4.1.$$

$$K_{EFF} = \frac{2Ak}{l} + k_i\left[\frac{f2A(1-\omega)}{l\omega} + g(1-f)\right]$$

7.4.4.4.2.

The equation for Q is quadratic in I and is expressed as:

$$A'I^2 + BT_{c_j}I - \left[C\Delta T_j + \mathcal{V}_c\right] = 0 \qquad 8.3.2.2.$$

where:

A', B, C are material property parameters defined as follows:

$$A' \equiv \frac{\omega R_{EFF}}{4A} \qquad 8.3.2.3.$$

$$B \equiv \frac{\omega \alpha_{np}}{2A} \qquad 8.3.2.4.$$

$$C = \frac{\omega K_{EFF}}{2A} \qquad 8.3.2.5.$$

By means of the quadratic formula the current for a given module configuration at known T_{c_j}, ΔT_j, $\mathcal{V}_c$ (cold side heat flux) is:

$$I = \frac{BT_{c_j} - \sqrt{[BT_{c_j}]^2 - 4A'[C\Delta T_j + \mathcal{V}_c]}}{2A'} \qquad 8.3.2.6.$$

The negative sign $-\sqrt{}$ is based on the singularity at power "off" operation $I = 0$, $\Delta T_j = 0$, $\mathcal{V}_c = 0$.

The electrical power per couple is expressed as:

$$P = \alpha_{np} I \Delta T_j + I^2 R_{EFF} \qquad 8.3.2.7.$$

The electrical power per unit of module area (A_m) is defined as:

$$\frac{P}{A_m} = \frac{\alpha_{np} I \Delta T_j \omega}{2A} + \frac{I^2 R_{EFF} \omega}{2A} \qquad 8.3.2.8.$$

and introducing the material property parameters

$$\frac{P}{A_m} = 2A' I^2 + B I \Delta T_j \qquad 8.3.2.8.$$

The C.O.P. by definition is:

$$C.O.P. = \frac{Q_c}{P} \qquad 8.3.2.10.$$

or

$$C.O.P. = \frac{\mathcal{V}_c}{P/A_m} \qquad 8.3.2.11.$$

The heat rejected per couple on the hot side of the module is expressed as:

$$Q_R = Q_c + P \qquad 8.3.2.12.$$

or

$$Q_R = Q_c \left[1 + \frac{1}{C.O.P.} \right] \qquad 8.3.2.13.$$

Introducing the hot side heat flux:

$$\vartheta_h = \frac{Q_R}{A_m} \qquad 8.3.2.14.$$

then equation 8.3.2.13 results:

$$\vartheta_h = \vartheta_c\left[1 + \frac{1}{C.O.P.}\right] \qquad 8.3.2.15.$$

8.3.3 Hot-Side Heat Exchanger.

Defining the hot side temperature drop as:

$$\Delta T_h = T_{hj} - T_{h\infty} \qquad 8.3.2.16.$$

and using the same procedure as used on the cold side the hot side temperature drop can be expressed as:

$$\Delta T_h = \left[\frac{\vartheta_h}{E_h}\right]^{\left[\frac{1}{1+N_h}\right]M_h} + \left[\frac{t_h \vartheta_h}{k_h}\right] \qquad 8.3.2.17.$$

where:

ϑ_h the heat flux through the electrical insulation on the hot side, watts/cm^2

E_h, N_h constants for the given heat exchanger (as defined by equation 8.3.1.1)

k_h, t_h equivalent thermal conductivity, electrical insulation on the hot side of the module (as defined by equation 8.3.1.2)

8.4 Calculation Procedure.

The computer program calculates the performance of the thermoelectric system at the balanced operating point by an iterative procedure. The type of heat source, heat sink, heat source temperature, heat sink temperature, material property, module configuration are input information. The desired heat flux (ν_c) on the cold side is specified. The cold side temperature drop (ΔT_c) is calculated by equation 8.3.1.4. The cold side junction temperature is calculated by $T_{c_j} = T_{c_\infty} - \Delta T_c$ An initial value of the hot junction temperature (T_{h_j}) is assumed and the hot to cold junction temperature difference is expressed as: $\Delta T_j = T_{h_j} - T_{c_j}$; then I, C.O.P., ν_h, ΔT_h and T_{h_j} are calculated in that order and recalling: $T_{h_j} = T_{h_\infty} + \Delta T_h$. At this point the calculated value of T_{h_j} is compared with the initial value. If they do not agree to some allowable error (eprs) a new value of T_{h_j} is assumed and the procedure is repeated until a desired limit of error is obtained. The iterative technique when satisfactorily completed yields the balance operating point and provides the C.O.P., I, ν_c, ν_h, T_{c_j}, T_{h_j}, ΔT_j (etc) at the operational current. Other performance parameters (section 7.4.4.4) can be calculated as required. To illustrate the basic output data available; two representative computer outputs are presented (non-pedestal, pedestal).

In using the iterative procedure on a digital computer the selection of the input variable (ν_c) must fall within the range of the device capability (i.e. for the given heat source and heat sink temperature) otherwise no interesting results will be obtained. To conserve computer time a statement has been incorporated into the basic program to avoid this difficulty. Details of control statements are illustrated in Appendix C.P.5.

In the evaluation of new designs, preliminary estimates of module performance can be made using the methods presented in section 7.4.

8.5 Input/Output Information.

For a given module configuration (with or without pedestal), there is required 35 pieces of input data. The data required is:

ω	packing density
Ratio	Ap/A
l	module height, cm
A_m, A_p	area of thermoelement, cm^2
ω	overelaxation factor (1.5 appears reasonable)
E	maximum number of iterative loops in numerical sweep
l_m, l_p	thermoelement height, cm

note:

$$l_m, l_p = l \times l^*$$

Table 8.5.1.

```
THIS PROGRAM CALCULATES FOR A GIVEN MODULAR MATERIAL OPERATING
BETWEEN A HEAT SOURCE AND HEAT SINK WITH FINITE HEAT TRANSFER COEFFICIENT
THE PERFORMANCE CHARACTERISTICS


MATERIAL CHARACTERISTICS OF THE GIVEN MODULE

ELEMENT HEIGHT  CM.         +0.200000
JUNCTION RESISTIVITY  OHM CM SQRD   +2.50⏨- 5
CONDUCTIVITY OF N-ELEMENT  1/OHM CM  TERMINOLOGY SIGMAN     +894.000000
CONDUCTIVITY OF P-ELEMENT  1/OHM CM  TERMINOLOGY SIGMAP     +894.000000
PACKING DENSITY        +0.877000
AREA OF N-ELEMENT  CM SQRD        +0.040000
AREA OF P-ELEMENT  CM SQRD        +0.040000
SEEBECK COEFFICIENT  VOLTS/DEG KELVIN   +4.43⏨- 4
HEIGHT OF PEDESTAL  CM         +0.000000
HEIGHT OF MODULE  CM         +0.200000
RIPPLE FACTOR         +1.001000
PERCENT RIPPLE         +0.001265
THERMAL CONDUCTIVITY N-ELEMENT  WATT/CM DEG KELVIN        +0.014700
THERMAL CONDUCTIVITY P-ELEMENT  WATT/CM DEG KELVIN        +0.014700
FREE STREAM HEAT SINK TEMPERATURE  DEG KELVIN =       +300.000000
FREE STREAM SOURCE TEMPERATURE  DEG KELVIN =       +250.000000


MATERIAL THERMOELECTRIC MODULE PERFORMANCE

THE HOT AND COLD JUNCTIONS ARE SEPERATED BY THE ELEMENT PROPER


EFFECTIVE MATERIAL PROPERTIES

SHAPE FACTOR FOR OPTIMIZING COP =         +1.000000
COUPLE ELEMENT INTERIOR RESISTANCE  OHMS =         +0.011186
EFFECTIVE RESISTANCE  OHMS = +1.37⏨- 2
COUPLE ELEMENT THERMAL CONDUCTANCE  WATTS/DEG KELVIN =        +0.005880
EFFECTIVE THERMAL CONDUCTANCE  WATTS/DEG KELVIN =     +5.89⏨- 3
EFFECTIVE FIGURE OF MERIT  1/DEG KELVIN =     +2.43⏨- 3
COUPLE ELEMENT THERMAL CONDUCTANCE  WATTS/DEG KELVIN =        +0.005880
SHAPE FACTOR FOR OPTIMIZING COP =         +1.000000
COUPLE ELEMENT INTERIOR RESISTANCE  OHMS =         +0.011186
MATERIAL FIGURE OF MERIT 1/DEG KELVIN = +2.98⏨- 3

THE OPTION OF USING THE FOR STATEMENT HAS BEEN EXERCIZED
THE COLD SIDE HEAT FLUX IS BEING INCREMENTALY STEPPED BY THE FOR LOOP
ESTIMATED JUNCTION TEMPERATURES ESTABLISHING THE UPPER VALUE IN THE FOR
STATEMENT FOLLOWS:
ESTIMATED COLD SIDE JUNCTION TEMPERATURE  DEG KELVIN =     +235.00
ESTIMATED HOT SIDE JUNCTION TEMPERATURE  DEG KELVIN =     +315.00
ESTIMATED TEMPERATURE DIFFERENCE ACROSS JUNCTION  DEG C =      +80.00

THE UNIFORM COLD SIDE HEAT FLUX HAS BEEN ASSIGNED A VALUE  WATTS/CM SQRD
```

cont

```
THE UNIFORM COLD SIDE HEAT FLUX HAS BEEN ASSIGNED A VALUE  WATTS/CM SQRD
XXXXXXXXXXXXXXXXXXXXXXXXXXXXXXXXXXXXXXXXXX
       +0.800000
XXXXXXXXXXXXXXXXXXXXXXXXXXXXXXXXXXXXXXXXXX
EXPONENT VALUE FOR COLD SIDE HEAT TRANSFER COEFFICIENT =        +0.000000

ITERATIVE SOLUTION FOLLOWS
ITERATIONS      TSUBH DEG KEL       COMPARISON TSUBH

+0.00         +3.02x+ 2        +0.000000
+1.00x+ 0     +3.04x+ 2      +305.710529
+2.00x+ 0     +3.05x+ 2      +306.116055
+3.00x+ 0     +3.06x+ 2      +306.403752
+4.00x+ 0     +3.06x+ 2      +306.606213
+5.00x+ 0     +3.06x+ 2      +306.748024
+6.00x+ 0     +3.07x+ 2      +306.847076
+7.00x+ 0     +3.07x+ 2      +306.916143

BALANCED OPERATION ACHIEVED

THE ITERATIONS FOR THE HOT SIDE TEMPERATURE AT THE JUNCTION HAS SUCCESSFULLY
TERMINATED TO THE REQUIRED ERROR  1° EPSO


EXPONENT VALUE FOR HOT SIDE HEAT TRANSFER COEFFICIENT =        +0.000000
COLD SIDE HEAT FLUX  WATTS/CM SQRD =          +0.800000
HOT JUNCTION TEMPERATURE  DEG KELVIN =        +306.875153
JUNCTION TEMPERATURE DIFFERENCE  DEG KELVIN =        +58.368605
COLD SIDE JUNCTION TEMPERATURE  DEG KELVIN =       +248.417453
ITERATIONS TO ACHIEVE BALANCED OPERATIONAL SOLUTION =        +8.0000
CURRENT PER COUPLE REQUIRED TO MAINTAIN HEAT BALANCE  AMPS =        +6.1319
ELECTRICAL POWER REQUIRED TO MAINTAIN HEAT BALANCE  WATTS/COUPLE =        +0.6742
ELECTRICAL POWER REQUIRED FOR A SYSTEM CONTAINING NO-COUPLES IN ELECTRICAL SERIES  KW =        +0.030338
COP  AT THE BALANCED OPERATION =         +0.108246
THE REQUIRED HEAT REJUCTION RATE/MODULAR AREA  WATTS/CM SQRD =        +8.190575
```

```
THE ASSUMPTION FOR THE DESIGN IS THAT THE NO-COUPLES ARE ELECTRICALLY IN SERIES
ELECTRICAL POWER REQUIREMENTS
VOLTAGE PER COUPLE AT BALANCED OPERATION  VOLTAGE =          +0.109944
VOLTAGE FOR A SYSTEM OF NO-COUPLES ELECTRIACALLY IN SERIES  VOLTAGE =        +4.9475
THE CURRENT THAT MAXIMIZES THE HEAT PUMP RATE  AMPS =        +8.025114
RATIO CURRENT AT BALANCED OPERATION TO CURRENT AT MAX HEAT PUMP RATE =          +0.764089
RATIO CURRENT AT MAX COP TO CURRENT AT MAX HEAT PUMP RATE =          +0.799610
THE CURRENT REQUIRED TO MAXIMIZE COP  AMPS =        +6.416963
RATIO CURRENT AT OPERATIONAL BALANCE TO CURRENT AT MAX COP =          +0.955577
VOLTAGE PER COUPLE FOR MAXIMIZING HEAT PUMP RATE  VOLTS =          +0.135946
RATIO VOLTAGE AT BALANCED OPERATION TO VOLTAGE AT MAX HEAT PUMP RATE =          +0.808738
VOLTAGE PER COUPLE FOR MAXIMIZING COP  VOLTS =      +1.14m- 1
RATIO VOLTAGE AT BALANCED OPERATION TO VOLTAGE AT MAX COP =          +0.965666
THE MAX TEMPERATURE DIFFERENCE IS BASED ON THE COLD JUNCTION TEMPERATURE BEING A REFERENCE
THE MAX TEMPERATURE DIFFERENCE BASED ON MATERIAL PROPERTIES  DEG C =        +92.07
MAX TEMPERATURE DIFFERENCE BASED ON EFFECTIVE FIGURE OF MERIT DEG C =        +74.92
MAX COP =         +0.109253
RATIO OPERATING COP TO MAX COP =         +0.990783
HEAT PUMP RATE PER ELEMENT VOL  WATTS/CM CUB =          +4.561003
THE NEXT COMPUTER OUTPUTS COMPARE THE OPERATIONAL SOLUTIONS FOR THE BALANCED SYSTEM
HEAT PUMP RATE /MODULAR AREA  WATTS/CM SQRD
QUMODARA =         +0.800000
NUC =         +0.800000

HEAT REJECTION RATE/MODULAR AREA  WATTS/CM SQRD
NUH =         +8.190575
QRMODARA =         +8.190575


HEAT PUMP RATE WITH NO-COUPLES THERMALLY PARALLEL  TONS =          +0.000937
HEAT PUMP RATE WITH NO-COUPLES THERMALLY PARALLEL  WATTS =          +3.283922
RATIO HEAT PUMP RATE AT BALANCED OPERATION TO MAX HEAT PUMP RATE =          +0.748076


THE FOLLOWING RESULTS ARE BASED ON APPROXIMATIONS .THE APPROXIMATIONS FOR A COUPLE
AND SUBSEQUENT IMPLICATIONS OF ASSUMING THE PARAMETERS LAMBDA AND RECIPRICAL FUNCTION EQUAL TO
UNITY IS FOUND IN SECTION      6.6          OF THIS THESIS

COP AT MAX Q =         +0.110458
MAX COP =         +0.141779
HEAT PUMP RATE AT MAX COP =          +0.076001
CURRENT PROVIDING MAX COP =          +6.252237
```

cont

k_m, k_p thermal element conductivity, watts/cm-^oC

δ_m, δ_p electrical conductivity $(\text{ohm-cm})^{-1}$

N_h, N_c exponent value for heat exchangers

$f(0,1)$ modification factors for heat exchangers pedestal or non-pedestal assembly

F ripple factor

α_{mp} Seebeck couple coefficient volts/^oC

incr stepping term for changing γ_c

epso error value for terminating numerical solution

ρ_{jp}, ρ_{jm} element junction resistivity, ohm-cm^2

k_i insulation thermal conductivity, watts/cm^oC

lower starting of γ_c , watts/cm^2

$T_{c\infty}$ free stream source temperature, ^oK

$T_{h\infty}$ free stream sink temperature, ^oK

thkcold, thkhot electrical insulation thickness, cm

E_h, E_c heat exchanger factor, watts/cm^2-^oC

L limit control on interative loop

NO number of thermoelectric couples in electrical series

The output from each module design and given set of input variables (as listed above) are tabulated by the computer. Typical output is presented on Table 8.5.1 and Table 8.5.2. The output consists of dimensionless parameters and operational values. The output can be modified to match the design problem and requirements of the engineer. The format may be considered elaborate for general engineering design; the purpose within the thesis is to illustrate the inform-

Table 8.5.2.

THIS PROGRAM CALCULATES FOR A GIVEN MODULAR MATERIAL OPERATING
BETWEEN A HEAT SOURCE AND HEAT SINK WITH FINITE HEAT TRANSFER COEFFICIENT
THE PERFORMANCE CHARACTERISTICS

MATERIAL CHARACTERISTICS OF THE GIVEN MODULE

ELEMENT HEIGHT CM. +0.600000
JUNCTION RESISTIVITY OHM CM SQRD +1.00₁₀- 5
CONDUCTIVITY OF N-ELEMENT 1/OHM CM TERMINOLOGY SIGMAN +1000.000000
CONDUCTIVITY OF P-ELEMENT 1/OHM CM TERMINOLOGY SIGMAP +1000.000000
PACKING DENSITY +0.010000
AREA OF N-ELEMENT CM SQRD +0.030000
AREA OF P-ELEMENT CM SQRD +0.030000
SEEBECK COEFFICIENT VOLTS/DEG KELVIN +4.60₁₀- 4
HEIGHT OF PEDESTAL CM +1.400000
HEIGHT OF MODULE CM +2.000000
RIPPLE FACTOR +1.001000
PERCENT RIPPLE +0.001265
THERMAL CONDUCTIVITY N-ELEMENT WATT/CM DEG KELVIN +0.017000
THERMAL CONDUCTIVITY P-ELEMENT WATT/CM DEG KELVIN +0.017000
FREE STREAM HEAT SINK TEMPERATURE DEG KELVIN = +302.700000
FREE STREAM SOURCE TEMPERATURE DEG KELVIN = +285.700000

MATERIAL THERMOELECTRIC MODULE PERFORMANCE

THE THERMOELECTRIC ELEMENTS ARE POSITIONED ON A PEDESTAL

THIS PROGRAM CALCULATES THE GEOMETRICAL PARAMETERS
ASSOCIATED WITH THE HEAT FLOW MODEL THAT YIELD THE VALUES OF Q/QSUBC!

DEFINITION OF GEOMETRICAL PARAMETERS

LSTAR = DIMENSIONLESS LENGTH OF THE THERMOELECTRIC
COLUMN
BSTAR = DIMENSIONLESS PARAMETER L/B
RSTAR = DIMENSIONLESS PARAMETER A/B

PROCEDURE OPTILAX AND SUBTAB WHEN INCLUDED
EXTEND THE COMPUTATIONAL ACCURACY OF THE PROCEDURE ITERATE

THREE REAL PROCEDURES CALCULATE THE DIMENSIONLESS PARAMETERS REQUIRED AS INPUT

PACKING DENSITY = +0.0100
CROSS SECTIONAL AREA OF ELEMENT = +0.0300
PEDESTAL AREA TO ELEMENT AREA = +6.0000
HEIGHT OF ELEMENT = +0.6000
EPSO = +0.0100

```
LSTAR =              +0.3000
RSTAR =            +0.1732
BSTAR =                 +1.4481
MATRIX SIZE  N =                  +12.0000
ITERATIONS =                 +49.0000
OMEGA =              +1.5000
TEMPERATURE =                  +0.8819
QSUBK =              +0.9293
RATIO =               +1.63721
HEAT LEAKAGE =               +49.64286

EFFECTIVE MATERIAL PROPERTIES

SHAPE FACTOR FOR OPTIMIZING COP =           +1.000000
COUPLE ELEMENT INTERIOR RESISTANCE  OHMS =           +0.040000
EFFECTIVE RESISTANCE  OHMS = +4.14m- 2
COUPLE ELEMENT THERMAL CONDUCTANCE  WATTS/DEG KELVIN =          +0.001700
EFFECTIVE THERMAL CONDUCTANCE  WATTS/DEG KELVIN =    +3.19m- 3
EFFECTIVE FIGURE OF MERIT  1/DEG KELVIN =      +1.60m- 3
COUPLE ELEMENT THERMAL CONDUCTANCE  WATTS/DEG KELVIN =          +0.001700
SHAPE FACTOR FOR OPTIMIZING COP =           +1.000000
COUPLE ELEMENT INTERIOR RESISTANCE  OHMS =           +0.040000
MATERIAL FIGURE OF MERIT 1/DEG KELVIN = +3.11m- 3

THE OPTION OF USING THE FOR STATEMENT HAS BEEN EXERCIZED
THE COLD SIDE HEAT FLUX IS BEING INCREMENTALY STEPPED BY THE FOR LOOP
ESTIMATED JUNCTION TEMPERATURES ESTABLISHING THE UPPER VALUE IN THE FOR
STATEMENT FOLLOWS:
ESTIMATED COLD SIDE JUNCTION TEMPERATURE  DEG KELVIN =     +270.70
ESTIMATED HOT SIDE JUNCTION TEMPERATURE  DEG KELVIN =     +317.70
ESTIMATED TEMPERATURE DIFFERENCE ACROSS JUNCTION  DEG C =      +47.00

THE UNIFORM COLD SIDE HEAT FLUX HAS BEEN ASSIGNED A VALUE  WATTS/CM SQRD
XXXXXXXXXXXXXXXXXXXXXXXXXXXXXXXXXXXXXXXX
      +0.017000
XXXXXXXXXXXXXXXXXXXXXXXXXXXXXXXXXXXXXXXX
EXPONENT VALUE FOR COLD SIDE HEAT TRANSFER COEFFICIENT =       +0.400000
```

,cont

cont

```
ITERATIVE SOLUTION FOLLOWS
ITERATIONS        TSUBH DEG KEL        COMPARISON TSUBH

+0.00          +3.06"+ 2          +0.000000
+1.00"+ 0      +3.04"+ 2       +303.325551
+2.00"+ 0      +3.04"+ 2       +303.314582

BALANCED OPERATION ACHIEVED

THE ITERATIONS FOR THE HOT SIDE TEMPERATURE AT THE JUNCTION HAS SUCCESSFULLY
TERMINATED TO THE REQUIRED ERROR 1° EPSO


EXPONENT VALUE FOR HOT SIDE HEAT TRANSFER COEFFICIENT =          +0.400000
COLD SIDE HEAT FLUX  WATTS/CM SQRD =            +0.017000
HOT JUNCTION TEMPERATURE  DEG KELVIN =          +303.593590
JUNCTION TEMPERATURE DIFFERENCE  DEG KELVIN =          +18.608854
COLD SIDE JUNCTION TEMPERATURE  DEG KELVIN =        +285.269075
ITERATIONS TO ACHIEVE BALANCED OPERATIONAL SOLUTION =        +3.0000
CURRENT PER COUPLE REQUIRED TO MAINTAIN HEAT BALANCE  AMPS =        +1.6693
ELECTRICAL POWER REQUIRED TO MAINTAIN HEAT BALANCE  WATTS/COUPLE =       + 0.1296
ELECTRICAL POWER REQUIRED FOR A SYSTEM CONTAINING NO-COUPLES IN ELECTRICAL SERIES  KW
COP  AT THE BALANCED OPERATION =         +0.786425                          + .002324
THE REQUIRED HEAT REJUCTION RATE/MODULAR AREA  WATTS/CM SQRD =          +0.038617
```

cont

```
THE ASSUMPTION FOR THE DESIGN IS THAT THE NO-COUPLES ARE ELECTRICALLY IN SERIES(18)
ELECTRICAL POWER REQUIREMENTS
VOLTAGE PER COUPLE AT BALANCED OPERATION  VOLTAGE =          + .07756
VOLTAGE FOR A SYSTEM OF NO-COUPLES ELECTRIACALLY IN SERIES  VOLTAGE =      + 1.400(18)
THE CURRENT THAT MAXIMIZES THE HEAT PUMP RATE  AMPS =        +3.168429
RATIO CURRENT AT BALANCED OPERATION TO CURRENT AT MAX HEAT PUMP RATE =        +0.526861
RATIO CURRENT AT MAX COP TO CURRENT AT MAX HEAT PUMP RATE =        +0.305944
THE CURRENT REQUIRED TO MAXIMIZE COP  AMPS =        +0.969361
RATIO CURRENT AT OPERATIONAL BALANCE TO CURRENT AT MAX COP =        +1.722083
VOLTAGE PER COUPLE FOR MAXIMIZING HEAT PUMP RATE  VOLTS =        +0.139653
RATIO VOLTAGE AT BALANCED OPERATION TO VOLTAGE AT MAX HEAT PUMP RATE =        + .5580
VOLTAGE PER COUPLE FOR MAXIMIZING COP  VOLTS =     +4.87#- 2
RATIO VOLTAGE AT BALANCED OPERATION TO VOLTAGE AT MAX COP =        + 1.594
THE MAX TEMPERATURE DIFFERENCE IS BASED ON THE COLD JUNCTION TEMPERATURE BEING A REFERENCE
THE MAX TEMPERATURE DIFFERENCE BASED ON MATERIAL PROPERTIES  DEG C =     +126.62
MAX TEMPERATURE DIFFERENCE BASED ON EFFECTIVE FIGURE OF MERIT  DEG C =     +65.18
MAX COP =        +1.025011
RATIO OPERATING COP TO MAX COP =        +0.767236
HEAT PUMP RATE PER ELEMENT VOL  WATTS/CM CUB =        +2.833333
THE NEXT COMPUTER OUTPUTS COMPARE THE OPERATIONAL SOLUTIONS FOR THE BALANCED SYSTEM
HEAT PUMP RATE /MODULAR AREA  WATTS/CM SQRD
QUMODARA =        +0.017000
NUC =        +0.017000
```

```
HEAT REJECTION RATE/MODULAR AREA  WATTS/CM SQRD
NUH =          +0.038617
QRMODARA =             +0.038617


HEAT PUMP RATE WITH NO-COUPLES THERMALLY PARALLEL  TONS =          +0.000524
HEAT PUMP RATE WITH NO-COUPLES THERMALLY PARALLEL  WATTS =          +1.836000
RATIO HEAT PUMP RATE AT BALANCED OPERATION TO MAX HEAT PUMP RATE =          +0.686695

THE FOLLOWING RESULTS ARE BASED ON APPROXIMATIONS .THE APPROXIMATIONS FOR A COUPLE
AND SUBSEQUENT IMPLICATIONS OF ASSUMING THE PARAMETERS LAMBDA AND RECIPRICAL FUNCTION EQUAL TO
UNITY IS FOUND IN SECTION  6.6                OF THIS THESIS

COP AT MAX Q =          +0.357256
MAX COP =          +1.251392
HEAT PUMP RATE AT MAX COP =          +0.042406
CURRENT PROVIDING MAX COP =          +0.904546
```

cont

ation available. In the next section engineering decisions based on a general sweep of results will be presented.

8.6 Material Utilization as a Performance Parameter.

8.6.1 Philosophy.

Advancements in material properties, demands which space applications make on thermoelectric devices, stimulates the need for a comprehensive computer model. In the general literature the internal energy process as reflected in the relationships of section 6.0 has been delt with and the author's approach is summarized in computer program C.P.2. In this type of analysis it is assumed that the junction temperature are known and are invariant with the current density passing through the couple.

In the actual system application, it is not the junction temperatures that are known but the temperatures of the environment to be regulated. When the coefficients of heat transfer are constant then the current-density changes the heat flow through the junctions and hence the temperature changes between the junction and environment consequently the junction temperature.

It is the basic object of this section to present examples of the energy balance for the case when the

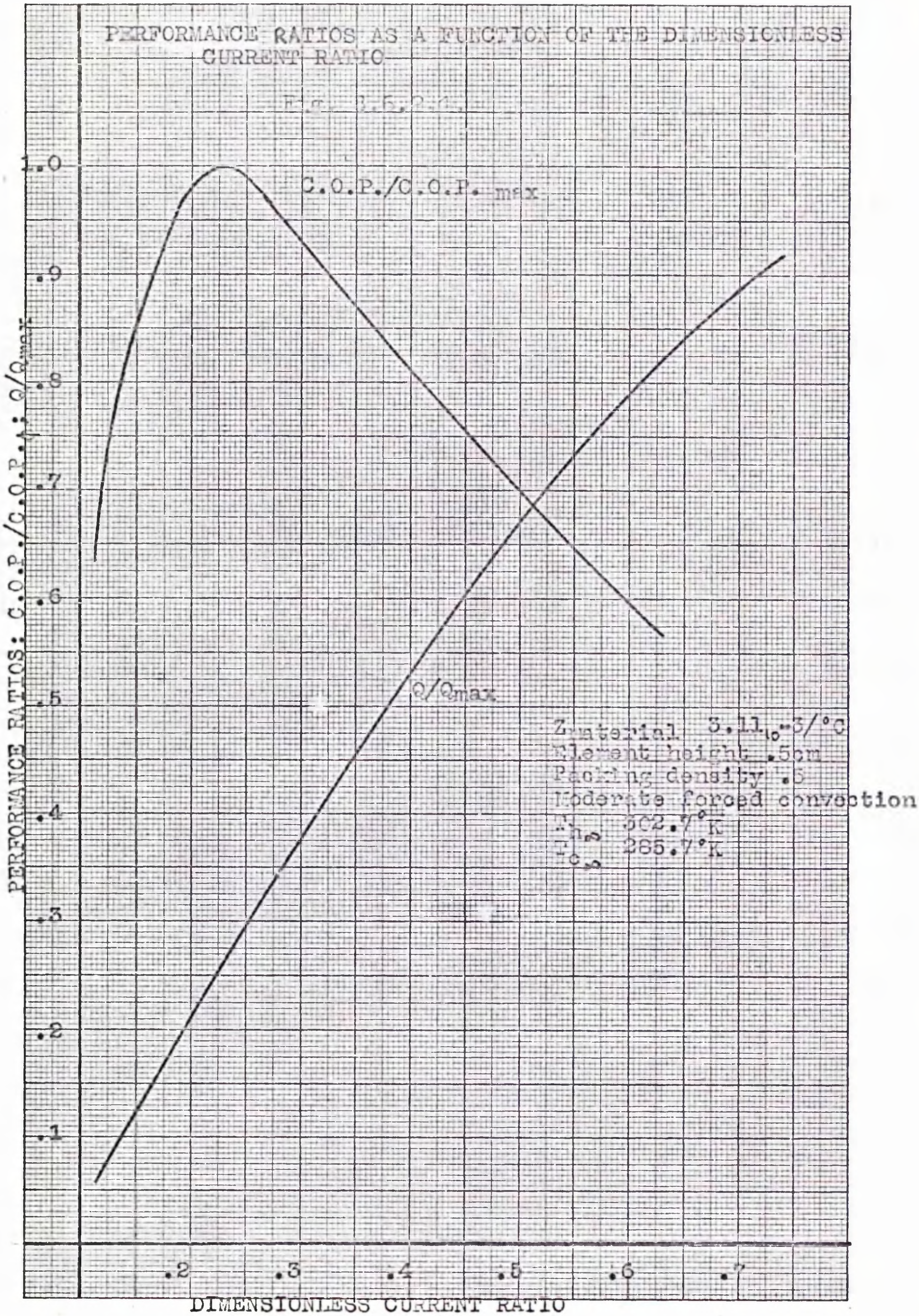

PERFORMANCE RATIOS AS A FUNCTION OF THE DIMENSIONLESS CURRENT RATIO

Fig. 3.5.2.4.

conditions of heat transfer between couple and environment are given by the coefficients of the heat exchangers. The quantitative result depends on the form of the function: $T_j = g\ (I)$ which depends on the nature of the interface between the thermoelectric couple and the media to be controlled.

The relations derived in this section reflect more accurately the "actual" process occuring in a "real" thermoelectric system. The result: 'A technique is proposed to account for the thermal/energetic heat balance of a thermoelectric device operating between known heat source and heat sink temperatures; taking into account the temperature dependence on current magnitude'.

8.6.2 General Results.

This section illustrates the general resulting output available from the computer program (C.P.5). Table 8.5.1 presents the computer output for a conventional thermoelectric module. Table 8.5.2 presents the computer output for a pedestal module thermoelectric assembly. Figure 8.6.2.1 indicates the functional parameters ($C.O.P./C.O.P._{max}$, $Q_s/Q_{s\,max}$) as a function of the current parameter (θ, I/I_Q). The current (I) is the required current to maintain thermal balance under the given boundry conditions. Figure 8.6.2.1 indicates the following characteristics: The parametric ratios exhibit an increasing-decreasing function which is similar to figure 6.7.1 and figure 6.7.2. Figure 8.6.2.2 illustrates the

OPERATIONAL CHARACTERISTICS AS A FUNCTION OF POWER INPUT

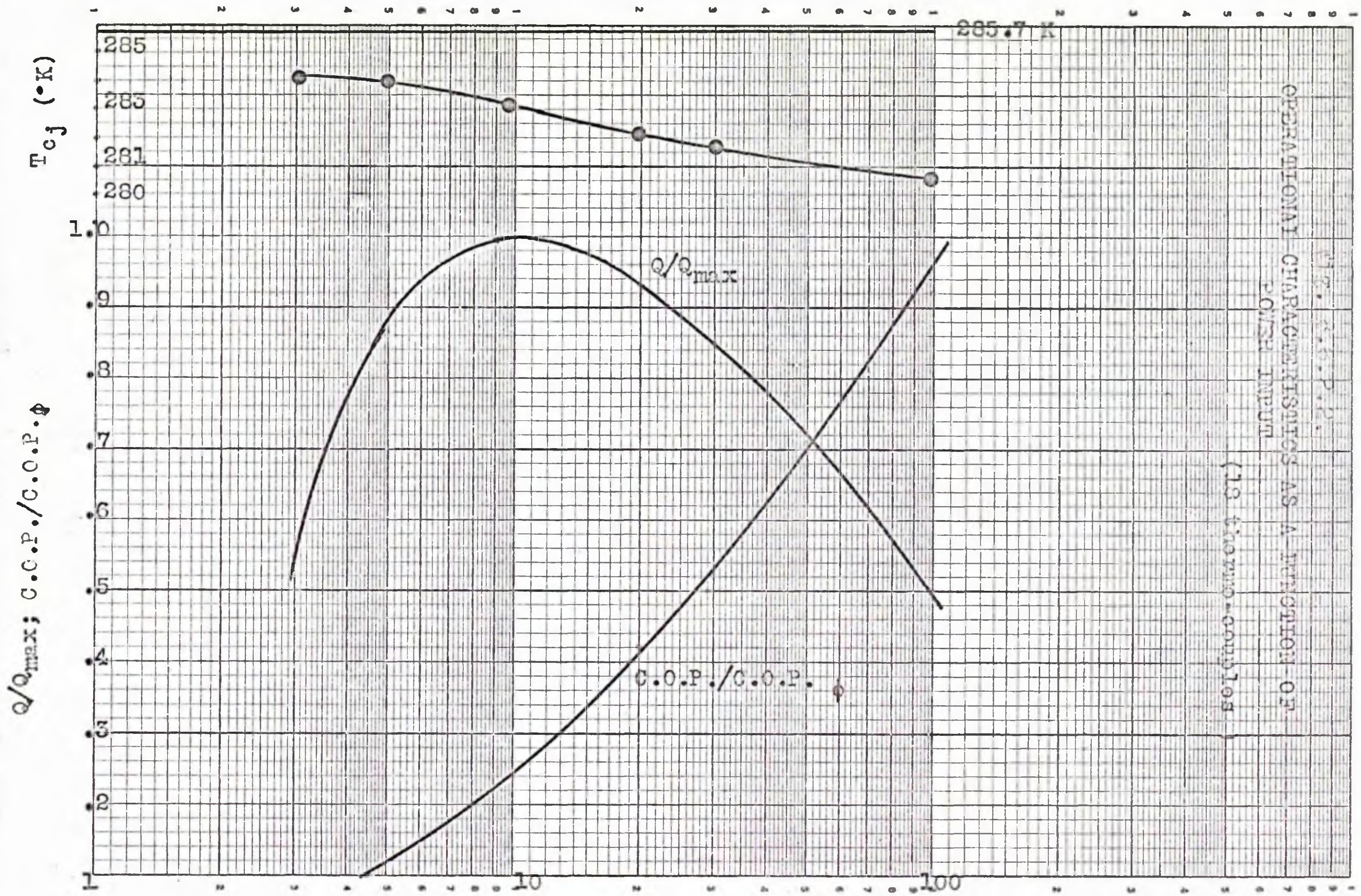

parametric ratios as a function of the power input. As the power increases the ratio $(Q_s/Q_{s_{max}})$ increases and reaches a maximum ratio of unity at a power input of approximately 10 watts. The cold side junction temperature (T_{cj}) decreases as a function of power input. At approximately 100 watt power input the cold side junction temperature exhibits a change in slope and T_{cj} starts to increase. The power input is based on 18 thermocouples in electrical series. Figure 8.6.2.3 is a plot of material utilization as a function of the operational C.O.P. At the lower portion of C.O.P. parameter a heat rejection rate of approximately 8 watts/cm^2 results. A heat rejection rate of $\cong$ 8 watts/cm^2 will require forced air convection or a water heat exchanger in order to control the hot side junction temperature. The heat rejection rate would increase as the height of the thermoelement decreases imposing a real design problem for the electrical insulation.

Figure 8.6.2.4 illustrates the material utilization parameters as a function of the operational C.O.P. for variation in the heat transfer exponent (N_i). Extracting the relationships from the computer program for (M_i = 0) the cold side temperature difference and the hot side temperature difference is expressed as:

$$\Delta T_c = \frac{t_c \mathcal{V}_c}{k_c} \qquad 8.6.2.1.$$

and

$$\Delta T_h = \frac{t_h \mathcal{V}_h}{k_h} \qquad 8.6.2.2.$$

Fig. 8.6.2.3.

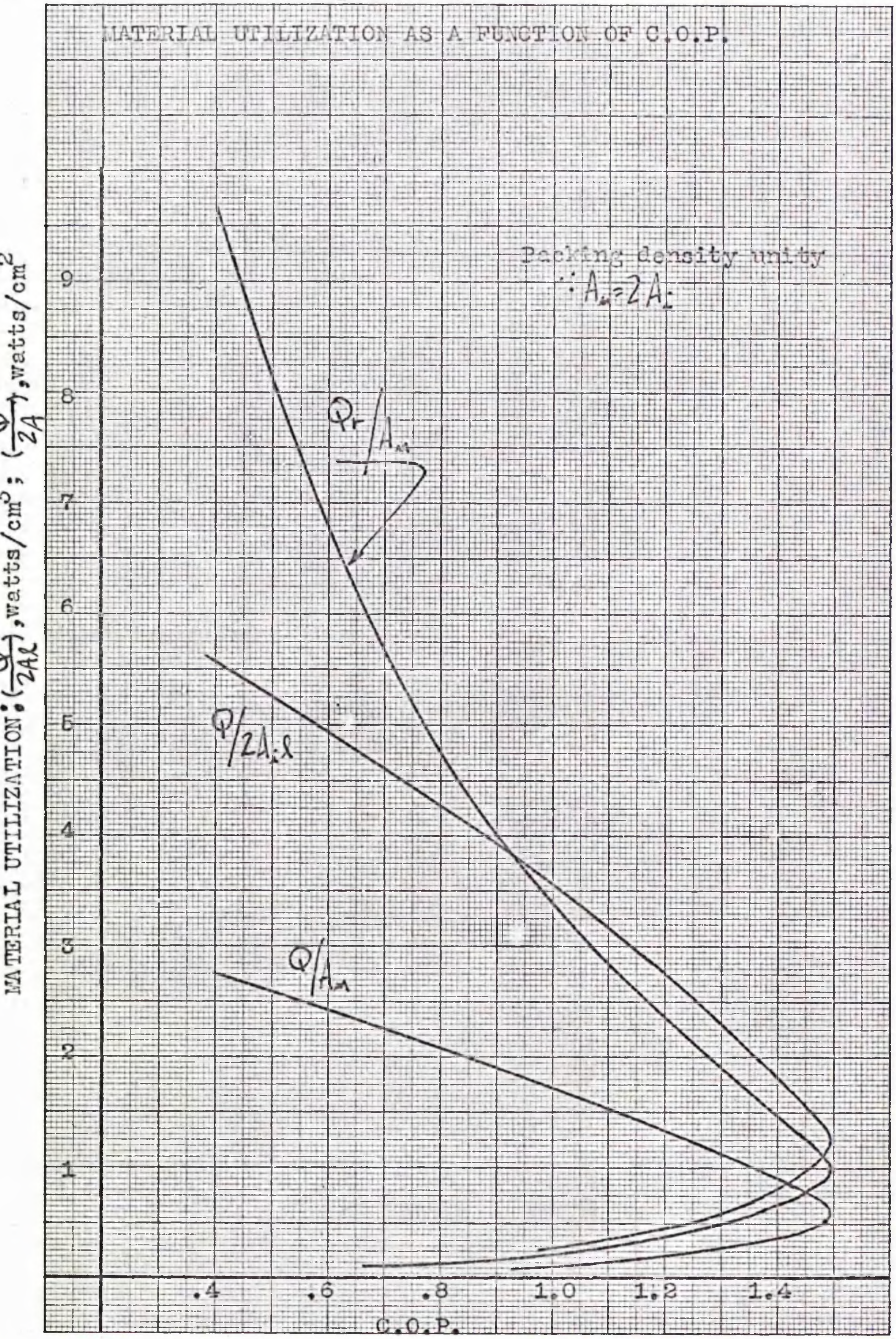
MATERIAL UTILIZATION AS A FUNCTION OF C.O.P.
Packing density unity
$\therefore A_m = 2A_i$
Q_r/A_m
$Q/2A_i\ell$
Q/A_m
MATERIAL UTILIZATION: $(\frac{Q}{2A\ell})$, watts/cm^3; $(\frac{Q}{2A})$, watts/cm^2
9
8
7
6
5
4
3
2
1
.4
.6
.8
1.0
1.2
1.4
C.O.P.

Fig. 8.6.2.4.

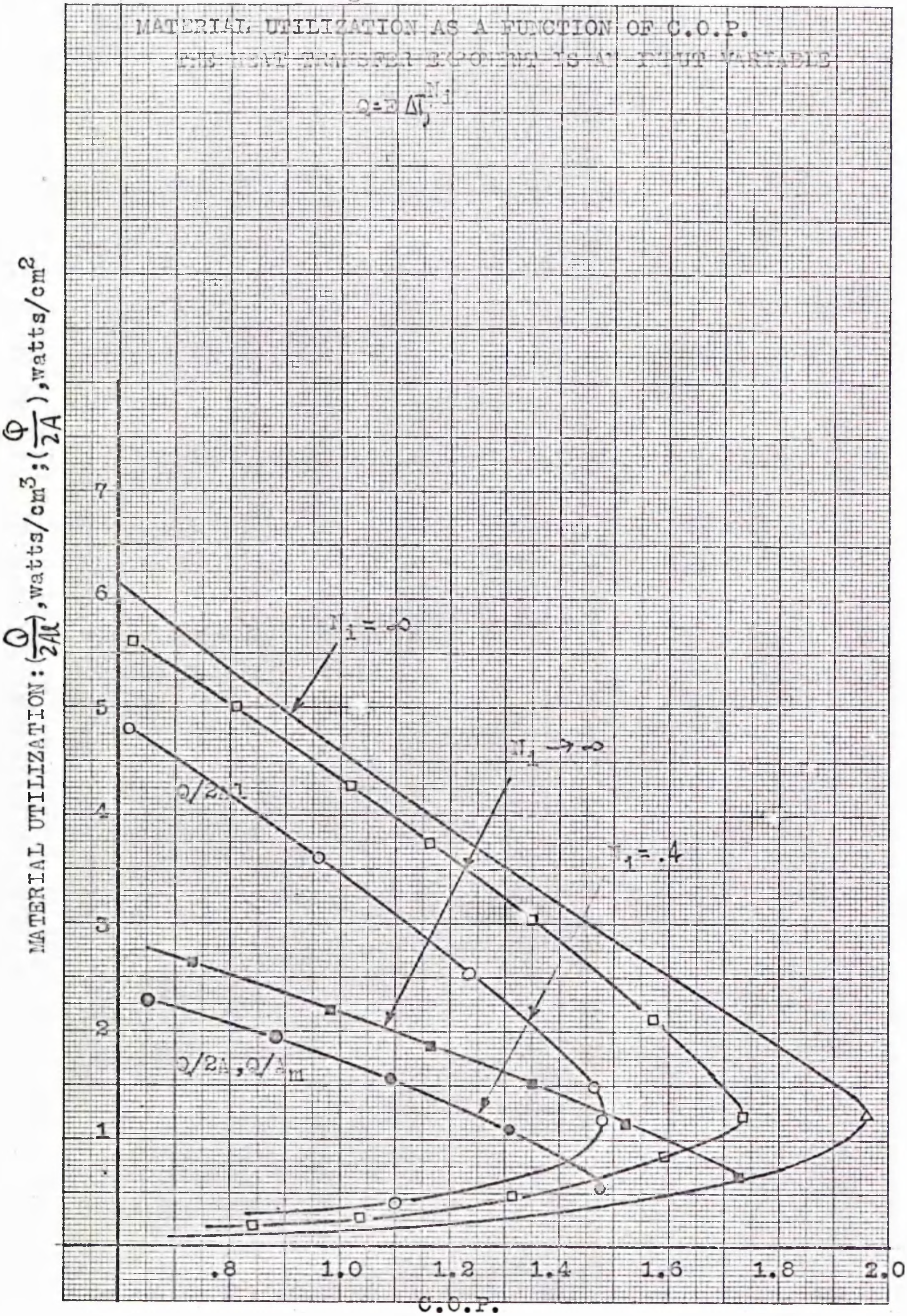
MATERIAL UTILIZATION AS A FUNCTION OF C.O.P.
Q=E ΔT^N1
MATERIAL UTILIZATION: (Q/2Al), watts/cm³; (Φ/2A), watts/cm²
N1 = ∞
N1 → ∞
N1 = .4
Q/2Al
Q/2A, Q/Am
1
2
3
4
5
6
7
.8
1.0
1.2
1.4
1.6
1.8
2.0
C.O.P.

The right hand side represents the "thermal-barrier" of the electrical insulation. For t_i = 0 equation 8.6.2.1 and 8.6.2.2 reduces to:

$$T_{c_j} = T_{c_\infty} \qquad 8.6.2.3.$$

$$T_{h_j} = T_{h_\infty} \qquad 8.6.2.4.$$

The condition illustrated by figure 8.6.2.4 for the heat transfer exponent ($N_i \longrightarrow \infty$) represents a 1°C temperature difference between the heat exchanger root and the free stream source/sink temperature. Increasing the heat transfer exponent increases substantially the maximum C.O.P. at I_ϕ.

8.7 Off-Balance Operation.

8.7.1 Computational Procedure.

To determine the "off" balance performance characteristic with a current (θ) not equal to the balanced current value determined by the computer program (C.P.5) the following technique is introduced:

(1) Use computer program (C.P.5.) based on module operation with finite heat transfer coefficients to determine the operational parameters. At the required cold side heat flux ($\mathfrak{V}_c$, watts/cm^2) record the following:

(a) Junction temperature difference, (ΔT_j)

(b) Cold junction temperature, T_{cj}.

(c) (θ) current ratio at balance point

(2) Introduce items (a), (b), (c) (above) into computer program (C.P.6.). The computer program incorporates procedure OFFBALANCE for performing the above calculations.

The approach utilized for determining the off balance effects is as follows:

At balanced operation $\theta = \theta_{BAL}$ with $\Delta T_j'$, T_{cj}' considered unique (fixed). For $\theta \angle \theta_{BAL}$ the heat removal rate is less than that required for balanced operation. It is expected that the free stream source temperature will increase ($\theta \angle \theta_{BAL}$) . Expressing the temperature across the cold side; i.e. from cold junction interface to free stream sink for balanced operation with "prim" notation then:

$$\Delta T_c' = \left[\frac{\nu_c'}{E_c}\right]^{\left[\frac{1}{1+N_c}\right]M_c} + \frac{t_c \nu_c'}{k_c} \qquad 8.7.1.1.$$

and for $\theta \angle \theta_{BAL}$ as:

$$\Delta T_c = \left[\frac{\nu_c}{E_c}\right]^{\left[\frac{1}{1+N_c}\right]M_c} + \frac{t_c \nu_c}{k_c} \qquad 8.7.1.2.$$

Expressing the left hand side of equation 8.7.1.1 and 8.7.1.2 as:

$$\Delta T_c' = T_{c_\infty}' - T_{c_j} \qquad 8.7.1.3.$$

$$\Delta T_c = T_{c_\infty} - T_{c_j} \qquad 8.7.1.4.$$

for T_{c_j} constant then:

$$T_{c_\infty}' < T_{c_\infty} \qquad 8.7.1.5.$$

Expressing the temperature difference for $\theta = \theta_{BAL}$ and $\theta < \theta_{BAL}$ then:

$$\Delta T_c - \Delta T_c' = T_{c_\infty} - T_{c_j} - T_{c_\infty}' + T_{c_j} \qquad 8.7.1.6.$$

and

$$\Delta T'' \equiv T_{c_\infty} - T_{c_\infty}'(\theta_{BAL}) \geq 0 \qquad 8.7.1.7.$$

Solving for $T_{c_\infty}(\theta < \theta_{BAL})$ results:

$$T_{c_\infty} = \Delta T'' + T_{c_\infty}'(\theta_{BAL}) \qquad 8.7.1.8.$$

where:

T_{c_∞}' free stream source temperature at balance operation, ^oK

$\Delta T''$ difference between ΔT_c (off-balance operation) and $\Delta T_c'$ (at balance operation), ^oC

T_{c_∞} free stream source temperature at 'off'

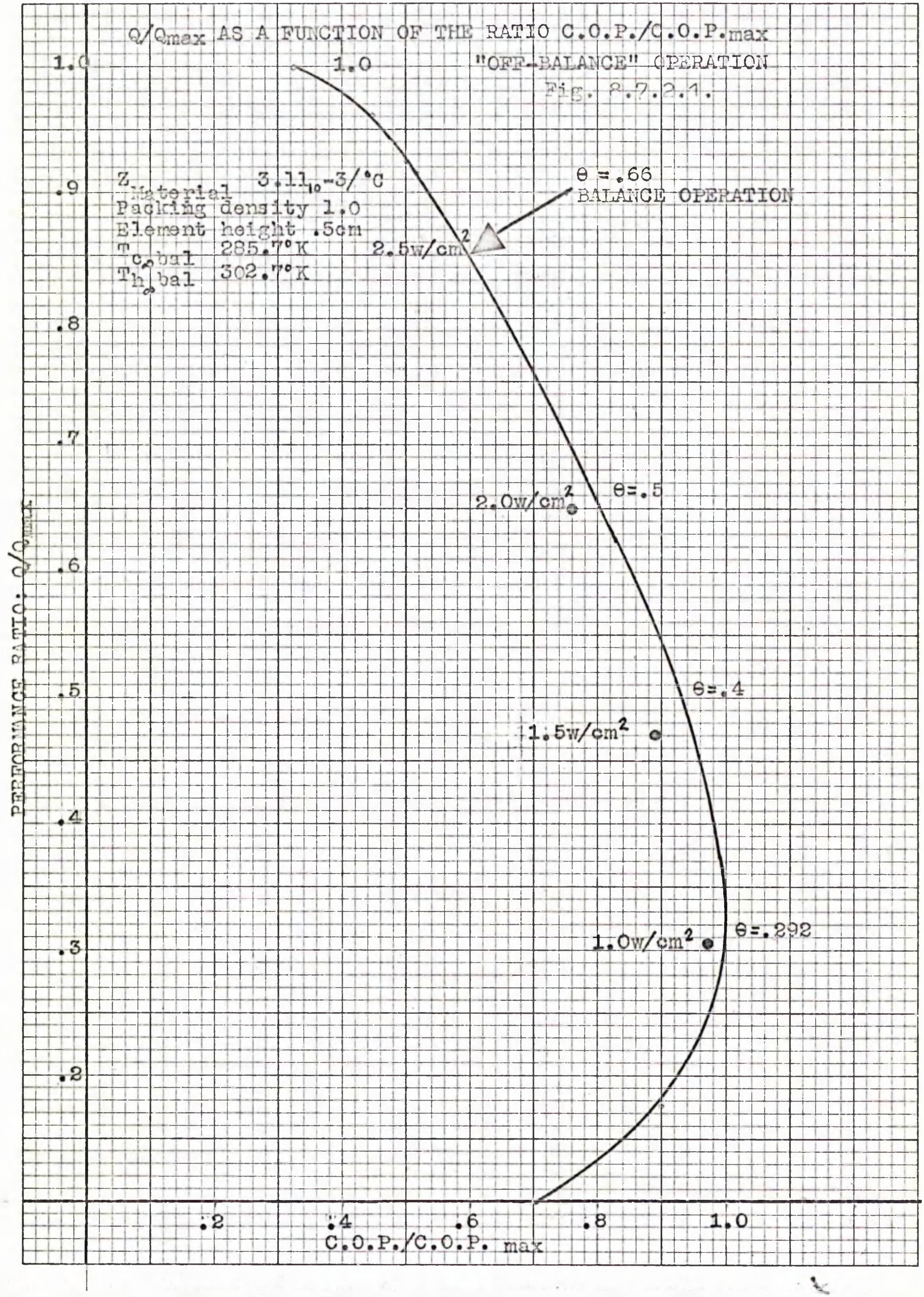

Q/Qmax AS A FUNCTION OF THE RATIO C.O.P./C.O.P.max
"OFF-BALANCE" OPERATION
Fig. 8.7.2.1.
Z Material 3.11 10-3/°C
Packing density 1.0
Element height .5cm
Tc∞ bal 285.7°K
Th∞ bal 302.7°K
θ = .66
BALANCE OPERATION
2.5w/cm2
2.0w/cm2
θ=.5
θ=.4
1.5w/cm2
1.0w/cm2
θ=.292
1.0
.9
.8
.7
.6
.5
.4
.3
.2
.2
.4
.6
.8
1.0
C.O.P./C.O.P. max
PERFORMANCE RATIO. Q/Qmax

balance operation, ^{o}K

SUMMARY COMMENT.

The proposed calculation technique is to fix ΔT_j, T_{c_j} based on the output from the balanced operation program. Procedure OFFBALANCE utilizes these values and performs a $I/I_Q(\theta)$ sweep about the balance point and uses the relationship of equation 8.7.1.8 to calculate the "off" balance free stream temperature.

8.7.2. Discussion and Results.

Figure 8.7.2.1 illustrates the parameter $(Q_s/Q_{s_{max}})$ as a function of the performance ratio $(C.O.P./C.O.P._{max})$. The module/thermoelectric couple has a material figure of merit of $\cong 3.11_{10}$ $-3/^{o}C$ with an element height of .50cm. The heat transfer exponent is .40 for both hot and cold heat exchangers. The balance operation with a cold side heat flux of 2.5 watts/cm^2 and T_{h_∞} = 302.7^{o}K, T_{c_∞} = 285.7^{o}K occurs at $\theta_{BAL} \cong$ .66, C.O.P./C.O.P.$_{max}$ $\cong$ .59 and a corresponding $Q_s/Q_{s_{max}} \cong$ .85. The heat balance for three discrete heat fluxes (2.0, 1.5, 1.0 watts/cm^2) are indicated on figure 8.7.2.1. The junction temperatures resulting for these heat fluxes would depend on the current level required to maintain thermal equilibrium with the environment. The 'sweep' variable (θ) has been incrementaly stepped from θ = 1.0 to $\theta \cong$ .180 to indicate the decrease in performance ratios. The values of the variable θ to the right of θ_{BAL} is for $\theta < \theta_{BAL}$ and to the left

Fig. 8.7.2.P.

HEAT PUMP RATE AND C.O.P. AS A FUNCTION OF THE CURRENT TO MAINTAIN BALANCED OPERATION

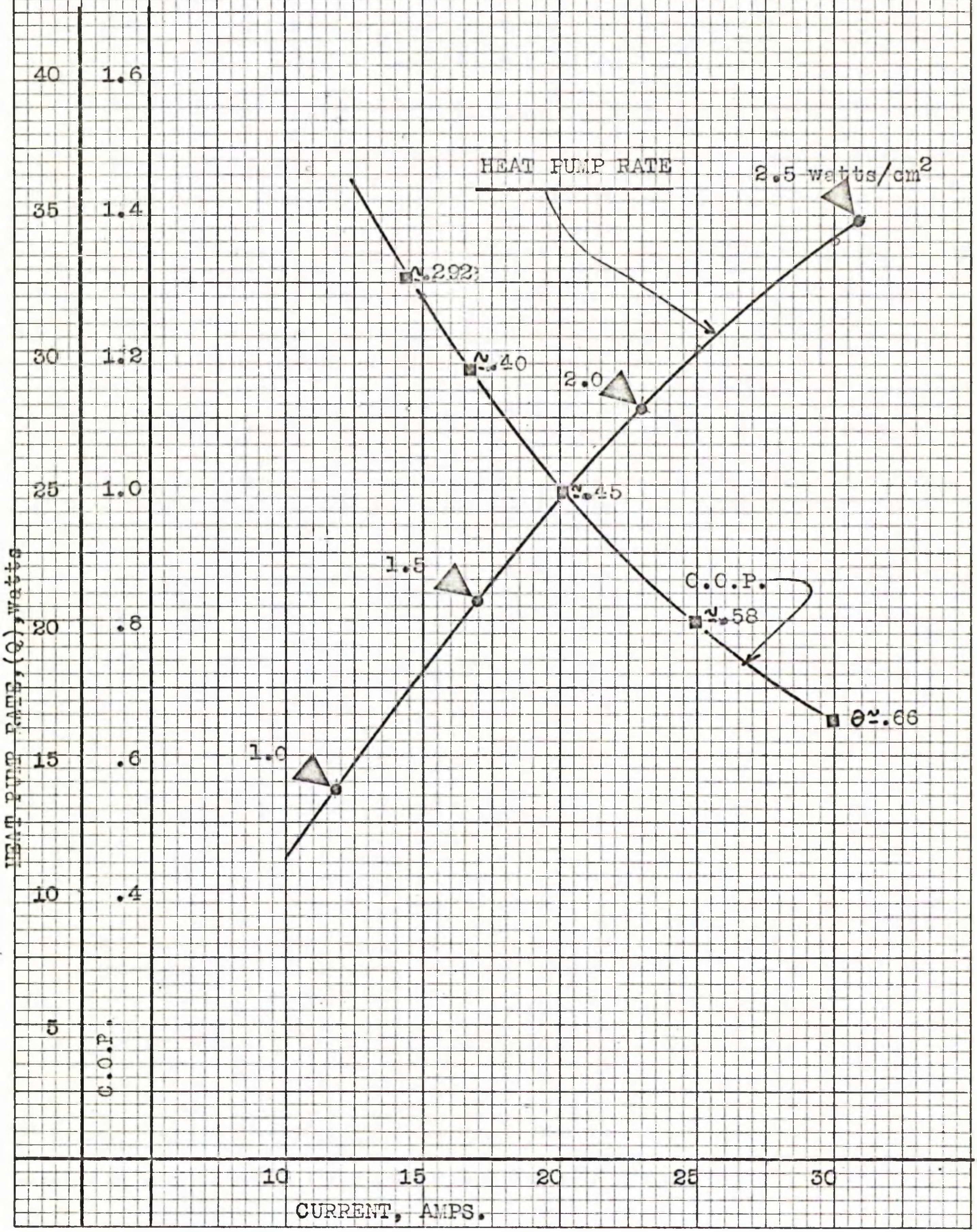

for $\theta > \theta_{BAL}$ Figure 8.7.2.2 illustrates the heat pump rate (Q_S) and C.O.P. as a function of the current required for thermal balance. For a 2.5 change in heat flux the C.O.P. exhibits a change of approximately the same ratio. The heat pump rate is based on 18-thermocouples in electrical series and thermally in parallel. The circuit arrangements will in a final design depend on the power supply available, cost, and a balance between current/voltage on a system weight analysis. Figure 8.7.2.3 indicates the change in source temperature as a function of the dimensionless current ratio (θ). At $\theta = \theta_{BAL} \simeq .660$, $\Delta T = 0$ indicating a balanced solution (singularity - figure 8.7.2.1). For $\theta < \theta_{BAL}$ figure 8.7.2.3 indicates $T_{c\infty} > T'_{c\infty}$ (balance) and for $\theta > \theta_{BAL}$ $T_{c\infty} < T'_{c\infty}$ (balance). If $\theta > 1$ $(I = I_Q)$ the freestream temperature approaches $T'_{c\infty}$ (balance) and will for $\theta \gtrsim 1.4$ become greater than $T'_{c\infty}$ (at balance).

Fig. 8.7.2.3.

CHANGE IN TEMPERATURE OF COLD SOURCE DUE TO "OFF-BALANCE" OPERATION AS A FUNCTION OF THE DIMENSIONLESS CURRENT RATIO (θ)

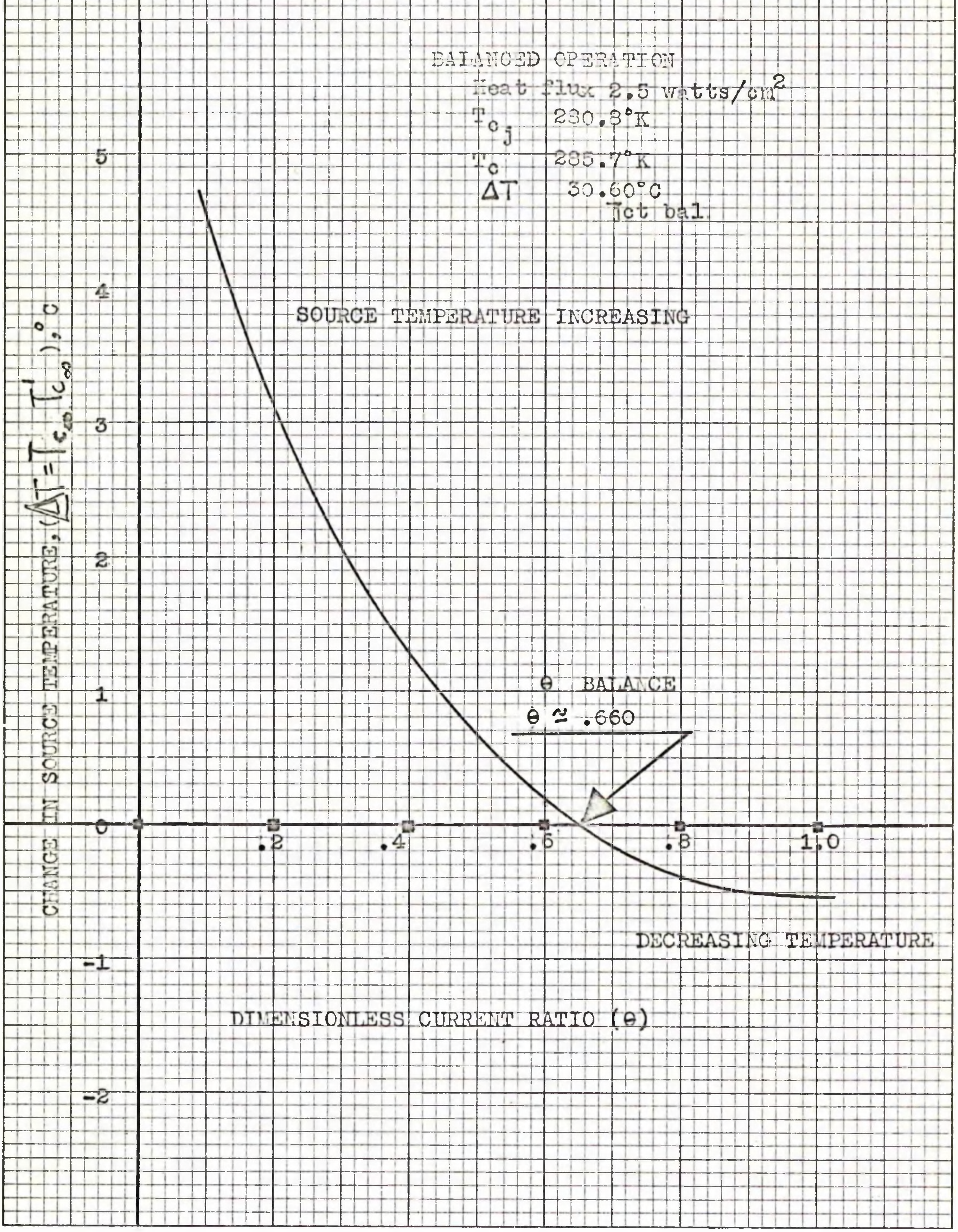

9.0. OPERATIONAL CONSIDERATION - PEDESTAL MODULE/ CONVENTIONAL CONFIGURATION.

9.1 Abstract.

Demands which space/military applications make on thermoelectric devices and ancillary systems are more stringent and require in particular a consideration of system weight. Operational properties of thermoelectric devices must be competitive and offer increases in material utilization (output/system burden). Cooling devices are essential in space or in orbiting vehicle applications. In some established designs the ambient temperature can be controlled by radiative cooling, several applications require supporting cooling devices. Examples of installations require cooling systems are cold-storage, de-humidification, electronic tracking devices such as infrared sensors or transistorized circuit components. Thermoelectric devices are particularly well suited to applications for space travel. Being electronic in nature, constructed of no moving parts infers good design with a dependable/reliable minimum maintenance system. In addition, the thermoelectric device would produce no vibration (cylic or random) or gyroscopic moments to be compensated or interfere with vehicle guidance/stabilization. The requirement for space application requires a minimum weight system consistent with its design objective. The problem proposed for analysis is: 'Which of two proposed thermoelectric devices (pedestal VS conventional assembly) is more orientated towards

Fig. 9.2.1.

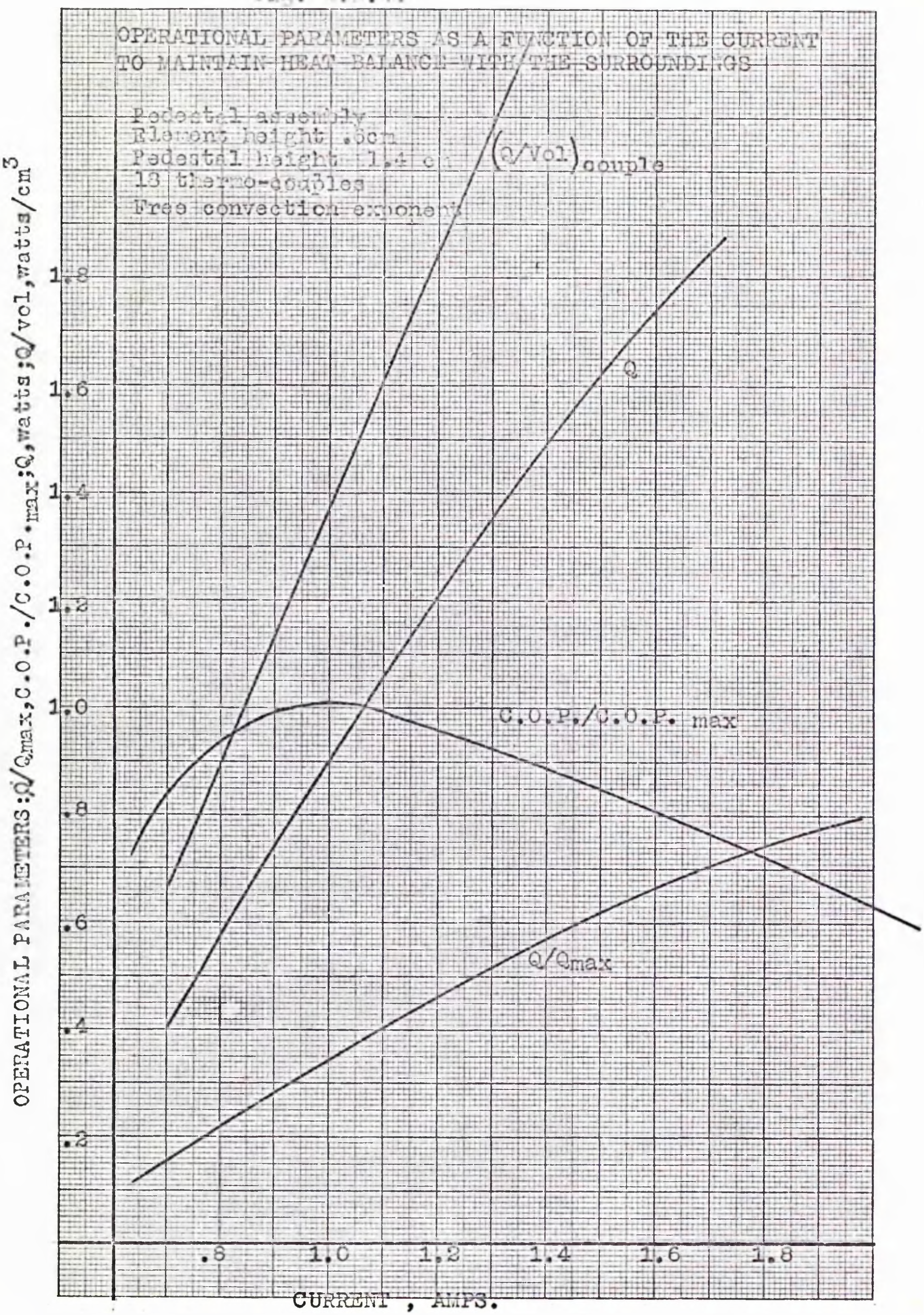
OPERATIONAL PARAMETERS AS A FUNCTION OF THE CURRENT
TO MAINTAIN HEAT BALANCE WITH THE SURROUNDINGS
Pedestal assembly
Element height .5cm
Pedestal height 1.4 cm
13 thermo-couples
Free convection exponent
(Q/Vol)couple
Q
C.O.P./C.O.P. max
Q/Qmax
OPERATIONAL PARAMETERS: Q/Qmax, C.O.P./C.O.P.max; Q, watts; Q/vol, watts/cm3
1.8
1.6
1.4
1.2
1.0
.8
.6
.4
.2
.8
1.0
1.2
1.4
1.6
1.8
CURRENT, AMPS.

space application?' The conclusions resulting are based on the illustrations presented in this section. It will be pointed-out in subsequent discussions the final answer can take many forms. The purpose of the analysis is to:

(1) Present the general characteristics of a pedestal-module operating between heat source and heat sink.

(2) Broaden the scope of the engineering data with the aid of the basic parametric variables available as output from the computer programs.

9.2 Operational Comparisons.

Figure 9.2.1 illustrates four operational parameters as a function of the current required to maintain thermal heat balance. The model consists of 18 thermocouples positioned on pedestals. Table 8.5.2 presents the basic module configuration incorporated into figure 9.2.1. The maximum C.O.P. (C.O.P./C.O.P.$_{max}$) occurs at approximately 1.0 amps with a corresponding heat pumping rate of $\cong$ .90 watts. The heat pump rate ($Q_s / Q_{s_{max}}$) parameter is somewhat linear for the current values illustrated. At 2.0 amps the $Q_s / Q_{s_{max}}$ ratio is $\cong$ .90 with a corresponding C.O.P./C.O.P.$_{max}$ $\cong$ .63.

Maintaining constant free stream conditions figure 9.2.2 introduces a comparison between a pedestal and non-pedestal (conventional) module assembly. The pedestal configuration has the element dimensions as illustrated

Fig. 9.2.2.

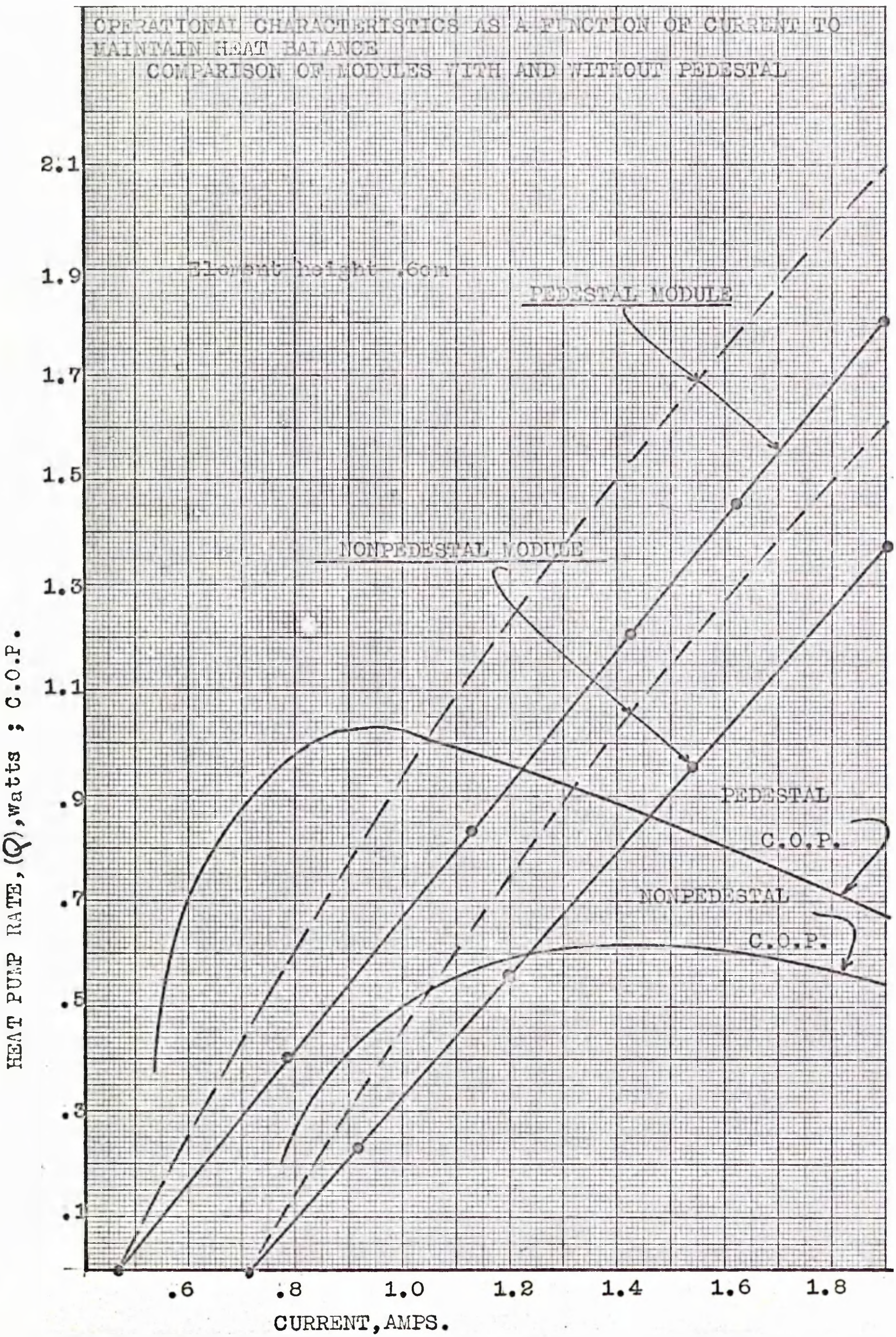

OPERATIONAL CHARACTERISTICS AS A FUNCTION OF CURRENT TO MAINTAIN HEAT BALANCE
COMPARISON OF MODULES WITH AND WITHOUT PEDESTAL
Element height .6cm
PEDESTAL MODULE
NONPEDESTAL MODULE
PEDESTAL
C.O.P.
NONPEDESTAL
C.O.P.
HEAT PUMP RATE, (Q), watts ; C.O.P.
CURRENT, AMPS.
2.1
1.9
1.7
1.5
1.3
1.1
.9
.7
.5
.3
.1
.6
.8
1.0
1.2
1.4
1.6
1.8

Fig. 9.2.3.

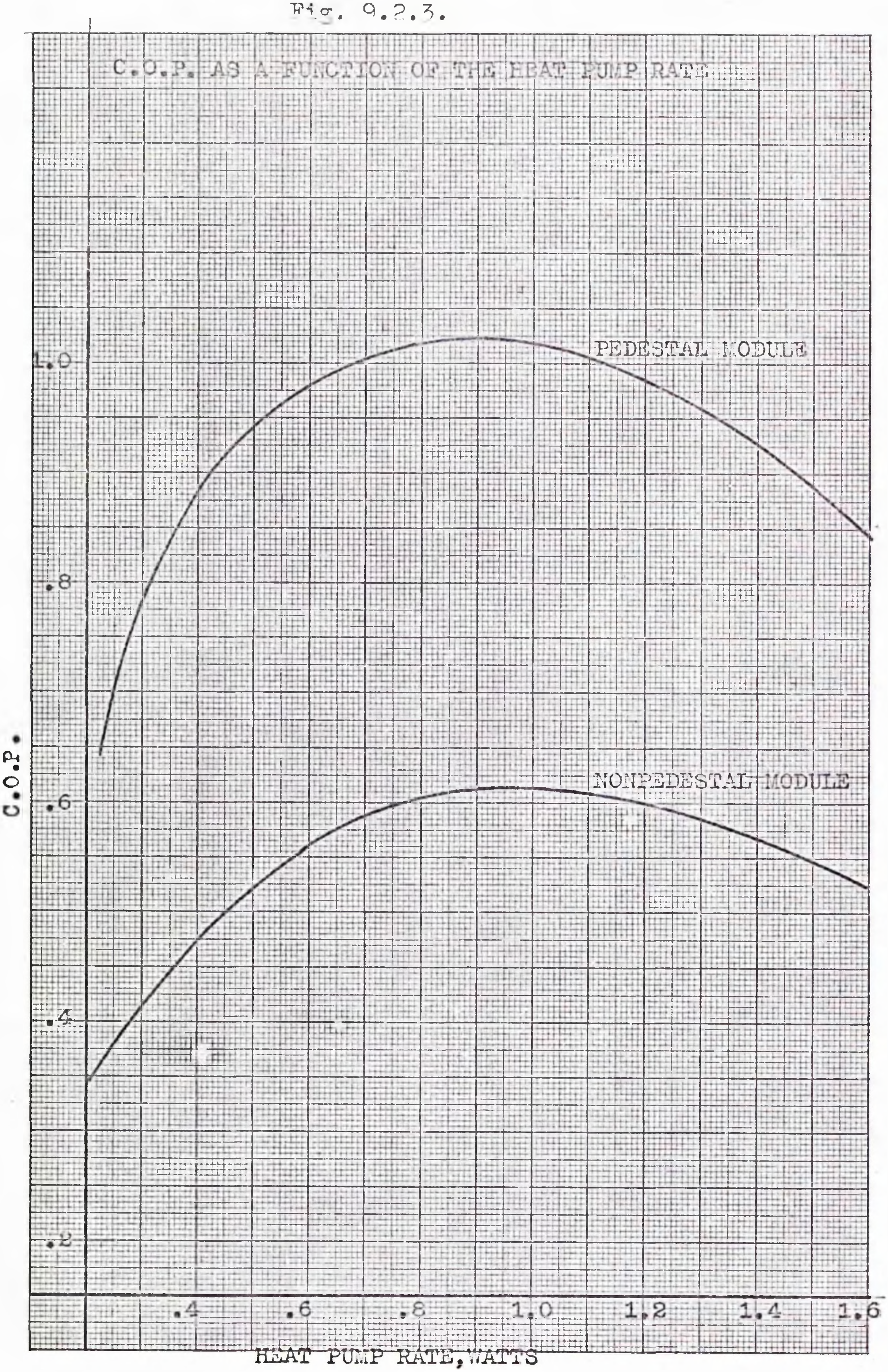
C.O.P. AS A FUNCTION OF THE HEAT PUMP RATE
PEDESTAL MODULE
NONPEDESTAL MODULE
C.O.P.
1.0
.8
.6
.4
.2
.4
.6
.8
1.0
1.2
1.4
1.6
HEAT PUMP RATE, WATTS

on table 8.5.2. The thermal insulation height is 2 cm. The pedestal column is assumed to be Alu with a density of $\cong$ 2.80 grams/cc, with a thermoelement density of 7.0 grams/cc. For a constant current input the pedestal module exhibits a higher heat pump rate and C.O.P. as compared to a conventional configuration. For a constant heat load of 1 watt the current required for the pedestal module is $\cong$ 1.05 amps. and for the non-pedestal assembly 1.39 amps (an increase of $\cong$ 33%). Incorporating the data from figure 9.2.2 at constant current results in figure 9.2.3. Figure 9.2.3 indicates that for a 1 watt heat pump rate input the pedestal C.O.P. is approximately 60% greater than the conventional module. On the basis of the previous data it appears that the pedestal module is a more favourable conclusion. The next question to be answered is: 'What is the weight penality imposed upon the system if the pedestal assembly is an acceptable conclusion?'

In the previous section (8.6) the parameter 'material utilization' was introduced as a 'comparison' criteria. The units of the 'material utilization' term is watts/cm^3 which can be interpreted as the module output: system burden (Weight $\sim$ ρ cm^3). The introduction of the system burden will increase the scope of the analysis and can alter the above conclusion.

Fig. 9.2.4.

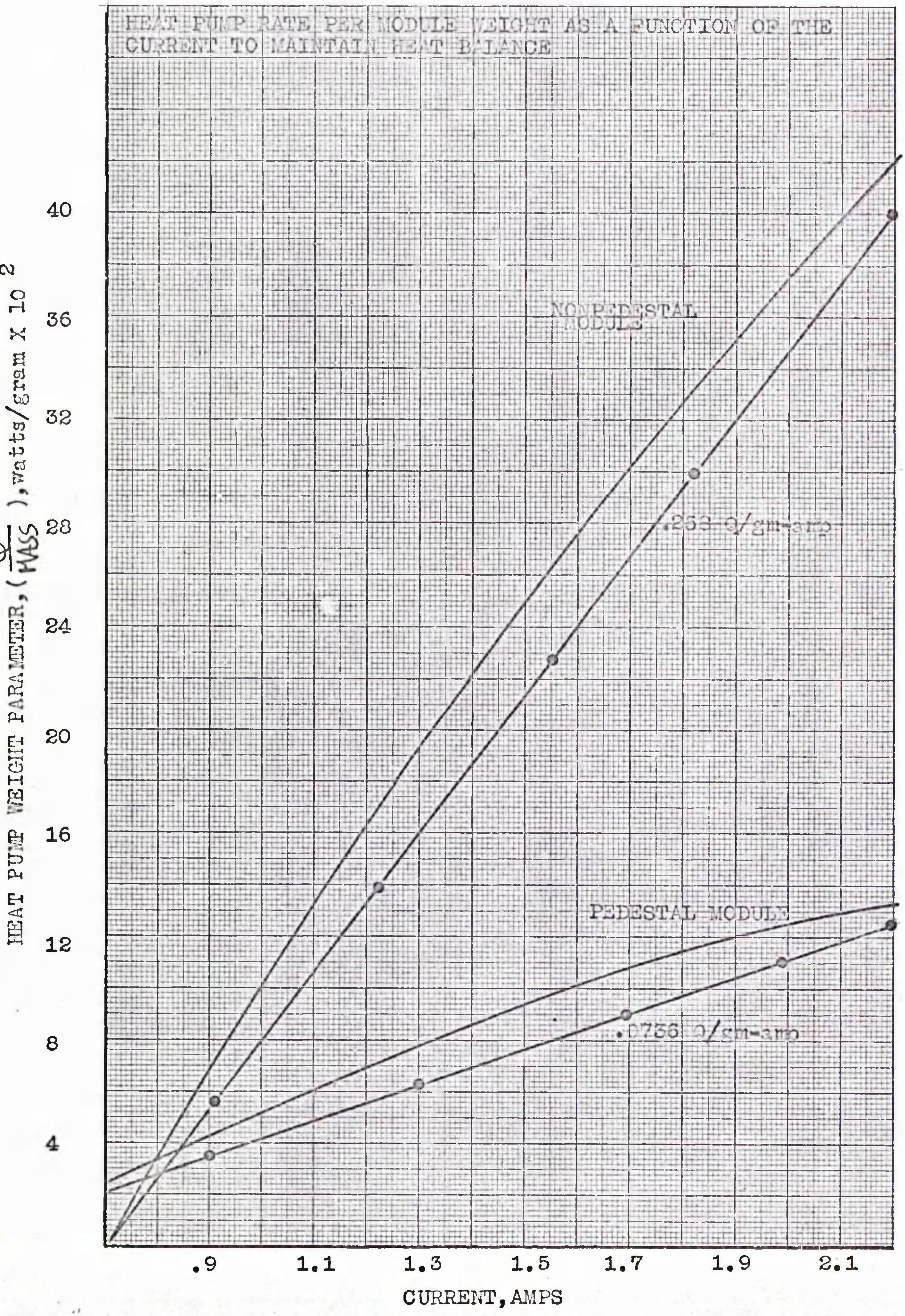
HEAT PUMP RATE PER MODULE WEIGHT AS A FUNCTION OF THE CURRENT TO MAINTAIN HEAT BALANCE
NONPEDESTAL MODULE
.253 Q/gm-amp
PEDESTAL MODULE
.0736 Q/gm-amp
40
36
32
28
24
20
16
12
8
4
HEAT PUMP WEIGHT PARAMETER, ($\frac{Q}{MASS}$), watts/gram X 10 2
.9
1.1
1.3
1.5
1.7
1.9
2.1
CURRENT, AMPS

The weight per couple is expressed as:

$$M_{NON-PEDESTAL} \cong \rho 2 A \ell \qquad 9.2.1.$$

$$M_{PEDESTAL} \cong \rho 2 A \ell + \rho_p A_p \ell_p \qquad 9.2.2.$$

Figure 9.2.4 illustrates the heat pump rate (Q_s) per unit mass of thermoelectric material (and pedestal) as a function of the current required for thermal heat balance. The weight allocation is:

(1) Alu-pedestal $\cong$ (2.8) (6) (.03) (1.4) $\cong$ .705 grams

or

(2) Cu - pedestal $\cong$ (7.7) (6) (.03) (1.4) $\cong$ 1.940 grams

(3) Thermoelectric couple $\cong$ (7.0) (2) (.03) (.6) $\cong$ .252 gr

(4) Pedestal/thermocouple module $\cong$ .252 + .705 $\cong$ .957 gr

The systems considered for further review are noted as items (3) and (4) above. Figure 7.4.1.1 outlines the basic pedestal assembly. The introduction of module weight has altered the relative position of each system. For a constant current input the non-pedestal assembly exhibits a higher heat pump rate parameter (figure 9.2.4) then the pedestal module. The slope of the non-pedestal module is approximately 3.5 times the pedestal assembly. The slope units are (watts/gram-amp) which reflects

Fig. 9.2.5.

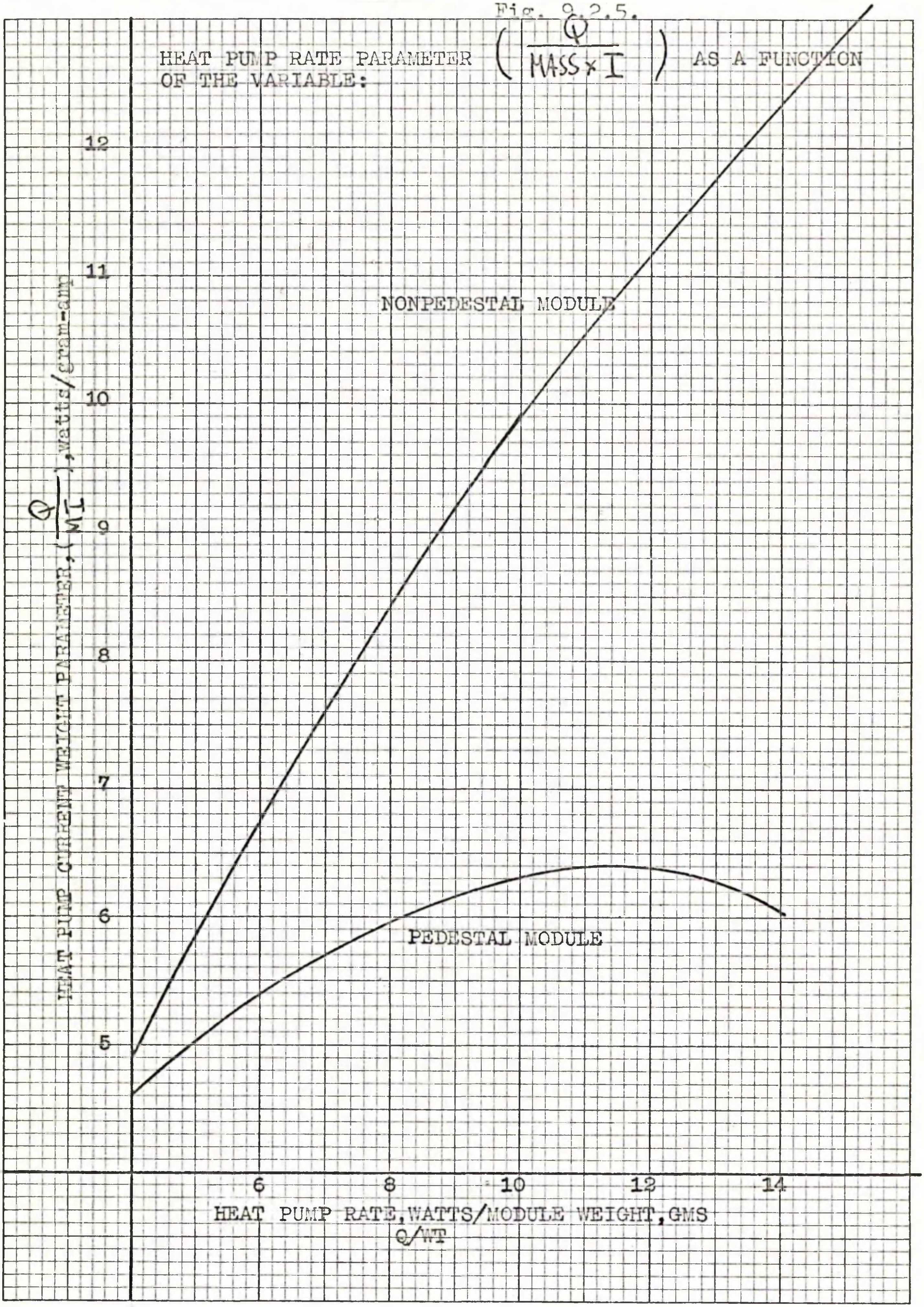
HEAT PUMP RATE PARAMETER $\left(\frac{Q}{MASS \times I}\right)$ AS A FUNCTION OF THE VARIABLE:
NONPEDESTAL MODULE
PEDESTAL MODULE
HEAT PUMP CURRENT WEIGHT PARAMETER, $\left(\frac{Q}{MI}\right)$, watts/gram-amp
12
11
10
9
8
7
6
5
6
8
10
12
14
HEAT PUMP RATE, WATTS/MODULE WEIGHT, GMS
Q/WT

the couple performance and introduces an additional performance criteria. To introduce the slope parameter the data available from figure 9.2.4 is expanded resulting in figure 9.2.5. The data illustrated on figure 9.2.5 is obtained as represented below:

From figure 9.2.4 (neglecting 10^2 exponent term)

$\frac{Q}{\text{Mass}}$	I Pedestal	I Non-Pedestal	$\frac{Q}{MI}$ Pedestal	$\frac{Q}{MI}$ Non-Pedestal
10.0	1.6	1.0	6.25	10.0

Figure 9.2.5 illustrates the functional current slope parameter Q/MI as a function of Q/M for both pedestal and conventional assemblies. The resulting figure (9.2.5) indicates that the conventional module exhibits a higher performance value. The previous conclusions, i.e. Q/vol figures 9.2.4, 9.2.5 has been based on a one: one couple performance. It therefore appears reasonable to ask the following question. 'How many couples of a non-pedestal (conventional) module is equivalent to a pedestal assembly and what is the resulting weight parameter with this criteria?' From figure 9.2.2 the heat pump rate per couple as a function of the current can be determined. The ordinate is divided by 18 to determine the heat pump rate per couple. The number of conventional couples to be equivalent to a pedestal module is a function of the current and may not be a whole number. Summarizing the results:

Fig. 9.2.6.

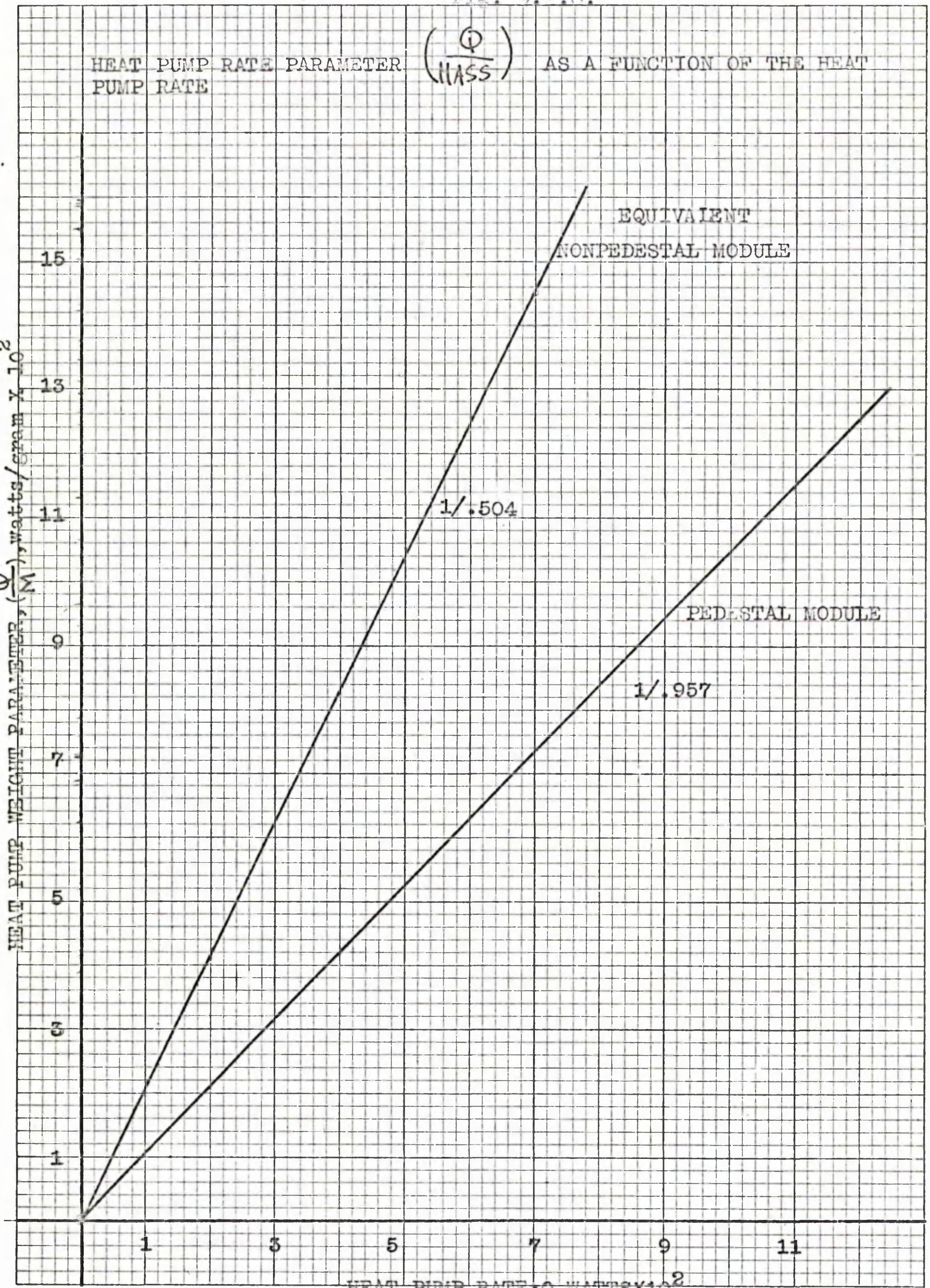

HEAT PUMP RATE PARAMETER (Q/MASS) AS A FUNCTION OF THE HEAT PUMP RATE
EQUIVALENT NONPEDESTAL MODULE
1/.504
PEDESTAL MODULE
1/.957
HEAT PUMP WEIGHT PARAMETER, (Q/M), watts/gram x 10^2
HEAT PUMP RATE, Q, WATTS×10^2
1
3
5
7
9
11
13
15

$$.9 \leq I \leq 2.4$$

$$2.54 \leq N \leq 1.25$$

where:

$$N = \frac{Q_{PEDESTAL}}{Q_{NON\text{-}PEDESTAL}}$$

Letting N = 2, the weight of the equivalent conventional module becomes (2) (.252) = .504 grams and the pedestal module remains at .957 grams. Figure 9.2.6 illustrates the parameter Q/M as a function of Q for the equivalent non-pedestal configuration. The equivalent conventional configuration exhibits a higher performance factor then the pedestal module. If N = 3 the non pedestal configuration will still exhibit a higher output/system weight than the conventional configuration. To explore a further parameter figure 9.2.4 indicates the following approximate slopes:

(1) Pedestal module $\cong$ .0736 $\frac{\text{watts}}{\text{amp-gram}}$

(2) Conventional module $\cong$ .258 $\frac{\text{watts}}{\text{amp-gram}}$

The data indicated above will be utilized to determine $Q|I$ parameter as a function of the module mass. To illustrate the technique for determining the parameters of figure 9.2.7 consider the following:

(1) Conventional Module

(a) Couples considered 30

HEAT PUMP RATE PARAMETER $\left(\frac{Q}{I}\right)$ AS A FUNCTION OF MODULE WEIGHT

Fig. 9.2.7.

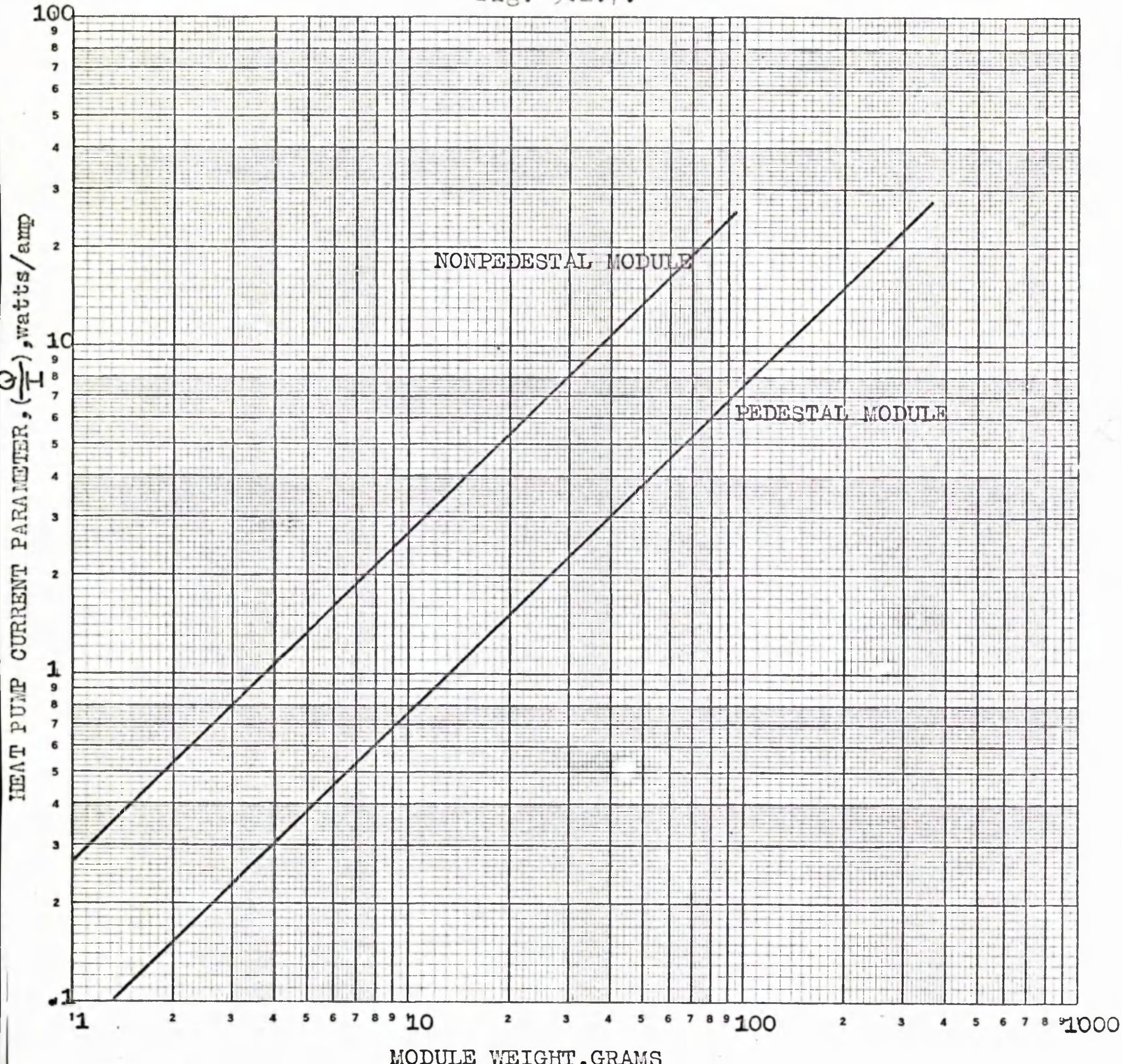

(b) Weight per couple .252 grams

(c) Weight of module (30) (.252) $\cong$ 7.56 grams

(d) Slope $\frac{.258 \text{ watts}}{\text{amp-gram}}$

(e) $Q|I$ parameter (.258) (7.56) $\cong$ 1.950 watts/amp.

(2) Pedestal Module

(a) Couples considered 30

(b) Weight per couple .957 grams

(c) Weight of module (30) (.957) $\cong$ 28.71 grams

(d) Slope $\frac{.0736 \text{ watts}}{\text{amp-gram}}$

(e) $Q|I$ parameter (.0736) (28.71) $\cong$ 2.10 watts/amp

Figure 9.2.7 illustrates $(Q|I)$ as a function of the module mass. The result indicates that for a constant module mass requirement the conventional module exhibits a higher heat pump rate current parameter.

Fig. 9.3.1.

MATERIAL UTILIZATION AS A FUNCTION OF C.O.P.

PEDESTAL MODULE ASSEMBLY
MODULE HEIGHT — 2cm.

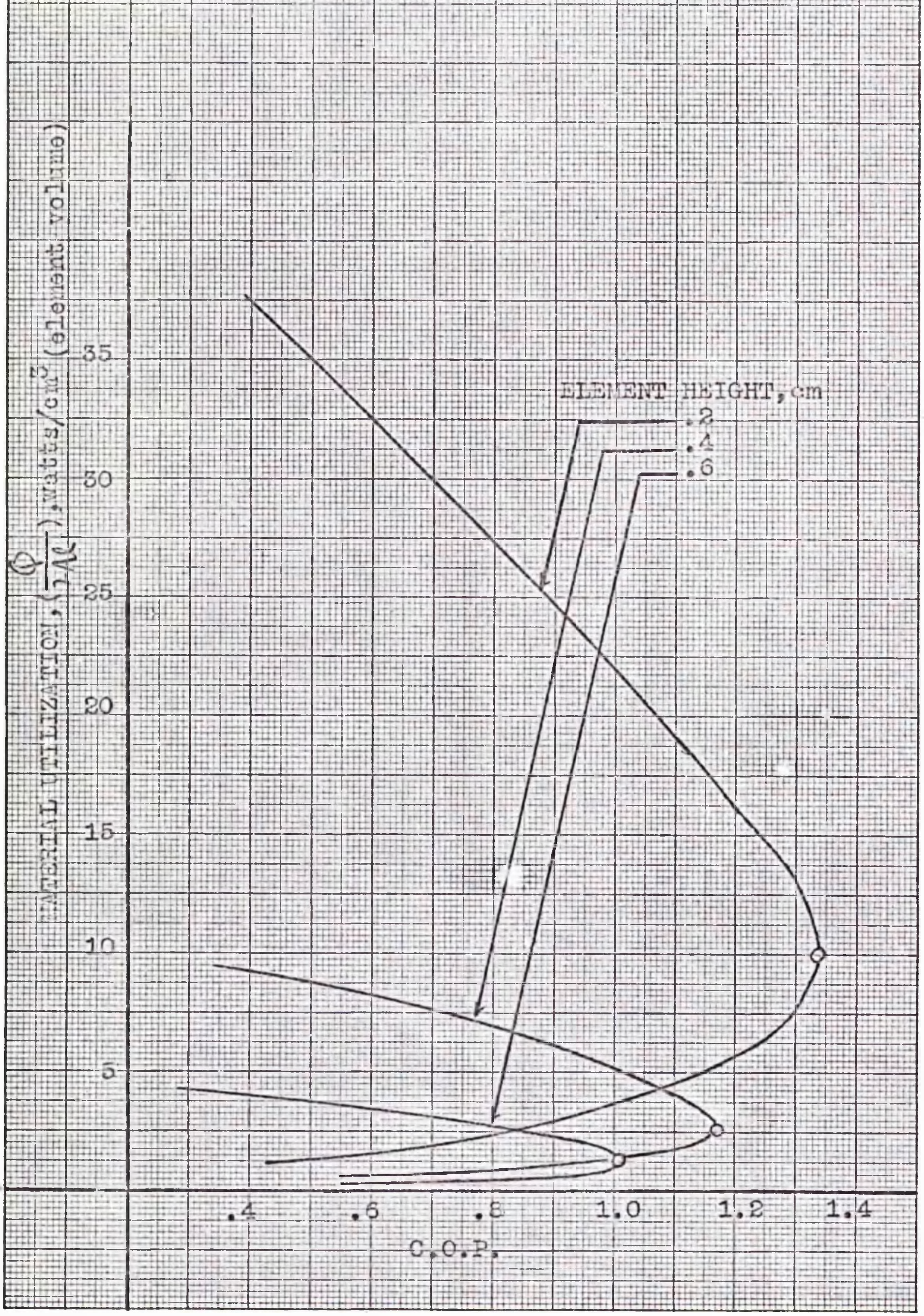

Fig. 9.3.2.

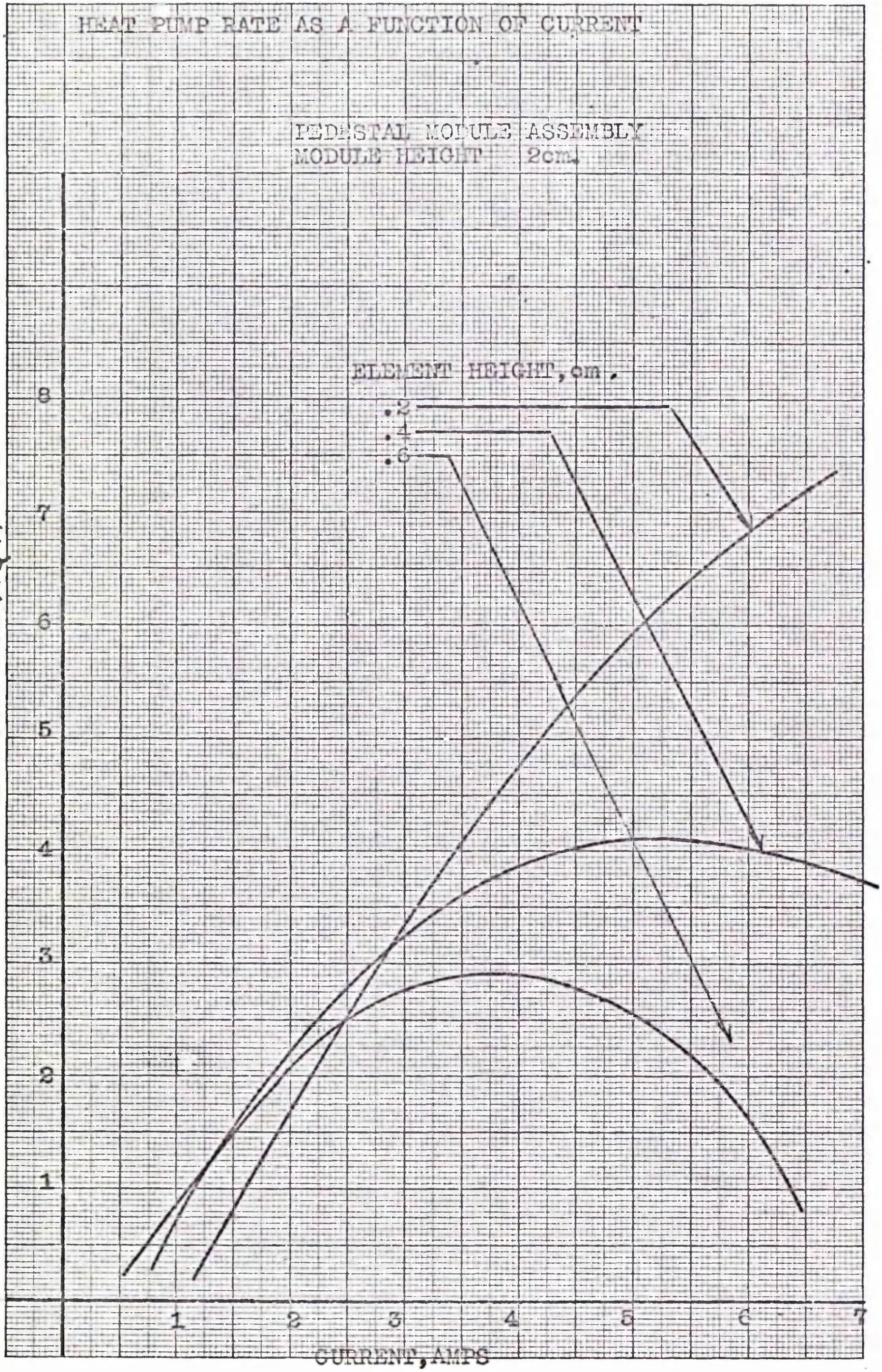
HEAT PUMP RATE AS A FUNCTION OF CURRENT
PEDESTAL MODULE ASSEMBLY
MODULE HEIGHT 2cm.
ELEMENT HEIGHT, cm.
.2
.4
.6
HEAT PUMP RATE, (Q), watts
1
2
3
4
5
6
7
8
CURRENT, AMPS
1
2
3
4
5
6
7

9.3 Effect of Element Height for a Module of Fixed Height.

Figure 9.3.1 illustrates the material utilization (watts/element mass) as a function of the C.O.P. For constant C.O.P. the smaller element height has the highest material utilization parameter. The maximum C.O.P. increases by approximately 30% for a decrease in element height from .6cm to .2cm. The heat leakage (g, equation 7.4.3.5.19) parameter decreased from a value of 49.6 to a value of 22.6 for a 3:1 decrease in element height (1). Figure 9.3.2 illustrates the heat pump rate for a module assembly consisting of 18 thermoelectric couples as a function of the current. Figure 9.3.2 indicates for a current > 3 amps the shorter element has a higher net heat pumping capability. Figure 9.3.3 shows the heat pump per couple mass as a function of the current required to maintain the thermal heat balance. For a constant current input the ($I >$ 2.5 amps) smaller element exhibits a higher heat pump weight parameter.

9.4 General Summary and Conclusion.

In order to undertake space travel of many days duration several cabin functions must be supported by thermoelectric devices. As was mentioned in section 9.1, desired ambient conditions within the cabin proper can be maintained by a proper balance within the cabinet by absorbing and/or emitting thermal radiation. However, there is a need for thermoelectric devices to provide

Fig. 9.3.3.

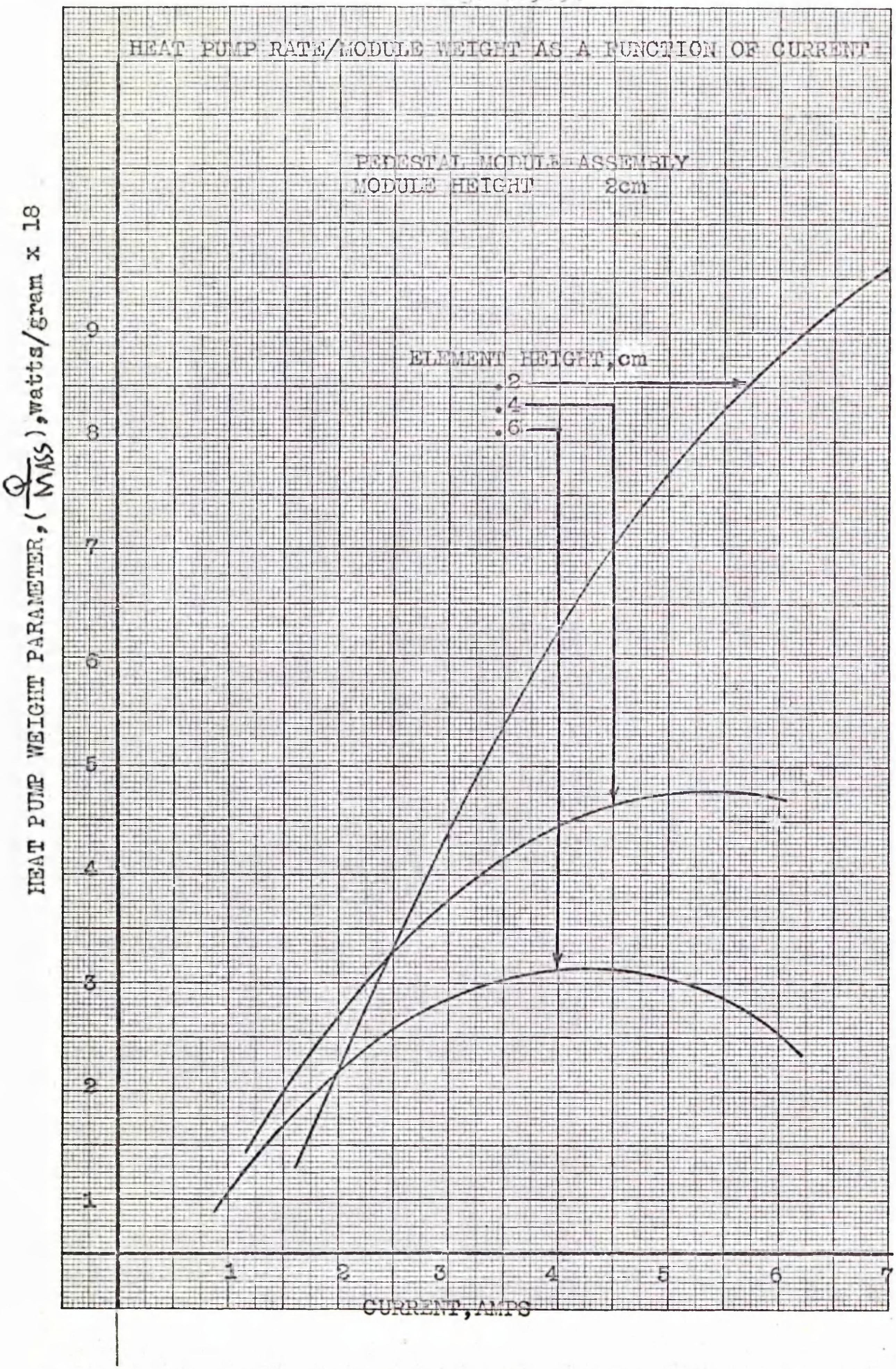

HEAT PUMP RATE/MODULE WEIGHT AS A FUNCTION OF CURRENT
PEDESTAL MODULE ASSEMBLY
MODULE HEIGHT 2cm
ELEMENT HEIGHT, cm
.2
.4
.6
HEAT PUMP WEIGHT PARAMETER, (Q/MASS), watts/gram x 18
1
2
3
4
5
6
7
8
9
CURRENT, AMPS

humidity control, space-area refrigeration, temperature control of electronic components and support basic water purification schemes. The strongest support for utilizing thermoelectricity is its versatility.

Perhaps one of the more difficult problem and subsequent solution on long space flights is to provide fresh water. The reclamation and reuse of all waste water will be mandatory. This means that a method of water purification is necessary. Certainly one method of obtaining pure water is through the basic distillation process. A thermoelectric system is well suited for this application. One of the unique properties of a thermoelectric system is the double function of cooling and heating. Through engineering design the thermoelectric device can become both evaporator and condenser. Such detail applications will require corresponding data and the general conclusions presented should be used as an 'indicator' of trends.

The data appearing in chapters 8.0 and 9.0 indicate the following:

(1) The operational parameter $C.O.P./C.O.P._{max}$ as a function of the dimensionless current parameter (θ) reaches a maximum value at a current parameter (θ) less than which is required to maximize $(Q_S / Q_{S\,max})$.

(2) The use of the material utilization parameter Q/Vol appears to be a good indicator of performance level. The highest value of volume occurs at $N_{\lambda} = \infty$ This condition is indicative of the junction temperature being the same for the corresponding surrounding media.

(3) Increasing the current above the condition of thermal balance is associated with decreasing the free-stream source temperature below the design value. (With the assumptions appearing in section 8.7.1)

(4) Comparison of the heat pump rate (Q_s) for constant input power with fixed element height (pedestal or conventional module) indicates a higher output value for the pedestal module. The heat pump weight parameters (Q/Vol, Q/gram) indicate a more favourable module is a conventional configuration. For a constant input power the C.O.P. for the conventional module is lower than the C.O.P. for the pedestal assembly. To make a final design decision as to the more effective system the application must be considered.
For a space application the thermoelectric system can be assumed to consist of two subassemblies:

(1) Basic thermoelectric module
(2) Power supply required

With the introduction of the power supply requirements the apparent advantages of the conventional module may be lost. The C.O.P. for the conventional assembly is lower than the C.O.P. for the pedestal module indicating the need for a larger power output reflected in an overall weight increase. An overall study should consider the ratio: (power supply/weight) as an input variable. For example an operational parameter could be (Q_s /System Weight) as a function of Q_s .

(5) Comparisons of pedestal modules indicate that the smaller thermoelectric element consistent with the heat load requirement offers the highest material utilization parameter.

COMMENT.

The purpose for this engineering analysis (pedestal Vs conventional module) is to indicate the operational design potential in the resulting Computer models. The establishing of what or how many parameters to be considered in any decision network can not be considered in detail for this presentation. It must be emphasized that good engineering practices must be applied in order to approach an optimized system performance. Optimization requirements for a thermoelectric device may be weight limited, volume restricted, or be bounded by the level of heat load. The 'limit' controls have excluded direct cost. Cost effectiveness is a valid and in many conditions the deciding factor between what configuration will be possible/ practical.

OPERATIONAL CHARACTERISTICS OF THERMOELECTRIC REFRIGERATION

BY WALLACE SHAKUN, B.S.M.E., M.S.M.E.

Advancements in contemporary physics in the field of semi-conductors now make it possible to effectively utilize thermo-electric phenomenon for cooling and environment heating. Refrigerator applications using thermoelectric cooling effect are being built and introduced into industrial and military engineering design. Calculations on semi-conductor thermoelectric refrigeration systems have been based on relationships derived from considering the basic thermoelectric couple to be in an isolated control volume. In the pseudo environment the cooling capacity and coefficient of performance are based on the assumption that junction temperatures of the thermoelements are independent of the current (arbitrary). Test results, on semi-conductor refrigeration systems indicate that the C.O.P. characteristic (C.O.P. = f(I)) with the absence of artificial restraints do not have extremal values. Such results can only be observed if an experiment is conducted in which the junction temperatures are controlled (constant). Conclusions which are obtained account only for internal energy processes occurring within the control volume. However, in actual practice the cooling capability, performance level are functions of the applied current. The results available (within this research program) indicate that there is a direct functional relation between the thermoelectric couple and the environment to be regulated.

The object of the thesis is to present the various operational parameters that relate system performance to the environment in which the thermoelectric module is required to perform and control. The mathematical coupling between the thermoelectric junctions and the environments are assumed to be represented by a m^{th} order function. The technique of utilizing a parametric analysis model enables a comprehensive engineering effort for establishing the mathematical tools for competitive evaluation.

Four major subcomponents sharply influence the design/performance of thermocouples for module assembly. The thermal and electrical material properties of the elements fall into the most fundamental category. Power supply and regulation control are in a second major category. Properties and technique of material construction and processing are a third consideration. Heat exchanger devices provide further requirements to be considered. The various problems to be encountered are considered and the inter-acting of the major components are indicated. The extent to which these conditions limit the design/performance and the determination of the most advantageous compromise is essentially the task considered.

Methods are developed to determine the quantative effects of parametric adjustment. The design problems considered result in the requirements for the solution of the heat transfer equation in which the boundary conditions are determined by an iterative procedure. The solution to this class of problem is solved by the application of numerical analysis. The technique for solution is by the method termed, "over-relaxation", thereby effectively increasing the convergence rate of the finite difference equations. Advances and more sophisticated methods of digital computer utilization resulted in a comprehensive mathematical tool being afforded to the design engineer.

Operational Characteristics of Thermoelectric Refrigeration.

VOLUME II.

By

Wallace Shakun, B.S.M.E., M.S.M.E.

A Thesis submitted for the degree of Doctor of Philosophy.

April 1969.

Department of Aeronautics and Fluid Mechanics,
University of Glasgow.

TABLE OF CONTENTS - VOLUME II.

The thesis consists of two bound volumes. Volume I contains: Chapter 1.0 to Chapter 9.0 (inclusive). Volume II contains: Chapter 10 to Chapter 13 (inclusive), Computer Program Index and Appendix.

Pg.

Pg.

COMPUTER PROGRAMME INDEX.

APPENDICES.

10.0 THOMSON PHENOMENA.

10.1 Introduction.

The treatment of the efficiency and subsequent operational equations for the thermoelectric refrigerators have been based on the exclusion of the Thomson effect (section 5.2.3). The exclusion of the Thomson effect results from the condition that material properties were assumed invariant with temperature. This ideal material condition resulted in:

$$\tau = T\frac{d\alpha}{dT} = 0 \qquad 10.1.1.$$

where:

τ the Thomson coefficient, Volts/°C

Previous authors (6) (13) have discussed the uniqueness of the Thomson effect as a phenomena associated with the basic Peltier Couple. Reference (13) introduced a series solution into the basic heat flux equation ($q = -k\nabla T$) in order to account for the Thomson effect. The concept proposed in this section is to use a modified Seebeck coefficient (α^*_{np}) to replace α_{np} of the preceeding sections.

10.2 Modified Seebeck Coefficient.

In the presence of a temperature gradient along a conducting material heat is absorbed or released in proportion to the current passing through it. This phenomena is called the Thomson effect. The rate at which heat is absorbed in a small segment of conductor dx is proportional to the current (I) and the temperature gradient dT/dx. The rate of heat absorbed is expressed as:

$$dQ_\tau = \tau[T]\, I \frac{dT}{dx} dx \qquad 10.2.1.$$

In the above expression positive (+) I is flowing in the direction of increasing X ($0 \rightarrow \ell$). A positive dQ_τ indicates that heat is absorbed from the surroundings. The significance of the sign of dQ_τ and τ(T) is similar to that of $q(T)_P$ for $\pi(T)$ from the Peltier effect. The coefficient π_{ab} is called the Peltier coefficient (couple) and is a function of the local temperature. Recalling that:

$$\pi_{ab}(T) = -\pi_{ba}(T) \qquad 10.2.2.$$

The Thomson coefficient $\tau(T)$ can be positive or negative depending on the material. Consider the energy balance of a basic thermocouple for an operating period of one second. Figure 10.2.1 illustrates the basic thermocouple circuit and the sign convention.

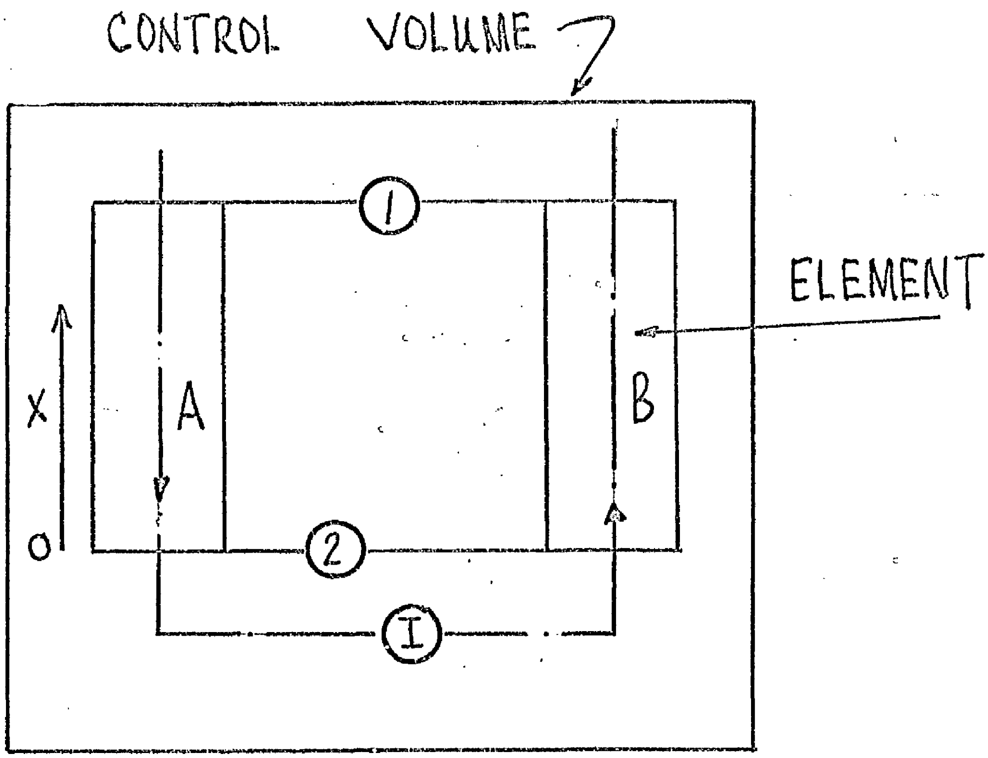

Figure 10.2.1.

Thomson Sign Convention.

The Thomson phenomena for conductor A is expressed as:

$$q_A = -I \int_{T_2}^{T_1} \tau_A(T) \frac{dT}{dx} dx \qquad 10.2.3.$$

then:

$$q_A = -I \int_{T_2}^{T_1} \tau_A(T) \, dT \qquad 10.2.4.$$

where:

$\tau_A(T)$ Thomson coefficient for element A

In element B the current I is in the direction ② to ①, which results in:

$$q_B = I \int_{T_2}^{T_1} \tau_B(T)\, dT \qquad 10.2.5.$$

The total Thomson heat input for the system is:

$$q_T = q_A + q_B \qquad 10.2.6.$$

$$q_T = I \int_{T_2}^{T_1} \left[\tau_B(T) - \tau_A(T) \right] dT \qquad 10.2.7.$$

The total heat input from reversible sources (less joule term and heat conduction effect) is:

$$Q = q_1 + q_2 + q_A + q_B \qquad 10.2.8.$$

where:

q_1, q_2 Peltier heat inputs at junctions ① and ② respectfully, introducing the basic effects into equation 10.2.8 results:

$$Q = \Pi_{AB}(T_1) I - \Pi_{AB}(T_2) I + I \int_{T_2}^{T_1} \left[\tau_B(T) - \tau_A(T) \right] dT \qquad 10.2.9.$$

then:

$$\frac{Q}{I} = \Pi_{AB}(T_1) - \Pi_{AB}(T_2) + \int_{T_2}^{T_1} \left[\tau_B(T) - \tau_A(T) \right] dT \qquad 10.2.10.$$

The Seebeck Coefficient is expressed as:

$$\alpha_{AB} = \frac{\Pi_{AB}}{T_i \,(\text{local value})} \qquad 10.2.11.$$

From Kelvin's second relation:

$$T\frac{d\alpha_{AB}}{dT} = \tau_A - \tau_B \qquad 10.2.12.$$

Introducing equation 10.2.11 and equation 10.2.12 into equation 10.2.10 results:

$$\frac{Q}{I} = \alpha_{AB}(T_1)T_1 - \alpha_{AB}(T_2)T_2 - \int_{T_2}^{T_1} T\frac{d\alpha_{AB}}{dT}\,dT \qquad 10.2.13.$$

The modified Seebeck coefficient is defined as:

$$\alpha^*_{AB} \equiv \frac{\left[\alpha_{AB}(T_1)T_1 - \alpha_{AB}(T_2)T_2 - \int_{T_2}^{T_1} T\frac{d\alpha_{AB}}{dT}\,dT\right]}{\left[T_1 - T_2\right]} \qquad 10.2.14.$$

when $\alpha_{AB}(T_i) \neq g(T_i)$; $\frac{d\alpha_{AB}}{dT} = 0$

then equation 10.2.14 reduces to:

$$\alpha^*_{AB} = \frac{\alpha_{AB}(T_1 - T_2)}{T_1 - T_2} = \alpha_{AB} \qquad 10.2.15.$$

where:

α_{AB} Seebeck couple coefficient as utilized in previous chapters, volts/^oC

Equation 10.2.14 is transformed by the introduction of the thermocouple junction temperatures into:

$$\alpha_{mp}^{*} \equiv \frac{\left[\alpha_{mp}(T_{h_j})T_{h_j} - \alpha_{mp}(T_{c_j})T_{c_j} - \int_{T_{c_j}}^{T_{h_j}} T\frac{d\alpha_{mp}}{dT}dT\right]}{\left[T_{h_j} - T_{c_j}\right]} \qquad 10.2.16.$$

The heat pump rate (Q_s) will be expressed as:

$$Q_s = T_{c_j} I \alpha_{mp}^{*} - \frac{1}{2}I^2 R_{EFF} - K_{EFF}\Delta T_j \qquad 10.2.17.$$

where:

α_{mp}^{*}	defined by equation 10.2.16
R_{EFF}	defined by equation 7.2.5.3.
K_{EFF}	defined by equation 7.2.3.4.

A computer program procedure C.P.7. (Polynomial) was developed to establish α_{mp} in a polynomial form with sufficient accuracy. This basic procedure can be applied to material properties i.e. $k(T)$, $\rho(T)$ to obtain a polynomial function or average material value by direct integration. The form required for $\alpha_{mp}(T)$ is expressed as:

$$\alpha_{mp}(T) = \alpha_0 T^0 + \alpha_1 T^1 + \alpha_2 T^2 + \alpha_n T^n \qquad 10.2.18.$$

Discrete values of $\alpha_{mp}(T)$ or array pairs are obtained from test data. An array pair takes the general form of:

$$\alpha[i], T[i] \qquad 10.2.19.$$

Figure 10.2.2 illustrates the general form of the Seebeck coefficient as a function of the absolute temperature (^{o}K)

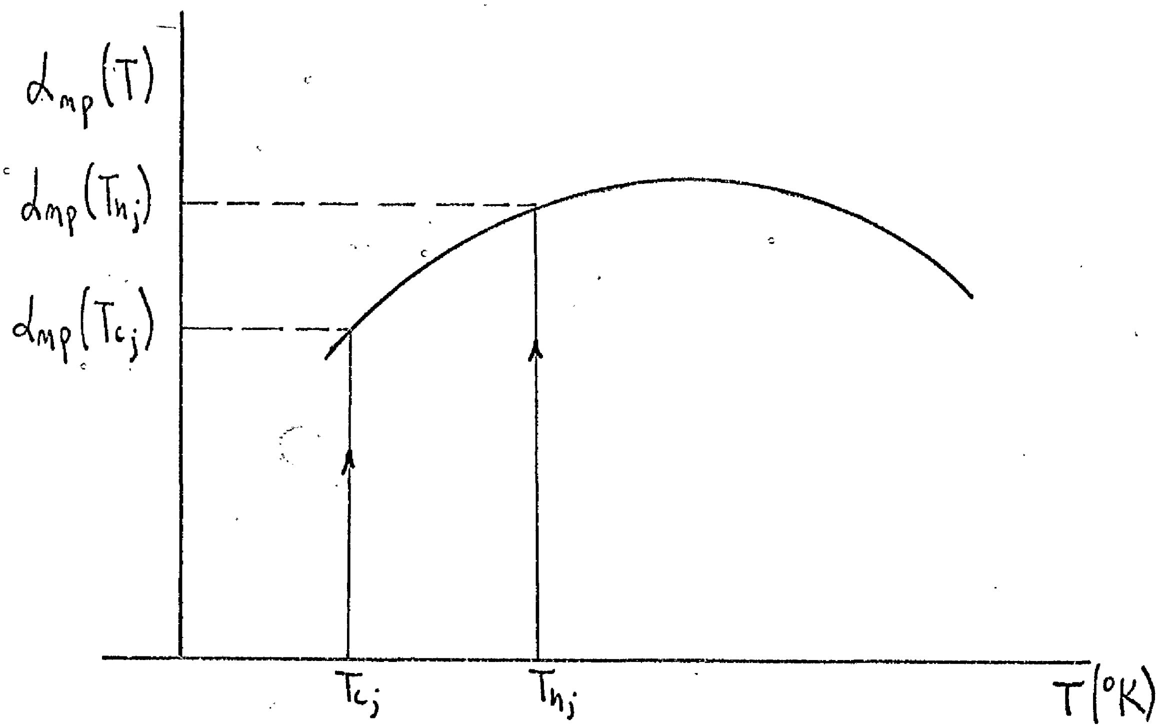

Figure 10.2.2.

Seebeck Couple Coefficient as a function of Temperature Absolute.

Taking the derivative of equation 10.2.18, multiplying the derivative by T results:

$$\int T\frac{d\alpha}{dT}dT = \frac{\alpha_1 T^2}{2} + \frac{2\alpha_2 T^3}{3} + \frac{3\alpha_3 T^4}{4} + \frac{m\alpha_m T^{m+1}}{m+1} \qquad 10.2.20.$$

Replacing the right hand side of equation 10.2.20 by a series summation; introducing the limits of integration and combining results:

$$\int_{T_{c_j}}^{T_{h_j}} T\frac{d\alpha}{dT}\,dT = \sum_{i=1}^{i=m} \frac{i\alpha_i}{[i+1]}\left[T_{h_j}^{\,i+1} - T_{c_j}^{\,i+1}\right]$$

10.2.21.

Introducing equation 10.2.21 into equation 10.2.16 results:

$$\alpha_{np}^{*} = \frac{\alpha(T_{h_j})T_{h_j} - \alpha(T_{c_j})T_{c_j} - \sum_{i=1}^{i=m}\frac{i\alpha_i}{[i+1]}\left[T_{h_j}^{\,i+1} - T_{c_j}^{\,i+1}\right]}{\left[T_{h_j} - T_{c_j}\right]}$$

10.2.22.

where:

$$\alpha(T_{h_j})T_{h_j} = \alpha_0 T_{h_j} + \alpha_1 T_{h_j}^2 + \alpha_m T_{h_j}^{m+1} \qquad 10.2.23.$$

$$\alpha(T_{c_j})T_{c_j} = \alpha_0 T_{c_j} + \alpha_1 T_{c_j}^2 + \alpha_m T_{c_j}^{m+1} \qquad 10.2.24.$$

Replacing equation 10.2.23 and equation 10.2.24 by corresponding series and introducing the result into equation 10.2.22 results:

$$\alpha_{np}^{*} = \alpha_0 + \frac{\sum_{i=1}^{i=m}\alpha_i\left[T_{h_j}^{\,i+1} - T_{c_j}^{\,i+1}\right]\left[1 - \frac{i}{i+1}\right]}{\left[T_{h_j} - T_{c_j}\right]}$$

10.2.25.

A computer procedure ALPHA was developed to solve for a n-order polynomial (output from procedure POLY).

To illustrate the basic concept consider the following:

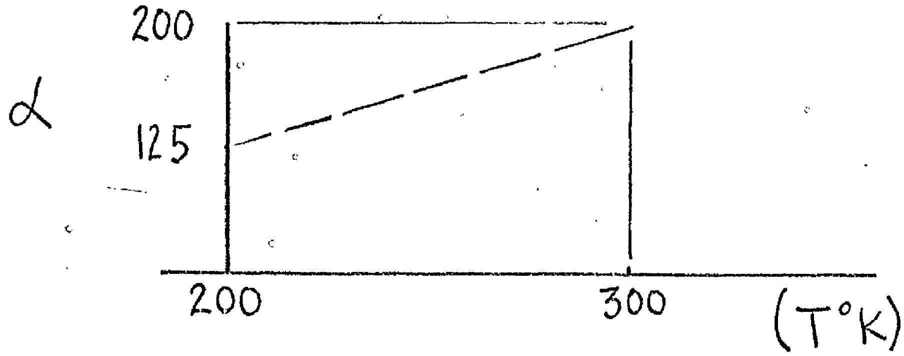

The curve equation is:

$$\alpha(T) = -25 + .75T \qquad 10.2.26.$$

where: $\alpha(T_{h_j}) = 200 \qquad \alpha(T_{c_j}) = 125$

and

$$\Delta T_j = 100$$

By direct integration and substituting into equation 10.2.16:

$$\alpha^*_{mp} = \frac{(200)(300) - (125)(200) - \frac{3}{8}(300)^2 + \frac{3}{8}(200)^2}{100} \qquad 10.2.27.$$

$$\alpha^*_{mp} = 162.5 \qquad 10.2.28.$$

The average value is expressable as:

$$\bar{\alpha}_{mp} = \int_{200}^{300} \frac{[-25 + 0.75T]\,dT}{100} \qquad 10.2.29.$$

$$\bar{\alpha}_{mp} = 162.5 \qquad 10.2.28.$$

The curve equation is:

$$\alpha(T) = -25 + .75T \qquad 10.2.26.$$

where:

$$\alpha_0 = -25$$

$$\alpha_i = .75 \quad \text{and} \quad i = 1$$

Introducing $\alpha_0, \alpha_1, T_{h_j}, T_{c_j}$ into equation 10.2.25 results as follows:

$$\alpha^*_{mp} = -25 + \frac{.75[(300)^2 - (200)^2]\frac{1}{2}}{100} \qquad 10.2.27.$$

$$\alpha^*_{mp} = 162.5 \qquad 10.2.28.$$

A first order polynomial of the form: $y = mx + b$ was utilized in equation 10.2.16., 10.2.25., 10.2.29 to determine the modified Seebeck Coefficient (α^*). The results for all three calculations were identical.

<u>COMMENT</u>.

To determine the modified Seebeck coefficient (α^*_{mp}) computer procedure ALPHA requires the input of the hot junction temperature (T_{h_j}) and the cold junction temperature

(T_{c_j}). Material parameters (i.e. α_i) are determined from procedure POLY. The junction temperatures are determined by procedure HEATFLUX. Procedure HEATFLUX is incorporated into computer program (CP.5). The computer program was developed to determine module performance for a system operating between heat source and heat sink with finite heat transfer coefficients.

10.3 Thomson Effect Influence on Thermoelement Temperature Distribution.

10.3.1 Abstract.

The temperature distribution along the arm of a thermoelement will be determined when the Thomson effect is included. A heat flux exists when a temperature gradient is present in a material and is given by:

$$q = -k \nabla T \qquad 10.3.1.1.$$

The heat flux is a vector and is not necessarily parallel to the temperature gradient. This section will be concerned with isotropic material where all thermodynamic-material properties are scalar. In addition a one-dimensional geometry will be examined. Practical device (developed today) performance have indicated that no advantage is to be gained by using two or three dimensional gradients. In applications utilizing magnetic fields the tensor properties of the medium as well as the three dimensional nature of the problem must be considered.

10.3.2 Solution of the Differential Equation for Determining Temperature Distribution.

The temperature distribution along an element can be determined from the following:

$$\frac{d}{dx}\left[k(T(x))\,A(x)\frac{dT}{dx}\right] + \frac{I^2\rho(T(x))}{A(x)} - T(x)\,I\,\frac{d\alpha}{dx}(T(x)) = 0$$

10.3.2.1.

and

$$\frac{d}{dx}\left[k(T(x))\,A(x)\frac{dT}{dx}\right] + \frac{I^2\rho(T(x))}{A(x)} + T(x)\,I\,\frac{d\alpha}{dx}(T(x)) = 0$$

10.3.2.2.

Equation 10.3.2.1 is for the A- element of figure 10.2.1 and equation 10.3.2.2 is for the B- element of figure 10.2.1. The symbol (A) is equivalent of the n-type thermoelement and the symbol (B) is equivalent to the p- type thermoelement. A program has been developed (14) where a numerical method coupled with a high capacity computer (IBM 709) successfully solved equation 10.3.2.1. The method of solution was relatively cumbersome for the level of analysis required for this study. A technique will be employed to introduce simplyfying assumptions with operational parameters. The first approximation is to replace the transport coefficients by average values. The method of using average values was first presented in reference (6) with a modified series solution extracted from (13). The solution presented in this section is for the n- type element (purpose of illustration).

Introducing average material values and a constant cross-sectional area equation 10.3.2.1 results:

$$A\hat{k}\frac{d^2T}{dx^2} + \frac{I^2\hat{\rho}}{A} - T(x)I\frac{d\alpha}{dx} = 0 \qquad 10.3.2.3.$$

From equation 10.2.12:

$$T\frac{d\alpha_{AB}}{dT} = \tau_A - \tau_B$$

and for a single element:

$$T\frac{d\alpha_m}{dT} = \tau_m \qquad 10.3.2.4.$$

Introducing equation 10.3.2.4 into equation 10.3.2.3 results:

$$A\hat{k}\frac{d^2T}{dx^2} + \frac{I^2\hat{\rho}}{A} - I\hat{\tau}_m\frac{dT}{dx} = 0 \qquad 10.3.2.5.$$

where:

$\hat{k}, \hat{\rho}, \hat{\tau}_m$ average material properties

For $\hat{\tau}_m = 0$ equation 10.3.2.5 reduces to the basic equation of appendix A . Equation 10.3.2.5 is a linear differential equation with constant coefficients. The solution will consist of a complementary function and particular integral. The complementary solution is as follows:

$$A\hat{k}\frac{d^2T}{dx^2} - I\hat{\tau}_m\frac{dT}{dx} = 0 \qquad 10.3.2.6.$$

The characteristic equation takes the form:

$$a m^2 + b m = 0 \qquad 10.3.2.7.$$

The roots of the equation are:

$$m_1 = 0$$

$$m_2 = \frac{-b}{a} \quad , \quad m_2 = \frac{\hat{\tau} I}{A \hat{k}} \qquad 10.3.2.8.$$

The complementary solution:

$$T(x) = C_1 e^{m_1 x} + C_2 e^{m_2 x} \qquad 10.3.2.9.$$

Introducing the roots of the solution (10.3.2.8) into equation 10.3.2.9 results

$$T(x) = C_1 + C_2 e^{\frac{\hat{\tau} I x}{A \hat{k}}} \qquad 10.3.2.10.$$

The particular solution is as follows:

$$T_p(x) = A'' x \qquad 10.3.2.11.$$

where:

A'' is a constant

Introducing equation 10.3.2.11 into equation 10.3.2.5 results:

$$\frac{I^2 \hat{\ell}}{A} - I \hat{\tau}_m A'' = 0 \qquad 10.3.2.12.$$

then:

$$A'' = \frac{I\hat{\rho}}{\hat{\tau}A} \qquad 10.3.2.13.$$

Substituting for A" (equation 10.3.2.13) into equation 10.3.2.11 results

$$T_p(x) = \frac{I\hat{\rho}x}{\hat{\tau}A} \qquad 10.3.2.15.$$

The total solution is the sum of the complementary solution and the particular solution resulting

$$T(x) = C_1 + C_2 e^{\frac{\hat{\tau}Ix}{A\hat{k}}} + \frac{I\hat{\rho}x}{\hat{\tau}A} \qquad 10.3.2.15.$$

The boundary conditions are introduced to determine the constants C_1 and C_2 The boundary conditions are:

$$T(0) = T_{h_j} \qquad T(\ell) = T_{c_j} \qquad 10.3.2.16.$$

Introducing the boundary conditions results in two equations:

$$T_{h_j} = C_1 + C_2 \qquad 10.3.2.17.$$

$$T_{c_j} = C_1 + C_2 e^{\frac{\hat{\tau}Ix}{A\hat{k}}} + \frac{I\hat{\rho}\ell}{\hat{\tau}A} \qquad 10.3.2.18.$$

Letting:

$$a = \frac{\hat{\tau}I\ell}{A\hat{k}} \qquad c = \frac{\hat{\tau}Ix}{A\hat{k}} \qquad 10.3.2.19.$$

$$b = \frac{I\hat{\rho}\ell}{\hat{\tau}A} \qquad d = \frac{\hat{\rho}Ix}{\hat{\tau}A}$$

Where:

a, b, c, d are the Thomson material parameters.

Solving for C_1 results:

$$C_1 = \frac{\left[T_{c_j} - T_{h_j} e^{a} - b\right]}{\left[1 - e^{a}\right]} \qquad 10.3.2.20.$$

Solving for C_2 results:

$$C_2 = T_{h_j} - C_1 \qquad 10.3.2.21.$$

Introducing equation 10.3.2.20 and equation 10.3.2.11 into equation 10.3.2.15 with:

$$C_{11} = \frac{\left[T_{c_j} - T_{h_j} e^{a} - b\right]}{\left[1 - e^{a}\right]} \qquad 10.3.2.22.$$

results:

$$T(x) = C_{11}\left[1 - e^{c}\right] + d + T_{h_j} e^{c} \qquad 10.3.2.23.$$

To verify the resulting equation 10.3.2.23 at $T(0) = T_{h_j}$ then:

$$T(0) = C_{11}\left[1 - 1\right] + T_{h_j} \qquad 10.3.2.24.$$

and $T(\ell) = T_{c_j}$

then:

$$T(\ell) = T_{c_j} - T_{h_j} e^{a} - b + b + T_{h_j} e^{a} \qquad 10.3.2.25.$$

$$T(\ell) = T_{c_j} \qquad 10.3.2.26.$$

Equation 10.3.2.24 and equation 10.3.2.26 indicates that the differential equation is satisfied by the boundary conditions. If no current passes through the element equation 10.3.2.5 reduces to

$$\hat{k}\frac{d^2T}{dx^2} = 0 \qquad 10.3.2.27.$$

Equation 10.3.2.27 illustrates that dT/dx is constant. The temperature T is linear with x from $T(0) = T_{h_j}$ to $T(\ell) = T_{c_j}$. This condition is indicated on the appropriate figures within this section. The characteristic resulting from equation 10.3.2.27 can also be obtained by applying ℓ' Hospital rule to the intermediate fraction of equation 10.3.2.23.

$$\frac{(1-e^c)}{(1-e^a)} = \frac{\left[1-e^{\left[\frac{\tau I x}{A k}\right]}\right]}{\left[1-e^{\left[\frac{\tau I \ell}{A k}\right]}\right]} \longrightarrow \frac{x}{\ell} \qquad 10.3.2.28.$$

and for I = 0 equation 10.3.2.23 reduces to:

$$T(x) = \left[T_{c_j} - T_{h_j}\right]\frac{x}{\ell} + T_{h_j} \qquad 10.3.2.29.$$

The boundary conditions are satisfied by equation 10.3.2.29.

10.3.3. Thomson Material Parameters With Optimized Current Ratios.

The temperature distribution along the element can be determined from the following equation:

$$T(x) = C_{11}\left[1-e^c\right] + d + T_{h_j}e^c$$

10.3.2.23.

where:

$$C_{11} = \frac{\left[T_{cj} - T_{hj} e^{a} - b\right]}{\left[1 - e^{a}\right]} \qquad 10.3.2.22.$$

The dimensionless current ratio is defined as:

$$\theta \equiv I / I_Q \qquad 6.7.1.$$

The current required to operate at maximum heat pump rate is:

$$I_Q = \alpha_{np} T_{cj} / 2R \qquad 6.5.4.1.$$

Equation 6.5.4.1 reflects the operation for the current required to operate at maximum heat pump rate. The current ratio at maximum C.O.P. is expressed as:

$$\theta = \mu_\phi = I_\phi / I_Q \qquad 7.4.4.5.3.$$

and

$$\mu_\phi = \frac{\Delta T_j \left[1 + \sqrt{1 + Z_{EFF}\left[\frac{\Delta T_j}{2} + T_{cj}\right]}\right]}{T_{cj} Z_{EFF}\left[\frac{\Delta T_j}{2} + T_{cj}\right]} \qquad 7.4.4.5.4.$$

Equation 6.5.4.1 and equation 7.4.4.5.4 reflect the operation for a thermoelectric couple, in order to utilize these diamensionless parameters in equation 10.3.23 (an element temperature function) the following transformations are introduced.

The Seebeck couple coefficient (α_{np}) is replaced by:

$$\alpha_{np} \cong 2\alpha_n \qquad 10.3.3.1.$$

where:

α_n Seebeck coefficient of n- type element

Introducing equation 10.3.31 into equation 6.5.4.1 results:

$$I_\varphi = \frac{\hat{\alpha}_n T_{cj} A}{\hat{\rho} l} \qquad 10.3.3.2.$$

In Soviet literature, the parameter

$$Z_A = \frac{\alpha_A^2}{\rho_A k_A} \qquad 10.3.3.3.$$

is used to indicate the figure of merit of material A. Transforming equation 7.4.4.5.4 to reflect the material figure of merit of an element results in letting:

$Z_{EFF} = Z_{n\text{-element}}$ (as defined by 10.3.3.3)

then:

$$\mu_\phi = \frac{\Delta T_j\left[1 + \sqrt{1 + Z_n\left[\frac{\Delta T_j}{2} + T_{cj}\right]}\right]}{T_{cj} Z_n \left[\frac{\Delta T_j}{2} + T_{cj}\right]} \qquad 10.3.3.4.$$

Equation 10.3.3.2 and equation 10.3.3.4 are identified as the optimized current ratios. The Thomson material parameters resulting from introducing equation 10.3.3.2 are:

$$a = \frac{\hat{\tau}\theta\hat{\alpha}T_{cj}}{\hat{\rho}k} \qquad c = \frac{\hat{\tau}\theta\hat{\alpha}T_{cj}}{\hat{\rho}\hat{k}}\left(\frac{X}{l}\right) \qquad 10.3.3.5$$

$$b = \frac{\theta\alpha T_{cj}}{\hat{\tau}} \qquad d = \frac{\theta\hat{\alpha}T_{cj}}{\hat{\tau}}\left(\frac{X}{l}\right)$$

The condition for operation at maximum heat pump rate occurs at $\theta = 1$. The current required for operation at max C.O.P. occurs at $\theta = \mu_\phi$. The derivation of the term μ_ϕ is presented in Appendix K. A computer program was developed to calculate $T(x)/T_{h_j}$ as a function of position ratio x/ℓ for variation in the dimensionless current ratio (θ). The average material values will be determined in the next section.

10.3.4 Determination of Average Material Properties.

(a) The thermal conductivity ($k(T)$) is assumed to have the following form:

$$k = k_0 / T \qquad 10.3.4.1.$$

and k_0 is a constant and is invariant with temperature, watts/cm.

(b) The electrical resistivity ($\rho(T)$) is assumed to have the following form:

$$\rho = \rho_0 T^0 + \rho_1 T^1 + \rho_2 T^2 + \rho_m T^m \qquad 10.3.4.2.$$

(c) The Seebeck coefficient ($\alpha(T)$) is assumed to have the following form:

$$\alpha = \alpha_0 T^0 + \alpha_1 T^1 + \alpha_2 T^2 + \alpha_m T^m \qquad 10.3.4.3.$$

and the Thomson coefficient for a single element:

$$\tau = T \frac{d\alpha}{dT} \qquad 10.3.4.4.$$

Fig. 10.3.4.1.

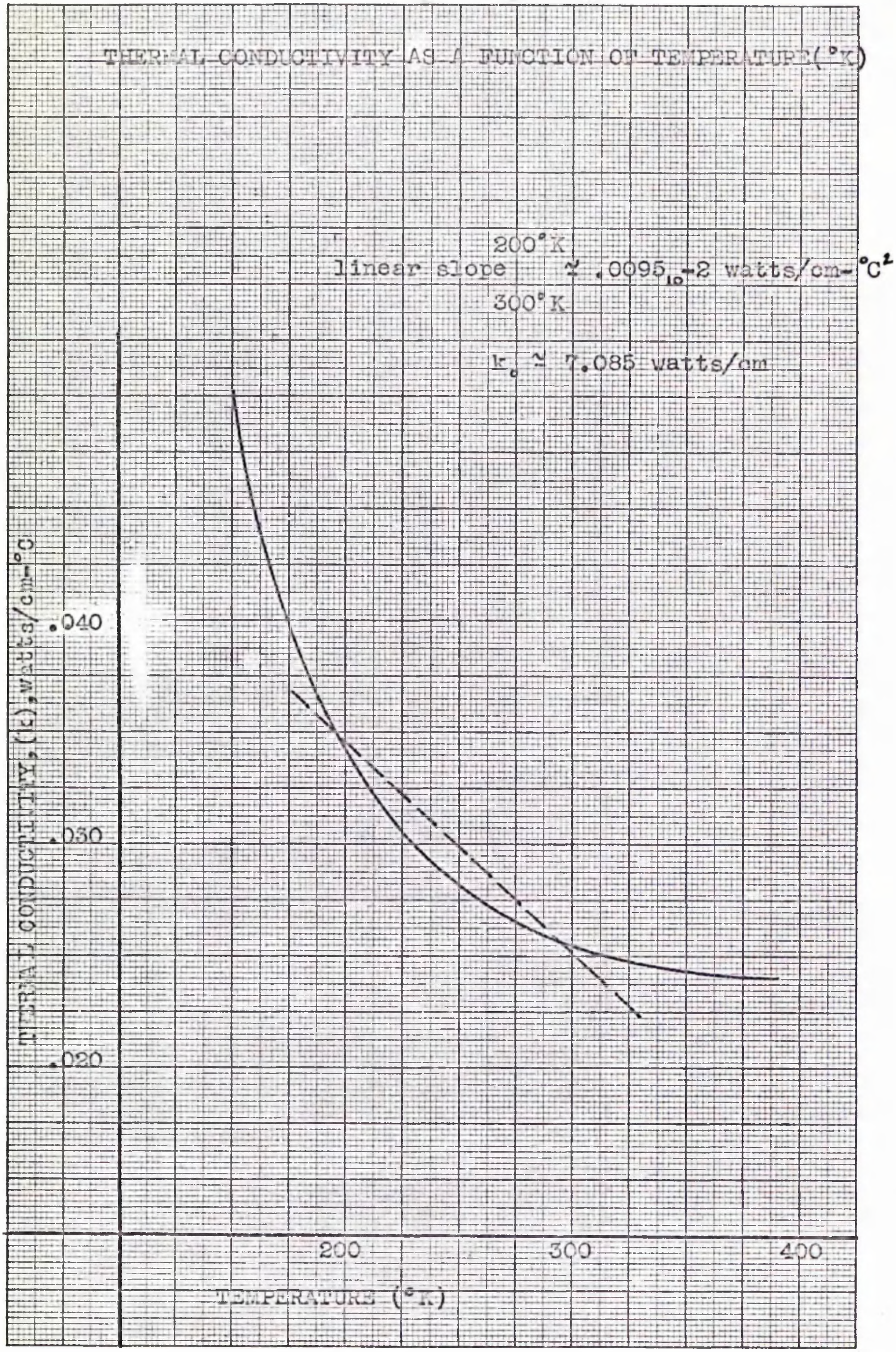
THERMAL CONDUCTIVITY AS A FUNCTION OF TEMPERATURE(°K)
200°K
linear slope ≃ .0095 10-2 watts/cm-°C²
300°K
k₀ ≃ 7.085 watts/cm
.040
.030
.020
THERMAL CONDUCTIVITY, (k), watts/cm-°C
200
300
400
TEMPERATURE (°K)

The coefficients are determined by experiment. The final property constants (α_n, ρ_n, k_n) will be determined by curve fitting the test data with a fourth order polynomial. Computer procedure POLY was developed as a curve fitting routine to a $n^{\underline{th}}$ order using orthogonal polynomials with statistical termination.

The average thermal conductivity will be expressed as:

$$\hat{k} = \int_{T_{c_j}}^{T_{h_j}} \frac{\frac{k_0}{T} dT}{\left[T_{h_j} - T_{c_j}\right]} \qquad 10.3.4.5.$$

Performing the integration results:

$$\hat{k} = \frac{k_0 \ln\left[\frac{T_{h_j}}{T_{c_j}}\right]}{\left[T_{h_j} - T_{c_j}\right]} \qquad 10.3.4.6.$$

Figure 10.3.4.1 illustrates the thermal conductivity as a function of temperature for a representative thermoelement.

The average electrical resistivity will be expressed as:

$$\hat{\rho} = \frac{\int_{T_{c_j}}^{T_{h_j}} \rho^n T^n dT}{\left[T_{h_j} - T_{c_j}\right]} \qquad 10.3.4.7.$$

Performing the integration yields:

$$\hat{\rho} = \rho_o + \sum_{i=1}^{i=n=4} \frac{\left[T_{h_j}^{\ i+1} - T_{c_j}^{\ i+1}\right]\rho_i}{\left[i+1\right]\left[T_{h_j} - T_{c_j}\right]} \qquad 10.3.4.8.$$

A fourth order polynomial curve fit will be sufficient

Fig. 10.3.4.2.

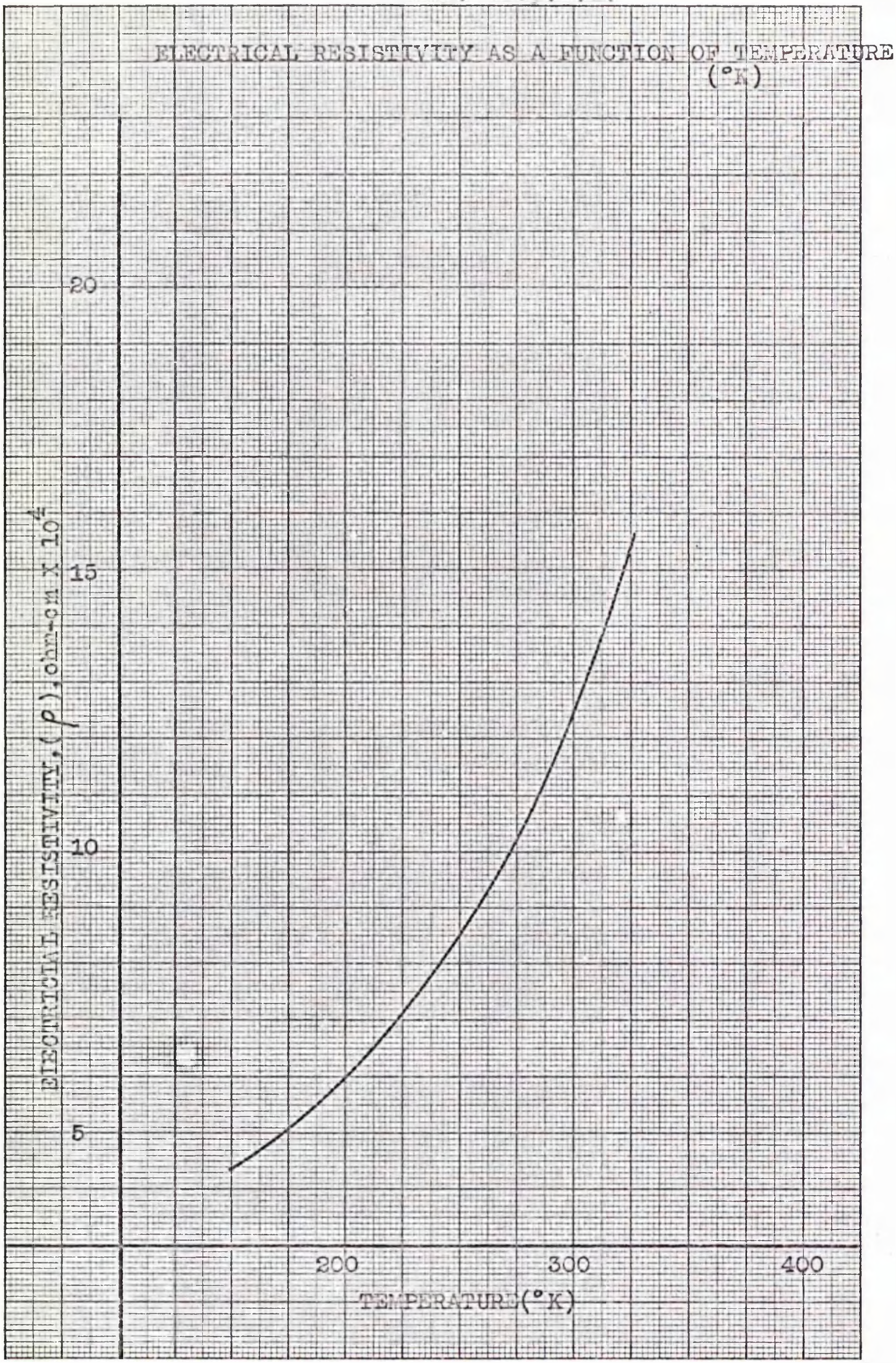
ELECTRICAL RESISTIVITY AS A FUNCTION OF TEMPERATURE (°K)
ELECTRICAL RESISTIVITY, (ρ), ohm-cm X 10^4
20
15
10
5
200
300
400
TEMPERATURE (°K)

for this analysis. Figure 10.3.4.2 illustrates the electrical resistivity as a function of temperature for a representative thermoelement. The average thermal conductivity will be expressed as:

$$\hat{k} = k_0 + \sum_{i=1}^{i=n=4} \frac{\left[T_{h_j}^{\,i+1} - T_{c_j}^{\,i+1}\right] k_i}{[i+1]\left[T_{h_j} - T_{c_j}\right]} \qquad 10.3.4.9.$$

which assumes that $k(T)$ is:

$$k = k_0 T^0 + k_1 T^1 + k_2 T^2 + k_n T^n \qquad 10.3.4.10.$$

The average Thomson coefficient will be expressed as:

$$\hat{\tau} = \sum_{i=1}^{i=4} \frac{i \alpha_i \left[T_{h_j}^{\,i+1} - T_{c_j}^{\,i+1}\right]}{[i+1]\left[T_{h_j} - T_{c_j}\right]} \qquad 10.3.4.11.$$

The average Seebeck coefficient is expressed as:

$$\hat{\alpha} = \alpha_0 + \sum_{i=1}^{i=4} \frac{\alpha_i \left[T_{h_j}^{\,i+1} - T_{c_j}^{\,i+1}\right]}{[i+1]\left[T_{h_j} - T_{c_j}\right]} \qquad 10.3.4.12.$$

Equation 10.2.25 (α^*) is equivalent to equation 10.3.4.12 ($\hat{\alpha}$). In order to establish the identity supporting:

$$\alpha^* = \hat{\alpha} \qquad 10.3.4.13.$$

then:

$$\left[1 - \frac{i}{i+1}\right] = \left[\frac{1}{i+1}\right] \qquad 10.3.4.14.$$

Fig. 10.3.4.3.

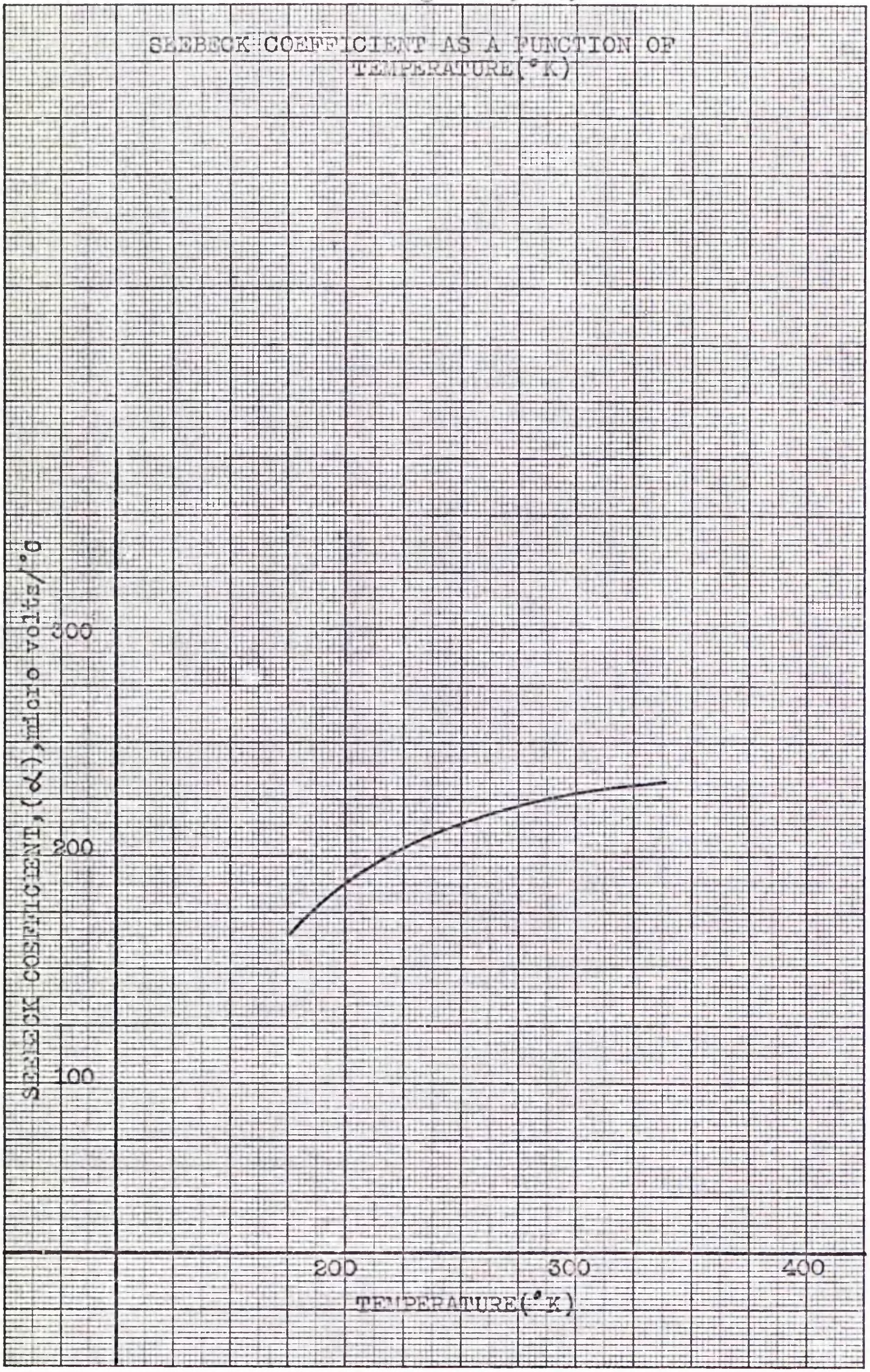
SEEBECK COEFFICIENT AS A FUNCTION OF TEMPERATURE(°K)
SEEBECK COEFFICIENT, (α), micro volts/°C
300
200
100
200
300
400
TEMPERATURE(°K)

hence:

$$\left[\frac{i+1-i}{i+1}\right] = \left[\frac{1}{i+1}\right] \qquad \text{Q.E.D.} \qquad 10.3.4.15.$$

and equation 10.3.4.13 is established. Figure 10.3.4.3 illustrates the Seebeck coefficient as a function of temperature for a representative thermoelement. Figure 10.3.4.3 can be used to estimate the magnitude of the Thomson coefficient. Kelvin's first relation requires the Seebeck coefficient and the Thomson coefficient be related in the following manner:

$$\frac{d\alpha}{dT} = \frac{\tau}{T} \qquad 10.3.2.4.$$

Assuming τ is invariant with absolute temperature then equation 10.3.2.4 can be integrated to yield:

$$\alpha = \tau \ln\left[\frac{T}{T_0}\right] \qquad 10.3.4.16.$$

where

T_0 is the constant of integration.

Solving for the τ (Thomson coefficient) results:

$$\tau = \frac{\alpha}{\ln\left[\frac{T}{T_0}\right]} \qquad 10.3.4.17.$$

Figure 10.3.4.4 shows the Seebeck coefficient (α) as a function of the $\ln$ (T) ($^{\circ}$K). The slope at any temperature is interpreted as the Thomson coefficient at the corresponding temperature. The average Thomson coefficient over the

Fig. 10.3.4.4.

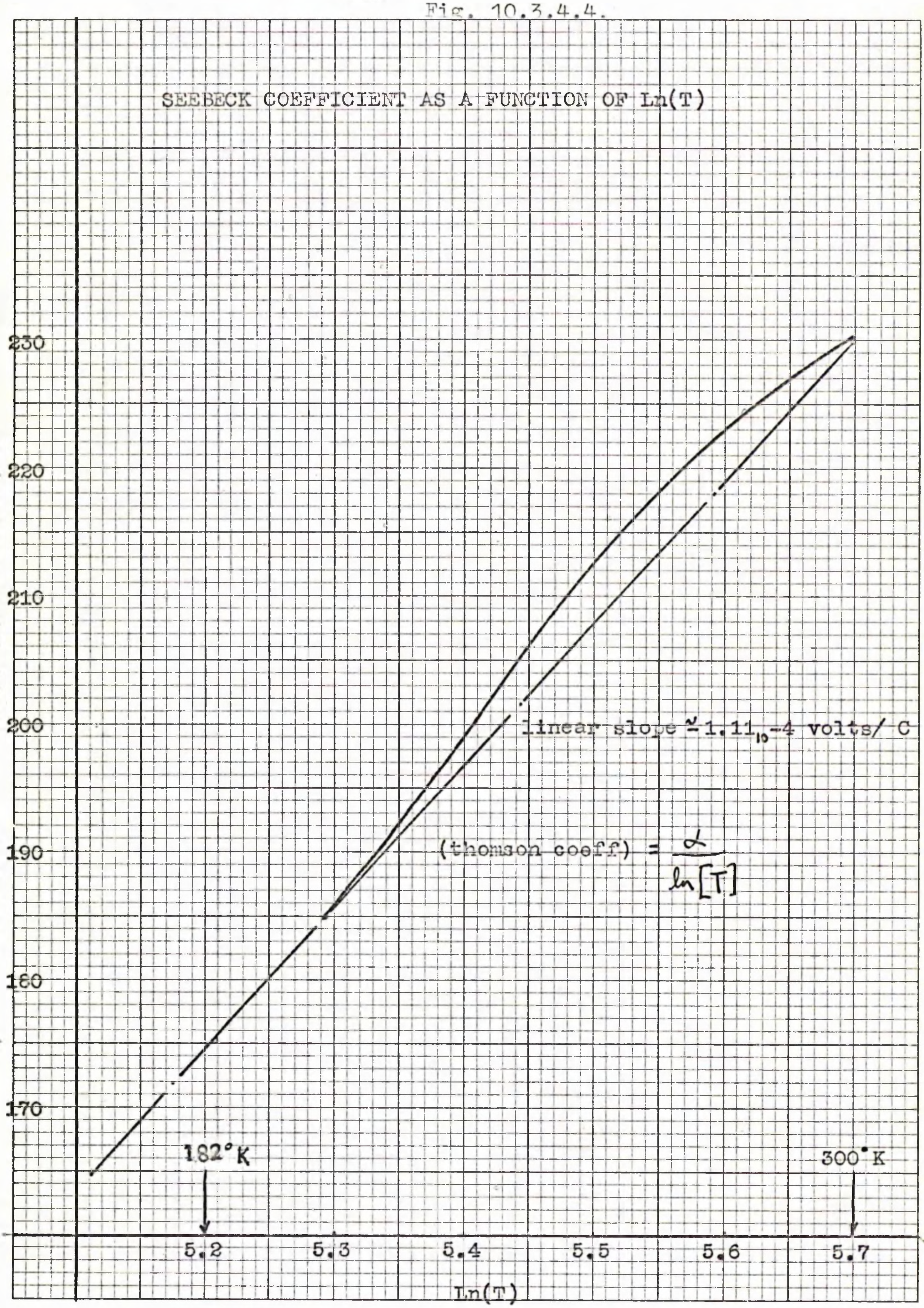
SEEBECK COEFFICIENT AS A FUNCTION OF Ln(T)
230
220
210
200
190
180
170
linear slope ≃1.11₁₀-4 volts/ C
(thomson coeff) = $\frac{\alpha}{\ln[T]}$
182°K
300°K
5.2
5.3
5.4
5.5
5.6
5.7
Ln(T)

range of temperature from $\cong$ 185°K to 300°K (slope of chord connecting these points) indicates a value of approximately $110_{10}{-6}$ volts/°K. The magnitude of the Thomson coefficient is approximately one-half of the Seebeck coefficient for the same temperature range. The local Thomson coefficient was calculated by equation 10.3.2.4 for ($185°K \leq T°K \leq 300$) with $\Delta T = 5°$ resulting in a Thomson coefficient of $\cong$ $102.5_{10}{-6}$ Volts/°K (numerical average 24 state points). The local Thomson coefficient was not constant but varied from $\cong$ $140_{10}{-6}$ Volts/°K to $30_{10}{-6}$ Volts/°K .

The values of the property constants (α_m, ρ_m, k_m) were determined by curve fitting experimental data with a fourth order polynomial. The polynomials have the following form:

(a) Thermal conductivity (k (T)), watts/cm°C

$$k(T) = 2.5703_{10}{-1} - 2.9711_{10}{-3}T + 1.5258_{10}{-5}T^2 - 3.6606_{10}{-10}T^3 + 3.3939_{10}{-11}T^4 \tag{10.3.4.18.}$$

The average thermal conductivity resulting from equation 10.3.4.9 is:

$$\hat{k}\Big|_{310°K}^{270°K} \cong .0259 \text{ watts/cm-°C}$$

and from equation 10.3.4.6:

$$\hat{k}\Big|_{310°K}^{270°K} \cong .0247 \text{ watts/cm-°C}$$

$\cong$ .0247 watts/cm-°C

(b) Electrical resistivity (ρ (T)), ohm-cm

$$\rho(T) = -4.0684_{10}-4 + 8.7421_{10}-6T - 2.7455_{10}-8T^2 + 2.7475_{10}-11T^3 + 9.6970_{10}-14T^4 \qquad 10.3.4.19.$$

The average electrical resistivity resulting from equation 10.3.4.8 is:

$$\hat{\rho}\Bigg|_{310°K}^{270°K} \cong .001181 \text{ ohm-cm}$$

(c) Element Seebeck coefficient (α (T)), volts/$^{\circ}$C

$$\alpha(T) = -1.2872_{10}^{+2} + 3.2242T - 1.4273_{10}-2T^2 + 3.9596_{10}-5T^3 - 4.8485_{10}-8T^4 \qquad 10.3.4.20.$$

The average element Seebeck coefficient resulting from equation 10.3.4.12 is:

$$\hat{\alpha}\Bigg|_{310°K}^{270°K} \cong .228.15_{10}-6 \text{ Volts/}^{\circ}\text{K}$$

The average Thomson coefficient resulting from equation 10.3.4.20 and equation 10.3.4.1 is:

$$\hat{\tau}\Bigg|_{310°K}^{270°K} \cong 56.638_{10}-6 \text{ Volts/}^{\circ}\text{K}$$

10.3.4.1 Thomson Effect Compensation.

It is stated in reference (6) that a technique for compensating for the Thomson effect is substitute average values for the material parameters. The couple figure of merit would be expressed as:

$$Z_{AV} = \left[\frac{\hat{\alpha}_{np}}{\left[\hat{\rho}_p \hat{k}_p\right]^{\frac{1}{2}} + \left[\hat{\rho}_n k_n\right]^{\frac{1}{2}}} \right]^2 \qquad 10.3.4.1.1.$$

Reference (6) indicates that for small τ the Thomson coefficient is correctly taken into account if $\hat{\alpha}$ is used for the calculation of Z (figure of merit). It is also stated that as a first approximation the temperature dependence of ρ and k can be taken in account by replacing the product (ρk) by $(\widehat{\rho k}) \approx (\hat{\rho}\ \hat{k})$. However the proof is not complete. Reference (4, 8) indicated that these approaches can result in accurate results in some cases and serious disagreement for other conditions. The authors (4) propose using the Seebeck coefficient defined as:

$$\alpha = \alpha_a - \tau \ln\left[\frac{T}{T_a}\right] \qquad 10.3.4.1.2.$$

where:

$$\alpha_a = \frac{1}{2}\left[\alpha_{h_j} + \alpha_{c_j}\right] \qquad 10.3.4.1.3.$$

and:

$\alpha_{h_j}, \alpha_{c_j}$ Seebeck coefficient at hot and cold junction respectfully

T_a absolute temperature at $\alpha = \alpha_a$

Equation 10.3.4.1.2 can be used when the average Seebeck coefficient (α_a) is constant and τ a variable.

The technique proposed (for this thesis) is to use $\hat{\alpha}$ (α^*) as derived in section 10.3.4, however $\hat{\rho}$ and $\hat{k}$ are individual determined. Private conversation with a number of United States thermoelectric system designers indicate that a 3% - 5% reduction in performance is expected if the Thomson heat is included in the basic heat balance equations. Reference (3) suggests the use of the mean value of the Seebeck coefficient expressed as:

$$\left[\frac{\alpha_{h_j}+\alpha_{c_j}}{2}\right]T_{c_j}I \cong \alpha_{c_j}T_{c_j}I + \frac{1}{2}I\int_{\alpha_{c_j}}^{\alpha_{h_j}} T\,d\alpha \qquad 10.3.4.1.4.$$

where:

α_{h_j} ; α_{c_j} Seebeck coefficients at hot and cold junction temperature

Equation 10.3.4.1.4 indicates that the Thomson effect can be accounted for by using the mean value of the Seebeck coefficient rather than the (α) Seebeck coefficient at the cold junction. The modified Seebeck coefficient (α^*) is approximately equal to $(\alpha_{h_j}+\alpha_{c_j}) \times 0.5$. When $\alpha(T)$ is a linear function (equation 10.2.26) of temperature:

$$\left[\frac{\alpha_{h_j}+\alpha_{c_j}}{2}\right] = \alpha^* \qquad 10.3.4.1.5.$$

From figure 10.3.4.3 the mean value of the Seebeck coefficient from equation 10.3.4.1.4 results:

$$\left[\frac{\alpha_{h_j}+\alpha_{c_j}}{2}\right]\Bigg|_{200^\circ K}^{300^\circ K} \cong 207.5_{10}{}^{-6} \text{ Volts}/{}^\circ K$$

Fig. 10.3.5.1.

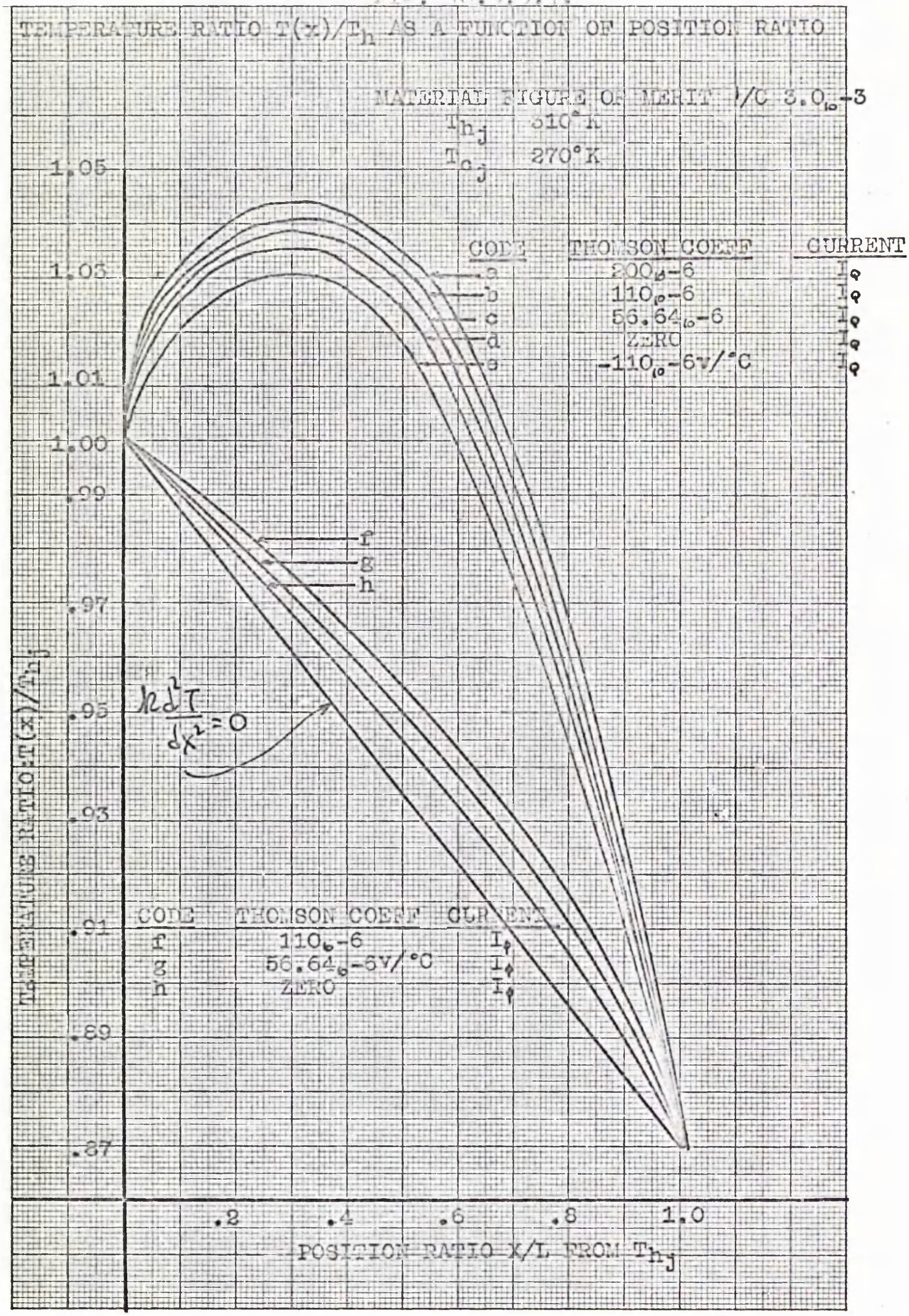
TEMPERATURE RATIO T(x)/Th AS A FUNCTION OF POSITION RATIO
MATERIAL FIGURE OF MERIT /C 3.0₁₀-3
Thj 310°K
Tcj 270°K
CODE THOMSON COEFF CURRENT
a 200₁₀-6 Iφ
b 110₁₀-6 Iφ
c 56.64₁₀-6 Iφ
d ZERO Iφ
e -110₁₀-6v/°C Iφ
f
g
h
kd²T/dx² = 0
CODE THOMSON COEFF CURRENT
f 110₁₀-6 Iφ
g 56.64₁₀-6v/°C Iφ
h ZERO Iφ
1.05
1.03
1.01
1.00
.99
.97
.95
.93
.91
.89
.87
.2
.4
.6
.8
1.0
TEMPERATURE RATIO T(x)/Thj
POSITION RATIO X/L FROM Thj

and the modified Seebeck coefficient from equation 10.2.25 results:

$$\alpha^* \Big|_{200^\circ K}^{300^\circ K} \cong 212.26 \text{ Volts}/^\circ K$$

Comparison of the results above indicate approximately 2.5% difference in value.

10.3.5 Discussion and Results.

There has been a few papers on the effect of the Thomson heat on the performance of thermoelectric power generation systems. Reference (4) and reference (13) present expressions for determining the temperature distribution with constant Thomson coefficient. Reference (13) indicates the influence of the Thomson effect on the heat conduction process. Reference (4) determines the expected degradation of efficiency and power output by using a mean Seebeck coefficient. The temperature range for thermoelectric generators may be between 300°K to 700°K. The thermoelectric refrigerator falls into a lower temperature of operation, 200 - 373°K (B.P. of water). The temperature distribution for an insulated thermoelement operating at the current ratios for maximum heat pump rate and maximum C.O.P. for both positive and negative Thomson coefficient will be presented in this section. To illustrate the general influence of the Thomson effect various numerical examples have been programmed on the digital computer.

Fig. 10.3.5.2.

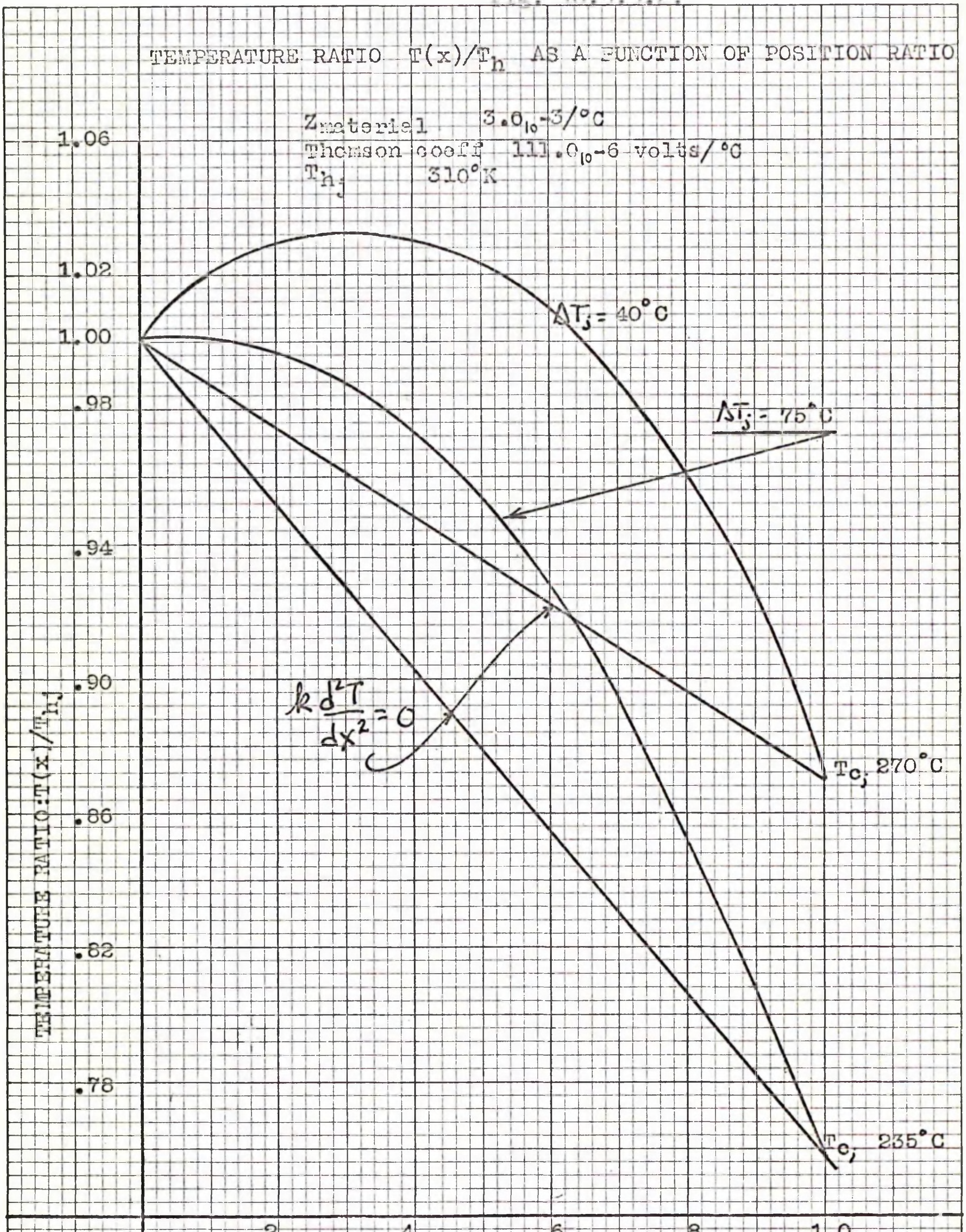
TEMPERATURE RATIO T(x)/T_h AS A FUNCTION OF POSITION RATIO
Z_material 3.0_10-3/°C
Thomson coeff 111.0_10-6 volts/°C
T_hj 310°K
1.06
1.02
1.00
.98
.94
.90
.86
.82
.78
ΔT_j = 40°C
ΔT_j = 75°C
k d²T/dx² = 0
T_cj 270°C
T_cj 235°C
TEMPERATURE RATIO:T(x)/T_hj
.2
.4
.6
.8
1.0
X/L

Figure 10.3.5.1 illustrates the temperature ratio $(T(x)/T_{h_j})$ as a function of position ratio (X/ℓ). Positive Thomson coefficients exhibit a higher operating temperature ratio for both current conditions. The critical position at which the maximum temperature ratio occur appears to be independent of the magnitude of the Thomson coefficient. The material properties employed are:

- Figure of Merit $3.0_{10}{-6}$ /°C
- Seebeck coefficient $228.15_{10}{-6}$ Volts/°C
- Thermal conductivity $1.71_{10}{-2}$ watts/cm - °C
- Electrical conductivity $1.022_{10}{-3}$ ohm-cm

Figure 10.3.5.2 illustrates the effect of increasing the junction temperature difference for fixed positive Thomson coefficient. The temperature ratio $(T(x)/T_{h_j})$ is based on fixed hot junction temperature with ΔT_j = 40°C, 75°C. For $\Delta T_j \longrightarrow \Delta T_{j_{max}}$ the temperature ratio $(T(x)/T_{h_j})$ $\longrightarrow$ unity. The slope at $T(0) = T_{h_j}$ for the current (I_Q) and $\Delta T_j = \Delta T_{j_{max}}$ is expressable as:

$$\left.\frac{d\left[T(x)/T_{h_j}\right]}{d\left[\frac{X}{\ell}\right]}\right|_{\frac{X}{\ell}=0} \longrightarrow 0 \qquad 10.3.5.1.$$

The derivation of equation 10.3.5.1 appears in Appendix A. Figure 10.3.5.3 illustrates the temperature ratio ($T(x)/T_{h_j}$) as a function of the position ratio for $\Delta T_j \overset{\longrightarrow}{=} \Delta T_{j_{max}}$ The maximum junction temperature difference is expressed as:

Fig. 10.3.5.3.

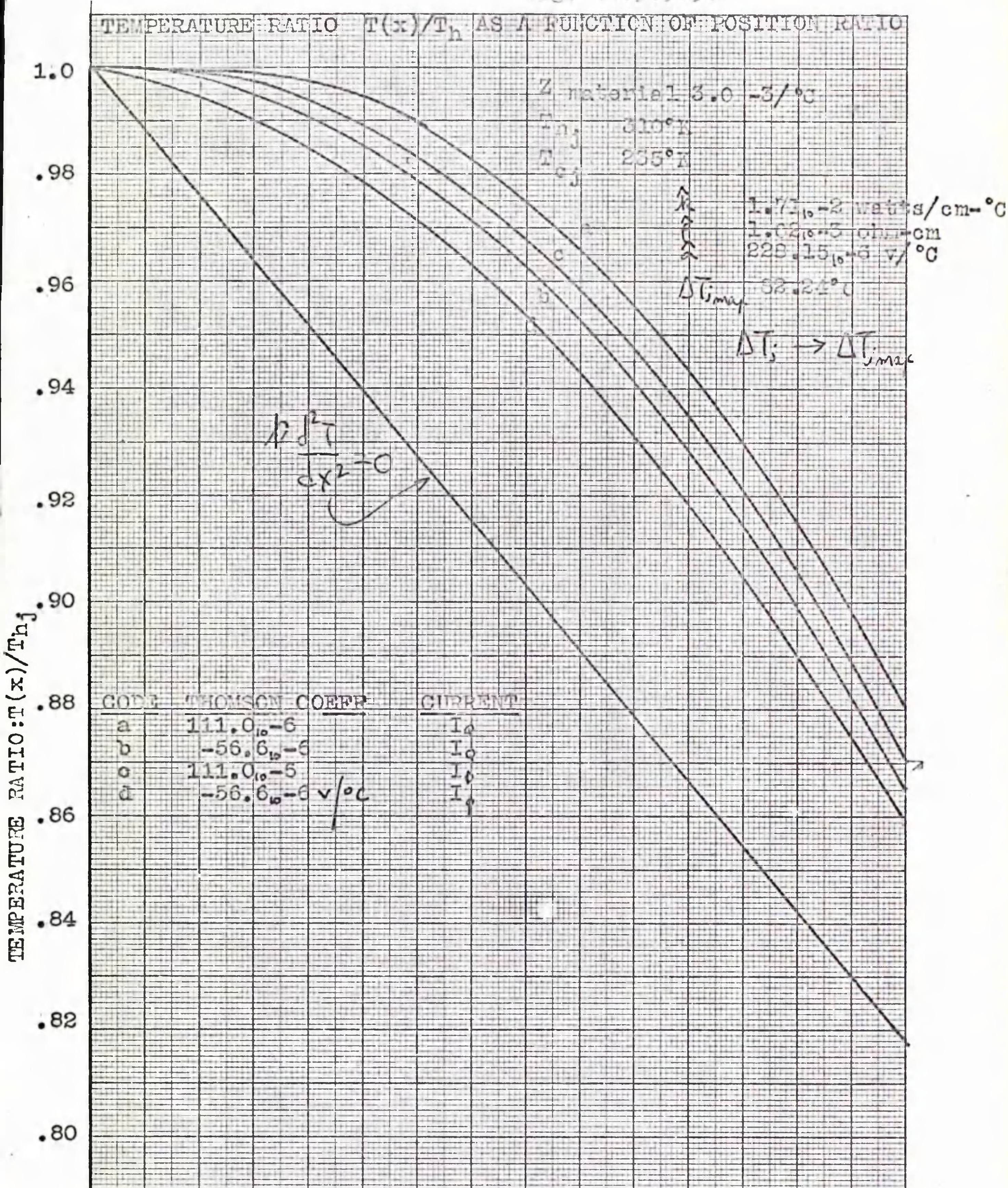
TEMPERATURE RATIO T(x)/Th AS A FUNCTION OF POSITION RATIO
Z material 3.0 -3/°C
Thj 310°K
Tcj 235°K
1.71 10-2 watts/cm-°C
1.02 10-3 ohm-cm
228.15 10-6 v/°C
ΔTjmax 82.24°C
ΔTj → ΔTjmax
a
b
c
d
1.0
.98
.96
.94
.92
.90
.88
.86
.84
.82
.80
TEMPERATURE RATIO:T(x)/Thj
CODE THOMSON COEFF. CURRENT
a 111.0 10-6 Iφ
b -56.6 10-6 Iφ
c 111.0 10-5 Iφ
d -56.6 10-6 v/°C Iφ
.1
.2
.3
.4
.5
.6
.7
X/L

$$\Delta T_{j_{max}} = \frac{1}{2} \frac{\alpha^2}{\hat{\rho}\,\hat{k}} T_{c_j}^2 \qquad 10.3.5.2.$$

For the operating condition of $\tau = 0$ the current required to maximize the C.O.P. is expressed as:

$$I_\phi \cong \frac{\Delta T_j}{\Delta T_{j_{max}}} I_Q \qquad 10.3.5.3.$$

With $\Delta T_j = \Delta T_{j_{max}}$ equation 10.3.5.3 reduces to:

$$I_\phi \cong I_Q \qquad 10.3.5.4.$$

Equation 10.3.5.1 indicates that the slope at $\left(\frac{X}{\ell}\right) = 0$ approaches zero as $\Delta T_j \longrightarrow \Delta T_{j_{max}}$ is verified by figure 10.3.5.3. To illustrate the proposed technique of using the modified Seebeck coefficient (α^*) in place of τ and α_{c_j} in order to account for the Thomson effect the following data was extracted from figure 10.3.4.1 - figure 10.3.4.4.

(a)

T_{h_j}	$310^{\circ}K$	ΔT_j	$40^{\circ}C$
T_{c_j}	$270^{\circ}K$		
α^*	$228.15_{10}{-6}$ Volts/$^{\circ}K$		
$\hat{\rho}$	.001181 ohm-cm		
$\hat{k}$	.025932 watts/cm$^{\circ}C$		
α_{c_j}	$220.0_{10}{-6}$ Volts/$^{\circ}K$		
$\hat{\tau}$	$56.638_{10}{-6}$ Volts/$^{\circ}C$		
$\Delta T_{j_{max}}$	$61.93^{\circ}C$ (based on α^*)		
$\Delta T_{j_{max}}$	$57.63^{\circ}C$ (based on α_{c_j})		

Fig. 10.3.5.4.

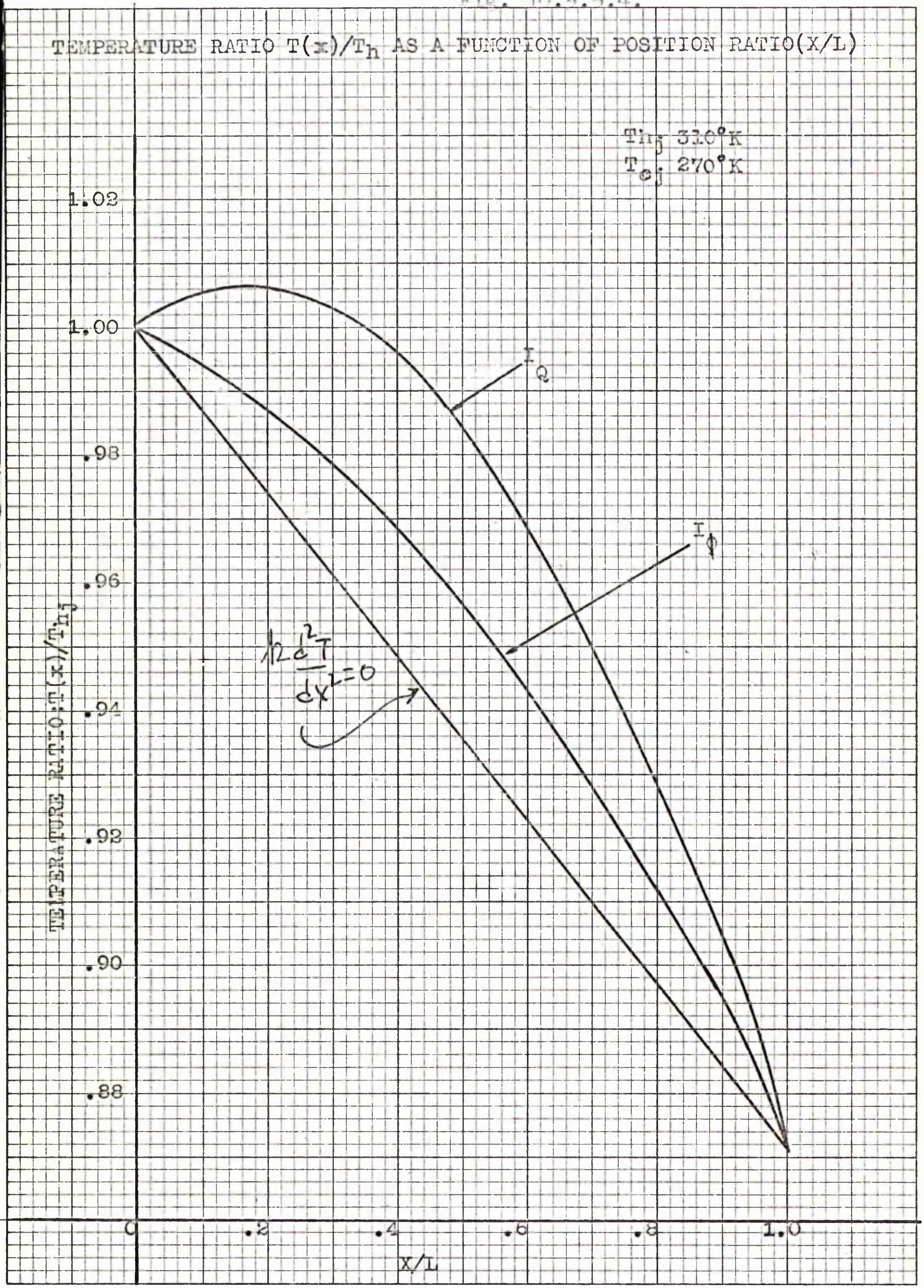
TEMPERATURE RATIO T(x)/Th AS A FUNCTION OF POSITION RATIO(X/L)
Thj 310°K
Tcj 270°K
1.02
1.00
.98
.96
.94
.92
.90
.88
TEMPERATURE RATIO:T(x)/Thj
I_Q
I_ϕ
$k\frac{d^2T}{dx^2}=0$
0
.2
.4
.6
.8
1.0
X/L

Figure 10.3.5.4 is based on the temperature distribution equation 10.3.2.23 for $\hat{\tau} \neq 0$ and for $\hat{\tau} = 0$ equation A9 from appendix A was used. The figure illustrates only one set of operational conditions for $I = I_{\varphi}, I_{\phi}$. The difference resulting from employing the modified Seebeck coefficient or accounting directly for the Thomson coefficient for the state conditions of figure 10.3.5.4 is less than 1%. Reference (3) suggests the use of the average (equation 10.3.4.1.4) Seebeck coefficient resulting in a value of $\cong$ 227.25$_{10}$-6 Volts/^{o}K. The average Seebeck coefficient and the modified value differ from each other in $\cong$ 1 part in 200 for a junction temperature difference of 40^{o}C. To illustrate the use of the modified Seebeck coefficient in place of τ and α_{c_j} for $\Delta T_j \longrightarrow \Delta T_{j\,max}$ the data (a) of figure 10.3.5.4 was used to construct figure 10.3.5.5. The hot side junction temperature is increased from 310^{o}K to 330^{o}K resulting in a ΔT_j of 60^{o}C ($\Delta T_{j\,max} \cong$ 61.93^{o}C). Figure 10.3.5.5. illustrates only one set of operational conditions, i.e. $I = I_{\phi}$ as $I_{\varphi} \cong I_{\phi}$ for $\Delta T_j \longrightarrow \Delta T_{j\,max}$. The difference resulting from employing the modified Seebeck coefficient is less than 1.5%. Figure 10.3.5.6 illustrates the temperature ratio ($T(x)/T_{h_j}$) as a function of (x/ℓ) for I_{ϕ} operation. The larger negative Thomson coefficient has a lower operational temperature ratio. The slope at (x/ℓ) = 0 is not equal to zero as $\Delta T_j \neq \Delta T_{j\,max}$.

Fig. 10.3.5.5.

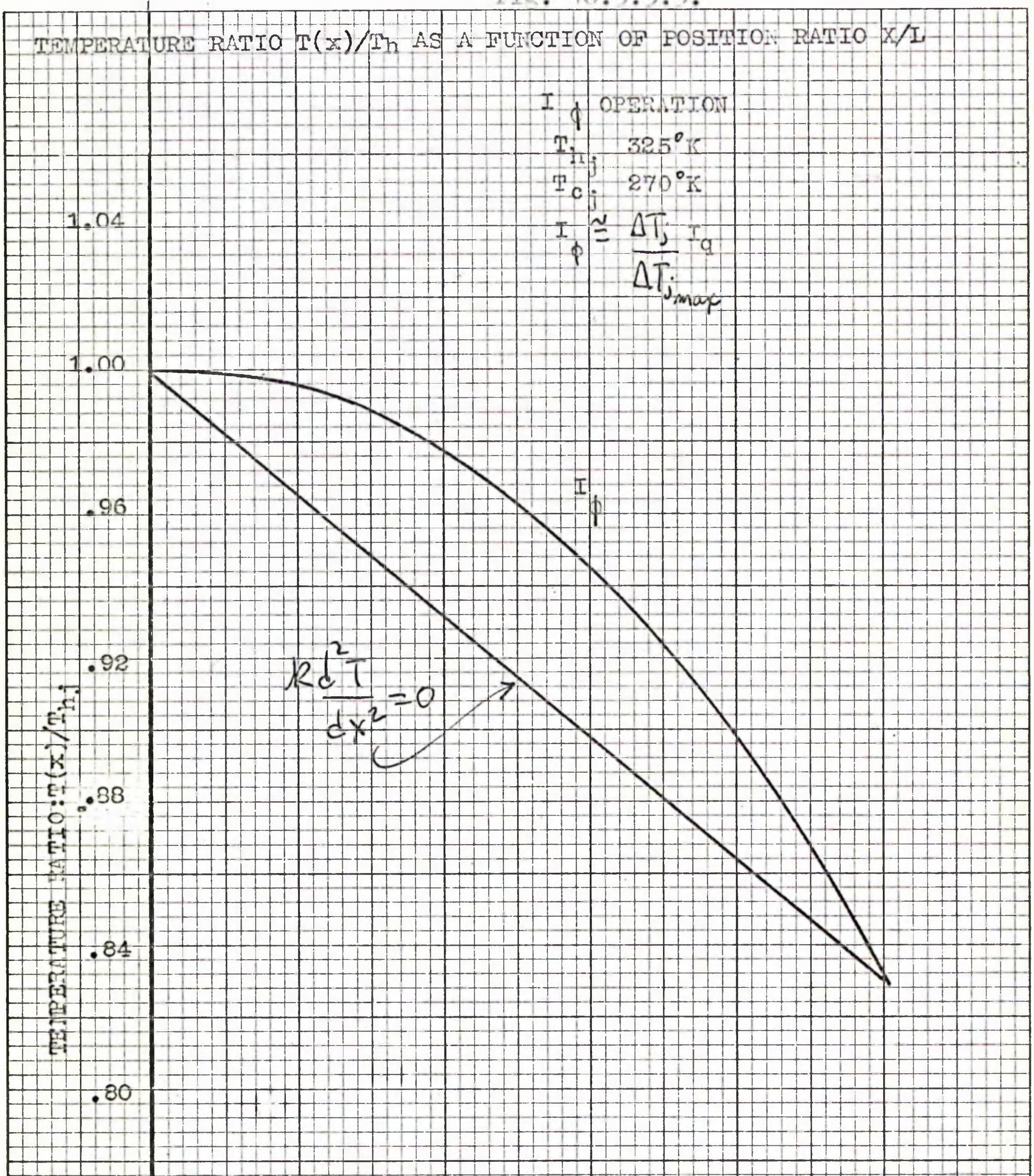

TEMPERATURE RATIO T(x)/Th AS A FUNCTION OF POSITION RATIO X/L
I ϕ OPERATION
T h j 325°K
T c j 270°K
I ϕ ≅ ΔTj/ΔTj max Iq
I ϕ
k d²T/dx² = 0
1.04
1.00
.96
.92
.88
.84
.80
.76
.2
.4
.6
.8
1.0
X/L
TEMPERATURE RATIO: T(x)/Thj

Fig. 10.3.5.6.

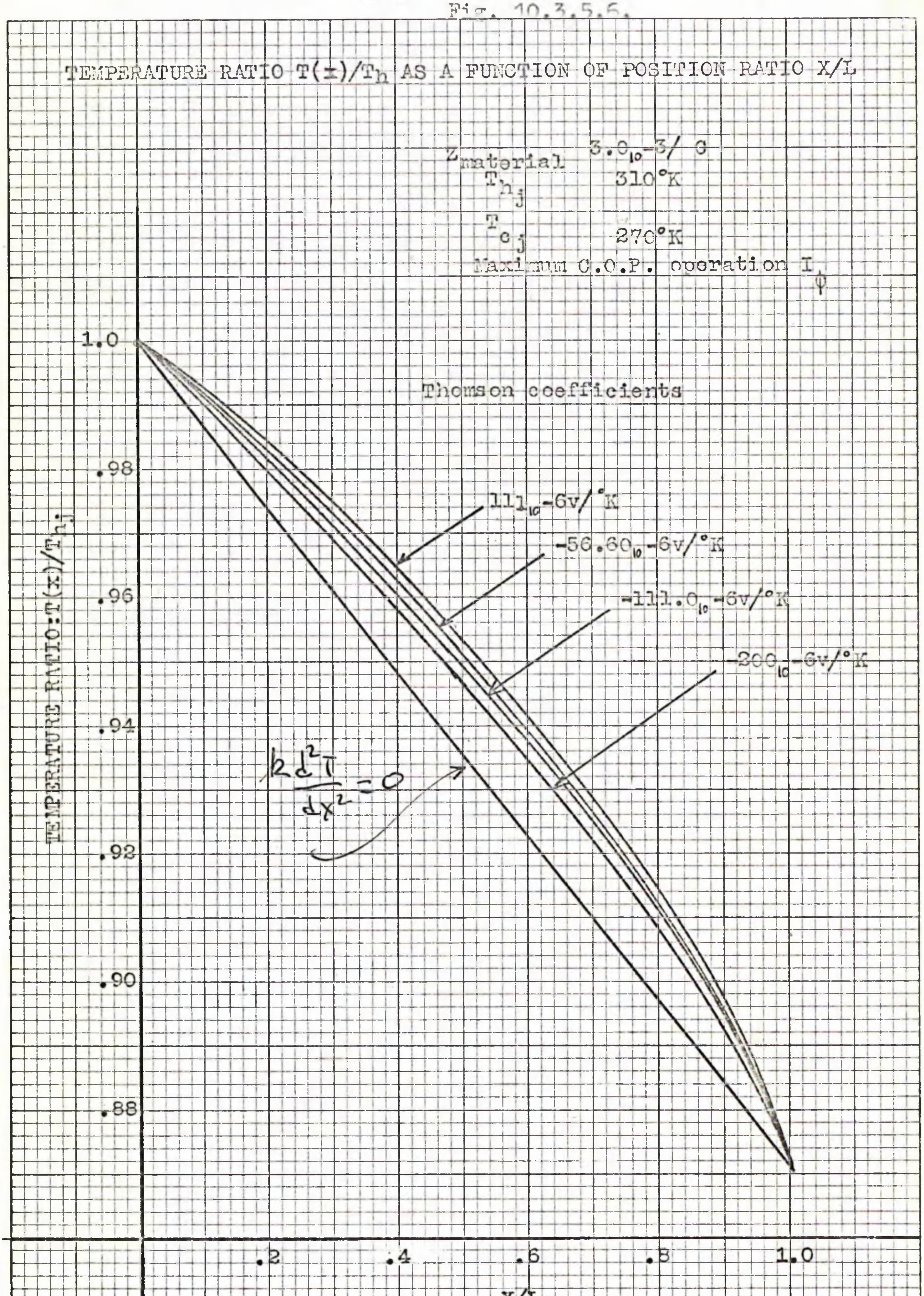

TEMPERATURE RATIO T(x)/Th AS A FUNCTION OF POSITION RATIO X/L
Zmaterial 3.0₁₀-3/ C
Thj 310°K
Tcj 270°K
Maximum C.O.P. operation Iφ
Thomson coefficients
111₁₀-6v/°K
-56.60₁₀-6v/°K
-111.0₁₀-6v/°K
-200₁₀-6v/°K
k d²T/dx² = 0
TEMPERATURE RATIO:T(x)/Thj
1.0
.98
.96
.94
.92
.90
.88
.2
.4
.6
.8
1.0
X/L

10.3.6 Summary.

The value of the Thomson coefficients and associated material properties are typical of the present state of the art. The figures within this section are for the specific cases considered.

Equations have been presented for predicting the temperature distribution of a single-thermoelement with constant average $(\hat{\tau})$ Thomson coefficients. The equations can be used for negative or positive coefficients with variation in the dimensionless current ratio (θ). The influence of the Thomson effect has been illustrated by introducing numerical examples. When this technique is employed the operational temperatures must be within the material capability, i.e. $\Delta T_j \leq \Delta T_{j\,max}$. The temperature distribution ($T(x)/T_{h_j}$) associated with the modified Seebeck coefficient (α^*) is within 2% of the temperature distribution when α^* replaces α_j and τ . For operation at maximum heat pump rate positive Thomson coefficients result in an increase in the temperature ratio $(T(x)/T_{h_j})$ in the interior of the element. The slope at X = 0 for positive Thomson coefficients is an increasing value ($\Delta T_j \neq \Delta T_{j\,max}$) indicating that the heat rejection rate is increased. For operation at maximum C.O.P. conditions negative Thomson coefficients decrease the $T(x)/T_{h_j}$ ratio as a function of (X/ℓ). Negative increasing Thomson coefficients depress the temperature ratio curve towards the (zero current) linear function ($k\dfrac{d^2T}{dx^2} = 0$).

Reference (4) concluded with the following summary:

$$(\Delta T_j = 400^\circ C, \quad T_{hj} = 700^\circ K, \quad T_{cj} = 300^\circ K)$$

Results show that "generators" made with materials having high positive Thomson coefficients have lower thermal efficiences than generators made with materials having low or negative values. The results also show that the power output of generators with high positive Thomson coefficients is higher than the power output of generators with low negative Thomson coefficients. These comparisons apply to generators with the same average Seebeck coefficient.

In applications where thermal efficiency is a prim importance, if materials available have $\cong$ the same average Seebeck coefficient over the temperature range considered than the lowest value of the Thomson coefficient should be used. If the prim concern is power output, materials with high positive Thomson coefficients should be selected.

11.0 PERFORMANCE OF A TWO-STAGE CASCADED PELTIER DEVICE OPERATING BETWEEN HEAT SOURCE AND HEAT SINK WITH FINITE HEAT TRANSFER COEFFICIENTS.

11.1 Abstract.

The operational characteristics of a two-stage cascaded Peltier device operating between heat sink and heat source with finite heat transfer coefficients can be determined by a proposed mathematical model. The solution considers the thermoelectric module to be operating between known heat source and heat sink temperatures ($^{\circ}K$). The solution employs an interative method and has been programmed for a digital computer utilizing a Fortran compiler.

The coupling of the basic 2-stage cascaded Peltier device to the surrounding environment is based on the assumption that an m-th order function can approximate the transfer function of the heat exchangers. The resulting iterative procedure yields the current required to maintain thermal equilibrium with the heat source and heat sink environment. Determination of the junction temperatures, inter-stage temperature are resulting functions of the current and hence are not arbitrary (as is the case presented in section 8.0).

The basic computer programme can be extended to consider additional variables as required. Some additional effects which may be considered are: insulation effects, packing density (ω), material properties variant with temperature,

m-th stages, variation of λ/A for the stages considered.

11.2 Technique for Determining Operational Characteristics.

11.2.1 Derivation of Equations.

The operational characteristic of a 2-stage thermoelectric heat pump (figure 11.2.1.1) operating between heat sink and heat source can be determined by the proposed mathematical model. The mathematical solution is an iterative method for obtaining the balanced operation for a system consisting of a 2-stage cascaded Peltier module acting as a heat pumping device between hot and cold side heat exchangers. The solution technique considers a given thermoelectric device operating between known heat source and heat sink temperatures.

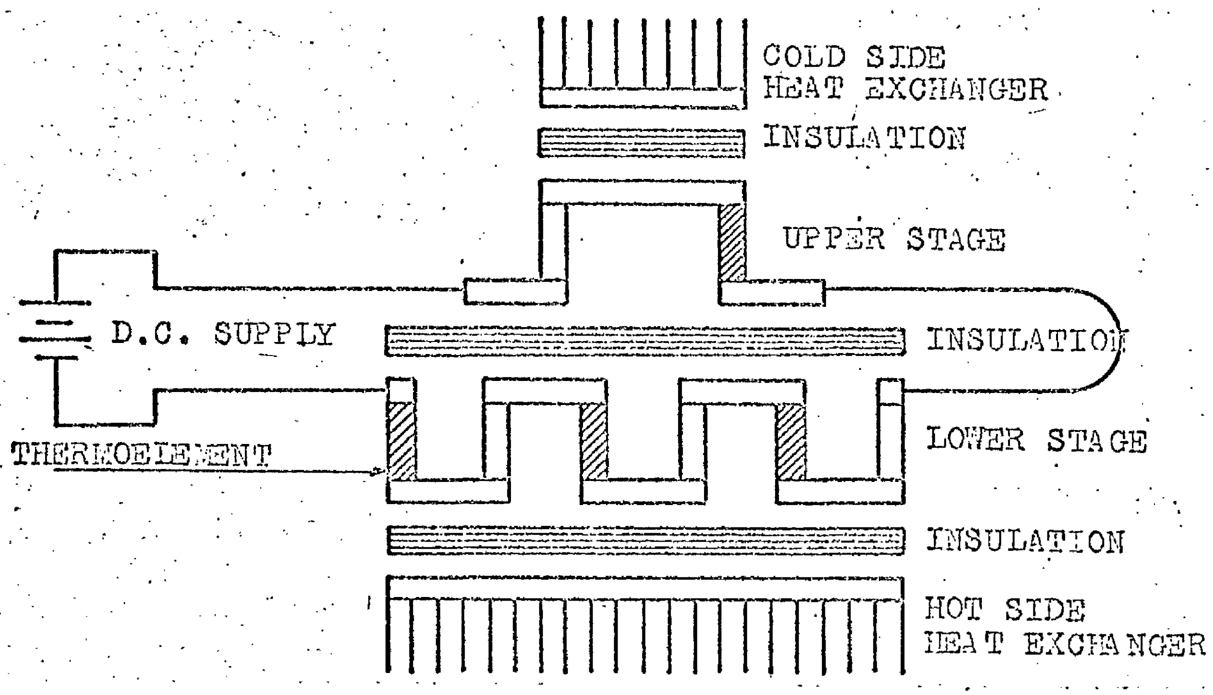

Figure 11.2.1.1.
Two-Stage Cascade Configuration.

The material properties can be expressed as:

(1) The internal couple electrical resistance is

$$R_{INT} = 2\rho l / A \qquad 11.2.1.6.$$

where:

ρ is the electrical resistivity, ohm-cm.

l is the height of the thermoelement, cm.

A is the cross sectional area of a thermoelement, cm^2

R_{INT} is the couple element resistance, ohms.

(2) The couple junction resistance (R_j) is expressed as:

$$R_j = 4\rho_j / A \qquad 11.2.1.7.$$

where: ρ_j is the junction thermoelement resistance, ohm-cm^2.

Defining the effective electrical resistance:

$$R_{EFF} = \left[\frac{2\rho l}{A} + \frac{4\rho_j}{A}\right] F^{2*} \qquad 11.2.1.8.$$

where:

$$F^* = I_{RMS} / I_{D.C.}^{(1)} \qquad 11.2.1.9.$$

2. The thermal conductance of the couple is:

$$K_{INT} = 2kA / l \qquad 11.2.1.10.$$

(1) Term defined in (2)

The overall system can be divided into three sub-assemblies for purpose of equation derivation:

1. The cold side heat exchanger and electrical insulation interface.
2. The 2-stage cascaded Peltier device.
3. The hot side heat exchanger and electrical insulation interface.

The symbols utilized to define the temperatures (^oK) of interest are shown in figure 11.2.1.2.

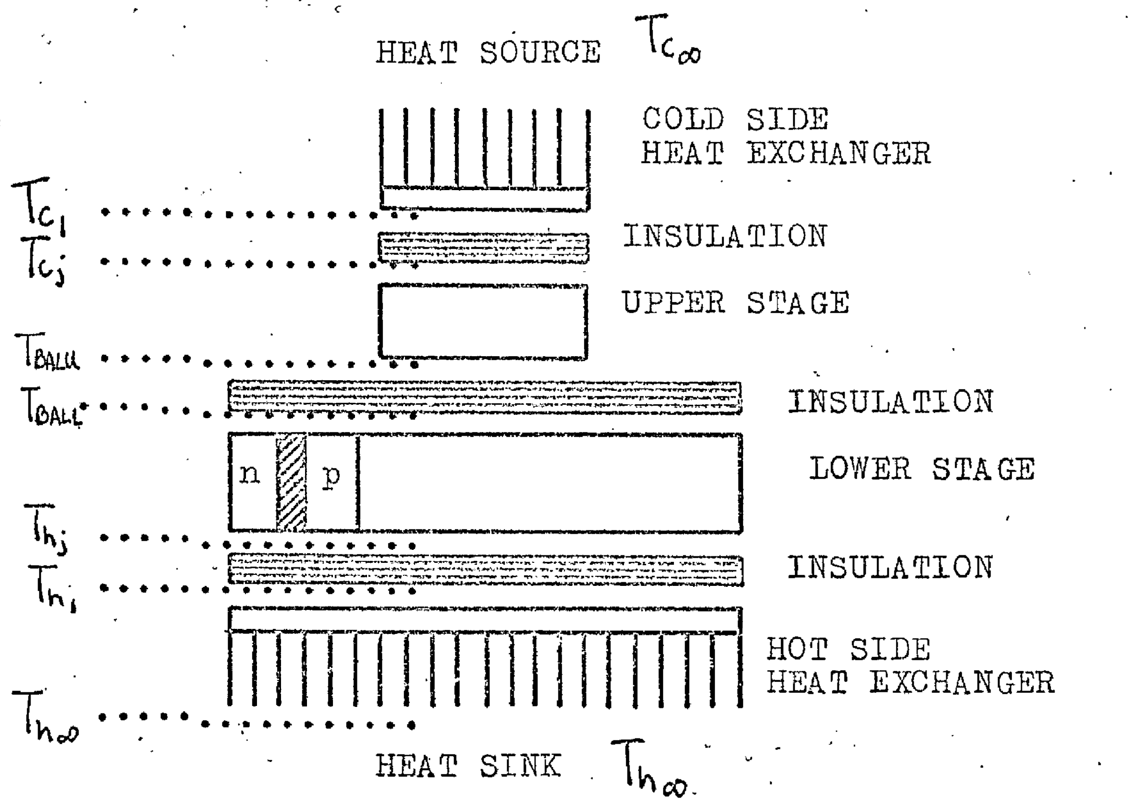

Figure 11.2.1.2.

Two-Stage Cascade Reference Temperatures.

The heat flux rate ($\mathcal{V}_c$ watts/cm^2) through the cold side heat exchanger will be approximated by

$$\mathcal{V}_c = E_c\left[T_{c_\infty} - T_{c_1}\right]^{1+N_c} \qquad 11.2.1.1.$$

where: E_c is a constant for a given heat exchanger, heat source, and is a function of the fin effectiveness, heat transfer coefficient, watts/cm^2-$^\circ$C.

N_c is the exponent constant introduced to account for variation in overall heat transfer coefficients due to variation in fin effectiveness and for the mode of heat transfer, i.e. free convection, forced convection.

The heat flux ($\mathcal{V}_c$ watts/cm^2) through the electrical insulation on the cold side is:

$$\mathcal{V}_c = \frac{k_c}{t_c}\left[T_{c_1} - T_{c_j}\right] \qquad 11.2.1.2.$$

where: k_c is the effective thermal conductivity of the cold side electrical insulation interface, watts/cm -$^\circ$C

t_c is the thickness of the cold side electrical insulation interface, cm.

The cold side junction temperature can be expressed as:

$$\Delta T_{upper} = \left[\frac{t_c \mathcal{V}_c}{k_c}\right] + \left[\frac{\mathcal{V}_c}{E_c}\right]^{\left[\frac{1}{1+N_c}\right]} \qquad 11.2.1.3.$$

where:

$$\Delta T_{upper} = T_{c_\infty} - T_{c_j} \qquad 11.2.1.4.$$

and:

$$T_{c_\infty} > T_{c_1} > T_{c_j} \; (^\circ K) \qquad 11.2.1.5.$$

where: k is the thermal conductivity of the thermoelement, watts/cm-^{o}C.

The inter-element thermal conductance will be expressed by introducing a term called packing density(12) where:

$$\omega \equiv 2A / A_m \qquad 11.2.1.11.$$

where:

ω is the packing density

A_m is the module area, cm^2

and

$$A_m = 2A + A_{INSL} \qquad 11.2.1.12.$$

where: A_{INSL} is the inter-element cross sectional area, cm^2 and is expressible as:

$$A_{INSL} = 2A(1-\omega)/\omega \qquad 11.2.1.13.$$

The inter-element thermal conductance is:

$$K_\omega = k_{INSL} \cdot A_{INSL} / \ell \qquad 11.2.1.14.$$

where: k_{INSL} is the thermal conductivity of the insulation material within the inter-element area, watts/cm-^{o}C, and K_ω is the thermal conductance of the insulation material within the inter-element area, watts/^{o}C.

The effective thermal conductance is

$$K_{EFF} = \frac{k_{INSL} A_{INSL}}{l} + \frac{2kA}{l} \qquad 11.2.1.15.$$

then:

$$K_{EFF} = \frac{k_{INSL} 2A(1-\omega)}{l\omega} + \frac{2kA}{l} \qquad 11.2.1.16.$$

The equations determining R_{EFF} and K_{EFF} are based on the assumption that the element heights are the same for n-: p- thermoelements and $\rho_n = \rho_p = \rho$; $k_n = k_p = k$. This is not a rigid requirement and is present in this form in order to simplify the equation. The effective figure of merit (Z_{EFF}) is expressed as:

$$Z_{EFF} = \frac{\alpha^2}{R_{EFF} \cdot K_{EFF}} \qquad 11.2.1.17.$$

The material figure of merit:

$$Z_{MAT} = \frac{\alpha^2}{\rho \cdot k} \qquad 11.2.1.8.$$

and

$$\alpha = |\alpha_n| + |\alpha_p| \qquad \text{Volts}/^{\circ}\text{C}$$

(2) The 2-stage cascaded Peltier heat flux capability can be expressed as

$$\mathcal{V}_c = \frac{T_{cj} I \alpha - \frac{1}{2} I^2 R_{EFF} - K_{EFF} \Delta T_{j_{upper}}}{A_m} \qquad 11.2.1.19.$$

where: T_{cj} is the cold junction temperature, $^{\circ}$K.

$\Delta T_{j_{upper}}$ is the junction temperature difference, ^{o}C

where:

$$\Delta T_{j_{upper}} = T_{BALL} - T_{c_j} \qquad 11.2.1.20.$$

and T_{BALL} is the hot junction temperature, ^{o}K. (upper stage)

I is the current required to maintain (balance) the heat flux load (ν_c watts/cm^2).

Introducing:

$$A_m = 2A/\omega \qquad 11.2.1.21.$$

into equation 11.2.1.19 results:

$$\nu_c = \frac{T_{c_j} I \alpha \omega}{2A} - \frac{I^2 R_{EFF} \omega}{4A} - \frac{\omega K_{EFF} \Delta T_{j_{upper}}}{2A} \qquad 11.2.1.22.$$

Equation (22) is a quadratic relation in I and is expressible as

$$0 = A' I^2 - B T_{c_j} I + A' \left[C \Delta T_{j_{upper}} + \nu_c \right] \qquad 11.2.1.23.$$

where:

$$A' = \omega R_{EFF}/4A \qquad 11.2.1.24.$$

$$B = \omega \alpha / 2A \qquad 11.2.1.25.$$

$$C = \omega K_{EFF}/2A \qquad 11.2.1.26.$$

By means of the quadratic relation:

$$I = \frac{BT_{c_j} \pm \sqrt{(BT_{c_j})^2 - 4A'\left[C\Delta T_{j_{upper}} + \nu_c\right]}}{2A} \qquad 11.2.1.27.$$

The sign before the $\sqrt{\quad}$ is determined by power off operation,

$$I = 0 \;, \nu_c = 0 \;, \; \Delta T_{j_{upper}} = 0 \qquad 11.2.1.28.$$

and the negative sign is the required solution.

The current equation 11.2.1.27 relates the current for the upper stage of the module at known T_{c_j}, $\Delta T_{j_{upper}}$ and heat flux load (ν_c).

The power flux input to the upper stage is:

$$\frac{P}{A_m} = 2A'I^2 + BI\Delta T_{j_{UPPER}} \qquad 11.2.1.29.$$

Symbolically

$$P_\nu = P/A_m \text{, watts}/cm^2 \qquad 11.2.1.30.$$

where:

$$\Delta T_{j_{UPPER}} = T_{BALU} - T_{c_j} (^\circ K) \qquad 11.2.1.31.$$

By definition:

$$\text{C.O.P.}_{\text{upper stage}} = \frac{\nu_c}{P_\nu} \qquad 11.2.1.32.$$

The hot side heat flux from the upper stage to the low stage is:

$$\vartheta_h = \vartheta_c \left[\frac{1}{C.O.P._{\substack{\text{UPPER}\\\text{STAGE}}}} + 1 \right] \qquad 11.2.1.33.$$

The solution requires a coupling of the upper stage to the lower stage. From a review of literature (3) (15) three assumptions appear reasonable.

(1) $$\frac{T_i}{T_{h_j}} = \frac{T_{c_j}}{T_i}$$

where T_i is the intermediate temperature (^{o}K)

(2) $C.O.P._{\text{upper stage}} = C.O.P._{\text{lower stage}}$

(3) ΔT_j upper stage $=$ ΔT_j lower stage

As a general approach the author prefers:

$$\Delta T_{j \text{ lower stage}} = N' \, \Delta T_{j \text{ upper stage}} \qquad 11.2.1.34.$$

For the computer output $N' = 1.2$

The heat rejection from the lower stage can be expressed:

$$\vartheta_h' = \vartheta^*_{h_{LWR}} + BI\Delta T_{j_{\substack{\text{LOWER}\\\text{STAGE}}}} + 2A'I^2 \qquad 11.2.1.35.$$

$$\vartheta^*_{h_{LWR}} = \frac{\vartheta_h \times N_{\text{UPPER COUPLES}}}{N_{\text{LOWER COUPLES}}}$$

where:

$$P_{\nu_{\substack{LOWER\\STAGE}}} = BI\Delta T_{j_{\substack{LOWER\\STAGE}}} + 2A'I^2 \qquad 11.2.1.36.$$

The upper and lower stages are assumed to be in electrical series hence I is the same for both units.

The temperature drop on the hot side of the lower unit is expressed as:

$$\Delta T_{LOWER} = \left[\frac{t_h \nu_h'}{k_h}\right] + \left[\frac{\nu_h}{E_h}\right]^{\left[\frac{1}{1+N_h}\right]} \qquad 11.2.1.37.$$

where:

$$\Delta T_{LOWER} = T_{h_j} - T_{h\infty} \qquad 11.2.1.38.$$

Equation 11.2.1.37 is in the form previously noted as equation 11.2.1.3.

The C.O.P. of the lower stage is expressible as

$$\text{C.O.P.}_{\text{lower stage}} = \frac{\nu_{hLWR}}{\nu_h' - \nu_{hLWR}} \qquad 11.2.1.39.$$

and the overall C.O.P. (γ) for a cascaded 2-stage device can be given as

$$1 + \frac{1}{\gamma} = \left[1 + \frac{1}{C.O.P._{\substack{LOWER\\STAGE}}}\right]\left[1 + \frac{1}{C.O.P._{\substack{UPPER\\STAGE}}}\right] \qquad 11.2.1.40.$$

as control values reference (3) presents the following relationship for γ_{max}:

$$\gamma_{max} = \gamma_1 + \frac{1}{8[2\gamma_1 + 1]} \qquad 11.2.1.41.$$

and

$$\gamma_1 = \frac{\frac{T_{cj}}{\Delta T_j}\sqrt{1 + Z_{EFF} T_{MEAN}} - \frac{T_{hj}}{T_{cj}}}{\sqrt{1 + Z_{EFF} T_{MEAN}} + 1} \qquad 11.2.1.42.$$

An approximate expression reference (15) shows that:

$$\frac{\text{C.O.P. single stage(max)}}{\text{C.O.P. 2-stage (max)}} \cong F\left[\frac{\left[\Delta T_{j_{max}} - \frac{\Delta T_j}{m}\right]^m}{\left[\Delta T_{j_{max}} + \frac{\Delta T_j}{m}\right]^m - \left[\Delta T_{j_{max}} - \frac{\Delta T_j}{m}\right]^m}\right]$$

$$F = 2\Delta T_j \Big/ \left[\Delta T_{j_{max}} - \Delta T_j\right] \qquad 11.2.1.43$$

where:

$$\Delta T_{j_{max}} = 2T_{MEAN}\left[\frac{\sqrt{1 + Z_{EFF} T_{MEAN}} - 1}{\sqrt{1 + Z_{EFF} T_{MEAN}} + 1}\right] \qquad 11.2.1.44.$$

11.2.2 Calculation Procedure.

The calculation procedure used to determine the balance operating mode is as follows:

The mode of heat source and heat sink transfer, heat source and sink temperatures, material properties, packing density (ω) and module dimensional characteristics are given information. The required heat flux (ν_c) on the cold side is specified. ν_c can be a single value or variable being incrementally stepped. The cold side temperature drop ΔT_{upper} is calculated by equation 11.2.1.3. The cold side junction temperature T_{cj} is determined by re-arranging equation 11.2.1.4 $T_{cj} = T_{c\infty} - \Delta T_{upper}$

In order to determine the current required to maintain the heat balance with the environment an initial estimate of T_{BAL} is made. The upper stage junction temperature is then determined: $\Delta T_{j_{upper}} = T_{BAL} - T_{c_j}$. The system current is determined by equation 11.2.1.27. The current has been established by the heat load imposed upon the upper stage and the T_{BAL} estimated value. The power flux of the upper stage is determined by equation 11.2.1.29 and the C.O.P. upper stage is determined by $C.O.P._{upper} = \mathcal{V}_c / P_{\mathcal{V}}$. The heat rejected ($\mathcal{V}_h$) from the upper stage to the lower stage is determined by $\mathcal{V}_h = \mathcal{V}_c \left[1/C.O.P._{upper} + 1 \right]$. Introducing the ratio of the number of couples to the number of thermoelectric couples in the lower stage as: N_{upper}/N_{lower} and the value of N' for the ratio of $\Delta T_{j_{lower}} / \Delta T_{j_{upper}}$. The power flux of the lower stage is determined by equation 11.2.1.36 combining this value with heat flux load from the upper stage to the lower results in the heat flux load to be dissipated into the sink reservoir. From equation 11.2.1.37 the lower temperature drop is determined and the hot junction temperature of the lower stage determined by $T_{h_j} = T_{h_\infty} + \Delta T_{lower}$. Using $T_{BAL} = T_{h_j} - \Delta T_{j_{lower}}$ where $\Delta T_{j_{lower}} = N' \Delta T_{j_{upper}}$ the solution for the calculated value of T_{BAL} is compared with the assumed value. If they do not agree by an acceptable error (epso = .05°K) a new value is assumed by the relationship $T_{BAL} = (T_{BAL1} + T_{BAL2})0.5$ and the procedure is repeated until agreement within a desired limit of error is obtained. The iterative procedure yields the balanced operating junction temperatures which provide values for determining $C.O.P._{max}$ and overall C.O.P. The junction temperatures: T_{h_j}, T_{c_j} ; T_{BAL}

(intermediate temperature) are then incorporated into equation 42, 43 and 44 to determine system potential.

11.2.3 Representative Computer Results. (C.P.8. contains the Computer Programme)

To illustrate the basic data output from the program the following is presented. ANUC represents the heat flux load to the upper stage of the thermoelectric module. 'BALANCED OPERATION ACHIEVED' indicates that the solution converged to an allowable epso of .05°K. MAXIMUM C.O.P. is based on equation (41) and OPERATIONAL C.O.P. is based on equation (40). COP RATIO 2/1 is the output of equations (43) (44). The heat flux input from the upper stage to the lower stage is:

$$\nabla^{*}_{h_{LWR}} = \nabla_{h} \times N_{upper}/N_{lower}$$

where:

$N_{upper} = 10$

$N_{lower} = 45$

VOLTS 1 is an additional check on the system voltage required to maintain thermal equilibrium. It is simple to check the results for C.O.P. by the following relationship:

$$\text{C.O.P.}_{\text{OVERALL}} = \frac{Q_{IN}}{Q_{REJ} - Q_{IN}}$$

where Q_{IN} is the input heat load (watts) to the upper stage, Q_{REJ} is the heat rejected to the sink environment. The Power input (IV) is equal to $Q_{REJ} - Q_{IN}$. The C.O.P. upper stage is

TWO STAGE CASCADED THERMOELECTRIC OPERATION

BETWEEN HEAT SOURCE AND HEAT SINK

WITH FINITE HEAT TRANSFER COEFFICIENTS

ELEMENT HEIGHT CM L 0.200

JUNCTION RESISTIVITY OHM CM SQRD RHOJI 0.250E-04

ELEMENT CONDUCTIVITY /OHM CM SIGMA 894.0000

PACKING DENSITY OMEGA 0.8770

SEEBECK COEFFICIENT VOLTS/K ALPHA 0.443E-03

RIPPLE FACTOR F 1.0010

PERCENT RIPPLE 0.00126523

THERMAL CONDUCTIVITY WATTS/CM K 0.0147

EFFECTIVE MATERIAL PROPERTIES

COUPLE ELEMENT INTERIOR RESISTANCE OHMS= 0.11185682E-01

EFFECTIVE RESISTANCE OHMS= 0.137131E-01

COUPLE ELEMENT THERMAL CONDUCTANCE WATTS/K= 0.588000E-02

EFFECTIVE THERMAL CONDUCTANCE WATTS/K= 0.589403E-02

EFFECTIVE FIGURE OF MERIT /K= 0.242807E-02

MATERIAL FIGURE OF MERIT /K= 0.298379E-02

ZMAT= 0.298379E-02/°K

EXPONENT HOT SIDE HEAT TRANSFER COEFFICIENT= 0.3333

EXPONENT COLD SIDE HEAT TRANSFER COEFFICIENT= 0.8333

ESUBC= 0.150

FREE STREAM CONDITIONS

SOURCE TEMPERATURE°K= 250.0000

SINK TEMPERATURE°K= 300.0000

ANUC= 1.000

BALANCED OPERATION ACHIEVED,

HEAT FLUX WATTS/CM SQRD= 1.0000

HOT JUNCTION TEMPERATURE°K= 304.0671

INTERMEDIATE TEMPERATURE°K= 271.5280

COLD JUNCTION TEMPERATURE°K= 244.4123

ITERATIONS REQUIRED NN= 3.

CIRCUIT CURRENT I= 2.823

C.O.P. UPPER STAGE= 0.637

C.O.P.LOWER STAGE= 0.347

MAXIMUM C.O.P.= 0.191

OPERATIONAL C.O.P.= 0.111

COP RATIO2/1= 2.285

HEAT REJ UPR WATTS/CMSQRD= 2.570

HEAT INPUT LOWER WATTS/CMSQRD= 0.571

HEAT REJ LWR WATTS/CMSQRD= 2.216

VOLTAGE TOTAL VOLTS = 2.898

VOLTS1= 2.898

COLD SIDE HEAT PUMPED WATTS = 0.912201D+00

UPPER STAGE REJECTION WATTS = 0.234457D+01

LOWER STAGE REJECTION WATTS = 0.909549D+01

Fig. 11.3.1

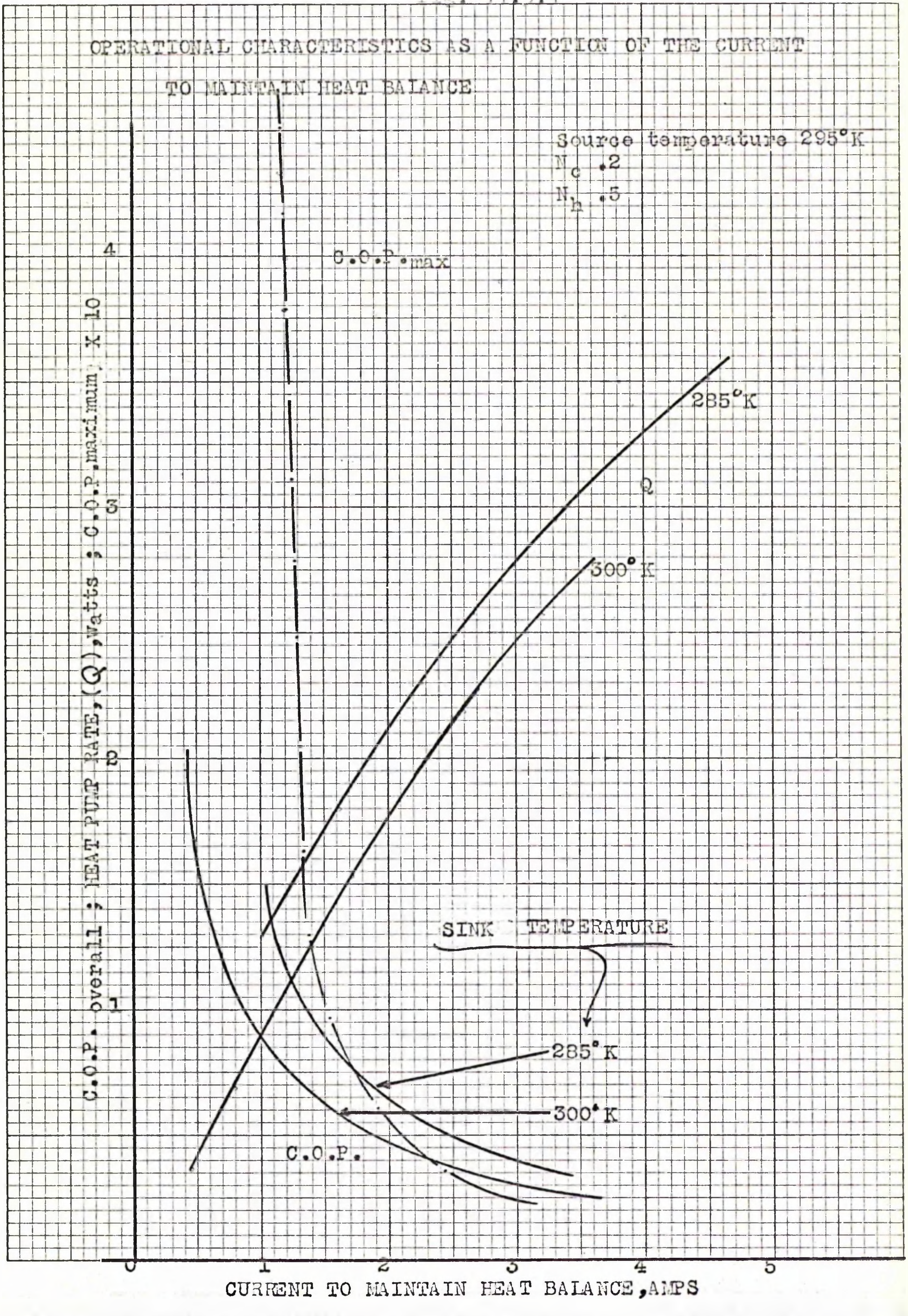
OPERATIONAL CHARACTERISTICS AS A FUNCTION OF THE CURRENT
TO MAINTAIN HEAT BALANCE
Source temperature 295°K
N_c .2
N_h .5
C.O.P.max
285°K
Q
300°K
SINK TEMPERATURE
285°K
300°K
C.O.P.
C.O.P. overall ; HEAT PUMP RATE, (Q), Watts ; C.O.P. maximum, X 10
CURRENT TO MAINTAIN HEAT BALANCE, AMPS
0
1
2
3
4
5

Fig. 11.3.2.

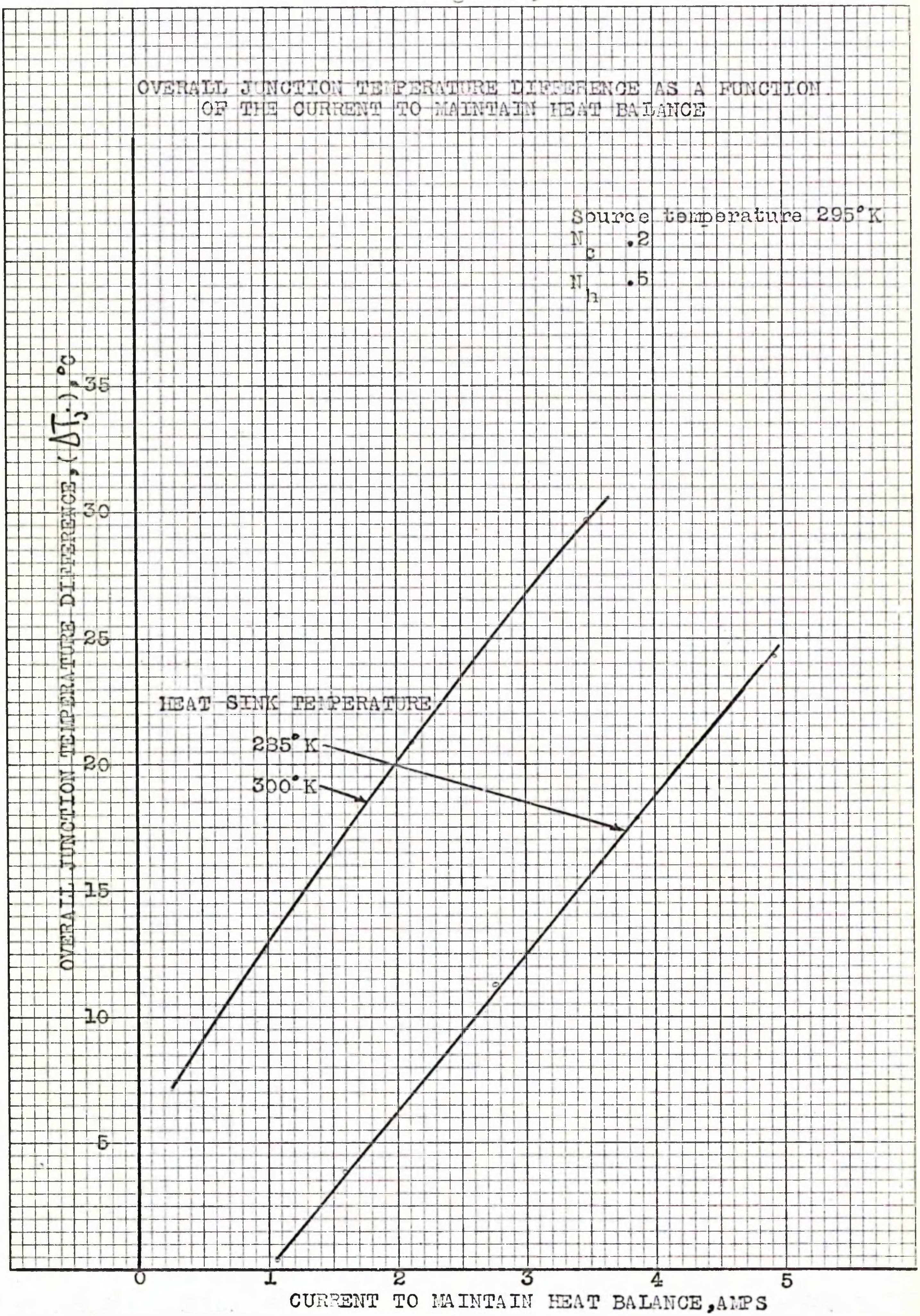
OVERALL JUNCTION TEMPERATURE DIFFERENCE AS A FUNCTION OF THE CURRENT TO MAINTAIN HEAT BALANCE
Source temperature 295°K
N_c .2
N_h .5
HEAT SINK TEMPERATURE
285°K
300°K
OVERALL JUNCTION TEMPERATURE DIFFERENCE, (ΔT_j), °C
CURRENT TO MAINTAIN HEAT BALANCE, AMPS
0
1
2
3
4
5
10
15
20
25
30
35

Fig. 11.3.3.

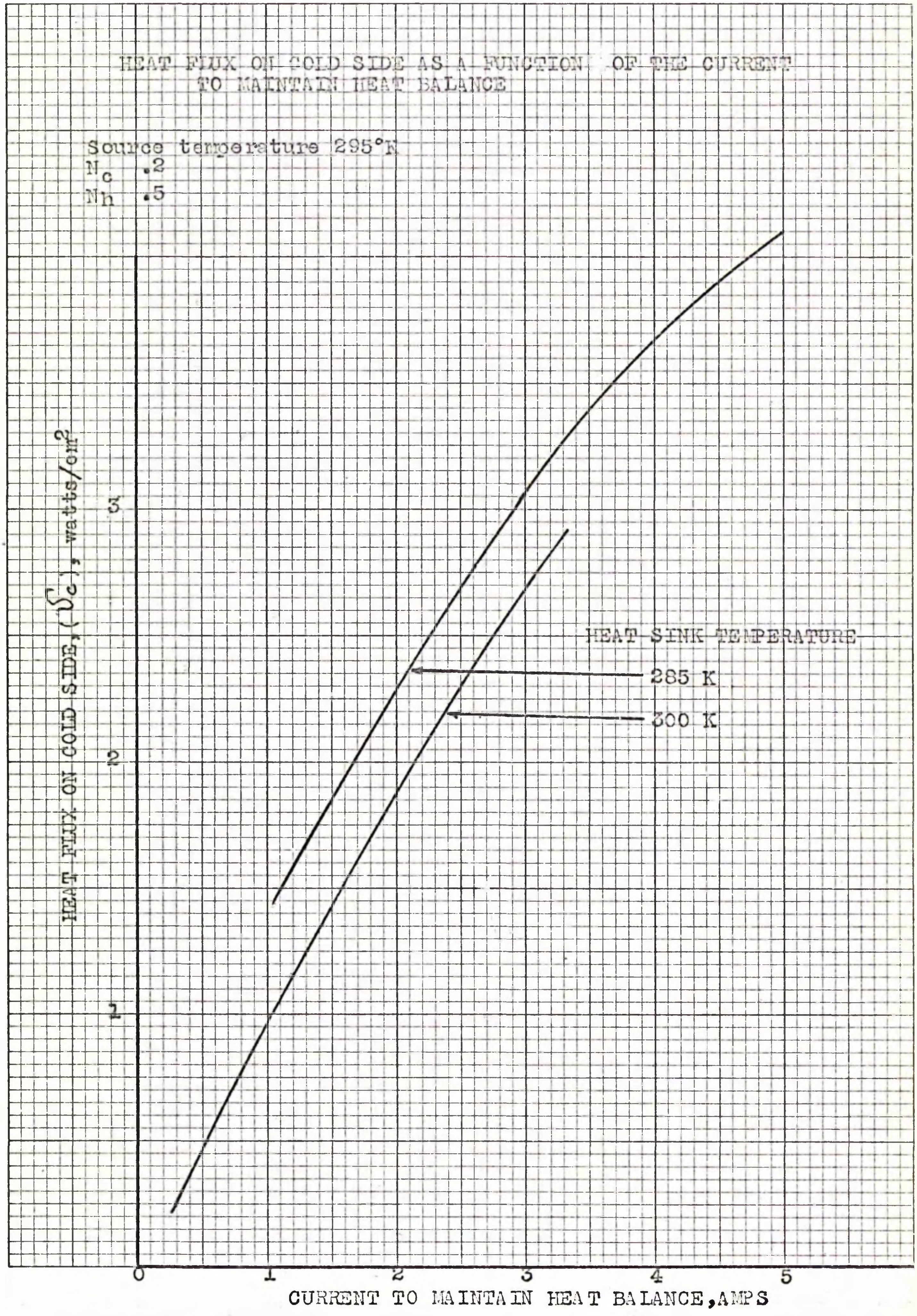

HEAT FLUX ON COLD SIDE AS A FUNCTION OF THE CURRENT
TO MAINTAIN HEAT BALANCE
Source temperature 295°K
N_c .2
N_h .5
HEAT SINK TEMPERATURE
285 K
300 K
HEAT FLUX ON COLD SIDE, (S_c), watts/cm²
CURRENT TO MAINTAIN HEAT BALANCE, AMPS
0
1
2
3
4
5

expressed as:

$$C.O.P._{\text{upper stage}} = \frac{Q_{IN}}{Q_{R_{\text{upper stage}}} - Q_{IN}}$$

where: Q_R upper stage is the upper stage heat rejection (watts) to the lower stage.

$$\text{and } C.O.P._{\text{lower stage}} = \frac{Q_{R_{\text{upper stage}}}}{Q_{REJ} - Q_{R_{\text{upper stage}}}}$$

11.3 Operational Characteristics of a Two-Stage Peltier Devices.

The figures presented in this section illustrate the general output from the computer programme. The results will be used to evaluate the ability of a 2-stage cascaded Peltier module to maintain a temperature difference under a given heat load. The basic computer programme can be extended to evaluate the performance of a 3-stage assembly or possible an m-stage (as an ultimate objective). The resulting equations would require additional assumptions about the inter-stage temperatures. Very little test data exists to support the assumptions required in extending the analysis beyond a 3-stage device.

Figure 11.3.1 illustrates the operational characteristics of a 2-stage module as a function of current with variation in sink temperature. The material properties are listed as computer output (Section 11.2.3 - Computer Results). The overall C.O.P. is approximately 1/10 of the maximum value

Fig. 11.3.4.

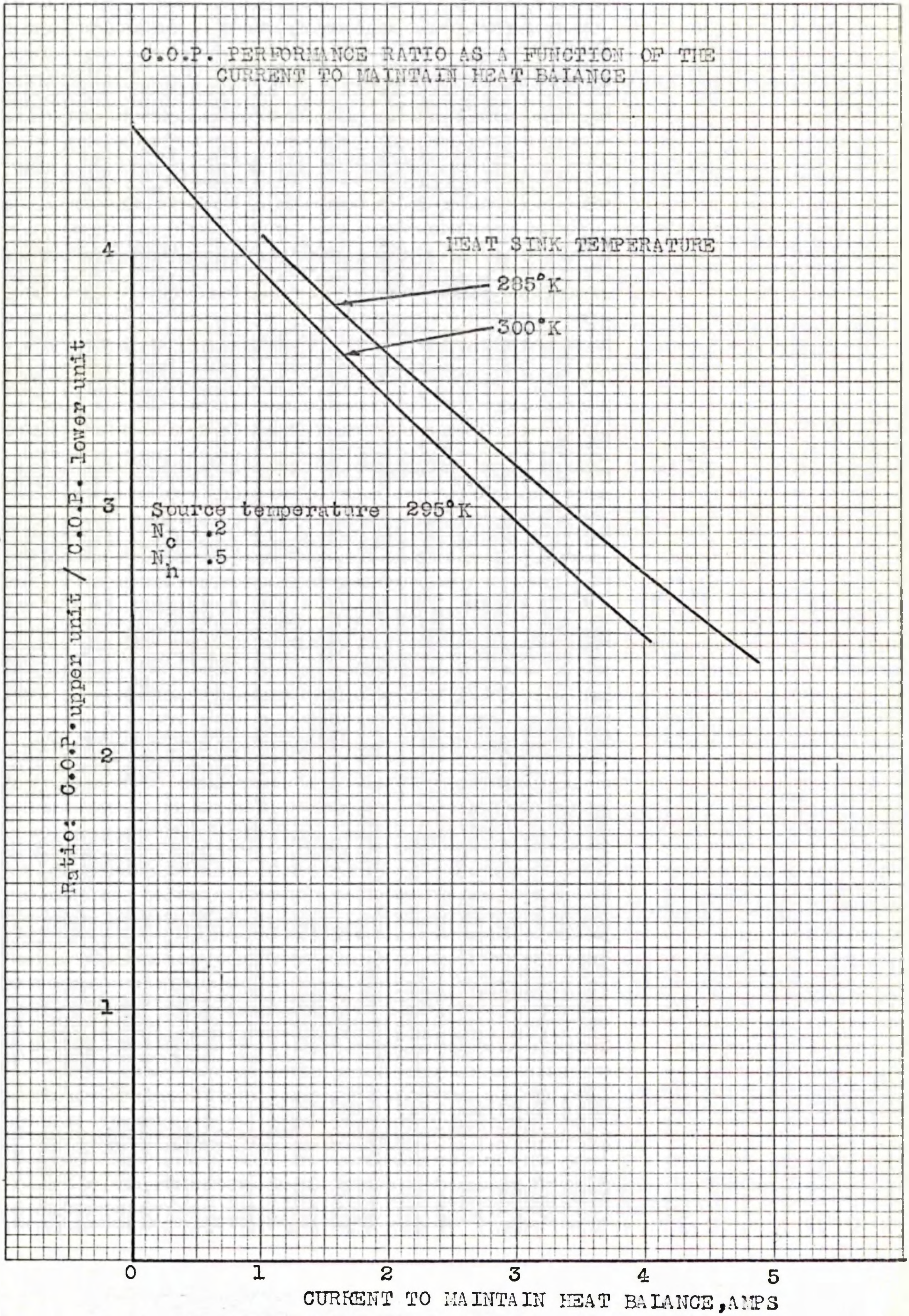

C.O.P. PERFORMANCE RATIO AS A FUNCTION OF THE CURRENT TO MAINTAIN HEAT BALANCE
HEAT SINK TEMPERATURE
285°K
300°K
Source temperature 295°K
N_c .2
N_h .5
Ratio: C.O.P. upper unit / C.O.P. lower unit
1
2
3
4
0
1
2
3
4
5
CURRENT TO MAINTAIN HEAT BALANCE, AMPS

Fig. 11.3.5.

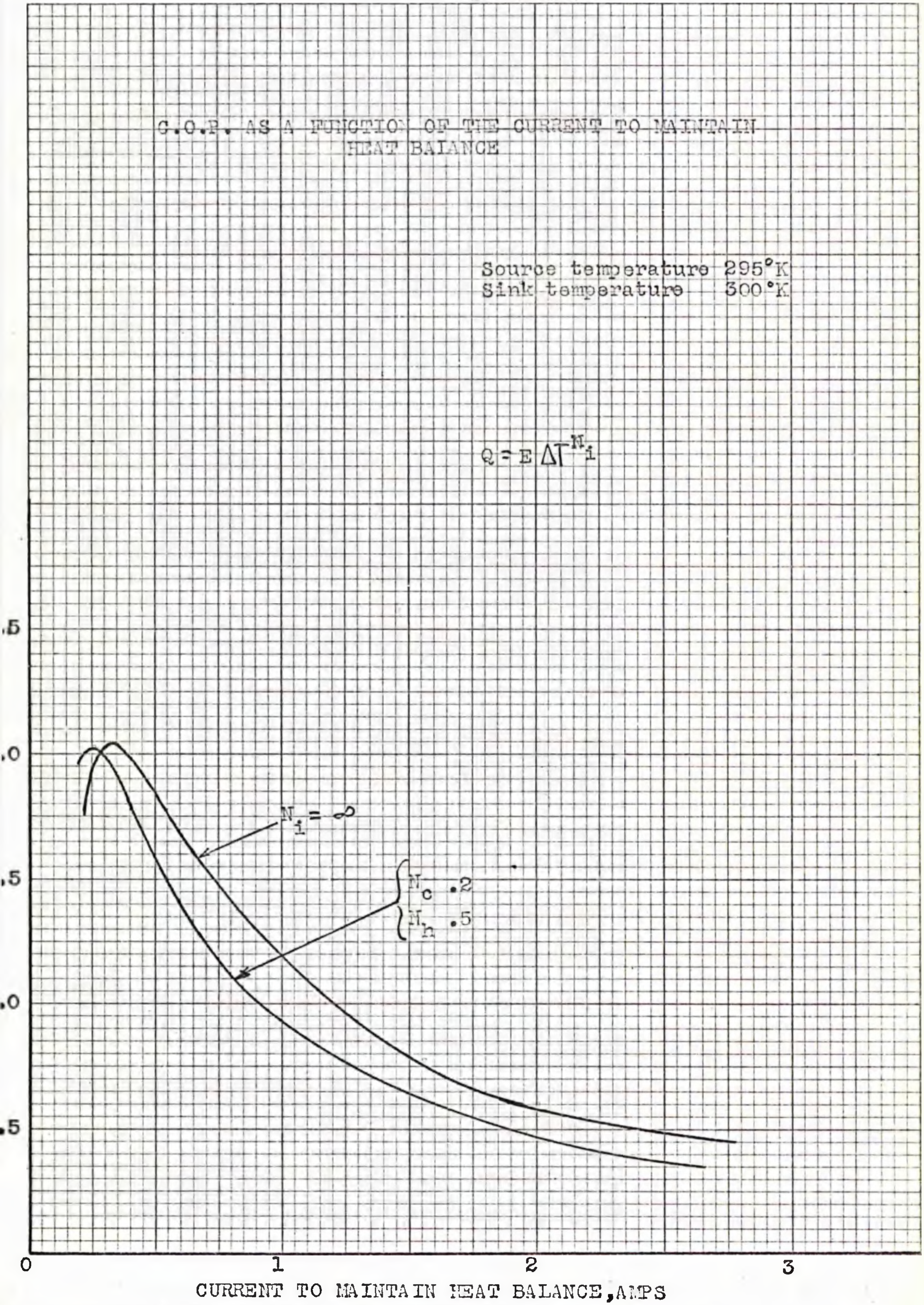
C.O.P. AS A FUNCTION OF THE CURRENT TO MAINTAIN HEAT BALANCE
Source temperature 295°K
Sink temperature 300°K
$Q = E\,\Delta T^{N_i}$
$N_i = \infty$
N_c .2
N_h .5
.5
.0
.5
.0
.5
0
1
2
3
CURRENT TO MAINTAIN HEAT BALANCE, AMPS

Fig. 11.3.6.

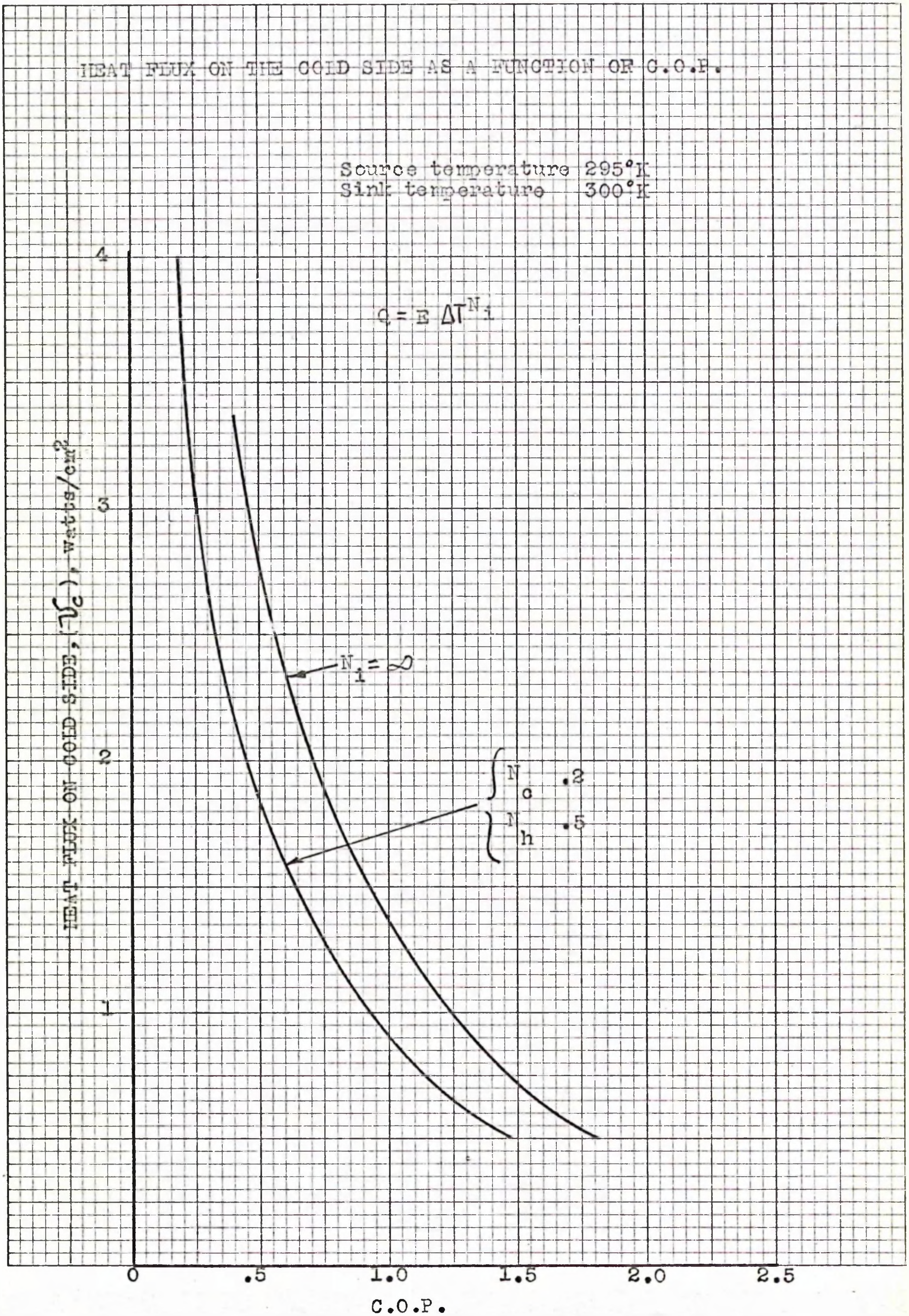
HEAT FLUX ON THE COLD SIDE AS A FUNCTION OF C.O.P.
Source temperature 295°K
Sink temperature 300°K
Q = E ΔT^N i
N i = ∞
N c .2
N h .5
HEAT FLUX ON COLD SIDE, watts/cm²
4
3
2
1
0
.5
1.0
1.5
2.0
2.5
C.O.P.

predicted by equation (42) section 11.2.1. The lower sink temperature exhibits a higher C.O.P. and higher heat pump rate than the higher heat sink temperature. The junction temperatures have been determined by an iterative routine. The iterative loop terminates at an error value (epso) of .05°C. Figure 11.3.2 illustrates the overall junction temperature difference as a function of current. For the heat sink temperature of 285°K at 1 amp the overall junction temperature is approximately zero with a correspondin heat flux rate of $\cong$ 1.4 watts/cm^2 (figure 11.3.3). Figure 11.3.4 illustrates the (C.O.P.$_{\text{upper stage}}$/C.O.P.$_{\text{lower stage}}$) as a function of current. For a fixed value of current the lower heat sink temperature has a higher operational C.O.P. ratio. Figure 11.3.5 indicates the C.O.P. overall as a function of current for variation in the heat transfer exponent. Two heat transfer coefficients were utilized to contract figure 11.3.5; a finite value and $N_h, N_c = \infty$ (equation (1) and equation (37); section 11.2.1). Figure 11.3.6 illustrates the cold side heat flux as a function of operational C.O.P. for variation in the heat transfer exponent (finite, ∞ value).

11.4 Comparison Between 2-stage Cascaded Device and Single Stage Module.

11.4.1 Introduction.

This section presents the available computer output to determine in a general way the operational trends associated with a 2-stage Peltier device and a single stage module

Fig. 11.4.2.1.

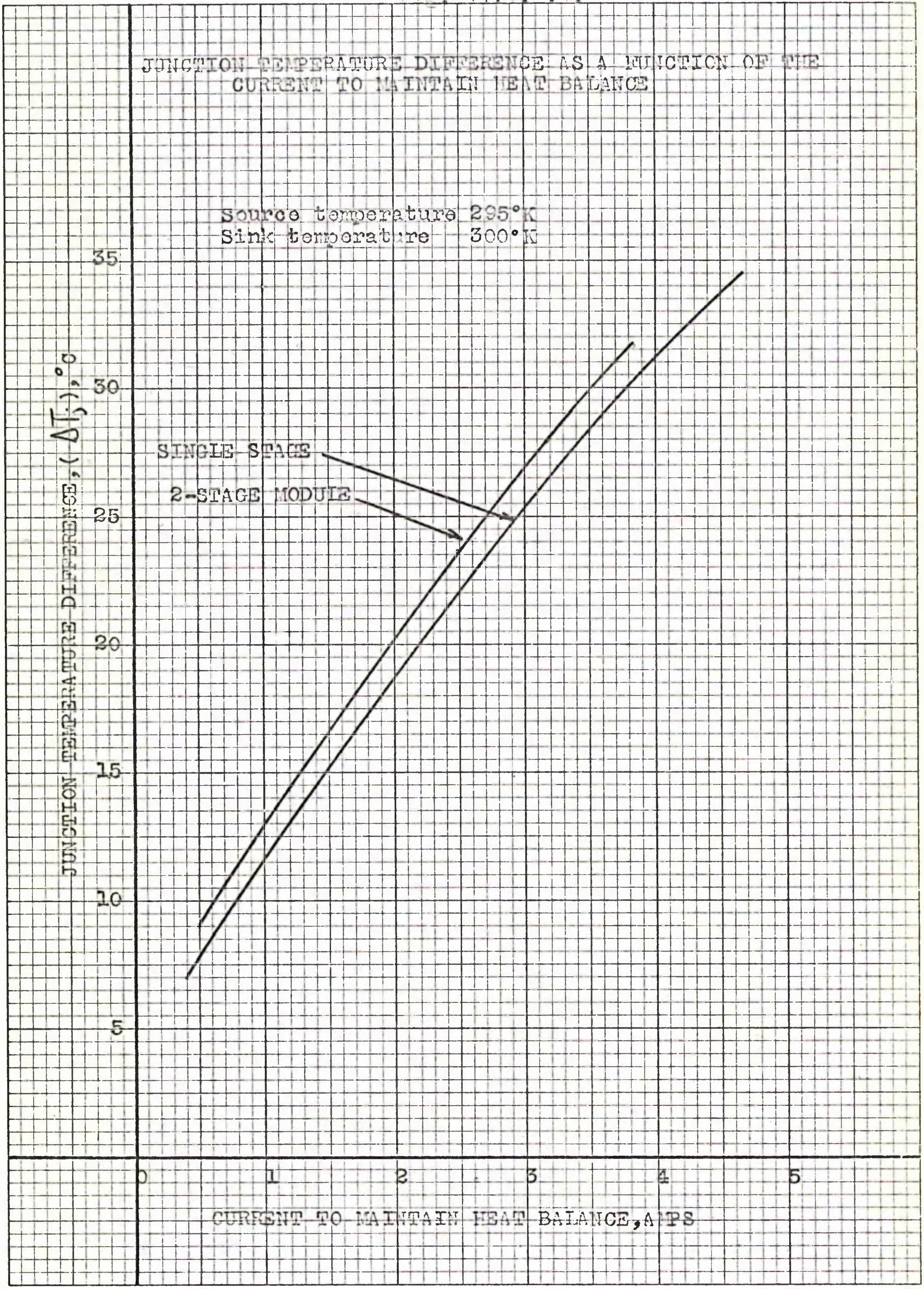

JUNCTION TEMPERATURE DIFFERENCE AS A FUNCTION OF THE CURRENT TO MAINTAIN HEAT BALANCE
Source temperature 295°K
Sink temperature 300°K
SINGLE STAGE
2-STAGE MODULE
JUNCTION TEMPERATURE DIFFERENCE, (ΔT_j), °C
5
10
15
20
25
30
35
0
1
2
3
4
5
CURRENT TO MAINTAIN HEAT BALANCE, AMPS

operating between heat source and heat sink. In addition, it is proposed to indicate that gains in C.O.P. through cascading may not be a - prior consequence of the cascaded module.

11.4.2 Discussion and Results.

Figure 11.4.2.1 to figure 11.4.2.5 compare the operational potential of a two-stage Peltier device and a single stage assembly. The heat source temperature is 295 K and the heat sink temperature is 300°K ($\Delta T_{\infty} = 5°C$). The heat transfer exponents are finite with material properties similar for both configurations (Section 11.2.1 - Computer Results). Figure 11.4.2.1 illustrates the overall junction temperature difference as a function of current. Figure 11.4.2.2 shows the overall C.O.P. as a function of current for both the 2-stage and single stage and single stage device. The results indicate that the overall C.O.P. for the 2-stage module is lessthan the C.O.P. for the single stage device (as indicated section 11.4.1.). This condition can be supported by considering the following.

From figure 11.4.2.1 ΔT_j 2 stage $\simeq \Delta T_j$ single stage 11.4.2.1.

(1) The C.O.P. for a single stage can be defined by:

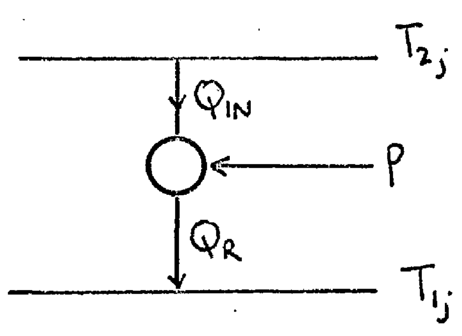

$T_{2j} < T_{1j}$

Fig. 11.4.2.2.

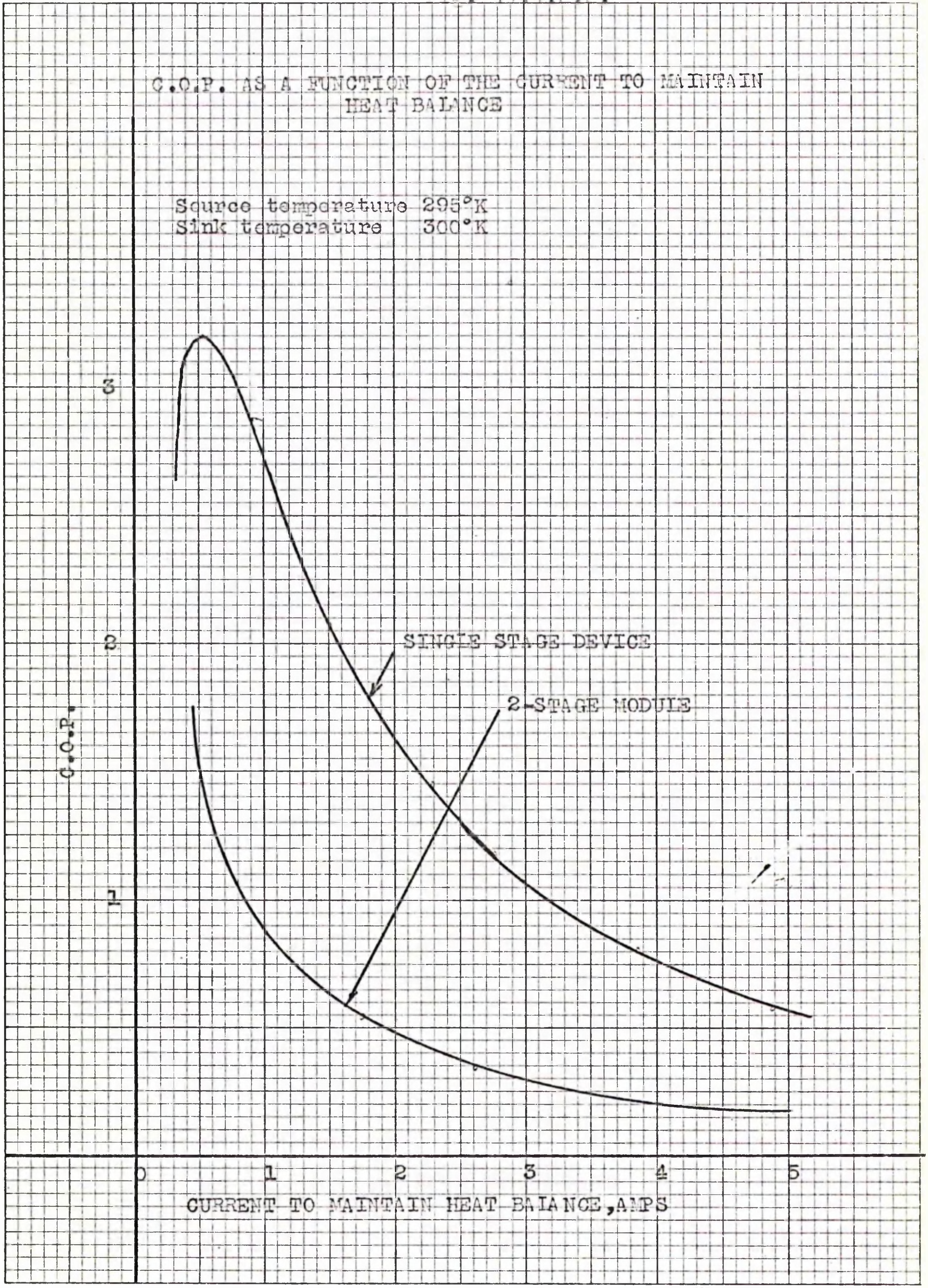
C.O.P. AS A FUNCTION OF THE CURRENT TO MAINTAIN HEAT BALANCE
Source temperature 295°K
Sink temperature 300°K
SINGLE STAGE DEVICE
2-STAGE MODULE
C.O.P.
1
2
3
0
1
2
3
4
5
CURRENT TO MAINTAIN HEAT BALANCE, AMPS

then from the illustration above:

$$\text{C.O.P.} \equiv Q_{IN} / P \qquad 11.4.2.2.$$

and

$$\text{C.O.P.} = Q_{IN} / \left[Q_R - Q_{IN} \right] \qquad 11.4.2.3.$$

(2) The C.O.P. for a two-stage device can be defined by:

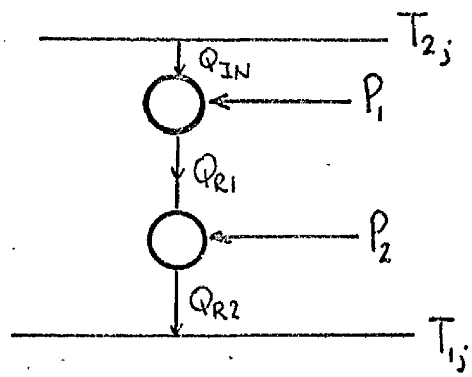

$$T_{2_j} < T_{1_j}$$

where:

$$\text{C.O.P.}\Big|_{\text{2-stage}} \equiv \frac{Q_{IN}}{P_1 + P_2} \qquad 11.4.2.4.$$

(3) With $P_1 + P_2 > P \quad \therefore \text{C.O.P.}\Big|_{\text{2-STAGE}} < \text{C.O.P.}\Big|_{\text{single stage}}$

$$\text{for} \quad \Delta T_j\Big|_{\text{2-STAGE}} \cong \Delta T_j\Big|_{\text{single stage}}$$

The overall C.O.P. for an m-stage device can be derived as follows:

$$\text{C.O.P.}\Big|_{\text{2-stage}} \equiv \frac{Q_{IN}}{P_1 + P_2} \qquad 11.4.2.4.$$

$$\text{C.O.P.}\Big|_{\text{upper stage}} \equiv \frac{Q_{IN}}{P_1} \qquad 11.4.2.5.$$

$$\text{C.O.P.}\Big|_{\text{lower stage}} \equiv \frac{Q_{R1}}{P_2} \qquad 11.4.2.6.$$

From the previous illustration:

$$Q_{R1} = Q_{IN} + P_1 \qquad 11.4.2.7.$$

Introducing equation 11.4.2.7, equation 11.4.2.6 and equation 11.4.2.5 into equation 11.4.2.4 results:

$$\text{C.O.P.}\Big|_{\text{2 stage}} = \frac{\left[\text{C.O.P}_{\text{upper}} \cdot P_1\right]}{\left[P_1 + \dfrac{Q_{IN} + P_1}{\text{C.O.P.}_{\text{lower}}}\right]} \qquad 11.4.2.8.$$

Expanding and dividing through results:

$$\text{C.O.P.} = \frac{1}{\dfrac{1}{\text{C.O.P.}_{\text{upper}}} + \dfrac{1}{\text{C.O.P.}_{\text{lower}}} + \dfrac{1}{\text{C.O.P.}\Big|_{\text{lower}} \times \text{C.O.P.}\Big|_{\text{upper stage}}}} \qquad 11.4.2.9.$$

which is extended to yield:

$$\text{C.O.P.}\Big|_{n\text{-stage}} = \prod_{i=1}^{n} \frac{1}{\left[1 + \dfrac{1}{\text{C.O.P.}_i}\right] - 1} \qquad 11.4.2.10.$$

Fig. 11.4.2.3.

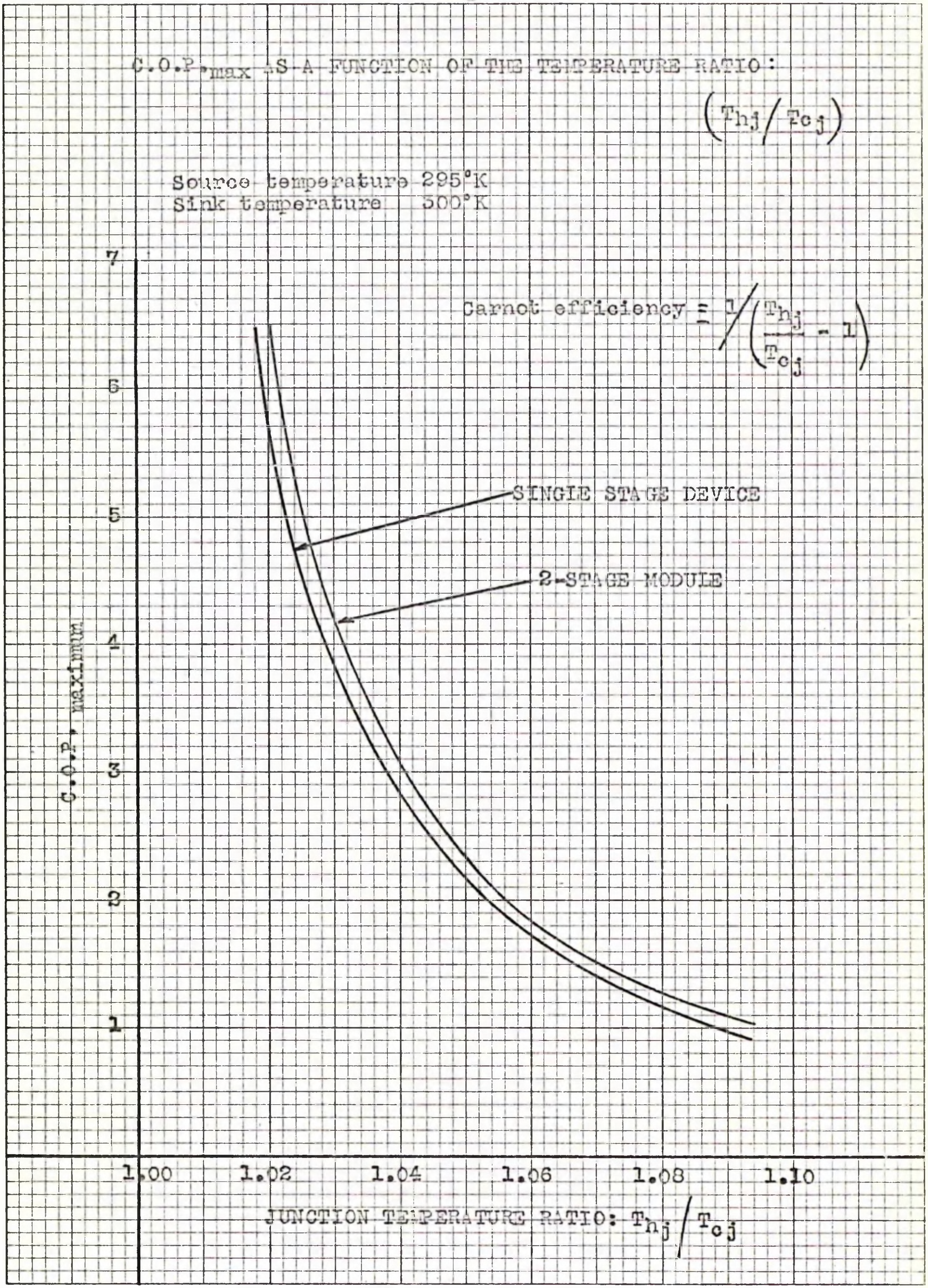

C.O.P.$_{max}$ AS A FUNCTION OF THE TEMPERATURE RATIO: $\left(T_{hj}/T_{cj}\right)$
Source temperature 295°K
Sink temperature 300°K
Carnot efficiency = $1\Big/\left(\frac{T_{hj}}{T_{cj}} - 1\right)$
SINGLE STAGE DEVICE
2-STAGE MODULE
C.O.P. maximum
7
6
5
4
3
2
1
1.00
1.02
1.04
1.06
1.08
1.10
JUNCTION TEMPERATURE RATIO: T_{hj}/T_{cj}

The C.O.P. for the 2-stage device (as utilized in the Computer programme) can be expressed as:

$$\text{C.O.P.}\Big|_{2\ \text{stage}} = \frac{1}{\left[1+\frac{1}{\text{C.O.P.}_1}\right]\left[1+\frac{1}{\text{C.O.P.}_2}\right]-1} \qquad 11.4.2.11.$$

Figure 11.4.2.3 shows the maximum C.O.P. (equation 41, section 11.2.1) as a function of the junction temperature ratio. The results indicate that the $\text{C.O.P.}_{max}\Big|_{2\ \text{stage}} \cong \text{C.O.P.}_{max}\Big|_{\text{single}}$. This condition was infered by (15) by the following relationship:

$$\lim_{Z\to\infty} \frac{\text{C.O.P. cascaded}}{\text{C.O.P.}_{\text{single stage}}}\Bigg|_{max} \longrightarrow 1 \qquad 11.4.2.12.$$

(Note: The limited refers to the figure of merit). The results (15) indicated that at $T_{cj} = 250^{\circ}K$, $T_{hj} = 300^{\circ}K$ for $Z = 3.0_{10}{-3}/^{\circ}K$ the ratio was $\cong 1.20$ (2 stage device) and for $\Delta T_{\infty} \ll 50^{\circ}C$ the ratio is expected to approach unity. To support the results indicated by figure 11.4.2.3 an approximate expression presented in reference (15) was incorporated into the basic computer programme. The computer results indicated the following:

$$.1 \cong \leq \sigma_c \leq \cong 3\ \text{watts/cm}^2$$

$$1.002 \cong \leq \left|\frac{\text{C.O.P.}_{2\ \text{stage}}}{\text{C.O.P.}_{\text{single}}}\right| \leq \cong 1.055$$

Fig. 11.4.2.4.

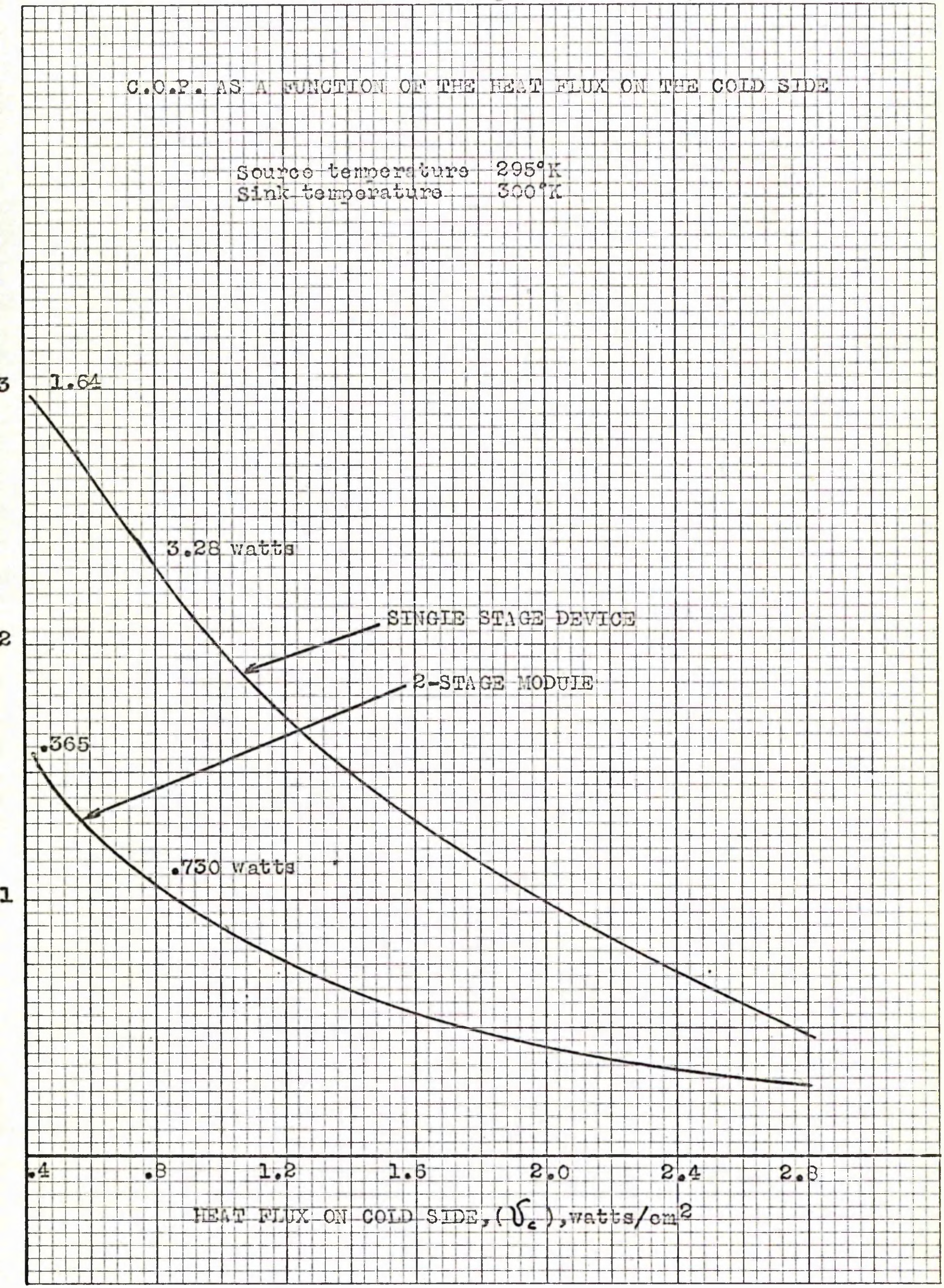

C.O.P. AS A FUNCTION OF THE HEAT FLUX ON THE COLD SIDE
Source temperature 295°K
Sink temperature 300°K
3
2
1
1.64
3.28 watts
SINGLE STAGE DEVICE
2-STAGE MODULE
.365
.730 watts
.4
.8
1.2
1.6
2.0
2.4
2.8
HEAT FLUX ON COLD SIDE, ($\mathcal{V}_c$), watts/cm^2

Fig. 11.4.2.5.

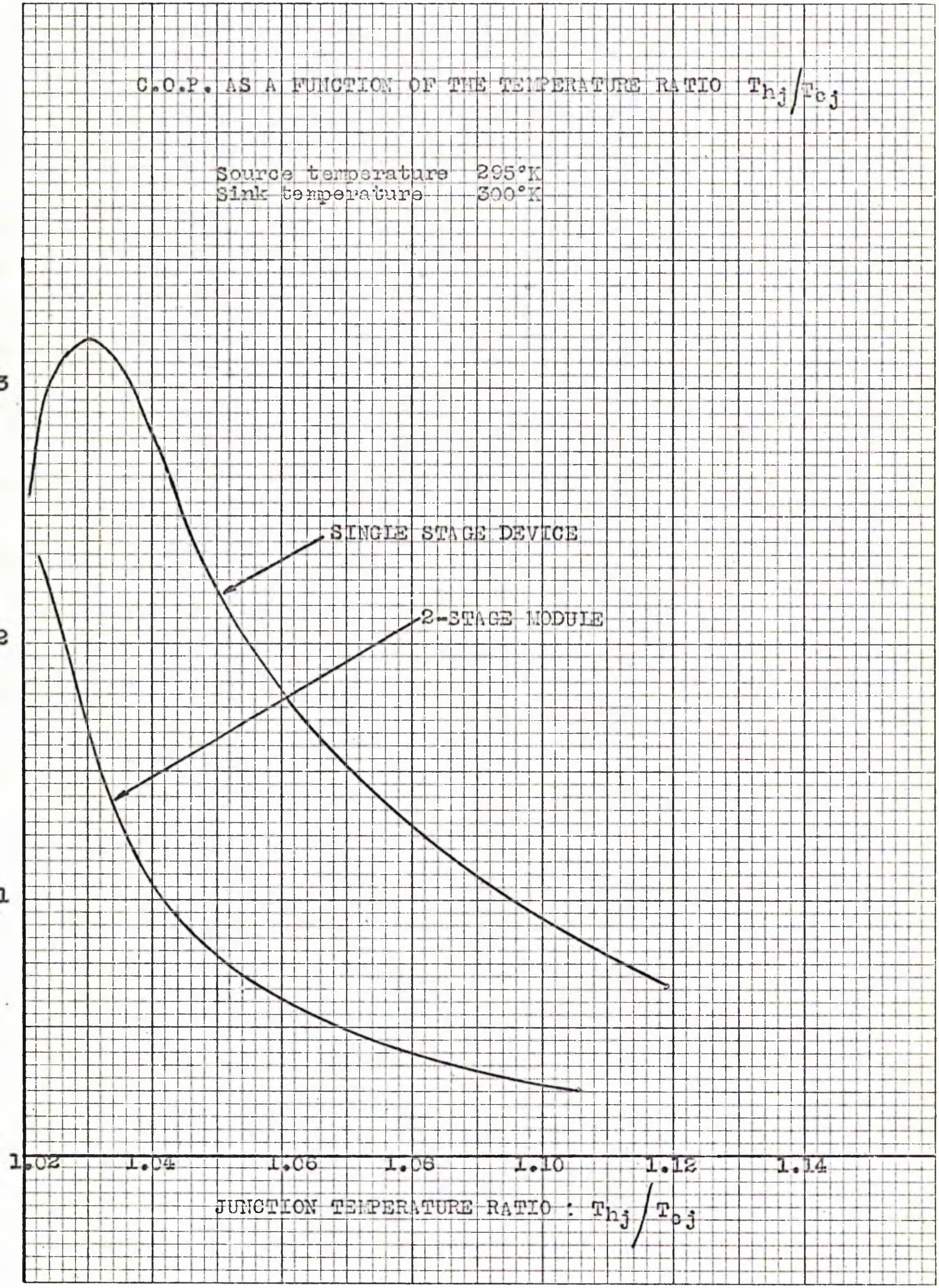
C.O.P. AS A FUNCTION OF THE TEMPERATURE RATIO T_{hj}/T_{cj}
Source temperature 295°K
Sink temperature 300°K
SINGLE STAGE DEVICE
2-STAGE MODULE
3
2
1
1.02
1.04
1.06
1.08
1.10
1.12
1.14
JUNCTION TEMPERATURE RATIO : T_{hj}/T_{cj}

with:

$$1.021 \quad \stackrel{\sim}{=} \; \leq T_{H_j} / T_{C_j} \leq \; \stackrel{\sim}{=} \quad 1.105$$

The results given above support the function illustrated by figure 11.4.2.3. Figure 11.4.2.4 illustrates the C.O.P. as a function of the heat flux on the cold side. For a constant heat flux input the single stage device exhibits a higher C.O.P. Figure 11.4.2.5 illustrates the overall C.O.P. as a function of the junction temperature ratio. The C.O.P. for the single stage device reaches a maximum C.O.P. of $\stackrel{\sim}{=}$ 3.20 at a temperature ratio of $\stackrel{\sim}{=}$ 1.03 with a corresponding carnot efficiency of $\stackrel{\sim}{=}$ 33 (operational C.O.P. $\stackrel{\sim}{=}$ 1/10 of the Carnot value). The computer program developed in section 8.3 is utilized to determine the operational characteristics of the single stage device. Two independent computer programmes were employed to determine the operational characteristics of the single stage device and the 2-stage module.

Figure 6.7.2 exhibits the general C.O.P. characteristic of a decreasing function as ΔT_j exceeds $\stackrel{\sim}{=}$ 20°C (representative value). It is proposed to illustrate that two-stage cascading can improve performance where the junction temperature difference exceeds $\stackrel{\sim}{=}$ 20°C (X% of $\Delta T_{j_{max}}$).(1) To support this conclusion the modular operational characteristics were obtained from two independent computer programmes. (Computer programme - C.P.5; Computer programme - C.P.8.). For the boundary conditions the heat sink temperature is 300°K and the heat source temperature

(1) Indicative of $\Delta T_j \longrightarrow \Delta T_{j_{max}}$

Fig. 11.4.2.6.

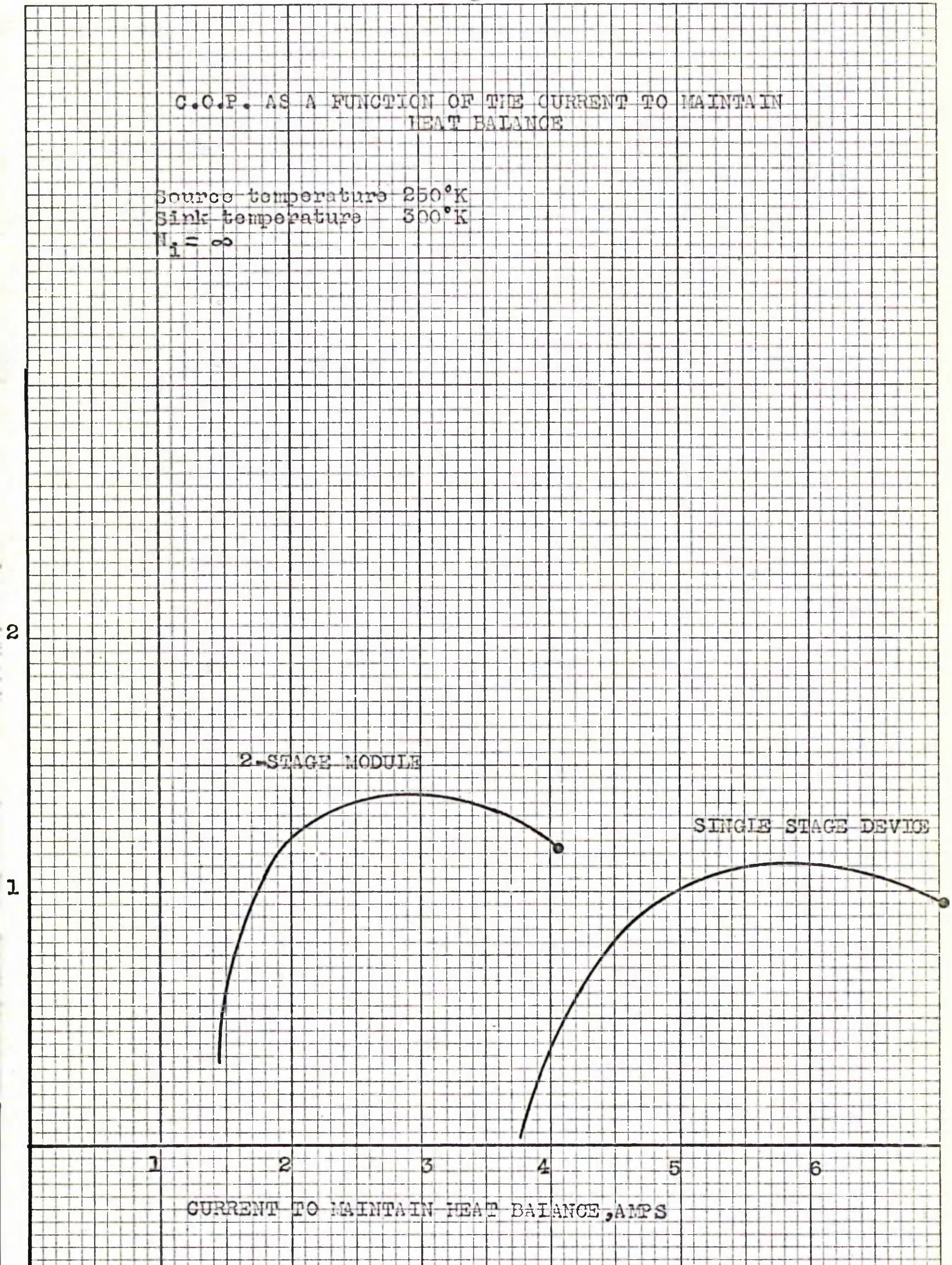
C.O.P. AS A FUNCTION OF THE CURRENT TO MAINTAIN HEAT BALANCE
Source temperature 250°K
Sink temperature 300°K
$N_1 = \infty$
2-STAGE MODULE
SINGLE STAGE DEVICE
2
1
1
2
3
4
5
6
CURRENT TO MAINTAIN HEAT BALANCE, AMPS

Fig. 11.4.2.7

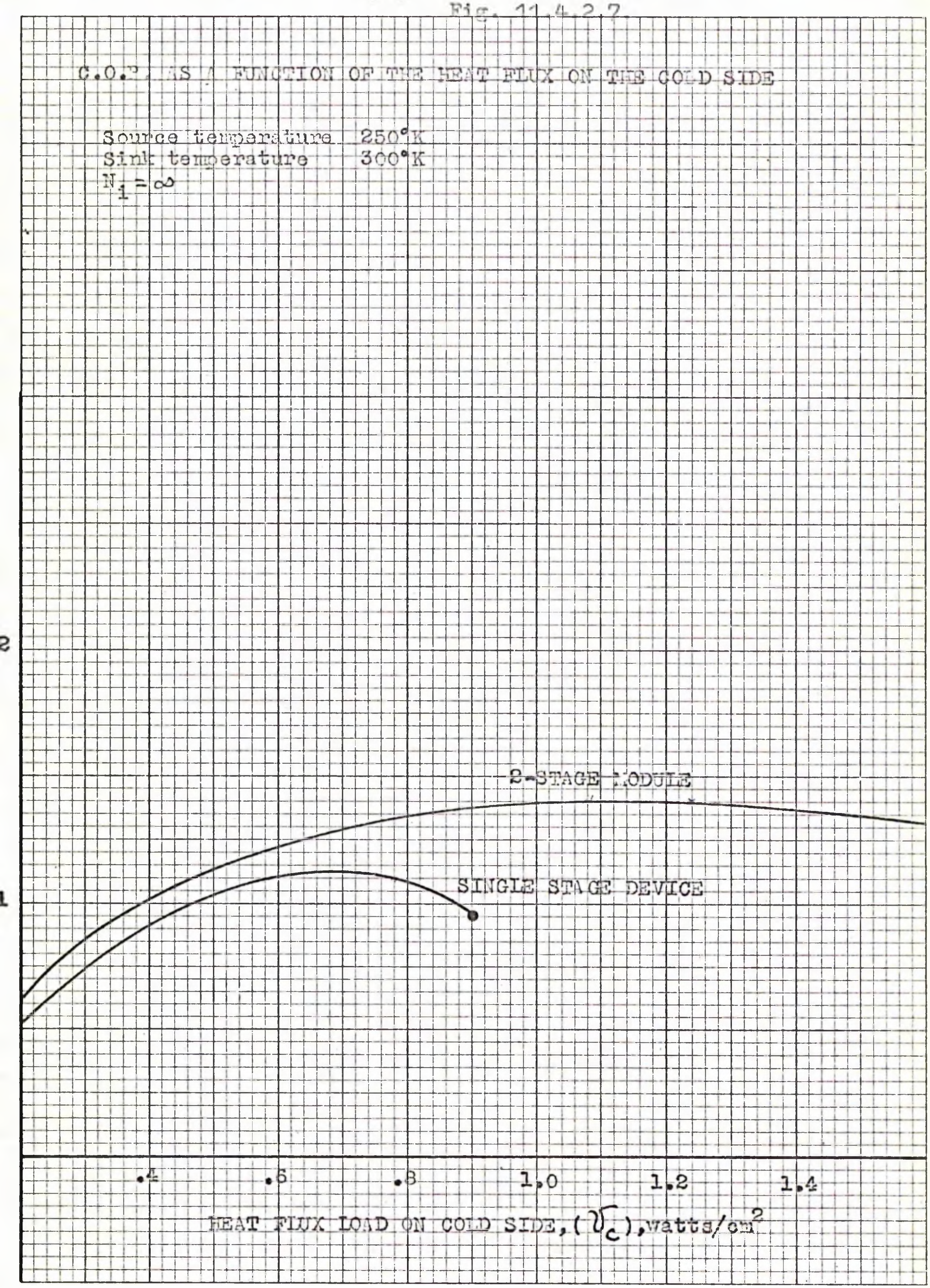
C.O.P. AS A FUNCTION OF THE HEAT FLUX ON THE COLD SIDE
Source temperature 250°K
Sink temperature 300°K
$N_1 = \infty$
2-STAGE MODULE
SINGLE STAGE DEVICE
2
1
.4
.6
.8
1.0
1.2
1.4
HEAT FLUX LOAD ON COLD SIDE, (ν_c), watts/cm^2

is 250°K (ΔT_{∞} = 50°C). The effective figure of merit is $\cong$ 2.43$_{10}$- 3/°K which can be used to approximate the overall maximum junction temperature difference. The overall maximum temperature is expressed as:

$$\Delta T_{j_{max}} \cong 0.5\, Z_{EFF}\, T_{c_{\infty}}^{2} \qquad 11.4.2.13.$$

where:-

$$T_{c_{\infty}} \geq T_{c_j}\ (°K) \qquad 11.4.2.14.$$

then:

$$\Delta T_{j_{max}} \cong 76°C \qquad 11.4.2.15.$$

Figure 11.4.2.6 illustrates the overall C.O.P. as a function of the current required to maintain thermal equilibrium. For constant C.O.P. operation the current for the 2-stage device is approximately half of that required for the single stage device. Figure 11.4.2.7 shows the C.O.P. as a function of the heat flux on the cold side. For a constant heat flux the 2-stage device exhibits a higher C.O.P. than the single stage device. The 2-stage module has a flatter C.O.P. as a function of the heat flux. ($.89 \leq \mathcal{V}_c \leq$ 2 watts/cm^2). Figure 11.4.2.8 illustrates the junction temperature difference as a function of the current. There is a modest increase in the junction temperature difference for the 2-stage device; however, the 2-stage device is operating under a higher heat flux load (i.e. from 2.5 to 10 times the single stage value). Figure 11.4.2.9 illustrates the C.O.P. as a function of the

Fig. 11.4.2.8.

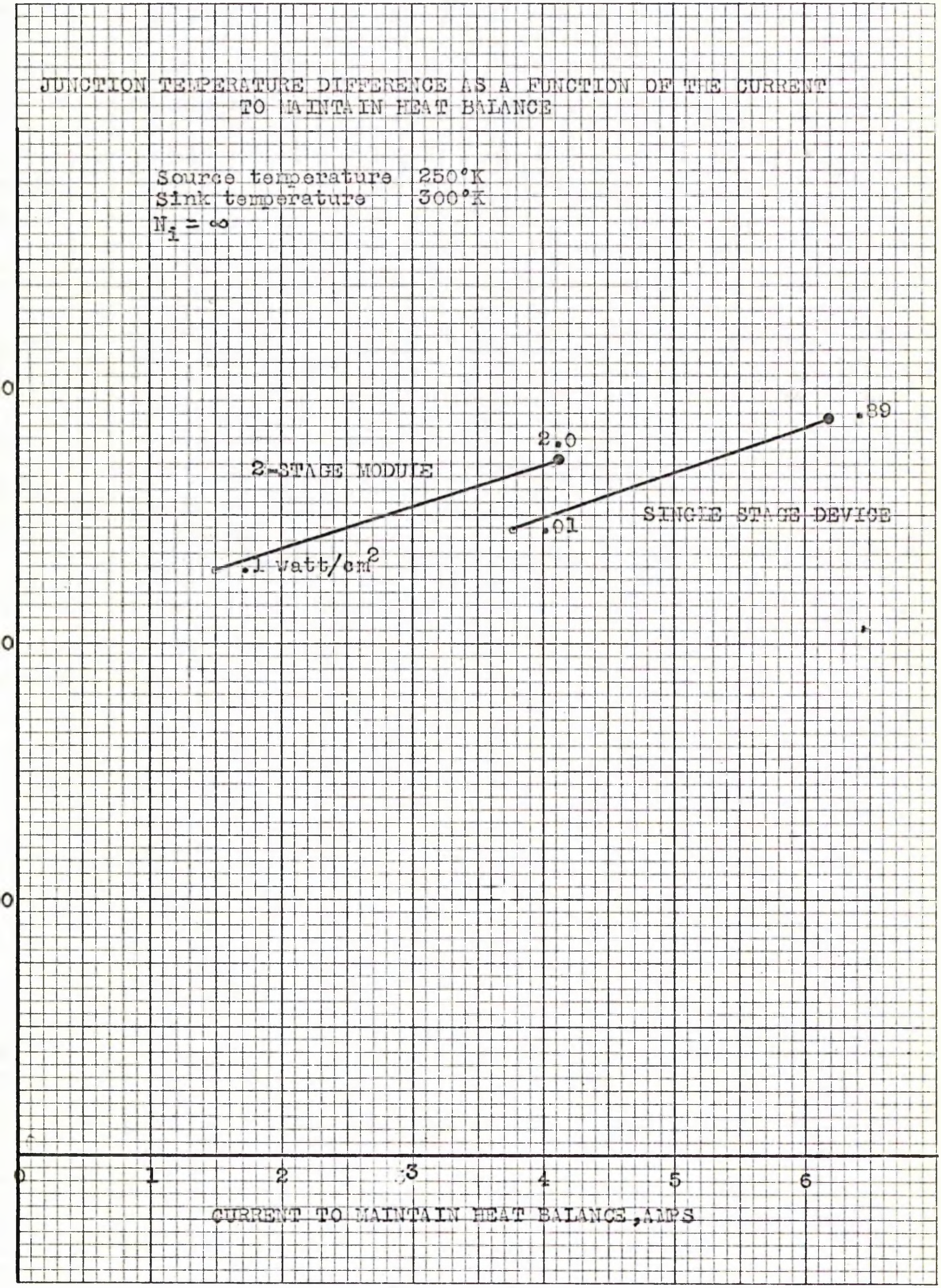
JUNCTION TEMPERATURE DIFFERENCE AS A FUNCTION OF THE CURRENT TO MAINTAIN HEAT BALANCE
Source temperature 250°K
Sink temperature 300°K
$N_i = \infty$
2.0
.89
2-STAGE MODULE
SINGLE STAGE DEVICE
.01
.1 Watt/cm²
0
1
2
3
4
5
6
CURRENT TO MAINTAIN HEAT BALANCE, AMPS

Fig. 11.4.2.9.

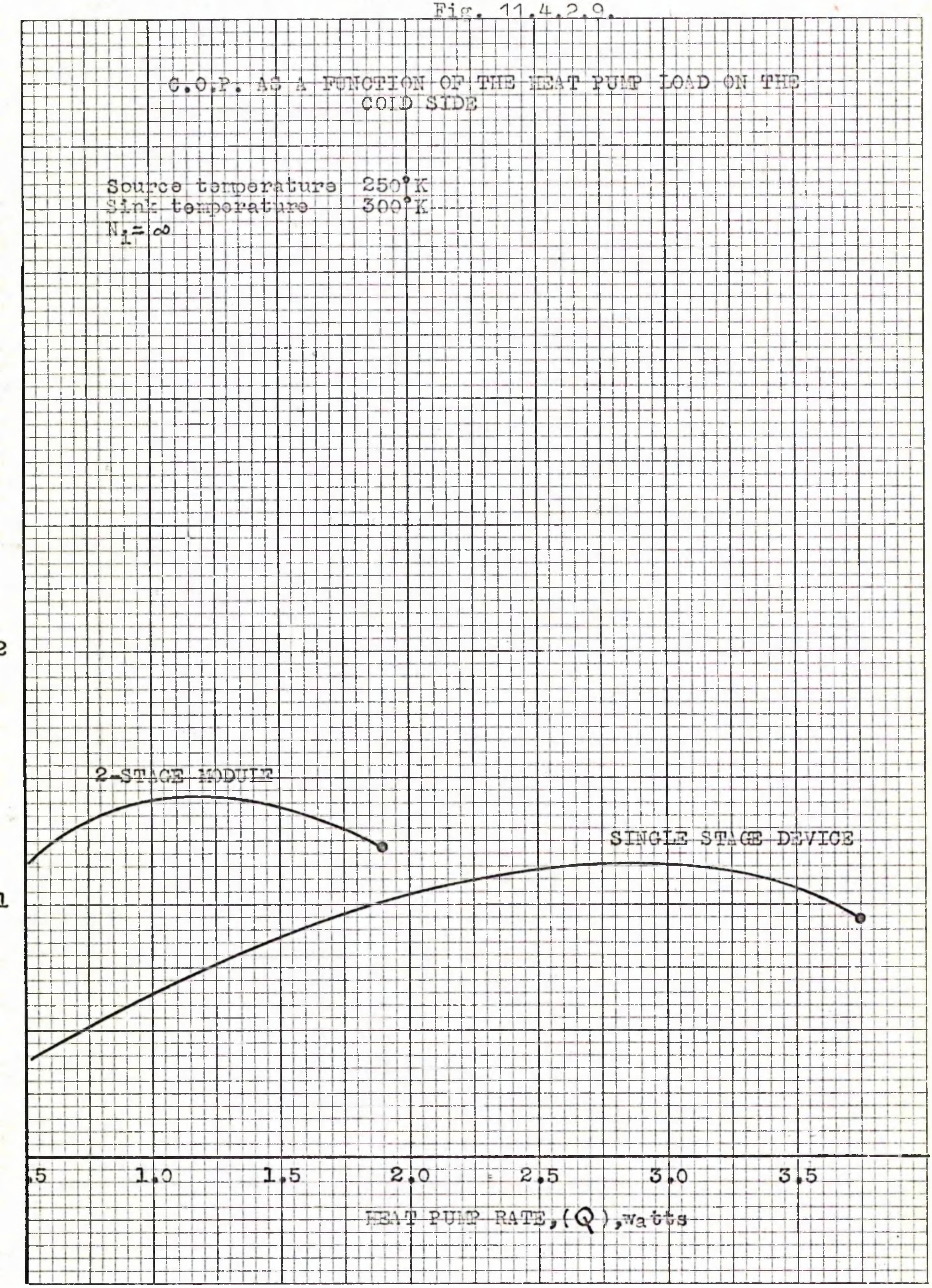
C.O.P. AS A FUNCTION OF THE HEAT PUMP LOAD ON THE COLD SIDE
Source temperature 250°K
Sink temperature 300°K
$N_1 = \infty$
2-STAGE MODULE
SINGLE STAGE DEVICE
2
1
.5
1.0
1.5
2.0
2.5
3.0
3.5
HEAT PUMP RATE, (Q), watts

heat load. The 2-stage device has a higher C.O.P. in the region ($.5 \leq Q \leq 2.0$ watts) than a single stage device. The maximum heat load predicted by the manufacturer is $\cong$ 2 watts under the computer boundary conditions, ($T_{h\infty}, T_{c\infty}, N_h, N_c$). The 2-stage unit was designed to operate with a maximum C.O.P. at an $\cong$ 1 watt heat load (figure 11.4.2.9 based on the computer programme supports the design objectives). The operational temperature difference is $\cong .75\,\Delta T_{j\,max}$ (equation 11.4.2.15). Figure 11.4.2.10 illustrates the potential gain ratio $\left[C.O.P._{max\ 2\text{-}stage} \,/\, C.O.P._{max\ single\ stage} \right]$ as a function of the heat flux load. The ratio exhibits an approximate linear function of the heat flux load. From figure 11.4.2.7 the single stage device saturates at $\cong$ .89 watts/cm^2, and the 2-stage saturates at approximately 2.0 watts/cm^2.

11.4.3 Synopsis.

A computer programme and a philosophy for analysis has been presented in the previous sections. The programme (2 stage device) incorporates a very limited number of assumptions. The results are presented in a form which enables an operational/parametric analysis to be conducted. The computer programme does not access the merits of one module as compared to the other, this appraisal must consider all variables which are weighted to the overall system requirements. The programme establishes the operational characteristic envelope on the basis of environmental conditions ($T_{h\infty}, T_{c\infty}, N_h, N_c$). The results

Fig. 11.4.2.10

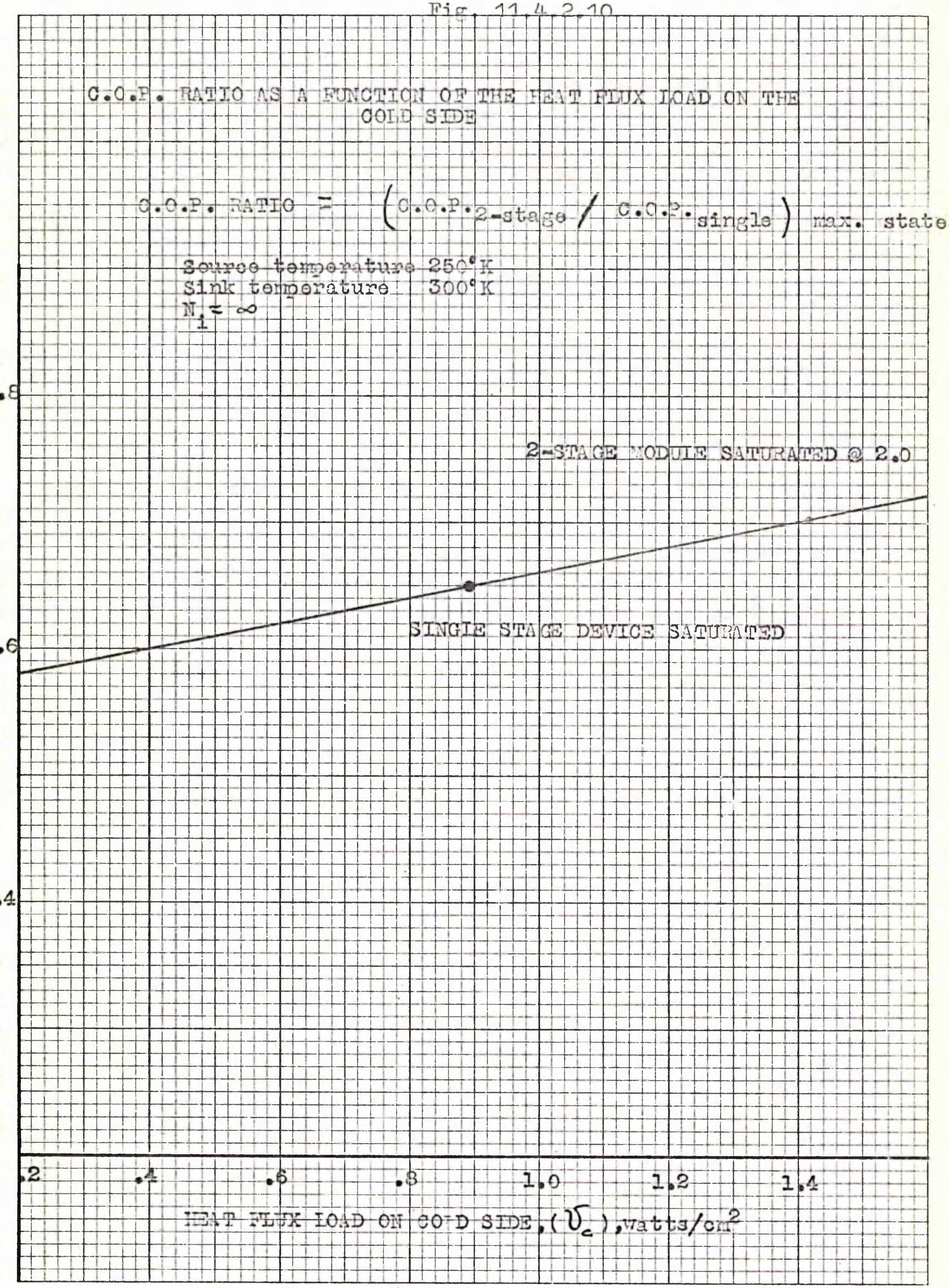
C.O.P. RATIO AS A FUNCTION OF THE HEAT FLUX LOAD ON THE COLD SIDE
C.O.P. RATIO = $\left(C.O.P._{2\text{-stage}} / C.O.P._{single} \right)$ max. state
~~Source temperature 250°K~~
Sink temperature 300°K
$N_i = \infty$
2-STAGE MODULE SATURATED @ 2.0
SINGLE STAGE DEVICE SATURATED
.8
.6
.4
.2
.4
.6
.8
1.0
1.2
1.4
HEAT FLUX LOAD ON COLD SIDE, (υ_c), watts/cm^2

within this section do not support the classical statement (16) , '..... more efficient than a single stage couple under all circumstances'. The statement deals with ideal cascading and neglects the effect of environment on the overall system ('real' devices). This section concludes that the cascaded device has an effectiveness envelope which can be determined by the programme developed in this study.

12.0 TEST AND THERMOELECTRIC MODULE EVALUATION.

12.1 Introduction.

This chapter summarizes the test results conducted with the experimental devices constructed using thermoelectric modules. The purpose of the testing was to compare the test data with the computer models. The test programme can be divided into three major areas. The areas of testing were:

(1) Thermoelectric module assembly (Plate 12.3.1.1) operating between heat source (ambient) and heat sink with finite heat convection fins on the cold side and water heat exchanger on hot side.

(2) Determination of maximum junction temperature difference for:

(a) Single stage device (Figure 12.4.1.1)

(b) Two stage device (Plate 12.4.1.1)

(3) Operational characteristic of basic thermoelectric module to determine: Q_{IN}, Q_R as a function of T_{hj}, T_{cj} (Plate 12.2.1).

12.2 Instrumentation and Control.

This section describes the basic instrumentation required to evaluate the operational characteristics of a Peltier module. Equipment and evaluation techniques were selected consistent with the required accuracy. Measurements were made of the steady state response of the thermoelectric devices to changes in current, heat load, and hot side junction temperatures. The computer models developed in the previous sections were compared to the test data in order to establish the validity of the model. The instrumentation philosophy imposed (author's concept) was to measure the major parameters independently of each other (i.e. Q_{IN}, Q_R, P_{IN}, T_{hj}, T_{cj})

The instrumentation used for the measurements will be divided into 3 subsections. The subsections are:

(1) Equipment for the control and measurement of the electrical current and voltage.

(2) Equipment for the control and measurement of the hot junction temperature.

(3) Equipment for the control and measurement of the cold junction temperature.

Figure 12.2.1 is a block diagram of the control and measurement equipment as utilized during the test portion of the research.

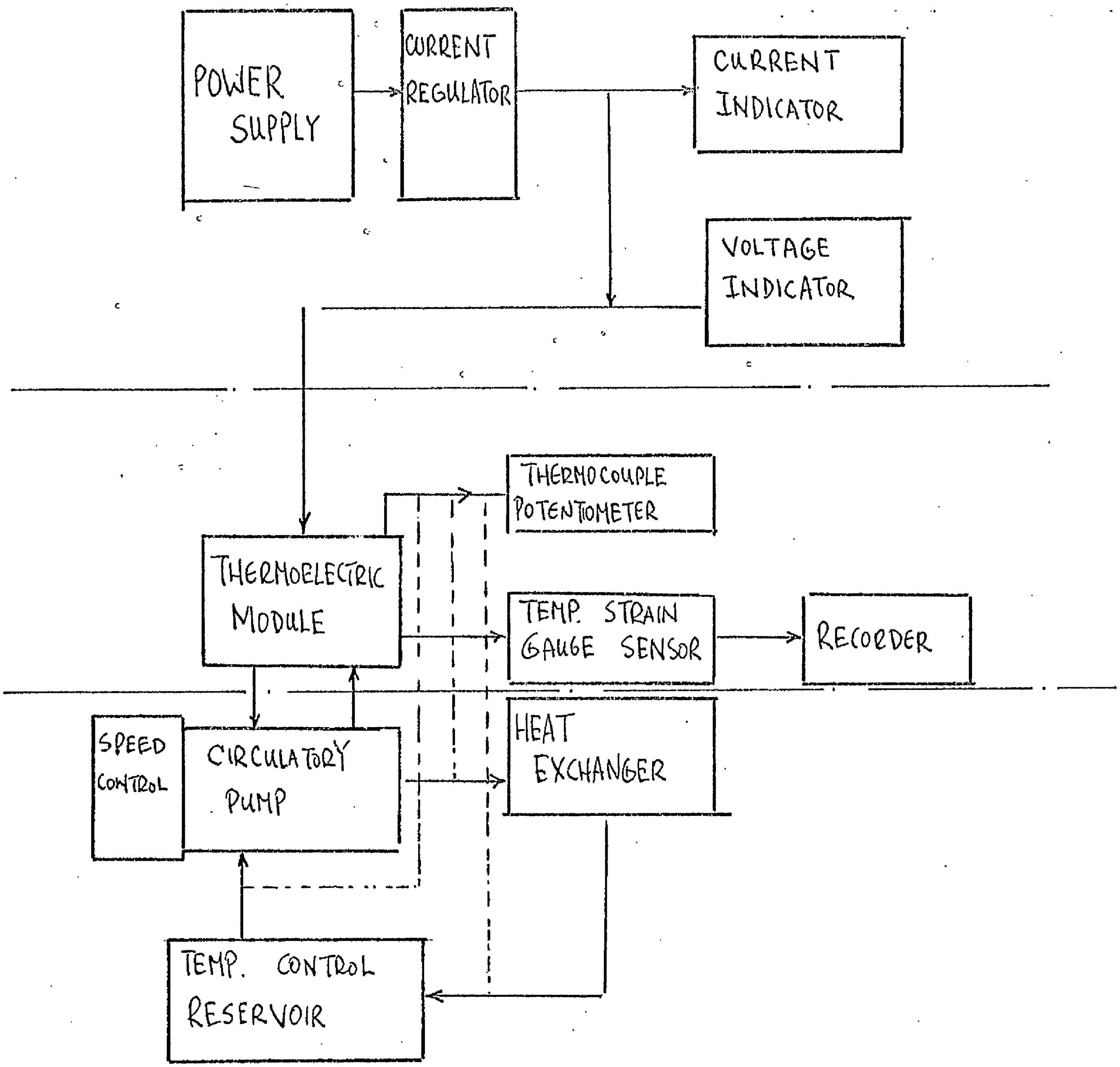

Figure 12.2.1.

Block Diagram of Basic Control and Instrumentation Facilities.

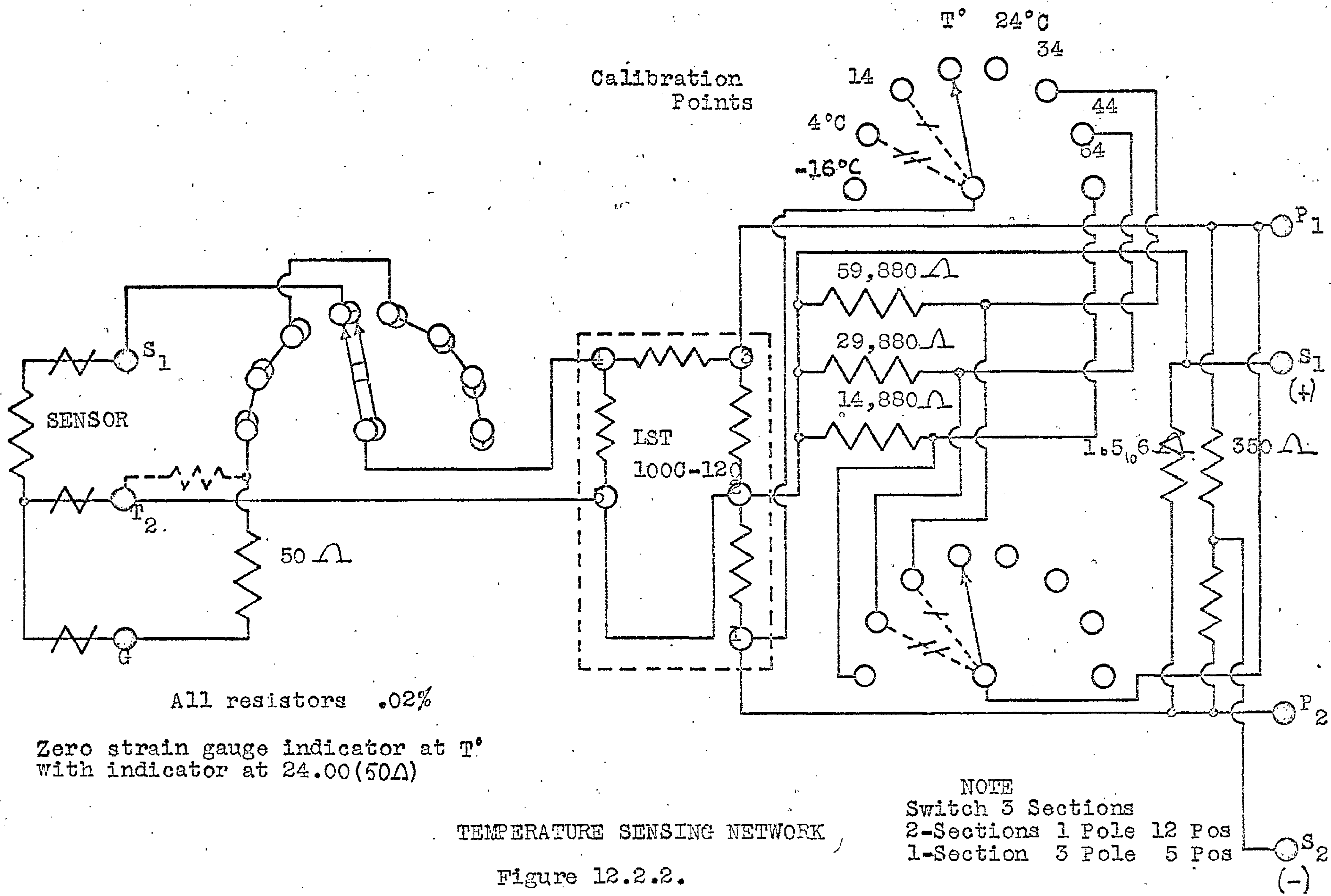

TEMPERATURE SENSING NETWORK

Figure 12.2.2.

The temperature at the hot junction (T_{hj}) was controlled by the heat exchanger and temperature controlled reservoir. The water circulatory pump rate was controlled by a thyristor circuit. The temperature drift during a single test event was less than $\pm .50^{\circ}C$. The steady state temperatures were measured by means of a calibrated Eureka-Constain thermcouple and a vernier potentiometer. Surface temperatures were measured by means of a bonded strain gauge coupled to a strain gauge indicator via a temperature sensing network (figure 12.2.2). The circuit provides a linear output, 120 Ω impedence to the recording instrument, a number of calibration points (in order to establish the absolute value of the temperature and characteristic slope). A test was conducted to compare the temperature readings of the thermocouple to the strain gauge sensor, (using the thermocouple as the base). The temperature range was from $+60^{\circ}C$ to $-70^{\circ}C$. The results indicated that the expected deviation was less than $\mp .50^{\circ}C$ at the extreme conditions.

In order to determine the operational characteristics of the basic thermoelectric module each variable was independently determined. To illiminate the heat losses to the ambient and hence facilitate an accurate heat balance the characteristic tests were conducted under vacuum conditions.($\cong 10_{-6}$" hg.) Plate 12.2.1 illustrates the basic configuration installed within the base of the vacuum chamber. Thermocouples were implanted in EN8 material (above and below the module) in order to determine the heat input and heat rejection rate as a function of junction

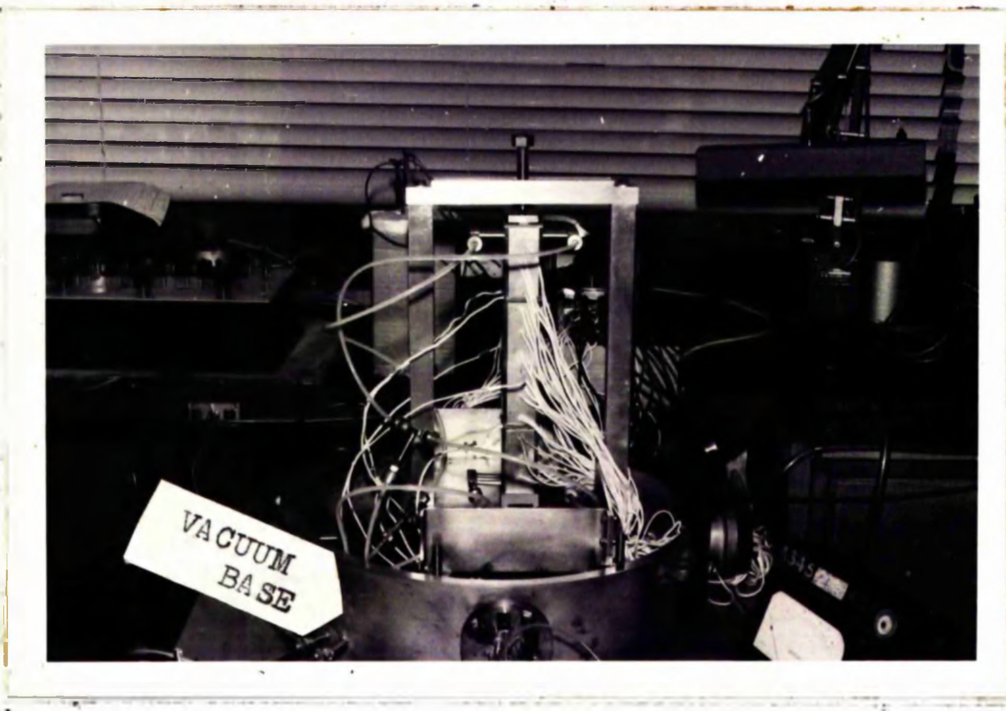

Plate 12.2.1.

Test Configuration for Determining Module Characteristics.

temperatures. The thermal conductivity of EN8 material as a function of temperature was made available to the author by Dr. H. Wong, Department of Aeronautics and Fluid Mechanics, University of Glasgow. The heat input to the thermoelectric module is expressed as:

$$Q_{IN} = \frac{k \Delta T_i A}{X} \qquad 12.2.1.$$

The heat rejection rate is expressed as:

$$Q_R = \frac{k \Delta T_R A}{X} \qquad 12.2.2.$$

The power input to each thermoelectric module is obtained by means of calibrated current and voltage meters ($\mp$ 1% full scale deflection). By measuring the three fundamental heat variables independently the overall module heat balance is expressed as:

$$Q_R = Q_{IN} + P_{IN} \qquad 12.2.3.$$

The results obtained by using equation 12.2.2 were compared to equation 12.2.3 for $\cong$ 480 test conditions. The average deviation was less than 3%. The water flow rate and temperature provides the temperature gradient on the hot side of the module with the heater providing the temperature gradient on the cold side. The junction temperatures are determined by projecting the temperature readings (3 per side, total of 6 per junction) to the positions corresponding the thermoelectric module interface. The test data indicated that the temperature slopes were linear (within $\mp$ 2% maximum) and the projected temperatures at the front and rear of the thermoelectric modules were within $\mp$ 3% (maximum) of each other.

The heat input to the thermoelectric module based on equation 12.2.1 can be compared to the heater power input measured by meters. The heat input to each module is approximately $\frac{1}{2}$ of the heater voltage x heater current. During this phase of testing a comparison was made of the heat input per module; the results indicated less than $\mp$ 3% deviation (full scale deflection) based on meter readings from the values calculated by equation 12.2.1.

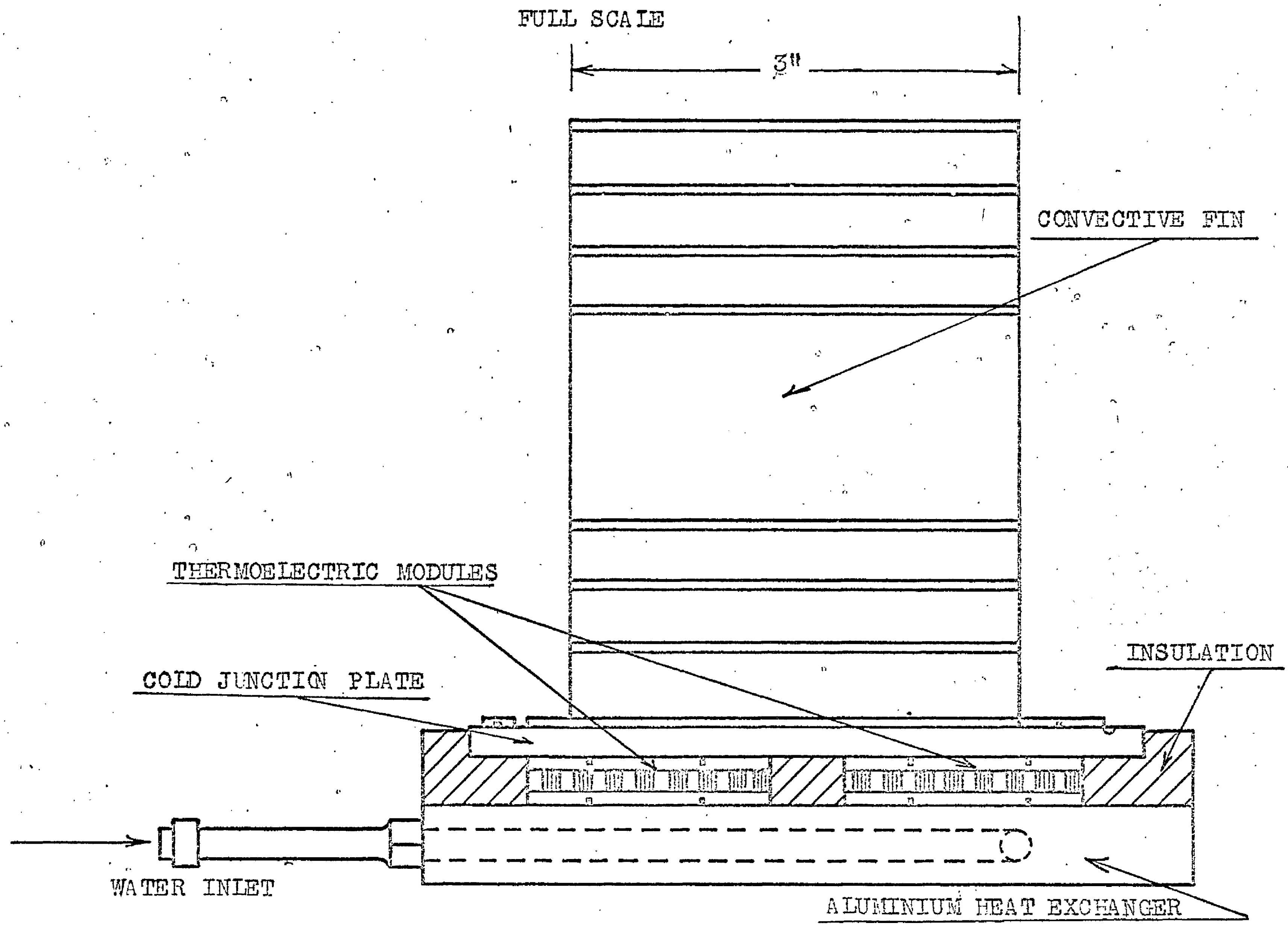
FULL SCALE
3"
CONVECTIVE FIN
THERMOELECTRIC MODULES
INSULATION
COLD JUNCTION PLATE
WATER INLET
ALUMINIUM HEAT EXCHANGER

Plate 12.3.1.1

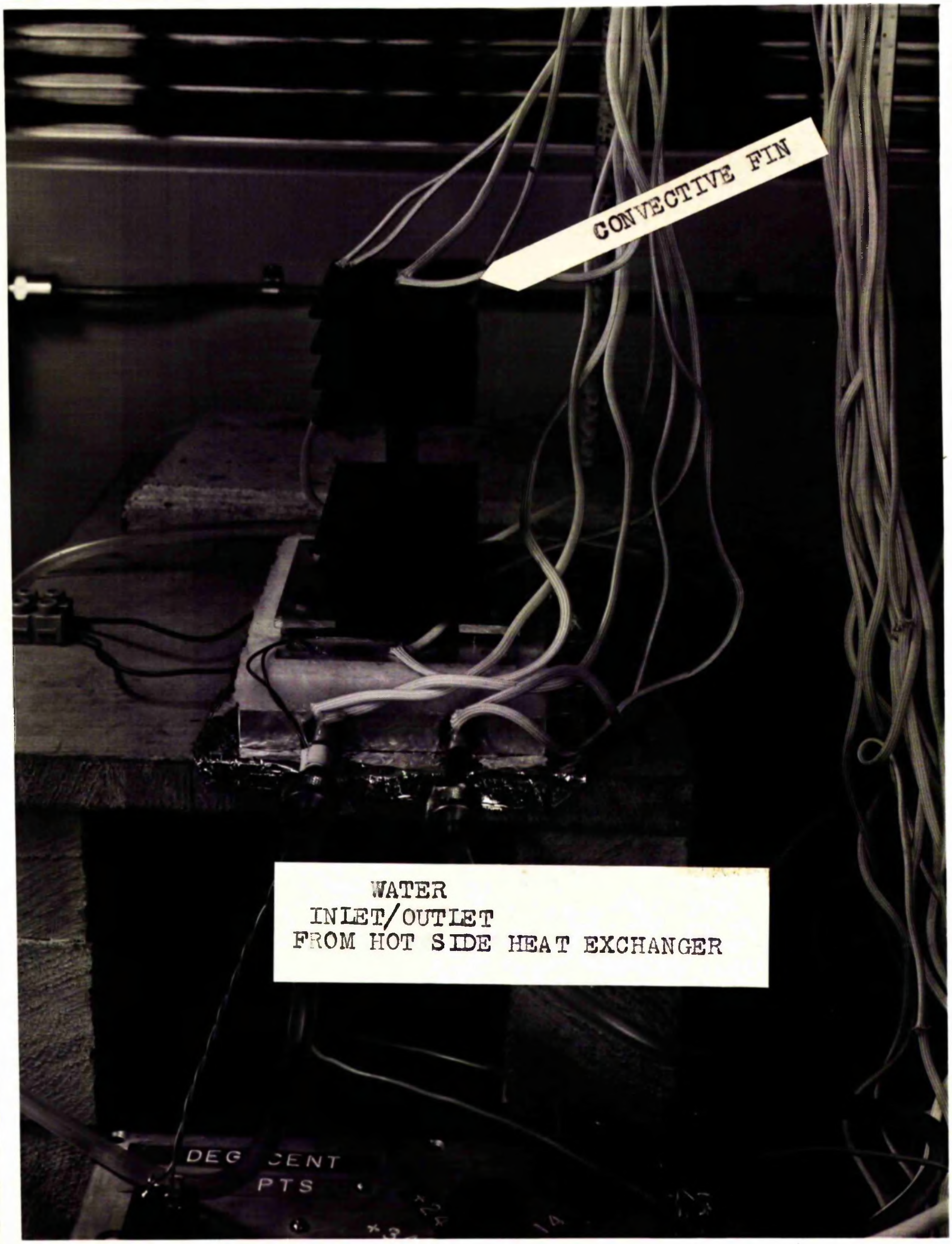

THERMOELECTRIC ASSEMBLY

12.3 Operational Test Between Heat Source and Heat Sink With Finite Heat Transfer Coefficient

12.3.1 Introduction.

The graphical data presented in this section (12.3) was based on two thermoelectric assemblies. Plate 12.3.1.1 shows a convection heat exchange 'tree' mounted to the cold surface of the thermoelectric module. Figure 12.3.1.1 is a cross sectional illustration of the thermoelectric configuration. Appendix N presents the basic material properties of the thermoelements. Plate 12.3.1.2 illustrates the basic equipment required for this test phase. Tests were conducted with andwithout the convective fin attached to the cold plate. The water flow rate on the hot side of the thermoelectric assembly was 755 ml/min ± 5 ml/min (during a data sweep). Statistical tests conducted on data repeatability concluded that at the 5% level of probable significance no difference was evident. Statistical tests were conducted during the testing phase to support the characteristic trends. The room temperature was maintained at 22^{o}C ± 1.5C with a minimum of room turbulence.

12.3.2 Discussion of Test Results.

12.3.2.1 Convection Fin Attached to Cold Side Thermoelectric Assembly.

Figure 12.3.2.1 illustrates the junction temperature

Plate 12.3.1.2


THERMOELECTRIC ASSEMBLY
CONVECTIVE HEAT EXCHANGER
TEMPERATURE THERMOCOUPLES
THERMAL STRAIN GAUGE METER
TEMPERATURE REGULATED WATER BATH
D.C. POWER SUPPLY

Fig. 12.3.2.1.1.

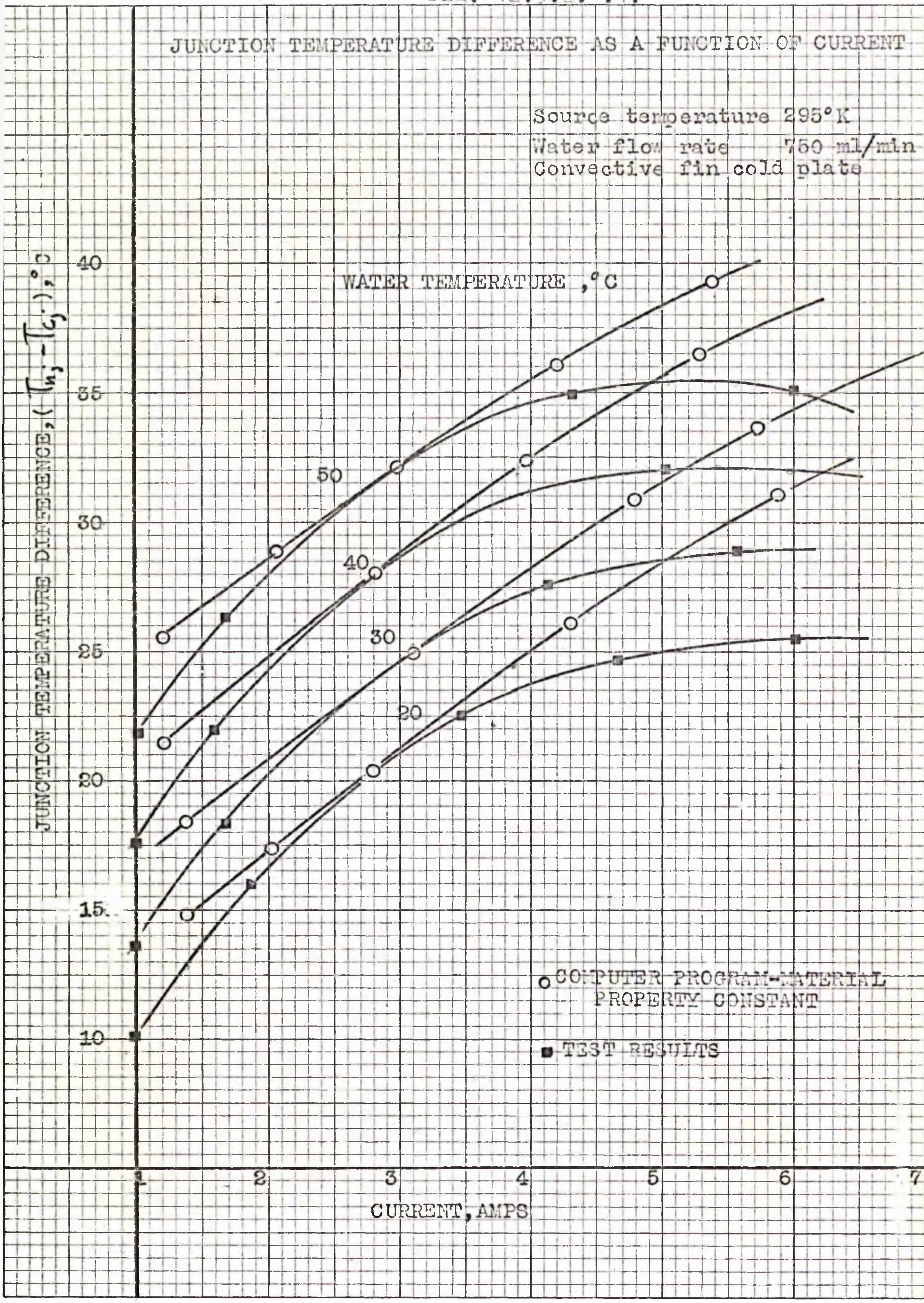
JUNCTION TEMPERATURE DIFFERENCE AS A FUNCTION OF CURRENT
Source temperature 295°K
Water flow rate 750 ml/min
Convective fin cold plate
WATER TEMPERATURE ,°C
50
40
30
20
JUNCTION TEMPERATURE DIFFERENCE, $(T_{h_j} - T_{c_j})$, °C
10
15
20
25
30
35
40
o COMPUTER PROGRAM-MATERIAL PROPERTY CONSTANT
■ TEST RESULTS
1
2
3
4
5
6
7
CURRENT, AMPS

difference as a function of current. The temperature parameters are based on an average value for the first and second thermoelectric module of the assembly (figure 12.3.1.1). A statistical "t" test was conducted of the corresponding temperatures for both modules. The results indicated that both modules exhibited insignificant differences. Computer programme (C.P.5.) output based on the mathematical model of chapter 8.0 is presented on figure 12.3.2.1.1. The computer programme in this instance utilized material properties invariant of temperature. The deviation between the test data and the computer model for $I > 4$ amps is attributed to the material properties exhibiting temperature dependence. The variance appears larger as the inlet water temperature to the hot side heat exchanger increases. The thermoelectric material property at 25°C was supplied by the manufacturer (Appendix N). The representative data points collected during the experiment and presented on figure 12.3.2.1.1 figure 12.3.2.1.2 correspond to the average of 30 to 40 test points with an extremely small standard deviation. Figure 12.3.2.1.2 illustrates the cold side junction (T_{cj}) as a function of inlet water temperature for variation in thermoelectric current. Each constant current line represents between 30 to 40 recorded data points. The thermoelectric assembly (plate 12.3.1.1) exhibited saturation at a current ≥ 3 amps, i.e. for $I > 3$ amps T_{cj} increased. At an inlet water temperature of 20°C with a current of 3 amps, condensation was evident on the thermoelectric assembly. Figure 12.3.

Fig. 12.3.2.1.2.

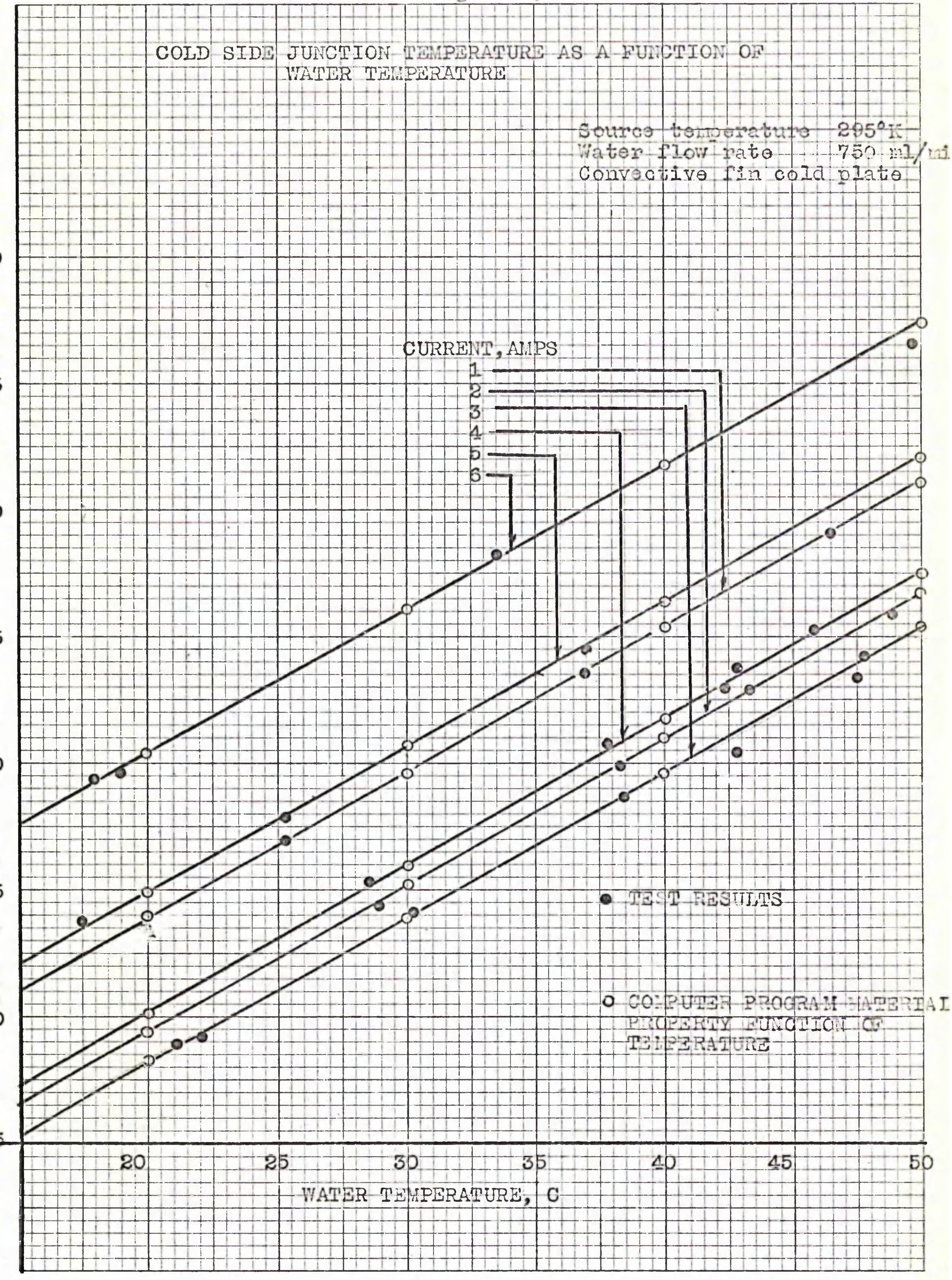
COLD SIDE JUNCTION TEMPERATURE AS A FUNCTION OF WATER TEMPERATURE
Source temperature 295°K
Water flow rate 750 ml/mi
Convective fin cold plate
CURRENT, AMPS
1
2
3
4
5
6
TEST RESULTS
COMPUTER PROGRAM MATERIAL PROPERTY FUNCTION OF TEMPERATURE
20
25
30
35
40
45
50
WATER TEMPERATURE, C

2.1.2 indicates extremely good agreement with the computer model and the test data. To obtain this close correspondence it was necessary to incorporate into the computer programme a temperature dependent linear function (degredration of material property as temperature increases). The incorporation of a material temperature function as a possible solution for the difference between the computer model and the test result was indicative of an appent high system voltage. A high system voltage indicates a large emf ($\alpha \Delta T_j$) indicating that the junction temperature on the hot side is excessive and hence the material properties will require adjustment. Figure 12.3.2.1.3 illustrates the temperature at the root (surface of thermo-electric assembly) of the convective 'tree'. The surface temperature was measured by four thermocouples and one thermo-strain gauge.

12.3.2.2 Thermoelectric Assembly with Flat Plate on Cold Surface.

The basic thermoelectric assembly illustrated on figure 12.3.1.1 is utilized for this test section. The convective fin is removed resulting in a flat plate in contact with the ambient. The purpose of this test section is to determine the adequacy of the computer model to predict module steady state response with a variation in heat transfer exponent (equation 8.3.1.4.). The removing of the convective fin will decrease the heat load and hence the cold surface temperature will decrease as compared to the assembly with the fin (plate 12.3.1.1). Comparison

Fig. 12.3.2.1.3.

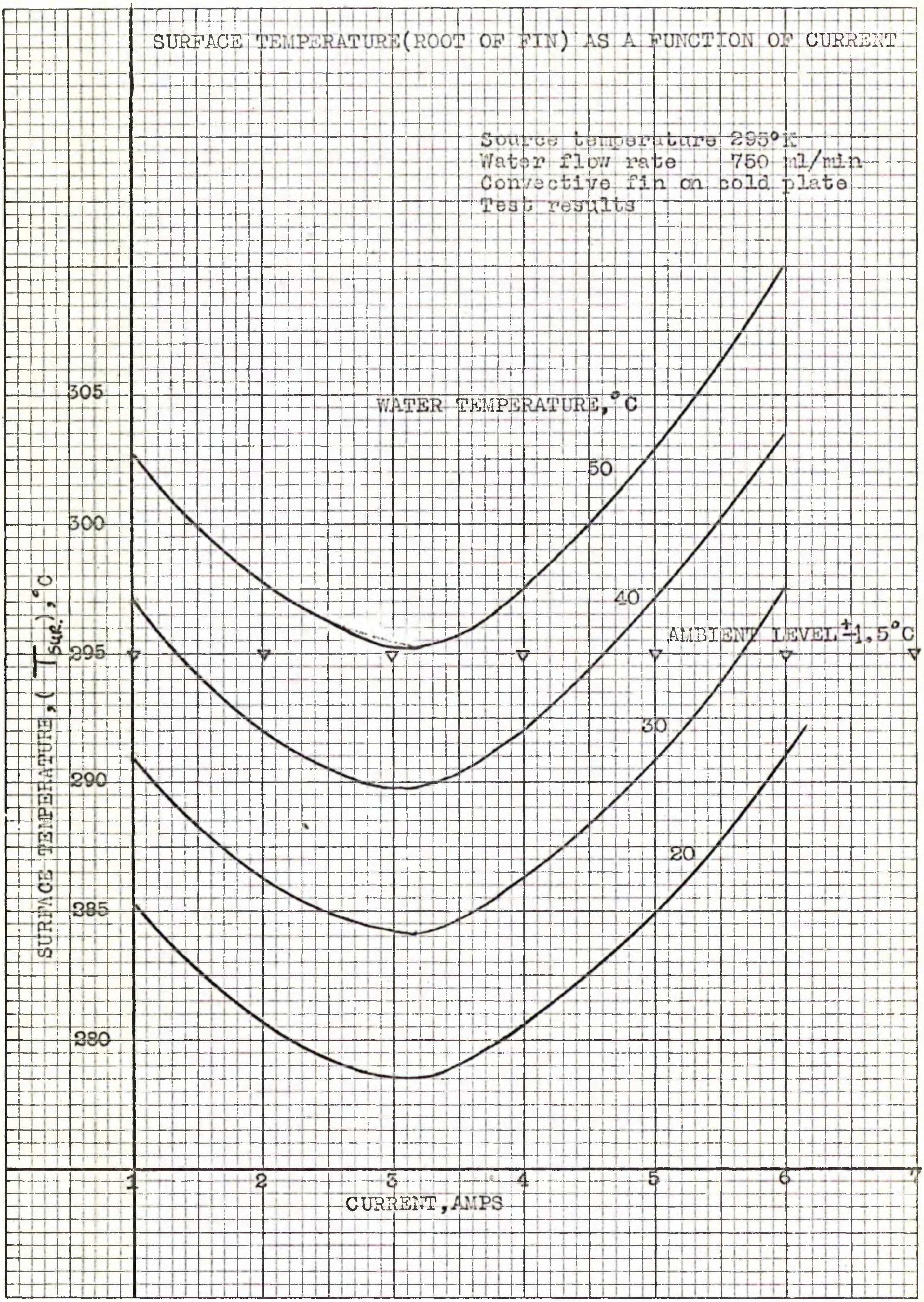
SURFACE TEMPERATURE(ROOT OF FIN) AS A FUNCTION OF CURRENT
Source temperature 295°K
Water flow rate 750 ml/min
Convective fin on cold plate
Test results
WATER TEMPERATURE, °C
50
40
30
20
AMBIENT LEVEL ±1,5°C
305
300
295
290
285
280
SURFACE TEMPERATURE, ($T_{sur.}$), °C
1
2
3
4
5
6
7
CURRENT, AMPS

Fig. 12.3.2.2.1.

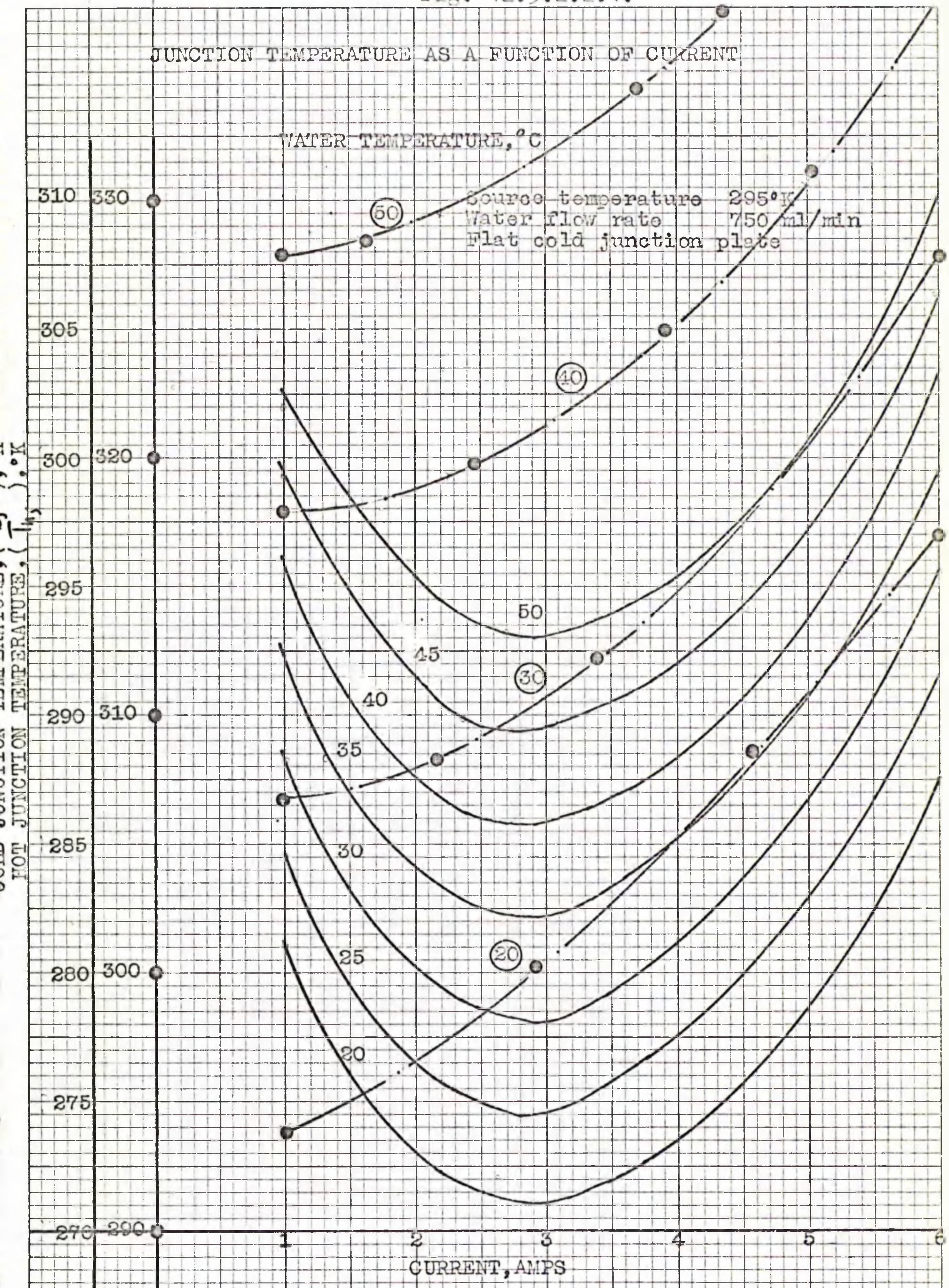
JUNCTION TEMPERATURE AS A FUNCTION OF CURRENT
WATER TEMPERATURE, °C
Source temperature 295°K
Water flow rate 750 ml/min
Flat cold junction plate
HOT JUNCTION TEMPERATURE, (T_H), °K
CURRENT, AMPS
50
40
30
20
50
45
40
35
30
25
20
310
305
300
295
290
285
280
275
270
330
320
310
300
290
1
2
3
4
5
6

of the results in this section can be made directly to the data presented in section 12.3.2.1. The operational variables for both test conditions were maintained constant to facilitate statistical comparisons. High emf (voltage) and high hot junction temperatures were again in evidence. Figure 12.3.2.2.1 shows the junction temperatures as a function of current for variation in the inlet water temperature. The cold side junction temperature reached a minimum of $\cong$ 271°K at 3 amps with a water temperature of 20°C. This is approximately 7.5°C lower than the value presented on figure 12.3.2.1.3 (convective fin attached). Figure 12.3.2.2.2 illustrates the assembly surface temperature as a function of current for variation in inlet water temperature. Figure 12.3.2.2.2 indicates a rapid decrease in surface temperature as a function of current. The minimum value occurs at a relatively low current magnitude. Figure 12.3.2.2.3 illustrates the junction temperature difference as a function of inlet water temperature for variation in current. The dots (⊙) represent a representative number of test points. There is good agreement between the computer programme and the test results. The computer programme employs a temperature dependent linear function as indicated by the results of the previous section.

The high voltage evident during the test was investigated. Figure 12.3.2.2.4 illustrates the hot side heat exchanger. The following conclusion results:

372

Fig. 12.3.2.2.2.

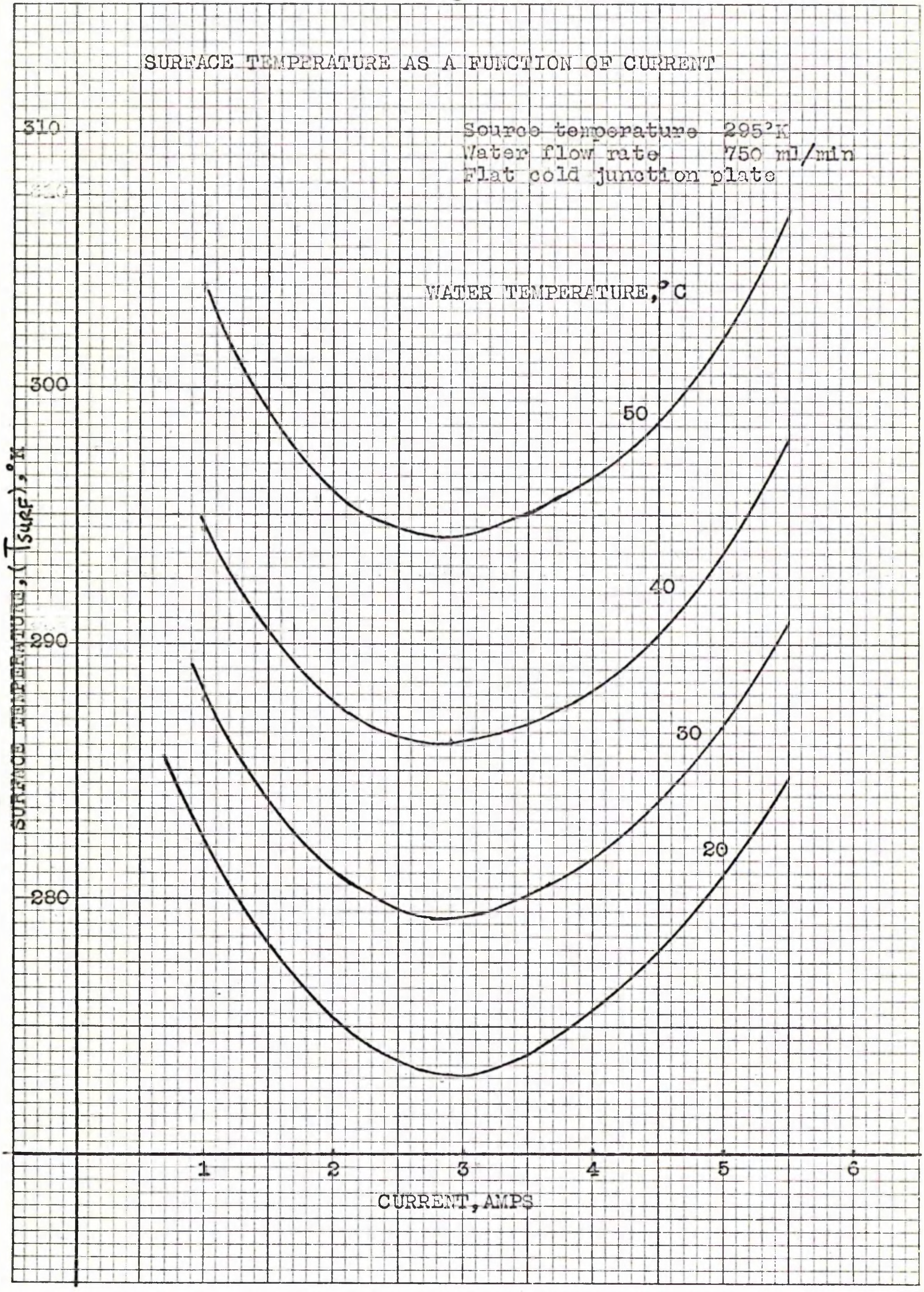

Fig. 12.3.2.2.3.

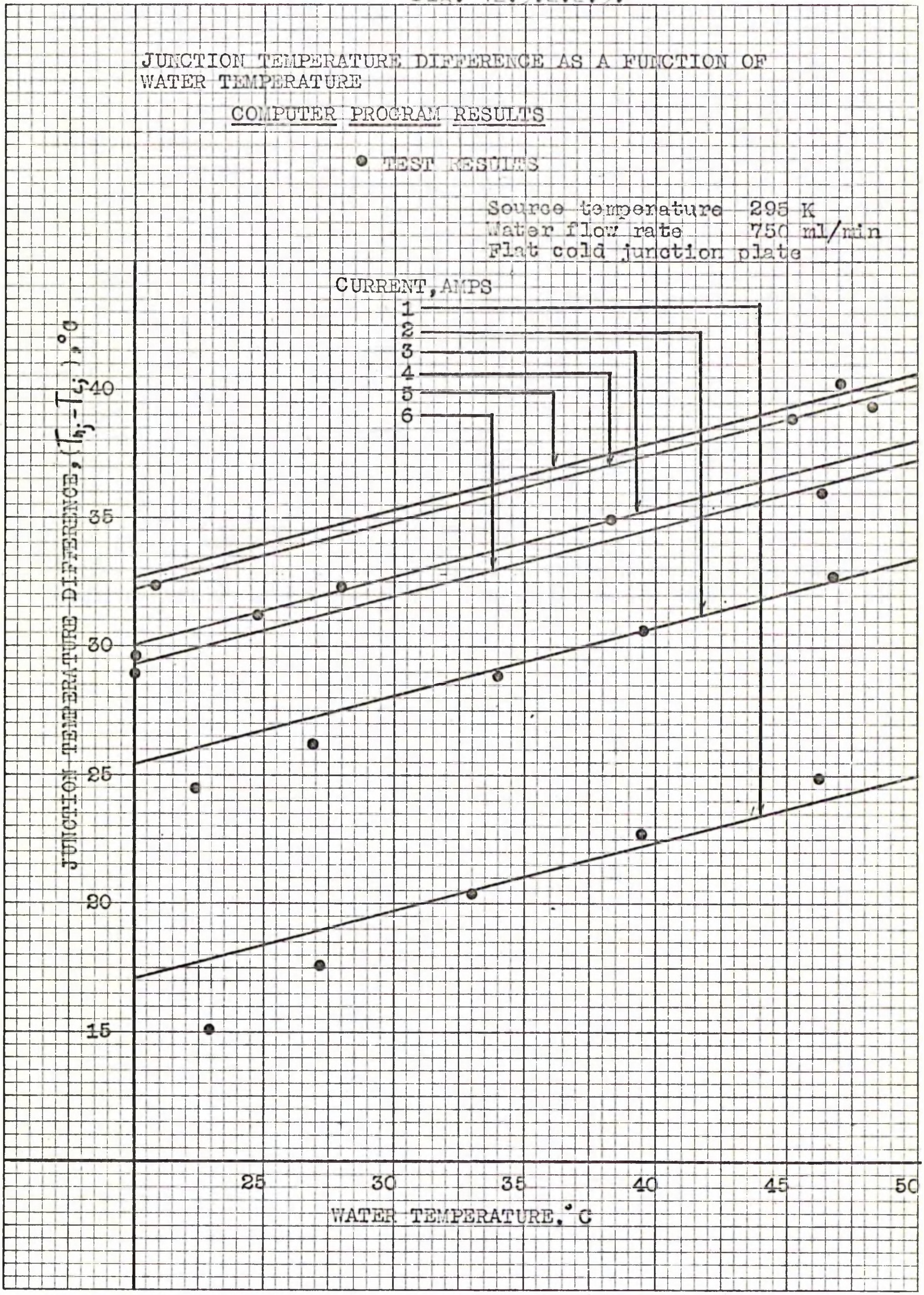
JUNCTION TEMPERATURE DIFFERENCE AS A FUNCTION OF WATER TEMPERATURE
COMPUTER PROGRAM RESULTS
TEST RESULTS
Source temperature 295 K
Water flow rate 750 ml/min
Flat cold junction plate
CURRENT, AMPS
1
2
3
4
5
6
JUNCTION TEMPERATURE DIFFERENCE, $(T_{hj}-T_{cj})$, °C
40
35
30
25
20
15
25
30
35
40
45
50
WATER TEMPERATURE, °C

(1) Internal damage to the thermoelectric modules during transit.

Measurement of the resistance using an A.C. bridge circuit indicated that the resistance is as specified by the manufacturer. The value corresponded to the calculated value (R_{EFF}).

(2) Poor design of the heat exchanger.

Figure 12.3.2.2.4 illustrates the water circulation path. The cooling appears to an 'edge' only.

The heat load and the operational C.O.P. as a function of current for variation in inlet water temperature will be presented in section 12.5.2; figure 12.5.3 and figure 12.5.4.

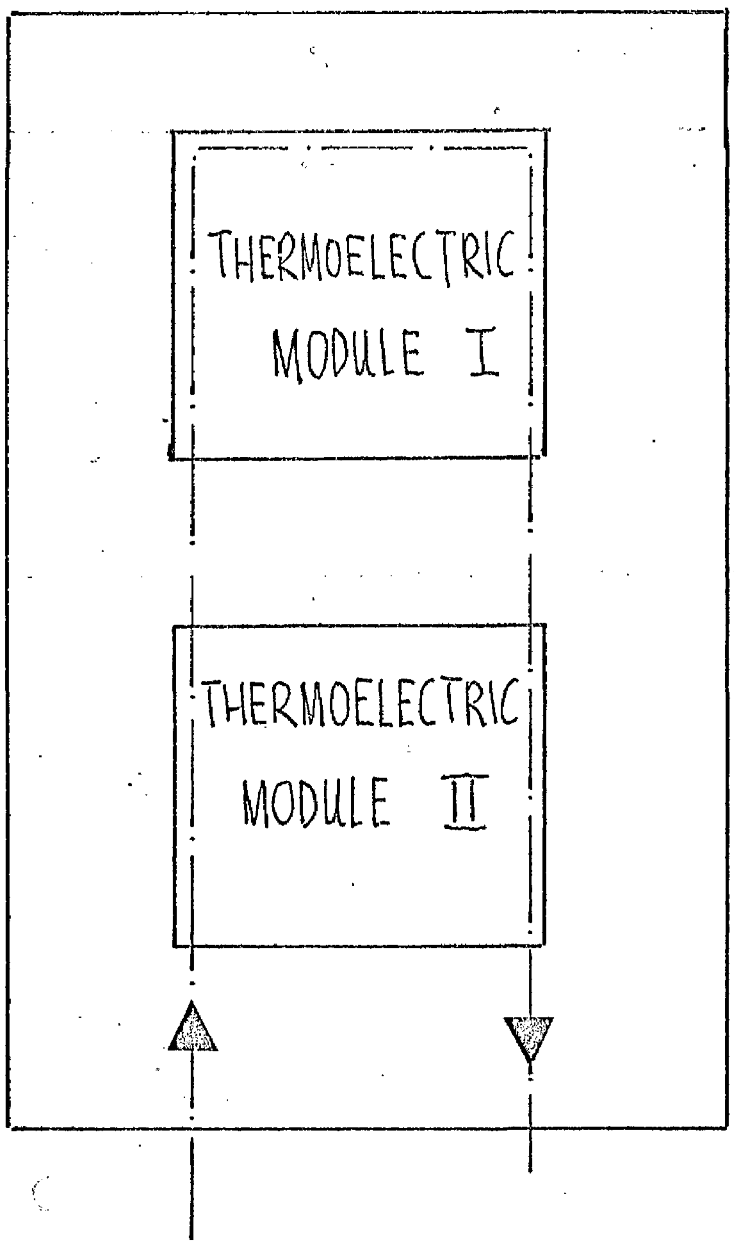

Figure 12.3.2.2.4.

Thermoelectric Assembly Heat Exchanger With Water Circulation Path Indicated.

12.3.2.3 Thermoelectric Module With/ Without Convective Fin Attached to Cold Junction Plate.

This section describes the results of testing a single module with and without a convective fin attached to the cold junction plate. Plate 12.3.2.3.1 shows the heat exchanger attached to the thermoelectric module. The thermoelectric module tested in this section is from the same production lot as those (2) illustrated on figure 12.3.2.2.4.

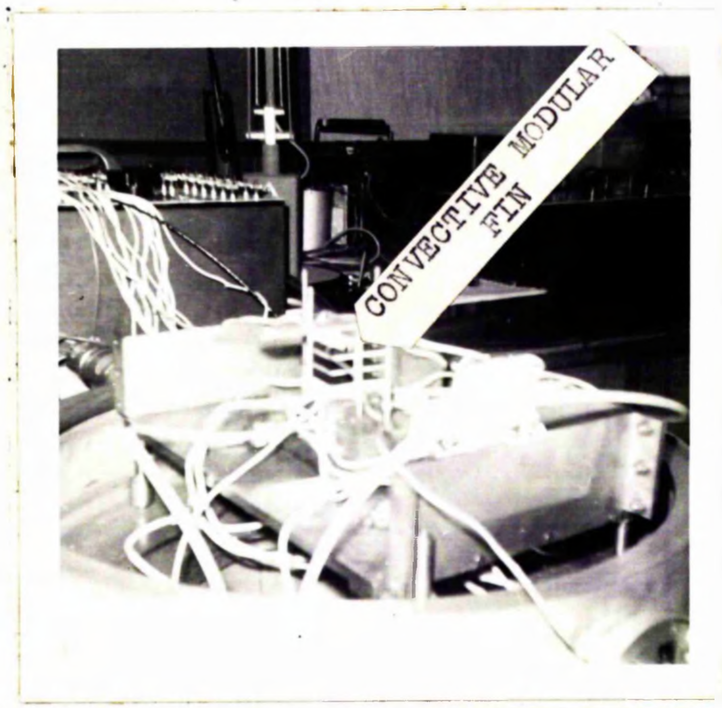

Plate 12.3.2.3.1.

Thermoelectric Module With Convective Fin Attached to Cold Junction Plate.

577

Fig. 12.3.2.3.1.

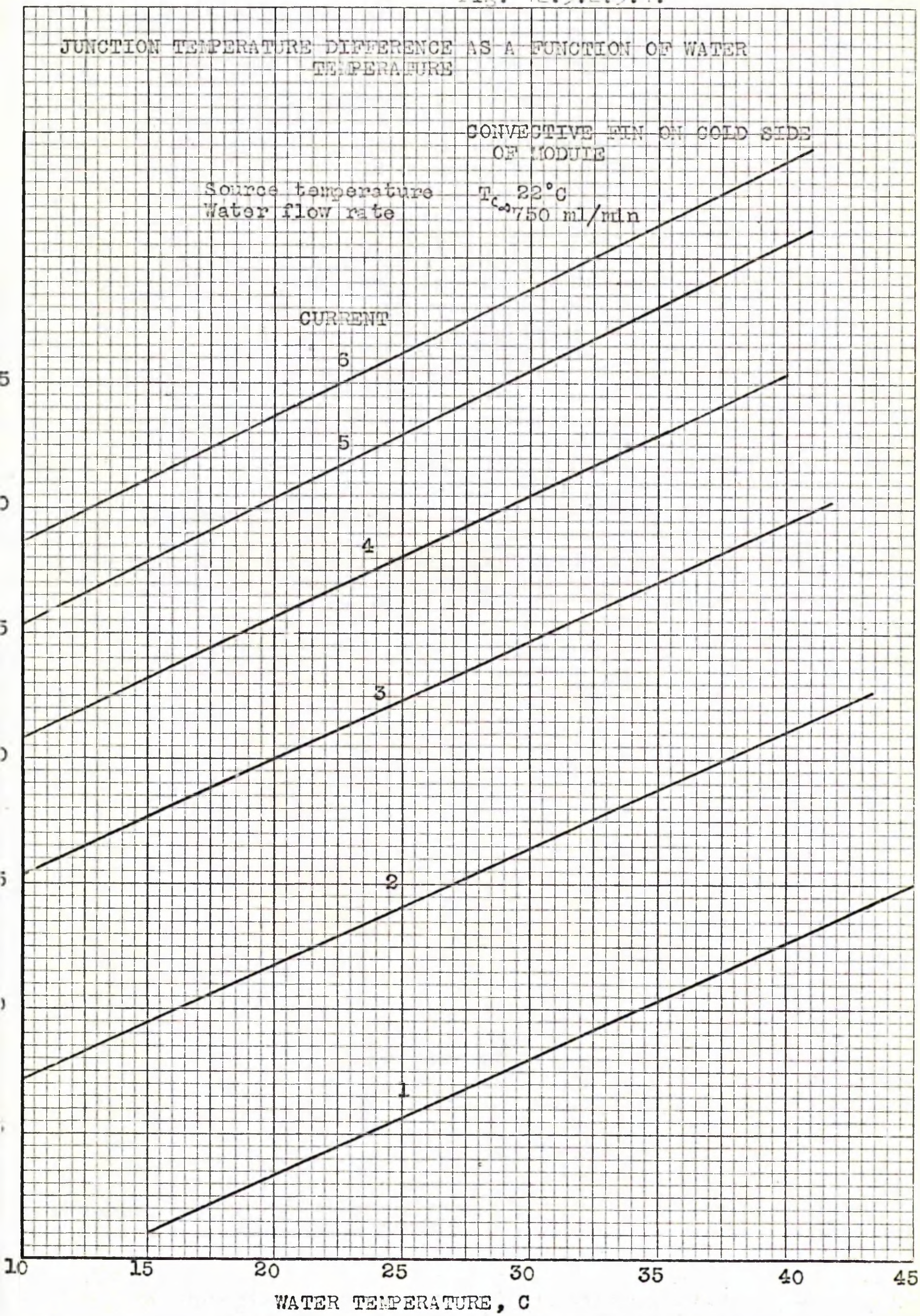

The heat exchanger is constructed from sheet Cu with all contact surfaces polished. Heat exchanger flow rates and ambient conditions are the same as in the previous section. Figure 12.3.2.3.1 illustrates the junction temperature difference as a function of inlet water temperature for variation in current. Comparison of the junction temperature trends with the previous section indicate a general improvement. Figure 12.3.2.3.2 illustrates the junction temperature difference with the cold junction plate exposed to the atmosphere. The junction temperature difference with the convective fin removed is larger than with the fin attached. With the fin removed the heat load on the module decreases and for fixed hot junction temperature the cold junction temperature will decrease thereby, ΔT_j increases. Figure 12.3.2.3.3 shows the cold side plate temperature as a function of inlet water temperature. The results support the feasibility of quick freezing biological specimens under ambient room conditions. For a water temperature of 20°C and a current of 5 amps the cold side temperature is $\cong 253^{\circ}$K (-20°C).

12.3.3 Summary.

The computer model formulated to determine the operational characteristics between heat source and heat sink is in good agreement with the test results.

Extreme care is required to match the heat rejection

Fig. 12.3.2.3.2.

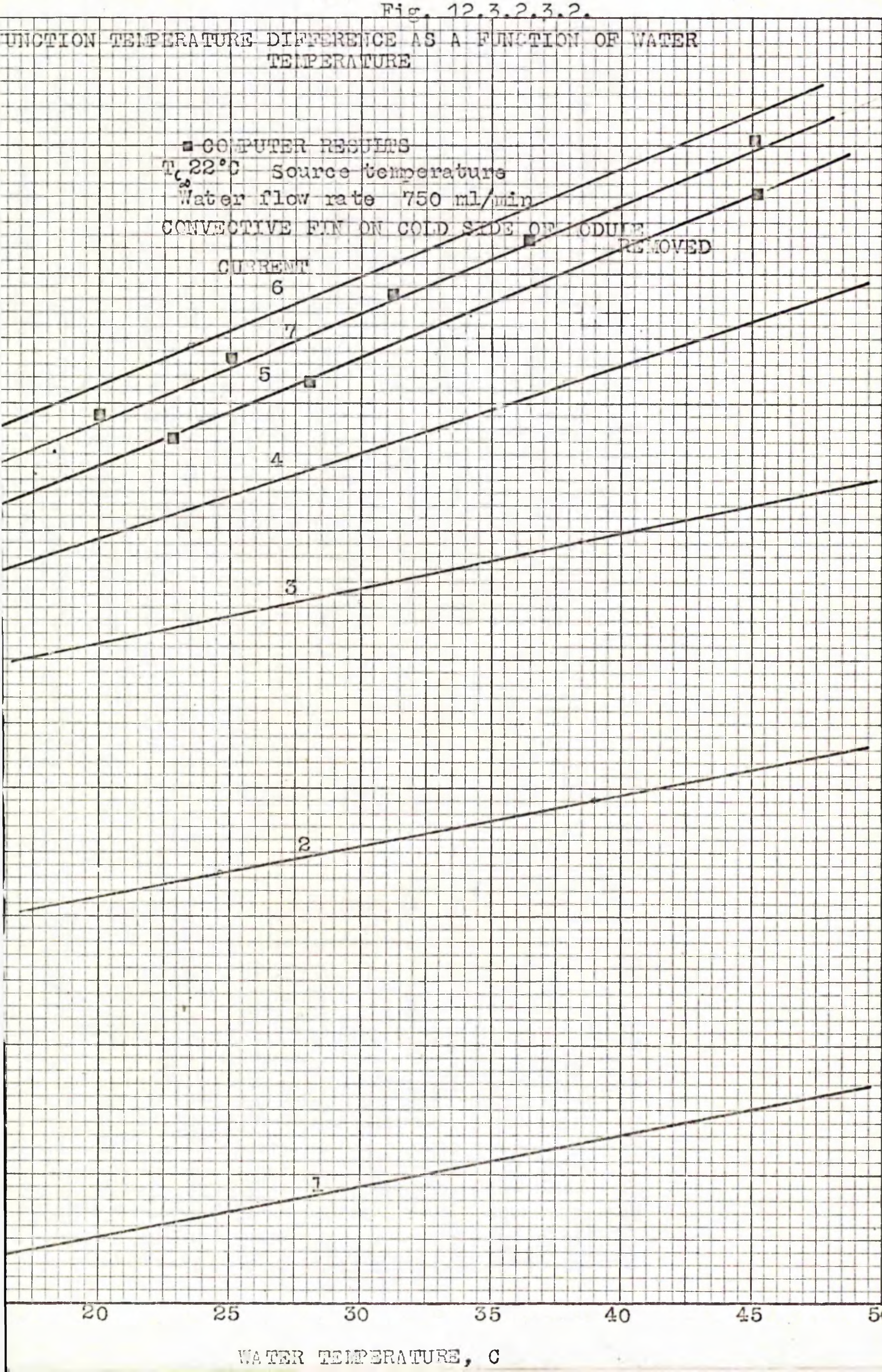
UNCTION TEMPERATURE DIFFERENCE AS A FUNCTION OF WATER TEMPERATURE
■ COMPUTER RESULTS
$T_{c\infty}$ 22°C Source temperature
Water flow rate 750 ml/min
CONVECTIVE FIN ON COLD SIDE OF MODULE REMOVED
CURRENT
6
7
5
4
3
2
1
20
25
30
35
40
45
50
WATER TEMPERATURE, C

Fig. 12.3.2.3.3.

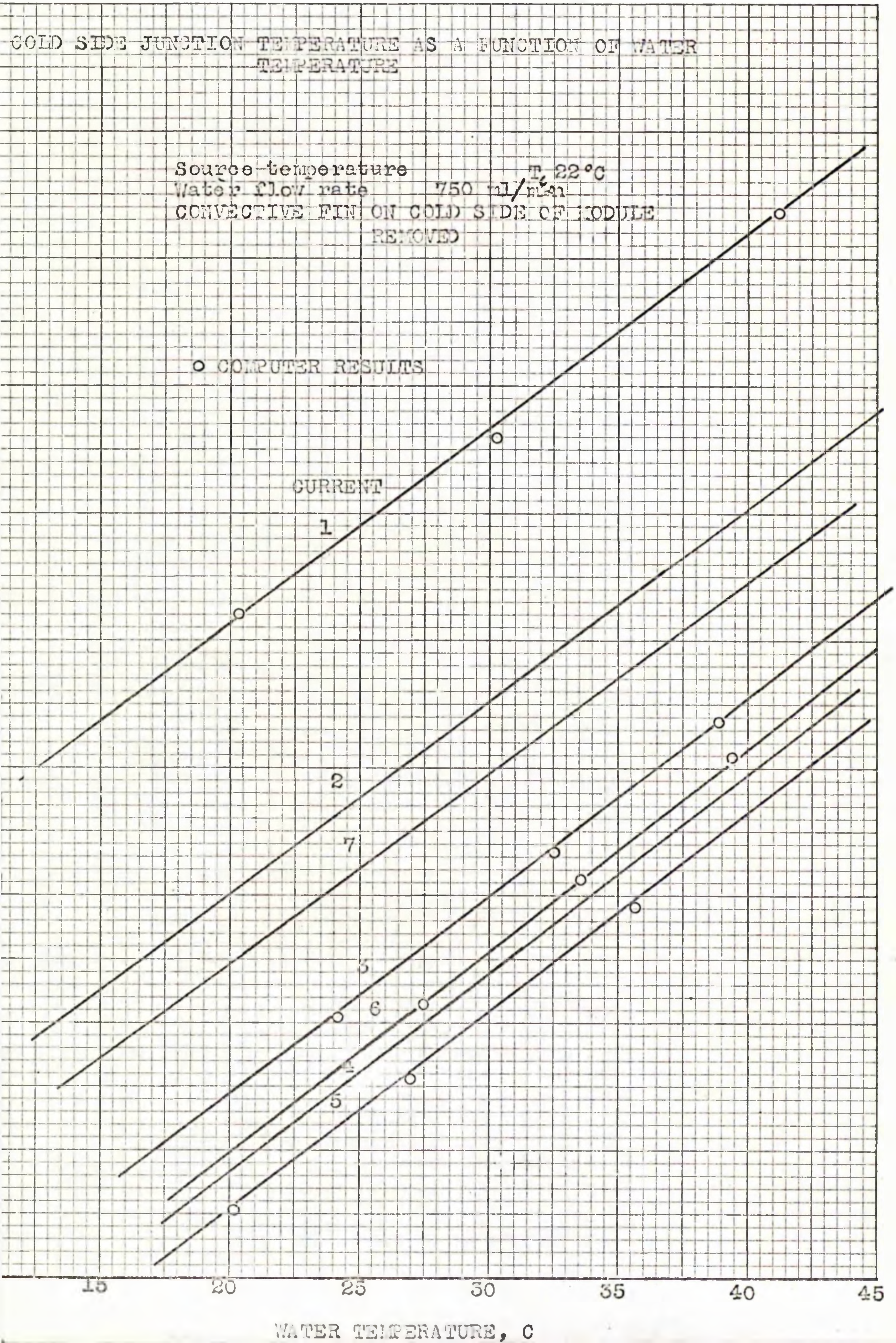

COLD SIDE JUNCTION TEMPERATURE AS A FUNCTION OF WATER TEMPERATURE
Source temperature T_c 22°C
Water flow rate 750 ml/min
CONVECTIVE FIN ON COLD SIDE OF MODULE REMOVED
o COMPUTER RESULTS
CURRENT
1
2
7
3
6
4
5
15
20
25
30
35
40
45
WATER TEMPERATURE, C

rate (Q_R) of the thermoelectric module to the capability of the heat exchanger. Considerable improvement in performance can result by increasing the heat exchange wetted area in contact with the module.

The contact resistance between the module assembly and the heat exchanger interface must be as low as economically feasible. Poor contact design (a relative term) results in large ΔT_j across the junction with subsequent loss in performance.

12.4 Maximum Junction Temperature Difference Determination.

12.4.1 Introduction.

Measurement of $\Delta T_{j_{max}}$ can assist in evaluating elementary forms of the Peltier device. The Peltier devices tested for this section were as follows:

(1) Single Stage Device

(a) Thermoelectric assembly (plate 12.3.1.1). A 2" thick polystyrene insulation sheet was attached to the cold junction plate. The insulation decreases the heat load on the thermoelectric assembly and is expected to simulate $Q_s \longrightarrow 0$ (a condition indicated in section 6.5.6. for obtaining $\Delta T_{j_{max}}$).

(b) Thermoelectric module (plate 12.3.2.3.1).

The tests were conducted in a vacuum chamber under a vacuum of $\cong 10_{-6}$"hg. Two test configurations were employed. The first test configuration positioned two thermoelectric modules with their cold junction plates opposed. Figure 12.4.1.1 illustrates the basic assembly configuration. The second configuration consisted of placing a highly polished plate in place of the upper module/heat exchanger as illustrated on figure 12.4.1.1 to act as a radiation shield. The flow rates are the same for both configuration.

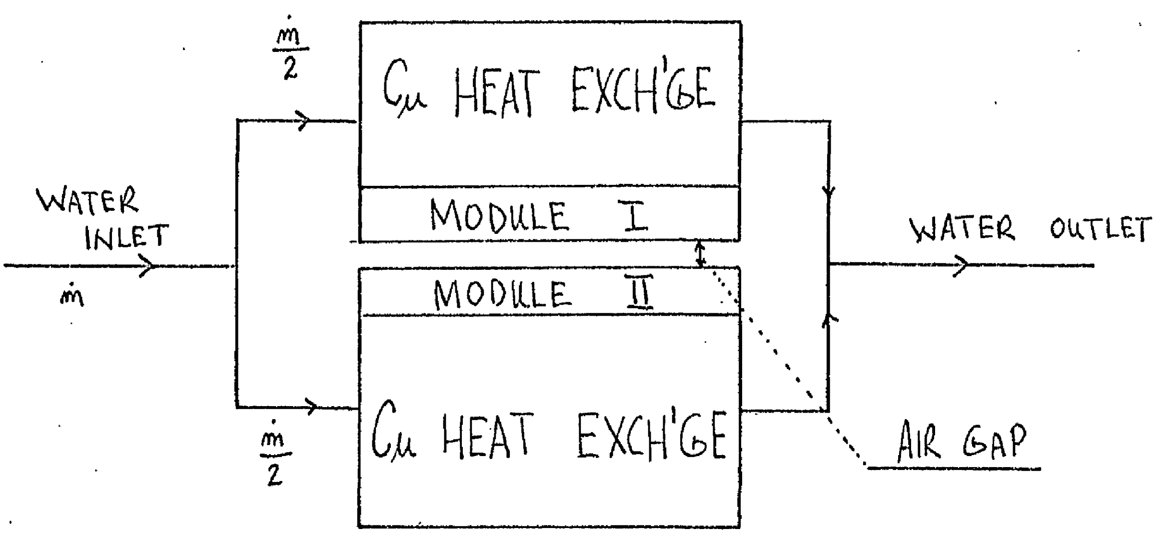

Figure 12.4.1.1.

Opposed Module Configuration.

(2) Two stage Device

A two stage device as shown on plate 12.4.1.1 was tested under vacuum conditions. The Cu heat exchanger of the previous section was utilized on the hot side of the two stage device. Plate 12.4.1.2 shows a side view of the two stage device, with a free convective 'tree' attached to the hot junction plate. A radiation shield was utilized near the upper stage to reduce any radiation heat.

12.4.2 <u>Background</u>.

When considering the quality of thermoelectric material to perform as a couple of a Peltier device the thermoelectric figure of merit is usually used. The material figure of merit, Z is expressed as:

$$Z = \frac{\alpha_{np}^2}{RK} \qquad 12.4.2.1.$$

where:

α_{np} Seebeck couple coefficient, volts/$^{\circ}$K
R Couple electrical resistance, ohms
K Couple thermal conductance, watts

The determination of Z is often made by measuring the three material parameters and computing Z by equation 12.4.2.1. An alternative method utilized is considered below:

In the following discussion it is convenient to

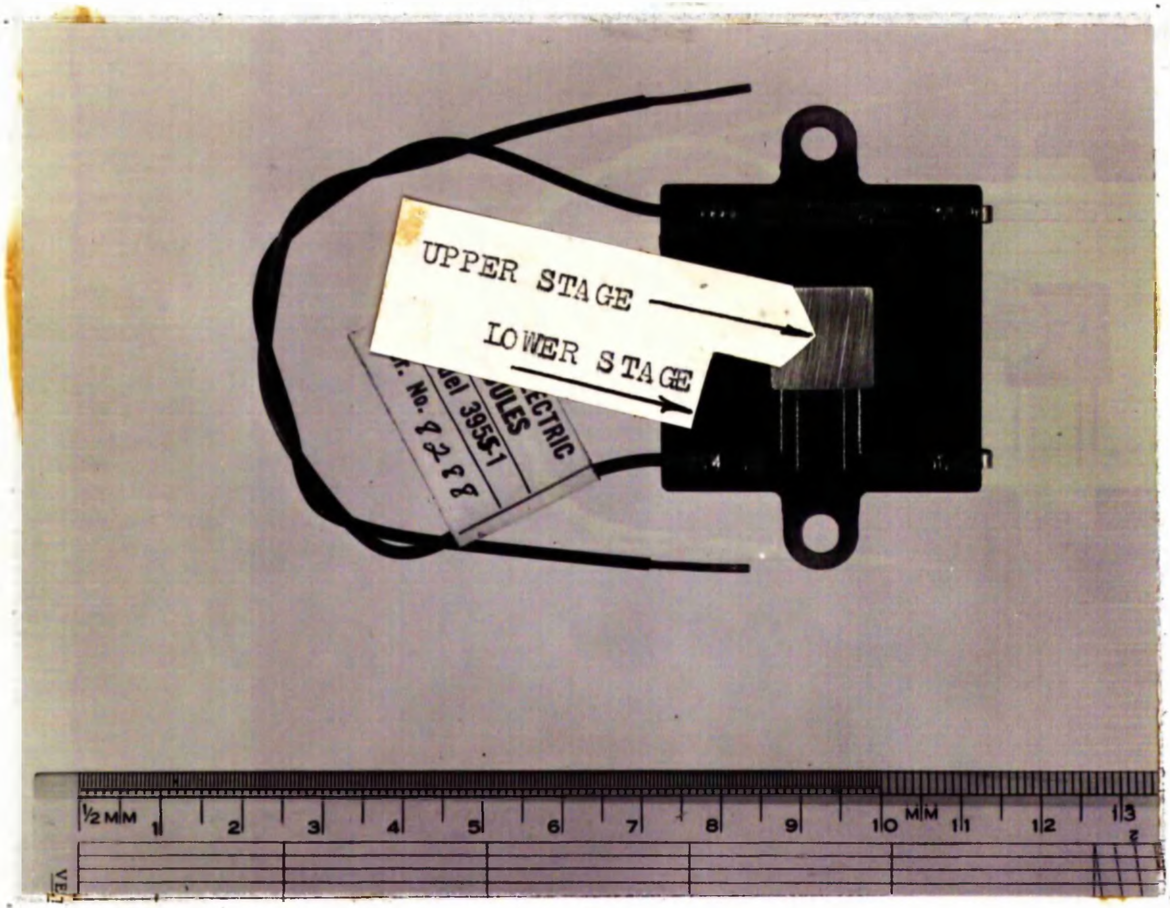

Plate 12.4.1.1

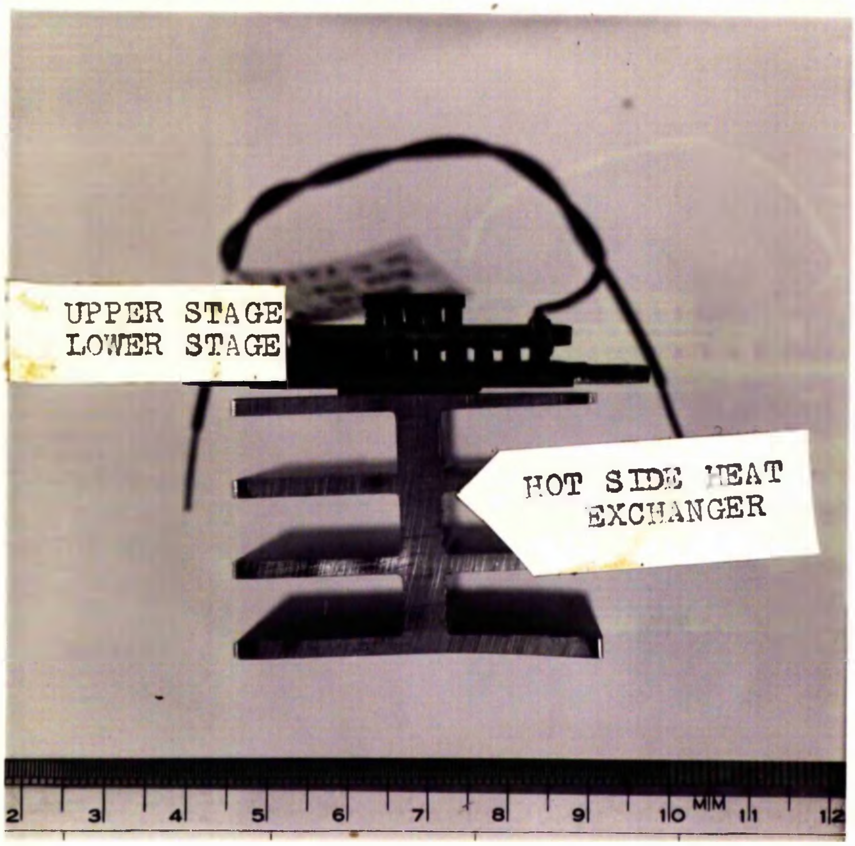

Plate 12.4.1.2

consider a Peltier couple as shown:

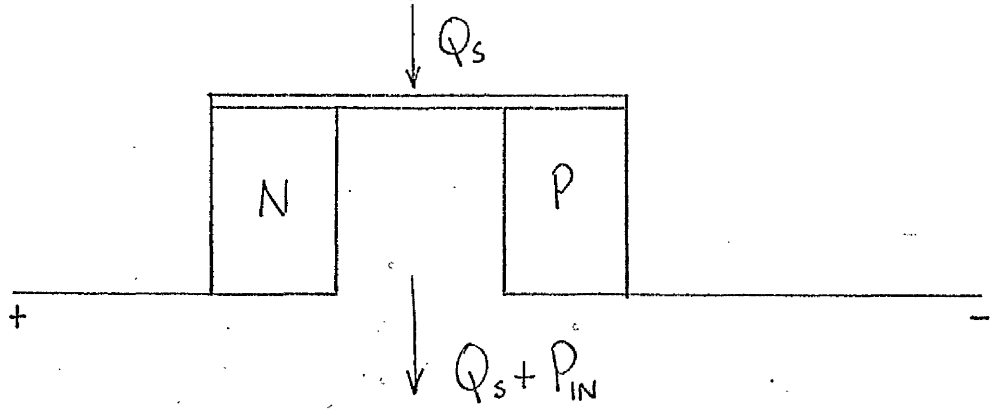

The net heat absorbed at the cold junction is:

$$Q_s = T_{cj} I \alpha_{np} - \frac{1}{2} I^2 R - K \Delta T_j \qquad 6.3.10.$$

The current required to maximize Q_s is:

$$I_Q = \frac{\alpha_{np} T_{cj}}{R} \qquad 6.5.4.1.$$

With this current and Q_s = 0 (the cold junction thermally insulated) then:

$$\Delta T_{j_{max}} = \frac{0.5\, T_{cj}^2\, \alpha_{np}^2}{R \cdot K} \qquad 6.5.4.6.$$

With the electrical resistance as:

$$R = \frac{l}{A}\left[\rho_n + \rho_p\right] \qquad 12.4.2.2.$$

and:

$$K = \frac{A}{l}\left[k_n + k_p\right] \qquad 12.4.2.4.$$

There is a fundamental assumption that is introduced into the analysis (and discussed in section 6.5.1, comment). It is that the temperatures are invariant of current. This assumption when applied to the derivative of Q_s with respect to the current results as follows:

$$\frac{dQ}{dI} = T_{cj}\, \alpha_{np} - IR \qquad 12.4.2.5.$$

Using equation 12.4.2.4 with the measured value of $\Delta T_{j\,max}$ (at I_Q) and Z the figure of merit may be computed. There is a distinction between Z so determined and one determined from measuring, $\alpha_n, \alpha_p, \rho, k,$ seperately. This test method (measuring $\Delta T_{j\,max}$) determines a composite or effective Z for the Peltier device. In the material measurement procedure the materials have a relatively small temperature difference; while in the $\Delta T_{j\,max}$ experiment a large temperature difference will exist. In the range: $(T_{hj} \leq T \leq T_{cj})$ the figure of merit is not necessarily constant; but is usually a function of temperature. In addition, it is difficult in the $\Delta T_{j\,max}$ method to separate the effects of thermal and electrical junction resistance. Consequently, the $\Delta T_{j\,max}$ method is expected to yield a Z - effective (as illustrated by equation 7.2.5.1) which is less than computed from the separate material parameter method.

These considerations not with standing, the measurements are useful as a direct indication of the expected performance of a Peltier device (the equations

Fig. 12.4.3.1.1.

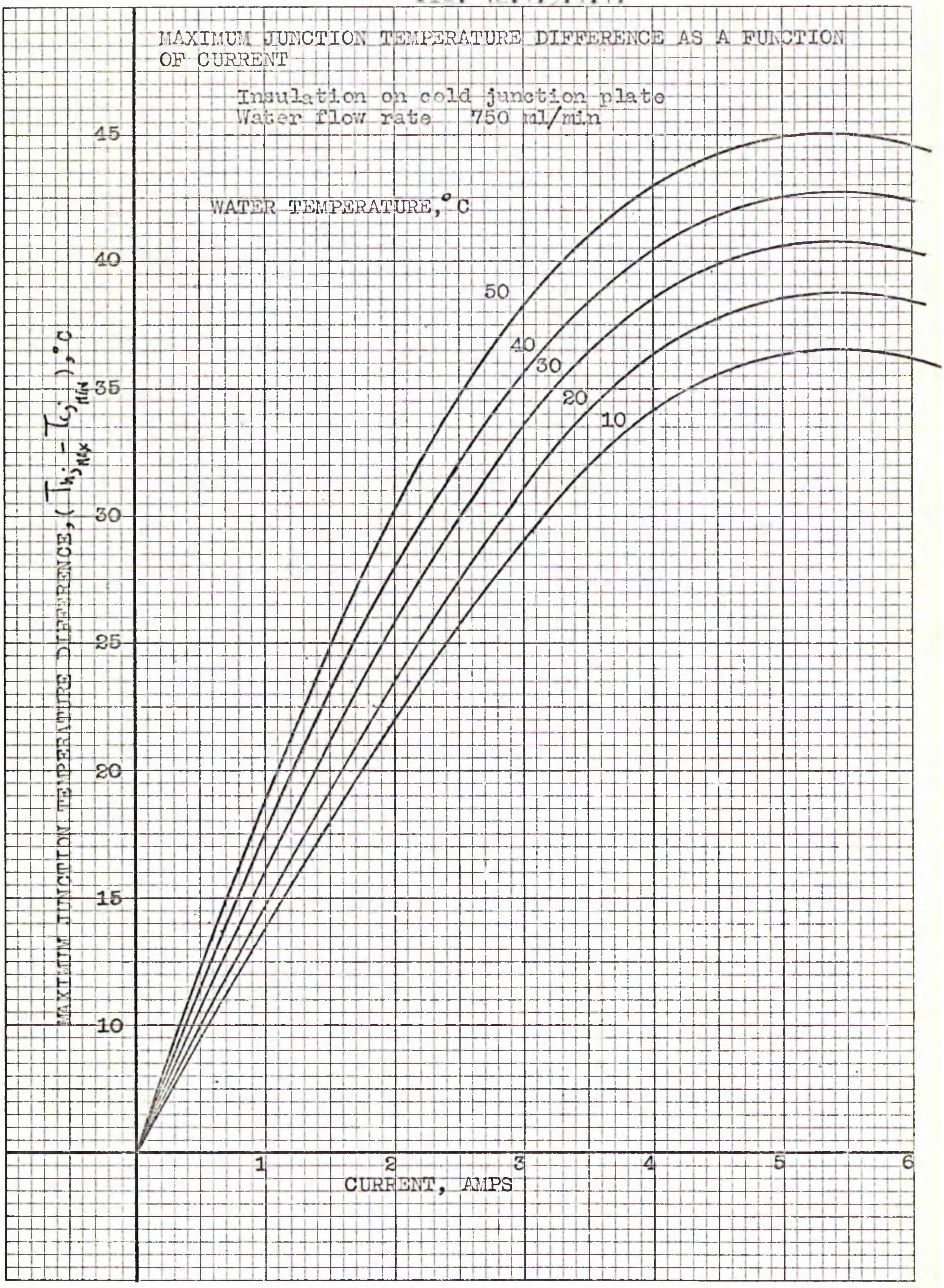
MAXIMUM JUNCTION TEMPERATURE DIFFERENCE AS A FUNCTION OF CURRENT
Insulation on cold junction plate
Water flow rate 750 ml/min
WATER TEMPERATURE, °C
50
40
30
20
10
MAXIMUM JUNCTION TEMPERATURE DIFFERENCE, $(T_{h_j,max} - T_{c_j,min})$, °C
45
40
35
30
25
20
15
10
1
2
3
4
5
6
CURRENT, AMPS

of section 6.6 can be utilized to determine expected performance). If the material characteristics comprising the thermoelectric couple are known then the figure of merit of the material may be compared with the effective figure of merit from the $\Delta T_{j_{max}}$ method. This allows for an evaluation in a quasi-quantitative fashion of the effect of junction resistance and material variation with temperature. In other words, this is a measure of the success of the fabrication processes employed. In addition to the figure of merit, the $\Delta T_{j_{max}}$ measurement establishes another useful parameter, the current required for maximizing the heat pump rate.

12.4.3 Single Stage Device.

12.4.3.1 Thermoelectric Assembly.

Figure 12.3.1.1 is the basic thermoelectric assembly that is modified to determine the maximum junction temperature difference ($\Delta T_{j_{max}}$) when $\varphi_S \longrightarrow 0$. The assembly without cold plate convection fin was encapsulated with insulation material. The insulation material acts as a thermal barrier between the room ambient and the cold face of the thermoelectric assembly. Figure 12.4.3.1.1 is a plot of $\Delta T_{j_{max}}$ ($\varphi \overset{\sim}{=}\!\!\longrightarrow 0$) as a function of current for variation in the water inlet temperature to the hot side heat exchanger. The maximum ΔT_j occurs at approximately 5.5 amps. The magnitude of ΔT_j ($\varphi \xrightarrow{\sim} 0$) as compared to figure 12.3.2.2.3 is not encouraging. The general trends appear to indicate a 5°C to 10°C increase in ΔT_j

Fig. 12.4.3.1.2.

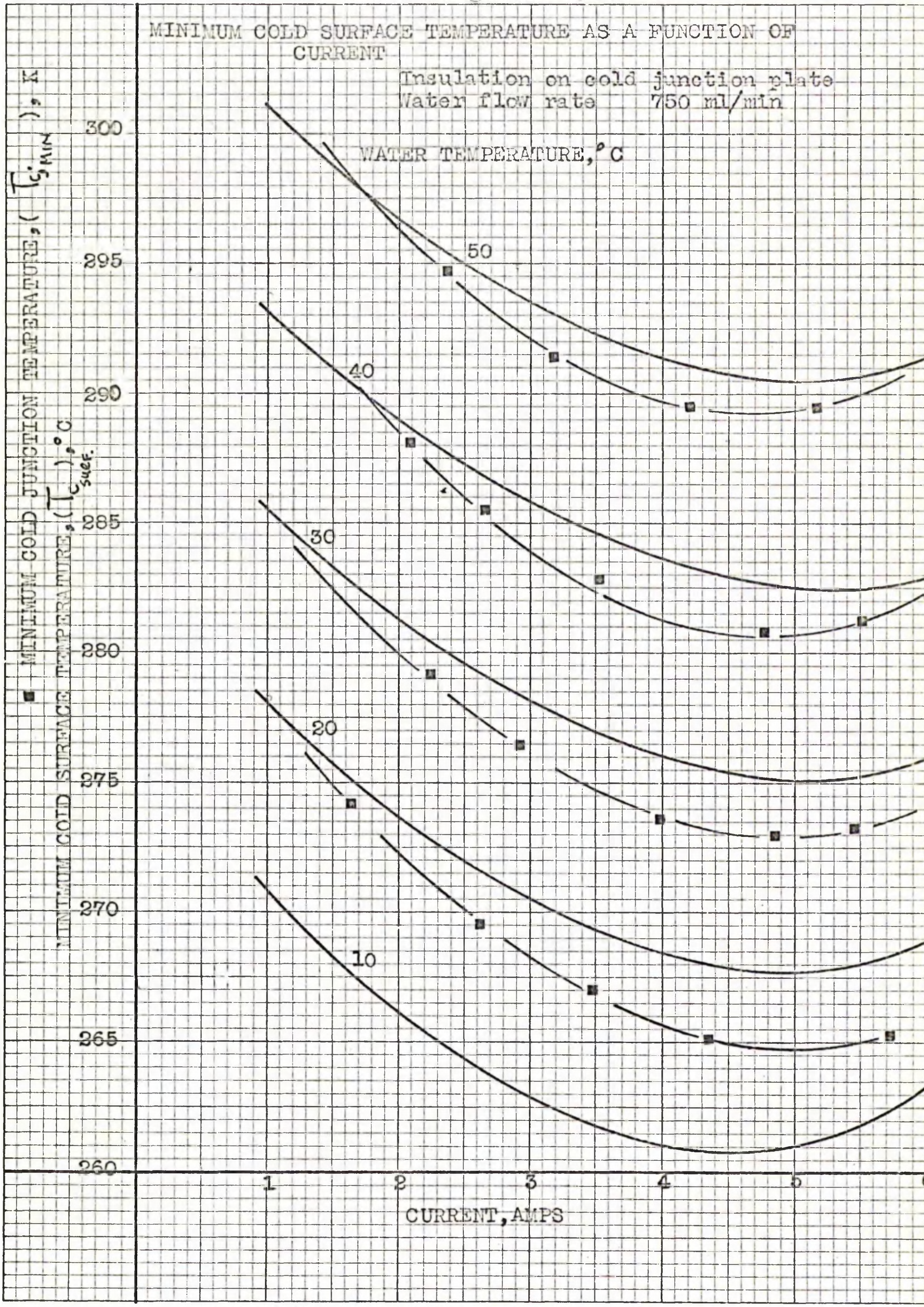
MINIMUM COLD SURFACE TEMPERATURE AS A FUNCTION OF CURRENT
Insulation on cold junction plate
Water flow rate 750 ml/min
WATER TEMPERATURE, °C
50
40
30
20
10
■ MINIMUM COLD JUNCTION TEMPERATURE, ($T_{cj, MIN}$), K
MINIMUM COLD SURFACE TEMPERATURE, ($T_{c_{surf.}}$), °C
300
295
290
285
280
275
270
265
260
1
2
3
4
5
6
CURRENT, AMPS

for $Q \cong 0$ as compared to the assembly where a flat plate is exposed to the ambient. Figure 12.4.3.1.2 indicates $T_{cj_{MIN}}$ and $T_{c_{SURFACE\ MIN}}$ as a function of current for variation in the inlet water temperature. To operate with a surface temperature below 273°K (0°C) requires an inlet water temperature of less than 20°C and $I \geq 3$ amps. Figure 12.4.3.1.1 and figure 12.4.3.1.2 contains the data required to calculate the effective figure of merit. To illustrate consider the water inlet temperature of 20°C then:

$$Z_{EFF} \cong \frac{2(38.8)}{(265)^2} \quad \text{at} \quad I_{\varphi} \cong 5.5 \text{ amps}$$

$$Z_{EFF} \cong 1.11_{10}{-3}/^{\circ}C$$

Data recorded by the manufacturer indicated the following:

$$Z_{EFF} \cong \frac{2(48)}{(246)^2} \quad \text{at} \quad I_{\varphi} \cong 6.0 \text{ amps}$$

with:

$$Z_{EFF} \cong 1.59_{10}{-3}/^{\circ}C$$

The test results in general indicate that the assembly exhibits a minimum temperature at a relatively low current value. From equation 6.5.4.1 and figure 12.4.3.1.2 the material sensitivity can be determined from:

$$\left(\frac{\alpha_{mp}}{\rho}\right) = \frac{K''}{T_{cj_{min}}} \qquad 12.4.3.1.1.$$

Fig. 12.4.3.2.1.

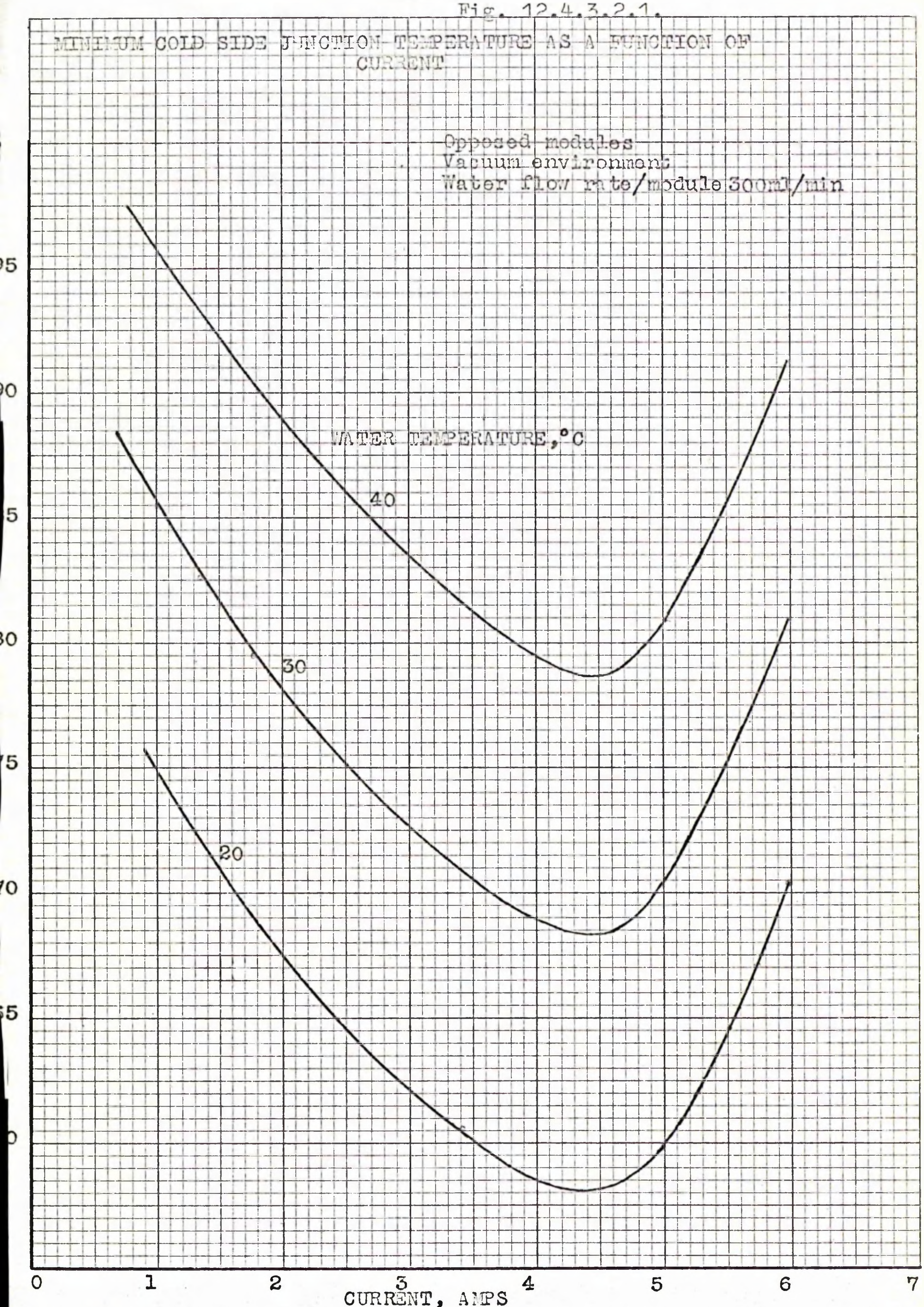
MINIMUM COLD SIDE JUNCTION TEMPERATURE AS A FUNCTION OF CURRENT
Opposed modules
Vacuum environment
Water flow rate/module 300ml/min
WATER TEMPERATURE, °C
40
30
20
95
90
80
75
70
0
1
2
3
4
5
6
7
CURRENT, AMPS

where:

$$K'' = I_Q \left[\frac{\ell}{A} \right]^2 \qquad 12.4.3.1.2.$$

The test configuration indicates: $I_Q \cong$ 5.5 amps with a $(\ell/A)A)$ of $\cong 5$. The minimum cold junction ($T_{cj_{MIN.}}$) is expressed in degrees Kelvin.

12.4.3.2 Opposed Modules (Vacuum Environment).

As illustrated by figure 12.4.1.1 a test was conducted under vacuum conditions. The upper and lower thermoelectric modules are the units incorporated into the thermoelectric assembly of section 12.4.3.1 (plate 12.3.1.1). Six thermocouples are positioned to each junction plate for each (2) of the modules. Throughout the test programme statistical sampling of the test data indicated that the temperature variation recorded by the thermocouples on the same and corresponding junction plates were insignificant. The data presented on figure 12.4.3.2.1 and figure 12.4.3.2.2 were based on thermocouple measurements for the lower module (as the upper module thermocouple data was statistically compared to the lower unit and the results indicated no significant difference). Figure 12.4.3.2.1 illustrates the cold junction temperature as a function of current for variation in inlet water temperature. The minimum cold junction temperature corresponds to a current of $\cong$ 4.5 amps. Figure 12.4.3.2.2 illustrates the junction temperature difference as a function of current for variation in inlet

Fig. 12.4.3.2.2.

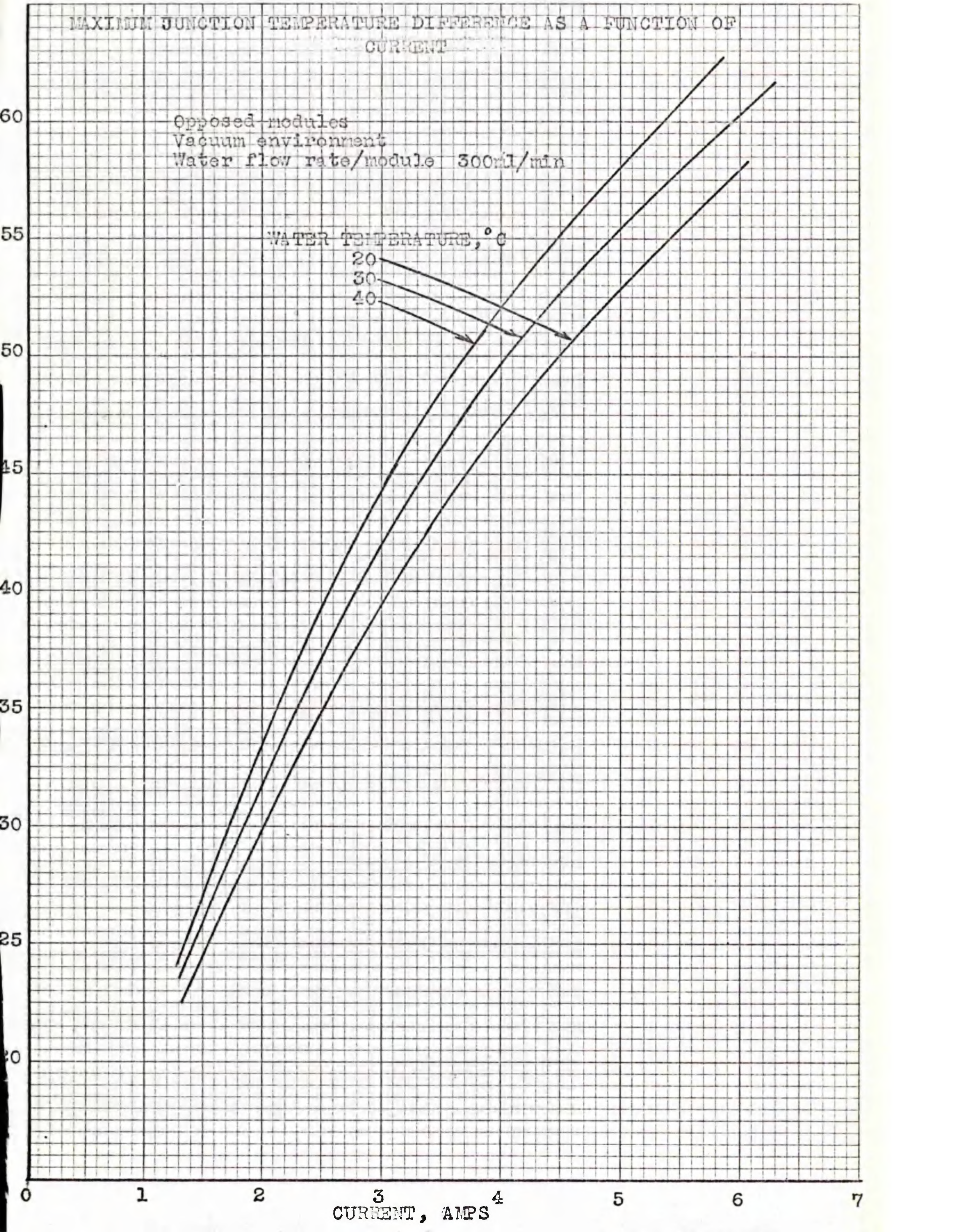
MAXIMUM JUNCTION TEMPERATURE DIFFERENCE AS A FUNCTION OF CURRENT
Opposed modules
Vacuum environment
Water flow rate/module 300ml/min
WATER TEMPERATURE, °C
20
30
40
60
55
50
45
40
35
30
25
20
0
1
2
3
4
5
6
7
CURRENT, AMPS

water temperature. Test results indicated that is an increasing (monotonic) function of current. This condition is associated with the characteristic of the hot junction temperature (i.e. n^{th} order curve). There is a hot side temperature limit imposed by the electrical tinned connectors. The manufacturer indicates the limit of material melt at 125°C (398°K). The results are indicative of a test programme in which the junction temperatures are not constant. Testing in which the hot junction temperature is maintained constant will be as illustrated by figure 12.4.3.2.3. The minimum cold junction temperature (Q_5 = 0) can be expressed as:

$$T_{cj_{MIN}} = \frac{\sqrt{1 + 2Z\,T_{hj}} - 1}{Z} \qquad 12.4.3.2.$$

and

$$\Delta T_{j_{max}} = T_{hj} - T_{cj_{MIN}} \qquad 12.4.3.3.$$

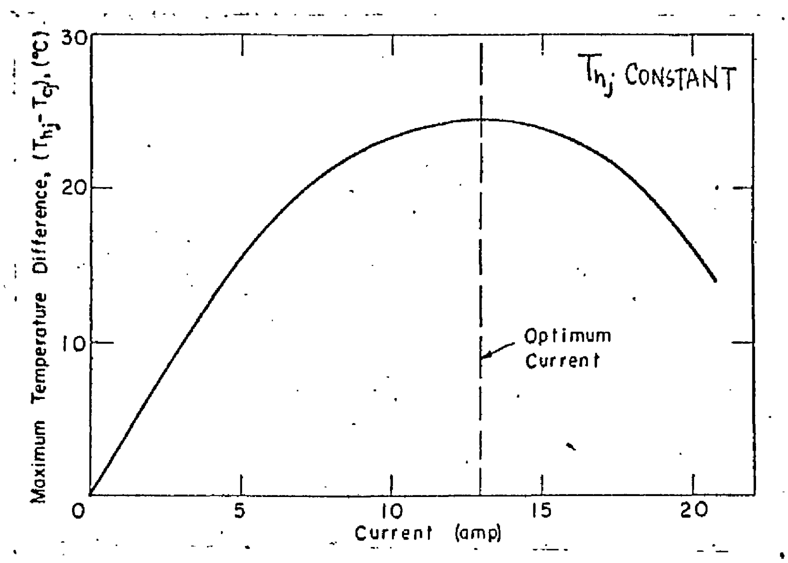

Figure 12.4.3.2.3.

Optimum Current for Maximum Temperature Difference.

The resulting equation (12.4.3.2) is based on the assumption that the hot side junction temperature is invariant of the current.

Comment.

It is the opinion (based on the tests conducted and the computer models) of the author that for conditions in which $Q_{IN} \geq 0$ and where thermoelectric operation is between heat source and heat sink the operational variable ΔT_j as a measure of efficiency can be a misleading parameter. For this 'real' operating condition the values of T_{cj}, T_{hj} should be considered in relationship to Q_S, Q_R and to the power requirements to maintain the heat balance.

12.4.3.3 Module With Radiation Shield (Vacuum Environment).

The purpose of the test performed under the above title was to compare $\Delta T_{j\,max}$ as determined by the opposed module technique (section 12.4.3.2) and the conventional configuration as illustrated by plate 12.4.3.3.1.

Fig. 12.4.3.3.1.

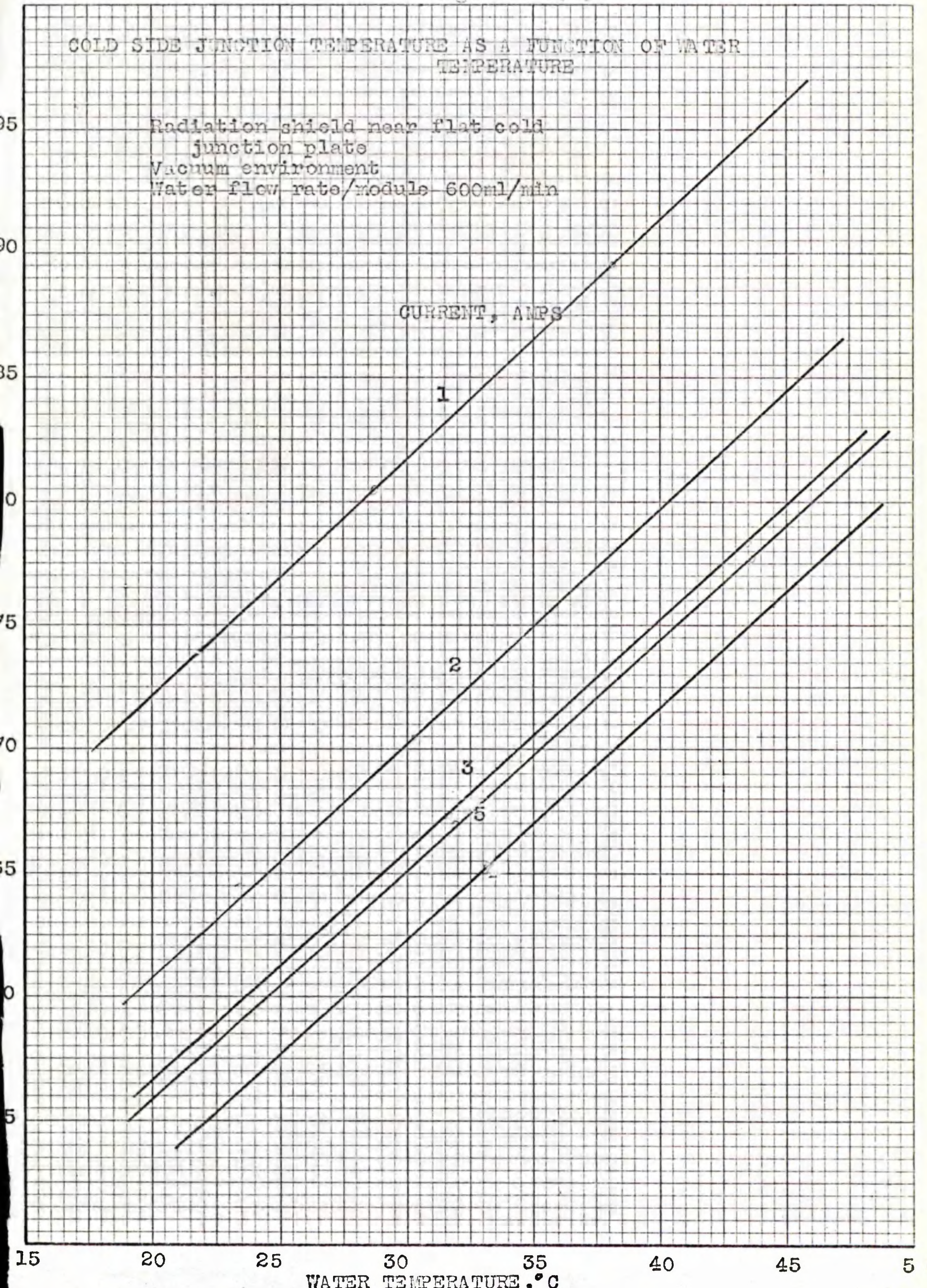
COLD SIDE JUNCTION TEMPERATURE AS A FUNCTION OF WATER TEMPERATURE
Radiation shield near flat cold junction plate
Vacuum environment
Water flow rate/module 600ml/min
CURRENT, AMPS
1
2
3
5
95
90
85
0
75
70
65
0
5
15
20
25
30
35
40
45
5 0
WATER TEMPERATURE, °C

Plate 12.4.3.3.1.

Radiation Shield Positioned Above Cold Junction Plate of Thermoelectric Module.

A radiation shield (highly polished Cu plate) is located at close proximity to the cold surface plate of the thermoelectric module. The flow rate and associated parameters are consistent with the previous section. The data was compared by computing the "t" test to determine if any significant statistical difference existed. The results at a confidence level of 95% indicated no significant difference. An additional test was conducted with the flow rate of twice the value of the previous section (section 12.4.3.3), to determine the relative increase in $\Delta T_{j\,max}$. Figure 12.4.3.3.1 shows the cold side junction temperature as a function of the inlet water temperature for variation in the current. Table 12.4.3.3.1 is indicative of the comparable results. Increasing

Table 12.4.3.3.1.

Current amps	flow rate ml/min	water temp. ^oC	$\cong T_{cj_{MIN}}$ ^oK	$\cong \Delta T_{j_{max}}$ ^oC
4	600	30^o	262.2	54.5
4	300	30^o	269.0	49.5
		Δ	6.8	5.0
1	600	30^o	281.5	22.3
1	300	30^o	285.5	19.5
		Δ	4.0	2.8

the flow rate decreases $T_{cj_{MIN}}$ and increases $\Delta T_{j_{max}}$. The magnitude of change $\Delta T_{cj_{MIN}}$, $\Delta(\Delta T_{j_{max}})$ appears to be a function of the current magnitude (indicative of joule heating effect). To justify the increase in performance will depend on the system requirements and the overall C.O.P. (including water pump efficiency).

Fig. 12.4.4.2.1.

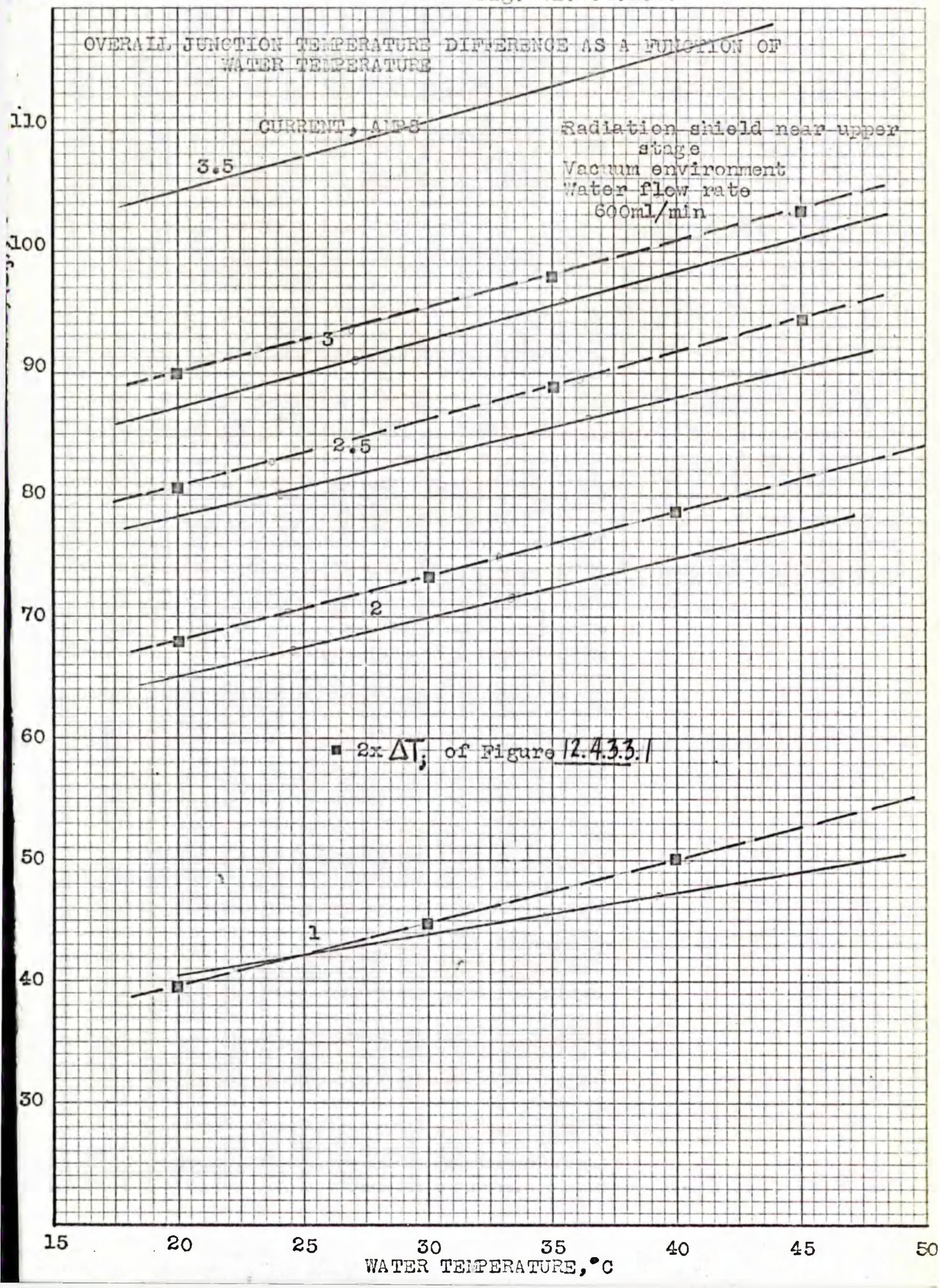
OVERALL JUNCTION TEMPERATURE DIFFERENCE AS A FUNCTION OF WATER TEMPERATURE
CURRENT, AMPS
Radiation shield near upper stage
Vacuum environment
Water flow rate 600ml/min
3.5
3
2.5
2
1
■ 2x ΔT_j of Figure 12.4.3.3.1
110
100
90
80
70
60
50
40
30
15
20
25
30
35
40
45
50
WATER TEMPERATURE, °C

12.4.4 Two Stage Device With Radiation Shield (Vacuum Environment).

12.4.4.1 Introduction.

The purpose of the tests conducted was to determine the effect of current and water temperature on $T_{c_{MIN}}$ (upper stage) and $\Delta T_{j_{max}}$ (overall). Plate 12.4.1.1 shows the top view of the two-stage cascade device. A radiation shield is positioned above the upper stage. The hot side heat exchanger and flow rate is as utilized in the previous section. The first stage of the two-stage device consists of 45 thermocouples (the single stage module of the previous section has the same number and element dimensions as the first stage of the two-stage device). The upper stage of the two-stage device consists of 10 couples which are in electrical series with the lower elements.

12.4.4.2 Results.

In reference (3) it is stated, "theoretically it should be possible to double the maximum ΔT_j using a 2-stage module but, practically it would be difficult to raise it more than one and a half times the value of a single couple". To indicate the expected increase in overall $\Delta T_{j_{max}}$ a two-stage device was attached to the hot side heat exchanger. The hot side heat exchanger was previously utilized in section 12.4.3.2 and in section 12.4.3.3. The flow rate and vacuum conditions were

Fig. 12.4.4.2.2.

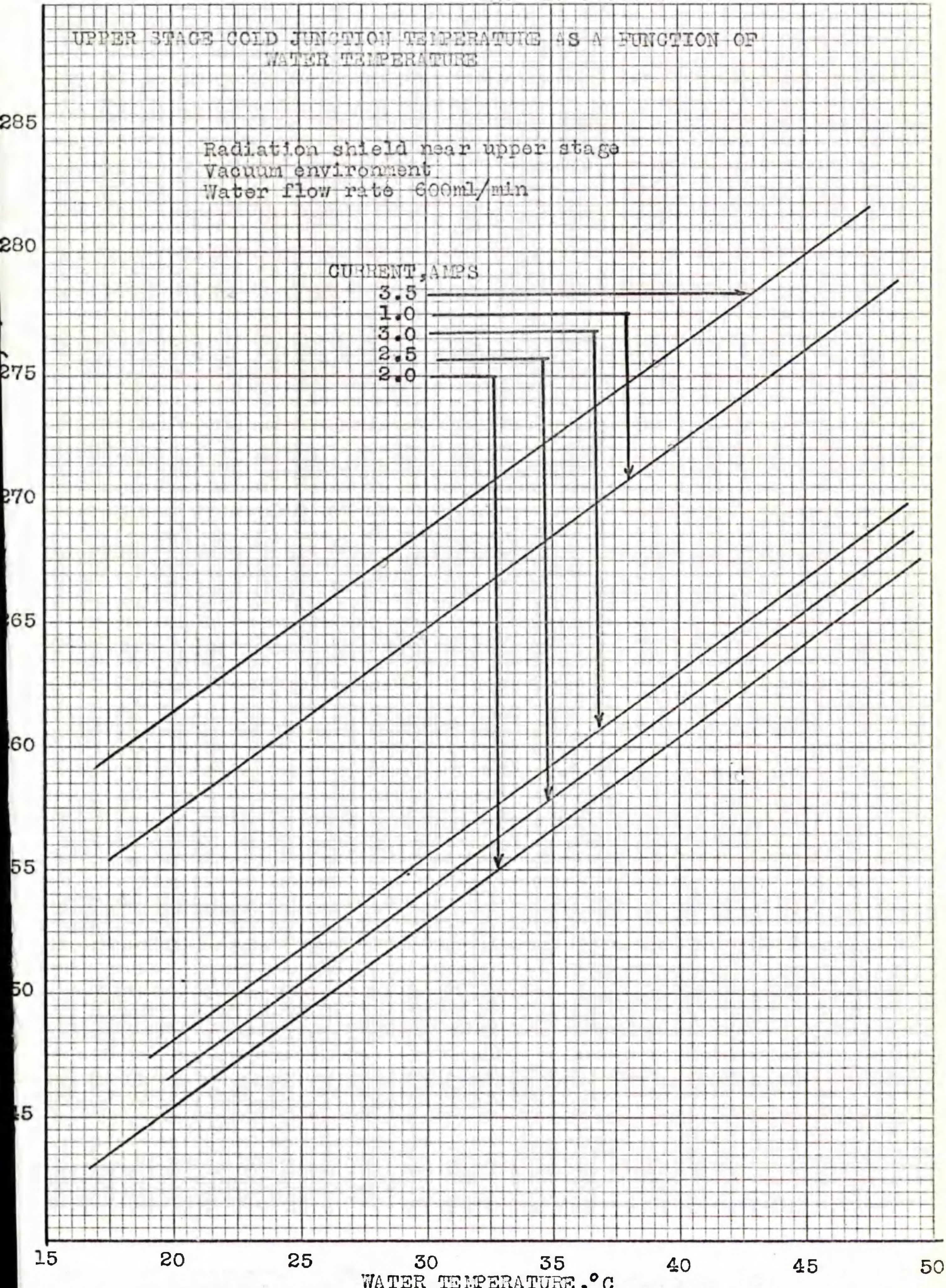
UPPER STAGE COLD JUNCTION TEMPERATURE AS A FUNCTION OF WATER TEMPERATURE
Radiation shield near upper stage
Vacuum environment
Water flow rate 600ml/min
CURRENT, AMPS
3.5
1.0
3.0
2.5
2.0
285
280
275
270
265
260
255
250
245
15
20
25
30
35
40
45
50
WATER TEMPERATURE, °C

maintained under the same conditions as the previous section. The junction temperature difference of the previous section was multiplied by the factor 2 (i.e. $2 \cdot \Delta T_{j_{max}}$ (single stage device)) and plotted with the test data of the 2-stage cascade module. Figure 12.4.4.2.1 illustrates the overall junction temperature difference as a function of water inlet temperature for variation in current. The results indicate that the 2-stage cascade module as tested (within experimental limits) appeared to be performing at a higher value than stated in the quote above. There are construction differences between the 2-stage module and the single stage unit. Some of the differences which were difficult to control are:

(1) The inter-element thermal insulation is different for both units.

(2) The contact pressure between the module hot junction plate and surface of the heat exchanger is difficult to torque test.

(3) Fluid flow rate is difficult to monitor.

Figure 12.4.4.2.2 illustrates the upper stage cold side junction temperature as a function of inlet water temperature. For a 20°C inlet water temperature with the current at 2 amps; the cold side junction temperature is $\cong$ 245°K (-28°C) and ΔT_j from figure 12.4.4.2.1 is $\cong$ 65°C. Figure 12.4.4.2.3 shows the circuit voltage as a function of the lower stage hot junction temperature with current a variable. For the test condition illustrated for $T_{h_j} \cong$ 310°K at 2 amps the voltage as indicated on figure 12.4.4.2.3

Fig. 12.4.4.2.5.

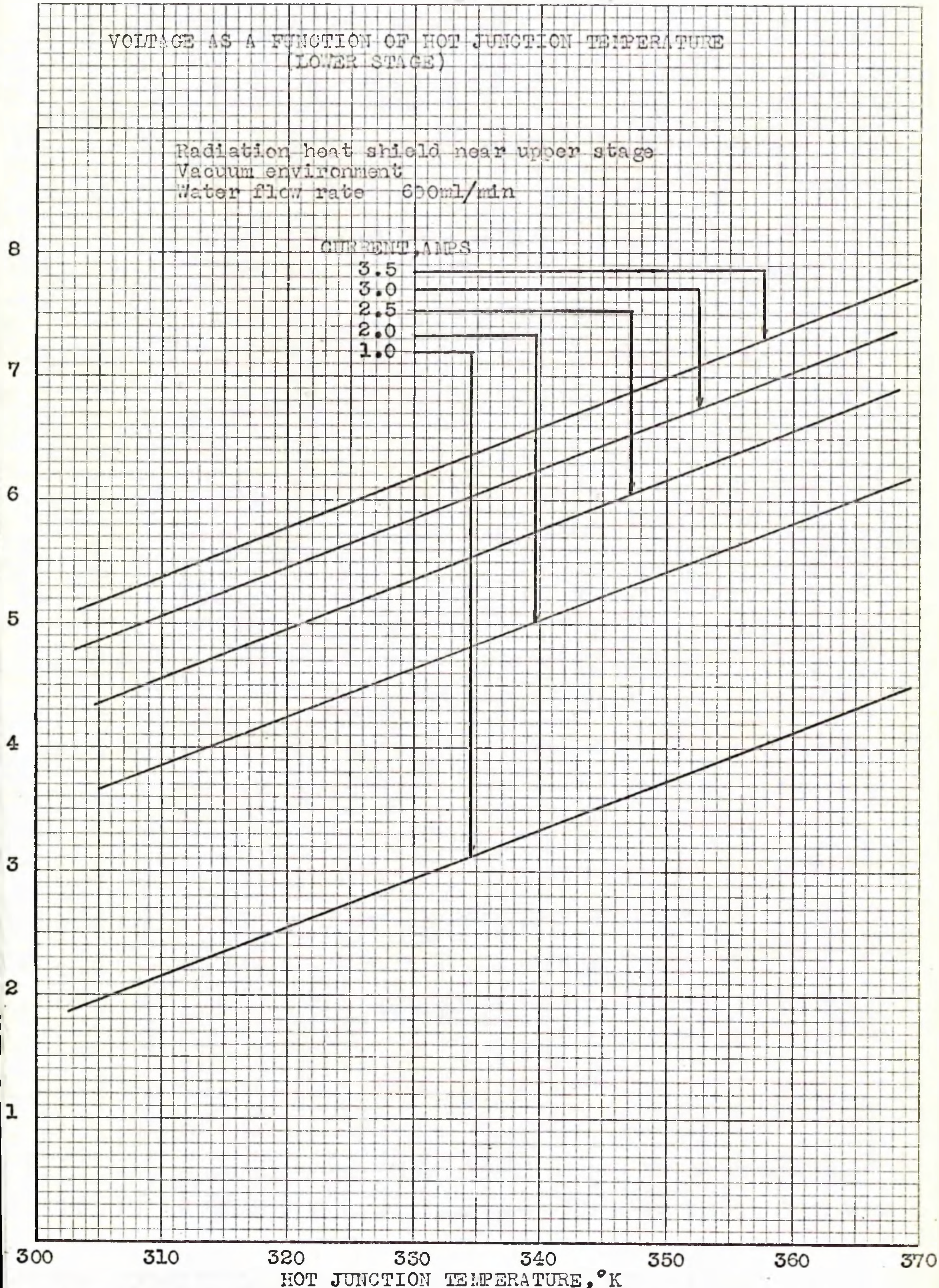
VOLTAGE AS A FUNCTION OF HOT JUNCTION TEMPERATURE
(LOWER STAGE)
Radiation heat shield near upper stage
Vacuum environment
Water flow rate 600ml/min
CURRENT,AMPS
3.5
3.0
2.5
2.0
1.0
8
7
6
5
4
3
2
1
300
310
320
330
340
350
360
370
HOT JUNCTION TEMPERATURE,°K

is $\cong$ 3.85V (power input 7.70 watts). The voltage is an approximate linear function of the hot side junction temperature. The average slope is $\cong$ 0.4 volts/^{o}C for ($1 \leq I \leq 3.5$ amps). The voltage function is expressed as:

$$V = m T_{hj} + B(I)$$

where:

m average slope, volts/^{o}C

B (I) parameter (current dependent)

The results indicate that the 2-stage cascade module can approach twice the junction temperature difference of a single stage module. The linear characteristic of $T_{cj_{MIN}}$ and Voltage as a function of temperature is encouraging. The minimum T_{cj} occurs at 2 amps (for this test configuration). The low value of current is representative of $Q_s \cong \longrightarrow 0$ (vacuum 10_{-6} Tors). In an actual design Q_s would be an input variable with subsequent solution as outlined in section 11.2.

A 2-stage module was utilized for cooling an optical decoder positioned within a vacuum housing. The heat rejection was by convective fins. Figure 12.4.4.2.4 illustrates the basic assembly.

OPERATIONAL TEST ASSEMBLY
Plate 12.4.4.1

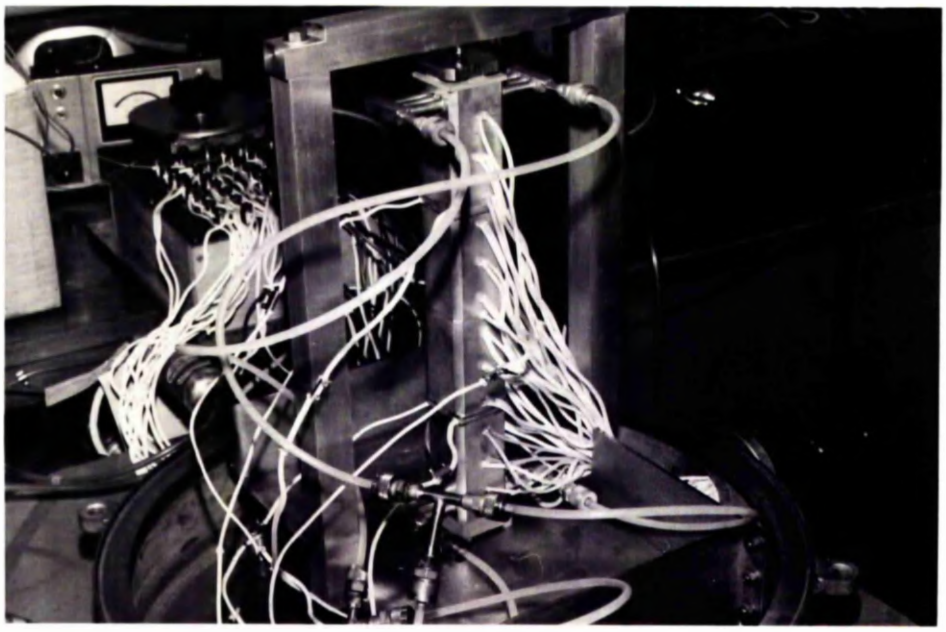

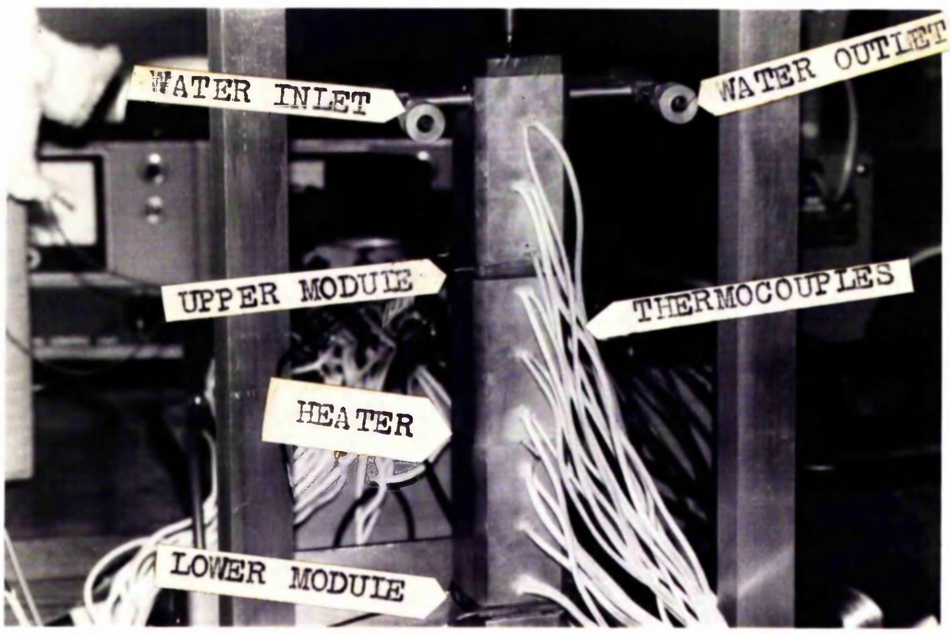

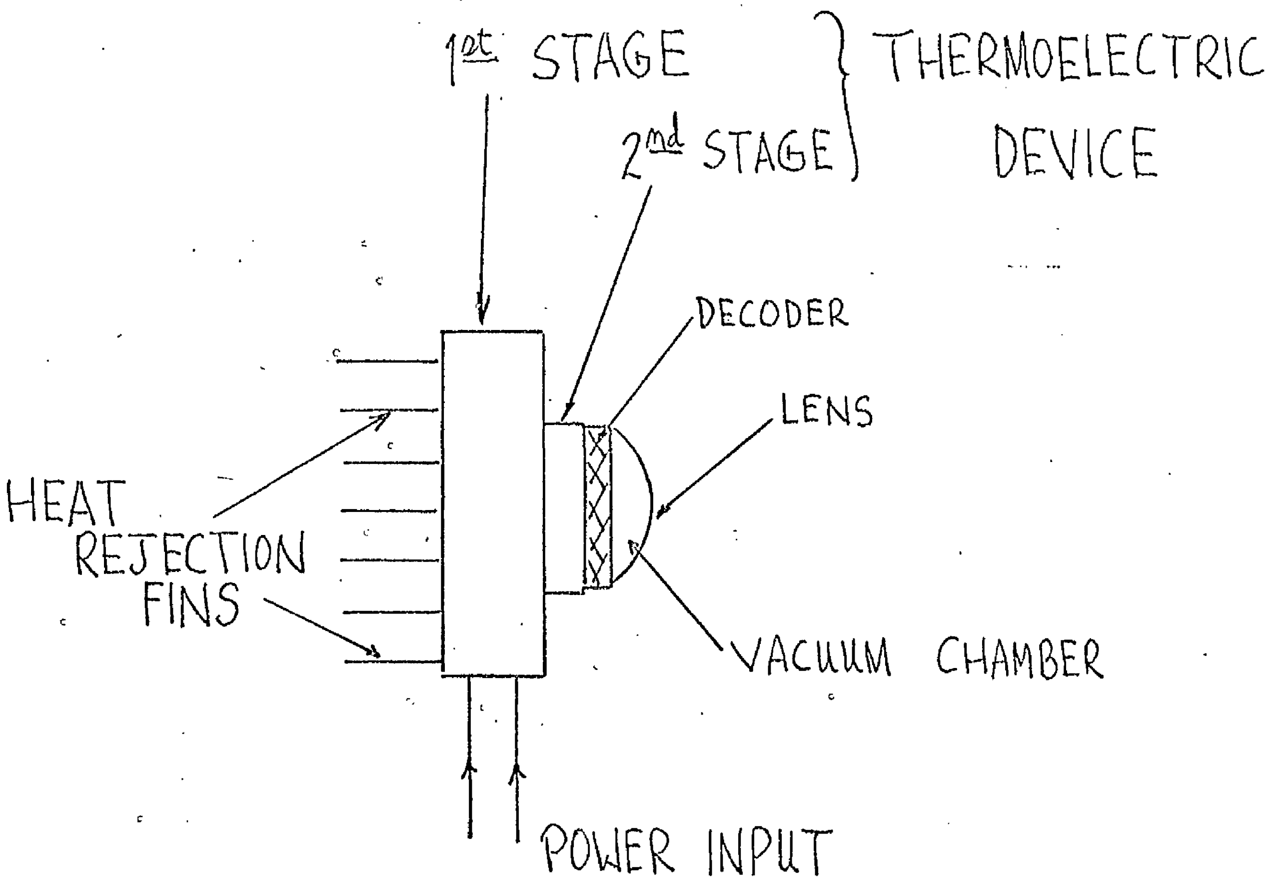

Figure 12.4.4.2.4.

Optical Decoder - Thermoelectric Assembly.

12.5 Operational Characteristics of a Thermoelectric Module.

12.5.1 Introduction.

In order to determine the operational characteristics of a thermoelectric module it is necessary to independently measure the following operational variables:

(1) Heat Pump Rate, i.e. watts input, Q_s

(2) Heat Rejection Rate, i.e. watts output, Q_R

(3) Electrical Power Input, i.e. IV, P_{IN}

In terms of measurable variables this can be expressed as:

$$Q_S = f(\ I, T_{c_j}, T_{h_j}, \ \ldots\ldots \text{ material properties})$$

and

$$Q_R = g(\ P_{IN}, Q_S, \ \ldots\ldots \text{ material properties})$$

The test was conducted under vacuum conditions in order to eliminate ambient effects. Two thermoelectric modules were tested congruently within the vacuum assembly. Plate 12.4.4.1 indicates the basic material geometry. The technique for measuring the operational variables is presented in section 12.4.2. Throughout the test programme statistical sampling indicated that there was no statistical significance between the data recorded for the upper module and the lower module. The data represented on the figures are based on the average for the upper and lower module.

12.5.2 Results and Synopsis.

Figure 12.5.2.1 and figure 12.5.2.2 illustrates T_{c_j} as a function of T_{h_j} for variation in Q_S (watts input) and C.O.P. with fixed current values. The assembled data was compared to the output from the computer model, (section 7.4.4.6). A statistical sampling technique was employed in which 844 points of the test data was compared with the computer model. The results indicated that the average

COLD JUNCTION TEMPERATURE AS A FUNCTION OF THE HOT JUNCTION TEMPERATURE FOR FIXED CURRENT VALUES WITH VARIABLE HEAT PUMP RATE(WATTS/MODULE)

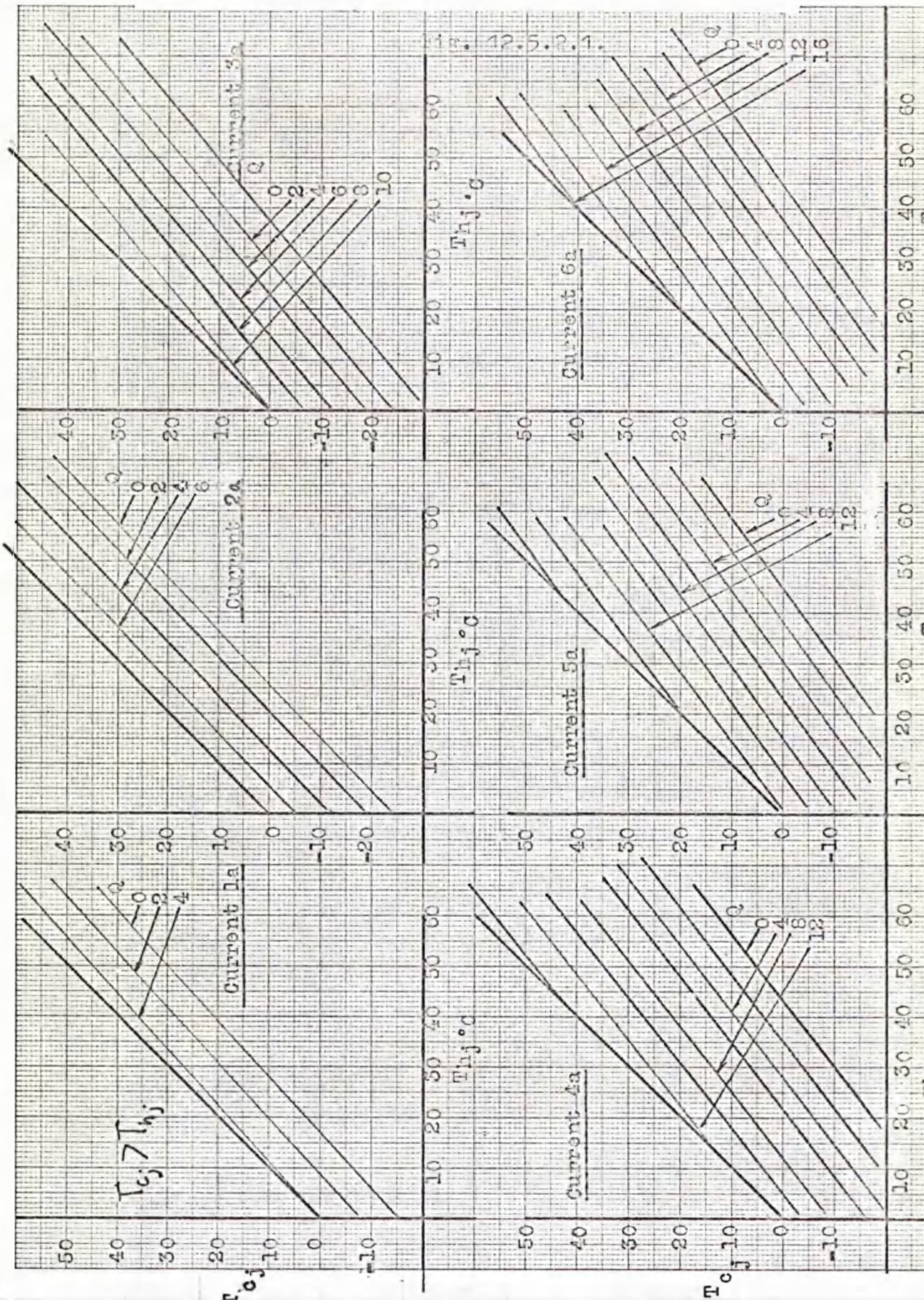

COLD JUNCTION TEMPERATURE AS A FUNCTION OF THE HOT JUNCTION TEMPERATURE FOR FIXED CURRENT VALUES WITH VARIABLE C.O.P.

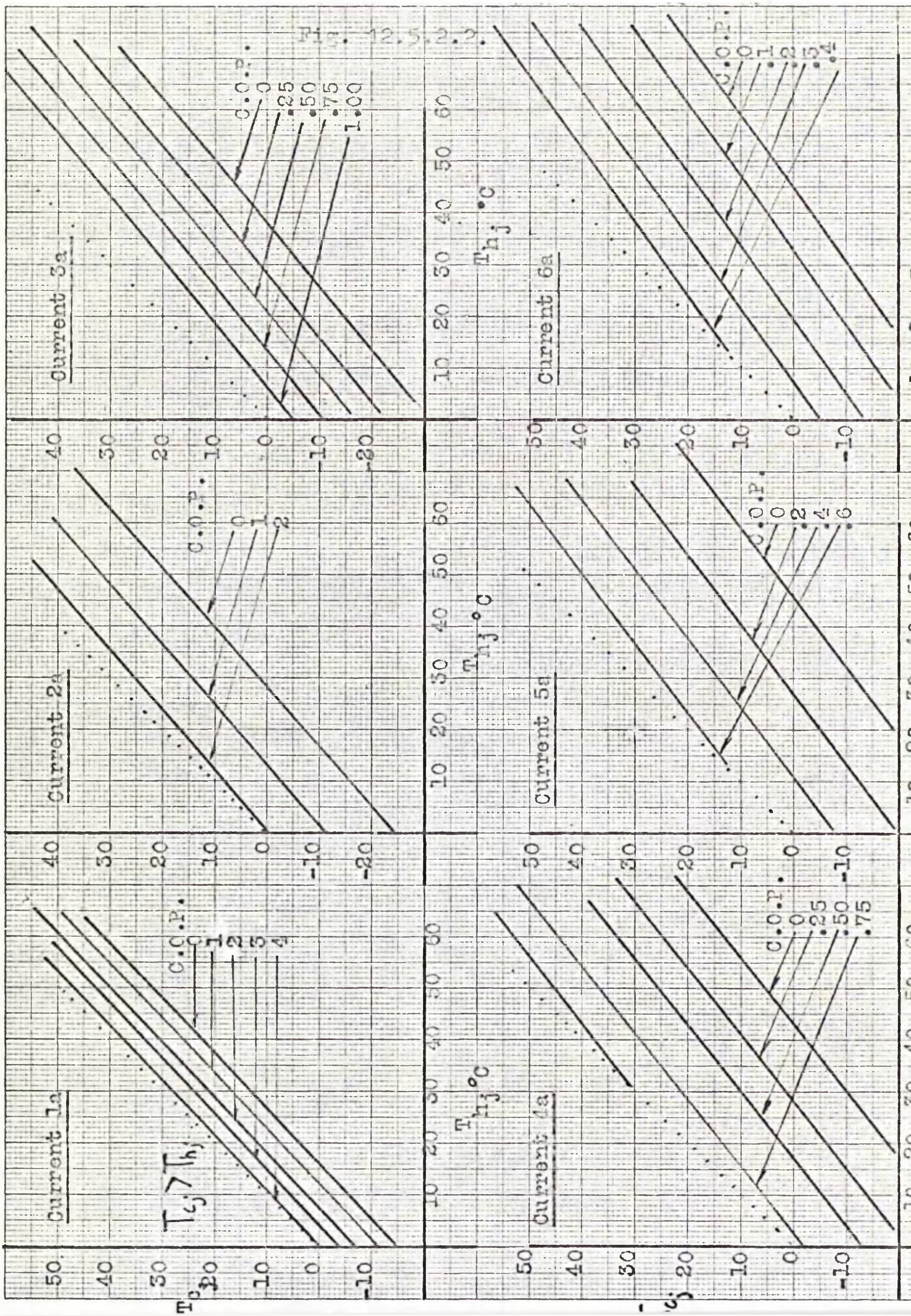

deviation was less than 3%. The deviation approached 5% with high hot junction temperatures ($T_{hj} \geq 60^\circ C$).

The heat load and the operational C.O.P. as a function of current for variation in inlet water temperature (to hot side heat exchanger) is determined as follows:

(a) The basic thermoelectric assembly with a flate plate on the cold junction plate (plate 12.3.1.1 - less 'tree') is the configuration considered.

(b) From figure 12.3.2.2.1 determine T_{hj} and T_{cj} corresponding to the current and inlet water temperature.

(c) From figure 12.5.2.1 and figure 12.5.2.2 locate T_{hj}, T_{cj} and I corresponding to (b). The heat pump rate (Q_s) and C.O.P. is then determined directly. From the data presented in section 12.3.2.1 and section 12.3.2.3 combined with figure 12.5.2.1 and figure 12.5.2.2 results similar to figure 12.5.2.3 and figure 12.5.2.4 can be constructed. A curve fit computer programme was utilized to construct figure 12.5.2.3 and figure 12.5.2.4.

Fig. 12.5.2.3.

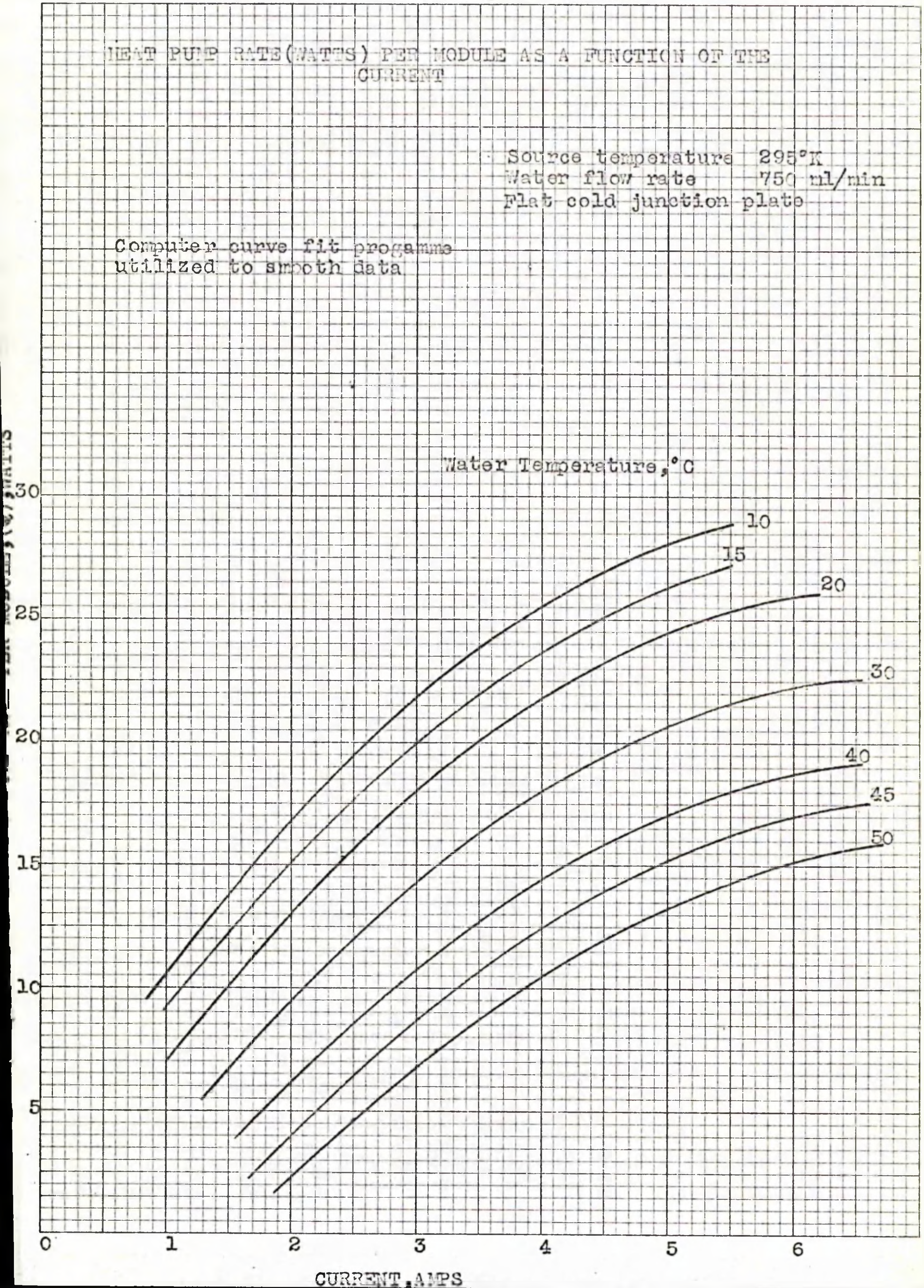

HEAT PUMP RATE(WATTS) PER MODULE AS A FUNCTION OF THE CURRENT
Source temperature 295°K
Water flow rate 750 ml/min
Flat cold junction plate
Computer curve fit progamme utilized to smooth data
Water Temperature,°C
10
15
20
30
40
45
50
30
25
20
15
10
5
0
1
2
3
4
5
6
CURRENT,AMPS

Fig.12.5.2.4.

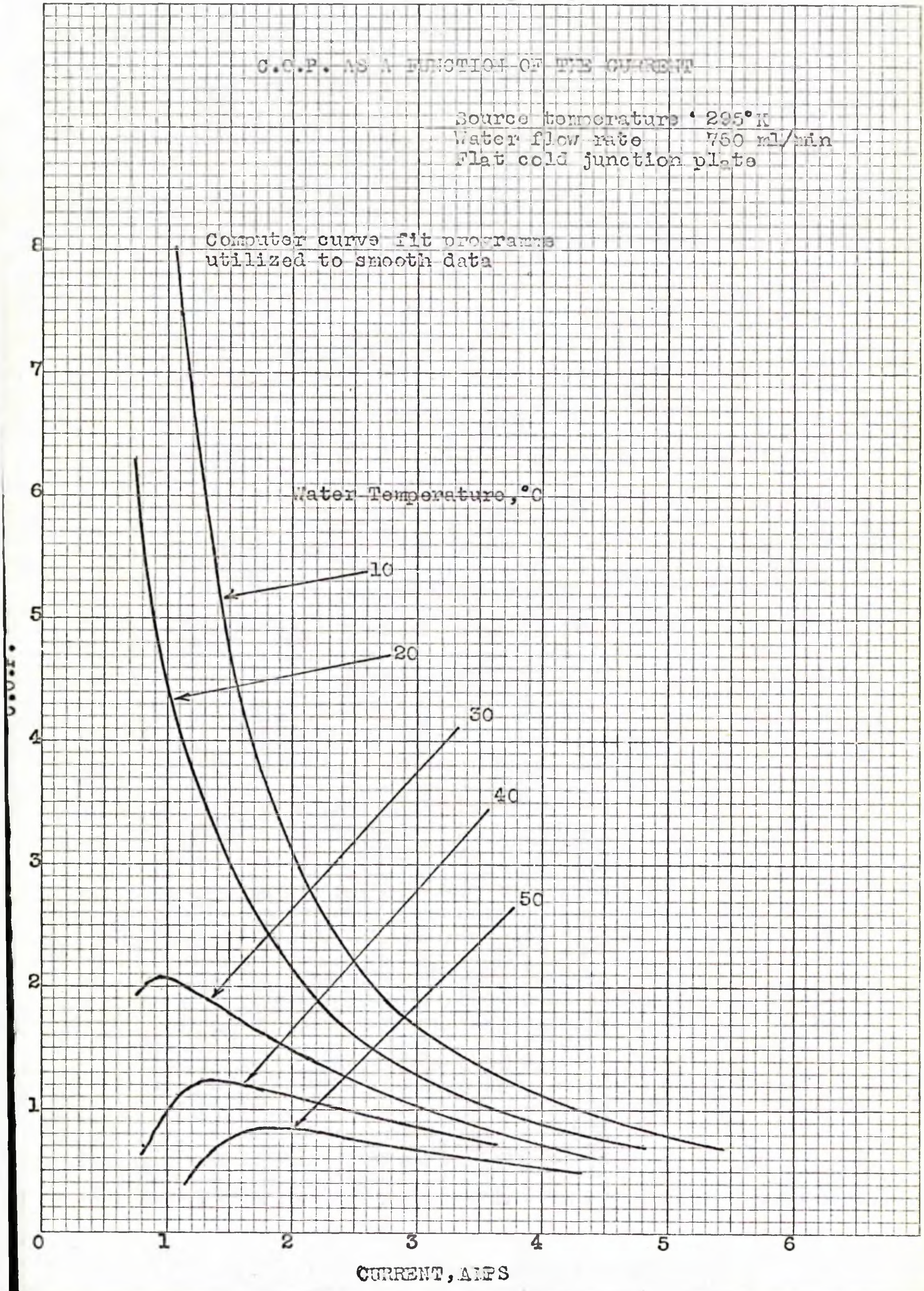
C.O.P. AS A FUNCTION OF THE CURRENT
Source temperature 295°K
Water flow rate 750 ml/min
Flat cold junction plate
Computer curve fit programme utilized to smooth data
Water Temperature,°C
10
20
30
40
50
C.O.P.
0
1
2
3
4
5
6
7
8
CURRENT,AMPS

13.0 REFERENCES.

(1) P.E. Gray, The Dynamic Behaviour of Thermoelectric Devices, John Wiley and Sons, Inc., New York (1960).

(2) Edited by I.B. Cadoff and E. Miller, Thermoelectric Materials and Devices, Reinhold Publishing, New York, (1960).

(3) H. J. Goldsmid, Thermoelectric Refrigeration, Temple Press Limited, London (1964).

(4) J.E. Sutherland and N.T. Burak, Solid-State Electronics, Vol. 7, pp. 465 - 471 (1964).

(5) B. Varga, A.D. Reich and J.R. Madigan, Journal of Applied Physics, Vol. 34, Number 12, pp. 3430 - 3441 (1963).

(6) A.F. Ioffe, Semiconductor Thermoelements and Thermoelectric Cooling, Infosearch Limited, London (1957).

(7) O.J. Mengate and M.R. Seiler, Advanced Energy Conversion, Vol. 2, pp. 59 - 68 (1962).

(8) Letter discussion with General Electric Company, U.S.A.

(9) R.R. Heikes and R.W. Ure, Jnr., Thermoelectricity: Science and Engineering, p. 521, Interscience Publishing, New York (1961).

(10) V.A. Naer and A. Rozhentseva, Soviet Physics - Solid State, Vol. 3, No. 4 (1961).

(11) G. Vikhosev and V. Naer, Odessa Tech. Institute of Food and Refrigeration Industry, pp. 824 - 828 (1958).

(12) J.R. Andersen, Advanced Energy Conversion, Vol. 2, pp. 241 - 248 (1962).

(13) A.I. Burshteyn, Semiconductor Thermoelectric Devices, Temple Press, London (1964).

(14) W.C. Lyon and T.S. Bustard, Advance Energy Conversion, Vol. 2, pp. 197 - 208 (1962).

(15) P.W. Cowling and J.E. Sunderland, Advance Energy Conversion, Vol. 7, pp. 289 - 295 (1968).

(16) B.J. O'Brien, C.S. Wallace and K. Landecker, Journal of Applied Physics, Vol. 27, No. 7, (1956).

(17) G.E. Forsythe and W.R. Wasow, Finite Difference Methods for Partial Differential Equations, John Wiley and Sons, London (1960).

(18) R.S. Varga, Matrix Iterative Analysis, Prentice Hall, New York (1962).

(19) R.S. Burington, Handbook of Mathematical Tables and Formulas, Mc.Graw-Hill, New York (1962).

COMPUTER PROGRAMME INDEX.

```
DD0179B00WPU+P1500079PSP→
begin comment This program calculates the effect of
   configuration geometry for maximizing the C.O.P.,
   four distinct ratios are presented as output data
   showing the expected degradation of performance;
 integer f1,f2,f3,f4;
 real sigman,sigmap,ASUBP,l,KSUBP,alpha,OMEGA,DELT,
   TSUBC,F,rhojn,rhojp,KSUBN,KSUBI;
 procedure owner;
 begin write text(70,[[2c]WALLACE*SHAKUN**AERO*ENGR[2c]]);
 end   LINE  10  owner;
 comment Examination of equations***********
   and************* show that there are two
   variables which can be adjusted to maximize the
   coefficient of performance,these are the
   parameter p and the shape factor fsubn/fsubp.The
   coefficient of performance being positive the
   shape factor is maximized by minimizing the
   product KR.The value of the maximized or
   optimized shape factor is designated in this
   computer progarm as N.The term factor×N is
   utilized to indicate  variations from the
   optimized shape factor . To limit the error when
   utilizing system operational approximations it is
   required to have a limit control on the ratios,
```

and . These limit controls are required inorder that the parameters lambda,reciprical function as found on pages and, figure and be as close to unity as possible,when absolute values are required . For relative comparison results as presented in this computer program values of lambda or reciprical function are not restrictive;

```
procedure CONFIG(sigman,sigmap,ASUBP,l,KSUBN,KSUBP,
  f1,f2,f3,f4,alpha,F,OMEGA,DELT,TSUBC,rho jn,rho jp,KSUBI);
  value sigman,sigmap,ASUBP,l,KSUBN,KSUBP,f1,f2,f3,
  f4,alpha,F,OMEGA,DELT,TSUBC,rho jn,rho jp,KSUBI;
  integer f1,f2,f3,f4;
  real sigman,sigmap,ASUBP,l,KSUBN,KSUBP,alpha,F,
  OMEGA,DELT,TSUBC,rho jn,rho jp,KSUBI;
begin real top,bottom,N,rhon,rhop,term1,term2,R,
        term3,K,ZMATERIAL,REFF,term4,term5,KEFF,
        ZEFF,DLTMX,DLTMXEFF,factor,M,term11,term22,
        RR,term33,KK,fREFF,term55,fKEFF,ZEFFf,
        COPMX,DLTMXf,COPMXf,A,QMAX,QMAXf,QATCOPX,
        QATCOPXf,B,C,COPATMXQ,COPMXQf,D;
     write text(70,[the*equations*utilized*are*
       approximations*and*are*found*in*section****
       ********[c]and*on*table*****************
       of*this*thesis[2c]]);
     write text(70,[cold*junction*temperature*=*]);
```

```
write(70,f2,TSUBC);
write text(70,[junction*temperature*difference*=*]);
write(70,f2,DELT);
write text(70,[hot*junction*temperature*=*]);
write(70,f2,TSUBC+DELT);   newline(70,2);
rhon:=1/sigman;   rhop:=1/sigmap;   top:=KSUBP×rhon;
bottom:=KSUBN×rhop;   N:=sqrt(top/bottom);
comment N is the ratio of ASUBN to ASUBP;
write text(70,[shape*ratio*=*]);   write (70,f3,N);
newline(70,2);   term1:=rhon/(N×ASUBP);
term2:=rhop/ASUBP;
comment l is assumed the same for the n-or*p-
  type element;
R:=l×(term1+term2);   term3:=KSUBN×N+KSUBP;
K:= ASUBP×term3/l;   ZMATERIAL:=(alpha↑2)/(R×K);
write text(70,[material*figure*of*merit*=*]);
write(70,f1,ZMATERIAL);
REFF:=(R+2×rhojp/ASUBP+2×rhojn/(N×ASUBP))×F↑2;
comment F is the ripple effect, rhoj is the
  junction resistivity ohm-cm*sqrd;
term4:=(1-OMEGA)/(l×OMEGA);
comment OMEGA is the packing density;
term5:=(ASUBP+N×ASUBP);   KEFF:=K+ KSUBI×term4×term5;
comment KSUBI is the insulation thermal conductivity;
ZEFF:=(alpha↑2)/(REFF×KEFF);
```

```
comment This is the effective figure of merit
  when the configuration is at the required
  value for maximizing the C.O.P., this
  configuration is known as the N-configuration;
write text(70,[figure*of*merit*for*
  N-configuration*=*]);
write(70,f1,ZEFF);    DLTMX:=(TSUBC↑2×ZMATERIAL)×0.5;
write text(70,[max*temperature*difference*
  corresponding*to*material*figure*of*merit*=*]);
write(70,f2,DLTMX);
write text(70,[max*temperature*difference*
  corresponding*to*N-configuration*=*]);
DLTMXEFF:=(TSUBC↑2×ZEFF)×0.5;
write(70,f2,DLTMXEFF);   newline (70,2);
for factor:= .8 step .05 until 1.50, 1.0 do
begin write text(70,[factor*=*]);
      write(70,f4,factor);   M:=N×factor;
      term11:=rhon/(M×ASUBP);   term22:=rhop/ASUBP;
      RR:=l×(term11+term22);   term33:=KSUBN×M+KSUBP;
      KK:= ASUBP×term33/l;
      fREFF:=(RR+2×rhojp/ASUBP+2×rhojn/(M×
        ASUBP))×F↑2;
      term55:=(ASUBP+M×ASUBP);
      fKEFF:= KK+KSUBI×term4×term55;
      ZEFFf:=(alpha↑2)/(fREFF×fKEFF);
```

```
comment The MN-configuration is based
  on the condition that the material
  geometry does not correspond to the
  N- configuration;
write text(70,[figure*of*merit*
  corresponding*to*MN-configuration*=*]);
write(70,f1,ZEFFf);
DLTMXf:=(TSUBC↑2×ZEFFf)×0.5;
write text(70,[max*temp*difference*
  corresponding*to*MN-configuration*=*]);
write(70,f2,DLTMXf);
COPMX:=0.5×(DLTMXEFF/DELT - 1);
comment COPMX,QMAX,QATCOPX,COPATMXQ are
  based on the N-configuration,the
  symbols ending with small case f are
  based on the NM-configuration;
COPMXf:=0.5×(DLTMXf/DELT - 1);
A:=COPMXf/COPMX;
write text(70,[ratio*of*max*cop*
  MN-configuartion*to*max*cop*
  N-configuration*=*]);
write(70,f3,A);
QMAX:=KEFF×DLTMXEFF×(1- DELT/DLTMXEFF);
QMAXf:=fKEFF×DLTMXf×(1-DELT/DLTMXf);
QATCOPX:=(DELT/DLTMXEFF×QMAX);
```

```
            QATCOPXf:=(DELT/DLTMXf×QMAXf);
            B:=QATCOPXf/QATCOPX;
            write text(70,[ratio*of*heat*pumping*
              rate*at*max*cop*MN-configuration*to*
              heat*pump*rate*N-configuration*=*]);
            write(70,f3,B);   C:=QMAXf/QMAX;
            write text(70,[ratio*max*heat*pump*
              rate*MN-configuration*to*max*heat*
              pump*rate*N-configuration*=*]);
            write(70,f3,C);
            COPATMXQ:=0.5×(1-DELT/DLTMXEFF);
            COPMXQf:=0.5×(1-DELT/DLTMXf);
            D:=COPMXQf/COPATMXQ;
            write text(70,[ratio*cop*at*max*q*
              MN-configuraton*to*cop*at*max*q*at*
              N-configuration*=*]);
            write(70,f3,D);   newline (70,2);
        end   LINE 142  innerloop;
    end   LINE 143  CONFIG;
    open(20);   open(70);   f1:=format([4s+d.dd₁₀±ndc]);
    f2:=format([4s+nddd.ddc]);   f3:=format([4s+nddd.dddddc]);
    f4:=format([6s+ndd.dddcc]);   owner;   sigman:=read(20);
    sigmap:=read(20);   rhojn:=read(20);   KSUBI:=read(20);
    rhojp:=read(20);   ASUBP:=read(20);   l:=read(20);
    KSUBN:=read(20);   KSUBP:=read(20);   alpha:=read(20);
```

```
F:=read(20);   OMEGA:=read(20);   DELT:=read(20);
TSUBC:=read(20);
CONFIG(sigman,sigmap,ASUBP,l,KSUBN,KSUBP,f1,f2,f3,
  f4,alpha,F,OMEGA,DELT,TSUBC,rhojp,rhojn,KSUBI);
close(20);  close(70);
end →
```

C.P. 2

DD017A000WPU+P1500079PSP→

```
begin comment This program calculates the design and
    operational characteristics of a modular
    thermoelectric couple;
  integer f1,f2,f3,f4,f5,f6,f7,f8,f11,f22,f33,f44,
    f55,f66,E,f;
  real sigma,l,rhoj,F,A,OMEGA,KSUBI,K,alpha,TSUBC,
    DELT,omega,density,ASUBI,ratio,lstar,ll;
  procedure owner;
  begin write text(70,[[2c]WALLACE*SHAKUN**AERO*ENGR[2c]]);
  end   LINE  10  owner;
  procedure concept1;
  begin write text(70,[[c]This*program*calculates*
          for*a*given*module*design*the*[c]
          performance*characteristics*for*various*
          cold*junction*temperatures*[c]
          hot*to*cold*junction*temperatures*and*
          currents[2c]]);
  end   LINE  18  concept1;
  procedure heading1;
  begin write text(70,[[c]OPERATIONAL*
          CHARACTERISTICS*OF*THE*GIVEN*MODULE[c]]);
        write text(70,[[c]ELEMENT*HEIGHT*=***********
          cm.[c]JUNCTION*RESISITIVITY*=**********
          ohm.*cm.*sqrd.[c]CONDUCTIVITY*OF*ELEMENT*=*
```

```
        ********1/ohm*cm[c]PACKING*DENSITY*=*******
        ****[c]ELEMENT*AREA*=*********cm*sqrd[c]
        SEEBECK*COEFFICIENT*=**********volts/deg*
        kel[c]HEIGHT*OF*MODULE*=****************
        cm[c]HEIGHT*OF*PEDESTAL*=***************
        cm[c]RIPPLE*FACTOR*=**************[3c]]);
end   LINE  31  heading1;
procedure heading;
begin write text(70,[[c]this*program*calculates*
        the*geometrical*parameters[c]
        associated*with*the*heat*flow*model*that*
        yield*the*values*of*q/qsubci[3c]]);
      write text(70,[[c]definition*of*geometrical*
        parameters[c]]);
      write text(70,[[c]lstar*=*dimensionless*
        length*of*the*thermoelectric*[c]column[c]]);
      write text(70,[bstar*=*dimensionless*
        parameter**l:b[c]rstar*=*dimensionless*
        parameter**a/b[c]]);
end   LINE  44  heading;
procedure concept;
begin write text(70,[[c]procedure*optilax*and*
        subtab*when*included*[c]extend*the*
        computational*accuracy*of*the*procedure*
        iterate[c]]);
```

```
      write text (70,[[2c]Three*real*procedures*
        calculate*the*dimensionless*parameters*
        required*as*input*for*procedure*iterate[2c]]);
end   LINE 53  concept;
real procedure rstar(density,ratio);
  value density, ratio; real density, ratio;
  rstar:= sqrt (density×0.5×ratio);
comment ratio is the pedestal area to element area;
comment density is thermoelectric packing density;
real procedure bstar (l,density,ASUBI);
  value l,density,ASUBI; real l,density,ASUBI;
  bstar:= l×sqrt((3.1456×density)/(2.0×ASUBI));
comment l is the height of insulation, density is
  packing density,ASUBI is cross sectional area of element;
real procedure zeta1(lstar); value lstar; real lstar;
  zeta1:= 1-lstar;
comment lstar is the ratio of height of element to
  height of insulation;
real procedure  phaseq(omega,E,f11,f22,f33,f44,f55,f66,FF);
  comment procedure phaseq is a numerical soulution
  of the heat transfer equation;
  comment t[i,j] is the value of tau at eta=i×h,
  zeta=j×h where h=1/n. Starting values must be
  assigned,which might all be zeros or else values
  previously derived,for i=1(1)n, j=1(1)n-1;
```

```
  value omega,E,f11,f22,f33,f44,f55,f66; label FF;
  integer  E,f11, f22,f33,f44,f55,f66;  real omega;
begin integer j,i,nm1,no,n,m,k;
      real d,s,b,h,lambda,mu,a,w,APRIM,BPRIM,YO,Y1,
        Y,c,f,tt,sl,r,QSUBK,Q,so,RATIO,epso;
      begin heading;   concept;
            no:= entier(0.5×(1.0/rstar(density,
              ratio) -1.0)) + 2.0;
            if lstar ≤ .8 then epso:= .01 else epso:= .001;
            if rstar (density,ratio) ≤ .1 then
            begin k:= 1;   goto F
            end   LINE  86;
            if rstar (density,ratio) ≤ .2 then
            begin k:= 3;   goto F
            end   LINE  89;
            if rstar (density,ratio) ≤ .3 then
            begin k:= 8;   goto F
            end   LINE  92;
            k:= 18;
            comment  the above if statements is the
              technique for minimising the matrix
              required  and maintaining an accuracy
              of approximately 4 per cent.  The
              iterative solution was compared with
              a closed solution for approximately
```

```
          144 points;
F: n:=no × k;   h:=1/n;
   begin real array t[0:n+1,0:n],tl[1:n-1];
         for j:= 1 step 1 until n-1 do
          for i:= 1 step 1 until n do t[i,j]:=0;
         comment the starting values have
          been assigned;
         d:= 1.0 - zeta1(lstar);
         s:=-zeta1(lstar)/d;   b:=h/d;
         nm1:= n-1;
         for j:= 1 step 1 until nm1 do
         begin tl[j]:=t[n,j];
               comment right side of
                 interior domain;
               s:=b+s;
               t[0,j]:=if s≤ 0 then 0 else s;
               comment boundary condition
                 left side;
               t[n+1,j]:=t[n-1,j];
               comment boundary condition
                 right side derivative
                 zero across r;
         end   LINE 122;
         for i:= n+1 step -1 until 0 do
         begin t[i,0]:= 0;
```

```
        comment lower boundary condition;
        t[i,n]:= 1;
        comment upper boundary condition;
end     LINE 128;
comment The above two for loops
  set up the boundary conditions
  for the difference equation;
lambda:=(rstar(density,ratio))/
  (1.0- rstar(density,ratio));
mu:= (1.0- rstar(density,ratio))
  /bstar(1,density,ASUBI);
a:=(lambda+ lambda)/h;   w:= 1-omega;
s:=mu×mu;   c:=0.5×omega/(1.0+s);
b:=s×c;   m:=0;
comment loop control term;
for sl:= 0, s while s> epso  do
begin r:=a;   s:= 0;
      for i:= 1 step 1 until nm1  do
      begin r:= r + 2.0;   d:= c/r;
            for j:= 1 step 1 until nm1 do
              t[i,j]:= t[i,j]×w +
              t[i+1,j]×(c+d) +
              (c-d)×t[i-1,j]+b×(t[i,j+1]
              + t[i,j-1])
      end   LINE 149;
```

```
        comment The above
          expression sweep equation
          is equivelent to equation three;
        for j:= 1 step 1 until nm1 do
        begin r:= t[n,j] :=
                t[n,j]×w  +(c+c)×t[nm1,j] +
                b×(t[n,j+1] + t[n,j-1]);
              s:= abs(tl[j] - r)+s;
              tl[j]:= r
        end   LINE 159;
        comment s is now the sum on
          the right hand side of
          equation ten;
        m:=m+1;
        if m=E then goto FF;
        if sl≠0 then QSUBK:=s/sl;
        comment there would follow
          a sequence of
          instructions using the
          adjustment of omega if
          this were to be optimized;
end     LINE 171;
write text (70,[PACKING*DENSITY*=*]);
write (70,f44,density);
write text (70, [Cross*sectional*
```

```
  area*of*element*=*]);
write (70,f11,ASUBI);
write text (70, [Pedestal*area*
  to*element*area*=*]);
write (70,f11,ratio);
write text (70, [Height*of*element*=*]);
write (70,f11,(lstar×l));
write text (70,[epso*=*]);
write (70,f11,epso);
write text(70,[lstar*=*]);
write(70,f11,lstar);
write text(70,[rstar*=*]);
write(70,f22,rstar(density,ratio));
write text(70,[bstar*=*]);
write (70,f33,bstar(l,density,ASUBI));
write text(70,[matrix*size**n*=*]);
write(70,f44,n);
write text(70,[iterations*=*]);
write (70,f44,m);
write text(70,[omega*=*]);
write (70,f11,omega);
write text(70,[temperature*=*]);
write(70,f44,t[n,n-1]);
write text(70,[QSUBK*=*]);
write(70,f55,QSUBK);
```

```
comment The Q ratio is next to be
  evaluated using a trapezoidal
  approximation for the integral;
APRIM:=(rstar(density,ratio)
  -rstar(density,ratio)
  ×rstar(density,ratio));
BPRIM:=(1.0-rstar(density,ratio))×(1.0 -
  rstar(density,ratio));
YO:=(1.0 - t[0,n-1]);
Y1:=(1.0- t[n,n-1]);   Q :=0;
so:=APRIM×YO + (APRIM+ BPRIM)× Y1;
for i:= 1 step 1 until n-1 do
begin Y :=(1.0- t[i,n-1]);
      f:=(APRIM+BPRIM×i×h)×Y;   Q:=Q+2×f;
end  LINE 214  loop;
RATIO:=Q+so;   write text(70,[RATIO*=*]);
write(70,f66,RATIO);
comment  The heat leakage is
  calculated as follows;
tt:=  phaseq:= RATIO×(lstar/
  density-.5×ratio×lstar)+(.5×ratio-1);
write text (70, [Heat*leakage*=*]);
write (70,f66,tt);
     end   LINE 223;
end   LINE 224;
```

```
end   LINE 225  phaseq iteration;
procedure module(f1,f2,f3,f4,f5,f6,f7,f8,sigma,ll,
  rhoj,F,A,f,OMEGA,KSUBI,K,alpha,TSUBC,DELT);
  value f1,f2,f3,f4,f5,f6,f7,f8,sigma,ll,rhoj,F,A,
  f,OMEGA,KSUBI,K,alpha,TSUBC,DELT;
  integer f1,f2,f3,f4,f5,f6,f7,f8,f;
  real sigma,ll,rhoj,F,A,OMEGA,KSUBI,K,alpha,TSUBC,DELT;
begin real rho,interior,junction,REFF,term1,g,
        term2,KEFF,ZEFF,DLTMXEFF,introd,bata,ISUBQ,
        muq,theta,muphi,VOLTCPL,I,bracket,QSUBS,
        denom,PHI,QUVOL,QUMODARA,QRMODARA,QUAREA;
      concept1;   heading1;
      write text(70,[MATERIAL*MODULE*PERFORMANCE[2c]]);
      if f=0 then
        write text(70,[The*thermoelectric*element*
        is*positioned*on*a*pedestal*]) else
        write text(70,[The*hot*and*cold*junctions*
        are*seperated*by*the*element]);
      new line(70,2);
      term1:=(f×2×A)×(1-OMEGA)/(ll×OMEGA);
      comment OMEGA is the packing density;
      if f=0 then
        g:=phaseq(omega,E,f11,f22,f33,f44,f55,f66,
        FF)×2×A/ll else g:=1;
      term2:=g×(1-f);
```

```
        comment f=0 for pedestal,f=1for non pedestal module;
        write text(70,[REFF[8s]KEFF[9s]ZEFF[2c]]);
        rho:= 1/sigma;   interior:= rho×11;
        comment 11  is height of thermoelement;
        junction:= 2×rhoj;
        REFF:= (2×F↑2/A)×(interior+junction);
        comment F is ripple effect;
        write (70,f1,REFF);
        KEFF:= (2×A×K/11)+KSUBI×(term1+term2);
        comment KSUBI conductivity of insulation;
        write (70,f2,KEFF);   ZEFF:= (alpha↑2)/(REFF×KEFF);
        write (70,f3,ZEFF);
READ: TSUBC:= read (20);   newline (70,2);
        write text (70,[TSUBC*=*]);   write (70,f4,TSUBC);
     write text (70,[[2c]DLTMXEFF[4s]MUPHI[8s]ISUBQ[2c]]);
     DLTMXEFF:=(TSUBC↑2×ZEFF)×0.5;
     write(70,f5,DLTMXEFF);
     introd:=DELT/((ZEFF×TSUBC)×(0.5×DELT+TSUBC));
     bata:=sqrt(1+ZEFF×(0.5×DELT+TSUBC));
     muphi:=introd×(1+bata);
     comment upper value of input variable has
       been asigned;
     write(70,f6,muphi);   ISUBQ:=alpha×TSUBC/REFF;
     comment section 1;
     write(70,f7,ISUBQ);   newline(70,2);   muq:=1.0;
```

```
comment lower value of dimensionless input variable;
for theta:= (muq + .06) step (-.02) until
  (muphi -.02) , muphi  do
begin VOLTCPL:=alpha×(theta×TSUBC+DELT);
      I:=theta×ISUBQ;
      bracket:=(2.0 ×theta-theta↑2-DELT/DLTMXEFF);
      QSUBS:=KEFF×DLTMXEFF×bracket;
      denom:=2×(theta↑2+theta×DELT/TSUBC);
      PHI:=bracket/denom;    QUVOL:=QSUBS/(2×A×11);
      QUMODARA:=QUVOL×OMEGA×11;
      QRMODARA:=QUMODARA×(1+1/PHI);
      QUAREA:=QUVOL×11;    write text(70,[THETA*=*]);
      write(70,f8,theta);
      write text(70,[VOLTAGE/COUPLE*=*]);
      write(70,f8,VOLTCPL);
      write text(70,[CURRENT*AMPS*=*]);
      write(70,f8,I);
      write text(70,[HEAT*PUMP*RATE--WATTS*=*]);
      write(70,f8,QSUBS);
      write text(70,[COEFF*OF*PERFORMANCE*=*]);
      write(70,f8,PHI);
      write text(70,[HEAT*PUMP*RATE/VOLUME*=*]);
      write(70,f8,QUVOL);
      write text(70,[HEAT*PUMP*RATE/MOD*AREA*=*]);
      write(70,f8,QUMODARA);
```

```
            write text(70,[HEAT*REJECTION/MOD*AREA*=*]);
            write(70,f8,QRMODARA);
            write text(70,[HEAT*PUMP*RATE/ELEMENT*
              AREA*=*]);
            write(70,f8,QUAREA);   newline(70,2);
         end   LINE 305  innerloop;
         write text(70,[[p]]);
         if read boolean(20) then goto READ;
   FF:   write text(70,[the*program*has*not*converged]);
      end   LINE 309  module;
      open(20);   open(70);   f1:=format([+d.dd10≠nd]);
      f2:=format([3s+d.dd10≠nd]);   f3:= format([4s+d.dd10≠ndc]);
      f4:= format([3s+nddd.dc]);   f5:=format([3s+nddd.d]);
      f6:=format([3s+ndd.ddd]);   f7:=format([4s+ndd.ddddcc]);
      f8:=format([4s+nddd.dddddc]);   f11:=format([9s+nd.ddddc]);
      f22:=format([9s+nd.ddddc]);   f33:=format([12s+nd.ddddc]);
      f44:=format([12s+ndd.ddddc]);   f55:=format([9s+nd.ddddc]);
      f66:=format([9s+ndd.dddddcc]);   owner;
      comment A is the same as ASUBI and OMEGA is
        equivelent to density;
      sigma:=read(20);   l:=read(20);   rhoj:=read(20);
      F:=read(20);   A:=read(20);   f:=read(20);
      OMEGA:=read(20);   KSUBI:=read(20);   K:= read(20);
      alpha:=read(20);   DELT:=read(20);   l1:=read(20);
      omega:=read(20);   E:= read(20);   lstar:=read(20);
```

```
  ratio:=read(20);   density:=read(20);   ASUBI:=read(20);
  module(f1,f2,f3,f4,f5,f6,f7,f8,sigma,ll,rhoj,F,A,f,
    OMEGA,KSUBI,K,alpha,TSUBC,DELT);
  close(20);   close(70);
end ->
```

C.P. 3

DD0172500WPU+P1500079PSP→

```
begin comment This program calculates the design and
    operational characteristics of a modular
    thermoelectric couple operating at maximum
    temperature difference;
  integer f1,f2,f3,f4,f5,f6,f7,f8,f;
  real sigma,l,rhoj,F,A,OMEGA,phaseq,KSUBI,k,alpha,TSUBC;
  procedure owner;
  begin write text(70,[[2c]WALLACE*SHAKUN**AERO*ENGR[2c]]);
  end   LINE   9  owner;
  procedure concept2;
  begin write text(70,[[c]This*program*calculates*
          for*a*given*module*design*the*[c]
          performance*characteristic*operating*at*a*
          maximum*temperature*[c]difference*the*
          parameter*is*the*dimensionless*current[2c]]);
  end   LINE   16  concept2;
  procedure heading2;
  begin write text(70,[[c]OPERATIONAL*
          CHARACTERISTICS*OF*THE*GIVEN*MODULE[c]]);
        write text(70,[[c]ELEMENT*HEIGHT*=***********
          cm.[c]JUNCTION*RESISITIVITY*=**********
          ohm.*cm.*sqrd.[c]CONDUCTIVITY*OF*ELEMENT*=*
          ********1/ohm*cm[c]PACKING*DENSITY*=*******
          ****[c]ELEMENT*AREA*=*********cm*sqrd[c]
```

```
        SEEBECK*COEFFICIENT*=**********volts/deg*
        kel[c]HEIGHT*OF*MODULE*=******************
        ***cm[c]HEIGHT*OF*PEDESTAL*=**************
        *cm[c]RIPPLE*FACTOR*=**************[3c]]);
end   LINE  29  heading2;
procedure MODMAXT(f1,f2,f3,f4,f5,f6,f7,f8,sigma,l,
  rhoj,F,A,f,OMEGA,phaseq,KSUBI,k,alpha,TSUBC);
  value f1,f2,f3,f4,f5,f6,f7,f8,sigma,l,rhoj,F,A,f,
  OMEGA,phaseq,KSUBI,k,alpha,TSUBC;
  integer f1,f2,f3,f4,f5,f6,f7,f8,f;
  real sigma,l,rhoj,F,A,OMEGA,phaseq,KSUBI,k,alpha,TSUBC;
begin real rho,interior,junction,REFF,term1,g,
        term2,KEFF,ZEFF,TSUBH,DLTMXEFF,introd,bata,
        ISUBQ,muq,theta,muphi,VOLTCPL,I,bracket,
        QSUBS,denom,PHI,QUVOL,QUMODARA,QRMODARA,QUAREA;
      write text(70,[MATERIAL*MODULE*PERFORMANCE[2c]]);
      write text(70,[REFF[8s]KEFF[9s]ZEFF[2c]]);
      rho:= 1/sigma;   interior:= rho×l;
      comment l is length of thermoelement;
      junction:= 2×rhoj;
      REFF:= (2×F↑2/A)×(interior+junction);
      comment F is ripple effect;
      write (70,f1,REFF);
      term1:= (f×2×A)/(l×OMEGA)×(1-OMEGA);
      comment  OMEGA is packing density;
```

```
        g:= phaseq×2×A/l;   term2:= g×(1-f);
        comment f=0 for pedestal, f=1 nonpedestal module;
        KEFF:= (2×A×k/l)+KSUBI×(term1+term2);
        write (70,f2,KEFF);   ZEFF:= (alpha↑2)/(REFF×KEFF);
        write (70,f3,ZEFF);
READ:   TSUBC:= read (20);   newline (70,2);
        write text (70,[TSUBC*=*]);   write (70,f4,TSUBC);
        DLTMXEFF:=(TSUBC↑2×ZEFF)×0.5;
        TSUBH:=DLTMXEFF+TSUBC;
        write text(70,[TSUBH*MAX*=*]);   write (70,f8,TSUBH);
        newline(70,2);
        comment this section is based on TSUBC being
          a fixed operating condition;
        write text(70,[[2c]DLTMXEFF[4s]MUPHI[8s]ISUBQ[2c]]);
        write(70,f5,DLTMXEFF);
        introd:=DLTMXEFF/((ZEFF×TSUBC)×(0.5×DLTMXEFF+TSUBC));
        bata:=sqrt(1+ZEFF×(0.5×DLTMXEFF+TSUBC));
        muphi:=introd×(1+bata);
        comment upper value of input variable has
          been assigned;
        comment muphi must be approximately unity by
          virtue of ISUBPHI approx equal to
          DLT×ISUBQ/DLTMXEFF;
        write(70,f6,muphi);   ISUBQ:=alpha×TSUBC/REFF;
        comment section 1;
```

```
write(70,f7,ISUBQ);   newline(70,2);   muq:=1.0;
comment lower value of dimensionless input variable;
for theta:= (muq+.06) step -.025 until
  (muphi-.20), muphi do
begin VOLTCPL:=alpha×(theta×TSUBC+DLTMXEFF);
      I:=theta×ISUBQ;
      bracket:=(2.0 ×theta-theta↑2-1.0);
      QSUBS:=KEFF×DLTMXEFF×bracket;
      denom:=2×(theta↑2+theta×DLTMXEFF/TSUBC);
      PHI:=bracket/denom;   QUVOL:=QSUBS/(2×A×l);
      QUMODARA:=QUVOL×OMEGA×l;
      QRMODARA:=QUMODARA×(1+1/PHI);
      QUAREA:=QUVOL×l;   write text(70,[THETA*=*]);
      write(70,f8,theta);
      write text(70,[VOLTAGE/COUPLE*=*]);
      write(70,f8,VOLTCPL);
      write text(70,[CURRENT*AMPS*=*]);
      write(70,f8,I);
      write text(70,[HEAT*PUMP*RATE--WATTS*=*]);
      write(70,f8,QSUBS);
      write text(70,[COEFF*OF*PERFORMANCE*=*]);
      write(70,f8,PHI);
      write text(70,[HEAT*PUMP*RATE/VOLUME*=*]);
      write(70,f8,QUVOL);
      write text(70,[HEAT*PUMP*RATE/MOD*AREA*=*]);
```

```
            write(70,f8,QUMODARA);
            write text(70,[HEAT*REJECTION/MOD*AREA*=*]);
            write(70,f8,QRMODARA);
            write text(70,[HEAT*PUMP*RATE/ELEMENT*
              AREA*=*]);
            write(70,f8,QUAREA);   newline(70,2);
        end   LINE 106  innerloop;
        write text(70,[[p]]);
        if read boolean(20) then goto READ;
    end    LINE 109  MODMAXT;
    open(20);   open(70);   f1:=format([+d.dd₁₀±nd]);
    f2:=format([3s+d.dd₁₀±nd]);   f3:= format([4s+d.dd₁₀±ndc]);
    f4:= format([3s+nddd.dc]);   f5:=format([3s+nddd.d]);
    f6:=format([3s+ndd.ddd]);   f7:=format([4s+ndd.ddddc]);
    f8:=format([4s+nddd.dddddc]);   owner;   concept2;
    heading2;   sigma:=read(20);   l:=read(20);
    rhoj:=read(20);   F:=read(20);   A:=read(20);
    f:=read(20);   OMEGA:=read(20);   phaseq:=read(20);
    KSUBI:=read(20);   k:= read(20);   alpha:=read(20);
    MODMAXT(f1,f2,f3,f4,f5,f6,f7,f8,sigma,l,rhoj,F,A,f,
      OMEGA,phaseq,KSUBI,k,alpha,TSUBC);
    close(20);   close(70);
  end →
```

C.P. 4

DD0172400WPU+P1500079PSP→

```
begin comment This program calculates the design and
     operational characteristics of a modular
     thermoelectric couple operating at a temperature
     difference of ZERO degrees;
   integer f1,f2,f3,f4,f5,f6,f7,f8,f;
   real sigma,l,rhoj,F,A,OMEGA,phaseq,KSUBI,k,alpha,TSUBC;
   procedure owner;
   begin write text(70,[[2c]WALLACE*SHAKUN**AERO*ENGR[2c]]);
   end   LINE   9   owner;
   procedure concept1;
   begin write text(70,[[c]This*program*calculates*
         the*operational*characteristics*of*a*
         thermoelectric[c]module*operating*at*a*
         temperature*difference*of*zero*degrees*
         with*input*of*a*[c]dimensionless*current*
         parameter*known*as*theta[2c]]);
   end   LINE   17   concept1;
   procedure heading1;
   begin write text(70,[[c]OPERATIONAL*
         CHARACTERISTICS*OF*THE*GIVEN*MODULE[c]]);
       write text(70,[[c]ELEMENT*HEIGHT*=***********
         cm.[c]JUNCTION*RESISITIVITY*=**********
         ohm.*cm.*sqrd.[c]CONDUCTIVITY*OF*ELEMENT*=*
         ********1/ohm*cm[c]PACKING*DENSITY*=*******
```

```
            ****[c]ELEMENT*AREA*=*********cm*sqrd[c]
            SEEBECK*COEFFICIENT*=**********volts/deg*
            kel[c]HEIGHT*OF*MODULE*=******************
            *cm[c]HEIGHT*OF*PEDESTAL*=***************
            cm[c]RIPPLE*FACTOR*=***************[3c]]);
end   LINE  30  heading1;
procedure MODZERO(f1,f2,f3,f4,f5,f6,f7,f8,sigma,l,
   rhoj,F,A,f,OMEGA,phaseq,KSUBI,k,alpha,TSUBC);
   value f1,f2,f3,f4,f5,f6,f7,f8,sigma,l,rhoj,F,A,f,
   OMEGA,phaseq,KSUBI,k,alpha,TSUBC;
   integer f1,f2,f3,f4,f5,f6,f7,f8,f;
   real sigma,l,rhoj,F,A,OMEGA,phaseq,KSUBI,k,alpha,TSUBC;
begin real rho,interior,junction,REFF,term1,g,
            term2,KEFF,ZEFF,DLTMXEFF,ISUBQ,muq,theta,
            muphi,VOLTCPL,I,bracket,QSUBS,denom,PHI,
            QUVOL,QUMODARA,QRMODARA,QUAREA;
      write text(70,[MATERIAL*MODULE*PERFORMANCE*
            FOR*DELT*=*ZERO*DEGREES*[2c]]);
      write text(70,[REFF[8s]KEFF[9s]ZEFF[2c]]);
      rho:= 1/sigma;   interior:= rho×l;
      comment l is length of thermoelement;
      junction:= 2×rhoj;
      REFF:= (2×F↑2/A)×(interior+junction);
      comment F is ripple effect;
      write (70,f1,REFF);
```

```
term1:= (f×2×A)/(l×OMEGA)×(1-OMEGA);
comment OMEGA is packing density;
g:= phaseq×2×A/l;    term2:= g×(1-f);
comment f=0 for pedestal, f=1 nonpedestal module;
KEFF:= (2×A×k/l)+KSUBI×(term1+term2);
write (70,f2,KEFF);   ZEFF:= (alpha↑2)/(REFF×KEFF);
write (70,f3,ZEFF);
READ: TSUBC:= read (20);   newline (70,2);
write text (70,[TSUBC*=*TSUBH*=*]);
write (70,f4,TSUBC);
write text (70,[[2c]DLTMXEFF[4s]MUPHI[8s]ISUBQ[2c]]);
DLTMXEFF:=(TSUBC↑2×ZEFF)×0.5;
comment THIS IS A POTENTIAL TERM BASED ON THE
  HOT JUNCTION TEMPERATURE;
write(70,f5,DLTMXEFF);
comment upper value of input variable is specified;
muphi:=0;   write(70,f6,muphi);
ISUBQ:=alpha×TSUBC/REFF;
comment section 1;
write(70,f7,ISUBQ);   newline(70,2);   muq:=1.0;
comment lower value of dimensionless input variable;
for theta:= muq step -.02 until muphi do
begin VOLTCPL:=alpha×(theta×TSUBC);   I:=theta×ISUBQ;
      bracket:=(2.0 ×theta-theta↑2);
      QSUBS:=KEFF×DLTMXEFF×bracket;
```

```
        denom:=2×(theta↑2);   PHI:=bracket/denom;
        QUVOL:=QSUBS/(2×A×l);
        QUMODARA:=QUVOL×OMEGA×l;
        QRMODARA:=QUMODARA×(1+1/PHI);
        QUAREA:=QUVOL×l;   write text(70,[THETA*=*]);
        write(70,f8,theta);
        write text(70,[VOLTAGE/COUPLE*=*]);
        write(70,f8,VOLTCPL);
        write text(70,[CURRENT*AMPS*=*]);
        write(70,f8,I);
        write text(70,[HEAT*PUMP*RATE--WATTS*=*]);
        write(70,f8,QSUBS);
        write text(70,[COEFF*OF*PERFORMANCE*=*]);
        write(70,f8,PHI);
        write text(70,[HEAT*PUMP*RATE/VOLUME*=*]);
        write(70,f8,QUVOL);
        write text(70,[HEAT*PUMP*RATE/MOD*AREA*=*]);
        write(70,f8,QUMODARA);
        write text(70,[HEAT*REJECTION/MOD*AREA*=*]);
        write(70,f8,QRMODARA);
        write text(70,[HEAT*PUMP*RATE/ELEMENT*
          AREA*=*]);
        write(70,f8,QUAREA);   newline(70,2);
end     LINE 98 innerloop;
write text(70,[[p]]);
```

```
        if read boolean(20) then goto READ;
    end   LINE 101 ' MODZERO;
    open(20);   open(70);   f1:=format([+d.dd₁₀≠nd]);
    f2:=format([3s+d.dd₁₀≠nd]);   f3:= format([4s+d.dd₁₀≠ndc]);
    f4:= format([3s+nddd.dc]);   f5:=format([3s+nddd.d]);
    f6:=format([3s+ndd.ddd]);   f7:=format([4s+ndd.ddddcc]);
    f8:=format([4s+nddd.dddddc]);   owner;   concept1;
    heading1;   sigma:=read(20);   l:=read(20);
    rhoj:=read(20);   F:=read(20);   A:=read(20);
    f:=read(20);   OMEGA:=read(20);   phaseq:=read(20);
    KSUBI:=read(20);   k:= read(20);   alpha:=read(20);
    MODZERO(f1,f2,f3,f4,f5,f6,f7,f8,sigma,l,rhoj,F,A,f,
     OMEGA,phaseq,KSUBI,k,alpha,TSUBC);
    close(20);   close(70);
end →
```

C.P. 5

DD0177COOWPU+P1500078PSP→

```
begin comment This program calculates the design and
        operational characteristics of a modular
        thermoelectric couple operating between heat
        source and heat sink with finite heat-transfer
        coefficients;
    integer f1,f2,f3,f4,f5,f6,f7,f11,f22,f33,f44,f55,
        f66,L,NO,f,E;
    real OMEGA,lstar,l,epso,ASUBN,ASUBP,rhojp,rhojn,F,
        KSUBI,alpha,incr,lower,TSUBCPRM,sigman,sigmap,
        omega,NSUBC,MC,NSUBH,ksubh,MH,KSUBP,KSUBN,LSUBN,
        LSUBP,density,ratio,ASUBI,TSUBHPRM,thkcold,ksubc,
        ESUBC,thkhot,ESUBH;
    procedure owner;
    begin write text(70,[[2c]WALLACE*SHAKUN**AERO*ENGR[2c]]);
    end   LINE  15  owner;
    procedure concept1;
    begin write text(70,[[2c]This*program*calculates*
              for*a*given*modular*material*operating*[c]
              between*a*heat*source*and*heat*sink*with*
              finite*heat*transfer*coefficients*[c]
              the*performance*characteristics[2c]]);
    end   LINE  22  concept1;
    procedure heading;
    begin write text(70,[[c]this*program*calculates*
```

```
          the*geometrical*parameters[c]
          associated*with*the*heat*flow*model*that*
          yield*the*values*of*q/qsubci[3c]]);
        write text(70,[[c]definition*of*geometrical*
          parameters[c]]);
        write text(70,[[c]lstar*=*dimensionless*
          length*of*the*thermoelectric*[c]column[c]]);
        write text(70,[bstar*=*dimensionless*
          parameter**l:b[c]rstar*=*dimensionless*
          parameter**a/b[c]]);
end     LINE 35 heading;
procedure concept;
begin write text(70,[[c]procedure*optilax*and*
          subtab*when*included*[c]extend*the*
          computational*accuracy*of*the*procedure*
          iterate[c]]);
        write text (70,[[2c]Three*real*procedures*
          calculate*the*dimensionless*parameters*
          required*as*input*for*procedure*iterate[2c]]);
end     LINE 44 concept;
real procedure rstar(density,ratio);
  value density, ratio; real density, ratio;
  rstar:= sqrt (density×0.5×ratio);
comment ratio is the pedestal area to element area;
comment density is thermoelectric packing density;
```

```
real procedure bstar (l,density,ASUBI);
  value l,density,ASUBI; real l,density,ASUBI;
  bstar:= l×sqrt((3.1456×density)/(2.0×ASUBI));
comment l is the height of insulation, density is
  packing density,ASUBI is cross sectional area of element
real procedure zeta1(lstar); value lstar; real lstar;
  zeta1:= 1-lstar;
comment lstar is the ratio of height of element to
  height of insulation;
real procedure  phaseq(omega,E,f11,f22,f33,f44,f55,f66,FF)
  comment procedure phaseq is a numerical soulution
  of the heat transfer equation;
  comment t[i,j] is the value of tau at eta=i×h,
  zeta=j×h where h=1/n. Starting values must be
  assigned,which might all be zeros or else values
  previously derived,for i=1(1)n, j=1(1)n-1;
  value omega,E,f11,f22,f33,f44,f55,f66; label FF;
  integer  E,f11, f22,f33,f44,f55,f66;  real omega;
begin integer j,i,nm1,no,n,m,k;
      real d,s,b,h,lambda,mu,a,w,APRIM,BPRIM,YO,Y1,
       Y,c,f,tt,sl,r,QSUBK,Q,so,RATIO,epso;
      begin heading;   concept;
            no:= entier(0.5×(1.0/rstar(density,
              ratio) -1.0)) + 2.0;
            if lstar ≤ .8 then epso:= .01 else epso:= .001
```

```
    if rstar (density,ratio) ≤ .1 then
    begin k:= 1;   goto F
    end   LINE  77;
    if rstar (density,ratio) ≤ .2 then
    begin k:= 3;   goto F
    end   LINE  80;
    if rstar (density,ratio) ≤ .3 then
    begin k:= 8;   goto F
    end   LINE  83;
    k:= 18;
    comment  the above if statements is the
      technique for minimising the matrix
      required  and maintaining an accuracy
      of approximately 4 per cent.  The
      iterative solution was compared with
      a closed solution for approximately
      144 points;
F:  n:=no × k;   h:=1/n;
    begin real array t[0:n+1,0:n],tl[1:n-1];
          for j:= 1 step 1 until n-1 do
            for i:= 1 step 1 until n do t[i,j]:=0;
          comment the starting values have
            been assigned;
          d:= 1.0 - zeta1(lstar);
          s:=-zeta1(lstar)/d;   b:=h/d;
```

```
nm1:= n-1;
for j:= 1 step 1 until nm1 do
begin t1[j]:=t[n,j];
      comment right side of
        interior domain;
      s:=b+s;
      t[0,j]:=if s≤ 0 then 0 else s;
      comment boundary condition
        left side;
      t[n+1,j]:=t[n-1,j];
      comment boundary condition
        right side derivative
        zero across r;
end   LINE 113;
for i:= n+1 step -1 until 0 do
begin t[i,0]:= 0;
      comment lower boundary condition;
      t[i,n]:= 1;
      comment upper boundary condition;
end   LINE 119;
comment The above two for loops
  set up the boundary conditions
  for the difference equation;
lambda:=(rstar(density,ratio))/
  (1.0- rstar(density,ratio));
```

```
mu:= (1.0- rstar(density,ratio))
  /bstar(1,density,ASUBI);
a:=(lambda+ lambda)/h;   w:= 1-omega;
s:=mu×mu;   c:=0.5×omega/(1.0+s);
b:=s×c;   m:=0;
comment loop control term;
for sl:= 0, s while s> epso  do
begin r:=a;   s:= 0;
    for i:= 1 step 1 until nm1  do
    begin r:= r + 2.0;   d:= c/r;
    for j:= 1 step 1 until nm1 do
   t[i,j]:= t[i,j]×w +
       t[i+1,j]×(c+d) +
             (c-d)×t[i-1,j]+b×(t[i,j+1]
+ t[i,j-1])
    end   LINE 140;
    comment The above
      expression sweep equation
      is equivelent to equation three;
    for j:= 1 step 1 until nm1 do
    begin r:= t[n,j] :=
         t[n,j]×w  +(c+c)×t[nm1,j] +
            b×(t[n,j+1] + t[n,j-1]);
         s:= abs(t1[j] - r)+s;
         t1[j]:= r
```

```
        end   LINE 150;
        comment s is now the sum on
          the right hand side of
          equation ten;
        m:=m+1;
        if m=E then goto FF;
        if s1≠0 then QSUBK:=s/s1;
        comment there would follow
          a sequence of
          instructions using the
          adjustment of omega if
          this were to be optimized;
    end   LINE 162;
    write text (70,[Packing*DENSITY*=*]);
    write (70,f44,density);
    write text (70, [Cross*sectional*
      area*of*element*=*]);
    write (70,f11,ASUBI);
    write text (70, [Pedestal*area*
      to*element*area*=*]);
    write (70,f11,ratio);
    write text (70, [Height*of*element*=*]);
    write (70,f11,(lstar×l));
    write text (70,[epso*=*]);
    write (70,f11,epso);
```

```
write text(70,[lstar*=*]);
write(70,f11,lstar);
write text(70,[rstar*=*]);
write(70,f22,rstar(density,ratio));
write text(70,[bstar*=*]);
write (70,f33,bstar(1,density,ASUBI));
write text(70,[matrix*size**n*=*]);
write(70,f44,n);
write text(70,[iterations*=*]);
write (70,f44,m);
write text(70,[omega*=*]);
write (70,f11,omega);
write text(70,[temperature*=*]);
write(70,f44,t[n,n-1]);
write text(70,[QSUBK*=*]);
write(70,f55,QSUBK);
comment The Q ratio is next to be
  evaluated using a trapezoidal
  approximation for the integral;
APRIM:=(rstar(density,ratio)
  -rstar(density,ratio)
  ×rstar(density,ratio));
BPRIM:=(1.0-rstar(density,ratio))×(1.0 -
  rstar(density,ratio));
YO:=(1.0 - t[0,n-1]);
```

```
            Y1:=(1.0- t[n,n-1]);   Q :=0;
            so:=APRIMxY0 + (APRIM+ BPRIM)x Y1;
            for i:= 1 step 1 until n-1 do
            begin Y :=(1.0- t[i,n-1]);
                f:=(APRIM+BPRIMxixh)xY;   Q:=Q+2xf;
            end  LINE 205  loop;
            RATIO:=Q+so;   write text(70,[RATIO*=*]);
            write(70,f66,RATIO);
            comment  The heat leakage is
              calculated as follows;
            tt:= phaseq:= RATIOx(lstar/
              density-.5xratioxlstar)+(.5xratio-1);
            write text (70, [Heat*leakage*=*]);
            write (70,f66,tt);
        end  LINE 214;
    end  LINE 215;
end  LINE 216  phaseq iteration;
procedure heading1;
begin write text(70,[[c]material*characteristics*
      of*the*given*module[c]]);
    write text(70,[[c]element*height**cm.]);
    write(70,f4,lxlstar);
    write text(70,[junction*resistivity**ohm*cm*sqrd]);
    write(70,f5,rhojn);
    write text(70,[conductivity*of*n-element**
```

```
  1/ohm*cm**terminology*sigman]);
write(70,f4,sigman);
write text(70,[conductivity*of*p-element**
  1/ohm*cm**terminology*sigmap]);
write(70,f4,sigmap);
write text(70,[packing*density]);
write(70,f4,OMEGA);
write text(70,[area*of*n-element**cm*sqrd]);
write(70,f4,ASUBN);
write text(70,[area*of*p-element**cm*sqrd]);
write(70,f4,ASUBP);
write text(70,[seebeck*coefficient**
  volts/deg*kelvin]);
write(70,f5,alpha);
write text(70,[height*of*pedestal**cm]);
write(70,f4,(l-lstar×l));
write text(70,[height*of*module**cm]);
write(70,f4,l);   write text(70,[ripple*factor]);
write(70,f4,F);   write text(70,[percent*ripple]);
write(70,f4,sqrt(8.0₁₀-4×(F↑2-1)));
write text(70,[thermal*conductivity*
  n-element**watt/cm*deg*kelvin]);
write(70,f4,KSUBN);
write text(70,[thermal*conductivity*
  p-element**watt/cm*deg*kelvin]);
```

```
    write(70,f4,KSUBP);
    write text(70,[free*stream*heat*sink*
      temperature**deg*kelvin*=*]);
    write(70,f4,TSUBHPRM);
    write text(70,[free*stream*source*
      temperature**deg*kelvin*=*]);
    write(70,f4,TSUBCPRM);
    comment when np pedestal is present set lstar
      equal to unity;
    newline(70,2);
end   LINE 260  heading1;
real procedure R(sigman,sigmap,KSUBP,KSUBN,LSUBN,LSUBP,f4);
  value sigman,sigmap,KSUBP,KSUBN,LSUBN,LSUBP,f4;
  integer f4; real sigman,sigmap,KSUBP,KSUBN,LSUBN,LSUBP;
begin real rhon,rhop,top,bottom,N,inter1,inter2,rr;
    rhon:=1/sigman;   rhop:=1/sigmap;   top:=KSUBP×rhon;
    bottom:=KSUBN×rhop;   N:=sqrt(top/bottom);
    write text(70,[shape*factor*for*optimizing*cop*=*]);
    write(70,f4,N);   inter1:=rhon/ASUBN×LSUBN;
    inter2:=rhop/ASUBP×LSUBP;   rr:=R:=inter1+inter2;
    write text(70,[couple*element*interior*
      resistance**ohms*=*]);
    write(70,f4,rr);
end   LINE 273  R;
real procedure K(ASUBN,KSUBN,LSUBN,ASUBP,KSUBP,LSUBP,f4);
```

```
  value ASUBN,KSUBN,LSUBN,ASUBP,KSUBP,LSUBP,f4;
  integer f4; real ASUBN,KSUBN,LSUBN,ASUBP,KSUBP,LSUBP;
begin real kk;
    kk:=K:=ASUBN×KSUBN/LSUBN + ASUBP×KSUBP/LSUBP;
    write text(70,[couple*element*thermal*
      conductance**watts/deg*kelvin*=*]);
    write(70,f4,kk);
end  LINE 282;
real procedure expcold(NSUBC,MC,f4);
  value NSUBC,MC,f4; integer f4; real NSUBC,MC;
  comment MC is introduced as a technique to study
  the effects of when NSUBC is at infinity,
  therefore the exponent is zero.In most cases of
  free convection the exponent value is between
  zero and unity;
begin real ee;
    ee:=expcold:=(1/(1+NSUBC))×MC;
    write text(70,[exponent*value*for*cold*side*
      heat*transfer*coefficient*=*]);
    write(70,f4,ee);
end  LINE 295  expcold;
real procedure exphot(NSUBH,MH); value NSUBH,MH;
  real NSUBH,MH;
begin real ff;
    ff:=exphot:=(1/(1+NSUBH))×MH;
```

```
end   LINE 300  exphot;
procedure HEATFLUX(f,OMEGA,l,lstar,ASUBP,ASUBN,F,
   alpha,KSUBP,epso,rhojp,rhojn,KSUBI,incr,lower,
   TSUBCPRM,TSUBHPRM,thkcold,ksubc,ESUBC,L,thkhot,
   ksubh,ESUBH,NO,f1,f2,f3,f4,NSUBH,MH,f6,f7,END);
   value f,OMEGA,l,lstar,ASUBP,ASUBN,F,alpha,KSUBP,
   epso,rhojp,rhojn,KSUBI,lower,TSUBCPRM,incr,NSUBH,
   MH,TSUBHPRM,thkcold,ksubc,ESUBC,L,thkhot,ksubh,
   ESUBH,NO,f1,f2,f3,f4,f6,f7; label END;
   integer f1,f2,f3,f4,f6,f7, L,NO,f;
   real OMEGA,l,lstar,ASUBP,ASUBN,F,alpha,KSUBP,
   epso,rhojn,rhojp,KSUBI,lower,TSUBCPRM,incr,NSUBH,
   MH,TSUBHPRM,thkcold,ksubc,ESUBC,thkhot,ksubh,ESUBH;
begin real termAA, termA;g,crossterm,termB,
      JUNCTION,REFF,KEFF,ZEFF,h,ZMATERIAL,A,B,C,
      guesstc,guessth,gssdltjt,NUC,TSUBCJ,TSUBH,
      DELTJCT,mm,termBB,CURRENT,I,POWERFLUX,COP,
      NUH,DELTHTSD,TSUBH2,POWER,VOLTCPL,ISUBQ,
      nucupper,muphi,bata,introd,IATCOP,VOLTPhI,
      DELTMAX,DELTMXEF,UPPER,LOWER,PHIMAX,theta,
      bracket,QSUBS,QUVOL,DELTTC,QUMODARA,
      QRMODARA,QUAREA,QSUCC,TONS,QMAX,RATIOQ;
    concept1;   heading1;
    write text(70,[material*thermoelectric*
      module*performance[2c]]);
```

```
if f = 0 then
  write text(70,[the*thermoelectric*elements*
  are*positioned*on*a*pedestal]) else
  write text(70,[the*hot*and*cold*junctions*
  are*seperated*by*the*element*proper]);
newline(70,2);
termA:=(f×(ASUBP+ASUBN))×(1-OMEGA)/(lstar×l×OMEGA);
comment lstar×l is the height of the
  thermoeleectric element,OMEGA is the
  packing density,l is the height of insulation;
comment it is assumed that LSUBN and LSUBP
  Are equal in length and lstar×l is the
  resulting element height;
crossterm:=(ASUBN+ASUBP)/(lstar×l);
if f=0 then
  g:=phaseq(omega,E,f11,f22,f33,f44,f55,f66,
  FF)×crossterm else g:=1;
termB:=g×(1-f);
comment f=0 for pedestal system,f=1 for
  non-pedestal module;
write text(70,[[c]effective*material*
  properties[2c]]);
JUNCTION:=(2×rhojp/ASUBP + 2×rhojn/ASUBN);
comment JUNCTION is the total contact
  resistance for a single thermoelectric couple;
```

```
REFF:=F↑2×(JUNCTION+R(sigman,sigmap,KSUBP,
  KSUBN,LSUBN,LSUBP,f4));
comment F is the term to include ripple effect;
write text(70,[effective*resistance**ohms*=*]);
write(70,f1,REFF);   newline(70,1);
KEFF:=K(ASUBN,KSUBN,LSUBN,ASUBP,KSUBP,LSUBP,
  f4)+KSUBI×(termA+termB);
write text(70,[effective*thermal*conductance*
  *watts/deg*kelvin*=*]);
write(70,f2,KEFF);   newline(70,1);
ZEFF:=(alpha↑2)/(REFF×KEFF);
write text(70,[effective*figure*of*merit**
  1/deg*kelvin*=*]);
write(70,f3,ZEFF);
h:=K(ASUBN,KSUBN,LSUBN,ASUBP,KSUBP,LSUBP,f4)
  ×R(sigman,sigmap,KSUBP,KSUBN,LSUBN,LSUBP,f4);
ZMATERIAL:=(alpha↑2)/h;
write text(70,[material*figure*of*merit*
  1/deg*kelvin*=*]);
write(70,f1,ZMATERIAL);   newline(70,2);
A:=(OMEGA×REFF)/(2×(ASUBP+ASUBN));
B:=(OMEGA×alpha)/(ASUBP+ASUBN);
C:=(OMEGA×KEFF)/(ASUBN+ASUBP);
if incr≠10 then
  write text(70,[the*option*of*using*the*for*
```

```
      statement*has*been*exercized*[c]
      the*cold*side*heat*flux*is*being*
      incrementaly*stepped*by*the*for*loop[c]]) else
      write text(70,[the*cold*side*heat*flux*
      input*is*a*single*value*determined*by*the*
      value*assigned*to*the*variable[c]
      designated*as*lower[c]]);
    if incr =0 then goto JUMP else
    begin write text(70,[estimated*junction*
          temperatures*establishing*the*upper*
          value*in*the*for*[c]statement*follows:[c]]);
       guesstc:=TSUBCPRM-15;
       write text(70,[estimated*cold*side*
         junction*temperature**deg*kelvin*=*]);
       write(70,f7,guesstc);   guessth:=TSUBHPRM+15;
       write text(70,[estimated*hot*side*
         junction*temperature**deg*kelvin*=*]);
       write(70,f7,guessth);
       gssdltjt:=guessth-guesstc;
       write text(70,[estimated*temperature*
         difference*across*junction**deg*c*=*]);
       write(70,f7,gssdltjt);
       nucupper:=((B×guesstc)↑2×.25)/A - C×gssdltjt;
    end   LINE 398;
JUMP: for NUC:= lower step incr until nucupper +
```

```
  5.00, nucupper do
begin write text(70,[[c]the*uniform*cold*
    side*heat*flux*has*been*assigned*a*
    value**watts/cm*sqrd[c]]);
   write text(70,
    [XXXXXXXXXXXXXXXXXXXXXXXXXXXXXXXXXXXXXXXXX[c
    ]]);
   write (70,f4,NUC);
   write text(70,
    [XXXXXXXXXXXXXXXXXXXXXXXXXXXXXXXXXXXXXXXXX[c
    ]]);
   DELTTC:=thkcold×NUC/ksubc+(NUC/ESUBC)
    ↑expcold(NSUBC,MC,f4);
   newline(70,1);    TSUBCJ:=TSUBCPRM-DELTTC;
   TSUBH:=TSUBHPRM+TSUBCPRM×0.01;
   comment this statement establishes a
    starting value for the hot side
    junction temperature sufficient to
    insure proper startng of the
    iterative solution;
   mm:=0;    TSUBH2:=0;
   write text(70,[iterative*solution*follows[c]]);
   write text(70,[iterations[6s]
    tsubh*deg*kel[7s]comparison*tsubh[2c]]);
   comment mm is a loop control term;
```

```
REPEAT: DELTJCT:=TSUBH-TSUBCJ;   write (70,f1,mm);
    write(70,f2,TSUBH);   write(70,f4,TSUBH2);
    mm:=mm+1;
    if mm = L then goto EXHAUST;
    termAA:=B×TSUBCJ;
    if (B×TSUBCJ)↑2-4×A×(C×DELTJCT+NUC)<0
      then goto ALARM;
    termBB:=sqrt((B×TSUBCJ)↑2-4×A×(C×DELTJCT+NUC));
    CURRENT:=(termAA-termBB)/(2×A);   I:=CURRENT;
    if I ≤ 0 then goto ALARM;
    comment when iteration is successfully
      completed;
    POWERFLUX:=B×I×DELTJCT+2×A×I↑2;
    COP:=NUC/POWERFLUX;   NUH:=NUC×(1/COP+1);
    DELTHTSD:= thkhot×NUH/ksubh+(NUH/ESUBH)
      ↑exphot(NSUBH,MH);
    TSUBH2:=DELTHTSD+TSUBHPRM;
    if abs(TSUBH-TSUBH2)≥ epso then
    begin TSUBH:=(TSUBH+TSUBH2)×0.5;
        goto REPEAT;
    end   LINE 445
      else TSUBH:=(TSUBH+TSUBH2)×0.5;
    write text(70,[[c]balanced*operation*
      achieved[2c]]);
    write text(70,[the*iterations*for*the*
```

```
  hot*side*temperature*at*the*junction*
  has*successfully[c]terminated*to*the*
  required*error****epso[c]]);
newline(70,3);
write text(70,[exponent*value*for*hot*
  side*heat*transfer*coefficient*=*]);
write(70,f4,(1/(1+NSUBH))×MH);
write text(70,[cold*side*heat*flux**
  watts/cm*sqrd*=*]);
write(70,f4,NUC);
write text(70,[hot*junction*
  temperature**deg*kelvin*=*]);
write(70,f4,TSUBH);
write text(70,[junction*temperature*
  difference**deg*kelvin*=*]);
write(70,f4,DELTJCT);
write text(70,[cold*side*junction*
  temperature**deg*kelvin*=*]);
write(70,f4,TSUBCJ);
write text(70,[iterations*to*achieve*
  balanced*operational*solution*=*]);
write (70,f6,mm);
write text(70,[current*per*couple*
  required*to*maintain*heat*balance**amps*=*]);
write (70,f6,I);
```

```
write text(70,[electrical*power*
  required*to*maintain*heat*balance**
  watts/couple*=*]);
write(70,f6,POWERFLUX×ASUBI×2/OMEGA);
write text(70,[electrical*power*
  required*for*a*system*containing*
  NO-couples*in*electrical*series**kw*=*]);
POWER:=POWERFLUX×NO×ASUBI×2/(OMEGA×1000);
write(70,f4,POWER);
write text(70,[COP**at*the*balanced*
  operation*=*]);
write(70,f4,COP);
write text(70,[the*required*heat*
  rejuction*rate/modular*area**
  watts/cm*sqrd*=*]);
write(70,f4,NUH);   newline(70,2);
write text(70,[the*assumption*for*the*
  design*is*that*the*NO-couples*are*
  electrically*in*series*[c]]);
write text(70,[electrical*power*
  requirements[c]]);
VOLTCPL:=alpha×DELTJCT + I×REFF;
write text(70,[voltage*per*couple*at*
  balanced*operation**voltage*=*]);
write(70,f4,VOLTCPL);
```

```
write text(70,[voltage*for*a*system*of*
  NO-couples*electriacally*in*series**
  voltage*=*]);
write(70,f6,VOLTCPL×NO);
ISUBQ:=alpha×TSUBCJ/REFF;
write text(70,[the*current*that*
  maximizes*the*heat*pump*rate**amps*=*]);
write(70,f4,ISUBQ);
write text(70,[ratio*current*at*
  balanced*operation*to*current*at*max*
  heat*pump*rate*=*]);
write(70,f4,I/ISUBQ);
introd:=DELTJCT/((ZEFF×TSUBCJ)
  ×(0.5×DELTJCT+TSUBCJ));
bata:=sqrt(1+ZEFF×(0.5×DELTJCT+TSUBCJ));
muphi:=introd×(1+bata);
write text(70,[ratio*current*at*max*
  cop*to*current*at*max*heat*pump*rate*=*]);
write (70,f4,muphi);    IATCOP:=muphi×ISUBQ;
write text(70,[the*current*required*to*
  maximize*cop**amps*=*]);
write(70,f4,IATCOP);
write text(70,[ratio*current*at*
  operational*balance*to*current*at*
  max*cop*=*]);
```

```
write(70,f4,I/IATCOP);
write text(70,[voltage*per*couple*for*
  maximizing*heat*pump*rate**volts*=*]);
write(70,f4,alpha×TSUBH);
write text(70,[ratio*voltage*at*
  balanced*operation*to*voltage*at*max*
  heat*pump*rate*=*]);
write(70,f4,VOLTCPL/(alpha×TSUBH));
write text(70,[voltage*per*couple*for*
  maximizing*cop**volts*=*]);
VOLTPHI:=alpha×(muphi×TSUBCJ+DELTJCT);
write(70,f2,VOLTPHI);   newline(70,1);
write text(70,[ratio*voltage*at*
  balanced*operation*to*voltage*at*max*
  cop*=*]);
write(70,f4,(VOLTCPL/VOLTPHI));
write text(70,[the*max*temperature*
  difference*is*based*on*the*cold*
  junction*temperature*being*a*reference[c]]);
write text(70,[the*max*temperature*
  difference*based*on*material*
  properties**deg*c*=*]);
DELTMAX:=(TSUBCJ↑2×ZMATERIAL)×0.5;
write(70,f7,DELTMAX);
write text(70,[max*temperature*
```

```
  difference*based*on*effective*figure*
  of*merit**deg*c*=*]);
DELTMXEF:=(TSUBCJ↑2×ZEFF)×0.5;
write(70,f7,DELTMXEF);
UPPER:=(2×muphi-muphi↑2-DELTJCT/DELTMXEF);
LOWER:=2×(muphi↑2+muphi×DELTJCT/TSUBCJ);
PHIMAX:=UPPER/LOWER;
write text(70,[max*cop*=*]);
write(70,f4,PHIMAX);
write text(70,[ratio*operating*cop*to*
  max*cop*=*]);
write(70,f4,COP/PHIMAX);
comment using the relation that
  theta=I/ISUBQ the following results;
theta:=I/ISUBQ;
bracket:=(2×theta-theta↑2-DELTJCT/DELTMXEF);
QSUBS:=KEFF×DELTMXEF×bracket;
QUVOL:=QSUBS/(LSUBN×ASUBN+LSUBP×ASUBP);
write text(70,[heat*pump*rate*per*
  element*vol**watts/cm*cub*=*]);
write (70,f4,QUVOL);
QUMODARA:=QSUBS×OMEGA/(ASUBN+ASUBP);
comment as a check on the iterative
  solution QUMODARA can be compared to NUC;
QRMODARA:=QUMODARA×(1+1/COP);
```

```
QUAREA:=QSUBS/(ASUBN+ASUBP);
comment as a check on the iterative
  solution NUH can be compared to QRMODARA;
write text(70,[the*next*computer*
  outputs*compare*the*operational*
  solutions*for*the*balanced*system[c]]);
write text(70,[heat*pump*rate*/modular*
  area**watts/cm*sqrd[c]]);
write text(70,[QUMODARA*=*]);
write(70,f4,QUMODARA);
write text(70,[NUC*=*]);  write(70,f4,NUC);
newline(70,2);
write text(70,[heat*rejection*
  rate/modular*area**watts/cm*sqrd[c]]);
write text(70,[NUH*=*]);  write(70,f4,NUH);
write text(70,[QRMODARA*=*]);
write(70,f4,QRMODARA);  newline(70,3);
comment this simple relation allows the
  calculation of NUC  when the heat
  load QSUCC is given in watts;
QSUCC:=(NUC)×(ASUBN+ASUBP)/OMEGA;
TONS:=(QSUCC×NO)/(17.52×200);
write text(70,[heat*pump*rate*with*
  NO-couples*thermally*parallel**tons*=*]);
write(70,f4,TONS);
```

```
        write text(70,[heat*pump*rate*with*
  NO-couples*thermally*parallel**watts*=*]);
write(70,f4,NO×QSUCC);
QMAX:=KEFF×DELTMXEF×(1-DELTJCT/DELTMXEF);
RATIOQ:=QSUCC/QMAX;
write text(70,[ratio*heat*pump*rate*at*
  balanced*operation*to*max*heat*pump*
  rate*=*]);
write(70,f4,RATIOQ);   newline(70,2);
write text(70,[the*following*results*
  are*based*on*approximations*.The*
  approximations*for*a*couple[c]
  and*subsequent*implications*of*
  assuming*the*parameters*lambda*and*
  reciprical*function*equal*to*[c]
  unity*is*found*in*section***********
  *******of*this*thesis[2c]]);
write text(70,[cop*at*max*q*=*]);
write(70,f4,(0.5×(1-DELTJCT/DELTMXEF)));
write text(70,[max*cop*=*]);
write (70,f4,(0.5×(DELTMXEF/DELTJCT-1)));
write text(70,[heat*pump*rate*at*max*cop*=*]);
write(70,f4,(DELTJCT/DELTMXEF×QMAX));
write text(70,[current*providing*max*cop*=*]);
write(70,f4,(DELTJCT/DELTMXEF×ISUBQ));
```

```
            write text(70,[[p]]);
        end    LINE 626   innerloop;
        write text(70,[[c]all*aspects*of*program*
          completed*successfully[c]]);
        goto END;
     ALARM: write text(70,[the*heat*flux*on*the*cold*
          side*has*exceeded*the*capabilities*of*the*
          [c]material*and*specified*free*stream*
          conditions*[2c]]);
        goto END;
   EXHAUST: write text(70,[[c]the*limit*value*for*the*
          number*of*iterations*has*been*exceeded*[c]
          in*procedure*HEATFLUX[2c]]);
        goto END;
      FF: write text(70,[the*program*has*not*converged*
          in*procedure*phaseq]);
    end    LINE 641   HEATFLUX;
    open(70);   open(20);   f1:=format([+d.dd₁₀±nd]);
    f2:=format([3s+d.dd₁₀±nd]);   f3:=format([4s+d.dd₁₀±ndc]);
    f4:=format([3s+ndddd.ddddddc]);
    f5:=format([3s+d.dd₁₀±ndc]);   f6:=format([3s+ndd.ddddc]);
    f7:=format([3s+nddd.ddc]);   f11:=format([9s+nd.ddddc]);
    f22:=format([8s+nd.ddddc]);   f33:=format([12s+nd.ddddc]);
    f44:=format([12s+ndd.ddddc]);   f55:=format([9s+nd.ddddc]);
    f66:=format([9s+ndd.dddddc]);   OMEGA:=density:=read(20);
```

```
ratio:=read(20);    l:=read(20);
ASUBN:=ASUBP:=ASUBI:=read(20);    lstar:=read(20);
omega:=read(20);    E:=read(20);    LSUBN:=LSUBP:=read(20);
KSUBP:=KSUBN:=read(20);    sigman:=sigmap:=read(20);
NSUBH:=read(20);    NSUBC:=read(20);    MC:=read(20);
MH:=read(20);    f:=read(20);    F:=read(20);
alpha:=read(20);    incr:=read(20);    epso:=read(20);
rhojp:=rhojn:=read(20);    KSUBI:=read(20);
lower:=read(20);    TSUBCPRM:=read(20);
TSUBHPRM:=read(20);    thkcold:=read(20);
thkhot:=read(20);    ksubc:=read(20);    ksubh:=read(20);
ESUBC:=read(20);    ESUBH:=read(20);    L:=read(20);
NO:=read(20);    owner;
HEATFLUX(f,OMEGA,l,lstar,ASUBP,ASUBN,F,
  alpha,KSUBP,epso,rhojp,rhojn,KSUBI,incr,lower,
  TSUBCPRM,TSUBHPRM,thkcold,ksubc,ESUBC,L,thkhot,
  ksubh,ESUBH,NO,f1,f2,f3,f4,NSUBH,MH,f6,f7,END);
END: close(20);    close(70);
end →
```

C.P. 6

DD0179R00WPU+P1500079PSP→

```
begin comment This program calculates the OFF  design and
      operational characteristics of a modular
      thermoelectric couple operating between junction
      temperatures;
   integer f1,f2,f3,f4,f5,f6,f7,f8,f,N;
   real sigma,l,rhoj,F,A,OMEGA,phaseq,KSUBI,k,alpha,
      TSUBC,DELT,MC,ESUBC,thkcold,NSUBC,ksubc,TSUBCPRM,
      NUCBAL,thetabal;
   procedure owner;
   begin write text(70,[[2c]WALLACE*SHAKUN**AERO*ENGR[2c]]);
   end   LINE  11  owner;
   procedure concept1;
   begin write text(70,[[c]This*program*calculates*
         for*a*given*module*design*the*off*balance*
         point[c]performance*characteristics*for*
         various*cold*junction*temperatures*[c]
         hot*to*cold*junction*temperatures*and*
         current*ratio*known*as*theta[2c]]);
   end   LINE  19  concept1;
   procedure heading1;
   begin write text(70,[[c]OPERATIONAL*
         CHARACTERISTICS*OF*THE*GIVEN*MODULE[c]]);
      write text(70,[[c]ELEMENT*HEIGHT*=***********
         cm.[c]JUNCTION*RESISITIVITY*=**********
```

```
        ohm.*cm.*sqrd.[c]CONDUCTIVITY*OF*ELEMENT*=*
        ********1/ohm*cm*sigma*terminology[c]
        PACKING*DENSITY*=***********[c]
        ELEMENT*AREA*=*********cm*sqrd[c]
        SEEBECK*COEFFICIENT*=**********volts/deg*
        kel[c]HEIGHT*OF*MODULE*=******************
        -*cm[c]HEIGHT*OF*PEDESTAL*=****************
        cm[c]RIPPLE*FACTOR*=***************[c]
        THERMAL*CONDUCTIVITY*=**************
        watt/cm*degree*cent[c]MATERIAL*FIGURE*
        OF--MERIT*=************/degree*Kelvin[3c]]);
end     LINE  36  heading1;
procedure OFFBALANCE(f1,f2,f3,f4,f5,f6,f7,f8,sigma,
    l,rhoj,F,A,f,OMEGA,phaseq,KSUBI,k,alpha,TSUBC,
    DELT,N,NSUBC,MC,ESUBC,thkcold,ksubc,TSUBCPRM,
    NUCBAL,thetabal);
    value f1,f2,f3,f4,f5,f6,f7,f8,sigma,l,rhoj,F,A,f,
    OMEGA,phaseq,KSUBI,k,alpha,TSUBC,DELT,N,NSUBC,MC,
    ESUBC,thkcold,ksubc,TSUBCPRM,NUCBAL,thetabal;
    integer f1,f2,f3,f4,f5,f6,f7,f8,f,N;
    real sigma,l,rhoj,F,A,OMEGA,phaseq,KSUBI,k,alpha,
    TSUBC,DELT,MC,ESUBC,thkcold,ksubc,NSUBC,TSUBCPRM,
    NUCBAL,thetabal;
begin real rho,interior,junction,REFF,term1,g,
        term2,KEFF,ZEFF,TSUBH,DLTMXEFF,introd,NUC,
```

```
        bata,ISUBQ,muq,theta,muphi,VOLTCPL,I,
        bracket,QSUBS,denom,PHI,QUVOL,QUMODARA,
        DELTCBAL,DELPRMPRM,TSUBCOF,INTERN,
        QRMODARA,QUAREA,POWER,TONS,RATIOQ,PHIMAX,
        RATIOPHI,QMAX,DELTC,raise;
      write text(70,[MATERIAL*MODULE*PERFORMANCE[2c]]);
      write text(70,[REFF[8s]KEFF[9s]ZEFF[2c]]);
      rho:= 1/sigma;   interior:= rho×l;
      comment l is length of thermoelement;
      junction:= 2×rhoj;
      REFF:= (2×F↑2/A)×(interior+junction);
      comment F is ripple effect;
      write (70,f1,REFF);
      term1:= (f×2×A)/(l×OMEGA)×(1-OMEGA);
      comment  OMEGA is packing density;
      g:= phaseq×2×A/l;   term2:= g×(1-f);
      comment f=0 for pedestal, f=1 nonpedestal module;
      KEFF:= (2×A×k/l)+KSUBI×(term1+term2);
      comment KSUBI is insulation thermal conductivity;
      write (70,f2,KEFF);   ZEFF:= (alpha↑2)/(REFF×KEFF);
      write (70,f3,ZEFF);
READ: TSUBC:= read (20);   newline (70,2);
      write text (70,[TSUBC*=*]);   write (70,f4,TSUBC);
      write text(70,[JUNCTION*TEMPERATURE*DIFFERENCE*=*]);
      write(70,f4,DELT);
```

```
comment the following section is based on
  TSUBC being at a fixed operating condition;
DLTMXEFF:=(TSUBC↑2×ZEFF)×0.5;
TSUBH:=TSUBC+DLTMXEFF;
write text(70,[TSUBH*MAX*=*]);   write(70,f8,TSUBH);
write text(70,[balance*free*stream*source*temp*=*]);
write(70,f8,TSUBCPRM);   newline(70,2);
write text (70,[[2c]DLTMXEFF[4s]MUPHI[8s]ISUBQ[2c]]);
write(70,f5,DLTMXEFF);
introd:=DELT/((ZEFF×TSUBC)×(0.5×DELT+TSUBC));
bata:=sqrt(1+ZEFF×(0.5×DELT+TSUBC));
muphi:=introd×(1+bata);
comment upper value of input variable has
  been asigned;
write(70,f6,muphi);   ISUBQ:=alpha×TSUBC/REFF;
comment section 1;
write(70,f7,ISUBQ);   newline(70,2);   muq:=1.0;
comment lower value of dimensionless input variable;
for theta:= (muq + .08) step (-.02) until
  (muphi -.20), muphi  do
begin VOLTCPL:=alpha×(theta×TSUBC+DELT);
    I:=theta×ISUBQ;
    bracket:=(2.0 ×theta-theta↑2-DELT/DLTMXEFF);
    QSUBS:=KEFF×DLTMXEFF×bracket;
    denom:=2×(theta↑2+theta×DELT/TSUBC);
```

```
PHI:=bracket/denom;    QUVOL:=QSUBS/(2×A×1);
QUMODARA:=QUVOL×OMEGA×1;
QRMODARA:=QUMODARA×(1+1/PHI);
QUAREA:=QUVOL×1;    POWER:=I×VOLTCPL×N/1000;
TONS:=QSUBS×N/(17.52×200);
QMAX:=KEFF×DLTMXEFF×(1-DELT/DLTMXEFF);
RATIOQ:=QSUBS/QMAX;
PHIMAX:=(2×muphi-muphi↑2-DELT/DLTMXEFF)
  /(2×(muphi↑2+muphi×DELT/TSUBC));
RATIOPHI:=PHI/PHIMAX;    NUC:=QUMODARA;
raise:=(1/(1+NSUBC))×MC;
DELTC:=(NUC/ESUBC)↑raise + (thkcold×NUC)/ksubc;
DELTCBAL:=(NUCBAL/ESUBC)↑raise +
  (thkcold×NUCBAL)/ksubc;
DELPRMPRM:=abs(DELTCBAL-DELTC);
if theta < thetabal then
  INTERN:=+DELPRMPRM else INTERN:=-DELPRMPRM;
comment TSUBCOF is the new free stream
  source temperature due to off
  balanced design;
TSUBCOF:=TSUBCPRM+INTERN;
write text(70,[N*couples*=*]);
write(70,f4,N);    write text(70,[THETA*=*]);
write(70,f8,theta);
write text(70,[VOLTAGE/COUPLE*=*]);
```

```
write(70,f8,VOLTCPL);
write text(70,[CURRENT*AMPS*=*]);
write(70,f8,I);
write text(70,[HEAT*PUMP*RATE--WATTS*=*]);
write(70,f8,QSUBS);
write text(70,[COEFF*OF*PERFORMANCE*=*]);
write(70,f8,PHI);
write text(70,[HEAT*PUMP*RATE/VOLUME*=*]);
write(70,f8,QUVOL);
write text(70,[HEAT*PUMP*RATE/MOD*AREA*=*]);
write(70,f8,QUMODARA);
write text(70,[HEAT*REJECTION/MOD*AREA*=*]);
write(70,f8,QRMODARA);
write text(70,[HEAT*PUMP*RATE/ELEMENT*
  AREA*=*]);
write(70,f8,QUAREA);
write text(70,[POWER*REQUIRED*KW*=*]);
write(70,f8,POWER);
write text(70,[HEAT*PUMP*RATE*Q*TONS*=*]);
write(70,f8,TONS);
write text(70,[RATIO*Q*TO*QMAX*=*]);
write(70,f8,RATIOQ);
write text(70,[RATIO*COP*TO*COP*MAX*=*]);
write(70,f8,RATIOPHI);
write text(70,[TEMPERATURE*DIFFERENCE*
```

```
            COLD-JUNCTION*to*source*STREAM*
            absolute*value*DEG*C*=*]);
          write(70,f8,DELPRMPRM);
          write text(70,[OFF*BALANCE*SOURCE*
            TEMPERATURE**DEG*CENT*=*]);
          write(70,f8,TSUBCOF);   newline(70,2);
      end   LINE 156  innerloop;
      write text (70,[The*following*results*are*
        based*on*approximations[c]]);
      write text (70,[COP*AT*MAXQ*=*]);
      write (70,f8,(0.5×(1-DELT/DLTMXEFF)));
      write text (70,[COP*MAX*=*]);
      write (70,f8,(0.5×(DLTMXEFF/DELT-1)));
      write text (70,[HEAT*PUMPRATE*AT*MAX*COP*=*]);
      write (70,f8,(DELT/DLTMXEFF×QMAX));
      write text (70,[CURRENT*PROVIDING*MAX*COP*=*]);
      write(70,f8,(DELT/DLTMXEFF×ISUBQ));
      write text (70,[The*approximation*formulas*
        are*found*in*section*******of*this*thesis]);
      newline (70,2);   write text(70,[[p]]);
      if read boolean(20) then goto READ;
  end   LINE 171  module;
  open(20);   open(70);   f1:=format([+d.dd₁₀±nd]);
  f2:=format([3s+d.dd₁₀±nd]);   f3:= format([4s+d.dd₁₀±ndc]);
  f4:= format([3s+nddd.ddc]);   f5:=format([3s+nddd.dd]);
```

```
f6:=format([3s+ndd.ddd]);    f7:=format([4s+ndd.ddddcc]);
f8:=format([4s+nddd.dddddc]);    owner;    concept1;
heading1;    sigma:=read(20);    l:=read(20);
rhoj:=read(20);    F:=read(20);    A:=read(20);
f:=read(20);    OMEGA:=read(20);    phaseq:=read(20);
KSUBI:=read(20);    k:= read(20);    alpha:=read(20);
DELT:=read(20);    N:=read(20);    ESUBC:=read(20);
MC:=read(20);    thkcold:=read(20);    ksubc:=read(20);
NSUBC:=read(20);    NUCBAL:=read(20);    thetabal:=read(20);
TSUBCPRM:=read(20);
OFFBALANCE(f1,f2,f3,f4,f5,f6,f7,f8,sigma,l,rhoj,F,
  A,f,OMEGA,phaseq,KSUBI,k,alpha,TSUBC,DELT,N,
  NSUBC,MC,ESUBC,thkcold,ksubc,TSUBCPRM,NUCBAL,thetabal);
close(20);    close(70);
end →
```

C.P. 7.

```
DD017PLOOWPU+P1500079PSP→

begin comment This program fits data in the least square
        sence to a set of data pairs which are
        represented by arrays: x[i] and f[i] using
        orthogonal polynomials;
      integer m,n,i;
      boolean PUNCHALL,RECALC;
      real array x,y,f[1:200];
      open(20);   open(70);
      write text(70,[[2c]WALLACE*SHAKUN**AERO*ENGR[2c]]);
      write text(70,[[c]THE*COEFFIENCIENTS*HAVE*THE*
        CONSTANT*TERM*FIRST.[3c]]);
      copy text(20,70,[;]);    m:= read(20);
      PUNCHALL:= read boolean(20);   RECALC:= read boolean(20);
      n:= read(20);
      for i := 1 step 1 until n do
      begin x[i]:= read(20);   f[i]:= read(20);
      end   LINE  17;
      comment The data must contain a heading for the polynomial;
      begin procedure POLY(m,n,x,y,f,PUNCHALL,RECALC);
           value m,n; integer m,n;
           boolean PUNCHALL,RECALC; real array x,y,f;
         begin if m≥n then
              begin write text(70,[[c]THE*MAXIMUM*
                    ORDER*OF*THE*OUTPUT*HAS*BEEN*
```

```
        REDUCED*TO*N-1.[c]]);
      m:= n-1
end   LINE 27;
begin integer i,j,k,l,fi,fx,fy,fe,frmse,fEc,fc
        c of y;
      real  a, SUM1,SUM2, SUM last e
        sq, SUM this p sq, SUM last p
        sq, alpha, beta, w, ;
      array  c of y, c last p, c this
        p, c next p, v this p, e[1:n];
      boolean e is uping, lm;
      SUMlastpsq:= n;   SUMlastesq:=₁₀37;
      l:= 0;    fi:= format([ndd;]);
      fx:= format([s-d.ddd₁₀-nd;]);
      fy:= fe:= format([ss-d.ddddd₁₀-nd;]);
      fEc:= format([ss-nd.dd;]);
      fccofy:= format([-
        d.ddddsddddsddd₁₀+nd;c]);
      frmse:= format([s-d.ddd₁₀+nd;cc]);
      SUM1:= SUM2:= 0.0;
      for  i:= 1 step 1 until n do
      begin X:= x[i];    SUM1:= X + SUM1;
            w:= f[i];    SUM2:= w + SUM2
      end   LINE  48;
      alpha:= SUM1/n;   cthisp[1]:= -alpha;
```

```
        cthisp[2]:= clastp[1]:= 1.0;
        w:= cofy[1]:= SUM2/n;
        for i:= 1 step 1 until n do
          e[i]:= f[i] - w;
NEXT:   l:= l+1;    k:= l+1;    lm:= l=m;
        SUM2:= SUMthispsq:= 0.0;
        for i:= 1 step 1 until n do
        begin SUM1:= cthisp[k];    X:= x[i];
              for j:= l step -1 until 1 do
                SUM1:= SUM1×X + cthisp[j];
              v this p[i]:= SUM1;
              SUM2:= e[i]×SUM1 + SUM2;
              SUMthispsq:= SUM1↑2 +
                SUMthispsq
        end   LINE 64   i;
        a:= SUM2/SUMthispsq;
        for j:= 1 step 1 until l do
          cofy[j]:= a×cthisp[j] + cofy[j];
        cofy[k]:= a×cthisp[k];    SUM2:= 0.0;
        for i:= 1 step 1 until n do
        begin SUM1:= cofy[k];    X:= x[i];
              for j:= l step -1 until 1 do
                SUM1:= SUM1×X + cofy[j];
              y[i]:= SUM1;
              w:= e[i]:= f[i] - SUM1;
```

```
        SUM2:= w×w + SUM2
end   LINE  76  i;
eisuping:= SUM2 > SUMlastesq;
SUMlastesq:= SUM2;
if PUNCH ALL or lm or eisuping then
begin write text(70,[[c]ORDER**OF**FIT]);
        write(70,fi,1);   w:= sqrt(SUM2);
        write text(70,[****R.M.S.**
          ERROR**=]);
        write(70,frmse,w/sqrt(n));
        if eisuping then
          write text(70,[RUN*
          TERMINATED*BECAUSE*THE*
          R.M.S.*ERROR*WAS*
          INCREASING.[c]]);
        write text(70,[COEFFICIENTS.*=*]);
        write(70,fi,k);   newline(70,1);
        for i:= 1 step 1 until k do
          write(70,fccofy,cofy[i]);
        newline(70,2);
        if RECALC or e is uping then
        begin write text(70,
                      [[2s]I[7s]X[13s]
                      F[13s]Y[13s]F-Y[10s]E[c]]);
                     for i:= 1 step 1 until n do
```

```
                              begin write(70,fi,i);
                                   write(70,fx,x[i]);
                              write(70,fx,f[i]);
                    write(70,fy,y[i]);
                        write(70,fe,e[i]);
                 * if w<10-2 then
                     write
                     text(70,[[2s]
                     EXACT*FIT]) else
              write(70,fEc,
                     e[i]×100.0/w);
                newline (70,1);
                   end   LINE 112  i
           end   LINE 113  RECALC or e
          is uping
                              end   LINE 115  PUNCH ALL;
           newline (70,3);
                   if lm or eisuping then goto END;
                              SUM1:= 0.0;
        for i:= 1 step 1 until n do
               SUM1:= x[i]×vthisp[i]↑2 + SUM1;
                              alpha:= SUM1/SUMthispsq;
        beta:= SUMthispsq/SUMlastpsq;
        SUMlastpsq:= SUMthispsq;
        cnextp[1]:= - alpha×cthisp[1] -
```

* if abs(e[i]) < abs (10-4 x f[i]) then............

```
                                    betaxclastp[1];
cnextp[k]:= cthisp[1] - alphaxcthisp[k];
       for i:= 2 step 1 until 1 do
 cnextp[i]:= cthisp[i-1] -
                alphaxcthisp[i] - betaxclastp[i];
for i:= 1 step 1 until k do
begin clastp[i]:= cthisp[i];
cthisp[i]:= cnextp[i]
end   LINE 133;
                                  cthisp[k+1]:= 1.0;   goto NEXT;
END:
                             end   LINE 136  arrays with dynamic bounds;
                       end   LINE 137  POLY;
                       POLY(m,n,x,y,f,PUNCHALL,RECALC);   close(20);
                       close(70);
                 end   LINE 140;
end →
```

COMPUTER PROGRAM. C.P. 8

The basic program was written for an English Electric KDF 9 computer configuration. The program consists of a driver section, two functions, and two subroutines. The data is introduced into SUBROUTINE BALANC. Defining the variables in SUBROUTINE BALANCE:

ASUBE,	cross sectional area thermoelement, cm^2
OMEGA,	packing density,
ALSUBE,	thermoelement height, cm
RHOJI,	junction resistivity, ohm-cm^2
F,	current form factor
AKSUBI,	insulation thermal conductivity, $\frac{\text{watts-cm}^2}{^oC}$
ALPHA,	Seebeck coefficient for couple volts/^oC
THKCLD,	thickness of cold side insulation, cm
ESUBC,	heat transfer factor, watts/cm^2
AKSUBC,	thermal conductivity of cold side insulation, watts-cm/^oC
SIGMA,	electrical conductivity of element 1/ohm-cm
AKSUBE,	thermal conductivity of element watts/cm-^oC
TBCPRM,	source temperature, ^oK

Defining the variables in function EXPCLD and EXPHOT

ANSUBH, ANSUBC, exponent in heat transfer equation relating module to free stream condition

AMC, AHH, introduced as an additional exponent term, with these terms ANSUBH and ANSUBC can be assumed to be , INFINITE, therefore AMC, AMH are introduced as zero for this condition.

```
1     FORMAT(20HW.SHAKUN. AERO ENGR,//)
      PRINT 1
      PRINT2
2     FORMAT(43HTWO STAGE CASCADED THERMOELECTRIC OPERATION,/)
3     FORMAT(33HBETWEEN HEAT SOURCE AND HEAT SINK,/)
      PRINT3
4     FORMAT(38HWITH FINITE HEAT TRANSFER COEFFICIENTS,//)
      PRINT4
      CALL BALANC
      CALL EXIT
      END
```

```
      FUNCTION EXPHOT(ANSUBH,AMH)
      FF=(1/(1+ANSUBH))*AMH
      EXPHOT=FF
8     FORMAT(44HEXPONENT HOT SIDE HEAT TRANSFER COEFFICIENT=,F7.4,//)
      PRINT8,FF
      RETURN
      END
```

```
      FUNCTION EXPCLD(ANSUBC,AMC)
C     AMC IS INTRODUCED AS UNITY EXCEPT WHEN ANSUBC IS AT INFINITY
      EE=(1/(1+ANSUBC))*AMC
      EXPCLD=EE
7     FORMAT(45HEXPONENT COLD SIDE HEAT TRANSFER COEFFICIENT=,F7.4,//)
      PRINT7,EE
      RETURN
      END
```

```
      SUBROUTINE HEADIN
      PUBLIC ALSUBE,RHOJI,SIGMA,OMEGA,ALPHA,F,AKSUBE
1     FORMAT(22HELEMENT HEIGHT  CM    L,F8.3,/)
      PRINT 1,ALSUBE
2     FORMAT(41HJUNCTION RESISTIVITY  OHM CM SQRD   RHOJI,E10.3,/)
      PRINT 2,RHOJI
3     FORMAT(35HELEMENT CONDUCTIVITY  OHM CM  SIGMA,F16.4,/)
      PRINT 3,SIGMA
4     FORMAT(23HPACKING DENSITY  OMEGA ,F8.4,/)
      PRINT 4,OMEGA
5     FORMAT(35HSEEBECK COEFFICIENT  VOLTS K ALPHA ,E10.3,/)
      PRINT 5,ALPHA
6     FORMAT(17HRIPPLE FACTOR    F,F8.4,/)
      PRINT 6,F
      RPLPER=SQRT(8.0E-4*(F**2-1))
7     FORMAT(17HPERCENT RIPPLE    ,F15.8,/)
      PRINT 7,RPLPER
8     FORMAT(33HTHERMAL CONDUCTIVITY  WATTS CM K ,F8.4,/)
      PRINT 8,AKSUBE
      RETURN
      END
```

```
      SUBROUTINE BALANC
      PUBLIC ALSUBE,RHOJI,SIGMA,OMEGA,ALPHA,F,AKSUBE
      ASUBE=.04
      OMEGA=.877
      ALSUBE=.20
      RHOJI=2.50E-5
      F=1.001
      AKSUBI=2.50E-4
      ALPHA=4.43E-4
      THKCLD=.0061
      ESUBC=.15
      AKSUBC=.008377
      ESUBH=ESUBC
      SIGMA=894.0
      AKSUBE=.0147
      TBCPRM=250.0
      CALL HEADIN
      TERMA=2.0*ASUBE*(1-OMEGA)/(ALSUBE*OMEGA)
 9    FORMAT(29HEFFECTIVE MATERIAL PROPERTIES,//)
      PRINT 9
      AJUNCT=4.0*RHOJI/ASUBE
C     JUNCTION IS CONTACT RESISTANCE FOR A COUPLE
     PAINTR=ALSUBE/(SIGMA*ASUBE)
     PRR=2.0*A   TR
      BIG=RR
 5    FORMAT(41HCOUPLE ELEMENT INTERIOR RESISTANCE  OHMS=,E18.8,//)
      PRINT5,RR
      REFF=(F**2)*(AJUNCT+BIG)
 99   FORMAT(27HEFFECTIVE RESISTANCE  OHMS=,E13.6,/)
      PRINT 99,REFF
      TERM=ASUBE*AKSUBE/ALSUBE
      AKK=2.0*TERM
      BAD=AKK
 6    FORMAT(44HCOUPLE ELEMENT THERMAL CONDUCTANCE  WATTS K=,E13.6,//)
      PRINT 6,AKK
     PAKEFF=BAD+AKSUBI*TERMA
 10   FORMAT(39HEFFECTIVE THERMAL CONDUCTANCE  WATTS K=,E15.6,/)
      PRINT 10,AKEFF
      ZEFF=(ALPHA**2)/(REFF*AKEFF)
 11   FORMAT(30HEFFECTIVE FIGURE OF MERIT   K=,E13.6,/)
      PRINT 11,ZEFF
      H=BAD*BIG
      ZMATER=(ALPHA**2)/H
 12   FORMAT(28HMATERIAL FIGURE OF MERIT  K=,E13.6,/)
      PRINT 12,ZMATER
      BALPHA=ALPHA*0.5
      ZMAT=(BALPHA**2)*SIGMA/AKSUBE
71    FORMAT(5HZMAT=,E13.6,/)
      PRINT 71,ZMAT
     PA=(OMEGA*REFF)/(4.0*ASUBE)
     PB=(OMEGA*ALPHA)/(2.0*ASUBE)
     PC=(OMEGA*AKEFF)/(2.0*ASUBE)
      RAB=EXPHOT(2.0,1.0)
      RIG=EXPCLD(.20,1.0)
 63   FORMAT(6HESUBC=,F10.3,/)
      PRINT 63,ESUBC
      DO 32 IBHPRM=300,320,5
      TBHPRM=IBHPRM
 19   FORMAT(22HFREE STREAM CONDITIONS,//)
      PRINT 19
 20   FORMAT(21HSOURCE TEMPERATURE K=,F9.4,/)
      PRINT 20,TBCPRM
```

```
21    FORMAT(19HSINK TEMPERATURE K=,F9.4,/)
      PRINT 21, TBHPRM
      I = 10.
     PNUC=I
      NN=0
      ALOWER=10.0
      ANUC=NUC/ALOWER
62    FORMAT(5HANUC=,F10.3,/)
      PRINT 62,ANUC
      THKHOT=THKCLD
      AKSUBH=AKSUBC
     PDELTTC=THKCLD*ANUC/AKSUBC+(ANUC/ESUBC)**RIG
     PTSUBCJ=TBCPRM-DELTTC
     PTBAL1=(TBCPRM+TBHPRM)*0.5+15
13    DLTJUR=TBAL1-TSUBCJ
      NN=NN+1
      IF(NN.GT.30)31
     PTERMAA=B*TSUBCJ
      ZED=(B*TSUBCJ)**2-4*A*(C*DLTJUR+ANUC)
      IF(ZED.LT.0.0)30
     PTERMBB=SQRT(ZED)
      CURREN=(TERMAA-TERMBB)/(2.0*A)
      PRFXUR=B*CURREN*DLTJUR+2.0*A*CURREN**2.0
      COPUPR=ANUC/PRFXUR
      ANUH=ANUC*(1/COPUPR+1)
      AN=1.2
      NLWR=45
      NUPR=10
      DLTJLR=AN*DLTJUR
      PRFXLR=B*CURREN*DLTJLR+2*A*CURREN**2
      ANUHPM=ANUH*NUPR/NLWR+PRFXLR
      DELTTH=THKHOT*ANUHPM/AKSUBH+(ANUHPM/ESUBH)**RAB
     PTSUBHJ=DELTTH+TBHPRM
     PTBAL2=TSUBHJ-DLTJLR
     PTRBL=ABS(TBAL2-TBAL1)
     PTBAL1=(TBAL1+TBAL2)*0.5
      IF(TRBL.GT.0.05)13
14    FORMAT(28HBALANCED OPERATION ACHIEVED,//)
      PRINT 14
15    FORMAT(25HHEAT FLUX  WATTS CM SQRD=,F8.4,//)
      PRINT 15,ANUC
16    FORMAT(27HHOT JUNCTION TEMPERATURE K=,F9.4,/)
      PRINT 16,TSUBHJ
17    FORMAT(27HINTERMEDIATE TEMPERATURE K=,F9.4,/)
      PRINT 17,TBAL1
18    FORMAT(28HCOLD JUNCTION TEMPERATURE K=,F9.4,/)
      PRINT18,TSUBCJ
22    FORMAT(23HITERATIONS REQUIRED NN=,F3.0,//)
      PRINT 22,NN
23    FORMAT(18HCIRCUIT CURRENT I=,F8.3,/)
      PRINT 23, CURREN
24    FORMAT(19HC.O.P. UPPER STAGE=,F8.3,/)
      PRINT 24,COPUPR
      COPLWR=(ANUH*NUPR)/(NLWR*PRFXLR)
25    FORMAT(18HC,O.P.LOWER STAGE=,F8.3,/)
      PRINT 25,COPLWR
      TERM1=TSUBCJ/(TSUBHJ-TSJBCJ)
      THEAN=(TSUBHJ+TSUBCJ)*0.5
      BATA=SQRT(1+ZEFF*TMEAN)
      RATIO=TSUBHJ/TSUBCJ
      TERM2=(BATA-RATIO)/(BATA+1)
      PHI1=TERM1*TERM2
      PHI2=PHI1+1/(8*(2*PHI1+1))
```

```
26    FORMAT(16H MAXIMUM C.O.P.=,F8.3,//)
      PRINT 26,PHI2
      GAMMA=(1+1/COPUPR)*(1+1/COPLWR)
      GAMBIT=GAMMA-1
      COPALL=1/GAMBIT
27    FORMAT(19HOPERATIONAL C.O.P.=,F8.3,//)
      PRINT 27,COPALL
      NOB=2.0
      DELTMX=(2.0*TMEAN*(BATA-1))/(BATA+1)
      DELT=TSUBHJ-TSUBCJ
      TRM=(2.0*DELT)/(DELTMX-DELT)
      RIGHT=(DELTMX-DELT/NOB)**NOB
      ALOP=(DELTMX+DELT/NOB)**NOB
      RATI=(TRM*RIGHT)/(ALOP-RIGHT)
64    FORMAT(13HCOP RATIO2 1=,F8.3,//)
      PRINT 64,RATI
41    FORMAT(26HHEAT REJ UPR WATTS CMSQRD=,F8.3,/)
      PRINT 41,ANUH
      ANNUH=ANUH*NUPR/NLWR
42    FORMAT(30HHEAT INPUT LOWER WATTS CMSQRD=,F8.3,/)
      PRINT 42,ANNUH
28    FORMAT(26HHEAT REJ LWR WATTS CMSQRD=,F8.3,/)
      PRINT 28,ANUHPM
      VLTPLR=ALPHA*DLTJLR+CURREN*REFF
      VLTPUR=ALPHA*DLTJUR+CURREN*REFF
      VOLTLR=NLWR*VLTPLR
      VOLTUR=NUPR*VLTPUR
      VOLTS=VOLTLR+VOLTUR
34    FORMAT(22HVOLTAGE TOTAL  VOLTS =,F8.3,/)
      PRINT 34,VOLTS
      QSUCC=ANUC*2.0*ASUBE*NUPR/OMEGA
      VOLTS1=QSUCC/(CURREN*COPALL)
43    FORMAT(7HVOLTS1=,F8.3,/)
      PRINT 43,VOLTS1
35    FORMAT(30HCOLD SIDE HEAT PUMPED  WATTS =,E15.6,/)
      PRINT 35,QSUCC
      QUREJ=ANUH*2*ASUBE*NUPR/OMEGA
36    FORMAT(30HUPPER STAGE REJECTION  WATTS =,E15.6,/)
      PRINT 36,QUREJ
      QLWREJ=ANUHPM*2*ASUBE*NLWR/OMEGA
37    FORMAT(30HLOWER STAGE REJECTION  WATTS =,E15.6,/)
      PRINT 37,QLWREJ
32    CONTINUE
29    FORMAT(32HALL ASPECTS OF PROGRAM COMPLETED,//)
      PRINT 29
      GOTO 33
30    FORMAT(30HHEAT FLUX EXCEEDS CAPABILITIES,//)
      PRINT30
      GOTO33
31    FORMAT(19HITERATIONS EXCEEDED,//)
      PRINT 31
      GOTO 33
33    RETURN
      END
```

APPENDICES.

Appendix A - Heat Conduction Differential Equation for the Temperature Distribution In a Current Conducting Element.

To determine the fraction of the joule heat appearing at the cold junction of the Peltier Couple (figure 6.2.1). The following is assumed:

(1) The thermoelements are homogeneous and invariant of temperature.

(2) The Thomson effect is neglected.

(3) Radiation and convective heat losses from the thermoelement is negligible.

(4) Additional assumptions as indicated in section 6.2.

For steady state operation the temperature distribution must satisfy the following one-dimensional equation (13)

$$k\frac{d^2u}{dx^2} + q_J = 0 \qquad \text{A.1}$$

where:

q_J joule heat term, watts/cm^3

and

$$q_J = \frac{I^2 R}{A l} \qquad \text{A.2}$$

$$q_J = J^2 \rho \qquad \text{A.3}$$

where:

- I current, amps
- R element resistance, ohm
- J current density, amps/cm^2
- ρ electrical resistivity, ohm-cm
- k thermal conductivity, watts/cm - $^{\circ}$C

The element junction temperatures (boundary conditions) are expressed as:

(a) at X = O $\quad u(0) = T_{h_j}$

(b) at X = L $\quad u(L) = T_{c_j}$

Replacing the partial derivative by d^2u/dx^2 as $u = u(x)$ The solution to equation A.1 is by two successive integrations. The integrations yield:

$$\frac{du}{dx} = -\frac{I^2Rx}{kAL} + C_1 \qquad \text{A.4}$$

and

$$u(x) = -\frac{I^2Rx^2}{kAL} + C_1x + C_2 \qquad \text{A.5}$$

where:

C_1, C_2 constants of integration, values to be determined from the boundary conditions.

Solving results:

$$\mu(x) = \frac{I^2 R x^2}{2Ak L} + x\left[\frac{T_{c_j} - T_{h_j}}{L} + \frac{I^2 R}{2kA}\right] + T_{h_j} \qquad \text{A.6}$$

Note: The temperatures are element junction temperatures,

Replacing:

$$\mu(x) = T(x) \qquad \text{A.7}$$

and:

$$\Delta T_j = T_{h_j} - T_{c_j} > 0 \qquad \text{A.8}$$

Substituting A.7 and A.8 into equation A.6 yields:

$$T(x) = \left[T_{h_j} - \frac{\Delta T_j x}{L}\right] + \frac{I^2 R x}{2ALk}\left[L - x\right] \qquad \text{A.9}$$

Equation A.9 is based on the assumptions that:

(1) One-dimensional heat flow

(2) All material properties invariant with temperature

(3) Materials are isotropic

The first term of equation A.9 is the "zero-current" heat and the second term is a joule heat term. The location (X_c) is found by differentiation of equation A.9 and equating the result to zero. Hence:

$$\frac{dT}{dx} = -\frac{\Delta T_j}{L} + \frac{I^2 R}{2Ak} - \frac{I^2 R x}{ALk} \qquad \text{A.10}$$

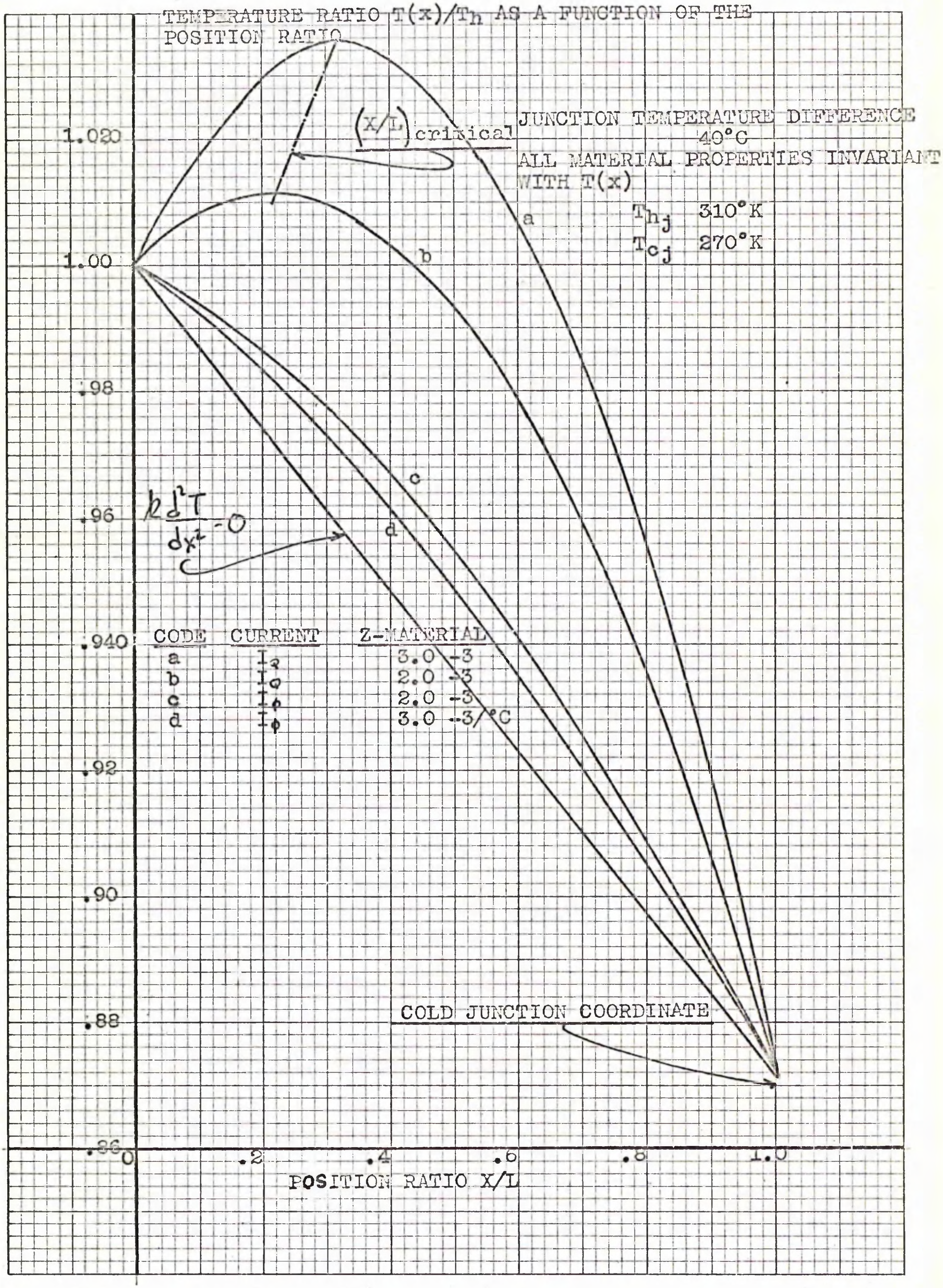

TEMPERATURE RATIO T(x)/Th AS A FUNCTION OF THE POSITION RATIO
(X/L)critical
JUNCTION TEMPERATURE DIFFERENCE 40°C
ALL MATERIAL PROPERTIES INVARIANT WITH T(x)
Thj 310°K
Tcj 270°K
1.020
1.00
.98
.96
.940
.92
.90
.88
.86
a
b
c
d
k d²T/dx² = 0
CODE CURRENT Z-MATERIAL
a I2 3.0 -3
b I2 2.0 -3
c Iφ 2.0 -3
d Iφ 3.0 -3/°C
COLD JUNCTION COORDINATE
0
.2
.4
.6
.8
1.0
POSITION RATIO X/L

With:

$$\frac{dT}{dX} = 0 \qquad \text{A.11}$$

$$X_c = \frac{L}{2} - \frac{\Delta T_j A^2 k}{I^2 \rho L} \qquad \text{A.12}$$

The maximum temperature ($T(X_c)$) occurs near the hot junction and is expressed as:

$$X_c < \frac{X}{2} \qquad \text{A.13}$$

The maximum temperature at X_c is:

$$T(X_c) = \left[T_{hj} - \frac{\Delta T_j X_c}{L}\right] + \frac{I^2 R X_c}{2ALk}\left[L - X_c\right] \qquad \text{A.14}$$

For normal operation the temperature $T(X_c)$ is greater than or equal to the temperature at the cold junction and hence conduction heat can not be transferred directly from the hot to cold junction. Figure A.1 indicates the expected temperature distribution for I_φ, I_ϕ operation. The I^2R heat generated within the element is transferred to both junctions. The part of the joule heat transferred to the cold junction is the fraction generated in the element between the cold junction (T_{cj}) and the point of maximum temperature $T(X_c)$. Thus the heat flow at $T(L) = T_{cj}$ is expressed as:

$$q = -kA \left.\frac{dT}{dx}\right|_{X=L} \qquad \text{A.15}$$

From equation A.9:

$$\left.\frac{dT}{dx}\right|_{X=L} = -\frac{\Delta T_j}{L} - \frac{I^2 R}{2Ak} \qquad \text{A.16}$$

Introducing equation A.16 into equation A.15 yields:

$$q_i = \frac{kA\Delta T_j}{L} + \frac{I^2 R}{2} \qquad \text{A.17}$$

A heat balance at the cold junction enclosed by a control volume can be illustrated by:

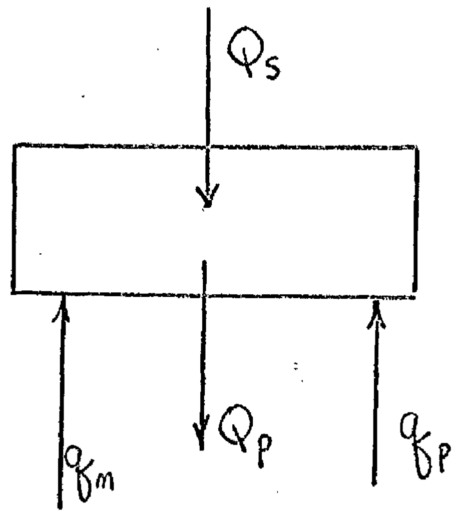

then:

$$Q_p = Q_s + q_m + q_p \qquad \text{A.18}$$

where:

Q_s	Peltier heat effect at the cold junction
q_m, q_p	heat conduction to cold junction along the element legs

Introducing the Peltier effect into equation A.18 and equation A.17 yields:

$$Q_s = T_{cj} I \alpha_{np} - \frac{I^2}{2}\left[R_n + R_p\right] - \left[\frac{k_n A_n}{L_n} + \frac{k_p A_p}{L_p}\right]\Delta T_j \qquad \text{A.19 (6.3.10)}$$

The temperature distribution $(T(X))$ at $Q_{s_{max}}$ and C.O.P.$_{max}$ can be expressed as:

$Q_{s_{max}}$ operation: $$I_Q = \frac{\alpha_{np} T_{cj}}{R_n + R_p}$$ 6.5.4.1.

Introducing $2R = R_n + R_p$

$$I_Q = \frac{\alpha_{np} T_{cj}}{2R} \qquad \text{A.20}$$

From equation 6.7.1

$$I = \Theta I_Q \qquad \text{A.21}$$

Substituting equation A.21 into equation A.20 yields:

$$I = \Theta \alpha_{np} T_{cj} / 2R \qquad \text{A.22}$$

Letting $L = 1$ (unit length)

$$T(X) = (T_{nj} - \Delta T_j X) + \frac{\theta^2 T_{cj}^2 X[1-X]\alpha_{np}^2}{8kp} \qquad \text{A.23}$$

Introducing the figure of merit (Z) as:

$$Z = \alpha_{np}^2 / R \cdot K \qquad \text{A.24}$$

where:

$$R = 2\rho l / A \qquad \text{A.25}$$

$$K = 2kA / l \qquad \text{A.26}$$

Substituting equation A.26 and equation A.25 into equation A.24 results:

$$Z = \frac{\alpha_{mp}^2}{4 \rho k} \qquad \text{A.27}$$

Substituting equation A.27 into equation A.23 yields:

$$T(x) = \left[T_{nj} - \Delta T_j x\right] + \frac{\theta^2 T_{cj}^2 x(1-x) Z}{2} \qquad \text{A.28}$$

The values of θ correspond as follows:

$\theta = 1, I_\varphi$ operation - maximum heat pump rate

$\theta = \mu_\phi, I_\phi$ operation - maximum C.O.P. (section 7.4.4.5)

Figure A.1 shows the temperature ratio (T (X)/Tnj) as a function of the position ratio (X/L). Two family of curves are illustrated. The upper series of curves is for the condition of maximum heat pump rate ($I = I_\varphi$) and the lower series is for maximum C.O.P. ($I = I_\phi$). The maximum temperature ratio approaches (X/L = .5) as the figure of merit increases. The shift can be expressed as:

$$X_c = \frac{1}{2} - \frac{\Delta T_j A k}{I^2 R} \qquad \text{A.12}$$

at $\theta = 1$ (maximum heat pump rate), $I = I_\varphi$ then:

$$X_c = \frac{1}{2} - \frac{\Delta T_j A k}{I_\varphi^2 R} \qquad \text{A.29}$$

Introducing equation A.20 into equation A.29 yields:

$$X_c = \frac{1}{2} - \frac{4 \Delta T_j k \rho}{\alpha_{mp}^2 T_{c_j}^2} \qquad \text{A.30}$$

Substituting the figure of merit relationship from A.27

$$X_c = \frac{1}{2} - \frac{\Delta T_j}{Z T_{c_j}^2} \qquad \text{A.31}$$

Equation A.31 indicates the locus of the X_c (critical position) as a function of Z From equation 6.5.6.3

$$\Delta T_{j_{max}} = \frac{1}{2} Z T_{c_j}^2 \qquad \text{6.5.6.3.}$$

Equation A.31 becomes:

$$X_c = \frac{1}{2} - \frac{\Delta T_j}{2 \Delta T_{j_{max}}} \qquad \text{A.32}$$

For X_c = 0 (at hot junction) $\Delta T_j = \Delta T_{j_{max}}$

This result is similar to the conclusion presented in reference (9) . Using the reference as a basis for further analysis equation A.10 is set equal to zero at X = 0 (boundary condition). The results are:

$$0 = -\Delta T_j + I^2 R / 2Ak \qquad \text{A.33}$$

The current to maximize $\Delta T_{j_{max}}$ (equation 6.5.4.1) is:

$$I_Q^2 = \alpha_{mp}^2 T_{c_j}^2 / 4R^2 \qquad \text{A.34}$$

Letting $I^2 = I_Q^2 \;(\theta = 1)$ then:

$$\Delta T_{j_{max}} = \frac{1}{2} Z T_{c_j}^2 \qquad 6.5.6.3.$$

When the system is operating at $Q_s = 0$ and the current maximized for ΔT_j the slope of the current at the hot junction $dT/dx\,|_{x=0}$ is zero (9) .
For operation at maximum heat pump rate the temperature ratio has a maximum value in the interior of the element.
A conclusion resulting is that as Z increases shorter elements can be utilized to pump the same amount of heat as a lower Z value with a longer element. The material utilization parameter ($Q_s/\text{vol.}$) increases with the shorter element. The C.O.P. for the shorter element would be higher as the interior resistance decreases; as the power input required decreases.

Appendix B - Parameter Optimization Technique.

A number of parameters have been optimized with respect to a single control variable. The technique is based on reference (19) and is summarized by the following rules:

(1) The quantity (y) to be maximized or minimized is expressed in terms of a single independent variable X.

(2) If y = f(X) is the quantity to be a maximum or a minimum find those values of X for which

$$dy/dx = 0$$

(3) Test each value of X for which $f'(X) = 0$ to determine whether it provides a maximum or minimum or neither. The tests employed were:

(a) If d^2y/dx^2 is positive when $dy/dx = 0$, y is a minimum.

(b) If d^2y/dx^2 is negative when $dy/dx = 0$, y is a maximum.

(c) If $d^2y/dx^2 \doteq 0$ when $dy/dx = 0$, test fails. This did not occur in the study.

Appendix C – Determination of the Current to Maximize the C.O.P. and Corresponding C.O.P.

Equation 6.4.9 indicates that the C.O.P. is a function of the current. The optimum value of the current is found by equating the first derivative to zero and solving for the current (I_ϕ).

From equation 6.4.9

$$\text{C.O.P.} = \frac{T_{cj} I \alpha_{mp} - \frac{1}{2} I^2 R - K \Delta T_j}{I \alpha_{mp} \Delta T_j + I^2 R} \qquad 6.4.9.$$

Letting

$\dfrac{d(\text{C.O.P.})}{dI} = 0$ results after expanding as:

where: $\alpha_{mp} = \alpha$

$$\frac{1}{2} I^2 R \alpha (T_{hj} + T_{cj}) = 2 I R K \Delta T_j + K \alpha \Delta T_j^{\,2} \qquad \text{C.1}$$

$$(\alpha | K)$$

Multiplying both sides by $(\alpha | K)$ and then adding $I^2 R^2$ yields:

$$I^2 R^2 + \frac{1}{2} \frac{\alpha^2 R^2 I^2}{KR} \left[T_{hj} + T_{cj} \right] = \alpha^2 \Delta T_j^{\,2} + 2 I R \alpha \Delta T_j + I^2 R^2 \qquad \text{C.2}$$

Factoring the left-hand side and letting:

$$B = 1 + \frac{1}{2}\frac{\alpha^2}{RK}\left[T_{h_j} + T_{c_j}\right] \qquad C.3$$

The right-hand side is a perfect square then:

$$R^2 I^2 B = \left[\alpha \Delta T_j + I R\right]^2 \qquad C.4$$

Solving for I (I_ϕ)

$$I_\phi = \frac{\alpha \Delta T_j}{R\left[\sqrt{B} - 1\right]} \qquad C.5 \quad (6.5.1.1)$$

Equation 6.5.11 expresses the current required to maximize the C.O.P. The maximum C.O.P. is expressed as:

$$C.O.P._\phi = \frac{\alpha I_\phi T_{c_j} - \frac{1}{2} I_\phi^2 R - K \Delta T_j}{I_\phi V_\phi} \qquad C.6$$

where:

$$V_\phi = I_\phi R + \alpha \Delta T_j \qquad C.7$$

Introducing equation C.5 into equation C.6 and C.7 yields after combining:

$$C.O.P._\phi = \frac{T_{c_j}\left[\sqrt{B} - 1\right]}{\Delta T_j \sqrt{B}} - \frac{1}{2\sqrt{B}} - \frac{KR\left[\sqrt{B} - 1\right]^2}{\alpha^2 \Delta T_j \sqrt{B}} \qquad C.8$$

Introducing:

$$RK = \frac{\alpha^2\left[T_{h_j} + T_{c_j}\right]}{2\left[B - 1\right]} \qquad C.9$$

and combining the three terms from equation C.8 yields:

$$\text{C.O.P.}_\phi = \frac{2[B-1]T_{c_j}[\sqrt{B}-1] - \Delta T_j[B-1] - [T_{h_j}+T_{c_j}][\sqrt{B}-1]^2}{2\Delta T_j\sqrt{B}[\sqrt{B}-1]} \qquad \text{C.10}$$

Factoring $\dfrac{1}{\Delta T_j[B-1]}$ and combining results:

$$\text{C.O.P.}_\phi = \frac{1}{\Delta T_j[B-1]}\left[BT_{c_j} + T_{h_j} - T_{c_j}\sqrt{B} - T_{h_j}\sqrt{B}\right] \qquad \text{C.11}$$

The term within the bracket is the product of two factors then:

$$\text{C.O.P.}_\phi = \frac{1}{\Delta T_j}\left[\frac{[T_{c_j}\sqrt{B} - T_{h_j}][\sqrt{B}-1]}{[B-1]}\right] \qquad \text{C.12}$$

The numerator of equation C.12 is equivalent to:

$$[T_{c_j}\sqrt{B} - T_{h_j}][\sqrt{B}-1] \equiv T_{c_j}\left[\left[\sqrt{B} - \frac{T_{h_j}}{T_{c_j}}\right][\sqrt{B}-1]\right] \qquad \text{C.13}$$

The term within the bracket is replaced which yields:

$$\text{C.O.P.}_\phi = \frac{T_{c_j}}{\Delta T_j}\left[\frac{\left[\sqrt{B} - \frac{T_{h_j}}{T_{c_j}}\right][\sqrt{B}-1]}{[B-1]}\right] \qquad \text{C.14.} \quad (6.5.13)$$

$$\text{C.O.P.}_\phi = \frac{T_{c_j}}{\Delta T_j}\left[\frac{\sqrt{B} - \frac{T_{h_j}}{T_{c_j}}}{\sqrt{B}+1}\right] \qquad \text{C.15.}$$

Appendix D - The Effect of Shape Factor Variation on Operational Performance Ratios.

In section 6.5.2 the shape factor required to maximize the C.O.P. is expressed as:

$$\frac{f_m}{f_p} = \left[\frac{k_p \rho_m}{k_m \rho_p}\right]^{0.5} \qquad 6.5.2.10.$$

where:

$$f_m = A_m / l_m \qquad 6.5.2.3.$$

$$f_p = A_p / l_p \qquad 6.5.2.4.$$

Assuming $l_m = l_p$ and introducing a multiplication factor, equation 6.5.2.10 is expressed as:

$$A_m = \left[\frac{k_p \rho_m}{k_m \rho_p}\right] \times Ap \text{ X Factor} \qquad D.1$$

In this appendix a technique is proposed to indicate the change in performance ratios as a function of 'factor'. Four operational criteria will be examined. The four operational ratios are:

(1) Operation at maximum C.O.P. ($C.O.P._\phi$)

(2) Operation at maximum heat pump rate ($Q_{s_{max}}$)

(3) Heat Pump Rate at C.O.P. ϕ (Q_ϕ)

(4) C.O.P. at maximum heat pump rate (ϕ_Q)

From section 7.2.3 and section 7.2.4

$$R_{EFF} = \left[\left[\frac{\rho_m}{A_p N} + \frac{\rho_p}{A_p}\right]\ell + \left[\frac{2\rho_{jp}}{A_p} + \frac{2\rho_{jm}}{A_p N}\right]\right] F^2 \qquad \text{D.2}$$

and

$$K_{EFF} = \frac{1}{\ell}\left[k_m A_p N + k_p A_p + \frac{K_i(1-\omega)}{\omega}\left[A_p + N A_p\right]\right] \qquad \text{D.3}$$

The effective material variables are expressed as:

$$R'_{EFF} = \left[\left[\frac{\rho_m}{A_p M} + \frac{\rho_p}{A_p}\right]\ell + \left[\frac{2\rho_{jp}}{A_p} + \frac{2\rho_{jm}}{M A_p}\right]\right] F^2 \qquad \text{D.4}$$

$$K'_{EFF} = \frac{1}{\ell}\left[k_m A_p M + k_p A_p + \frac{K_i(1-\omega)}{\omega}\left[A_p + M A_p\right]\right] \qquad \text{D.5}$$

where:

$$M = \left[\frac{k_p \cdot \rho_m}{k_m\ \rho_p}\right]^{0.5} \text{X "factor"} \qquad \text{D.6}$$

and

$$N = \left[\frac{k_p \rho_m}{k_m \rho_p}\right]^{0.5}$$

The effective figure of merit is expressed as:

$$Z_{EFF} = \alpha_{np}^{2} / R_{EFF} \cdot K_{EFF} \qquad D.7$$

The effective figure of merit is expressed as:

$$Z'_{EFF} = \alpha_{np}^{2} / R'_{EFF} \cdot K'_{EFF} \qquad D.8$$

The maximum temperature difference is:

$$\Delta T_{j_{max}} = 0.5\, T_{cj}^{2}\, Z_{EFF} \qquad D.9$$

and

$$\Delta T'_{j_{max}} = 0.5\, T_{cj}^{2}\, Z'_{EFF} \qquad D.10$$

The multiplication 'factor' is assumed to vary from .8 to 1.5. The operational ratios are based on approximations (section 6.6) and hence figure 6.5.2.6 is indicative of the general trends. The operational ratios are determined as follows:

(1) C.O.P.$_{\phi}$ ratio:

From Equation 6.7.13:

$$\frac{C.O.P.'}{C.O.P.} \cong \left[\frac{\Delta T'_{j_{max}}}{\Delta T_j} - 1 \right] \Bigg/ \left[\frac{\Delta T_{j_{max}}}{\Delta T_j} - 1 \right] \qquad D.11$$

(2) $Q_{s_{max}}$ ratio:

From Equation 6.5.4.8:

$$\frac{Q'_{s_{max}}}{Q_{s_{max}}} \cong \frac{K'_{EFF}\,\Delta T'_{j_{max}}\left[1-\frac{\Delta T_j}{\Delta T'_{j_{max}}}\right]}{K_{EFF}\,\Delta T_{j_{max}}\left[1-\frac{\Delta T_j}{\Delta T_{j_{max}}}\right]} \qquad D.11$$

(3) Q_ϕ ratio:

From Equation 6.6.14:

$$\left[\frac{Q'_s}{Q_s}\right]_\phi \cong \frac{Q'_{s_{max}}\,\Delta T_{j_{max}}}{\Delta T'_{j_{max}}\,Q_{s_{max}}} \qquad D.12$$

(4) C.O.P. $_Q$ ratio:

From Equation 6.7.12:

$$\left.\frac{C.O.P.'}{C.O.P.}\right|_{Q_{s_{max}}} \cong \frac{\left[1-\frac{\Delta T_j}{\Delta T'_{j_{max}}}\right]}{\left[1-\frac{\Delta T_j}{\Delta T_{j_{max}}}\right]} \qquad D.13$$

The prim notation in equation D.10 - D.13 denate that the multiplication factor (equation D.4) is not equal to unity. Figure 6.5.2.6 illustrates the performance ratio as a function of the multiplication factor. An interesting result occurs for the performance ratio $(Q'_s / Q_s)_{max}$ and $(Q'_s / Q_s)_{C.O.P.}$ with the multiplication factor > 1. The heat pump rate performance ratio indicates an increase in performance level. To rationalize this occurance consider the following:

For:

$$.8 \leq \text{`factor'} \leq 1.5$$

$$1.95_{10}{-3}/^{o}C \leq Z \leq 1.88_{10}{-3}/^{o}C$$

hence:

$$\Delta T_{j_{max}} \simeq \Delta T_{j_{max}}'$$

and equation D.10 becomes:

$$\left(\frac{Q_s'}{Q_s}\right)_{max} \cong \frac{K_{EFF}'}{K_{EFF}} \qquad D.14$$

With the multiplication factor being greater than unity then $K_{EFF}' > K_{EFF}$ and $(Q_s'/Q_s)_{max} > 1$ and from equation D.12 $(Q_s'/Q_s)_{\phi} > 1$.

Appendix E — Determination of Configuration Geometry for Optimizing the Parameter Q_s/A_T

From equation 6.5.4.2 the maximum heat pump rate is expressed as:

$$Q_{s_{max}} = \frac{\alpha_{mp}^2 T_{cj}}{2R} - K \Delta T_j \qquad \text{E.1}$$

where:

$$R = L\left[\frac{A_p \rho_n + A_n \rho_p}{A_n A_p}\right] \qquad \text{E.2}$$

and

$$K = \frac{1}{L}\left[k_n A_n + k_p A_p\right] \qquad \text{E.3}$$

Introducing equation E.2, E.3 into equation E.1 and dividing through by A_T (Total element cross section area) yields:

$$\frac{Q_{s_{max}}}{A_T} = \frac{\alpha^2 T_{cj}^2 - 2\left[k_n A_n + k_p A_p\right]\left[A_p \rho_n + A_n \rho_p\right]\Delta T_j}{2 L A_T \left[A_p \rho_n + A_n \rho_p\right]} \qquad \text{E.4}$$

Substituting $A_T = A_n + A_p$ into equation E.4 and taking the partial derivative of: $\partial(Q/A_T)/\partial A_p = 0$. The partial with respect to A_p is arbitrary, the partial with respect to A_n will give the same final result.

Factoring and combining results:

$$A_m^2\left[1-\frac{2\Delta T_j k_p \rho_p}{\alpha^2 T_{cj}^2}+\frac{2\Delta T_j k_m \rho_p}{\alpha^2 T_{cj}^2}\right]+A_m A_p\left[\frac{4\Delta T_j k_m A_m \rho_m}{\alpha^2 T_{cj}^2}-\frac{4\Delta T_j k_p A_m \rho_m}{\alpha^2 T_{cj}^2}\right]-$$

$$A_p^2\left[\frac{\rho_m}{\rho_p}+\frac{2\Delta T_j \rho_m^2 (k_p-k_m)}{\alpha^2 T_{cj}^2 \rho_p}\right]=0$$

E.5

Letting:

$$\varsigma=\frac{2(k_p-k_m)\Delta T_j}{\alpha^2 T_{cj}^2}$$ E.6

Introducing equation E.6 into equation E.5 and simplifing yields:

$$\frac{A_m}{A_p}=\frac{\mathcal{M}^{0.5}+\rho_m\varsigma}{[1-\varsigma\rho_p]}$$ E.7 (6.5.7.3)

where:

$$\mathcal{M}=\frac{\rho_m+\rho_m^2\varsigma-\varsigma\rho_p\rho_m}{\rho_p}$$ E.8 (6.5.7.4)

Appendix F - C.O.P.$_{max}$ Identity.

From equation 6.6.20

$$\frac{\left[1-\frac{\Delta T_j}{\Delta T_{j_{max}}}\right]}{2\left[\frac{\Delta T_j}{T_{c_j}}+\frac{\Delta T_j}{\Delta T_{j_{max}}}\right]}=\frac{1}{2}\frac{\Delta T_{j_{max}}}{\Delta T_j}\left[1-\frac{\Delta T_j}{\Delta T_{j_{max}}}\right]\left[1-\frac{\Delta T_j}{T_{h_j}}\right]\left[\frac{1}{1+\frac{\Delta T_{j_{max}}-\Delta T_j}{T_{h_j}}}\right] \quad \text{F.1}$$

Cancelling alike terms and cross multiplying with a reorganization of the right-hand side terms of equation F.1 results:

$$1=\frac{\Delta T_{j_{max}}}{\Delta T_j}\left[1-\frac{\Delta T_j}{T_{h_j}}\right]\left[\frac{T_{h_j}}{T_{h_j}+\Delta T_{j_{max}}-\Delta T_j}\right]\left[\frac{\Delta T_j}{T_{c_j}}+\frac{\Delta T_j}{\Delta T_{j_{max}}}\right] \quad \text{F.2}$$

$$1=\left[\frac{T_{h_j}-\Delta T_j}{T_{h_j}}\right]\left[\frac{T_{h_j}}{T_{h_j}+\Delta T_{j_{max}}-\Delta T_j}\right]\left[\frac{\Delta T_{j_{max}}}{T_{c_j}}+1\right] \quad \text{F.3}$$

Expanding the right-hand side of equation F.3 and cancelling like terms results:

$$\Delta T_{j_{max}}\cdot T_{c_j}=\Delta T_{j_{max}}\cdot T_{h_j}-\Delta T_{j_{max}}\cdot\Delta T_j \quad \text{F.4}$$

with:

$$\Delta T_j=T_{h_j}-T_{c_j} \quad \text{F.5}$$

Substituting equation F.5 into equation F.4 results:

$$\Delta T_{j_{max}}\cdot T_{c_j}=\Delta T_{j_{max}}\cdot T_{c_j} \quad \text{F.6}$$

Q.E.D.

Appendix G - Upper Limit of the Parameter $Z\bar{T}$

The upper limit of the parameter $Z\bar{T}$ will be determined as follows:

Let: $$Z\bar{T} = Z\left[\frac{T_{hj} + T_{cj}}{2}\right] \qquad \text{G.1}$$

From Appendix N:

$$Z \cong 3.00_{10}{-3}/^{o}K \text{ at room temperature}$$

The upper material limit imposed by the insulation within the matrix assembly is 200°C (473°K). From equation G.1 with $T_{hj} = T_{cj}$

$$\therefore Z\bar{T} \cong 1.419$$

Assuming an optimistic value for the figure of merit of $5.0_{10}{-3}/^{o}K$ then:

$$Z\bar{T} \cong 2.36$$

Hence the probable upper limit range is:

$$1.419 \leq Z\bar{T} \leq 2.36$$

From reference (3) based on the properties of semiconductors a $Z\bar{T}$ value exceeding two is unlikely.

Appendix H - C.O.P. Identity.

From equation 6.5.5.1 and equation 6.6.22:

$$\frac{\left[1-\frac{\Delta T_j}{\Delta T_{j_{max}}}\right]}{2\left[1+\frac{\Delta T_j}{T_{c_j}}\right]} = \frac{1}{2}\left[1-\frac{\Delta T_j}{\Delta T_{j_{max}}}\right]\left[1-\frac{\Delta T_j}{T_{h_j}}\right] \qquad \text{H.1}$$

Cross multiplying and cancelling like terms results:

$$1 = \left[1-\frac{\Delta T_j}{T_{h_j}}\right]\left[1+\frac{\Delta T_j}{T_{c_j}}\right] \qquad \text{H.2}$$

Expanding the right-hand side and combining like terms yields:

$$1 = 1 + \frac{T_{h_j}\Delta T_j - \Delta T_j T_{c_j}}{T_{h_j} T_{c_j}} - \frac{\Delta T_j^2}{T_{h_j} T_{c_j}} \qquad \text{H.3}$$

Operating on equation H.3 results:

$$T_{h_j}\Delta T_j - \Delta T_j T_{c_j} = \Delta T_j^2 \qquad \text{H.4}$$

Introducing $\Delta T_j = T_{h_j} - T_{c_j}$ into equation H.4 yields:

$$\Delta T_j^2 = \Delta T_j^2 \qquad \text{H.5}$$

Q.E.D.

Appendix I - Functional Relation Between Form Factor (F) and Percent Ripple.

In Section 7.3.2 an equation is presented to relate form factor (F) as a function of % ripple. The equation was given as:

$$F^2 = 1 + \frac{(\%\ \text{RIPPLE})^2}{8 \times 10^4} \qquad 7.3.2.2.$$

The derivation of equation 7.3.2.2 is as follows:

(1) Definition of Terms

(a) Average Current

Consider the following figure:

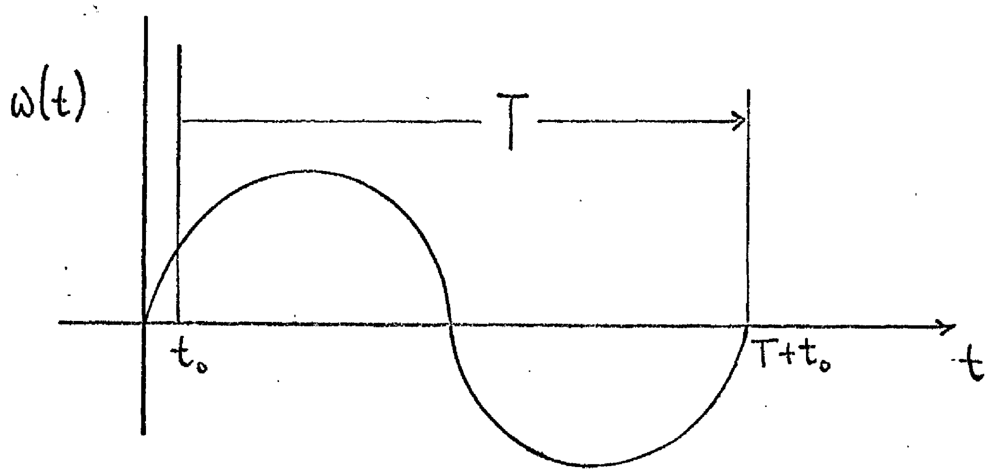

Figure I.1

Current Wave Form.

The average current is expressed as:

$$\bar{I} = \frac{1}{T}\int_{t_0}^{T+t_0} \omega(t)\, dt \qquad I.1$$

where:

$$\omega(t) = I_0 \sin \omega t \qquad \text{I.2}$$

(b) Mean Squared Current

The mean squared current is defined as:

$$\bar{\bar{I}} \equiv \frac{1}{T}\int_{t_0}^{T+t_0} [\omega(t)]^2 \, dt \qquad \text{I.3}$$

(c) Root Mean Squared Current

The root mean squared current is defined as:

$$I_{RMS} = \sqrt{\frac{1}{T}\int_{t_0}^{T+t_0} [\omega(t)]^2 \, dt} \qquad \text{I.4}$$

(2) Derivation of Equations

The form factor is defined as:

$$F \equiv \frac{I_{RMS}}{I_{D.C.}} \qquad \text{7.3.2.1.}$$

Percent Ripple is defined as:

$$\% \text{ Ripple} \equiv \frac{\text{Peak to Peak Variation} \times 100}{\text{Average Current}} \qquad \text{I.5}$$

The instantaneous power dissipated in a resistor is:

$$P(t) = \omega(t)^2 R \qquad \text{I.6}$$

The average power dissipated in a resistor is:

$$\overline{P(t)} = \int_0^T \frac{\omega(t)^2}{T} R\,dt \qquad \text{I.7}$$

$$\overline{P(t)} = (I_{RMS})^2 R \qquad \text{I.8}$$

To relate form factor (F) to % Ripple an assumption on the wave form is required. Assuming a small ripple from a filtered power supply is sinusodial (figure I.2)

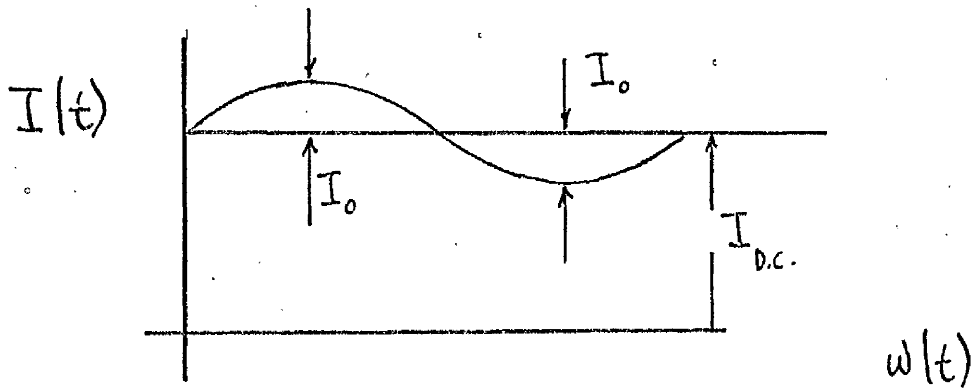

Figure I.2

<u>Sinusodial Ripple Form</u>.

From figure I.2 at ripple current: $I(t) = I_0 \sin \omega t$ is superimposed on a steady d.c. current ($I_{D.C.}$). The rms current is expressed as:

$$I_{RMS} = \sqrt{I_{D.C.}^2 + \frac{1}{2} I_0^2} \qquad \text{I.9}$$

Substituting equation I.9 into equation 7.3.2.1 yields:

$$F = \frac{\sqrt{I_{D.C.}^2 + \frac{1}{2} I_0^2}}{I_{D.C.}} \qquad \text{I.10}$$

and percent ripple from equation I.5 is:

$$\% \text{ Ripple} = \frac{2I_o \times 100}{I_{D.C.}} \qquad \text{I.11}$$

Squaring equation I.10 and equation I.11 yields:

$$F^2 = \frac{I_{D.C.}^2 + \frac{1}{2} I_o^2}{I_{D.C.}^2} \qquad \text{I.12}$$

$$(\% \text{ Ripple})^2 = \frac{4I_o^2 \times (100)^2}{I_{D.C.}^2} \qquad \text{I.13}$$

Combining equation I.13 and I.12 with $\left(I_o^2 / I_{D.C.}^2\right)$ as the common term and solving for F^2 results:

$$F^2 = 1 + \frac{(\% \text{ Ripple})^2}{8 \times 10^4} \qquad \text{I.14} \; (7.3.2.2)$$

To determine the % ripple corresponding to a non-filtered, full wave sinusodial ripple consider the following.

From equation 7.3.2.1

$$F = I_{RMS} / I_{D.C.} \qquad 7.3.2.1$$

then:

$$F = \frac{\int_0^{\pi} \frac{1}{\pi} (\omega(t))^2 \, dt}{\int_0^{\pi} \frac{1}{\pi} \omega(t) \, dt} \qquad \text{I.15}$$

where: $$\omega(t) = I_o \sin \omega t \qquad \text{I.16}$$

Performing the integration results:

$$F \cong \frac{.707\ Io}{.637\ Io} \cong 1.110 \qquad \text{I.17}$$

Substituting the value from equation I.17 into equation I.14 gives the % ripple as $\cong$ 136%.

Appendix J - The Effect of Power Supply Ripple on System Performance.

(a) The C.O.P.* can be expressed with current ripple as:

$$C.O.P.^* = \frac{T_{cj} I^* \alpha_{np} - \frac{1}{2} R_{EFF} I^{2*} F^2 - K_{EFF} \Delta T_j}{F^2 I^{2*} R_{EFF} + I^* \alpha_{np} \Delta T_j} \qquad 7.3.2.9.$$

Taking the $\frac{d\, C.O.P.^*}{d\, I} = 0$ and solving for I_ϕ^* yields:
(utilizing equation C.2 and equation C.3)

$$\beta I_\phi^{2*} R^2 = \frac{\alpha^2 \Delta T_j}{F^2} + 2 I_\phi R \alpha \Delta T_j + I_\phi^{2*} R^2 \qquad J.1$$

Assuming as an approximation that the right-hand side of equation J.1 is a perfect square then:

$$I_\phi^2 R^2 \beta \cong (\alpha \Delta T_j + I_\phi^* R)^2 \qquad J.2$$

As an intermediate relation:

$$I_\phi^* R \sqrt{B} = \alpha \Delta T_j + I_\phi^* R \qquad 7.3.2.10$$

and

$$I_\phi^* \cong \frac{\alpha_{np} \Delta T_j}{R_{EFF}\left[\sqrt{B} - 1\right]} \qquad 7.3.2.11$$

(b) The maximum junction temperature difference ($\Delta T_{j_{max}}{}^*$) with current ripple can be expressed as:

From equation 6.6.10

$$I_\phi \cong \frac{\Delta T_j}{\Delta T_{j_{max}}} I_Q \qquad 6.6.10.$$

and

$$I_\phi^* \cong \frac{\Delta T_j}{\Delta T_{j_{max}}{}^*} I_Q^* \qquad J.3$$

Solving for the maximum junction temperature ratio yields:

$$\frac{\Delta T_{j_{max}}{}^*}{\Delta T_{j_{max}}} \cong \frac{I_\phi}{I_\phi^*} \cdot \frac{I_Q^*}{I_Q} \qquad J.4$$

Introducing equation 7.3.2.7 and equation 7.3.2.8 into equation J.4 results:

$$\frac{\Delta T_{j_{max}}{}^*}{\Delta T_{j_{max}}} \cong \frac{1}{F^2} \qquad 7.3.2.12.$$

(c) The heat pump capacity at maximum C.O.P. ($Q_\phi{}^*$) and the C.O.P. at maximum heat pump rate (C.O.P.$_Q{}^*$) with current ripple can be expressed as:

From equation 6.6.13:

$$\frac{Q_{s\phi}^*}{Q_{s\phi}} \cong \frac{\left[1 - \frac{\Delta T_j}{\Delta T_{j_{max}}{}^*}\right]}{\left[1 - \frac{\Delta T_j}{\Delta T_{j_{max}}}\right]} \qquad J.5$$

Introducing equation 7.3.2.12 into equation J.5 yields:

$$\frac{Q_{s\phi}^{*}}{Q_{s\phi}} \cong \frac{\left[1 - \dfrac{F^2 \Delta T_j}{\Delta T_{j_{max}}}\right]}{\left[1 - \dfrac{\Delta T_j}{\Delta T_{j_{max}}}\right]} \qquad 7.3.2.14$$

From equation 6.7.12

$$\frac{C.O.P._{\phi}{}^{*}}{C.O.P._{\phi}} \cong \frac{\left[1 - \dfrac{\Delta T_j}{\Delta T_{j_{max}}^{*}}\right]}{\left[1 - \dfrac{\Delta T_j}{\Delta T_{j_{max}}}\right]} \qquad J.6$$

Introducing equation 7.3.2.12 into equation J.6 yields:

$$\frac{C.O.P._{\phi}{}^{*}}{C.O.P._{\phi}} \cong \frac{\left[1 - \dfrac{F^2 \Delta T_j}{\Delta T_{j_{max}}}\right]}{\left[1 - \dfrac{\Delta T_j}{\Delta T_{j_{max}}}\right]} \qquad J.7$$

and:

$$\left(\frac{C.O.P.^{*}}{C.O.P.}\right)_{\phi} = \left[\frac{Q_s^{*}}{Q_s}\right]_{\phi} \qquad 7.3.2.15$$

(d) The maximum $C.O.P.^{*}_{max}$ and maximum heat pump rate ($Q_{s_{max}}{}^{*}$) with current ripple can be expressed as:

From equation 6.6.21:

$$\left.\frac{C.O.P.^{*}}{C.O.P.}\right|_{max} \cong \frac{\Delta T_{j_{max}}{}^{*}\left[1 - \dfrac{\Delta T_j}{\Delta T_j{}^{*}_{max}}\right]}{\Delta T_{j_{max}}\left[1 - \dfrac{\Delta T_j}{\Delta T_{j_{max}}}\right]} \qquad J.8$$

Introducing equation 7.3.2.12 into equation J.8 yields:

$$\frac{C.O.P._{\phi}^{*}}{C.O.P._{\phi}} \cong \frac{1}{F^2} \frac{\left[1 - \frac{F^2 \Delta T_j}{\Delta T_{j\,max}}\right]}{\left[1 - \frac{\Delta T_j}{\Delta T_{j\,max}}\right]} \qquad 7.3.2.16.$$

and from equation 6.5.4.8 coupled with equation 7.3.2.12 results:

$$\frac{Q_{s\,max}^{*}}{Q_{s\,max}} = \frac{\left[1 - \frac{F^2 \Delta T_j}{\Delta T_{j\,max}}\right]}{F^2 \left[1 - \frac{\Delta T_j}{\Delta T_{j\,max}}\right]} \qquad J.9$$

Hence:

$$\left.\frac{C.O.P.^{*}}{C.O.P.}\right|_{\phi} = \left[\frac{Q_s^{*}}{Q_s}\right]_{Q_{max}} \qquad 7.3.2.16.$$

(e) The heat pump rate Q_s^{*} and the C.O.P.* with current ripple can be expressed as:

From equation 6.7.5:

$$\frac{Q_s^{*}}{Q_s} = \frac{\left[2\theta - \theta^{2*} - \frac{\Delta T_j}{\Delta T_{j\,max}}\right]}{\left[2\theta - \theta^2 - \frac{\Delta T_j}{\Delta T_{j\,max}}\right]} \qquad J.10$$

From equation 6.7.10:

$$\frac{C.O.P.^{*}}{C.O.P.} = \frac{\left[2\theta - \theta^{2*} - \frac{\Delta T_j}{\Delta T_{j\,max}}\right]\left[\theta^2 + \theta \frac{\Delta T_j}{\Delta T_{j\,max}}\right]}{\left[\theta^{2*} + \frac{\theta \Delta T_j}{\Delta T_{j\,max}}\right]\left[2\theta - \theta^2 - \frac{\Delta T_j}{\Delta T_{j\,max}}\right]} \qquad J.11$$

For the general operating conditions considered by equation J.10 and equation J.11 it is assumed that the boundary conditions are fixed (i.e. T_{cj}, T_{hj} constant with and without current ripple) therefore the only term to be modified is the θ^2 term (joule current variable). The assumption yields:

$$\frac{Q_s^*}{Q_s} = \frac{\left[2\theta - F^2\theta^2 - \frac{\Delta T_j}{\Delta T_{j\,max}}\right]}{\left[2\theta - \theta^2 - \frac{\Delta T_j}{\Delta T_{j\,max}}\right]} \qquad 7.3.2.17$$

and

$$\frac{\text{C.O.P.}^*}{\text{C.O.P.}} = \frac{\left[2\theta - F^2\theta^2 - \frac{\Delta T_j}{\Delta T_{j\,max}}\right]\left[\theta^2 + \theta\frac{\Delta T_j}{\Delta T_{j\,max}}\right]}{\left[F^2\theta^2 + \theta\frac{\Delta T_j}{\Delta T_{j\,max}}\right]\left[2\theta - \theta^2 - \frac{\Delta T_j}{\Delta T_{j\,max}}\right]} \qquad 7.3.2.18$$

where:

$$\frac{\text{C.O.P.}^*}{\text{C.O.P.}} = \frac{Q_s^* \cdot \text{Power}_{INPUT}}{\text{Power}^*_{INPUT} \cdot Q_s} \qquad J.12$$

Appendix K - Determination of the Dimensionless Current Ratio at Maximum C.O.P.

From equation 6.4.9

$$\text{C.O.P.} = \frac{T_{cj} I \alpha_{mp} - \frac{1}{2} I^2 R_{EFF} - K_{EFF} \Delta T_j}{I \alpha_{mp} \Delta T_j + I^2 R_{EFF}} \qquad 6.4.9.$$

Letting:

$$\frac{d\,COP}{dI} = 0$$ expanding and illiminating results:

$$I^2 \left[\alpha I R + \tfrac{1}{2} R \alpha \Delta T_j \right] - 2 I R K \Delta T_j - K \alpha \Delta T_j^2 = 0 \qquad \text{K.1}$$

Solving equation K.1 by the quadratic relation yields:

$$I_\phi = \frac{\alpha_{mp} \Delta T_j \left[1 + \left[1 + Z_{EFF} \left[T_{cj} + \frac{\Delta T_j}{2} \right] \right]^{0.5} \right]}{R_{EFF} Z_{EFF} \left[\frac{\Delta T_j}{2} + T_{cj} \right]} \qquad 7.4.4.5.$$

and from equation 6.5.1.1:

$$I_\phi = \frac{\alpha_{mp} \Delta T_j}{R_{EFF} \left[\sqrt{B} - 1 \right]} \qquad \text{C.5}$$

where:

$$B = 1 + Z_{EFF} \left[\frac{T_{hj} + T_{cj}}{2} \right] \qquad \text{C.3}$$

Equation 7.4.4.5.2 is identical to equation C.5

Defining the dimensionless current ratio at maximum C.O.P. (μ_ϕ) as:

$$\mu_\phi = \frac{I_\phi}{I_\varphi} \qquad 7.4.4.5.$$

where:

$$I_\varphi = \alpha_{mp} T_{cj} / R_{EFF} \qquad 7.4.4.4.$$

Substituting equation 7.4.4.5.2 and equation 7.4.4.4.5 into equation 7.4.4.5.3 yields:

$$\mu_\phi = \frac{\Delta T_j \left[1 + \sqrt{1 + Z_{EFF}\left[\frac{\Delta T_j}{2} + T_{cj} \right]} \right]}{T_{cj} Z_{EFF} \left[\frac{\Delta T_j}{2} + T_{cj} \right]} \qquad 7.4.4.5.$$

or

$$\mu_\phi = \frac{\Delta T_j}{T_{cj}\left[\sqrt{\beta} - 1\right]} \qquad K.2$$

From section 6.6 equation 6.6.10 (Λ = 1):

$$\frac{I_\phi}{I_\varphi} \simeq \frac{\Delta T_j}{\Delta T_{j_{max}}} \qquad K.3$$

Appendix L - Heat Exchanger Transfer Function.

The problem considered is to express the heat transfer from an extended surface into a fluid at a different temperature. Such extended surfaces have been utilized to increase the rate of cooling or heating. The requirement for this analysis is to express the heat transfer rate in a general form. The form that will be considered is:

$$Q = D \Delta T^{n} \tag{L.1}$$

The form utilized in equation 8.3.1.1 was:

$$Q_i = E_i A_m \left[T_{i\infty} - T_x \right]^{1+N_i} \tag{8.3.1.1.}$$

From reference (17) the heat transfer from an extended surface can be expressed as:

$$Q = A' \Delta T \tanh(B) \tag{L.2}$$

Equation L.2 is in a form that is too specific for a general operational analysis. The selection of a heat sink requires analysis of many parameters. Attention must be given to scores of small detail which in themselves appear insignificant and yet may compromise the overall performance of the final design. However, the overall performance can be only determined after series of tests; to evaluate the

Fig. K.1.

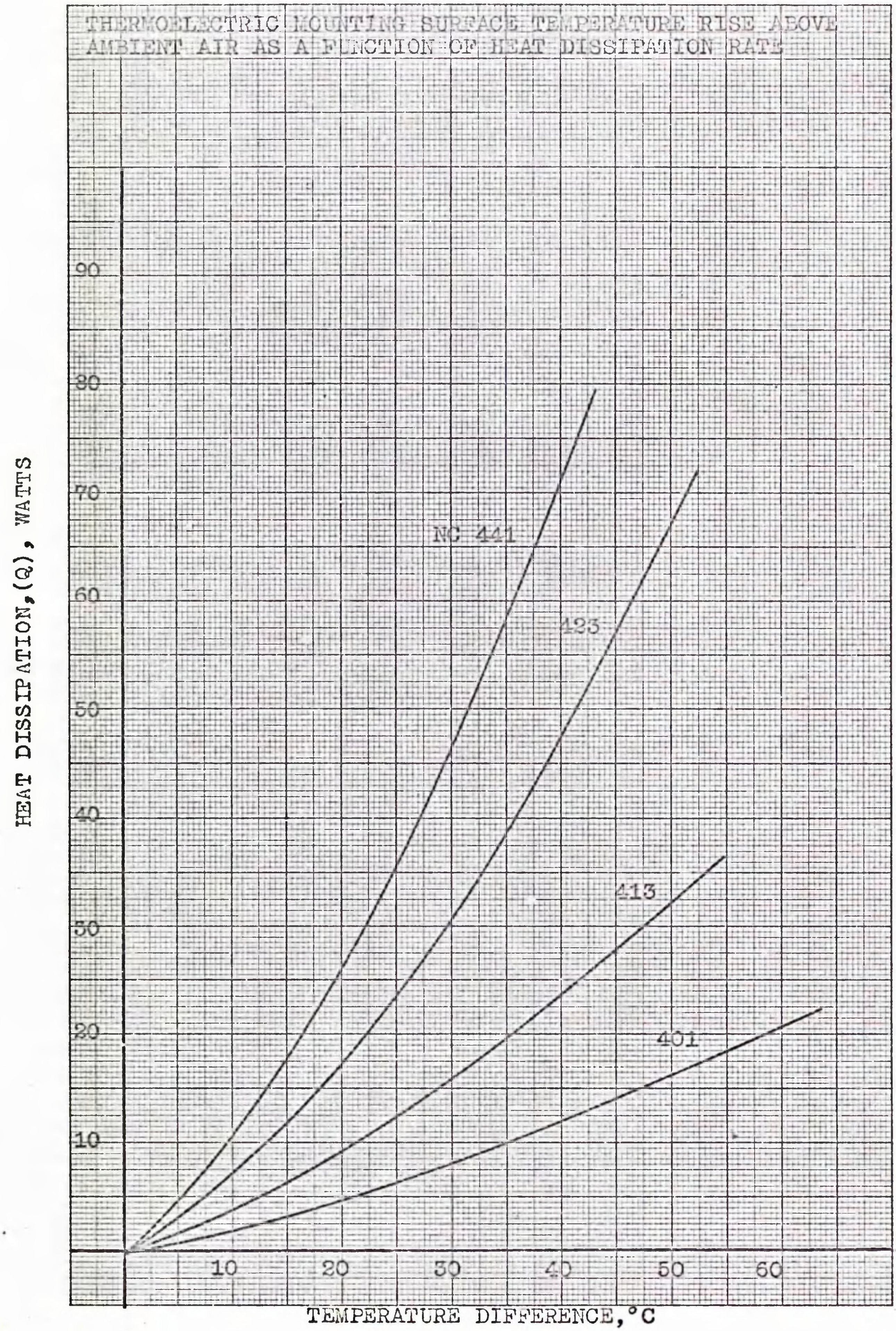
THERMOELECTRIC MOUNTING SURFACE TEMPERATURE RISE ABOVE AMBIENT AIR AS A FUNCTION OF HEAT DISSIPATION RATE
HEAT DISSIPATION,(Q), WATTS
90
80
70
60
50
40
30
20
10
NC 441
423
413
401
10
20
30
40
50
60
TEMPERATURE DIFFERENCE,°C

particular optimum features of each heat exchanger interface. By utilizing test data the problems and subsequent solution can generally be solved within the allowable envelope (space, cost). Figure K.1 illustrates the natural convection heat dissipation by means of a finned heat exchanger as a function of the mounting surface temperature rise above free stream ambient. The data is based on the 400 series Wakefield natural convection heat sinks. The general form of the equation representing the family of curves from figure K.1 is:

$$Q = D \Delta T^{m} \qquad \text{L.1}$$

where:

D,n are constants to be determined replotting figure K.1 into log-log paper results in figure K.2. From figure K.2 the resulting slope is approximately .75 which corresponds to m (power) of equation L.1. From figure K.1 (or figure K.2) the heat dissipation at $\Delta T = 40^{\circ}C$ can be determined (representative value) and hence the values of D for each heat exchanger is evaluated from equation L.1. The results indicated that: $(1.00 \leq D \leq 5.00)$ for the heat exchangers considered.

The constant slope (n) is considered to be representative of the constant characteristics for each heat exchanger.

(1) Material, Alu alloy 6603 - T5
(2) Black anodized finish
(3) Natural convection mode

Fig. K.2.

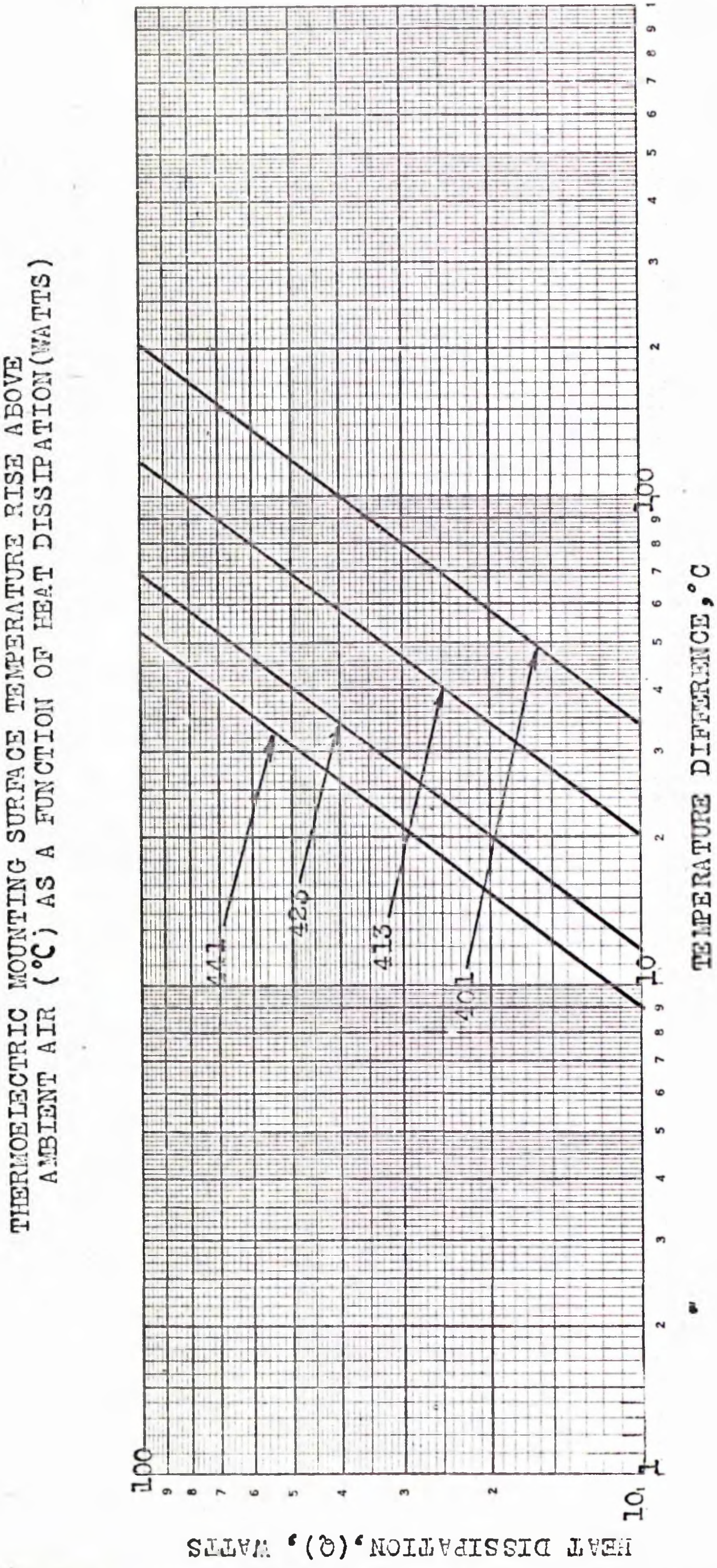
THERMOELECTRIC MOUNTING SURFACE TEMPERATURE RISE ABOVE
AMBIENT AIR (°C) AS A FUNCTION OF HEAT DISSIPATION (WATTS)
441
426
413
401
TEMPERATURE DIFFERENCE, °C
HEAT DISSIPATION, (Q), WATTS
1
10
100
10
100

The variation of D is considered to be a function of:

(1) Differences in fin area

(2) The variation in fin thermal resistance. The thermal resistance is defined as:

$$\text{Thermal resistance} \equiv \frac{\Delta T}{Q} \qquad \text{L.3}$$

where:

ΔT, temperature difference between root of fin and free stream, $^{\circ}C$.

Q, heat flow rate, watts.

Appendix M - Determination of the Heat Flux Ratio for the Interelement Insulation.

In section 7.4 the heat flux ratio $\left(q_{ACT}/q_{mi}\right)$ was introduced as a technique for determining the interelement heat leakage for the pedestal/element configuration (figure 7.4.1.1). The major assumptions made in developing a solution for the mathematical model is found in section 7.4.3.3. Figure 7.4.3.3.1 illustrates the boundary conditions for the interelement insulation. The mathematical model for the interelement insulation is defined by the following equations:

$$\frac{\partial^2 T(r,z)}{\partial r^2} + \frac{1}{r}\frac{\partial T(r,z)}{\partial r} + \frac{\partial^2 T(r,z)}{\partial z^2} = 0 \qquad \text{M.1}$$

Left-hand boundary condition:

$$T(a,z) = f(z) \qquad \text{M.2}$$

where:

$$f(z) = 0 \qquad 0 < z < z_1$$

$$f(z) = \left[\frac{z - z_1}{l - z_1}\right] T_0 \qquad z_1 < z < l_i$$

Right-hand boundary condition:

$$\frac{\partial T(b,z)}{\partial r} = 0 \qquad \text{M.3}$$

$T(b,z)$ finite value

Upper boundary condition:

$$T(r, l_i) = T_o \qquad \text{M.4}$$

Lower boundary condition:

$$T(r, 0) = 0 \qquad \text{M.5}$$

The temperature distribution will be determined by the finite difference method utilizing the technique of 'over-relaxation' to increase the convergence rate of the iterative cycle. The results are then employed in equation 7.4.3.3.1 yielding the heat flux ratio (q_{ACT}/q_{mi}) The nomenclature and symbols used are defined in section 7.4.3.4. The basic nomenclature is as follows:

a radius of pedestal column, cm

b outer radius of insulation, cm

l_i height of insulation; distance between hot and cold junction plates, cm

l^* dimensionless height of column,

$$l^* = 1 - \frac{z_1}{l_i} \qquad \text{7.4.3.5.13.}$$

r radial coordinate, cm

r^* dimensionless parameter

$$r^* = \frac{a}{b} \qquad \text{7.4.3.5.6.}$$

T_{h_j} hot junction temperature, upper boundary condition, ^oK

T_{c_j} cold junction temperature, lower boundary condition, ^oK

T_o reference temperature, $T_{h_j} - T_{c_j}$ = To, upper boundary condition

z axial co-ordinate, cm

β^* dimensionless parameter

$$\beta^* = \frac{l_i}{b} \qquad 7.4.3.5.3.$$

l_p, z_1 height of support pedestal, cm

Introducing the following variable transformations:

$$r = a + (b - a)\eta \qquad z = l_i \zeta \qquad M.6$$

$$T(r,z) = T_o \tau(\eta, \zeta) \qquad \lambda = r^* / [1 - r^*]$$

$$\mu = [1 - r^*] / \beta^* \qquad \zeta = z_1 / l_i$$

then: $$\frac{\partial T}{\partial r} = \frac{T_o}{b-a}\frac{\partial \tau}{\partial \eta} \qquad \frac{\partial^2 T}{\partial z^2} = \frac{T_o}{l_i^2}\frac{\partial^2 \tau}{\partial \zeta^2} \qquad M.7$$

and $$\frac{\partial^2 T}{\partial r^2} = \frac{T_o}{(b-a)^2}\frac{\partial^2 \tau}{\partial \eta^2}$$

Introducing equation M.7 into equation M.1 results:

$$\tau_{\eta\eta} + \frac{b-a}{r}\tau_{\eta} + \frac{(b-a)^2}{\ell_i^2}\tau_{\varphi\varphi} = 0 \qquad \text{M.8}$$

and

$$\lambda + \eta = \frac{r}{b-a} \qquad \text{M.9}$$

$$\mu^2 = \frac{(b-a)^2}{\ell_i^2} \qquad \text{M.10}$$

Substituting equation M.9 and M.10 into equation M.8 yields:

$$\tau_{\eta\eta} + \frac{1}{\lambda+\eta} t_{\eta} + \mu^2 \tau_{\varphi\varphi} = 0 \qquad \text{M.9}$$

Subject to the boundary conditions:

1. $\tau(0,\varphi) \equiv f(\varphi) = \dfrac{\varphi - \varphi_1}{1 - \varphi_1}$ left boundary $1 \geq \varphi \geq \varphi_1$

   $= 0$ $\qquad \varphi_1 \geq \varphi \geq 0$

2. $\tau_{\eta}(1,\varphi)$ $= 0$, Right boundary
3. $\tau(\eta, 1)$ $= 1$, Upper boundary
4. $\tau(\eta, 0)$ $= 0$, Lower boundary

The finite difference approximation to equation M.9 is:

$$\frac{\tau(\eta+h,\xi) - 2\tau(\eta,\xi) + \tau(\eta-h;\xi)}{h^2} + \frac{1}{\lambda+\eta}\left[\frac{\tau(\eta+h,\xi) - \tau(\eta,\xi)}{h}\right]$$

$$+ \frac{\mu^2}{h^2}\left[\tau(\eta,\xi+h) - 2\tau(\eta,\xi) + \tau(\eta,\xi-h)\right] = 0$$

M.10

Rearranging equation M.10 yields:

$$2\tau(\eta,\xi)(1+\mu^2) = \mu^2\left[\tau(\eta,\xi+h) - \tau(\eta,\xi-h)\right] + \tau(\eta+h,\xi) -$$

$$\tau(\eta-h,\xi) + \frac{h}{\lambda+\eta}\left[\frac{1}{2}\right]\left[\tau(\eta+h,\xi) - \tau(\eta-h,\xi)\right]$$

M.11

Equation M.11 can be transformed where: $h = 1/m$ and m is a positive integer. Equation M.9 reflects the boundary conditions where:

$$0 \leq \xi \leq 1$$
$$0 \leq \eta \leq 1 \qquad \text{square domain}$$

Hence:

$$L_h \tau(\eta,\varsigma) \equiv -\tau(\eta,\varsigma) + \frac{1}{2(1+\mu^2)}\Bigg[\left[1+\frac{\frac{1}{2}h}{\lambda+\eta}\right]\tau(\eta+h,\varsigma) + \left[1-\frac{\frac{1}{2}h}{\lambda+\eta}\right]\times$$

$$\times\, \tau\left[\eta-h,\varsigma\right] + \mu^2 \tau\left[\eta,\varsigma+h\right] + \mu^2 \tau\left[\eta,\varsigma-h\right]\Bigg]$$

M.12

where L_h is the difference operator.

Introducing the operator parameter into the boundary conditions of equation M.9 yields:

$$\begin{aligned}
L_h \tau(0,\varsigma) &\equiv -\tau(0,\varsigma) = -f(\varsigma) \\
L_h \tau(1+h,\varsigma) &\equiv -\tau(1+h,\varsigma) + \tau(1-h,\varsigma) = 0 \\
L_h \tau(\eta,0) &\equiv \tau(\eta,0) = 0 \\
L_h \tau(\eta,1) &\equiv \tau(\eta,1) = 0
\end{aligned}$$

M.13

To express the difference equations (M.12) and (M.13) as matrix equations proceeding as follows: For any point P (ih, jh) of the working domain R_h defined as the generality of pts. for integer i, j in the intervals i = 0(1) n + 1, j = 0(1) n we suppose τ (P) is the value of which satisfies equations (M.12) and (M.13). There are N = (n + 2) (n + 1) such points in R_h and consequently N equations of the form:

$$L_h \tau(P) = \sum_{Q \varepsilon R_h} C(P,Q)\tau(Q) = D(P) \qquad \text{M.14}$$

where:

$Q \varepsilon R_h$ represents the points in the working domain R_h

Equation M.12 embodies $m(m-1)$ of these N equations for the interior points of R_h , each of the first two of the equations (M.13) embodies $(m-1)$ (for $j = 1(\ )(m-1)$ and the two latter each embody $(m+2)$ (for $i = D(1)(m+1)$ giving:

$$N = m(m-1) + 2(m-1) + 2\,(m+2) \qquad \text{M.15}$$

where:

N expresses the number of equations of type M.14

If $\underset{\sim}{\tau}$ is now regarded as an N-pt. vector representing the ordered set of values of τ (P), then the linear operator L_h is represented as a square matrix $\underset{\sim}{C}$ of order N. Similarly $\underset{\sim}{D}$ can be taken as the vector of the constants D (P) in equation M.14. Note that all the principle diagonal elements of $\underset{\sim}{C}$ equal - 1, and this matrix has the property of diagonal dominance. (i.e. for sufficiently small h, the sum of the absolute values of any row of $\underset{\sim}{C}$ is ≤ 1 the critical value of h being 2λ , i.e. for $m > \frac{1}{2} = \frac{1}{2}\,(1/r^{4} - 1)$). Equation M.14 can be considered as the matrix equation

$$\mathbf{C}\,\mathbf{T} = \mathbf{D} \qquad \text{M.16}$$

This may be solved by any of the numerous iterative schemes which are known to converge if $\mathbf{C}$ has the property of diagonal dominance. The method of explicit successive over-relaxation is proposed as the solution technique.

Let $\mathbf{T}^{(1)}$, $\mathbf{T}^{(2)}$, $\mathbf{T}^{(3)}$ .....denote successive values of $\mathbf{T}$ at the completion of each stage of the iterative process begun by supposing any starting set $\mathbf{T}^{(0)}$. Further suppose the calculation for each component $T_i^{(k)}$ of $\mathbf{T}^{(k)}$ are in the order in which they are represented in the vector. Then the method consists of calculating:

$$\mathbf{T}^{(k)} = (1-\omega)\mathbf{T}^{(k-1)} + \omega\left[\mathbf{L}\,\mathbf{T}^{(k)} + \mathbf{U}\,\mathbf{T}^{(k-1)} - \mathbf{D}\right] \qquad \text{M.17}$$

where:

$$\mathbf{C} = \mathbf{L} + \mathbf{U} - \mathbf{I} \qquad \text{M.18}$$

and

$\mathbf{L}$ and $\mathbf{U}$ represent respectively the triangular matrices formed by the values of the elements of $\mathbf{C}$ below or above the main diagonal. The upper and lower triangular matrices form a commutative group under the operation of addition.

$\mathbf{I}$ is the unit matrix; a diagonal matrix with all its diagonal element equal to unity. The diagonal matrix has zero elements everywhere except in the leading diagonal.

The proposed iteration technique is based on a modified "Gauss-Seidel" method. The over-relaxation method for the solution of the system of equations: $\underset{\sim}{C}\,\underset{\sim}{T} = \underset{\sim}{D}$; where $\underset{\sim}{C}$ is the matrix of coefficients, $\underset{\sim}{T}$ column matrix (vector) and $\underset{\sim}{D}$ column matrix on right define a sequence of vectors $T^{(k)}$. When $T_1^{(k)}$ is thus evaluated $L\underset{\sim}{T}^{(k)}$ depends only on the values of $T_1^{(k)}, T_2^{(k)} \ldots\ldots T_{i-1}^{(k)}$ already formed. It can be shown (18) that the iteration implied by (M.17) converges for all $0 < \omega < 2$ the value $\omega = 1$ leads to the special case of the so-called iteration by successive displacements (Gauss-Seidel method), but values of ω between 1 and 2 (implying over-relaxation) lead to a much more rapid rate of convergence.

The best value of ω is determined by the use of the property that the average convergence factor ($\rho(\omega)$, here in after to be defined) is related to the best value ω_{OPT} by the equation (18).

$$\frac{\omega_{OPT}}{\omega} = \frac{2}{\left[\omega + (1+\rho)^{0.5}\left[1-(\omega-1)^2/\rho\right]^{0.5}\right]} \qquad \text{M.19}$$

$$\omega < \omega_{OPT}$$

and

$$\rho(\omega) = \omega - 1 \qquad \omega > \omega_{OPT}$$

The average convergence factor is the limit of many sequences. Thus if:

$$\underset{\sim}{Y}^{(k)} = \underset{\sim}{T}^{(k+1)} - \underset{\sim}{T}^{(k)} . \qquad \text{M.20}$$

then:

$$\lim_{k \to \infty} Q_k = \rho(\omega)$$ where:

$$Q_k = \frac{\| Y^{(k)} \|}{\| Y^{(k-1)} \|}$$ and

$$\| Y^{(k)} \| = \sum_{P \in R_h} | Y^{(k)}(P) |$$

where by definition:

$$\| X \| = \left[\sum_{i=1}^{m} | X_i |^2 \right]^{0.5}$$ is the Euclidean norm or length of X (Column vector)

The boundary condition introduces a maximum value of T along η = 1, therefore:

$$\| \underset{\sim}{Y}^{(k)} \| = \sum_{j=0}^{m} \left| T^{(k+1)}(1, jh) - T^{k}(1, jh) \right| \qquad \text{M.21}$$

However, the convergence of Q_k towards its limit Q_∞ is usually very irregular if ω is already close to ω_{OPT} Further if (inadvertantly) a value of ω is used which is $> \omega_{OPT}$ then as shown by M.19 the limit is of no use in determining ω_{OPT} (since $Q_k \longrightarrow \omega - 1$). The procedure for finding ω_{OPT} is as follows:

Select an initial value of ω (1.5 was used in the computer programme with success) not too large to be $> \omega_{OPT}$. Carry out the iterative generation of $\underset{\sim}{T}^{(1)}$, $\underset{\sim}{T}^{(2)}$ by M.17. After forming each $\underset{\sim}{T}^{(k)}$ for $k \geq 2$ find Q_k For $k \geq 3$, test values of (Q_k - Q_{k-1}): if this difference is sufficiently small (say ≤ 0.05) and if $Q_k > N^{1/k} (\omega - 1)$, then suppose $\rho(\omega) \simeq Q_k$ and use the first of the equations (M.19) to determine a better value of ω to be used in (M.17) for forming $\underset{\sim}{T}^{(k+1)}$, $\underset{\sim}{T}^{(k+2)}$, ... etc. The inequality $Q_k > N^{1/k} \times (\omega - 1)$ serves to reject values of which are (apparently) derived with $\omega > \omega_{OPT}$.

With the improved value of ω the process of finding a better value may be re-instated by generating a new sequence of Q_k, but usually one such approximation (ω = 1.5 starting value) is very close to ω_{OPT}. The gain of speed of computation by working at or close to ω_{OPT} will be pronounced and is considered to be well worth the effort.

With fixed h (i.e. fixed n and N), the iterative solution of $\underset{\sim}{T}$ by (M.17) proceeds until some error norm of the vector $\left(\underset{\sim}{T}^{k+1} - \underset{\sim}{T}^{k} \leq eps\sigma\right)$ is sufficiently small. Thus the norm given by M.21 and stop the process for $\| Y^k \| < \varepsilon h$

The value of h must be sufficiently small so that the difference between the solution of the difference equations M.16 for τ, and the solution of the differential equation M.12, be $< \varepsilon$. In other words, the discretisation error must be $< \varepsilon$, as well as the error in solving the difference equation (truncation error E). The discretisation error using Taylor's theorem is $E = O(h^4)$ which gives a rough estimate of the size for h consistent with the error tolerance. The starting value incorporated into the computer process was a small n (large h) equal to:

$$\text{entier}\ (0.5 \times (1.0 / r^* - 1.0)) + 2$$

storing the values of τ (1, jh) for j = 1(1)(n-1), formed by solving M.17 repeated until $\| Y^{(k)} \| < \varepsilon_m$. Then double the value of n and use $\underset{\sim}{\tau}^0$ the values of $\underset{\sim}{\tau}$ formed for the previous solution, the values of τ at the gird points not coincident with those of the former gird being interpolated. Relax the solution for $\underset{\sim}{\tau}$ in this new R_h, and then compare the converged values of τ (1, jh) for j = 2(2)(n-2) with those previously stored. If the sum of the absolute values of these differences is $< \varepsilon_m$ then the new solution has an acceptable discretisation error, else store the values of τ (1, jh) for j = 1 (1) n-1 and repeat the process.

There is thus a three fold iteration: an outer iteration of n (orh) and an inner iteration of $\underset{\sim}{\tau}$ by (M.17), with an intermediate process watching the values of ω and iterating a solution for ω_{opt}. The final form of the computer program (C.P.5.) (procedure phaseq) uses ω and n as variable parameters to form $\tilde{\tilde{\tau}}$ with an error tolerance $\mathcal{E}$ (epso).

The heat flux ratio $\left(q_{ACT}/q_{mi}\right)$ will be evaluated as follows:

From equation 7.4.2.1. and equation 7.4.3.3.1.

$$\frac{q_{ACT}}{q_{mi}} = \frac{\ell \int_a^b 2r \left.\frac{\partial T}{\partial z}\right|_{z=l_i} dr}{T_0 b^2} \qquad M.22$$

From equation M.6

$$\frac{\partial T}{\partial z} = \frac{T_0}{l_i}\frac{\partial \tau}{\partial \zeta} \qquad M.23$$

Substituting equation M.23 into equation M.22 with the integration limits, a = 0, b = 1 yields:

$$\frac{q_{ACT}}{q_{mi}} = \frac{\int_0^1 2r \left.\frac{\partial \tau}{\partial \zeta}\right|_{\zeta=1} dr}{b^2} \qquad M.24$$

where:

$$r = a + (b - a) \qquad M.25$$

$$dr = (b - a)\,d\eta$$

Introducing equation M.25 into M.24 and expanding gives:

$$\frac{q_{ACT}}{q_{mi}} = \int_0^1 2\left[r^* - r^{*2} + \eta\,(1 - r^*)^2\right] \frac{\partial \tau}{\partial \xi}\bigg|_{\xi=1} d\eta \qquad \text{M.26}$$

where:

η = i x h or discute value along ξ = 1

From equation M.10 the $\partial\tau/\partial\xi\,\big|_{\xi=1}$ is replaced by the central difference quotient yielding:

$$\frac{\partial \tau}{\partial \xi}\bigg|_{\xi=1} = \frac{1 - \tau[i, m-1]}{h} \qquad \text{M.27}$$

This can also be obtained by the backward difference method. Substituting equation M.27 into equation M.26:.

$$\frac{q_{ACT}}{q_{mi}} = \frac{\int_0^1 2\left[r^* - r^{*2} + \eta\,(1 - r^*)^2\right]\left[1 - \tau[i, m-1]\right]}{h} \qquad \text{M.28}$$

Letting:

$A = 2\,{}^* - 2r^{*2}$

$B = 2\,(1 - r^*)$

$Y(\eta) = 1 - \tau[i, m-1]$

then:

$$\frac{q_{ACT}}{q_{mi}} = \frac{\int_0^1 [A + B\eta] Y(\eta) d\eta}{h} \quad \eta = i \times h$$

M.29

Applying the trapezoidal rule for integration gives:

$$\int_a^b f(x) dx \cong \Delta x \left[\frac{f(a)}{2} + \frac{f(b)}{2} + f(x) + \dots f(x_{n-1}) \right] \qquad \text{M.30}$$

where:

$$\Delta x = \frac{b - a}{n} = \frac{1}{n} = h$$

$$\int_0^1 f(x) dx \cong \left[\frac{AY(0)}{2} + \left[\frac{A+B}{2} \right] Y(1) + \sum_{i=1}^{n-1} [A + B(ih)] Y(ih) \right]$$

M.31

Redefining terms:

$$'A' = \frac{A}{2} \qquad B' = \frac{A + B}{2} \qquad \text{M.32}$$

$$Y(0) = (1 - \tau[0, n - 1] \quad)$$

$$Y(1) = (1 - \tau[n, n - 1] \quad)$$

HEAT FLUX RATIO AS A FUNCTION OF GEOMETRICAL PEDESTAL PARAMETERS

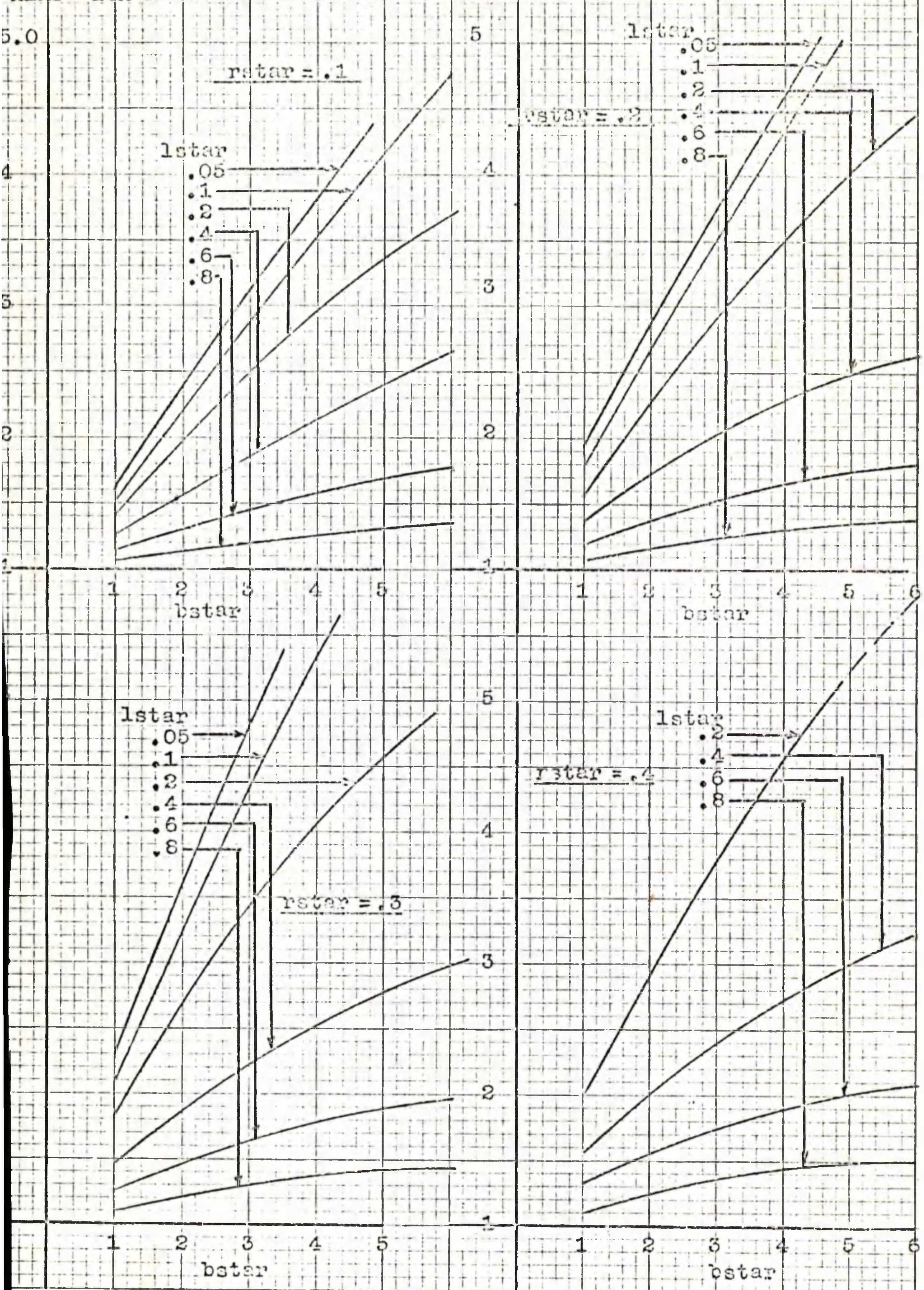

then:

$$\frac{q_{\delta ACT}}{q_{\delta mi}} \cong \left[A'Y(0) + B'Y(1) + 2\sum_{i=1}^{i=n-1} \left[A' + B'(ih)\right] Y(ih) \right] \qquad \text{M.33}$$

where:

$$Y(ih) = (1 - \quad I\left[i,\ n-1\right] \quad)$$

Figure M.1 illustrates $(q_{\delta ACT} / q_{\delta mi})$ as a function of the dimensionless parameters: B*, r*, l*.